

The Design and Synthesis of Novel Epigenetic Modulators

Katherine Jones



Epinova Discovery Performance Unit, GlaxoSmithKline

Department of Pure & Applied Chemistry, University of Strathclyde

Supervised by Rino Bit and Professor Colin Suckling

Declarations of Authenticity and Author's Rights

This thesis is the result of the author's original research. It has been completed by the author and has not been previously submitted for examination which has led to the award of a degree.

The copyright of this thesis belongs to GSK in accordance with the author's contract of employment with GSK under the terms of the United Kingdom Copyright Acts. Due acknowledgement must always be made of the use of any material contained in, or derived from, this thesis.

Signed:

Date:

Katherine Jones

Research Involving Animals

All animal studies were ethically reviewed and carried out in accordance with Animals (Scientific Procedures) Act 1986 and the GSK Policy on the Care, Welfare and Treatment of Animals.

Copyright Details

Figure 1.02 copyright (2005) National Academy of Sciences, USA. (*Proc. Natl. Acad. Sci. U. S. A.* **2005**, *102*, 10604-10609)

Figure 1.07 reprinted from *Prog. Med. Chem.*, 51, C. Chung, Small molecule bromodomain inhibitors: extending the druggable genome, Pages 1-55, copyright (2012), with permission from Elsevier.

Figure 1.10 reprinted by permission from Macmillan Publishers Ltd: NATURE (*Nature* **2010**, *468*, 1067-1073), copyright (2010).

Figure 1.12 reprinted by permission from Macmillan Publishers Ltd: NATURE (*Nature* **2010**, *468*, 1119-1123), copyright (2010).

Figures 1.18 and 1.19 reprinted by permission from Macmillan Publishers Ltd: NATURE CHEMICAL BIOLOGY (*Nat. Chem. Biol.* **2009**, *5*, 647-654), copyright (2009).

Figure 1.20 reprinted by permission from Macmillan Publishers Ltd: NATURE REVIEWS DRUG DISCOVERY (*Nat. Rev. Drug Discovery* **2004**, *3*, 711-715), copyright (2004).

Figure 1.27 reprinted with permission from (*J. Med. Chem.* **2010**, *53*, 1098-1108). Copyright (2010) American Chemical Society.

Abstract

This thesis describes the design and synthesis of small molecule epigenetic inhibitors, motivated by the identification of disease treatments which will provide innovative medicines for patients. The work reported is focused on the identification of compounds which bind to the bromodomains of the BET family of proteins. These bromodomains have been implicated in a number of therapeutic areas, including oncology and immuno-inflammatory diseases.

In Part I, an introduction to current challenges in drug discovery sets the scene for the work reported within this thesis. The science of epigenetics is introduced, and key medicinal chemistry themes relevant to these PhD studies are presented.

In Part II, an orally bioavailable BET bromodomain inhibitor suitable for clinical progression was identified, the first such example from the dimethylisoxazole series of compounds. Medicinal chemistry was focused on SAR generation, and the control of physicochemical properties by the use of *in silico* profiling. Ultimately, the pre-clinical candidate molecule was synthesised on a large scale to provide material for further *in vivo* safety and efficacy studies.

In Part III, esterase sensitive motif (ESM) technology was used to target molecules to cells of the monocyte/macrophage lineage with the aim of improving tolerability. ESM technology was incorporated into BET bromodomain inhibitors, and molecules were identified to probe the viability of this approach in the BET bromodomain area.

In Chapter 3, preliminary work was undertaken to establish a successful proof of principle for the use of ESM technology within the BET bromodomain area. In Chapter 4, the chemical series was further developed, resulting in an increased cellular potency of the molecules. As a result, an *in vitro* probe molecule was identified which could be used to further elucidate BET-ESM technology.

In Chapter 5, medicinal chemistry design was focused on improving the drug-like properties of the series, increasing cellular permeability, and reducing *in vitro* clearance. By balancing these properties, a molecule was identified for *in vivo* profiling, and is currently under investigation to assess its suitability as a pre-clinical candidate molecule.

Table of Contents

<i>PART I: INTRODUCTION</i>	1
Chapter 1: Introduction	
Title page	2
1.1 Prologue.....	3
1.2 Epigenetics	6
1.3 BET Bromodomains.....	10
1.3.1 Therapeutic Relevance of the BET Protein Family	12
1.3.2 Small Molecule BET Bromodomain Inhibitors	17
1.4 Medicinal Chemistry Strategies in Epigenetic Research.....	22
1.4.1 Structure of an Epigenetic Research Programme	22
1.4.2 Hit Identification Using Encoded Library Technology	24
1.4.3 Monitoring Physicochemical Properties during Drug Discovery	28
1.4.4 Requirements for Oral Administration of Drugs	34
1.5 Areas for Research	37
<i>PART II: BET BROMODOMAIN INHIBITORS</i>	38
Chapter 2: The Design and Synthesis of BET-Bromodomain Inhibitors for Oral Administration	
Synopsis.....	39
2.1 Background	40
2.2 Medicinal Chemistry Design of Compounds for Synthesis	44
2.3 Synthesis of Target Molecules	47
2.3.1 Scale-up of Key Intermediate 2.33	47
2.3.2 Synthesis of Imidazoquinolone Analogues.....	49
2.3.3 Synthesis of Imidazoquinoline Analogues.....	51
2.3.4 Synthesis of Enantiopure α -Methyl Tetrahydropyran Analogues.....	56
2.3.5 Synthesis of Dimethylamino Analogue	59
2.3.6 Remake of Compound 2.06 and its α -Methyl Analogue	60
2.3.7 Separation of Enantiomers of Compound 2.02	62
2.4 Biological Results and Analysis.....	63
2.4.1 Primary Data for Imidazoquinolone Compounds	64

2.4.2 Primary Data for Imidazoquinoline Compounds.....	65
2.4.3 Secondary Data for Compounds of Interest.....	68
2.5 Scale-Up of Lead Molecule 2.67	72
2.6 Salt Formation.....	76
2.6.1 Selection and Synthesis of Salts.....	76
2.6.2 Results.....	78
2.7 Conclusions and Future Work.....	80
<i>PART III: ESTERASE SENSITIVE MOTIFS</i>	83

Chapter 3: Targeting BET Bromodomain Inhibitors to Macrophages Using Esterase-Sensitive Motifs: Background and Preliminary Work

Synopsis.....	84
3.1 Targeted Drug Delivery and Esterase Sensitive Motifs.....	85
3.2 Aims of Esterase-Sensitive Motif Programme of Work.....	90
3.3 Current Status of Dimethylphenol Series.....	91
3.4 Incorporation of an ESM within a BET Chemotype.....	97
3.4.1 Design of Initial ESM-containing Compounds.....	97
3.4.2 Synthesis of Initial ESM-containing Compounds.....	99
3.4.2.1 Synthesis of Key Intermediate 3.25	99
3.4.2.2 Synthesis of Parent Molecule 3.22	99
3.4.2.3 Synthesis of ESM-containing Compounds.....	101
3.4.3 Biological Results and Analysis.....	103
3.4.3.1 Primary Screening Data.....	104
3.4.3.2 Secondary Screening Data.....	105
3.5 Summary of Proof of Concept Studies.....	108

Chapter 4: The Identification of a Molecule to Probe the *In Vitro* Biology of BET Bromodomain Inhibitors Containing an Esterase Sensitive Motif

Synopsis.....	109
4.1 Criteria for a BET-ESM <i>In Vitro Probe Molecule</i>	110
4.2 Medicinal Chemistry Design of Changes to the Benzimidazole Core.....	111
4.3 Synthesis of Compounds with Benzimidazole Core Changes.....	114
4.3.1 Synthesis of Compounds with Benzimidazole Core Replacements.....	114
4.3.2 Synthesis of Aza-benzimidazole Templates.....	115

4.4 Primary Data for Compounds with Benzimidazole Core Replacements.....	118
4.5 ESM-containing Compounds with Monoaryl Cores	121
4.5.1 Synthesis of ESM-containing Compounds with Monoaryl Cores	121
4.5.2 Biological Data on ESM-containing Compounds with Monoaryl Cores.....	122
4.6 Design of Compounds to Investigate <i>N</i> -Substituent.....	125
4.7 Synthesis of Benzimidazole <i>N</i> -Substituent Analogues	129
4.8 Primary Data for Benzimidazole <i>N</i> -Substituent Changes	130
4.9 Incorporation of ESMs into Pyridone Benzimidazole Template.....	134
4.10 Biological Data on ESM-containing Compounds from Pyridone Benzimidazole Template.....	136
4.11 Conclusions and Future Work Within the ESM Programme.....	140

Chapter 5: Discovery of an *In Vivo* Tool BET Bromodomain Inhibitor Containing an Esterase Sensitive Motif

Synopsis.....	142
5.1 Aims of BET-ESM Compound Optimisation.....	143
5.2 Medicinal Chemistry Design of Compounds for Synthesis.....	145
5.3 Synthesis of Initial Target Molecules	153
5.4 Biological Results and Analysis	162
5.4.1 Primary Screening Data	163
5.4.2 Secondary Screening Data for Compounds of Interest	172
5.5 Further Medicinal Chemistry Design	175
5.6 Further Synthesis of Target Molecules.....	178
5.7 Further Biological Results and Analysis	183
5.8 Conclusions and Further Work.....	187

Chapter 6: Epilogue

Conclusions.....	190
------------------	-----

Experimental

General Experimental Details	195
Chapter 2.....	198
Chapter 3.....	231
Chapter 4.....	240

Chapter 5	273
-----------------	-----

Appendix 1: Assay Details

<i>In Vitro</i> Assay Protocols	307
<i>In Silico</i> Modelling Details	314

Appendix 2: Benzimidazole *N*-Substituent Changes

Table 1: Full List of Compounds for Synthesis	316
Table 2: Yields of Reactions in Chapter 4, Scheme 4.07.....	320
Table 3: Assay Data for Ester Hydrolysis Products for Compounds 5.01 – 5.12	322

Appendix 3: Abbreviations

Abbreviation list.....	323
------------------------	-----

References

Chapter 1	331
Chapter 2	336
Chapter 3	338
Chapter 4	339
Chapter 5	340

Acknowledgements

Firstly, I would like to thank Rino Bit and Professor Colin Suckling for their supervision throughout this PhD, and for the comments and suggestions they gave me whilst compiling this thesis. I would also like to thank Ann Walker, Nigel Parr, and Jack Brown, my managers during this work, for their guidance and support, as well as the time they have dedicated to helping me despite their busy schedules. This has been very much appreciated. I am also grateful to Sue Westaway, Rob Sheppard and Dominique Amans for their comments on various sections of the thesis, as well as Dom Beaumont, Laurie Gordon, Zhengrong Zhu and Adriana De Simone for help with answering questions that came up during its compilation.

Many colleagues within Epinova have made suggestions around the medicinal and synthetic chemistry reported. This particularly includes programme chemistry leaders Jack Brown and Ann Walker; my supervisor Rino Bit; as well as other group members Jon Seal, Bob Watson, Emmanuel Demont and Matt Walker. In addition, the progress of the last four years would have been much less significant without my excellent industrial placement students Juliet Foster, Matt Keeling, Suil Collins, Anet Varghese and Piotr Wojciechowski, as well as other students within the group including Luke Donnellan and Robin Carton.

It would have been impossible to compile this thesis without the support of many colleagues throughout GSK. The majority of biological data in this thesis has been generated by the Biological Sciences group: in particular Laurie Gordon, Toni Lewis and Jon Hutchinson. Additionally, within the iiTAU, human whole blood assays were run by Pete Soden and Sharon Bernard, macrophage retention studies by Pal Mander and Rich Gregory, and DMPK experiments by James Gray. X-ray crystallographic support has been provided by Chun-wa Chung, and structural modelling support by Pam Thomas. The assistance of many colleagues in completing a large data integrity package to support this thesis is also very much appreciated. Analytical chemistry support was provided by the Chemical Sciences group, and I am particularly grateful to Andy Knaggs for large scale chiral separation work.

I would like to thank the Epinova DPU for supporting my involvement in the PhD programme; and both Harry Kelly and the University of Strathclyde for all their hard work in putting the programme together. And last, but not least, Robert Whittaker for suggestions on layout that have made this report significantly more readable, his academic-industry translation service, and putting up with weekend working despite the fact that chemistry is a vastly more inferior member of the science family than mathematics.

PART I:
INTRODUCTION

Chapter 1

Introduction

“It was love at first sight.”

Joseph Heller, Catch-22

1.1 Prologue

These are currently challenging times for small-molecule drug discovery within the pharmaceutical industry. Prior to a new drug being approved for use, regulatory agencies have increasingly demanding requirements to demonstrate a sufficient safety and efficacy profile, and payers are increasingly concerned with the cost–benefit ratio. Stringent regulatory requirements, and high levels of attrition throughout the research and development (R&D) process, led to a R&D cost estimated in 2010 of \$1.8bn per approved medicine.^{1.01} Data indicates that only 10% of compounds that are selected as clinical candidates reach the market.^{1.02} These factors have made it increasingly difficult to produce reimbursable medicines.

One strategy employed to increase the success rate in drug discovery is to focus on the physicochemical properties of the molecule, which have been identified to impact on attrition.^{1.03, 1.04} This approach has been followed to some extent within drug discovery since Lipinski's initial paper on the subject in 1997.^{1.05} Although this has significantly changed the way people approach drug discovery, there has been limited success in reducing the overall levels of small molecule attrition.^{1.06} This may in part be due to the challenges associated with designing and discovering potent and selective molecules that fulfil the desired physicochemical criteria, which has meant that clinical candidates still often lie outside the desired physicochemical space. Keeping physicochemical properties, such as molecular weight and lipophilicity, at the forefront of medicinal chemistry thinking is undoubtedly a critical part of reducing attrition. However, in isolation it will not overcome all of the industry's challenges.

To improve the chance of success in discovering innovative medicines, it is necessary to investigate the potential of novel biological mechanisms to deliver positive clinical outcomes. Novel biological mechanisms, which have not been studied in great depth, can be described as a “high risk, high reward” method of delivering a medicine that will meet unmet medical need in patients. If successful, these medicines have the opportunity to make it easier to show clinicians and payers a benefit of the medicine compared with its side effects and cost.

Epigenetics is a rapidly expanding new area of science, with fewer than 5000 articles in the scientific literature prior to 2005, and over 15,000 between 2005 and the commencement of these PhD studies in July 2010 (Figure 1.01). This can be compared to more comprehensively studied areas of science, such as kinases, where between 1990 and 2010 there had been over 400,000 articles in the scientific literature, and GPCR's, where between 1990 and 2010 there had been over 200,000 articles.

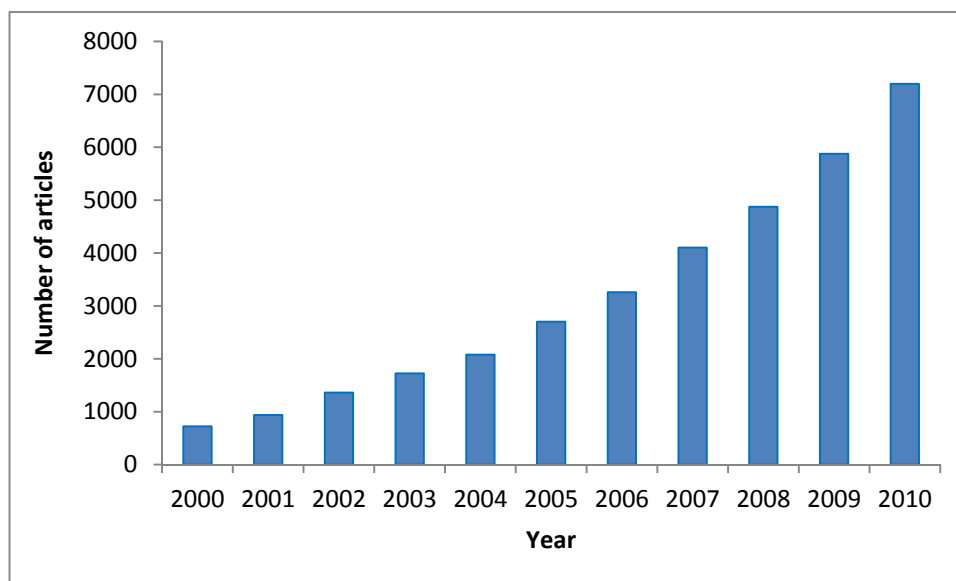


Figure 1.01: The number of articles mentioning epigenetics published in the scientific literature from 2000 to 2010.

To explore the biological potential of modulating the activities of epigenetic proteins, a number of techniques may be employed. These include the use of siRNA, knockout models, and small-molecule chemical probes. The latter are of particular interest in drug discovery as they most closely display the effects that would be seen by small-molecule drugs. The discovery of selective small-molecule probe molecules, for use in *in vitro* and *in vivo* biological models, would allow a greater understanding of the potential within the epigenetic area to deliver novel medicines. Where probe molecules have demonstrated a biological rationale for targeting a specific protein, candidate-quality molecules with good physicochemical and pharmacokinetic properties can then be used to study the safety profiles of epigenetic modulators. The information gained from these studies can then be used to provide a detailed rationale to begin clinical trials in patients.

The research described within this thesis encompasses the design of novel compounds via a number of different medicinal chemistry strategies, as well as the design and implementation of synthetic routes to access compounds for biological screening. Analysis of the data from these screens is then performed, and used to either direct further compound design, or to decide which compounds to progress into further biological studies to better understand their value as probe or drug candidate molecules.

Throughout this work, robust medicinal chemistry principles are applied. When designing a probe molecule, the physicochemical properties required are dictated by whether the probe molecule will be used as an *in vitro* intracellular probe, or an *in vivo* probe. When aiming for candidate molecules, physicochemical properties that give the best chance of seeing a high level of efficacy and safety *in vivo* are always required. Hit molecules and series are ranked by considering the attractiveness of the physicochemical properties, and these are monitored as the design process progresses. There is also a focus on achieving high levels of biological activity and, where relevant, high levels of selectivity against related biological targets.

In order to maximise the knowledge gained of epigenetic proteins in this competitive area, with the chemistry resource and time frame available within our laboratories, there are specific requirements for the synthetic chemistry undertaken. Synthetic routes are initially designed to access the desired molecules as quickly as possible, and routes are favoured which allow for rapid diversification of chemical structure in parts of the molecule identified for structure–activity relationship (SAR) investigation. Novel final compounds are synthesised, wherever possible, in greater than 25 mg quantities and greater than 95% purity by ¹H NMR. This allows sufficient compound availability for full *in vitro* profiling of compounds, and initial *in vitro* and *in vivo* DMPK studies.

1.2 Epigenetics

Epigenetics can be defined as the study of traits heritable through meiosis or mitosis that are not dependent on the primary DNA sequence.^{1.07} Different epigenetic modifications to genetically identical cells or individuals can lead to different gene expression patterns and therefore different phenotypes.

In 2005, Fraga *et al.* studied the global and locus-specific differences in the epigenome of a large cohort of monozygotic twins.^{1.08} They found that twins were epigenetically indistinguishable during early life, but exhibited marked differences in their epigenome in later life (Figure 1.02). The change in the epigenome of monozygotic twins was proposed as one possible explanation for their differences in susceptibility to disease.

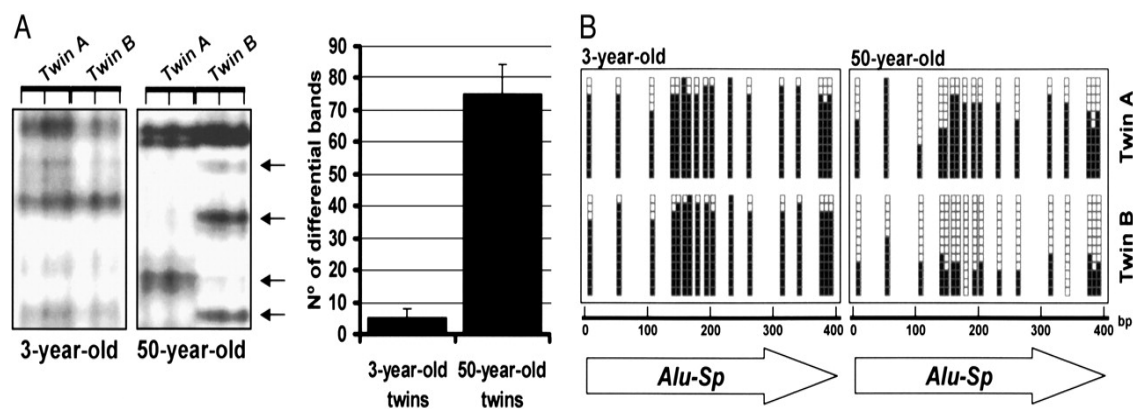


Figure 1.02:^{1.08} Mapping sequences with differential DNA methylation between monozygotic twins. A (left): Example of an AIMS (Amplification of Intermethylated Sites) analysis in 3- and 50-year-old twins. A (right): Number of differential bands obtained by AIMS. B: Bisulfite genomic sequencing of 12 clones of the repetitive DNA sequence Alu-SP obtained by AIMS in 3- and 50-year-old twin pairs. Schematic representations of the methylation status of each CpG dinucleotide. Black and white dots indicate methylated and unmethylated CpGs, respectively.

There are two main components of the epigenetic code (Figure 1.03).^{1.09} The first is DNA-methylation, where methyl groups (or ‘marks’) are added to DNA bases, usually adding to a cytosine where it is followed by guanine. The presence of the methyl mark affects the structure of chromatin, the combination of DNA and proteins which form the contents of the nucleus. This change in chromatin structure usually leads to the long term down-regulation of gene activity. The second component of the epigenetic code is histone modification. Histones are proteins around which DNA winds to form nucleosomes, and are the major protein components

of chromatin. A combination of modifications to the ‘tails’ of histones determines whether chromatin is tightly packed, shutting down gene expression, or more open, where gene expression may be active.

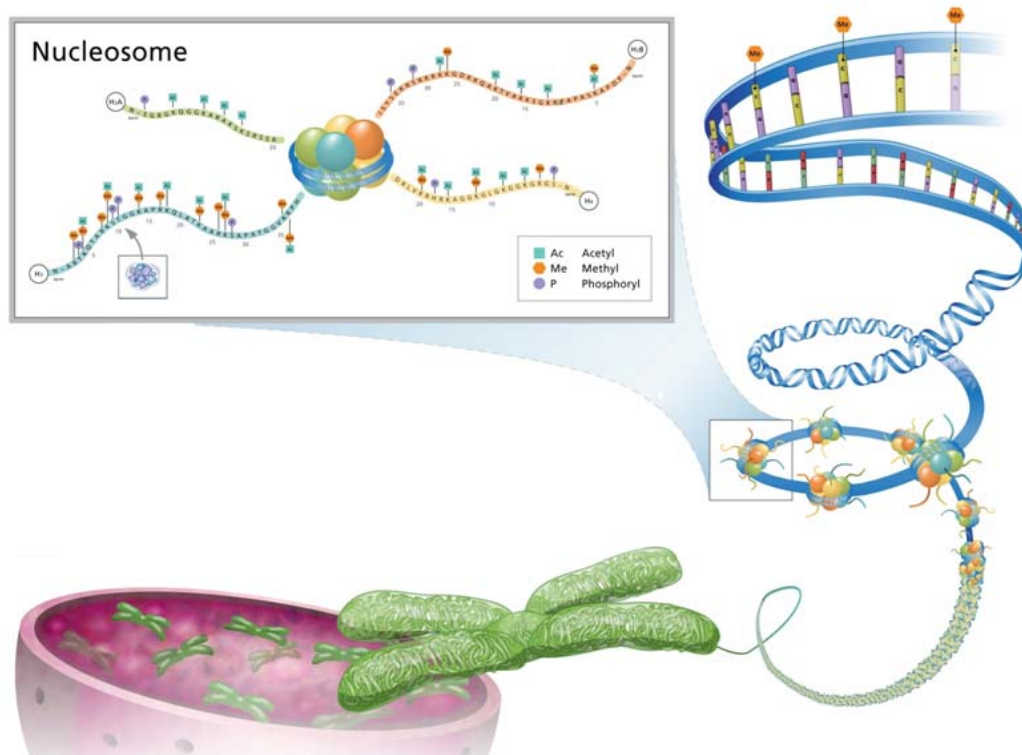


Figure 1.03: The main components of the epigenetic code: DNA methylation and histone modification.

There are a variety of epigenetic modifications known to occur on histone tails, including methylation, acetylation, phosphorylation, citrullination and ubiquitination.^{1,10} The processes involved in governing the epigenetic code can be grouped into the writing, erasing and reading of these modifications (Figure 1.04). Enzymes known to catalyse the transfer (‘writing’) of epigenetic marks onto histone tails include histone methyl and acetyl transferases, and those known to catalyse the removal (‘erasing’) of epigenetic marks include histone demethylases and deacetylases. There are also a number of protein domains which are involved in recognising (‘reading’) these epigenetic marks. These include bromodomains, which recognise acetylated lysine residues, and tudor domains, which recognise methylated lysines.

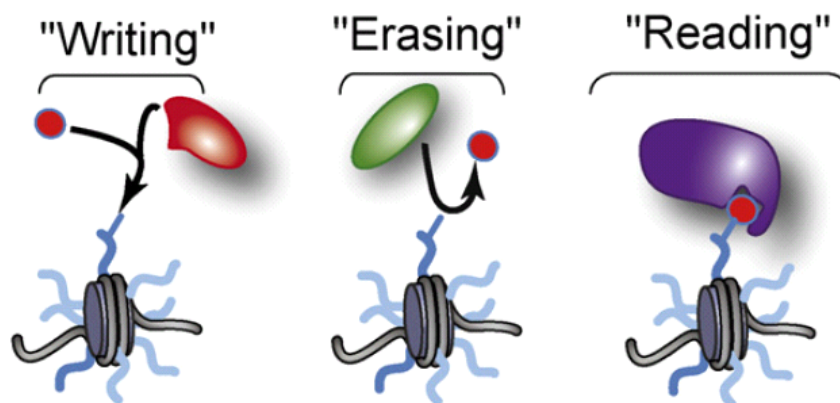


Figure 1.04:^{1.11} A cartoon depicting the three types of processes involved in altering the epigenetic code. The cartoon shows structural marks on histone tails being written, erased, or read by epigenetic proteins.

Over the past decade, there has been an increasing interest in the idea that the manipulation of epigenetic modifications by small-molecule inhibitors could have an impact on the progress of, or susceptibility towards, disease. At the outset of these PhD studies, there was evidence suggesting that epigenetic modulators could have an impact in a wide range of disease areas including oncology, immuno–inflammation, virology, and metabolic diseases.^{1.12}

Currently, there are only two classes of drugs on the market that are known to work as epigenetic modulators (Figure 1.05). The first class are the DNA methyltransferase inhibitors azacitidine (**1.01**) and decitabine (**1.02**), although these were initially discovered before their epigenetic mechanism was fully understood.^{1.12} The second class of drugs are histone deacetylase (HDAC) inhibitors.

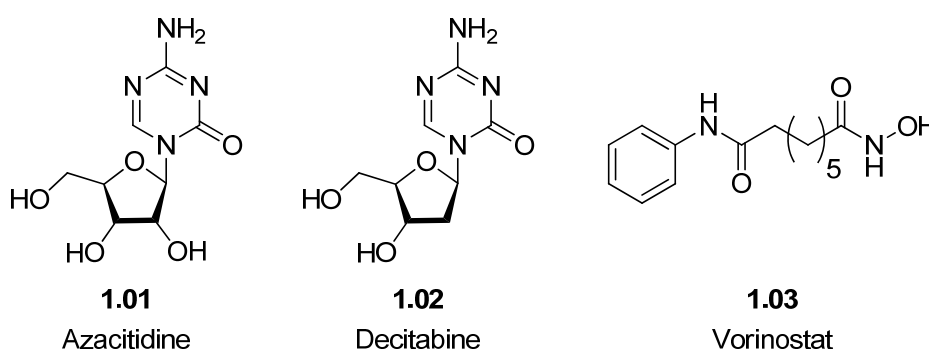


Figure 1.05: Structures of marketed drugs which are known to work as epigenetic modulators.

In 2006, the FDA gave the first approval of an HDAC inhibitor, Zolinza (vorinostat, **1.03**), for the treatment of cutaneous T-cell lymphoma (CTCL), a type of skin cancer.^{1.13} Vorinostat is a

non-selective inhibitor of both Class I and Class II HDACs,^{1.14} which erase acetyl groups near the *N*-termini of histones.^{1.15} The HDACs have a wide range of biological functions,^{1.16} although at present the main therapeutic application of HDAC inhibitors is in oncology. Vorinostat was shown to inhibit tumour growth in animal models, and clinical trials showed a significant response rate in studies in patients with CTCL.^{1.14}

The value of epigenetic targets has been predominantly investigated in oncology indications. This is due to the strong therapeutic rationale, as well as a greater tolerance of side-effects, which is important in this highly novel area. As well as the study of HDAC inhibitors for cancers beyond CTCL, there is evidence to suggest that targeting histone methyl transferases and acetyl lysine reader domains may be beneficial in the oncology field.^{1.17, 1.18}

Additionally, there is *in vitro* and *in vivo* evidence for the application of epigenetics in the immuno–inflammation therapeutic area, which is of particular interest within our laboratories. Acetyl lysine reader domains have been shown to have anti-inflammatory effects in mice, HDAC11 has been shown to regulate the expression of the anti-inflammatory cytokine IL-10 in antigen-presenting cells, and the inflammatory transcription factor NF-κB causes the lysine demethylase JMJD3 to be expressed in macrophages.^{1.19–1.21} Significant scientific evidence also exists for a role of epigenetics in neuroscience, such as Alzheimer’s disease, type I and type II diabetes, and virology resulting from HIV, HSV and EBV infections.^{1.12}

The challenge in progressing epigenetic science beyond the use of HDAC inhibitors in CTCL is great, but the wide range of potential applications in areas of high unmet medical need suggests the value to patients of succeeding. The development of potent, selective, small-molecule chemical probes would allow further study of biological mechanisms and their potential therapeutic effects. Translation of promising results from these studies to molecules suitable for progression into clinical trials has a high probability of meeting the needs of patients. In addition, in progressing molecules towards the clinic, pre-clinical toxicity models would allow a greater understanding of the potential for side effects when modulating epigenetic processes, as well as the likely size of the therapeutic window available.

1.3 BET Bromodomains

As a result of exciting emerging biology, there has recently been significant interest in the impact of the inhibition of functions of the BET family of proteins by small molecule inhibitors of their bromodomains. The biology and therapeutic relevance of BET bromodomain inhibition is discussed below. In addition, the structural features of the BET bromodomains as understood from X-ray crystallographic data are presented, along with the chemical structures of recently identified small molecule BET bromodomain inhibitors.

Bromodomains are short amino acid sequence domains within proteins that were first reported in 1992.^{1,22,1.23} Structural and site-directed mutagenesis studies of the bromodomain of P300/CBP-associated factor (PCAF) provided evidence that the bromodomain interacts specifically with acetylated lysine residues (Figure 1.06), an epigenetic histone modification that is important for transcription.^{1.24}

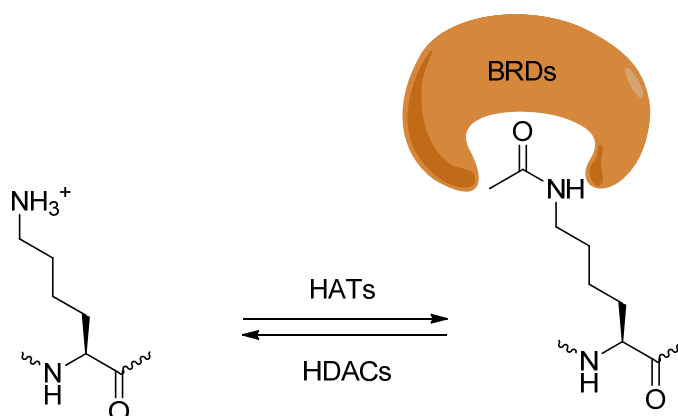


Figure 1.06: A cartoon depicting the interaction of acetylated lysine residues with bromodomain-containing proteins.

The acetylation of lysine residues on histone tails has a direct effect on the structure of chromatin. This is due to the neutralisation of the charge present on lysine amino acid side-chains at physiological pH. This results in activated states of chromatin, as the DNA is more accessible to transcription factors.^{1.25}

There are currently 42 known bromodomain-containing proteins, which have a total of 56 bromodomain sequence domains. A current phylogenetic tree used to visualise these proteins is shown below (Figure 1.07).^{1.26}

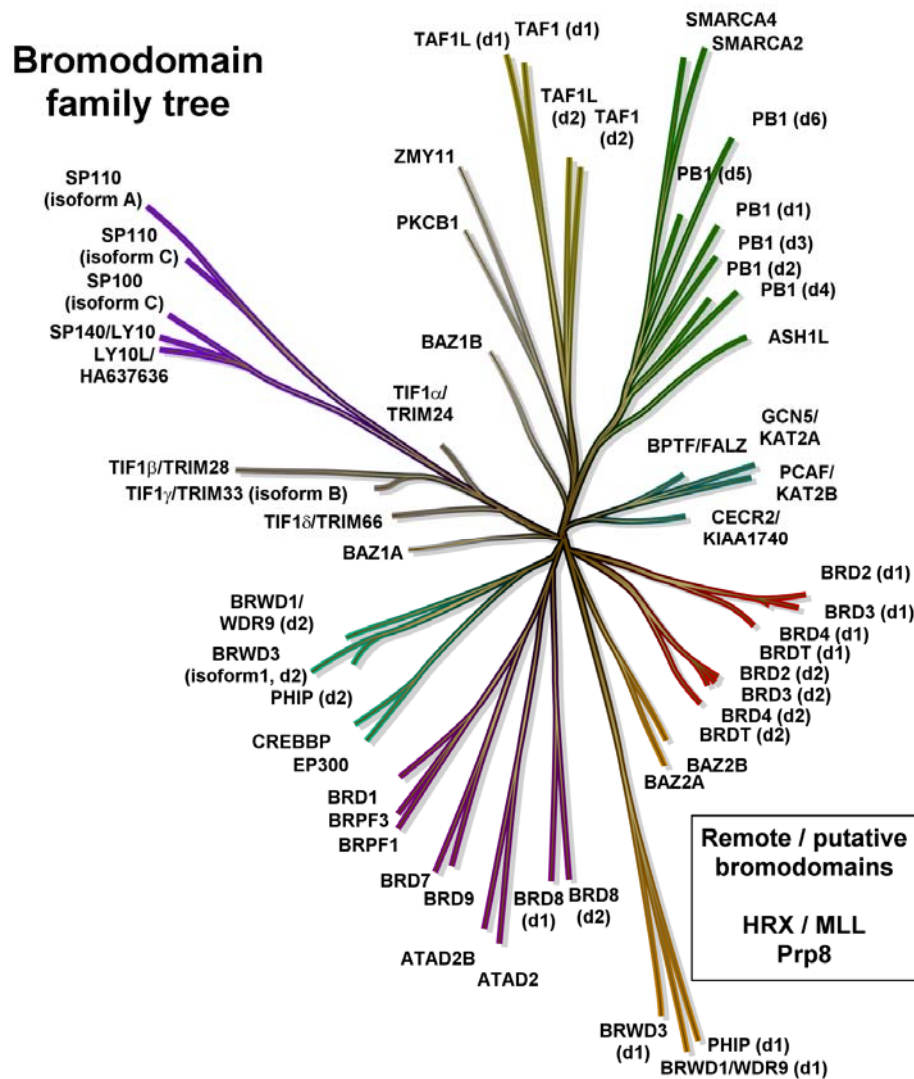


Figure 1.07:^{1,26} A phylogenetic tree of bromodomain-containing proteins.

Proteins containing bromodomains can be classified into several families, one of which is the ‘bromodomain (B) and extra-terminal (ET)’, or BET, proteins. BET proteins in animals are defined as having two bromodomains, labelled BD1 and BD2, and one ET domain. Early data suggested that BET proteins associate with (or ‘read’) acetylated chromatin via both of their two bromodomains, and that they may be involved in events such as opening chromatin structure and/or transcriptional initiation.^{1,27}

In humans, there are four BET proteins (BRD2, BRD3, BRD4 and BRDt) which exhibit similar gene arrangements, domain organisations, and some functional properties (Figure 1.08).^{1,28} Except for BRDt, which is expressed only in the testes and ovaries, BRD2, BRD3 and BRD4 are widely distributed. The four BET proteins have all been shown to bind acetylated lysines,

although their preference for which lysine mark, and on which histone, differs. There is over 75% homology between each of the *N*-terminals (BD1) and each of the *C*-terminals (BD2) across the BET family proteins, although only approximately 44% homology between the *N*-terminal and *C*-terminal bromodomain within the same protein (Figure 1.08).^{1.29} However, in all cases the amino acid residues critical for binding acetylated lysine residues are conserved.

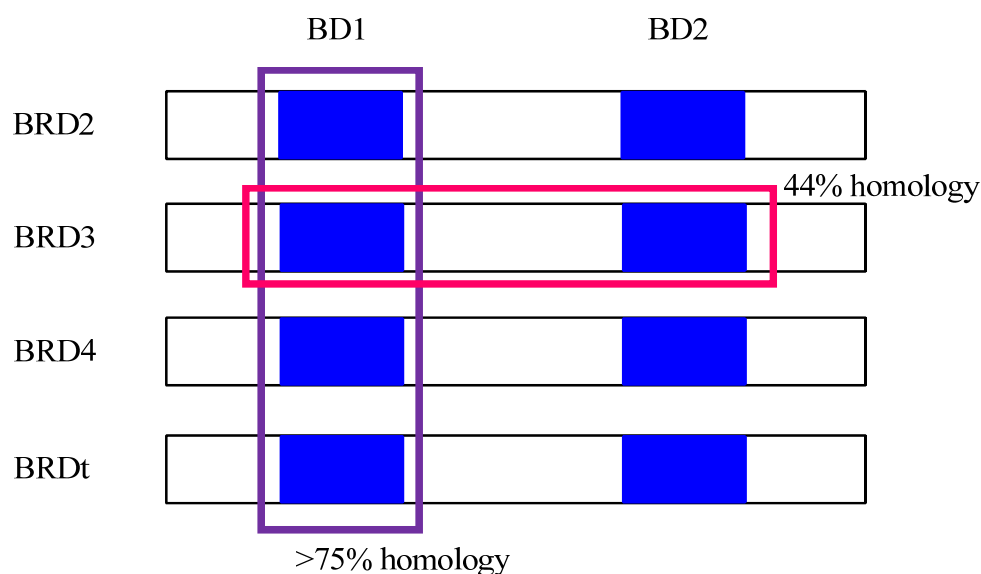


Figure 1.08: Schematic diagram of the bromodomain organisation of human BET family proteins BRD2, BRD3, BRD4 and BRDt. All four proteins contain two bromodomains, BD1 and BD2, which are indicated by blue boxes. The four *N*-terminal (BD1) domains are highlighted with a purple box, the two domains within BRD3 are highlighted with a pink box.

1.3.1 Therapeutic Relevance of the BET Protein Family

At the outset of these PhD studies, in addition to data generated within our laboratories, recent published research also provided a rationale for targeting BET proteins in cancer. A cell-penetrant small molecule inhibitor, (+)-JQ1 (**1.04**, Figure 1.09), of the BET family of bromodomains was shown to have antitumour efficacy in xenograft models of nuclear protein in testes (NUT) midline carcinoma (NMC).^{1.30} NMC is an aggressive disease which, except in the one recorded case where tumour resection was possible, has proven fatal.^{1.31} As of 2012, median survival time for sufferers is only 6.7 months.^{1.32} NMC is characterised by a recurrent t(15;19) chromosomal translocation, and the expression of a fusion protein containing NUT and BRD3/4.^{1.18}

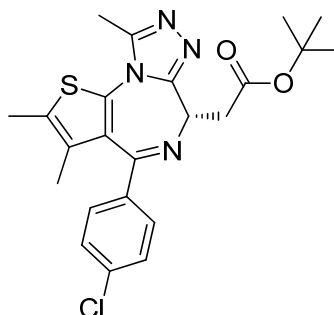
**1.04**

Figure 1.09: Chemical structure of (+)-JQ1, (**1.04**), a small molecule inhibitor of the BET bromodomain family proteins.^{1,30}

(+)-JQ1 has been shown to be a potent and highly selective inhibitor of the BET family of bromodomains *in vitro*.^{1,30} A luminescence proximity homogeneous assay was used to show that (+)-JQ1 inhibited binding of a tetra-acetylated H4 peptide to the first and second bromodomains of BRD4 with IC₅₀ values of 77 nM and 33 nM respectively. Differential scanning fluorimetry was used to establish the selectivity of (+)-JQ1 for the BET family over other bromodomains (Figure 1.10). (+)-JQ1 significantly increased the thermal stability of all the proteins of the BET family with ΔT_m^{obs} values from 4.2 to 10.1 °C. No significant stability shifts were seen for the 30 other bromodomains tested.

Critically, data also showed that (+)-JQ1 has efficacy *in vivo*. Three models of NMC were developed in which mice were engrafted with patient-derived tumour material. This was obtained from discarded clinical samples produced during the treatment of patients with metastatic NMC. After 18 days of therapy with (+)-JQ1, marked tumour regression and prolonged overall survival were observed.^{1,30} Taken together, both this data and *in vivo* models run within our laboratories established a proof of concept for targeting BRD/NUT in NMC.

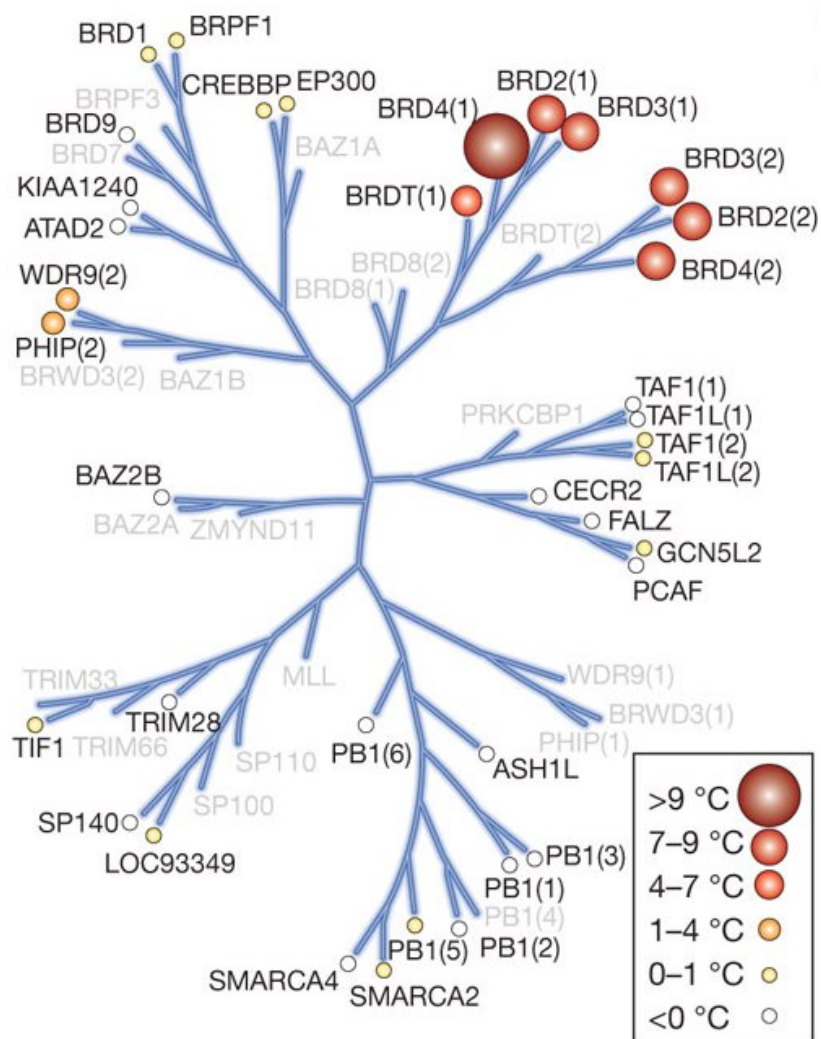


Figure 1.10.^{1.30} Assessment of bromodomain selectivity of (+)-JQ1 using differential scanning fluorimetry. Shown are averaged temperature shifts (ΔT_m^{obs}) upon binding of 10 μM (+)-JQ1, represented by spheres as indicated in the inset. Screened bromodomains are labelled in black; those not included in the selectivity panel are shown in grey.

As well as their potential utility as anti-cancer agents, strong evidence has also been provided for targeting BET bromodomains in inflammation. Recent literature from our laboratories showed that a potent, selective inhibitor of the BET family bromodomains, I-BET762 (**1.05**), has anti-inflammatory potential. I-BET762, which has a similar structure (Figure 1.11), as well as *in vitro* potency and selectivity profile, to (+)-JQ1 (**1.04**, Figure 1.09) was shown to disrupt chromatin complexes responsible for the expression of key inflammatory genes in activated macrophages.^{1.33}

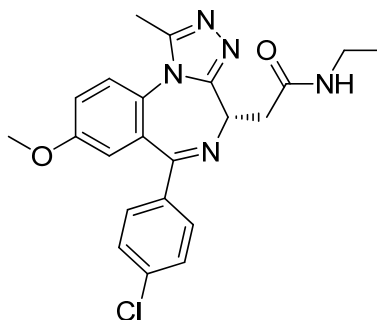
**1.05**

Figure 1.11: Chemical structure of I-BET762 (**1.05**), a small molecule inhibitor of the BET bromodomain family proteins.^{1,33}

In an *in vivo* model of LPS-induced endotoxic shock, administration of I-BET762 1 hour prior to stimulation prevented or attenuated the death of the mice (Figure 1.12). In the LPS-induced model, administration of I-BET762 1.5 hours after stimulation also prevented lethality in the mice, which is promising for therapeutic use.

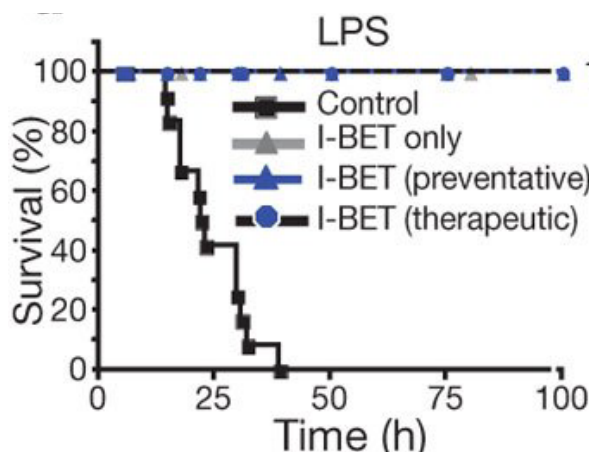


Figure 1.12:^{1,33} Kaplan–Meier survival curves of LPS-treated mice injected intravenously with a solvent control (black squares), 30 mg/kg I-BET762 1 hour before LPS-administration (blue triangles) or 30 mg/kg I-BET762 1.5 hour after LPS administration (blue circles). A control group of non LPS-treated mice dosed with 30 mg/kg of I-BET762 (grey triangles) is also shown.

Subsequent to the initial research on (+)-JQ1 and I-BET762, it has been shown that BET inhibitors may have therapeutic potential in a wider range of cancers. BET inhibitors have been shown to down regulate key genes in cell-proliferation such as c-Myc, and have shown efficacy in *in vivo* models of multiple myeloma and leukaemia.^{1,34,1,35}

The relevance of BET proteins in immuno–inflammatory diseases has also recently been further validated. Disease-associated single nucleotide polymorphisms (SNPs) have been identified for BRD2 in rheumatoid arthritis.^{1.36} BRD4 has also been shown to have a role in immune pathways, as it plays a role in activating inflammatory genes after LPS-stimulation.^{1.37}

Outside the oncology and immuno–inflammatory areas, it has been shown that BRD4 has a role in virus-induced pathogenesis, and is a potential target for drug development with a view to controlling HPV-induced human diseases, including genital warts, skin tumours, and cervical cancers.^{1.38} In addition, whole-body disruption of BRD2 in mice led to enhanced glucose tolerance and avoided the development of Type 2 diabetes. This suggests that the BET family of proteins may also be relevant in metabolic diseases.^{1.39}

BET bromodomain inhibitors may have an even wider therapeutic use than that currently predicted. Given the wide range of effects across many different therapeutic areas, the potential of bromodomain inhibitors, and the BET family in particular, is worthy of serious investigation with the view of providing novel medicines to patients.

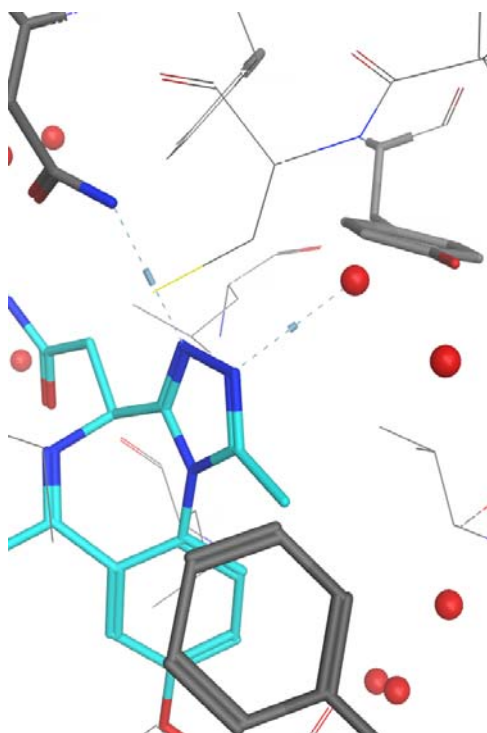
Since the commencement of these PhD studies, a small number of BET bromodomain inhibitors are being assessed in clinical trials. These include I-BET762 (**1.05**) from within our laboratories, which is currently in a Phase I/II study to investigate safety and activity in subjects with NMC and other cancers.^{1.40} Two other BET-bromodomain inhibitors have been reported to be in Phase I clinical trials in oncology patients. These are the Oncoethix/Mitsubishi compound OTX015, in a clinical trial for patients with haematological malignancies,^{1.41} and the Constellation Pharmaceuticals compound CPI-0610, in a clinical trial for patients with progressive lymphoma.^{1.42}

In addition, a compound initially identified as an ApoA1 upregulator by Resverlogix Corporation, RVX-208 (structure shown in Figure 1.16, **1.09**),^{1.43} was later shown to be acting via BET-bromodomain inhibition.^{1.44} this compound has been evaluated in a number of clinical studies, including a Phase II trial in patients with stable coronary artery disease.^{1.45}

1.3.2 Small Molecule BET Bromodomain Inhibitors

To understand how to identify, and optimise the potency of, BET bromodomain inhibitors, X-ray crystallography is of significant value. X-ray crystallography was applied to a number of examples within our laboratories, to identify structural features of the protein that are important for potency.^{1,26} The most important of these are the acetyl lysine binding site, the WPF shelf region, and the ZA channel. These are discussed further below, using I-BET762 (**1.05**, Figure 1.11) to illustrate compound binding.

Unsurprisingly, as the function of bromodomains is critical to their binding acetylated lysine residues on histone tails, small molecule BET bromodomain inhibitors possess acetyl-lysine mimetics which bind into the acetyl lysine recognition pocket. The binding of I-BET762 into the acetyl lysine binding site of the BRD4-BD1 bromodomain is shown below (Figure 1.13).



*Figure 1.13: A section of the X-ray crystal structure of I-BET762, **1.05**, bound to the first bromodomain of BRD4, showing the acetyl lysine binding site. I-BET762 is shown in cyan, and the protein in grey. The side-chains of Asn140, Tyr 97 and Phe83 are highlighted in bold. Water molecules are shown as red spheres, and hydrogen bonding contacts as blue dotted lines.*

The methyltriazole of I-BET762 acts as the acetyl lysine mimetic, binding into the acetyl lysine binding site of the bromodomain. The triazole nitrogen atoms form hydrogen bonding

interactions with both the side-chain of Asn140, as well as a conserved water network, as is seen for the acetyl group of acetylated lysines. The water network is conserved across over one hundred X-ray crystal structures which have been determined within our laboratories.^{1,26} It is held in place by hydrogen bonding interactions with Asn140, as well as water-bridged to Tyr 97. In addition to the hydrogen bonding interactions made by the triazole nitrogen atoms, the methyl substituent on the triazole of I-BET762 interacts with a small hydrophobic pocket, formed by the side-chain of Phe83. This mimics the interaction made between the bromodomain and the methyl of acetylated lysine residues.

In addition to the acetyl lysine binding site, a hydrophobic region of the protein named the ‘WPF shelf’ is also important in the binding of compounds to the BET bromodomains. The interaction of the 4-chlorophenyl of I-BET762 with the WPF shelf is shown below (Figure 1.14).

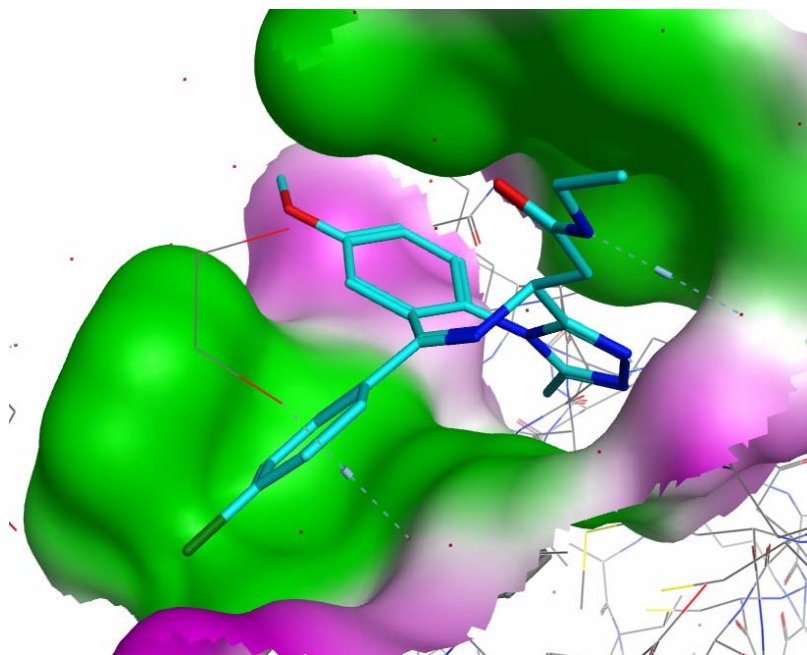


Figure 1.14: An X-ray crystal structure of I-BET762, 1.05, bound to the first bromodomain of BRD4. I-BET762 is shown in cyan, and the protein in grey. A molecular surface has been added to the protein, with lipophilic regions shown in green and polar regions in magenta.

The WPF shelf is named such as it is formed by the side-chains of Trp81 (W), Pro82 (P), and Phe83 (F). It is flat and hydrophobic, and provides a region for binding lipophilic and aromatic substituents, such as the 4-chlorophenyl of I-BET762.

The final key region for binding of small molecules within BET bromodomains is the ZA channel. The interaction of the fused methoxyphenyl ring of the benzodiazepine core of I-BET762 with the ZA channel is shown below (Figure 1.15). The ZA loop forms a fairly narrow channel, named the ‘ZA channel’. Introducing flatness in molecules which bind in this area of the protein would therefore be likely to aid binding. The directionality of any substituent would also be important. The good directionality and shape complementarity of the methoxyphenyl of I-BET762 with the ZA channel confers potency to the compound.

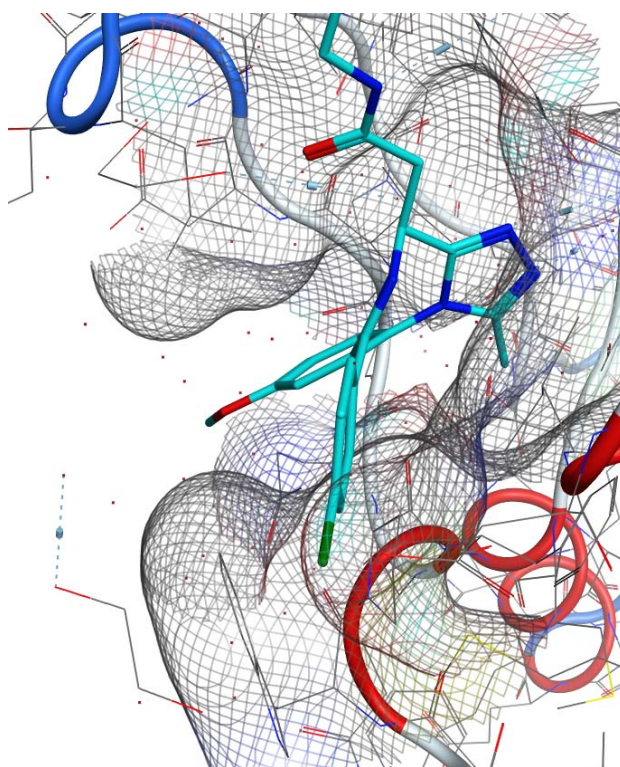


Figure 1.15: I-BET762, **1.05**, bound to the first bromodomain of BRD4. I-BET762 is shown in cyan and the protein in grey. The ZA-loop is shown as a ribbon from the top left to bottom centre. A molecular surface is added to the protein as a grey mesh, highlighting the ZA channel with the methoxyphenyl of the benzodiazepine ring system of I-BET762 bound in this region.

At the outset of these PhD studies, the only chemotypes of BET bromodomain inhibitors known within the literature were structurally similar to either I-BET762 (**1.05**) or (+)-JQ1 (**1.04**), which both bind similarly into the bromodomain of the protein, with the methyltriazole as the acetyl lysine mimetic. However, within our laboratories, there were chemotypes with alternative structural features acting as the acetyl lysine mimetic also known at this time. These, as well as the recently published *in vitro* tool molecule PFI-1 (**1.08**),^{1,46} and the clinical molecule RVX-

208 (**1.09**)^{1.44} are shown below (Figure 1.16). These structures represent a variety of chemotypes, however all show the same key binding interactions already described for I-BET762.

Compounds of the dimethylisoxazole family, exemplified by I-BET151 (**1.06**), were discovered within our laboratories.^{1.47} Here, the dimethylisoxazole moiety acts as the acetyl lysine mimetic, with the pyridine sat on the WPF-shelf and the quinoline ring system in the ZA channel. The dimethylisoxazole motif has, since the outset of these PhD studies, also been used within a range of other compounds to provide small molecule BET bromodomain inhibitors.^{1.48, 1.49}

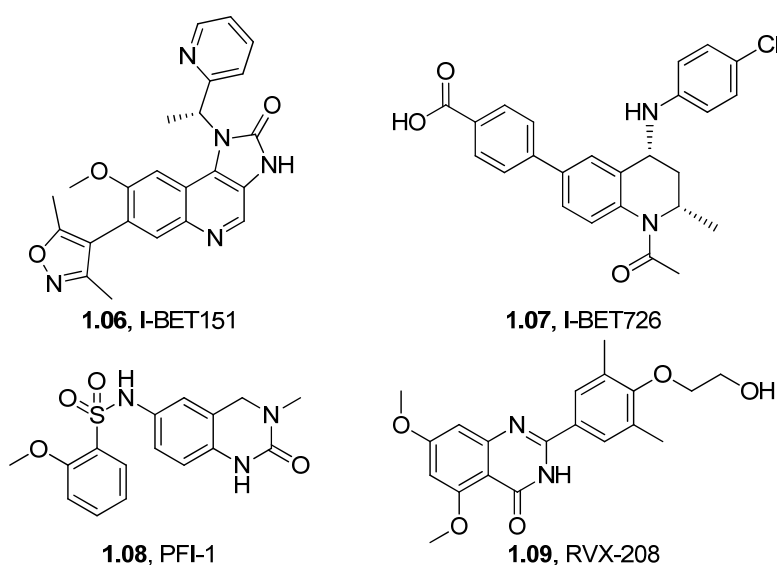


Figure 1.16: The chemical structures of key small molecule BET bromodomain inhibitors.

The tetrahydroquinoline (THQ) family, exemplified by I-BET726 (**1.07**),^{1.50} have the most recognisable acetyl lysine mimetics, with the *N*-acyl of the THQ sitting in the acetyl lysine binding site. In I-BET726, the 4-chlorophenyl sits on the WPF shelf in a similar position to that of I-BET762 and the aromatic ring of the 4-benzoic acid is directed through the ZA channel.

Recently, a novel chemical series, containing a methyl-dihydroquinazolinone acetyl lysine mimetic, has also been discovered, and has yielded PFI-1 as an *in vitro* tool BET bromodomain inhibitor.^{1.46} As with the previously discussed chemical series, the WPF shelf again makes an interaction with an aromatic ring, in this case the methoxyphenyl substituent. An interesting feature of the binding of PFI-1 is that instead of incorporating a largely lipophilic interaction with the ZA channel, it is postulated that the sulfonamide NH makes a water-mediated hydrogen bond with a ZA loop backbone carbonyl moiety.

These known chemotypes, and access to X-ray crystallography within our laboratories, make the identification of BET bromodomain inhibitors as drug candidate molecules an attractive prospect. This is supported by a strong therapeutic rationale, both within our laboratories and in the wider scientific community, for the relevance of the BET bromodomains in disease.

1.4 Medicinal Chemistry Strategies in Epigenetic Research

Working in epigenetic research requires an increased focus on certain medicinal chemistry strategies. The aims of the programme, as well as the biological screening to be undertaken, have to be designed with only a limited understanding of the target area. It is also necessary to complement classical hit identification with innovative ways to increase the chemical space covered by the current compound collection, owing to the novelty of structure of the proteins being targeted. At the same time, it is important to follow good medicinal chemistry practices. This ensures that high-quality compounds are designed, which stand the best chance possible of becoming successful drugs if a therapeutic rationale can be developed..

1.4.1 Structure of an Epigenetic Research Programme

Epigenetics is a new area of science where there is a limited amount of scientific knowledge currently available. The aim of scientific research underway in this area is twofold. First, the aim is to gain a greater understanding of specific epigenetic processes and their implications in disease. Secondly, where understanding of epigenetic processes suggests the possibility of delivering transformational medicines to patients, the aim is to develop candidate molecules which can be progressed into clinical studies. An overview of the stages to be followed in a drug discovery programme within the epigenetics area are summarised below (Figure 1.17).

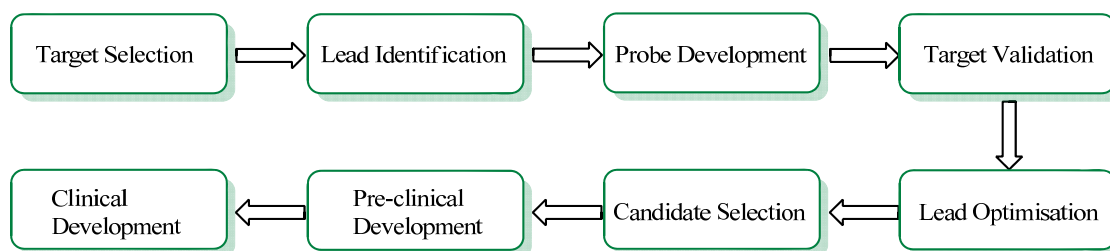


Figure 1.17: The stages of a drug discovery programme within the epigenetics area.

The first stage is target selection, deciding which epigenetic processes are of interest and which protein, or protein domain, should be targeted. Ideally, there is some scientific rationale (i.e. genetics, disease association), either within our laboratories or within the scientific literature, as to how this epigenetic process is involved in one or more diseases. Diseases with a high unmet medical need are preferred, due to a greater potential benefit to patients and a greater likelihood of development of a reimbursable medicine. Targets with implication in a number of different diseases are also attractive since this gives potential for developing the underlying science in a number of different directions.

Once a target has been selected, it is essential to find hit molecules that show some efficacy. Traditionally, hit molecules come from a variety of sources, including high-throughput screening (HTS), natural ligands, focused screening, virtual screening, and phenotypic ('black-box') screening. A range of different techniques are commonly used on the same programme to maximise the possibility of success, and recently encoded library technology (ELT) (Section 1.4.2) and fragment screening have been used to complement traditional techniques. In the epigenetic area, it has also been necessary to ensure the compound collection used for HTS and focussed screening is enriched with chemotypes which are likely to interfere with epigenetic proteins. For example, bromodomains interact with acetylated lysine residues; therefore it is advantageous to ensure the compound collection contains chemotypes which contain similar structural features to an acetylated lysine residue.

Once a target has been selected, and a hit identified, it is necessary to build on the biological data currently available to further validate the target. Various *in vitro* and *in vivo* biological studies can be undertaken to develop the rationale for targeting the specific protein in disease. Novel strategies and technologies, such as targeting to a sub-population of cell types, may also be considered. To complete these studies, a probe molecule is required. A probe molecule is a compound with sufficient potency and a pharmacokinetic profile to allow evaluation in these biological studies. The compounds must also be selective against other targets which may impede biological evaluation, and be cellular and nuclear penetrant to reach the target protein. At this stage, a number of properties including exposure after oral dosing, and developability issues such as CYP450 and hERG inhibition, are not of prime importance, although it is good practice to consider them where possible.

If the scientific rationale is further validated by studies undertaken with the probe molecule, it gives greater rationale to invest time and resource in lead optimisation. At this stage, the aim of the ongoing research becomes a candidate-quality molecule with an appropriate safety and efficacy profile in *in vitro* and *in vivo* models. Greater consideration is given to properties including the overall selectivity profile (including CYP450 and hERG inhibition), physical properties (including solubility and stability) and a suitable pharmacokinetic profile for dosing patients with the target disease. Depending on how well the probe molecule meets these requirements, the candidate may come from the same chemical series as the probe, or a different family of compounds.

Once a candidate molecule has been identified, its safety profile is analysed further through *in vitro* and *in vivo* pre-clinical studies. These studies are critical prior to clinical studies being

undertaken as they increase patient safety, and include the investigation of genotoxicity, cardiovascular effects, and medium-term *in vivo* toxicity studies. In a new area of science such as epigenetics, the priority given to the specific safety studies being undertaken changes as more information about the possible side-effects becomes available. The information gained during the pre-clinical studies is used to help design clinical protocols and support ‘Investigational New Drug’ (IND) applications with the appropriate regulatory agencies.

1.4.2 Hit Identification Using Encoded Library Technology

High-throughput screening (HTS) is commonly used within the pharmaceutical industry to provide hit molecules at the outset of medicinal chemistry programmes. HTS is the process of screening a large number of compounds against a biological target.^{1.51} Typically, 0.5–3 million compounds from a company’s in-house screening collection are tested. Their activity is measured as percent inhibition, or efficacy, at a single concentration. Compounds of interest are re-tested, and approximately 2000–5000 IC₅₀, or EC₅₀, values are generated. From this, a number of hit molecules with verified structural integrity and purity, as well as a reproducible result in the biological screen, are identified.

In 1992, it was proposed that by encoding individual members of a large library with unique nucleotide sequences, chemical synthesis and genetics could be combined to provide a powerful, versatile method for drug screening.^{1.52} Since then, the techniques and technology have developed to the point where DNA-encoded libraries (DELs) can be used to discover novel inhibitors for pharmaceutically relevant enzymes.^{1.53} In contrast to HTS, where each molecule is screened individually against the target, in encoded library technology (ELT) a large DEL is subjected to selective pressure until it is enriched with compounds with improved affinity for the biological target.

DELs have historically been prepared by using the appended DNA to control the synthetic destiny of the library members. It was shown, in 2002, that multistep syntheses of small molecules could be directed by DNA-templated synthesis, where sequence complementarity brings into proximity DNA-appended reactants.^{1.54} This methodology is compatible with a wide range of reactions, including organometallic coupling, amide coupling and carbon–carbon bond-forming reactions.^{1.55} DNA-programmed chemistry allowed one-pot library synthesis of DELs where the library members could be amplified by PCR and resynthesis.^{1.56} DNA-programmed chemistry was further developed by attaching building blocks to DNA prior to synthesis, allowing the use of off the shelf reagents. Resin-bound single-stranded DNA

(ssDNA) was used to separate DNA-tagged templates into various compartments, where solid phase synthesis was performed.^{1.57} This is an example of the use of traditional combinatorial ‘split-and-pool’ methodology^{1.58} to DEL preparation. Subsequently, a 100 million compound library of 8-mer peptides was constructed using this method.^{1.59}

Within our laboratories, it has been shown that DELs can be synthesised using DNA sequences to record the synthetic history of the library members, rather than using DNA to direct the course of synthesis.^{1.60} A combination of enzymatic and chemical syntheses in a ‘split-and-pool’ format was used (Figure 1.18). The starting material is tagged with DNA, followed by reaction and purification. The solution was split into 384 wells, reacted with an appropriate DNA tag solution, and reacted and purified again. This gave libraries where the DNA sequence represented the component reagents used to synthesise the final molecule. In contrast to previous methods, double-stranded DNA was used to encode the library, allowing for greater variability in synthetic chemistry available and therefore greater structural diversity.

Once DELs have been synthesised, they are subjected to selective pressure to enrich the DEL with compounds which interact with an immobilised target protein.^{1.61} The immobilised protein is added to the DEL, incubated, and the beads washed to remove unbound library members. The bound library molecules are then eluted from the beads by heating at 72 °C. The eluted compound library is subjected to three or four further rounds of selection using the immobilised protein to give a DEL enriched in molecules which bind to the protein. Physical losses during the selection process preclude a greater number of rounds of selection.

The enriched DEL is then characterised using high-throughput sequencing technologies which yield over 100,000 individual sequences in a single experiment.^{1.62} The selection output is viewed as a cubic scatter plot (Figure 1.19) where each axis on the plot represents one cycle of synthesis, therefore one structural feature, or synthon, within the molecule. The visualisation allows families of related structures enriched within the library to be picked out as planes (one synthon in common) or lines (two synthons in common). Molecules which bind more strongly to the target protein will be present in higher number in the DEL after selections have been performed, therefore will show up with higher copy numbers during DNA sequencing.

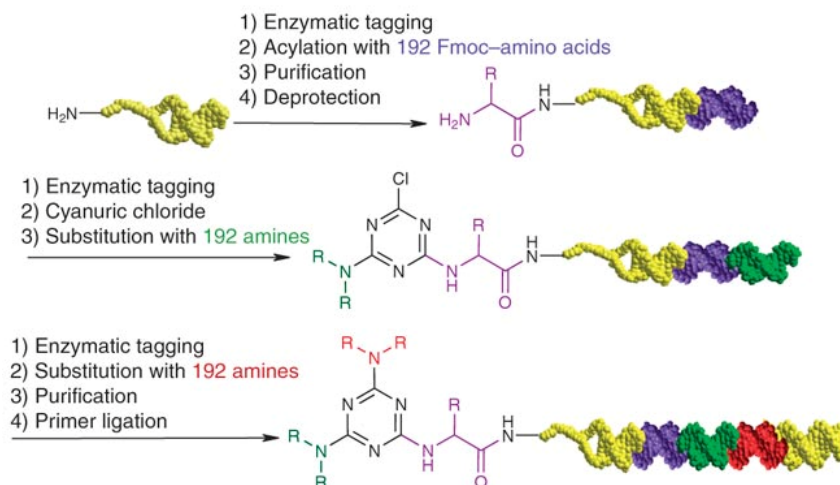


Figure 1.18:^{1.61} Synthetic scheme towards synthesis of a DEL using a 'split-and-pool' format. Double-stranded DNA tags are used to record the substituent parts of the molecule during library synthesis.

Once the enriched DEL has been characterised and analysed, it is possible to select families of compounds, or structural features, which are preferred for interaction with the target molecule. Exemplars from these families are synthesised without the DNA tag and screened in binding or functional assays to confirm activity. Once activity has been confirmed, the compound is designated as a hit molecule, and the chemotype can be studied further by the programme medicinal chemists. The output from the DEL can also be used to provide SAR for future medicinal chemistry.

Encoded library technology within our laboratories has been used to interrogate an 800-million-member DEL, from which inhibitors for Aurora A kinase and p38 MAP kinase have been discovered (Figure 1.19).^{1.61} Within these PhD studies, ELT identified a hit molecule for the esterase-sensitive motif programme of work (Part III). In this case, the use of ELT technology provided a novel structural series of BET bromodomain inhibitors which had previously not been discovered by high throughput screening of the GSK compound collection.

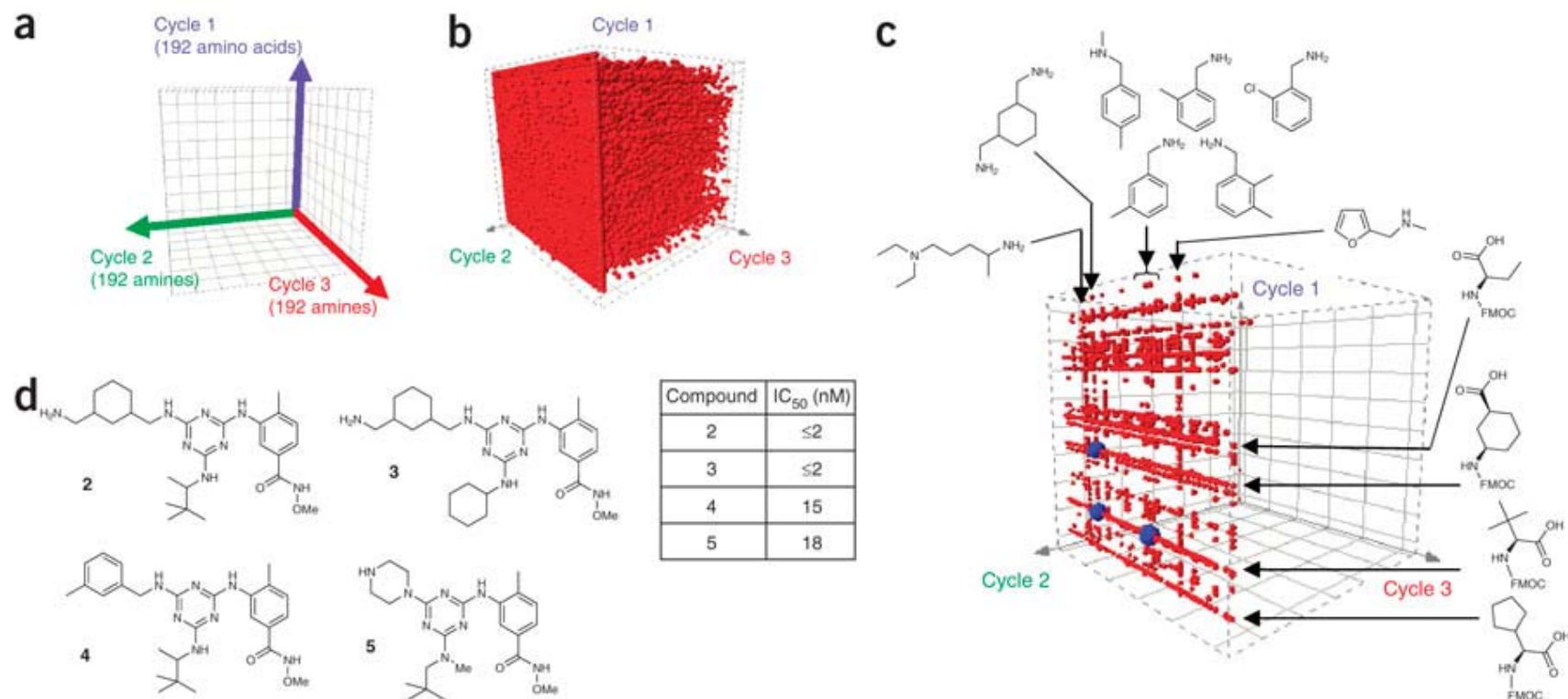


Figure 1.19:^{1,61} (a) Library populations can be viewed in three dimensions using Spotfire. Each of the DEL components can be uniquely identified by a single point in the cubic space. (b) An example unfiltered population obtained from a DEL selection with an enzyme (p38 MAP Kinase). (c) The same population after removing the low occurring molecules. Points corresponding to compounds 2, 3 and 4 are coloured blue. The structures and locations of some selected synthons are shown. (d) Structures and assay results of selected compounds 2, 3 and 4. The structures are very similar to reported p38 MAP kinase inhibitors such as compound 5.

Work is still ongoing to develop the use of DELs even further. The ‘split-and-pool’ synthetic methodology can lead to compounds with a higher molecular weight and lipophilicity than would be desired within a lead, and there is a concerted effort to improve the quality and diversity of the molecules within the library. The use of the technology is also limited by the availability of solid supported protein to use during selections, although within our laboratories we have not found this to be a limiting factor for the use of DELs to interrogate targets we are interested in within the epigenetic area.

1.4.3 Monitoring Physicochemical Properties during Drug Discovery

In the early 1990’s, the greatest cause of the attrition of drug candidates was poor human pharmacokinetics (Figure 1.20).^{1.63} The improved prediction of human pharmacokinetics from preclinical animal studies has since significantly reduced the impact of this on attrition. By 2000, poor efficacy, commercial decisions, and toxicology had become the most significant causes of drug attrition. Of these, as for the pharmacokinetic profile, efficacy and toxicology are in the hands of the medicinal chemist.

Since the seminal paper by Lipinski *et al.*^{1.05} there has been a significant focus on the use of physicochemical properties in drug discovery. This began with Lipinski’s ‘Rule of Five’ (Ro5), which identified physicochemical properties associated with good oral absorption, and has subsequently been developed towards the prediction of a wide range of properties which are important in drug discovery. Recently, due to the challenges faced by the industry, this has become focussed on the reduction of attrition in drug development by identifying those properties which correlate with a reduced risk of toxicology.

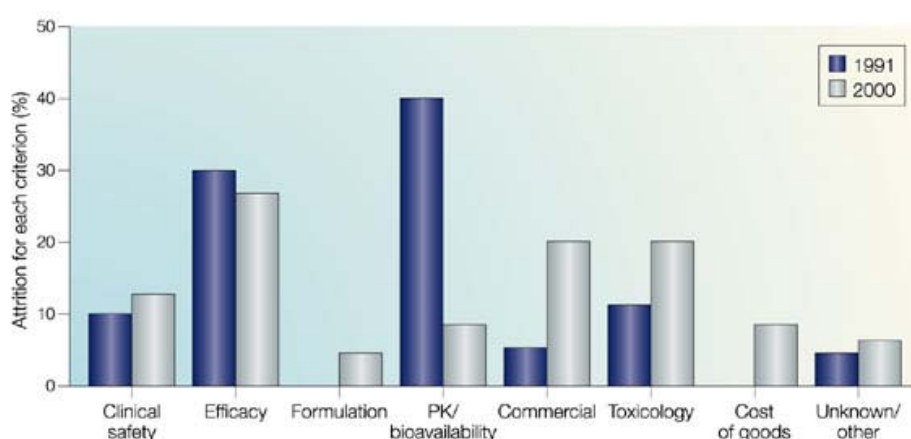


Figure 1.20:^{1.63} Causes of drug candidate attrition in 1991 and 2000.

As a result of this area of research, a number of guidelines have been developed which are useful to the medicinal chemist, and a subset of these are described below. These are based around *in silico* profiling of compounds prior to synthesis. *In silico* physicochemical profiling involves the use of computational models to predict the physicochemical profile of potential compounds for synthesis. This includes properties such as solubility, lipophilicity, and polar surface area. The *in silico* profiling of compounds during the medicinal chemistry design process is critical to the identification of high-quality drug molecules. It can also significantly reduce time and costs, by removing the synthesis and biological profiling of compounds which are not likely to have drug-like properties.

Inspection of the various physicochemical guidelines which have been developed show that the themes of low lipophilicity, reduced size, and reduced flatness are common across the majority of approaches. Lipinski's Ro5 (Figure 1.21), developed within the Pfizer research laboratories, is based on the premise that good oral activity is a result of not only high intrinsic potency, but good oral bioavailability.^{1.05} Oral bioavailability is primarily governed by the solubility and permeability of compounds, and by following the Ro5 the probability of identifying a compound with good solubility and permeability is increased. In Lipinski's Ro5, lipophilicity is defined as the octanol/water partition coefficient (logP).

- $mwt \leq 500$
- $\log P \leq 5$
- $\#hbd \leq 5, \#hba \leq 10$

Figure 1.21: Lipinski's Ro5 for the prediction of good oral bioavailability.^{1.05} Mwt is the molecular weight, logP the octanol/water partition coefficient, #hbd and #hba denote the number of hydrogen bond donors and acceptors.

A similar study by Veber *et al*, within our laboratories, also identified physicochemical properties which predicted good oral bioavailability.^{1.64} It was proposed that molecular weight had been identified by Lipinski as a result of its close correlation with polar surface area. This led to an updated set of criteria to predict good oral bioavailability, focussed instead on polar surface area and the number of rotatable bonds (Figure 1.22).

- $\#rb \leq 10$
- $PSA \leq 140 \text{ \AA}^2$

Figure 1.22: The criteria described by Veber et al to predict good oral bioavailability.^{1.65} $\#rb$ denotes the number of rotatable bonds. PSA denotes the polar surface area.

It has since been shown that physicochemical properties can be used to predict not only oral bioavailability, but a wide range of drug-like properties. This is evidenced by the detailed analysis performed by Ghose *et al*, within the Amgen research laboratories.^{1.65} In this study, the physicochemical properties of known drug molecules were calculated, and a set of rules for drug-likeness developed, with the aim of better designing chemical libraries (Figure 1.23). As with the Ro5, lipophilicity is amongst the descriptors, here as a calculated logP (clogP) value.

- $1.3 \leq \text{clogP} \leq 4.1$
- $70 \leq \text{cmr} \leq 110$
- $230 \leq \text{mwt} \leq 390$
- $30 \leq \#atoms \leq 55$

Figure 1.23: Criteria identified for drug-likeness, as described by Ghose *et al*.^{1.66} clogP denotes the calculated logP, cmr the calculated molar refractivity, mwt the molecular weight, and $\#atoms$ the number of atoms.

Ghose's rules for drug-likeness were supported by the work of Gleeson *et al*, again within our laboratories, which also identified molecular weight and clogP as the key predictors of drug-likeness.^{1.66} In this case, physicochemical properties were correlated with absorption, distribution, metabolism, and excretion–toxicity (ADMET) parameters such as solubility, plasma protein binding and *in vivo* clearance. This work resulted in the simple and easily-applied '4/400' rule (Figure 1.24).

- $\text{clogP} \leq 4$
- $\text{mwt} \leq 400$

Figure 1.24: The '4/400' rule for good ADMET properties identified by Gleeson *et al*.^{1.66}

At the outset of these PhD studies, research within the Pfizer research laboratories to predict both good oral properties and toxicity was identified as the gold standard of good drug discovery. This work is well represented by two publications, the first showing a rule for

increasing the likelihood of a good pharmacokinetic profile,^{1.67} and the second showing a rule for lowering the probability of toxicity of compounds.^{1.68}

To optimise the key pharmacokinetic parameters of clearance and oral absorption, the ‘Golden Triangle’ was developed, giving an optimum combination of molecular weight and lipophilicity, here denoted by the estimated octanol/buffer distribution coefficient $\text{eLogD}_{\text{pH}7.4}$ (Figure 1.25).^{1.67} Compounds with properties which are predicted to lead to a good pharmacokinetic profile lie inside the depicted ‘golden triangle’ area.

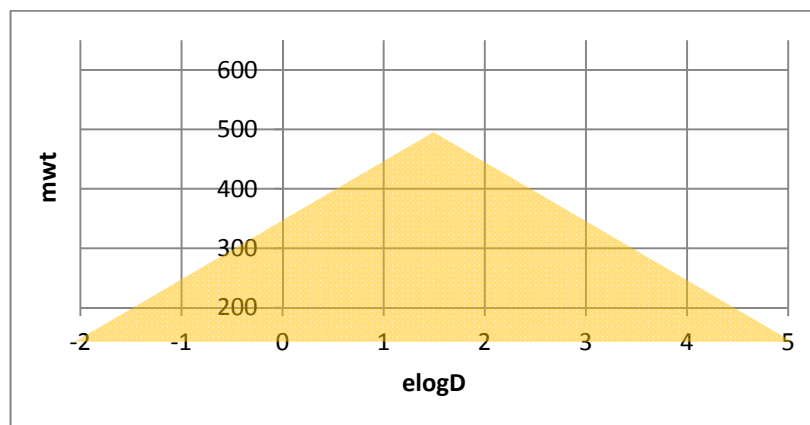


Figure 1.25: The ‘Golden Triangle’ rule for good pharmacokinetic profile.^{1.67} The estimated $\text{logD}_{\text{pH}7.4}$ (eLogD) is plotted on the x-axis, and the molecular weight (mwt) on the y-axis. Compounds with properties which are predicted to lead to a good pharmacokinetic profile lie inside the depicted ‘golden triangle’ area.

This work was supplemented by a second set of guidelines which identified physicochemical parameters associated with a reduced likelihood of *in vivo* toxicology, commonly named the ‘3/75’ rule (Figure 1.26).^{1.68}

- $\text{clogP} \leq 3$
- $\text{PSA} \geq 75 \text{ \AA}^2$

Figure 1.26: The ‘3/75’ rule for a reduced likelihood of *in vivo* toxicology.^{1.68}

This study showed that compounds with a polar surface area less than 75 and a calculated lipophilicity (clogP) greater than 3.0 were over six times more likely to be toxic than compounds with a polar surface area greater than 75 and a clogP less than 3.0. An increased lipophilicity may lead to increased toxicity for a number of reasons, including the compound having increased pharmacological promiscuity and nonspecific accumulation effects.^{1.69}

The overall theme of these various rules was distilled, at the outset of these PhD studies, to a commitment to the control of both lipophilicity, in the guise of clogP, as well as molecular weight wherever possible during the optimisation process. This was identified as being particularly critical when developing compounds which were designed to be either *in vivo* tool molecules or pre-clinical candidates. It is, however, important to note that these various specific rules were therefore being used as guidelines for improved compound design rather than as specific cut-off values. The risks of adhering strictly to one set of rules has also been documented,^{1.70} and using these various parameters as guidelines to improve the probability of success rather than blanket rules is in line with Lipinski's original intentions.^{1.71}

As described above, lipophilicity was identified as a critical physicochemical property for these PhD studies. The importance of lipophilicity is supported by the fact that the parabolic relationship of lipophilicity with oral bioavailability (Figure 1.27) can be rationalised scientifically as well as predicted by computational modelling.^{1.72} Low intestinal absorption for compounds which are very hydrophilic, combined with an increase in first-pass metabolism as lipophilicity increases, drive the parabolic relationship. Although the permeability of biological membranes, and therefore oral absorption of drug molecules, is governed by both passive diffusion and carrier-mediated mechanisms, passive diffusion is probably the primary route of intestinal permeation in most drugs.^{1.73} Intestinal absorption is therefore higher for more lipophilic compounds. The positive effect from lipophilicity of increased absorption is overtaken by an increase in first pass metabolism for more lipophilic compounds due to their greater affinity for enzymes such as cytochrome P450's.^{1.74}

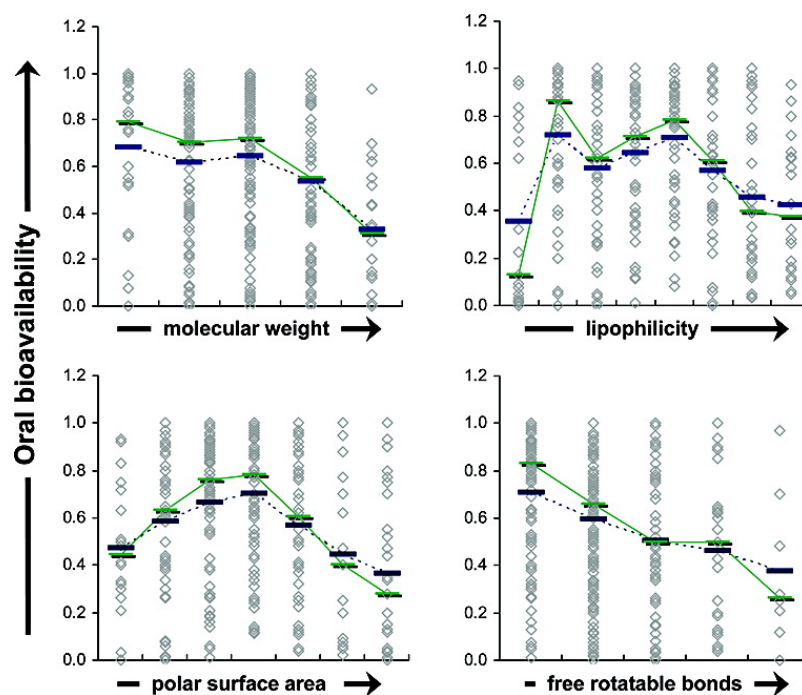


Figure 1.27:^{1.72} The relationship between oral bioavailability and a range of physicochemical characteristics. The molecular weight range is 200–500; the lipophilicity range is a clogP of -2–5; the polar surface area range is 25–150 Å²; the free rotatable bonds range is 0–12.

To aid decision making in medicinal chemistry, various descriptors have been described which simultaneously monitor potency and physicochemical properties. Commonly used descriptors include ligand efficiency (LE) and lipophilic ligand efficiency (LLE).^{1.03,1.74} Ligand efficiency is a measure of potency with relation to heavy atom count, and lipophilic ligand efficiency is a measure of potency with relation to lipophilicity. There are a number of methods for calculating LE and LLE; the methods used in this thesis are detailed below (Figure 1.28).

$$\text{LE} = \frac{-\Delta G}{\text{HAC}} \sim \frac{1.36 \times \text{pIC}_{50}}{\text{HAC}}$$

$$\text{LLE} = \text{pIC}_{50} - \text{clogP}$$

Figure 1.28: Definition of ligand efficiency (LE) and lipophilic ligand efficiency (LLE) used throughout this thesis, where ΔG is the change in Gibbs Free Energy, pIC_{50} is the negative logarithm of the half maximal inhibitory concentration, HAC is the heavy atom count and the clogP is the calculated $\log P$.

A typical compound with a pIC_{50} of 7, molecular weight of 350 and $clogP$ of 3 will have an LE of 0.36 and an LLE of 4. The optimum values of LE and LLE depend on the stage of the programme, but during the drug discovery process the aim is to keep both these values as high as possible.

Since the commencement of these PhD studies, there have been further developments in using physicochemical parameters to reduce attrition during pre-clinical and clinical development. A significant contribution to this area comes from within our laboratories, with the property forecast index (PFI). This is the sum of a chromatographically measured distribution coefficient $mChromlogD_{pH7.4}$ and the number of aromatic rings (Figure 1.29).^{1.75}

$$PFI = mChromlogD_{pH7.4} + \#Ar$$

Figure 1.29: Definition of the property forecast index (PFI). The $mChromlogD_{pH7.4}$ denotes the chromatographically measured distribution coefficient at pH7.4, and $\#Ar$ the number of aromatic rings.

The number of aromatic rings has previously been described as being a factor in compound-related attrition.^{1.76} However, the key development associated with the use of PFI is the incorporation of a chromatographically measured value of lipophilicity rather than an *in silico* prediction. This was shown to significantly increase the correlation of lipophilicity with a number of key factors, including solubility and intrinsic clearance, in comparison with previous approaches.^{1.75} The development of PFI during these PhD studies is reflected by a change in use of $clogP$ to $ChromlogD_{pH7.4}$ as the key lipophilicity measure during the later work reported.

1.4.4 Requirements for Oral Administration of Drugs

When designing a compound where the ultimate aim is the production of a drug treatment for patients, the behaviour of the compound in a whole animal system is critical for its ultimate efficacy. In medicinal chemistry, it is therefore important to control the pharmacokinetic (PK) profile of compounds during the design process. Pharmacokinetics is the study of the absorption, distribution, metabolism and excretion (ADME) of drug molecules.^{1.77}

To achieve activity *in vivo* from an orally administered drug, the compound must reach the site of action at sufficient concentration, and thus must be orally bioavailable. The main

requirements for this are solubility in gastrointestinal fluids, permeability across the gut wall, and low first pass metabolism by the liver.^{1.78}

The requirements for oral bioavailability can be measured in isolation during drug discovery to aid compound design. Solubility may be measured in many relevant systems, the most informative for oral dosing being fasted state simulated intestinal fluid (FaSSIF).^{1.79} This provides a measure of solubility relevant to the likely site of oral absorption.

An estimate of the permeability of compounds can be gained using *in vitro* systems such as artificial membrane permeability assays, Caco-2 cells, and PGP substrate assays.^{1.80} In combination, these can be used to assess the intestinal permeability of molecules.

For oral dosing, moderating the clearance of compounds by the liver in the form of first pass metabolism is critical for gaining good oral exposure. This can initially be estimated using *in vitro* systems such as microsomal,^{1.81} hepatocyte,^{1.82} and S9 fraction^{1.83} stability assays. Translation to an *in vivo* animal model allows the rate of clearance of the molecule from the bloodstream to be measured, as well as the half life of the compound.

A full assessment of a compound's suitability for oral dosing, which combines the parameters described above, can be made by performing an orally dosed *in vivo* PK study. Oral bioavailability *F* can then be determined, and is a dose-normalised ratio of oral to intravenous AUC's (areas under the curve) (Figure 1.30). The AUC is a measure of the quantity of the drug in the body, and is the total area under the blood/plasma concentration–time curve.^{1.84}

$$F = \frac{AUC_{po} \cdot dose_{iv}}{AUC_{iv} \cdot dose_{po}}$$

Figure 1.30: The method used to calculate oral bioavailability, F, in terms of the area under the curve (AUC) and dose after intravenous (iv) and oral (po) dosing.

The AUC measured after oral dosing is impacted by both oral absorption of the compound across the gut wall, and clearance of the compound from the blood. Measuring the bioavailability, by comparing the AUC after oral and intravenous dosing, indicates the fraction of the orally administered dose which enters the systemic circulation and is available to perform its predicted biological effect.

As described previously (Section 1.4.3), the PK properties of a compound, such as its oral absorption, may be improved by altering the physicochemical properties of the molecule. If

these are not successful alternative strategies may also be employed, such as the design of prodrugs of the active molecule. Prodrugs are pharmacologically inactive, or less active, chemical derivatives of the drug which are transformed within the body in order to release the active drug molecule.^{1.85}

The prodrug strategy has inspired the science of targeted drug discovery, where the chemical modification of molecules alters their pharmacodynamic, as well as pharmacokinetic, properties. This is achieved by modifications such as antibody-drug conjugates^{1.86} or esterase sensitive motifs^{1.87} which result in molecules being targeted to specific tissues or cell types. In these cases, the aim is to deliver a higher concentration of active compound to tissues of interest than to the rest of the body. In contrast to the prodrug strategy, the delivered drug molecules may retain a significant level of potency at the biological target. Targeted drug discovery, and its application within these PhD studies, will be discussed further in Part III of this thesis (Section 3.1).

1.5 Areas for Research

In this thesis a number of approaches to epigenetic drug discovery are described, ranging from probe development to the identification of a pre-clinical candidate. These focus on the design and synthesis of small molecule BET bromodomain inhibitors. Ultimately, the aim of the research described is the discovery of molecules which can be used as novel medicines to treat patients with a high unmet medical need.

Part II of this thesis describes the identification of classic small molecule inhibitors of the BET family of bromodomain-containing proteins. In particular, the design of molecules for oral administration for use in oncology indications is described. This required a focus on balancing potency and physicochemical properties, and subsequently pharmacokinetic profiles. The ultimate aim was the identification of a molecule with a profile suitable for progression into pre-clinical safety studies, and the implementation of an appropriate synthetic route to provide material for these studies.

As a result of challenging pre-clinical safety findings within our laboratories, targeted drug delivery strategies to increase the therapeutic index of BET bromodomain inhibitors were also considered. To this end, Part III describes the design and synthesis of molecules containing esterase-sensitive motifs (ESMs) to target the compound to a subset of cell types. The aim was to establish whether ESM technology was applicable to BET bromodomain inhibitors by the design of tool molecules. If *in vitro* biological studies proved successful, the aim would be to identify molecules with profiles suitable for assessment in *in vivo* studies. The ultimate aim would then be to identify a molecule suitable for pre-clinical evaluation. The identification and biological profiling of these ESM-containing tool molecules would enable the value of ESM technology in the BET area to macrophage-based diseases such as rheumatoid arthritis to be assessed.

PART II:
BET BROMODOMAIN INHIBITORS

Chapter 2

The Design and Synthesis of BET–Bromodomain Inhibitors for Oral Administration

“... and it was all yellow.”

Yellow, Coldplay

Synopsis

At the time this work was undertaken, a lead compound from an oral BET bromodomain inhibitor programme within our laboratory was undergoing preclinical toxicity studies. The ultimate aim of these studies was to enable progression of this compound into patients with NUT midline carcinoma, as the first step in a clinical expansion strategy.^{2,01} To mitigate the risk of attrition of this compound, a back-up molecule in a structurally distinct series with an equivalent biological profile was required. The profiles of compounds already synthesised within the quinoline–isoxazole series were interrogated and a number of further analogues were designed using the SAR knowledge gained from these interrogations, as well as the use of *in silico* profiling. The potency of these compounds was analysed using biological screening, and the more attractive compounds were profiled in a range of selectivity assays. From these compounds a preferred molecule was identified and synthesised on a large scale to provide material for a variety of *in vitro* and *in vivo* pre-candidate selection studies.

2.1 Background

At the time the work described within this chapter commenced, a lead compound from the oral BET bromodomain inhibitor programme, I-BET762 (**2.01**, Figure 2.02) was undergoing preclinical toxicity studies. These studies included 28-day rat and dog toxicological evaluations as part of a pre-clinical package initially aimed at progression of the compound into a clinical trial for patients with NMC (Section 1.3.1). To mitigate the risk of attrition of the lead compound, and safeguard future development opportunities in the highly novel BET bromodomain area, a molecule in a structurally distinct series, with a profile suitable for clinical development, was required. The backup compound could therefore replace the pre-clinical candidate if structurally related, rather than mechanism related, toxicity was seen in pre-clinical or clinical trials. It could also be used for progression into clinical trials for alternative BET bromodomain implicated diseases if safety and efficacy data was supportive. This chapter will deal with the work performed to identify a backup molecule from the quinoline–isoxazole series.

For the back-up molecule, a number of stringent criteria were established, which are shown below. These guarantee that the properties of the compound are comparable to, or better than, the current pre-clinical candidate in terms of potency, selectivity and pharmacokinetic profile.

- Human whole blood (HWB) (IL-6 assay)^{A1} pIC₅₀ > 6.5
- > 100 times selectivity over other known bromodomains
- Oral bioavailability in rat > 20%
- hERG pIC₅₀ < 4.0 in the *in vitro* FP assay^{A2}
- CYP450 IC₅₀ > 3 µM across isoforms^{A3}

Figure 2.01: The desired profile for a compound to move into pre-clinical studies, and that aimed for by the work described within this chapter.

At the commencement of the work described in this chapter, there had already been over 1300 compounds synthesised within the quinoline–isoxazole series within our laboratories. These were predominantly the result of an earlier oral ApoA1 agonist programme, as well as a programme undertaken to identify intravenously administered BET bromodomain inhibitors. A small number had also been specifically designed as oral BET bromodomain inhibitors. The

^{A1, B1, etc} refer to *in vitro* assay protocols (A) and *in silico* modelling details (B), which are detailed in Appendix 1.

biological profiles of all compounds previously synthesised were interrogated using the criteria above to identify compounds already displaying the required profile, as well as attractive starting points for optimisation. Data was extracted and manipulated using the in-house software ‘Helium for Excel’,^{2.02} and visualised using TIBCO Spotfire.^{2.03} The resulting shortlist of compounds is shown below (Figure 2.02) along with the current lead molecule **2.01**, and comprises the compounds with the most attractive overall profiles. The biological and physicochemical profiles of these compounds are also shown (Table 2.01). Details of the assays used to generate the data are provided in Section 2.5.

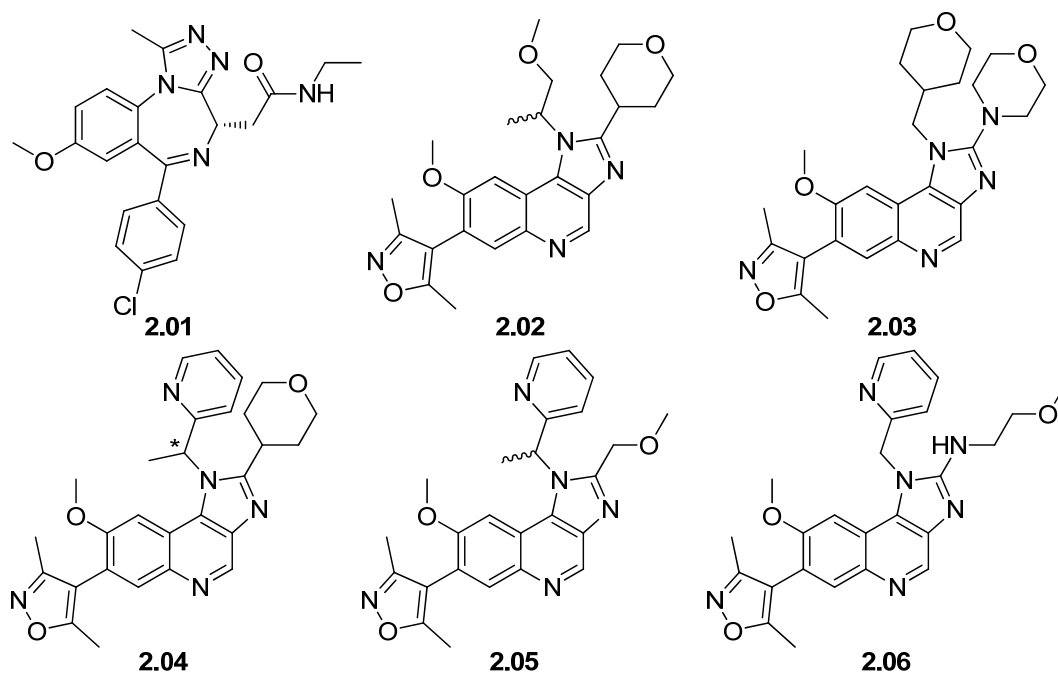


Figure 2.02: *l*-BET762, **2.01**, and the shortlisted **2.02–2.06**. Compounds **2.02** and **2.05** are racemic, and compound **2.04** is a single undefined enantiomer.

Compound	2.01	2.02	2.03	2.04	2.05	2.06
mwt	423	450	477	483	443	458
clogP	2.4	1.7	1.8	2.0	1.8	2.2
BRD4 (n) pIC ₅₀	6.8 (13)	6.9 (6)	7.1 (6)	7.0 (2)	6.9 (4)	7.0 (8)
HWB pIC ₅₀ (n)	6.2 (12)	6.4 (4)	6.6 (4)	7.0 (2)	6.1 (2)	6.4 (6)
CYP450 IC ₅₀ (μM)	All > 50	All > 12	All > 6	N/A	All > 6	All > 15
CLND solubility (μM)	311	453	256	> 337	≥ 391	387
hERG FP pIC ₅₀	< 4.3 (13)	4.2 (2)	N/A	N/A	N/A	4.4 (3), <4.0 (1)

Table 2.01: Profiles of the shortlisted quinoline–isoxazole compounds identified using the desired compound criteria. The BRD4 potency was measured in an HTRF assay.^{A4}

Further analysis of these compounds clarified that the combination of suitable physicochemical properties and human whole blood (HWB) potency was critical in identifying a suitable backup compound from this series. Compounds with higher HWB potency, such as compound **2.04**, contained five aromatic rings. This is undesirable in a candidate molecule, since the number of aromatic rings has been shown to correlate with an increased rate of attrition during development.^{2.04} Where an aromatic ring had been removed, compounds had lower HWB potency, with compound **2.03** being the most potent with a pIC₅₀ of 6.6. In addition, all of the compounds identified had molecular weights at the higher end of what is desired for a candidate molecule.^{2.05} The pharmacokinetic profiles of these compounds had not yet been investigated. Compounds **2.02** and **2.05** had been synthesised as the racemate, and **2.04** as a single enantiomer with undefined chirality. In these cases, single enantiomers of known configuration needed to be prepared and profiled to progress the compounds further.^{2.06}

After this thorough review of the available data, a set of priorities for the design and progression of compounds within the quinoline–isoxazole template was developed:

- Restriction of the number of aromatic rings to a maximum of four.
- Prioritisation of compounds for synthesis with a lower molecular weight, ideally less than 450.
- Investigation of the SAR with a view to increasing the HWB potency, including:
 - Position of heteroatoms in the R¹ and R² substituents (Figure 2.03).
 - Effect of α -methyl branching in R¹ on potency.
 - Introduction of π -character by using a cyclopropyl unit.^{2.07}
- Preparation of sufficient quantities of single known enantiomers of any compound of interest before profiling further.
- Establishment of the pharmacokinetic profile of lead compounds.

2.2 Medicinal Chemistry Design of Compounds for Synthesis

A set of compounds for synthesis was designed by inspection of the existing SAR, as well as physicochemical profiling. The compounds designed were restricted to changes at the R¹ and R² positions (Figure 2.03) and the core structure remained constant. Investigation of the quinoline–isoxazole series was well advanced by this stage, and provided confidence that the core structure was already optimal.

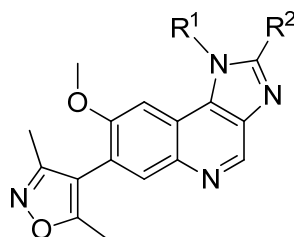


Figure 2.03: General structure, with changes to be made at the R¹ and R² positions.

Analysis of available SAR suggested a small number of R¹ groups with the potential to improve either the cellular potency or physicochemical properties of the molecules (Figure 2.04).

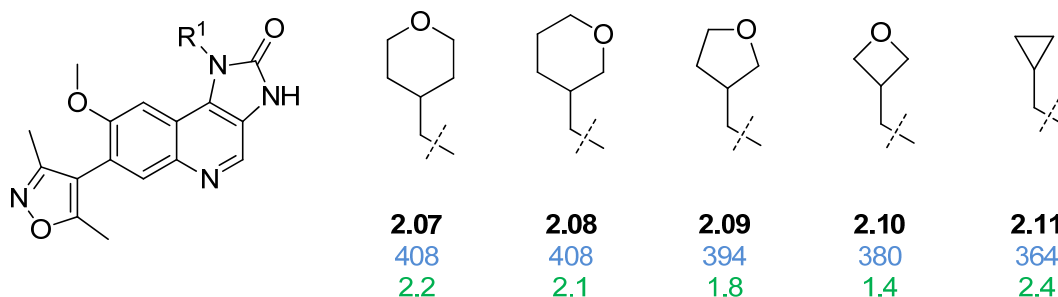


Figure 2.04: Compounds designed to investigate effect on potency of small changes to R¹. The compound number (bolded) is followed by molecular weight (blue) and clogP (green).^{B1}

In order to rapidly investigate the effect of changes at R¹, the compounds would be synthesised in the imidazoquinolone series, where the final compounds can be accessed in only two steps from an available intermediate. The 4-methyltetrahydro-2H-pyran of compound **2.07** is present in compound **2.03**, and a number of other potent analogues, and would be used to benchmark the effect of the changes to R¹. Any promising R¹ groups could be combined with attractive R² groups in a second iteration of chemistry.

The synthesis of compound **2.08** would identify whether altering the position of the heteroatom within the tetrahydropyran ring would affect the potency. Compounds containing 3-methyltetrahydrofuran (**2.09**) and 3-methyloxetane (**2.10**) may also have increased potency due to the altered position of the heteroatom, as well as having reduced molecular weight and lipophilicity compared to compounds **2.07** and **2.08**. The cyclopropyl group in compound **2.11** has some π -character^{2.07} and, by analogy to compounds **2.04** and **2.05**, may therefore have increased potency. Compound **2.11** has significantly reduced molecular weight over compound **2.07**, although the calculated lipophilicity is slightly increased.

Concurrently, a second set of compounds was designed to investigate the result of combining R¹ and R² groups into the same molecule that had been seen individually, in previous SAR, to have good cellular potency. The compounds designed after analysis of existing SAR and physicochemical profiling, particularly focusing on molecular weight, clogP and number of aromatic rings, are shown below (Table 2.02).

Compounds which were given a high priority for synthesis included **2.12** and **2.13**, to determine the effect of the α -methyl substituent, and compounds **2.14** and **2.16**, which have among the lowest molecular weights. Novel R² groups were also included for synthesis, such as a cyclopropyl group to introduce π -character whilst maintaining a low molecular weight. Another such example is the dimethylamino R² group to give a truncated version of the morpholine compound **2.03**. The dimethylamino has a more tractable synthesis than the morpholine example, and also a lower molecular weight. For the novel R² groups, compounds **2.17** and **2.20** were prioritised for synthesis as direct analogues of compound **2.12**, thus identifying the effect of the R² changes on potency.

The compounds shown in Figure 2.04 and Table 2.02 were not an exhaustive list of those to be synthesised. As data were produced, the SAR would be used to design changes likely to provide a precandidate molecule that met the required criteria. In addition, compound **2.02**, one of the most attractive compounds already synthesised (Table 2.01), would be prepared as its two constituent enantiomers and each profiled further. Compound **2.06** (Table 2.06), another with an attractive profile, would be resynthesised in sufficient quantity for pharmacokinetic evaluation, and the direct analogue with an additional α -methyl substituent, as seen in compounds **2.04** and **2.05**, was also to be synthesised as SAR indicates that this change may increase potency.

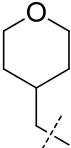
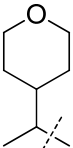
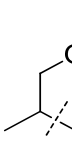
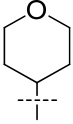
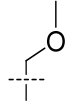
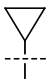
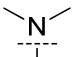
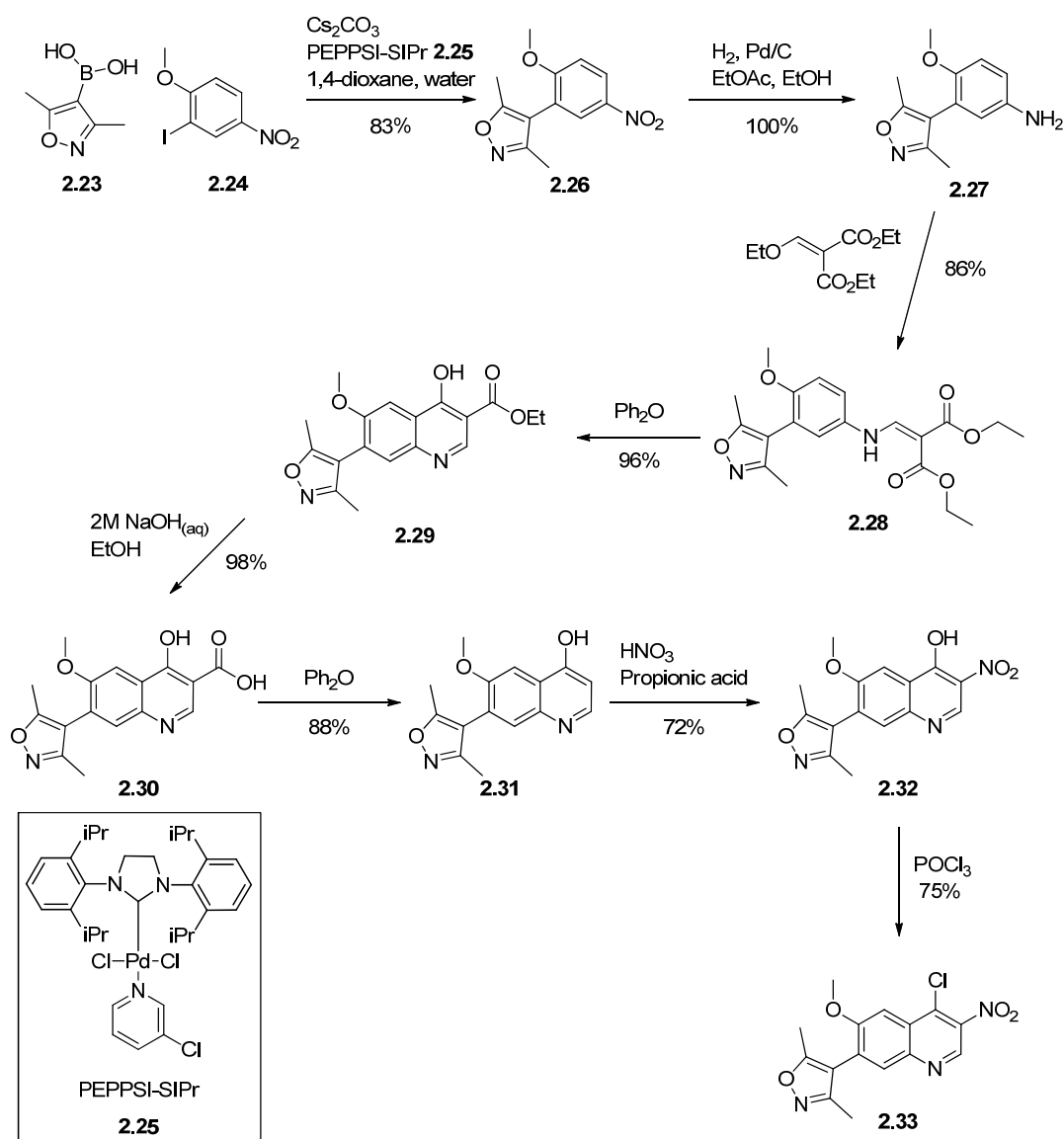
Structure of substituent, rationale. $R^2 \downarrow R^1 \rightarrow$				
		Historically most potent non-aromatic R^1 , e.g. 2.03 .	Does introducing α -methyl increase potency, as in 2.04?	Historically lowest mwt R^1 with good cellular potency, e.g. 2.02 .
	Historically potent non-aromatic R^2 , e.g. 2.02 and 2.04 .	2.12 476 3.5	2.13 490 3.8	2.02 450 3.3
	Historically lowest mwt R^2 with good cellular potency, e.g. 2.05 .	2.14 436 2.8	2.15 450 3.1	2.16 410 2.5
	Novel R^2 , introduce π -character whilst keeping low mwt.	2.17 432 4.7	2.18 446 5.0	2.19 406 4.5
	Novel R^2 , truncated secondary amine, analogous to morpholine in 2.03 .	2.20 435 3.6	2.21 449 3.9	2.22 409 3.3

Table 2.02: Compounds designed on the quinoline–isoxazole core (Figure 2.04), with rationale for selected R^1 and R^2 groups. Each cell contains compound number (bolded) followed by molecular weight (blue) and ACD clogP (green).^{B1}

2.3 Synthesis of Target Molecules

2.3.1 Scale-up of Key Intermediate 2.33

The majority of the compounds discussed in the subsequent sections within this chapter required the same common 4-chloroquinoline intermediate, **2.33**, as starting material. The synthesis of this compound from commercial starting materials is described below and used chemistry which had previously been validated within our laboratories (Scheme 2.01).



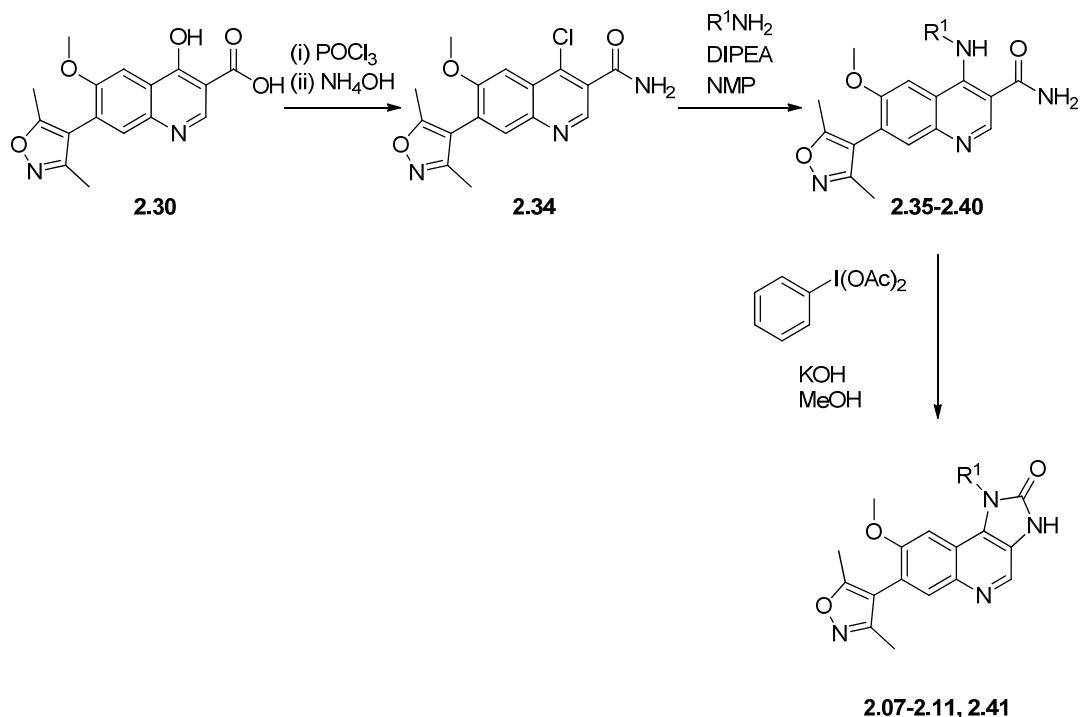
Scheme 2.01: Synthesis of common intermediate **2.33**, used throughout chapter 2.

Compound **2.28** was synthesised elsewhere in our laboratory^{2.08} in three steps and 71% yield from commercial starting materials. A Suzuki reaction between the boronic acid **2.23** and aryl iodide **2.24** using PEPPSI-SIPr **2.25** as the catalyst gave compound **2.26** in 83% isolated yield. The nitro group of compound **2.26** was reduced using palladium on carbon to form compound **2.27** in quantitative yield. This was reacted with diethyl ethoxymethylenemalonate to form compound **2.28**, in 86% yield, in preparation for the cyclisation to form the quinoline.^{2.09} At this point, the synthetic route was continued as part of the work described within this thesis. Cyclisation of compound **2.28** to form the 4-hydroxyquinoline **2.29** was performed in 96% isolated yield by adding compound **2.28** to boiling diphenyl ether in an open flask, and stirring for approximately 15 minutes. Continuing the heating beyond this point led to a significant reduction in yield, apparently caused by the reaction mixture charring in the flask. Any attempts to reduce the temperature, so the diphenyl ether was not at reflux, gave little conversion of compound **2.28** to compound **2.29** and predominantly starting material remained.

The ethyl ester of compound **2.29** was converted cleanly into the acid **2.30** in 98% isolated yield using aqueous sodium hydroxide. The acid **2.30** was decarboxylated in 88% isolated yield, again by addition to refluxing diphenyl ether, to give compound **2.31**.^{2.10} As in the conversion of compound **2.28** to compound **2.29**, it was important to ensure the diphenyl ether was at reflux, and to not heat for longer than 15 minutes, to avoid degradation. Compound **2.31** was nitrated using nitric acid in propionic acid^{2.11} to give compound **2.32** in 72% isolated yield. The material was chlorinated in small batches as required, using phosphorus oxychloride, to give compound **2.33** in a typical yield of 75%. The eight steps from commercial starting material were completed in 32% overall yield providing 7.3 g of compound **2.33**. This synthetic route was subsequently successfully scaled up by an outsourcing partner to give 58 g of compound **2.33**.

2.3.2 Synthesis of Imidazoquinolone Analogues

The synthetic route to the desired imidazoquinolone analogues was based on the use of a Hofmann-type rearrangement, via quinoline-isoxazole intermediate **2.34**.



Scheme 2.02: Synthetic route used to synthesise imidazoquinolone analogues. The structures of R^1 that were synthesised are shown previously (Figure 2.04).

The imidazoquinolone analogues **2.07–2.11** and **2.41** were prepared in two steps from the 4-chloroquinoline intermediate **2.34**. The intermediate had been prepared on a large scale from compound **2.30** via chlorination, followed by amide formation.^{2.08} Compound **2.34** underwent nucleophilic aromatic substitution ($\text{S}_{\text{N}}\text{Ar}$) with the appropriate aliphatic amines giving compounds **2.35–2.37**, and **2.39–2.40**, in moderate yields (Table 2.03). Conventional heating in NMP was used with DIPEA added to neutralise the hydrochloric acid produced.

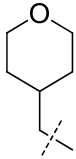
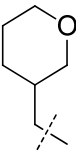
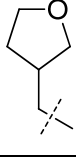
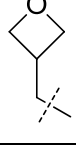
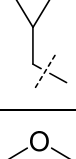

Final product	R ¹ substituent	Conversion of 2.34 to 2.35–2.40 . (Isolated yield, conversion)	Conversion of 2.35–2.40 to 2.07–2.09, 2.11, 2.41 . (Isolated yield, conversion)
2.07		(2.35) 71%, 92%	89%, N/A%
2.08		(2.36) 50%, 81%	67%, 91%
2.09		(2.37) 56%, 91%	84%, 90%
2.10		(2.38) Failed, 0% conversion.	N/A
2.11		(2.39) 67%, 80%	N/A, 90%
2.30		(2.29) 14%, 21%	24%, 65%

Table 2.03: The reaction conversion and isolated yields for the synthesis of compounds **2.07–2.11** and **2.41**, using the synthetic route shown in Scheme 2.02. The isolated yield is shown in blue; the conversion by LCMS of the reaction mixture is shown in green. The isolated yield for compound **2.11** is not shown as only a portion of the crude material was purified.

Compounds **2.35–2.37**, **2.39** and **2.40** were then converted to final products **2.07–2.09**, **2.11**, and **2.41** in moderate yields (Table 2.03). Conditions were identified for the conversion,^{2,12} and the reaction proceeds *via* a Hoffman-type rearrangement using hypervalent iodine and potassium hydroxide.^{2,13} The proposed reaction mechanism for this reaction is shown below (Figure 2.05).

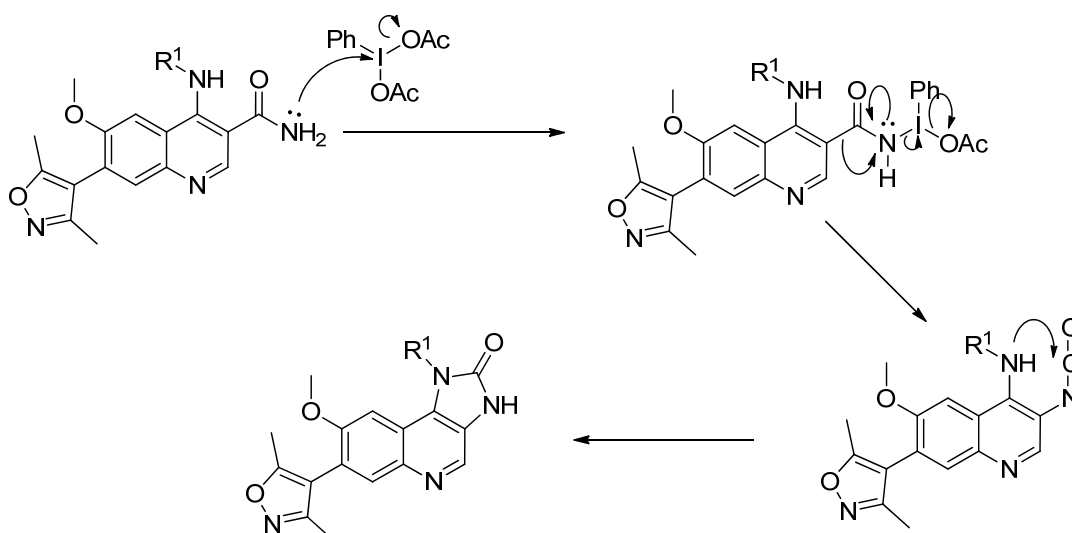


Figure 2.05: Reaction mechanism for the formation of imidazoquinolone analogues using hypervalent iodine via a Hoffman-type rearrangement.

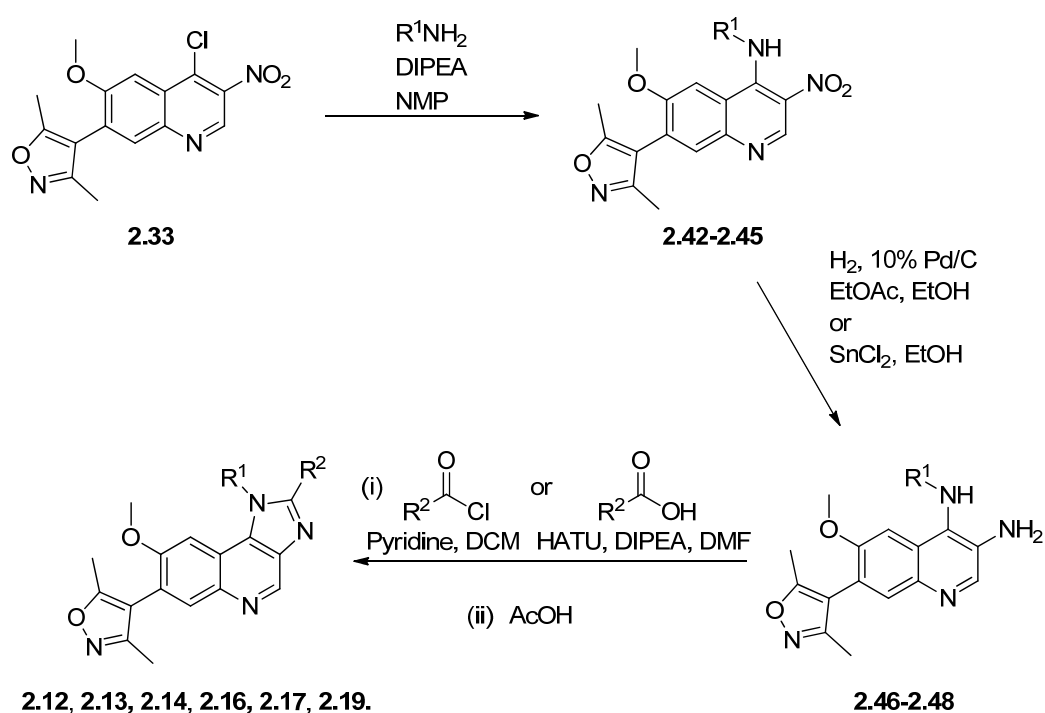
The majority of the planned compounds were successfully synthesised using the chemistry described. The only compound that was not successfully synthesised using this route was compound **2.10**. In this case, the nucleophilic aromatic substitution using oxetanylmethanamine was unsuccessful, and the starting material **2.34** had been completely converted to the 4-hydroxyquinoline side product. It was possible that the amine was not sufficiently nucleophilic, or was of poor quality. The synthesis of this compound was not investigated further due to the reduced potency of the 5-membered **2.09** over the six-membered **2.07** (Section 2.5).

One further compound, **2.41**, was synthesised in addition to those originally designed (Figure 2.04). Addition of the α -methyl substituent in similar compounds showed some increase in potency, so it was added to compound **2.07** to identify if this SAR transferred to the tetrahydropyran analogues. The amine starting material **2.55** had been previously synthesised elsewhere in our laboratory^{2.08} using the route described in Section 2.4.4 (Scheme 2.05).

2.3.3 Synthesis of Imidazoquinoline Analogues

The route to imidazoquinoline compounds where R² was carbon-linked to the core was based on an acid-catalysed benzimidazole cyclisation reaction. The *N*-substituent was to be installed prior to cyclisation in an S_NAr reaction, avoiding the need to alkylate the ring system and separate the isomers which would be formed.

Where R² was carbon-linked to the triaryl core, the majority of the imidazoquinoline analogues were synthesised using the synthetic route above (Scheme 2.03). The 4-chloroquinoline **2.33** underwent S_NAr with the appropriate amine R¹NH₂ to give compounds **2.42–2.45** with varying isolated yields from 23–85% (Table 2.04). This displacement was facile due to the *ortho*-nitro group, but despite similar conversions by LCMS, the yields of compounds **2.42**, **2.44**, and **2.45** varied due to the low solubility of the products causing difficulties in the isolation of material. The amine used to synthesise compound **2.43** contained large amounts of water, accounting for the low conversion and yield of this reaction and the presence of significant amounts of the 4-hydroxyquinoline side-product. The synthesis of this amine is discussed further in Section 2.4.4.



Scheme 2.03: Synthetic route used to synthesise imidazoquinoline analogues **2.12**, **2.13**, **2.14**, **2.16**, **2.17**, **2.19**.

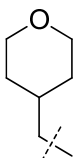
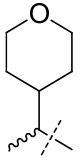
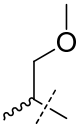
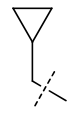
Product	R ¹ substituent	Isolated yield, conversion by LCMS
2.42		85%, 79%
2.43		19%, 31%
2.44		62%, 93%
2.45		23%, 92%

Table 2.04: The conversion and yields for the synthesis of compounds 2.42–2.45 by S_NAr .

Compounds 2.42–2.44 were reduced to compounds 2.46–2.48 (Table 2.05). Reduction was initially performed using an H-cube flow apparatus with a 10% Pd/C catalyst cartridge, in yields of 16–96%. During the reduction of compound 2.42, the low solubility of both the starting material and the product caused a blockage in the H-cube flow apparatus and some material was lost. The reduction was subsequently repeated using tin (II) chloride, refluxing the reaction mixture in ethanol, and this increased the isolated yield to 96%. Compound 2.45 was not reduced as a different synthetic route was used to produce the final products (Scheme 2.04).

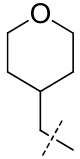
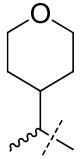
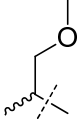
Compound	R ¹ substituent	Reduction conditions	Isolated yield
2.46		10% Pd/C, H-cube™	16%
		SnCl ₂	96%
2.47		10% Pd/C, H-cube™	93%
2.48		10% Pd/C, H-cube™	96%

Table 2.05: The synthesis of compounds **2.46–2.48**, via reduction with Pd/C or SnCl₂. The isolated yields of the reactions are shown.

Compounds **2.46–2.48** were converted to the final products shown below (Table 2.06) via amide formation followed by a dehydrative imidazole ring closure. The amide formation proceeded via reaction of the bis-amine **2.46–2.48** with either the appropriate acid chloride or activated acid, formed from the acid using HATU. After the amide intermediate was isolated, the cyclisation was performed by heating in acetic acid to give the final compound, except in the case of compound **2.14**. In this instance, the cyclisation was almost complete (91% by LCMS) during the isolation of the intermediate. This had occurred whilst the solvent was being removed in a nitrogen blow down apparatus at 45 °C after the MDAP purification. The solution being removed was a mixture of 10 mM ammonium bicarbonate in water (adjusted to pH10 with ammonia solution) and acetonitrile. This cyclisation was not seen at a significant level (over 10% by LCMS) in any of the other isolations; this does not seem to be for any obvious structural reason and it was speculated that a lower nitrogen flow in the case of compound **2.14** may have led to the solution being heated in solution for significantly longer.

Compounds **2.13**, **2.14**, **2.16**, **2.17** and **2.19** were successfully produced using this methodology. In addition, compound **2.12** was isolated from an impurity generated during the synthesis of compound **2.13**. This impurity was due to impure amine **2.55** (synthesis described in Scheme 2.05) being used in the S_NAr reaction to form compound **2.43**, and the impurity being carried through the synthetic route.

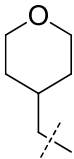
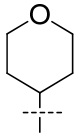
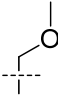
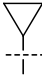
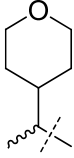
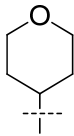
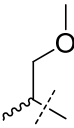
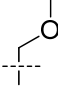
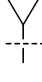
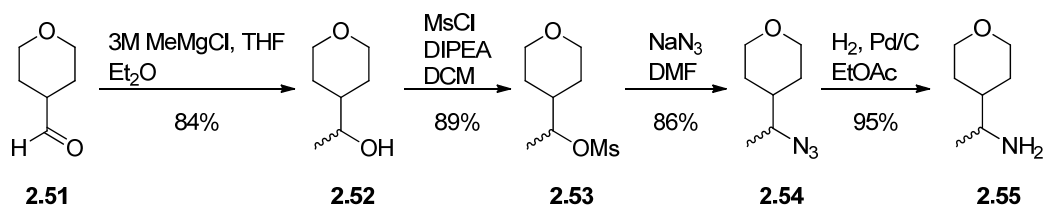
Compound	R ¹ substituent	R ² substituent	Overall yield of amide formation and cyclisation.
2.12			N/A*
2.14			52%
2.17			37%
2.13			15%
2.16			21%
2.19			69%

Table 2.06: The synthesis of final compounds, via amide formation and dehydrative cyclisation, for biological screening. The isolated yields over the two steps are shown. *The isolated yield for the formation of compound **2.12** cannot be calculated as the compound was synthesised using an impurity isolated during the formation of compound **2.13**.

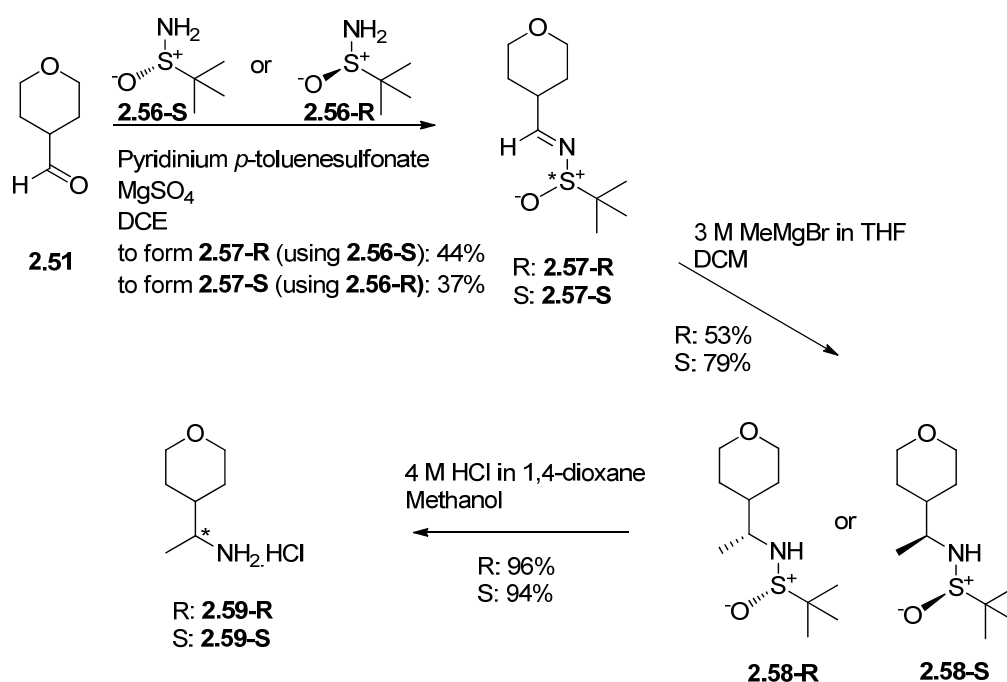
After the synthesis of the compounds above (Table 2.06), an alternative method (Scheme 2.04, below) was trialled to improve the initial route, and this was used to synthesise compounds **2.49** and **2.50**.^{2.14} This method is described in more detail in a subsequent part of this thesis (Section 3.4.2.2), where it was used extensively. Compound **2.45** was converted directly to the final products **2.49** and **2.50**, using the appropriate aldehyde and sodium hydrosulfite (Scheme 2.04), in 27–30% isolated yield.



Scheme 2.05: Synthesis of racemic 1-(tetrahydro-2H-pyran-4-yl)ethanamine **2.55**.^{2.08}

Due to the lack of reproducibility of this route, and encouraging data seen for both the racemic compound **2.13** and the *R*-enantiomer of compound **2.02** (compound **2.67**) (Section 2.5.2), it was decided to investigate an enantioselective synthesis of the *R*-enantiomer of compound **2.13**, as well as enabling the *R*-enantiomer of amine **2.55** to be available for the synthesis of further analogues if required. The *S*-enantiomer was also synthesised for analytical comparison.

A route was designed using chiral 2-methylpropane-2-sulfinamide, compound **2.56-R** and **2.56-S**, as chiral auxiliaries, based on methodology described in the literature (Scheme 2.06).^{2.15}



Scheme 2.06: Synthetic route used to prepare the enantiopure amines **2.59-R** and **2.59-S**.

The chiral sulfinamides **2.57-R** and **2.57-S** were formed using the commercially available aldehyde **2.51** and chiral auxiliaries **2.56-S** and **2.57-R** respectively. The Grignard reagent,

methylmagnesium bromide, was delivered selectively to form compounds **2.58-R** and **2.58-S**. The proposed reaction mechanism is shown below for the preparation of compound **2.58-R** (Figure 2.06). In the proposed chair transition state, the larger tetrahydropyran (THP) and tertiary butyl (^tBu) groups are fixed in equatorial positions. Coordination of the magnesium of methylmagnesium bromide with the sulfinamide oxygen holds the two reacting partners in the configuration which would produce the *R*-enantiomer at the reacting centre. Removal of the chiral auxiliary under acidic conditions produced the required *R*-amine **2.59-R** in 96% yield, and *S*-amine **2.59-S** in 94% yield, as hydrochloride salts.

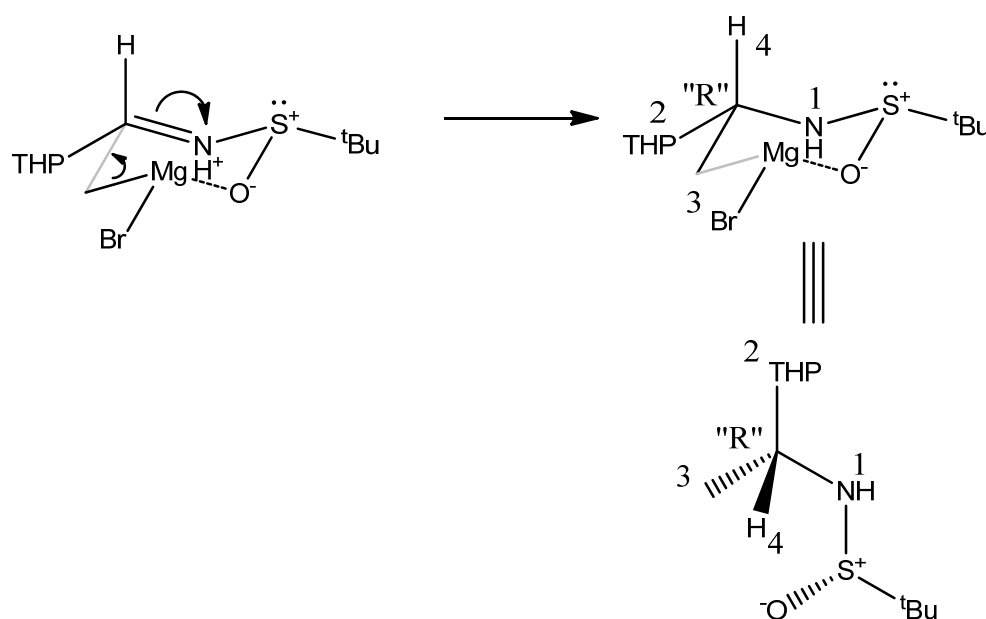
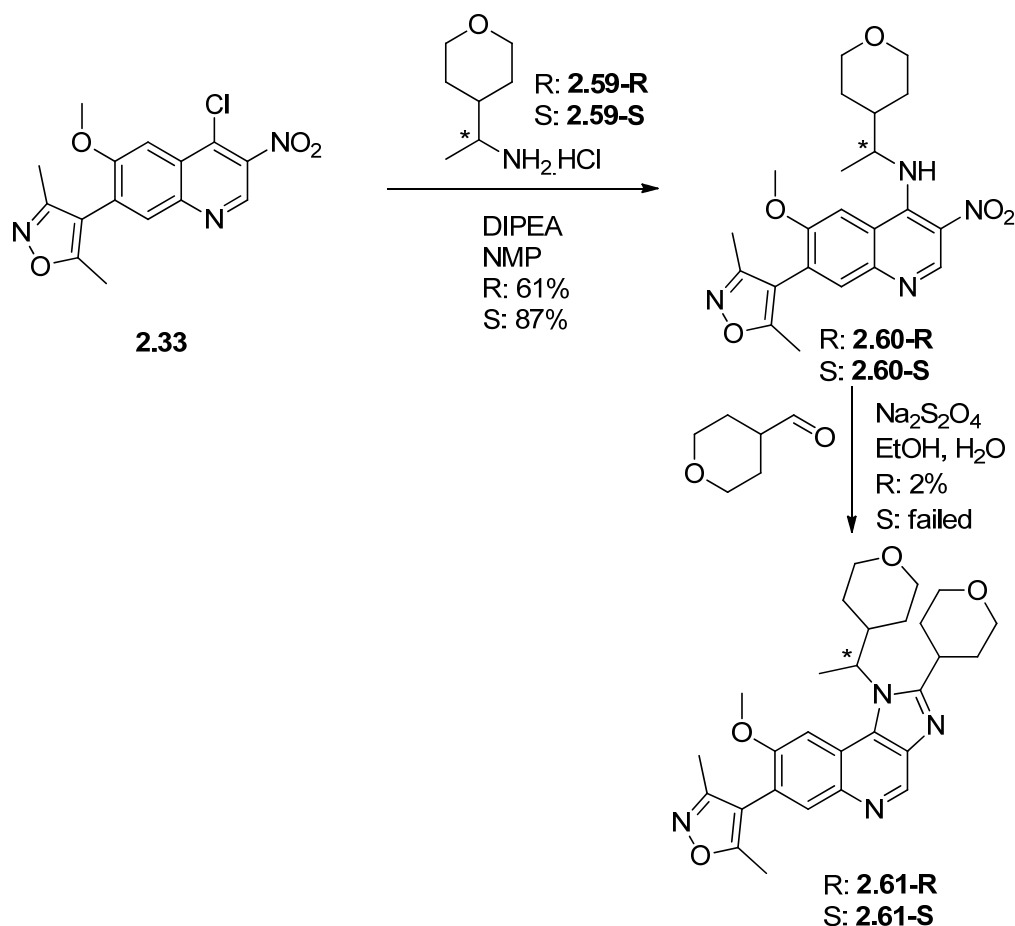


Figure 2.06: The enantioselective Grignard reaction used to form compound **2.58-R** (Scheme 2.08). A pale grey line is used to show the chair structure, where a bond is not present.

The chiral amines **2.59-R** and **2.59-S** were successfully used in an S_NAr reaction with intermediate **2.33** to produce compound **2.60-R** in 67% yield and compound **2.60-S** in 87% yield (Scheme 2.07). This is consistent with the yields seen in this reaction previously (Table 2.04). These intermediates were analysed using chiral analytical HPLC to confirm an enantiomeric excess of >99% in both cases, and that they were opposite enantiomers. The final compound **2.61-R** was prepared directly from the described intermediate using sodium hydrosulfite, as previously described (Scheme 2.04). This reaction gave only a very low isolated yield of 2%, which was consistent on repetition of the reaction.

The product **2.61-R** was isolated and submitted for biological screening, and the synthetic route would be revisited if the results were promising. Use of the route containing the acid-catalysed

cyclisation reaction may give a higher overall yield. Compound **2.61-S** was not isolated due to the failure of the benzimidazole cyclisation reaction. The synthesis of compound **2.61-S** was not repeated as this was the less desired enantiomer, and the chiral purity of compound **2.60-R** had already been confirmed by comparison with compound **2.60-S** during the previous reaction.



Scheme 2.07: Route used to prepare chirally pure compound **2.61** for biological profiling.

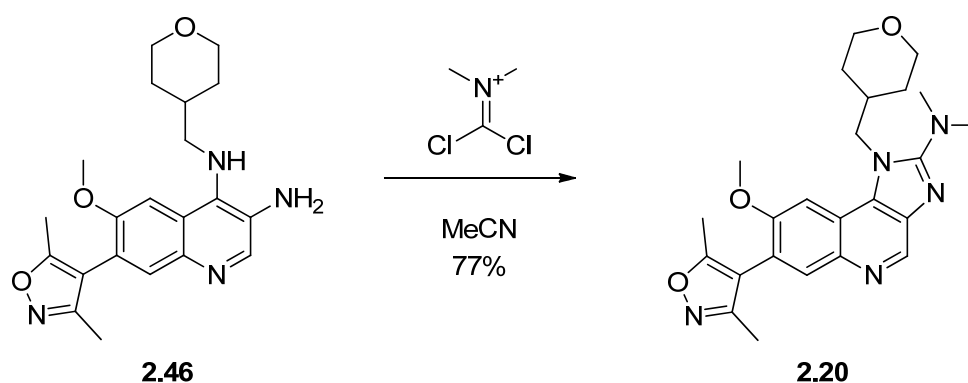
2.3.5 Synthesis of Dimethylamino Analogue

The morpholino-compound **2.03** was one of the most promising compounds identified at the outset of this work (Table 2.01). Resynthesis to provide material for hERG screening and pharmacokinetic profiling was attempted by a number of methods (below), but sufficient material could not be obtained.

- Scale-up of original reaction: formation of the 2-chloroimidazole from the imidazolone using phosphorus oxychloride and phosphorus pentachloride, followed by reaction with morpholine.^{2.16} This had previously been performed in 2% isolated yield.^{2.08}

- Addition of *N,N*-dimethylaniline^{2.17} to the 2-chloroimidazole formation.
- Phosphorus oxybromide to form the 2-bromoimidazole, and react with morpholine.^{2.18}

At this stage a decision was taken to prepare the more synthetically accessible, and more attractive in terms of physicochemical profile, dimethylamino analogue **2.20** to provide some indication of the biological profile of a similar molecule. This would also provide insight into whether more resource should be dedicated to the synthesis of the morpholine analogue. Compound **2.20** was prepared in one step (Scheme 2.07) from the previously described intermediate **2.46** (Scheme 2.03) by heating with commercially available *N*-(dichloromethylene)-*N*-methylmethanaminium chloride under microwave conditions.^{2.19}

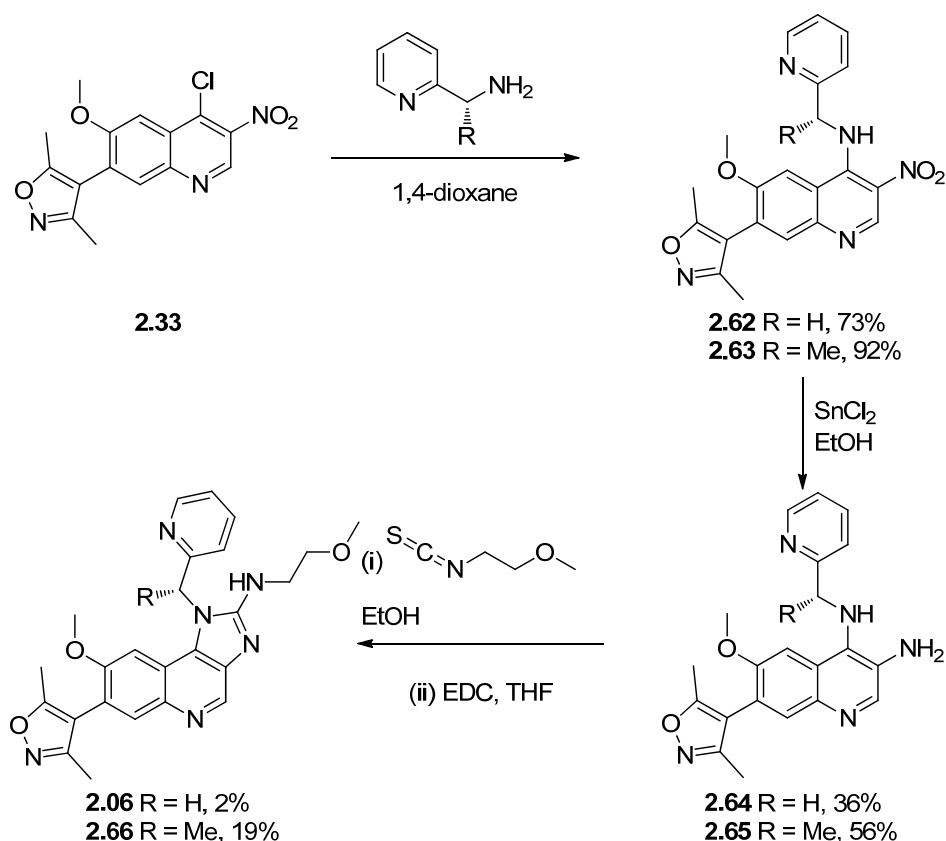


Scheme 2.08: Synthetic route used to dimethylamino analogue **2.20** for biological profiling.

The isolated yield of the reaction was 77% and, as well as providing compound **2.20** for biological profiling, this approach also identified a possible method for formation of compound **2.03**, as the corresponding morpholine reagent is known in the literature.^{2.20}

2.3.6 Remake of Compound 2.06 and its α -Methyl Analogue 2.66

Compound **2.06** was resynthesised for evaluation of its hERG channel inhibition, as well as for rat pharmacokinetic studies. As addition of an *R*-methyl group alpha to the pyridine ring improved potency of a wide range of analogues previously prepared in this series, compound **2.66** was also prepared. These analogues were prepared using the route established elsewhere within our laboratories during the initial synthesis of compound **2.06**, using the commercially available isothiocyanate shown (Scheme 2.08).

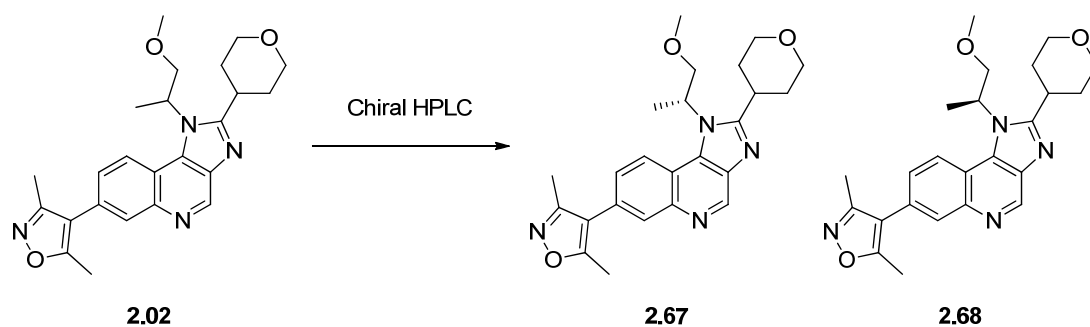


Scheme 2.09: Route used to synthesise compound **2.06**, and its α -methyl analogue **2.66**.

Compounds **2.62** and **2.63** were prepared in 73% and 92% isolated yield via an S_NAr reaction from the previously described chloro-quinoline intermediate **2.33** and commercially available amines. The DIPEA–NMP conditions used previously (Scheme 2.03) were replaced with heating in 1,4-dioxane without any base present. The nitro group was successfully reduced using tin chloride in ethanol, to give compounds **2.64** and **2.65** in 36% and 56% isolated yield, respectively. These were reacted with 1-isothiocyanato-2-methoxyethane in ethanol, followed by EDC in THF, to give the final products **2.06** and **2.66** in 2% and 19% yield, respectively. The yield of **2.06** is only 2% as only a portion of the crude reaction mixture was purified to the high standard required for the subsequent biological profiling; if this were extrapolated to purification of the whole reaction mixture, an overall yield of 17% would be predicted.

2.3.7 Separation of Enantiomers of Compound 2.02

Compound **2.02** had been identified as one of the compounds with the most attractive profile (Section 2.2). To progress this compound further, access to its constituent enantiomers would be required.^{2.06} This would enable identification of whether one enantiomer was more potent, as would be expected from previous SAR in the quinoline-isoxazole series, and also allow the selectivity and pharmacokinetic profile to be determined for the preferred enantiomer.



Scheme 2.10: Separation of compound **2.02** into its constituent R-(**2.67**) and S-(**2.68**) enantiomers.

Compound **2.02** was separated into the *R*-enantiomer **2.67** and *S*-enantiomer **2.68** (Scheme 2.10). The separation was performed by preparative chiral HPLC, with a Chiralpak AD-H column and a heptane/ethanol mobile phase. This purification gave compound **2.67** in 46% yield and 97% enantiomeric excess (ee), and compound **2.68** in 45% yield and > 99% ee. The chirality of the compounds was originally assigned as unknown but opposite; later X-ray crystallography of compound **2.67** (Figure 2.13), as well as comparison with material made from optically pure starting materials, identified this as the *R*-enantiomer.

2.4 Biological Results and Analysis

To assess whether the compounds synthesised in this chapter met the criteria set out at the outset (Section 2.2), they were profiled in a range of biological and physicochemical assays (Figure 2.07).

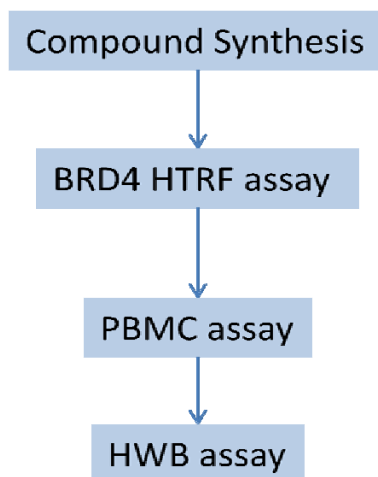


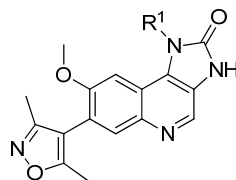
Figure 2.07: Primary screening cascade displaying the assays used to profile the compounds synthesised in Section 2.4.

Initially, the potency of the compounds at BRD4 was measured using a homogeneous time resolved fluorescence (HTRF) assay.^{A4} In this assay, HTRF is used to measure binding of the tetra acetylated histone H4 peptide to the protein. The protein:protein interaction is detected through binding of the labelled peptide to tagged BRD protein. The tight-binding limit of the BRD4 HTRF assay is a pIC_{50} of 7.3.

The effect of the compounds on the production of IL-6 in peripheral blood mononuclear cells (PBMC)^{A5} and in human whole blood (HWB)^{A1} was also measured. In the PBMC assay, PBMC's were incubated with appropriate concentrations of compound and then stimulated with LPS overnight. The reduction in the level of IL-6 produced was quantified to generate a pIC_{50} . The HWB assay was performed in a similar way to the PBMC assay, where the effect of the compound on the production of IL-6 was measured. The PBMC assay was used as a downstream measure of BRD4 inhibition and also requires the compound to be cell-penetrant. In the HWB assay, as well as the compound needing to be cell-penetrant, the effect of the other constituents in the blood, such as plasma proteins, also impacts potency.

2.4.1 Primary Data for Imidazoquinolone Compounds

The compounds prepared within the imidazoquinolone series were profiled in the BRD4 HTRF assay, as well as the programme's PBMC and HWB assays (Table 2.07).



General structure

	R ¹	BRD4 HTRF pIC ₅₀ (n)	PBMC pIC ₅₀ (n)	HWB pIC ₅₀ (n)
2.07		6.7 (10)	6.7 (12)	5.5 (2)
2.08		6.7 (8)	5.9 (4)	5.8 (2)
2.09		6.4 (4)	5.4 (4)	5.4 (2)
2.11		6.6 (6)	6.4 (4)	5.2 (2)
2.41		6.7 (6)	6.7 (8)	6.1 (2)

Table 2.07: Biological assay results for compounds synthesised within the imidazoquinolone series.

All compounds prepared within this series had pIC₅₀'s of 6.4–6.9 in the HTRF assay measuring potency against BRD4; this range of variation was within the error of the assay. We therefore used the PBMC and HWB assays to distinguish between the biological effectiveness of the compounds. Compound **2.07**, containing the baseline 4-substituted tetrahydropyran, had a pIC₅₀ of 6.7 in the PBMC assay, whereas the 3-substituted tetrahydropyran **2.08** had a lower pIC₅₀ of

6.0. As the HWB potency of the two compounds was similar, it was believed that the 3-substituted tetrahydropyran offered no advantage, and this group was not investigated further. Compound **2.09**, containing the 3-tetrahydrofuran, also had lower PBMC and HWB potency than compound **2.07** and therefore it was also not investigated further.

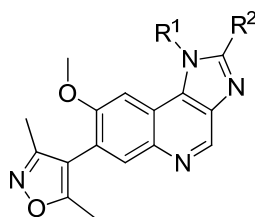
The cyclopropylmethyl-containing compound **2.11** had PBMC and HWB potency that were both slightly lower than compound **2.07**. As this was within the error of the assay, and introduction of the cyclopropylmethyl rather than the tetrahydropyran reduced the molecular weight of the compound, this substituent was of interest and therefore subsequently further examples (**2.49** and **2.50**) were synthesised within the preferred imidazoquinoline series.

The introduction of the α -methyl into compound **2.07** to give **2.30** gave similar potency in the PBMC assay, and an increase in pIC_{50} from 5.5 to 6.1 in the HWB assay. This supported the initial hypothesis that introduction of the α -methyl may lead to an increase in potency, and further examples (**2.13** and **2.61**) were therefore subsequently synthesised within the imidazoquinoline series.

2.4.2 Primary Data for Imidazoquinoline Compounds

The compounds prepared within the imidazoquinoline series were profiled in the BRD4 HTRF assay, as well as the programme's PBMC and HWB assays (Table 2.08).

As for the imidazoquinolone compounds, all compounds prepared within the imidazoquinoline series had similar pIC_{50} 's in the HTRF assay, in this case between 6.7 and 7.5. Therefore, the PBMC and HWB assays were, again, used to distinguish between the effectiveness of the compounds.



Substructure of compounds in Table 2.08 overleaf.

	R¹	R²	BRD4 HTRF pIC ₅₀ (n)	PBMC pIC ₅₀ (n)	HWB pIC ₅₀ (n)
2.02			6.9 (6)	6.9 (6)	6.4 (4)
2.67			7.1 (26)	7.0 (12)	6.5 (24)
2.68			6.7 (4)	6.3 (4)	not tested
2.06			7.0 (8)	7.0 (6)	6.4 (6)
2.66			7.1 (4)	7.5 (2)	6.8 (4)
2.12			7.3 (2)	7.0 (4)	6.3 (4)
2.13			6.9 (4)	6.7 (2)	6.7 (4)
2.61 -R			7.5 (2)	8.0 (2)	not tested
2.14			6.8 (4)	6.4 (4)	not tested
2.16			6.6 (4)	6.2 (4)	not tested

	R¹	R²	BRD4 HTRF pIC ₅₀ (n)	PBMC pIC ₅₀ (n)	HWB pIC ₅₀ (n)
2.17			7.0 (4)	6.9 (4)	5.8 (2)
2.19			6.7 (4)	6.4 (4)	5.5 (2)
2.20			7.1 (4)	7.4 (4)	6.6 (2)
2.49			6.8 (4)	6.7 (4)	5.7 (2)
2.50			7.0 (4)	6.4 (6)	5.2 (2)

Table 2.08: Primary biological results for compounds synthesised within the imidazoquinolone series.

The two enantiomers **2.67** and **2.68** of the racemic **2.02** showed different potency in the PBMC assay, with the *R*-enantiomer **2.67** being around 5-fold more potent. This was consistent with previous SAR in the series, where α -methyl substituted pyridines analogous to compound **2.04** were more potent as the *R*-enantiomer. Compound **2.67** also had a pIC₅₀ of 6.4 in the HWB assay, and was therefore selected as a compound for further profiling (Section 2.4.3).

Addition of the α -methyl to compound **2.06**, giving compound **2.66**, also gave an increase in potency in the PBMC and HWB assays. The compounds appeared equipotent in the HTRF assay, but this can be attributed to their potency being at the tight binding limit of the assay. Both these compounds were selected for further profiling (Section 2.4.3).

The effect on potency of the α -methyl in compound **2.13** compared to compound **2.12** is less clear. Compound **2.12** itself was borderline in terms of the required HWB potency, and was therefore selected for further profiling (Section 2.4.3). Compound **2.13** was prepared enantioselectively as the *R*-enantiomer to give compound **2.61**, but although this seemed to give a significant increase in potency, the synthesis had been sufficiently lengthy that by the time this

data was generated other compounds had already shown the desired compound profile. This compound was therefore not progressed further. In addition, the PBMC data for compound **2.61** was not consistent with that for compound **2.13**, and more test occasions would have been needed to confirm the robustness of the data.

Compounds with the R¹ group as tetrahydropyran (cf. compound **2.12**) or as methoxyethanamine (cf. compound **2.02**), where R² was C-linked to the imidazole and reduced in size, all showed a significant drop in potency. The methoxymethyl R² analogues **2.14** and **2.16** showed lower potency in the PBMC assay than compounds **2.12** and **2.02**, respectively. The cyclopropyl R² analogues **2.17** and **2.19** showed correspondingly lower potency in the HWB assay. These compounds were not profiled any further. In compound **2.20**, however, containing the N-linked dimethylamino R² group, the compound showed encouraging data in both the PBMC (pIC₅₀ = 7.5) and HWB (pIC₅₀ = 6.6) assays. This compound was therefore taken forward for further profiling (Section 2.4.3).

The remaining two compounds profiled, **2.49** and **2.50**, both contain cyclopropylmethyl groups at R¹. In both cases the HWB potency was reduced compared to their tetrahydropyran analogues **2.12** and **2.17**, and therefore these compounds were not progressed further.

2.4.3 Secondary Data for Compounds of Interest

Compounds identified that showed sufficient potency in the HWB assay were the chirally pure **2.67**, the bis-THP **2.12**, as well as the N-linked imidazolo-compound **2.06**, its α -methyl analogue **2.66**, and the dimethylamino **2.20**. These compounds were profiled further, in order to select a molecule that met the criteria for further progression (Figure 2.08).

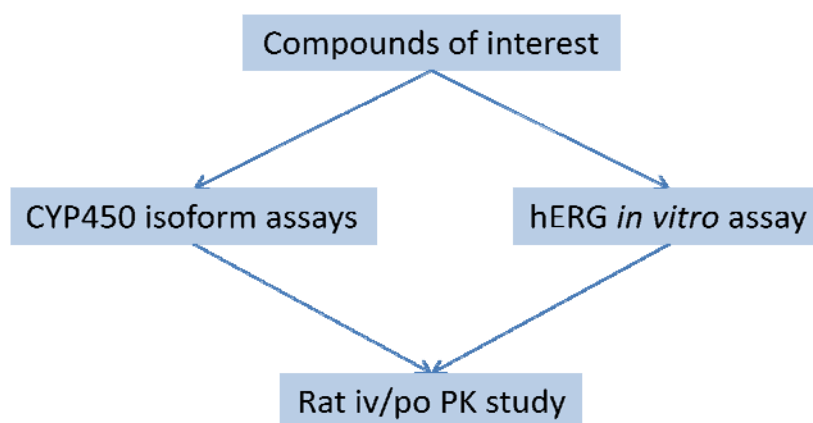


Figure 2.08: Secondary screening cascade displaying the assays used to profile the compounds identified as having sufficient potency in the PBMC and HWB assays.

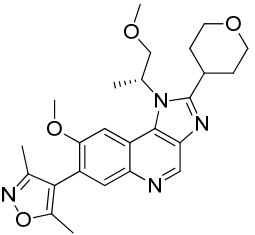
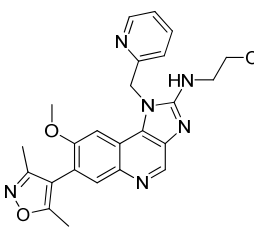
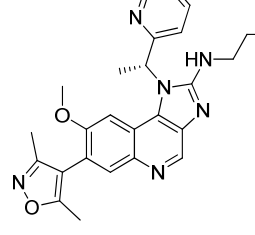
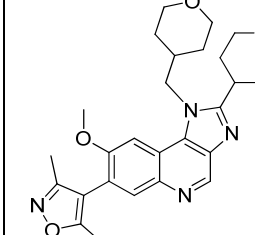
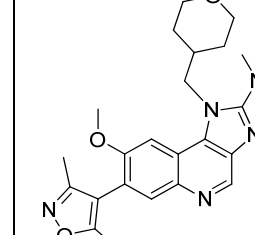
					
	2.67	2.06	2.66	2.12	2.20
CYP450 IC₅₀ (μM)	2C19 > 50 2C9 > 50 2D6 > 50 3A4VR > 50 3A4VG > 25.1	2C19 = 39.8 2C9 = 31.6 2D6 > 50 3A4VR > 50 3A4VG = 15.8	2C19 = 6.3 2C9 = 7.9 2D6 > 50 3A4VR > 50 3A4VG = 7.9	2C19 = 15.8 2C9 = 39.8 2D6 > 50 3A4VR > 50 3A4VG = 25.1	2C19 = 6.3 2C9 = 1.3 2D6 > 50 3A4VR > 50 3A4VG = 10.0
hERG pIC₅₀ (n)	4.4 (2)	4.4 (3), < 4.0 (1)	Not tested	4.2 (2)	< 4.0 (2)

Table 2.09: Secondary data generated on compounds of interest. Potency in the CYP450^{A3} and hERG^{A2} in vitro assays are shown. The compounds were tested against a variety of CYP450 isoforms: 1A2, 2C19, 2C9, 2D6, and 3A4 (vivid red, VR, and vivid green, VG assay formats).

Compounds were profiled in *in vitro* hERG and CYP450 assays to identify compounds which had potential *in vivo* safety issues and therefore could not be taken forward for development. The level of inhibition at the various CYP450 isoforms was measured in a FLINT (fluorescence intensity) assay.^{A3} The level of hERG inhibition was measured in an FP (fluorescence polarization) assay^{A2} where compounds compete with a fluorescent ligand to bind to the hERG ion channel. The data generated on the compounds is shown below (Table 2.09).

An IC₅₀ of greater than 3 µM was desired at all CYP450 isoforms tested to progress a compound into development. This is to reduce the risk of adverse drug–drug interactions due to the compound affecting metabolism and clearance of co-administered drugs by the P450 enzymes. It was pleasing to see that compounds from this series showed attractive P450 inhibition profiles. Of the compounds tested, only compound **2.20** did not meet the criteria with a potency of 1.3 µM at 2C9, and therefore this compound was not progressed further.

All compounds that were tested in the hERG FP assay showed a low potency, with all pIC₅₀ values below 4.5. This level of activity was deemed acceptable for further progression, and further studies would be performed on any compound that was progressed into development, including an *in vitro* hERG PatchXpress assay and *in vivo* dog cardiovascular studies.

Based on all the data generated, compounds **2.67** and **2.06** were selected to be profiled in rat pharmacokinetic studies. Compound **2.12** had a very similar profile to compound **2.67**, and therefore only one of these compounds was taken forward. Compound **2.67** was chosen as it had a significantly lower clogP (1.7 vs. 3.5), and a slightly lower molecular weight (450 vs. 476) and therefore better drug-like physicochemical properties. Compound **2.06** was chosen over the structurally similar **2.66** due to the more attractive CYP450 profile, and compound **2.66** would then be profiled later if the results for compound **2.06** were encouraging.

From the data generated, *in vivo* clearance and half-life in rat, as well as oral AUC and bioavailability, were determined (Table 2.10).

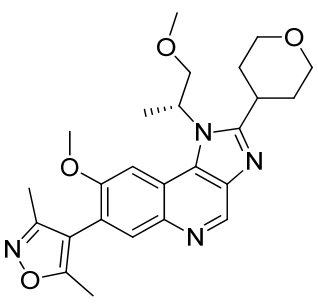
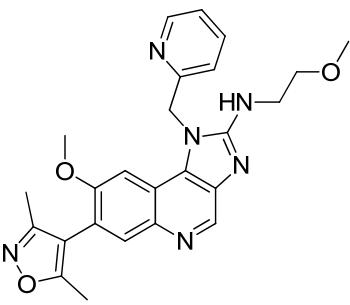
		
	2.67	2.06
Cl_b (ml/min/kg)	20	32
LBF	22%	35%
V_{ss} (l/kg)	2.2	3.0
t_{1/2} (i.v.) (h)	1.4	1.8
C_{max} (p.o.) (ng/ml)	665	218
AUC_{0-inf} (p.o.) (ng.h/ml)	1931	976
F	74%	64%

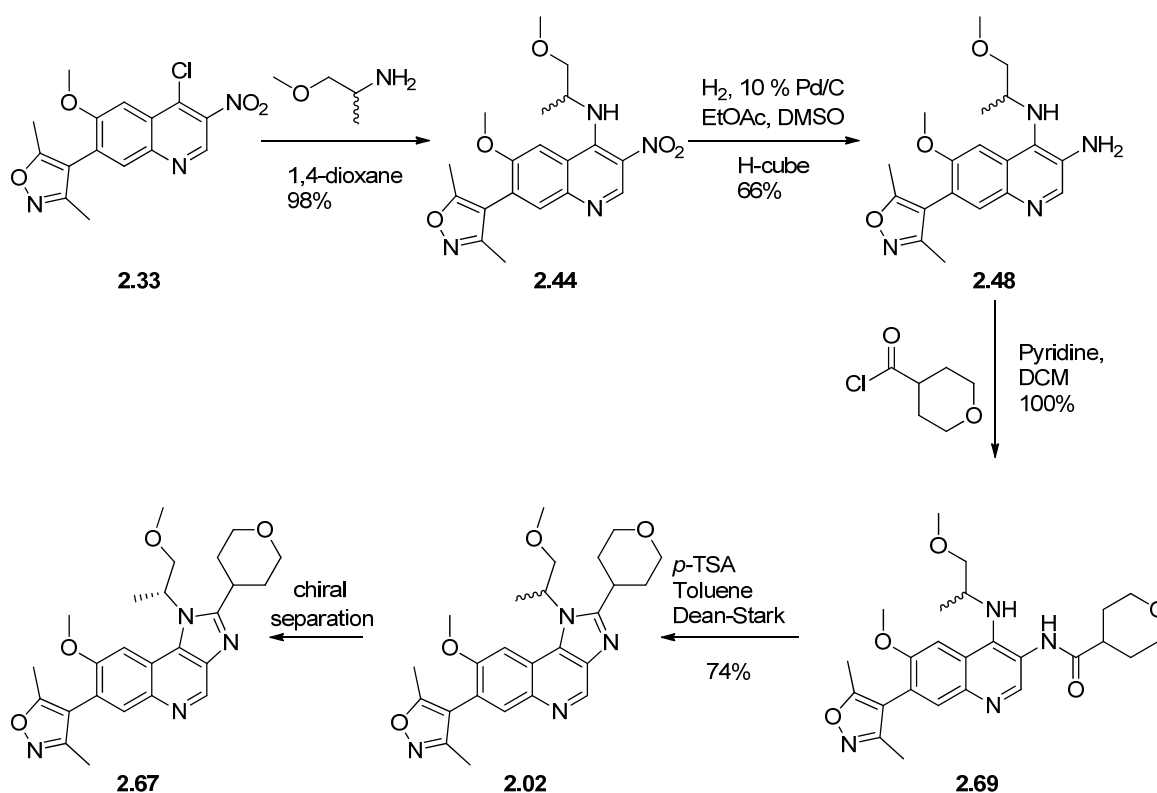
Table 2.10: Pharmacokinetic profile of compounds **2.67** and **2.06** in rats. Intravenous dosing was by infusion at 1 mg/kg (**2.67**) or 1.5 mg/kg (**2.06**), oral dosing was at 3 mg/kg. Compound **2.67** was dosed to three male Wistar Hans rats intravenously and orally, compound **2.06** was dosed to one male CD rat intravenously and three male CD rats orally. Cl_b denotes the blood clearance and LBF the clearance as a percentage of liver blood flow. V_{ss} is the volume of distribution, t_{1/2} the half life, C_{max} the maximum concentration, AUC the area under the curve, and F the bioavailability.

Both compounds **2.67** and **2.06** had low to moderate intravenous blood clearance which would be suitable for progression of the molecules in *in vivo* safety studies. Both compounds also showed high oral AUC's, resulting in good oral bioavailability. However, as compound **2.67** had the higher AUC, lower clearance, and cleaner CYP450 profile than compound **2.06**, as well as a lower aromatic ring count, this was selected as the preferred molecule for further development.

2.5 Scale-Up of Lead Molecule 2.67

To fulfil further studies on compound **2.67**, a medium scale synthesis to provide a minimum of 6 g of high quality material was required. This material would supply a package of studies required to identify whether the compound could be progressed towards pre-clinical development. The key compound-intensive studies were the Ames^{2.21} and MLA^{2.22} genotoxicity screens (350 mg), dog DMPK studies (1.0 g), dog cardiovascular studies (1.5 g), formulation and developability testing (900 mg), and rat 7-day safety studies (1.0 g). The remaining material was used to cover a wide range of *in vitro* and *in vivo* efficacy and selectivity studies.

Due to the short timescale available to provide material, a similar route and conditions to those described previously (Scheme 2.03) were employed to synthesise the compound. However, where possible, the reaction conditions and purification were optimised to achieve as favourable an overall yield as possible. The synthetic route and reagents used after the optimisation of conditions are shown below (Scheme 2.11).



Scheme 2.11: Synthetic route used to prepare large-scale batch of the lead molecule **2.67** after optimisation of conditions.

The S_NAr reaction to convert compound **2.33** to compound **2.44** had previously been performed in NMP using DIPEA to quench the hydrochloric acid produced. The removal of NMP on a large scale would be likely to be problematic, so the solvent was changed to the lower boiling 1,4-dioxane. Instead of the addition of DIPEA, the cheap and readily available 1-methoxypropan-2-amine was used in excess (5 equivalents), and the reaction proceeded in 1.5 hours at 70 °C. To isolate the desired product, the solvent was removed under reduced pressure and a simple aqueous workup was performed. These optimised conditions provided compound **2.44** in a 98% isolated yield.

The hydrogenation of compound **2.44** to form the bis-amine **2.48** was problematic due to the low solubility of both the starting material and product making the H-cube flow apparatus prone to blockages. In addition, hydrogenation using standard apparatus had been seen to cause reduction of the isoxazole ring as a significant side-product on a number of close analogues. Previously, where low solubility precluded use of the H-cube, tin (II) chloride was used as a reducing agent. However, as the material was to be used for *in vivo* toxicity studies the introduction of tin into the synthetic route was deemed inappropriate for toxicity reasons.

After testing the hydrogenation on a small scale using a number of solvent systems (including methanol, ethanol, ethyl acetate and DMSO), 5% DMSO in ethyl acetate was selected as it gave the best results. The addition of DMSO significantly increased the solubility of both the starting material and product in solution, and 5% DMSO is the maximum concentration that can be tolerated by the H-cube apparatus without damaging the interior of the equipment. In addition, the hydrogenation was tested using a solution of compound **2.44** in ethyl acetate that had not been isolated as a solid from the aqueous workup performed during the S_NAr reaction. Although this material appeared to be in solution at the start of the hydrogenation, the H-cube blocked quickly during the reaction, presumably due to the low solubility of the product.

Further optimisation in subsequent scale-up campaigns^{2,23} identified iron in acetic acid as the preferred reduction method, giving an isolated yield of 93%. In attempts to progress this chemistry in a timely fashion, it was decided to proceed with the best option available to us at this point. The hydrogenation was performed on a large scale using H-cube apparatus, 10% Pd/C catalyst cartridges, and 5% DMSO in ethyl acetate as the solvent. Blockages of the catalyst cartridge occasionally occurred, and these were resolved by fitting a new cartridge. The DMSO was removed by washing the reaction mixture with water, and, as the hydrogenation was incomplete, silica column chromatography was performed to separate the product from unreacted starting material. The starting material was recycled into a second hydrogenation and the

overall isolated yield of compound **2.48** was 66%. This yield was sufficient to prepare the material required at this stage.

Compound **2.69** was formed by reaction of the bis-amine **2.48** with 1.6 equivalents of tetrahydro-2*H*-pyran-4-carbonyl chloride, the lowest excess which was found to achieve complete conversion to product. The material was isolated using a basic aqueous workup (sodium hydrogen carbonate) to remove any tetrahydro-2*H*-pyran-4-carbonyl acid produced, followed by trituration of the crude material in diethyl ether, to give the product **2.69** in 100% isolated yield.

The dehydrative cyclisation had previously always been performed using acetic acid when products were synthesised on a small scale (Scheme 2.03). This was trialled for the conversion of compound **2.69** to compound **2.02** on a larger scale, and the reaction proceeded unacceptably slowly. To remove the water produced, 3 Å molecular sieves were added and this successfully enabled the reaction to reach completion in approximately 48 hours. However, the stirring of the large scale reaction caused destruction of the molecular sieves and produced a sludge which made the subsequent workup of the reaction very difficult and time-consuming, and reduced the isolated yield to 42%. Alternative cyclisation conditions were attempted, where one equivalent of *para*-toluenesulfonic acid was used to promote the cyclisation, and a Dean–Stark apparatus was used to remove the water and drive the reaction to completion.^{2,24} Compound **2.69** was successfully converted to the racemic product **2.02** using these conditions. A simple basic aqueous workup (sodium hydrogen carbonate) removed the acid, followed by trituration of the crude material in diethyl ether, giving the product in 74% isolated yield.

This optimised synthetic route gave 17.6 g of compound **2.02** in 48% yield in four steps from compound **2.33**; this is a significant improvement over the 26% yield seen for the first synthesis of the compound. The yield of compound **2.02** under these improved reaction conditions equates to a 15% yield in 12 steps from commercial starting materials. The racemic material was separated using chiral preparative HPLC using a Chiralpak AD-H column eluted with an *n*-hexane/ethanol gradient, as in the small scale described previously (Section 2.4.7). Isolation of the correct enantiomer, followed by trituration in diethyl ether, gave 6.7 g of solid **2.67** at > 99% ee, with a recovery of 76% of the desired enantiomer. Compound **2.67** underwent the extensive package of analysis required within our laboratories to unequivocally confirm structure and purity prior to *in vivo* toxicity studies.

Subsequent to this synthesis, work was underway to provide a chiral route to compound **2.67**, as this would be expected to at least double the yield of the synthesis. As the (*R*)-1-methoxypropan-2-amine required is analogous to the non-naturally occurring *D*-alanine, this was not readily commercially available. Attempts to repeat the synthesis of (*R*)-1-methoxypropan-2-amine using literature methods^{2,25} were unsuccessful. However, a supplier was eventually identified (ChemInstock) who were able to supply the material on a multi-gram scale. This material was sourced, and the chemistry shown (Scheme 2.11) repeated under almost identical conditions elsewhere within our laboratories^{2,23} to provide a 15 g batch of the product **2.67** in 13% yield from commercial starting materials in 12 steps, which was used in further *in vivo* safety studies.

2.6 Salt Formation

During the preparation of large scale batches of the lead molecule **2.67**, X-ray powder diffraction studies revealed that later batches of material were a different crystalline form from initial batches. This is undesirable as the presence of multiple crystalline forms can have significant impact during late stage drug development, as well as on marketed drugs.^{2.26} Additionally, the new Form 2 material was found to have a lower measured simulated fasted state (FaSSIF) solubility (Table 2.11).^{2.27}

Crystalline Form	FaSSIF solubility (4 hours)
“ 2.67 Form 1”	0.47 mg/ml
First preparation of “ 2.67 Form 2”	0.13 mg/ml

*Table 2.11: Solubility of the two crystalline forms of compound **2.67** in fasted state simulated intestinal fluid (FaSSIF).*

Subsequent studies on the isolation and crystallisation of compound **2.67** identified Form 2 as the most thermodynamically stable.^{2.28} Robust isolation conditions were only able to be identified for the preparation of Form 2; it was no longer possible to produce Form 1 material. Compound **2.67** was therefore not developable as Form 1. The low solubility of Form 2, as well as indications that this solubility may be pH dependent, led to concerns that Form 2 material may also not be suitable for long term development. The identification of a salt of compound **2.67** was therefore considered as an option to improve the physical properties of the material.

2.6.1 Selection and Synthesis of Salts

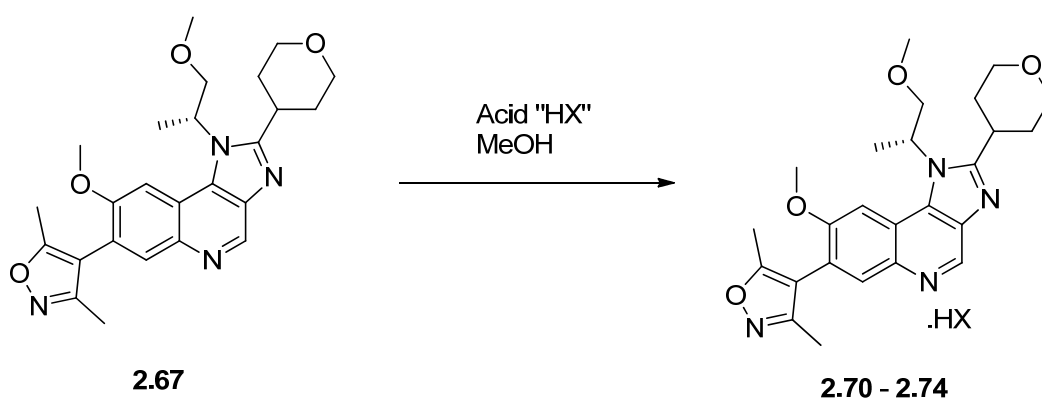
The acids to be used for salt formation were selected using two criteria. Firstly, the acid chosen had precedence for oral dosing. Secondly, the acid pK_a was generally greater than three units lower than the pK_a of compound **2.67**, which was predicted to be 5.0, to reduce the risk of disproportionation.^{2.29} These criteria led to the selection of the acids below for initial salt studies (Table 2.12). The hydrochloride salt was not considered as it had previously been synthesised during large scale route development work and was not suitable for progression due to a high water uptake.

The salts of compound **2.67** were initially synthesised on approximately a one gram scale from the parent free base (Scheme 2.12).

Salt	Salt name	Acid	Acid pK _a
2.70	Mesylate ^{2.30}		-1.9 ^{2.31}
2.71	Maleate ^{2.32}		2.0 ^{2.33}
2.72	Tosylate ^{2.34}		-1.9 ^{2.30}
2.73	Citrate ^{2.35}		3.1 ^{2.36}
2.74	Sulfate ^{2.37}		-2.8 ^{2.31}

Table 2.12: Selection of salts to be formed of compound 2.67.

The general procedure for salt formation was dissolution of the free base 2.67 in a minimum amount of hot methanol, followed by addition of one equivalent of the appropriate acid. The solvent was removed and the resulting material triturated in diethyl ether or cyclohexane to form a solid, which was dried in a vacuum oven. This procedure successfully produced the five salts 2.70 to 2.74 as solids.



Scheme 2.12: Salt formation from compound 2.67. The acids (HX) used are shown in Table 2.12.

2.6.2 Results

The salts were profiled in a range of assays to assess their physical properties and suitability for development. The most important amongst these is crystallinity, measured by X-ray powder diffraction. The results of these studies are shown below (Table 2.13).

	Salt	Crystallinity
2.67	Free base (Form 2)	Crystalline
2.70	Mesylate	Crystalline
2.71	Maleate	Semi-crystalline
2.72	Tosylate	Semi-crystalline
2.73	Citrate	Amorphous
2.74	Sulfate	Crystalline

Table 2.13: Crystallinity of salts of compound 2.67 as assessed by X-ray powder diffraction. The solubility of the citrate salt 2.73 was not measured as the material was amorphous.

As the only two fully crystalline salts, the mesylate **2.70** and the sulfate **2.74** were taken forward for further studies. Upon assessment of the stability of the salts under one month accelerated storage conditions, the sulfate **2.74** had formed a hemi-hydrate which was not developable due to a low dehydration temperature. The mesylate **2.70** was stable under three month accelerated storage conditions and therefore was the only salt suitable for further development.

At this stage, more comprehensive solubility experiments were carried out (Table 2.14). These indicated that the scale-up and purification of the Form 2 free base **2.67** had led to material with a reduced solubility over the initial batch (Table 2.11).

As salt formation impacts the kinetic, rather than thermodynamic, solubility of a compound,^{2,38} the solubility at three time points of both the free base **2.67** and mesylate salt **2.70** was determined. Although the solubility at 24 hours is similar for the two compounds, the formation of the mesylate salt **2.70** has provided approximately a twenty-fold increase in solubility over the free base after 30 minutes, and therefore it conveys a vastly improved dissolution profile.

Time point	2.70	Large scale batch of 2.67 (Form 2)
30 minutes	1.85 mg/ml	0.09 mg/ml
4 hours	0.70 mg/ml	0.11 mg/ml
24 hours	0.11 mg/ml	0.09 mg/ml

*Table 2.14: The solubility of the mesylate **2.70** and free base **2.67** at 30 minutes, 4 hours, and 24 hours in simulated fasted state fluid (FaSSIF).*

Due to these very encouraging initial data, extensive studies were undertaken to ensure that the mesylate salt **2.70** showed an appropriate physical profile for clinical development. These included solubility studies over time in buffered systems at a variety of pH's, which showed significantly reduced pH dependence on the solubility of the mesylate **2.70** compared with the free base **2.67**.^{2,39} These data, along with polymorph screening to confirm that the issues with multiple crystalline forms of the free base **2.67** were not present in the mesylate **2.70**, led to the selection of the mesylate salt as the salt form of choice for ongoing pre-clinical development activities.

2.7 Conclusions and Future Work

Compound **2.67** is a potent, selective, orally bioavailable inhibitor of the BET family of bromodomains. It shows a comparable profile to the lead pre-clinical candidate **2.01**, and favourable comparison with the criteria set out at the outset of this programme (Section 2.2), as shown below (Figure 2.09).

- | |
|--|
| <ul style="list-style-type: none"> • Human whole blood (HWB) (IL-6 assay) pIC₅₀ > 6.5 <ul style="list-style-type: none"> ○ pIC₅₀ = 6.4 (n = 20) • > 100 times selective over other known bromodomains <ul style="list-style-type: none"> ○ Shows this level of selectivity against an in-house panel of bromodomains, with the exception of a single example showing only 35-fold selectivity. • Oral bioavailability in rat > 20% <ul style="list-style-type: none"> ○ Oral bioavailability in rat = 78% (n = 6). • hERG pIC₅₀ < 4.0 in the <i>in vitro</i> FP assay <ul style="list-style-type: none"> ○ pIC₅₀ = 4.4 (n = 2) • CYP450 IC₅₀ > 3 μM across isoforms <ul style="list-style-type: none"> ○ IC₅₀ > 50 μM across isoforms |
|--|

Figure 2.09: Comparison of the profile of compound **2.67** with the criteria set out by the programme team for the back-up molecule. The required profile is shown in black, the assessment of compound **2.67** is shown underneath in blue.

Compound **2.67** met all the efficacy, pharmacokinetic, and safety criteria as set out within the goals of this programme. The oral bioavailability and CYP450 data were excellent; the bromodomain selectivity was judged to be acceptable for further progression of the molecule. The HWB potency was at an appropriate level, and also slightly greater than that of the lead molecule **2.01** (pIC₅₀ = 6.2). The hERG potency was, however, slightly higher than was set out initially and this was consistent with data seen for the template as a whole. The decision was made to progress with the molecule at risk, and both hERG PatchXpress and rabbit wedge^{2.40} studies were scheduled to better understand whether there was a hERG liability with the compound at the doses we intended to use *in vivo*.

After a wide variety of studies were completed, including *in vivo* safety and efficacy studies, compound **2.67** was chosen as the pre-clinical candidate molecule for the BET back-up

programme, and will be assessed in more comprehensive pre-clinical safety studies. These will guide the future strategy for the progression of this molecule. The issues with low solubility of the parent **2.67**, as well as the multiple crystalline forms present, were mitigated by the selection of the mesylate salt **2.70** for any clinical development work. A patent application was subsequently filed and published to cover compound **2.67**, and its various crystalline and salt forms (Figure 2.10).^{2.41} A scientific publication disclosing the work described within this chapter is also in preparation,^{2.42} and the work has been presented at a scientific conference.^{2.43}



(12) INTERNATIONAL APPLICATION PUBLISHED UNDER THE PATENT COOPERATION TREATY (PCT)		
(19) World Intellectual Property Organization International Bureau		
(43) International Publication Date 21 February 2013 (21.02.2013)		(10) International Publication Number WO 2013/024104 A1
(51) International Patent Classification: C07D 471/04 (2006.01) A61P 29/00 (2006.01) A61K 31/4745 (2006.01) A61P 37/00 (2006.01)		 AO, AT, AU, AZ, BA, BB, BG, BH, BN, BR, BW, BY, BZ, CA, CH, CL, CN, CO, CR, CU, CZ, DE, DK, DM, DO, DZ, EC, EE, EG, ES, FI, GB, GD, GE, GH, GM, GT, HN, HR, HU, ID, IL, IN, IS, JP, KE, KG, KM, KN, KP, KR, KZ, LA, LC, LK, LR, LS, LT, LU, LY, MA, MD, ME, MG, MK, MN, MW, MX, MY, MZ, NA, NG, NI, NO, NZ, OM, PE, PG, PH, PL, PT, QA, RO, RS, RU, RW, SC, SD, SE, SG, SK, SL, SM, ST, SV, SY, TH, TJ, TM, TN, TR, TT, TZ, UA, UG, US, UZ, VC, VN, ZA, ZM, ZW.
(21) International Application Number: PCT/EP2012/065918		
(22) International Filing Date: 15 August 2012 (15.08.2012)		
(25) Filing Language: English		
(26) Publication Language: English		
(30) Priority Data: 1114103.3 17 August 2011 (17.08.2011) GB		
(71) Applicant (for all designated States except US): GLAXO-SMITHKLINE LLC [US/US]; One Franklin Plaza, 200 North 16th Street, Philadelphia, Pennsylvania 19102 (US).		
(72) Inventors; and		
(75) Inventors/Applicants (for US only): DEMONT, Emmanuel, Hubert [FR/GB]; GlaxoSmithKline, Gunnels Wood Road, Stevenage Hertfordshire SG1 2NY (GB). JONES, Katherine, Louise [GB/GB]; GlaxoSmithKline, Gunnels Wood Road, Stevenage Hertfordshire SG1 2NY (GB). WATSON, Robert J [GB/GB]; GlaxoSmithKline, Gunnels Wood Road, Stevenage Hertfordshire SG1 2NY (GB).		
(84) Designated States (unless otherwise indicated, for every kind of regional protection available): ARIPO (BW, GH, GM, KE, LR, LS, MW, MZ, NA, RW, SD, SL, SZ, TZ, UG, ZM, ZW), Eurasian (AM, AZ, BY, KG, KZ, RU, TJ, TM), European (AL, AT, BE, BG, CH, CY, CZ, DE, DK, EE, ES, FI, FR, GB, GR, HR, HU, IE, IS, IT, LT, LU, LV, MC, MK, MT, NL, NO, PL, PT, RO, RS, SE, SI, SK, SM, TR), OAPI (BF, BJ, CF, CG, CI, CM, GA, GN, GQ, GW, ML, MR, NE, SN, TD, TG).		
Declarations under Rule 4.17:		
— as to applicant's entitlement to apply for and be granted a patent (Rule 4.17(ii))		
— as to the applicant's entitlement to claim the priority of the earlier application (Rule 4.17(iii))		
— of inventorship (Rule 4.17(iv))		

Figure 2.10: Screenshot of international patent application filed to cover compound **2.67** and its various crystalline and salt forms.^{2.41}

X-ray crystallography of compound **2.67** bound to the N-terminal bromodomain of BRD4 (Figure 2.11), overlaid with that of tetraacetylated H4 peptide, shows that the molecule binds to the acetylated lysine recognition pocket of BRD4. The heteroatoms of the isoxazole ring make a hydrogen bond to Asn140 as well as to the well-conserved water molecule within the acetyl-lysine recognition pocket. This is consistent with the binding mode seen with numerous other exemplars within this template within our laboratories. This X-ray crystallographic data also confirms the assignment of **2.67** as the *R*-enantiomer.

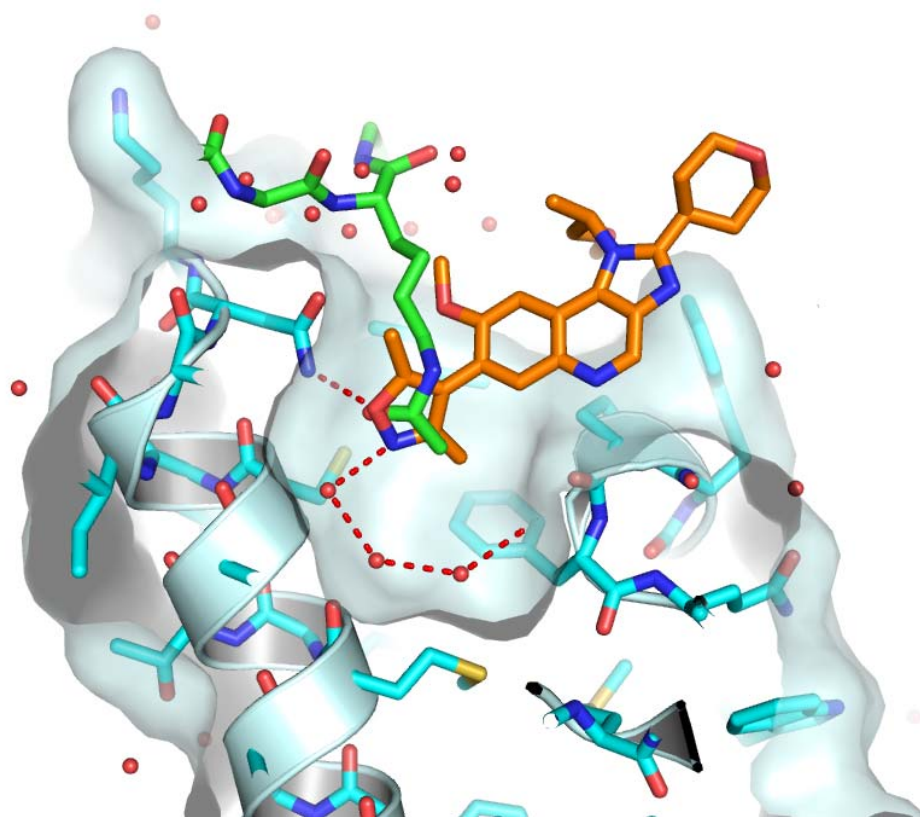


Figure 2.11: X-ray crystal structure of compound 2.67 in a truncated BRD4 N-terminal bromodomain.

With the successful discovery of compound **2.67**, any further medicinal chemistry on the quinoline–isoxazole series, as well as other chemical series within the BET oral backup programme, was discontinued. Compound **2.67**, and its mesylate salt **2.70**, are currently undergoing a wide range of studies designed to support their further progression within our laboratories.

PART III:
ESTERASE SENSITIVE MOTIFS

Chapter 3

Targeting BET Bromodomain Inhibitors to Macrophages Using Esterase-Sensitive Motifs: Background and Preliminary Work

“Thou art to shoot an apple from his head!”

Albrecht Gessler, Wilhelm Tell, Friedrich von Schiller.

Synopsis

As a result of findings in pre-clinical safety studies with a number of pan-BET bromodomain inhibitors, including the pre-clinical back-up molecule **2.67**, novel approaches to increase therapeutic index were under investigation within our laboratories. One of these approaches was the use of esterase-sensitive motifs (ESMs) to target molecules to specific cell types. From a novel chemical series, containing a 3-methylpyridone acetyl lysine mimetic, an ESM-containing BET bromodomain inhibitor was designed and synthesised. This tool molecule was used in *in vitro* proof of concept studies to establish confidence in the use of ESM technology to target BET-bromodomain inhibitors to cells of the monocyte-macrophage lineage.

3.1 Targeted Drug Delivery and Esterase Sensitive Motifs

Traditional drug delivery methods involve distributing the medicine via oral or intravenous administration into the systemic blood circulation. As a consequence, the drug can affect the whole body, rather than only the tissues of interest. The practice of targeted drug delivery encompasses a wide range of strategies used to deliver medication at a higher concentration in some parts of the body relative to others. These methods aim to achieve a greater interaction of the drug with the tissues of interest than with the remainder of the body, thereby reducing the severity of side-effects and increasing the therapeutic index (TI) of the drug. The therapeutic index of a drug molecule is the ratio of the lethal dose to the efficacious dose, therefore a greater TI implies a drug is safer.

One area of targeted drug delivery involves the enclosure of the drug within a macromolecular drug delivery vehicle, such as a liposome^{3.01} or micelle.^{3.02} The drug molecule can be encompassed by a lipid bilayer, and the liposome carries a homing peptide which allows for accumulation in specific pathological areas. Liposomes are currently used as drug delivery vehicles in a number of prescribed medicines, including Visudyne and DaunoXome.^{3.03}

Alternative drug delivery systems can also be designed by the covalent attachment of macromolecules, such as antibodies, to small molecule medicines. Within the oncology area, the concept of the conjugation of antibodies with antitumour activity to potent small-molecule cytotoxic agents to form antibody-drug conjugates (ADCs) is currently being studied in late-stage clinical trials.^{3.04} This strategy aims to use the antibody specificity for tumour cells to deliver the cytotoxic agent to the tumour and enhance the activities of both the antibody and the small molecule agent.

Recently, the use of esterase-sensitive motifs (ESMs) to intracellularly target monocytes and macrophages has been reported in the literature.^{3.05} A pharmacologically active drug molecule, containing an ester, is hydrolysed to a similarly active acid by an enzyme specific to cells of the monocyte and macrophage lineage. The resulting acid is therefore produced only within these cells and, due to its physicochemical properties, that is its low lipophilicity and zwitterionic nature, it has lower permeability through the cell membrane. This leads to a higher concentration of pharmacologically active compound in these cell types compared to other cells within the body.

In the reported example of ESM technology, the pharmacophore of an ESM has been overlaid with that of known small molecule inhibitors of proteins. The ESM pharmacophore was shown to be a benzyl or phenethyl substituted amino ester, such as the cyclopentyl ester of leucine. ESM technology was incorporated into a number of chemotypes, exemplified below (Figure 3.01) by the HDAC inhibitor Vorinostat **3.01**^{3.06} and p38 MAP kinase inhibitor **3.03**.^{3.05}

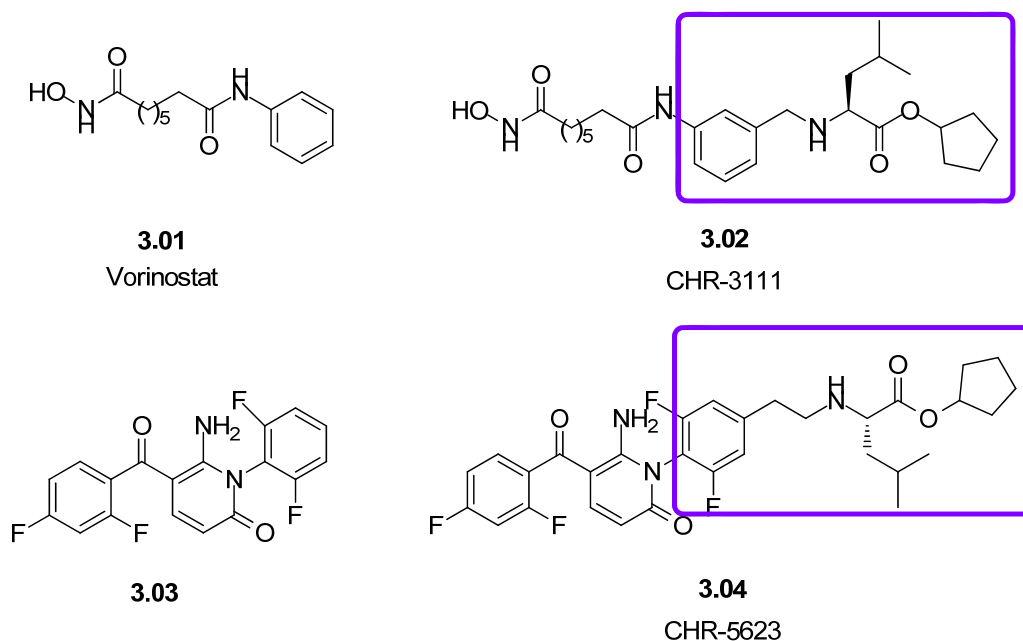


Figure 3.01: Known HDAC inhibitor Vorinostat **3.01**, and CHR-3111 **3.02**, an HDAC inhibitor containing an esterase-sensitive motif (ESM); along with p38 kinase inhibitor **3.03** and its analogue CHR-5623 containing an ESM. The ESM is highlighted in purple.^{3.05}

The development of treatments for autoimmune inflammatory diseases, such as rheumatoid arthritis (RA), is a key objective within our laboratories as this is an area with high unmet medical need. Macrophages have been shown to play a profound role in rheumatoid arthritis,^{3.07} including the production of proinflammatory cytokines such as TNF_α and IL-6, as well as contribution to cartilage and bone destruction. Therefore targeting compounds specifically to macrophages is of great interest in the treatment of RA. As the ESM esters were designed to be selectively cleaved by human carboxyesterase-1 (hCE-1, also known as CES-1), which is expressed in a subset of cell types including monocytes and macrophages,^{3.08} the use of ESM technology in treatments for RA is attractive.

Human carboxyesterase-1 (hCE-1) is a serine hydrolase, and ester hydrolysis by hCE-1 occurs via a two step hydrolysis mechanism (Figure 3.02).

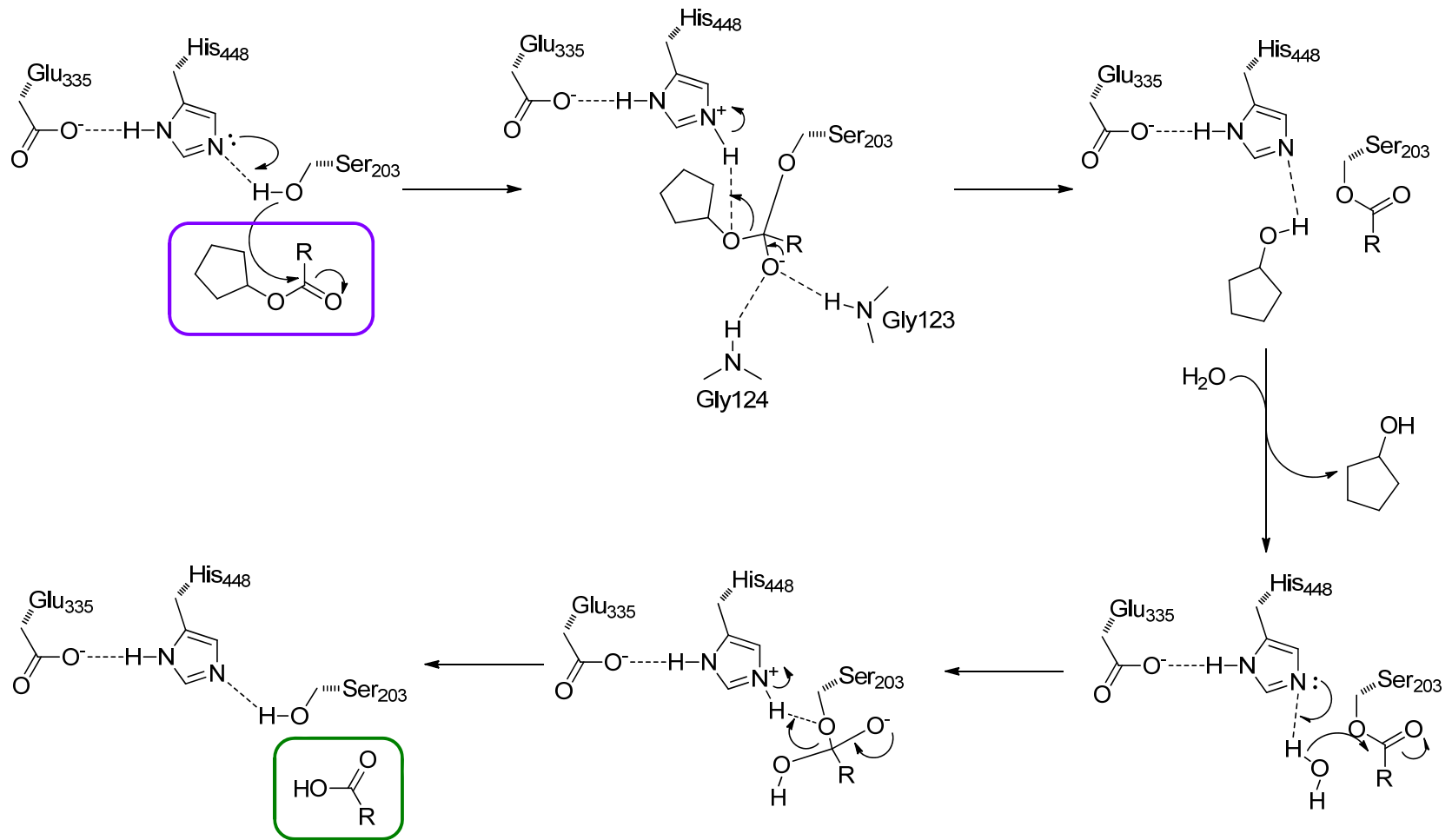


Figure 3.02: The proposed mechanism of hydrolysis of an ESM-containing cyclopentyl ester (purple box) to an acid (green box) by hCE-1.^{3,09}

Firstly, the ESM-containing ester acetylates Ser203, which has been activated by a neighbouring His448, releasing cyclopentanol. The tetrahedral intermediate is stabilised by hydrogen bonds from His448, Gly123 and Gly124. A water molecule then substitutes for the leaving alcohol, which leads to production of the acid hydrolysis product via a similar tetrahedral intermediate.

The theoretical proposal that ESM-containing esters are selectively hydrolysed by hCE-1 is supported by promising *in vitro* data.^{3,05} The ester in compound **3.02** was shown to be hydrolysed only in hCE-1 expressing cells to a pharmacologically active acid. This acid would be expected to be, from its physicochemical properties, poorly membrane permeable. It was therefore hypothesised that the acid could be retained within these cells (Figure 3.03).

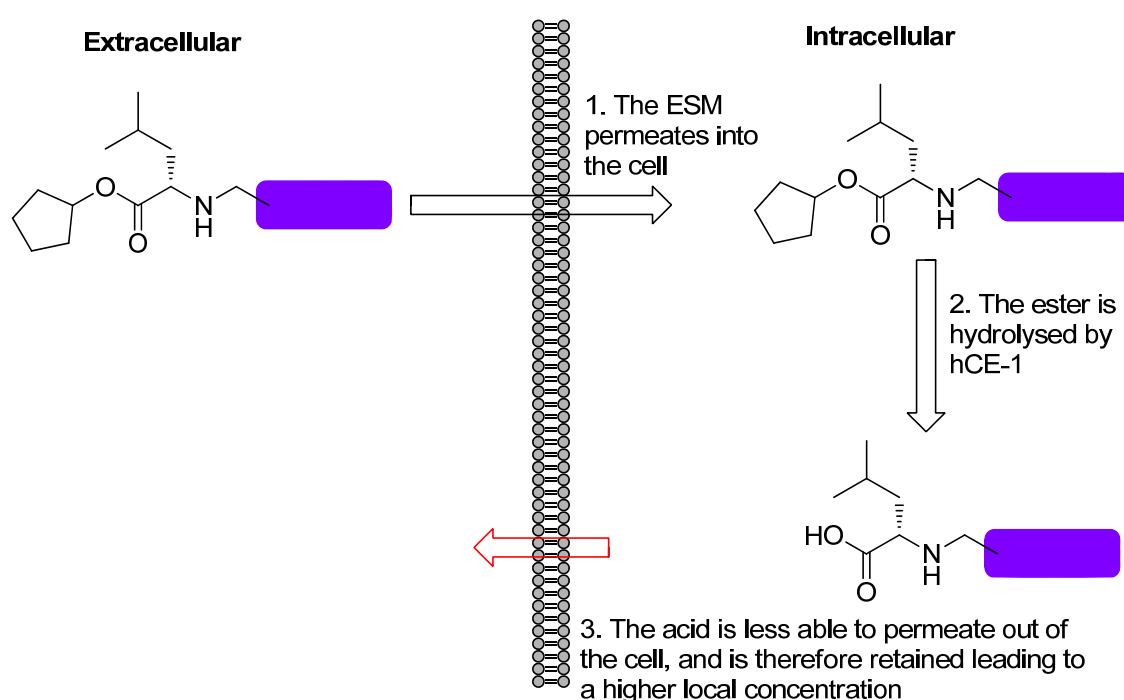


Figure 3.03: A cartoon showing the process by which an ESM-containing compound is hydrolysed within cells containing hCE-1 to an acid which is retained within the cell.

The ESM-containing compound is proposed to permeate into all cell types across the cell membrane. Once within cells where hCE-1 is present, the molecule is hydrolysed to the corresponding acid. The reduced permeability of the acid leads to its retention within these cells. Therefore, cells with hCE-1 present would have a higher local concentration of active compound than cells without hCE-1 present. This would produce a positive physiological effect at a lower systemic concentration of the ESM-containing compound than a traditional small

molecule drug, and therefore would potentially increase the therapeutic window. The use of ESMs to target small molecules to specific cells is therefore applicable in cases where the standard small molecule treatment cannot be progressed due to a low therapeutic index.

Since the outset of these PhD studies, it has been reported that a successful phase I first time in human study in oncology patients has been performed with a monocyte/macrophage targeted HDAC inhibitor which uses ESM technology.^{3,10} Early signs of efficacy and the absence of significant toxicity support the use of ESM technology in patients. In addition to this reported study, a second ESM-containing HDAC inhibitor is being progressed towards human clinical development in the chronic inflammatory disease area,^{3,11} a first for such epigenetic modulators of disease.

3.2 Aims of Esterase-Sensitive Motif Programme of Work

As has been seen for non-targeted HDAC inhibitors, current pan-BET bromodomain inhibitors, such as the pre-clinical lead molecule **2.67** described in Chapter 2, are predicted to have a low therapeutic index (TI) as a result of toxicology seen in pre-clinical safety studies. The toxicology seen has been attributed to on-target BET-bromodomain inhibition. Within our laboratories, approaches for targeting BET inhibitors to specific cell types are therefore being explored. This strategy aims to reduce systemic exposure, and therefore increase the TI, in the event that a lack of tolerability to BET-bromodomain inhibitors precludes traditional dosing to efficacious levels *in vivo* in humans.

The use of esterase-sensitive motifs (ESMs) to target bioactive molecules to monocytes and macrophages has the potential value of inhibiting the action of BET bromodomains in chronic inflammatory disease.^{3,12} The application of ESM technology to BET-bromodomain inhibitors is therefore of interest, with a view to the development of drugs for use in inflammatory diseases. Although ESM technology has been applied to multiple protein targets, there are no examples of its successful application in the bromodomain area. Our priority was to establish a proof of concept which would provide confidence that ESM technology is applicable to BET-bromodomain inhibitors. To do this, the aim was to produce a tool molecule with the profile shown below (Figure 3.04).

- The ESM is incorporated with minimal effect on BET-bromodomain activity in biochemical assays.
- The ester of the ESM is hydrolysed to the acid within macrophages, which express hCE-1.
- The acid is retained within the cell over a time-course of six hours.

Figure 3.04: The desired profile of an in vitro tool molecule to study the proof of concept of ESM technology within the BET bromodomain area.

This chapter describes a programme of work to establish whether an ESM can be incorporated within a recently identified ‘dimethylphenol’ series with minimal impact on BET-bromodomain activity in biochemical assays. If successful, the further aim was to conclude whether ESM-containing compounds within this series are hydrolysed to the acid within macrophages, and whether the acid concentration within the cell increases with time.

3.3 Current Status of Dimethylphenol Series

Compound **3.05** (Table 3.01) was identified as a potent BET-bromodomain inhibitor using encoded library technology (ELT) (Section 1.4.2). This compound showed good potency for BRD4-BD1, and was 100-fold selective for BRD4-BD1 over BRD4-BD2. The lack of activity for BRD4-BD2 was not a concern as it has been shown within our laboratories (data not shown) that BD1-selective compounds maintain a strong macrophage phenotype.

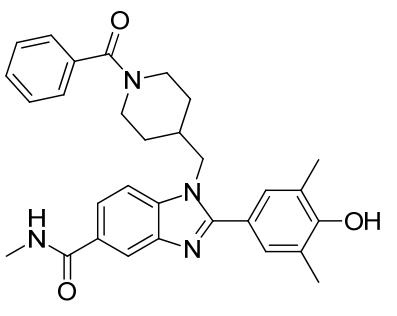
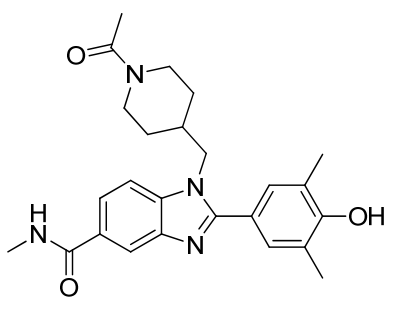
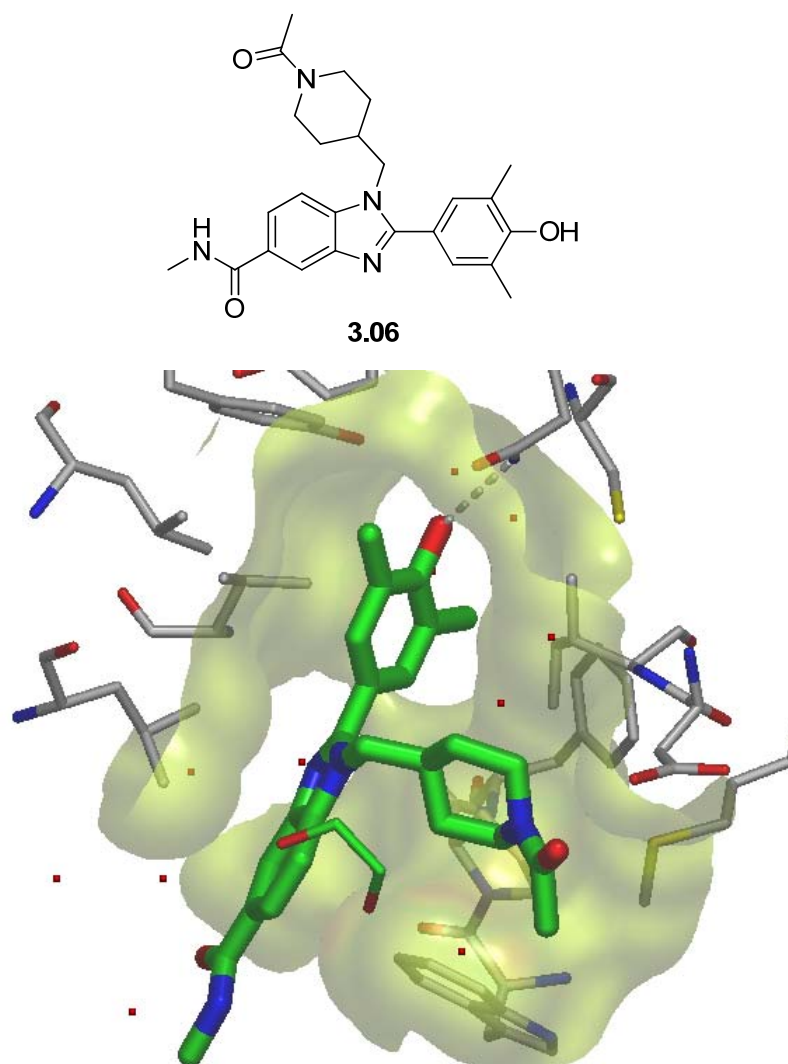
Structure		
Compound	3.05	3.06
mwt, #Ar	496, 4	435, 3
clogP	4.4	2.6
mChromlogD_{pH7.4}	3.2	2.0
BRD4-BD1 pIC₅₀ (n)	6.9 (2)	6.6 (2)
BRD4-BD2 pIC₅₀ (n)	4.9 (2)	4.7 (2)
CLND solubility (μM)	191	≥ 400

Table 3.01: Profiles of the initial hit molecule **3.05** identified by ELT, and of the subsequent lead **3.06**. The BRD4-BD1 and BD2 activity are measured in an FP assay. The solubility is assessed by CLND^{A6}. The molecular weight (mwt), number of aromatic rings (#Ar), clogP^{B1} and mChromlogD_{pH7.4} are also shown. Both compounds are TFA salts.

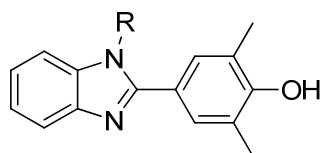
Initial medicinal chemistry carried out elsewhere within our laboratories^{3,13} focussed on bringing the series into a more lead-like physicochemical space. This led to the identification of compound **3.06** (Table 3.01). This compound maintains a similar potency and selectivity profile, whilst having significantly lower lipophilicity and a reduced aromatic ring count.

The DNA attachment point used in the ELT library was through the benzimidazole 5-amide of compound **3.05**, and the dimethylphenol was shown by X-ray crystallography of compound **3.06** to be the acetyl lysine mimetic (Figure 3.05).



*Figure 3.05: X-ray crystal structure of compound **3.06** bound to the first bromodomain of BRD4. Key protein residues are shown in grey, the protein surface in light green, and the hydrogen bonding interaction between the phenol of **3.06** and Asn140 with a grey dotted line.*

Prior to the commencement of this programme of work, a small number of changes had also been made to the benzimidazole *N*-substituent to investigate the SAR in this position.^{3,14} The key findings of this work are summarised below (Table 3.02). The compounds shown include only those where the benzimidazole *N*-substituent is not aromatic, as this provides starting-points for further medicinal chemistry in a more desirable physicochemical space.



	R	BRD4-BD1 pIC₅₀ (n)	clogP / mChromlogD_{pH7.4}	LLE
3.07	Me	4.8 (2)	4.1 / 4.1	0.7
3.08		6.5 (2)	6.1 / 6.5	0.4
3.09		5.9 (4)	3.7 / 1.2	2.2
3.10		5.6 (4)	4.3 / 1.4	1.3
3.11		5.7 (4)	3.8 / 1.0	1.9
3.12		6.1 (4)	4.2 / 1.6	1.9
3.13		4.8 (3)	3.2 / 1.1	1.6

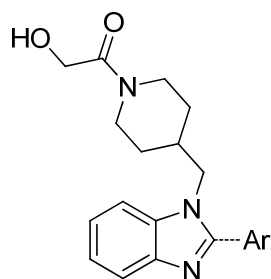
Table 3.02: Summary of the BRD4 potency and physicochemical data generated to investigate the SAR of the benzimidazole *N*-substituent. The BRD4-BD1 data is measured using a FRET assay.⁴⁸ Compound **3.07** is the HCl salt, compounds **3.07–3.13** are the bis-HCl salts.

The data shown above (Table 3.02) indicates that increasing the benzimidazole *N*-substituent in size from methyl to cyclohexyl (**3.07** vs. **3.08**) increases the potency at BRD4-BD1 approximately 100-fold, but has a small negative impact on the LLE. Introduction of a 4-nitrogen atom into the cyclohexyl ring (**3.08** vs. **3.09**) leads to a slight decrease in potency, but in this instance the LLE is significantly increased. Comparison of compounds **3.09** and **3.10** shows that where the ring is attached directly, rather than via a methylene linker, the potency is similar but the LLE is significantly higher. The potency of compounds **3.10** to **3.12** indicate that

reducing the heterocyclic ring size leads to a reduction in LLE. This may be due to the basic centre being placed in a less favourable position within the protein. By considering the LLE, the directly-linked piperidine of compound **3.09** was identified as the optimum substituent of those synthesised to be used when the ESM pharmacophore is incorporated.

Further SAR generated within this series^{3.14} showed the potential for replacing the dimethylphenol acetyl lysine mimetic with a pyridone without a significant loss in potency (Table 3.03). This was important for the future utility of this chemical series as the dimethylphenol group would be expected to contribute to a high *in vivo* clearance of these compounds. This was the case in the single analogue, **3.06**, whose PK had been evaluated *in vivo* in this series. This compound had a very high blood clearance in mouse of 346 ml/min/kg after intravenous infusion, which is nearly four times liver blood flow.^{3.15} This indicated that other mechanisms of clearance, such as renal clearance, were also occurring.

The biochemical data generated shows that the 1,3-dimethylphenol of compound **3.14** can be replaced by the dimethylpyridone of compound **3.15** with a small increase in potency. Pleasingly, a greater than 100-fold increase in LLE is seen when this structural change is made. Removal of the *N*-methyl of compound **3.15** to give **3.16** led to a reduction in potency, but a similar LLE, which makes both the *N*-H and *N*-methyl pyridones an attractive starting point for compounds where an ESM is to be incorporated. Removal of the 3-methyl substituent of the pyridone in compounds **3.17** and **3.18** showed a lower potency, and LLE, than compounds **3.15** and **3.16**, which indicated the former were not attractive options for further optimisation.



	Ar	BRD4-BD1 pIC ₅₀ (n)	clogP / mChromlogD _{pH7.4}	LLE
3.14		6.2 (2)	3.6 / N/A	2.6
3.15		6.6 (4)	1.6 / 1.8	5.0
3.16		5.8 (6)	1.1 / 1.7	4.7
3.17		5.0 (2)	1.1 / N/A	3.9
3.18		< 4.3 (3), <4.8 (1)	0.6 / 1.1	N/A

Table 3.03: Biochemical and physicochemical data generated on replacing the dimethylphenol with substituted pyridones. The BRD4-BD1 data is measured using a FRET assay.^{A8} Compounds **3.15** and **3.16** are hydrochloride salts.

X-ray crystallography of compound **3.16** established that the 3-methylpyridone bound in the acetyl lysine pocket of BRD4-BD1, and the overlay with the crystal structure of compound **3.06** verified that the binding mode was not altered on changing from the dimethylphenol to the 3-methylpyridone acetyl lysine mimetic (Figure 3.06).

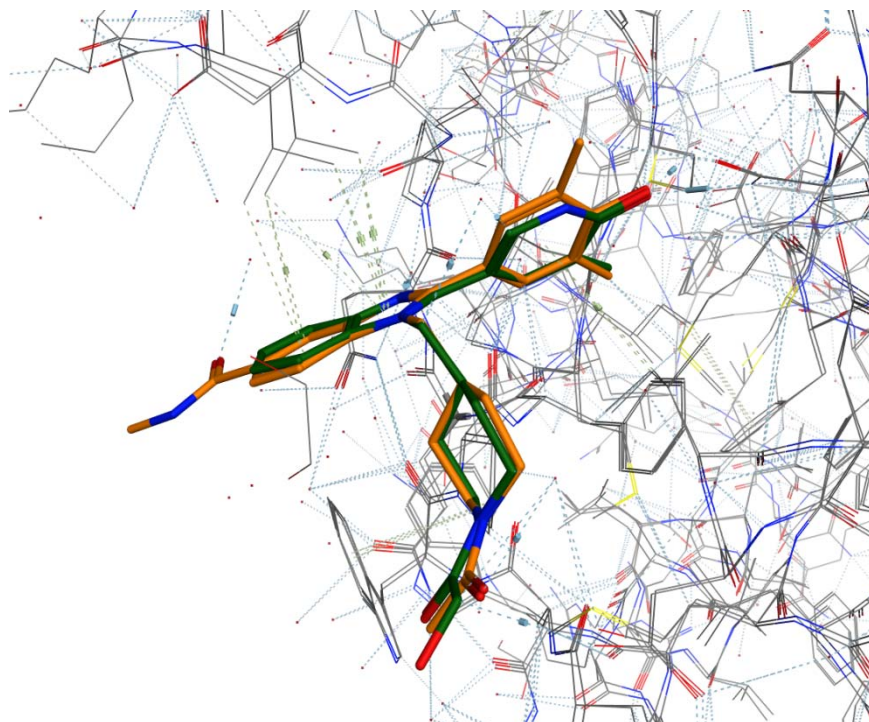
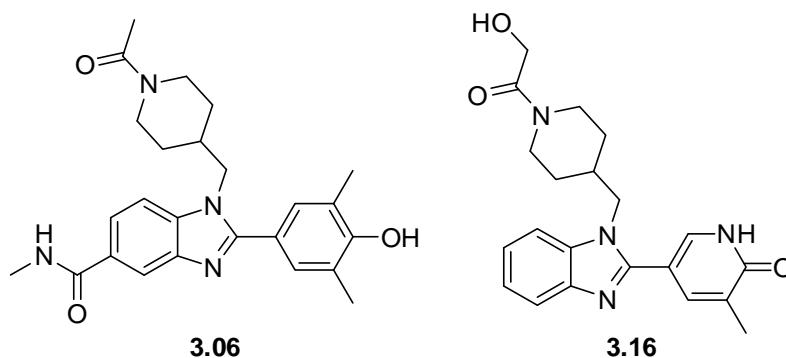


Figure 3.06: The overlaid X-ray crystal structures of compound 3.06 (orange) and compound 3.16 (dark green) bound into the first bromodomain of BRD4. The protein structures are shown in light grey. The chemical structures are shown above the figure.

Thorough analysis of the data presented above, as well as inspection of the X-ray crystal structure, gave sufficient confidence that this chemical series was a good candidate for optimisation and incorporation of an ESM. The key medicinal chemistry challenge was to achieve ESM incorporation whilst designing BET-ESM compounds within a good physicochemical space, and retaining sufficient BRD4-BD1 potency.

3.4 Incorporation of an ESM within a BET Chemotype

To perform experiments to understand the applicability of ESM technology within BET-bromodomain inhibitors, an initial ESM-containing BET bromodomain inhibitor was designed for use in initial *in vitro* studies. This section describes the design and synthesis of this compound, and the data subsequently generated.

3.4.1 Design of Initial ESM-containing Compounds

The key aim of the initial medicinal chemistry strategy was to establish whether an ESM could be incorporated within the pyridone template identified above whilst maintaining BET potency. As the pyridone template was identified using ELT (Section 1.4.2), the DNA-attachment point provided a vector where large groups are known to be tolerated without being deleterious to potency. In this chemical series, the DNA attachment point was the benzimidazole 5-position.

It was also understood, using examples within the literature,^{3,05} that the hCE-1 protein tolerates the ESM motif attached via a methylene linker to an aromatic ring system (Section 3.1, Figure 3.01, Compound **3.02**). As a result of these observations, the compounds below (Figure 3.07) were designed, with an established ESM attached to the 5-position of the benzimidazole ring.

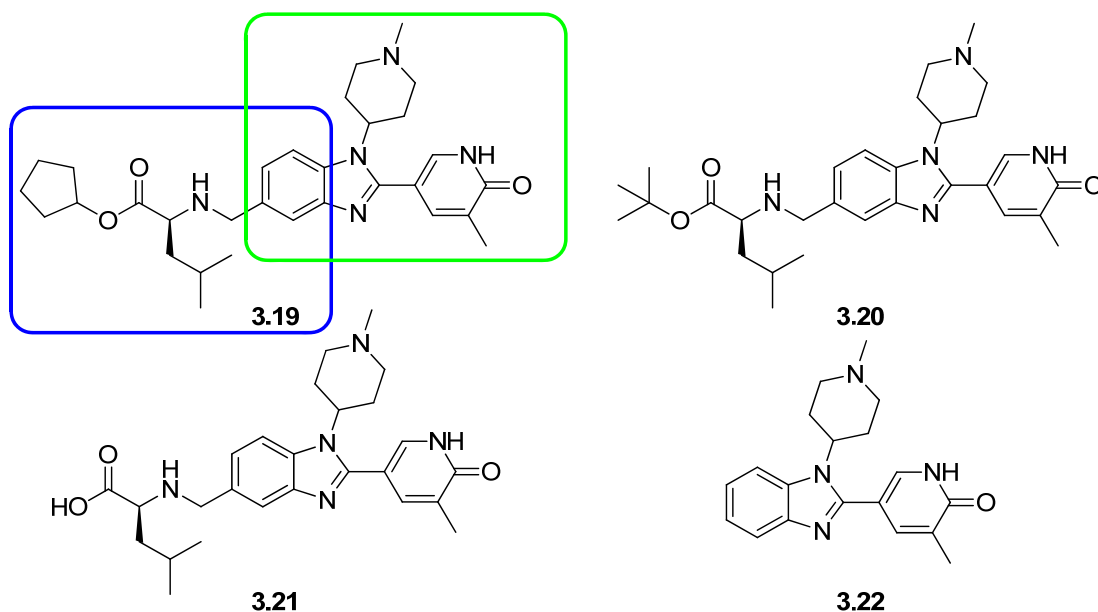


Figure 3.07: Compounds designed to establish whether an ESM could be incorporated into a compound from the pyridone series, and the comparator compound **3.22** without ESM. On compound **3.19** the BET inhibitor portion is highlighted in green and the ESM in blue.

The 3-methylpyridone of **3.16** was selected as the acetyl lysine mimetic due to its high LLE and low clogP (Table 3.03). The directly linked *N*-methylpiperidine benzimidazole substituent was inspired by compound **3.09** (Table 3.02) as the most potent and efficient substituent made in this position. Prior to initiation of the synthesis of compounds **3.19** to **3.21**, compound **3.22** would be synthesised to confirm baseline BRD4-BD1 potency without the ESM attached.

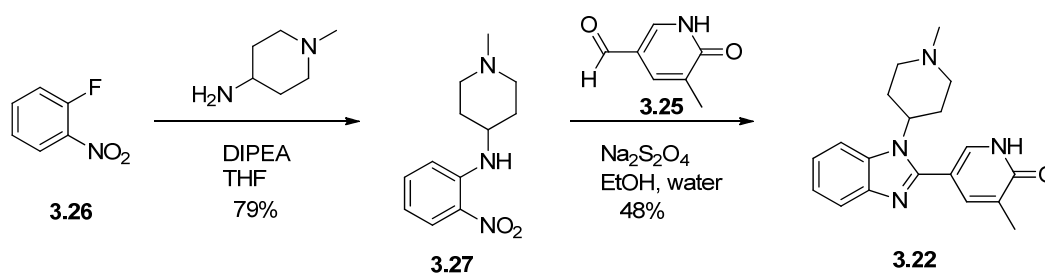
The cyclopentyl leucine ester **3.19** was designed as the ESM-containing tool molecule, as this would be expected to convey hCE-1 selective cleavage in our *in vitro* macrophage studies, and as examples of non-BET chemotypes using this ESM have already been studied.^{3.05} The *tert*-butyl leucine ester **3.20** was designed as a control compound which would not be expected to be hydrolysed by hCE-1. The acid **3.21** is the intended product of hCE-1 hydrolysis, and therefore required synthesis to enable the biochemical potency of the hydrolysis product to be determined.

To enable the ESM technology to be successful, high membrane permeability of the ester was required to allow the compound to be present within macrophages. However, after ester hydrolysis, an acid with low permeability was required to drive retention of the acid within the cell. To ensure compounds **3.19** and **3.21** met these criteria, their *in silico* profiles were generated and compared with the desired profile for these compounds (Table 3.04).

	Desired ester	Desired acid	3.19	3.21
cChromlogD_{pH7.4}	≤ 4	≤ 0	4.1	-0.7
Passive permeability	Medium/high	Low	Medium	Low

Table 3.04: Summary of the predicted physicochemical parameters of compounds **3.19** and **3.20**, and comparison with a desired ester and acid profile. The calculated ChromlogD_{pH7.4}^{B2} and the predicted passive permeability at pH7.4^{B3} are shown.

The ESM-containing ester **3.19** was predicted to have medium passive permeability,^{B3} and the calculated lipophilicity^{B2} was within a reasonable drug-like space.^{3.16} The acid hydrolysis product **3.21** was predicted to have low passive permeability, which is presumably driven by its low lipophilicity and ionic character. In combination these are hypothesised to cause cellular penetration of the ester, followed by cellular retention of the acid.



Scheme 3.02: Preparation of parent benzimidazole compound **3.22**.

The commercially available 1-fluoro-2-nitrobenzene **3.26** was reacted with 1-methylpiperidin-4-amine in an $\text{S}_{\text{N}}\text{Ar}$ reaction to give intermediate **3.27** in 79% yield. The intermediate **3.27** was reacted with aldehyde **3.25** in a reductive cyclisation using sodium hydrosulfite. The product **3.22** was isolated in 48% yield.

The key one-pot benzimidazole ring forming reaction is proposed to proceed via the mechanism below (Figure 3.08).

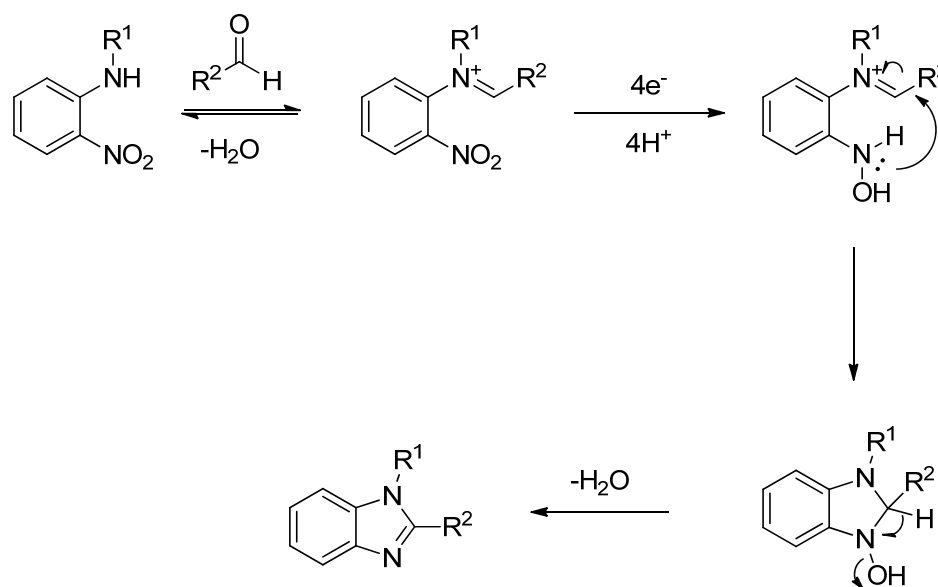


Figure 3.08: Proposed mechanism for the benzimidazole ring formation via an in situ nitro group reduction using sodium hydrosulfite reduction.^{3.17}

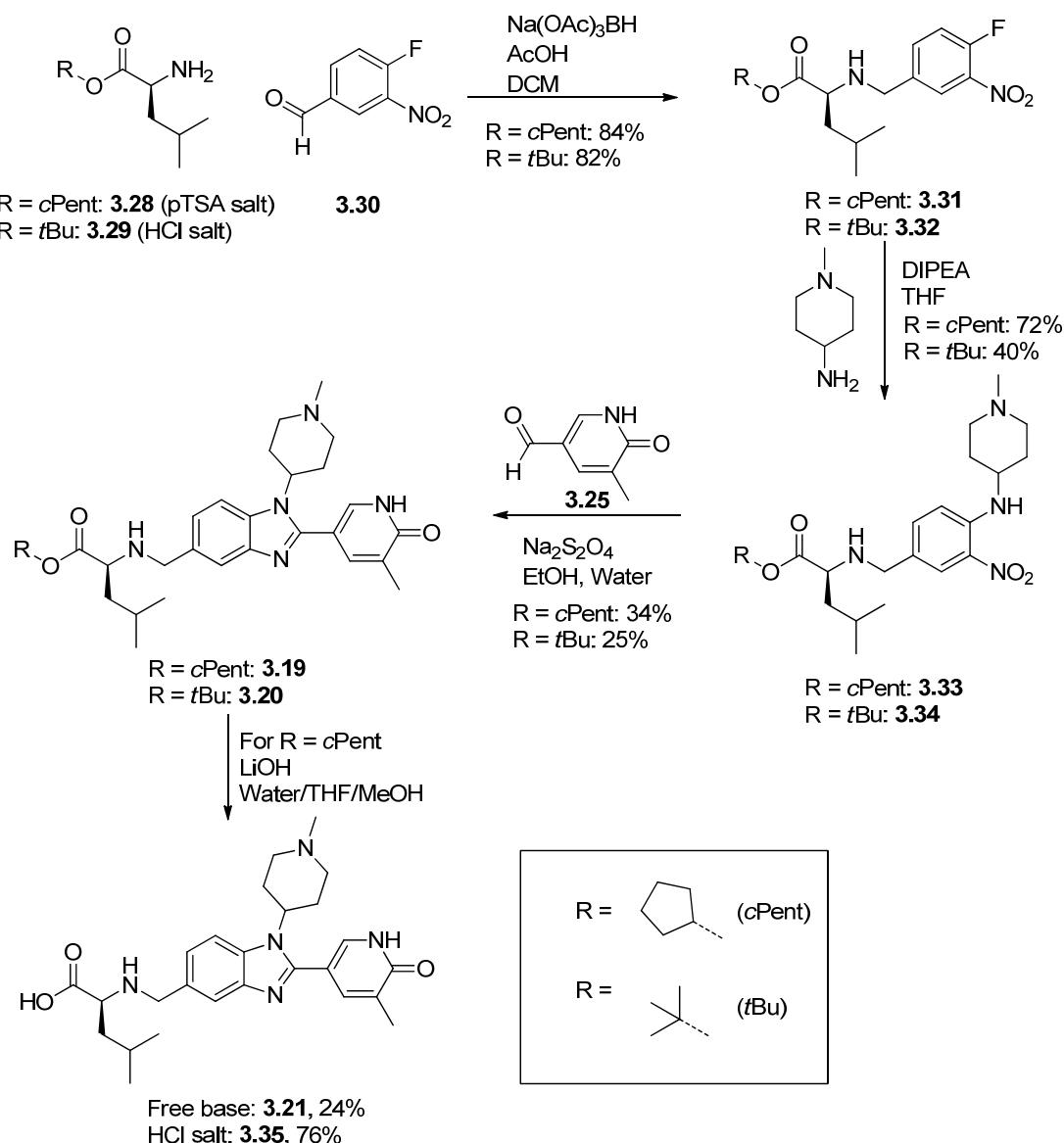
Firstly, an iminium species is formed between the aldehyde and the *N*-methyl aryl amine, followed by the four electron reduction of the nitro group to a hydroxylamine. Intramolecular reaction to form the benzimidazoline, followed by dehydration, would account for the formation

of the benzimidazole product. This reaction is an efficient method of benzimidazole formation as it is performed in one step and without the need for protecting groups.

3.4.2.3 Synthesis of ESM-containing Compounds

The synthetic route to the ESM-containing compounds within the benzimidazole series was designed based on that used to synthesise the parent molecule **3.22** (Scheme 3.02). The relevant ESM group was incorporated in the initial step, and then taken through the synthesis, to give the final compounds **3.19** to **3.21** (Scheme 3.03).

The cyclopentyl amino acid ester **3.28** was synthesised from *L*-leucine,^{3,07} and the *tert*-butyl amino acid ester **3.29** was commercially available. These were reacted with the commercially available aldehyde **3.30** under standard reductive amination conditions. The products **3.31** and **3.32** were isolated in 84% and 82% yields, respectively. Compounds **3.31** and **3.32** were converted by S_NAr chemistry, using microwave heating, to compounds **3.33** and **3.34** in 72% and 40% isolated yields. The lower yield of compound **3.34** was a result of difficulties during purification, rather than the conversion to product being less efficient in this reaction. The amines **3.33** and **3.34** were reacted with aldehyde **3.25** under reductive cyclisation conditions to give benzimidazoles **3.19** and **3.20** in 34% and 25% yield, respectively. There was not one clear impurity seen in the reaction mixture LCMS which would indicate options for reaction optimisation. However, the current yields allowed production of sufficient of the ESM-containing esters **3.19** and **3.20** for biological evaluation. The overall yield to the cyclopentyl ester **3.19** was 21%, and the *tert*-butyl ester **3.20** 8%, in three steps from available intermediates.



Scheme 3.03: Synthesis of ESM-containing compound **3.18** and acid hydrolysis product **3.20**. $\text{R} = \text{cPent}$ is the cyclopentyl substituent, $\text{R} = \text{tBu}$ is the tert-butyl substituent.

The cyclopentyl ester of compound **3.19** was hydrolysed using lithium hydroxide, after heating overnight at 50 °C, to give the acid **3.21** in 24% isolated yield. The low isolated yield was due to the sample coming out of solution during MDAP purification. It was subsequently found that compound **3.21** was not sufficiently soluble to allow determination of potency in the BRD4-BD1 biochemical assay. To enable the determination of the biochemical potency of the acid hydrolysis product **3.19**, it was therefore necessary to synthesise the hydrochloride salt **3.35**. This was done by the addition of hydrochloric acid after purification of the ester hydrolysis mixture. The isolated yield of the formation of **3.35** from cyclopentyl ester **3.19** was 76%.

3.4.3 Biological Results and Analysis

A number of biological assays were run to determine whether the molecules synthesised show that an ESM can be incorporated within the BET-bromodomain pharmacophore (Figure 3.09). The initial aim was to show that the ESM could be incorporated without impacting the BRD4-BD1 potency. Subsequently, the aim was to determine whether the ESM technology allows ester hydrolysis within macrophages, as well as a corresponding increase in concentration of the acid with time.

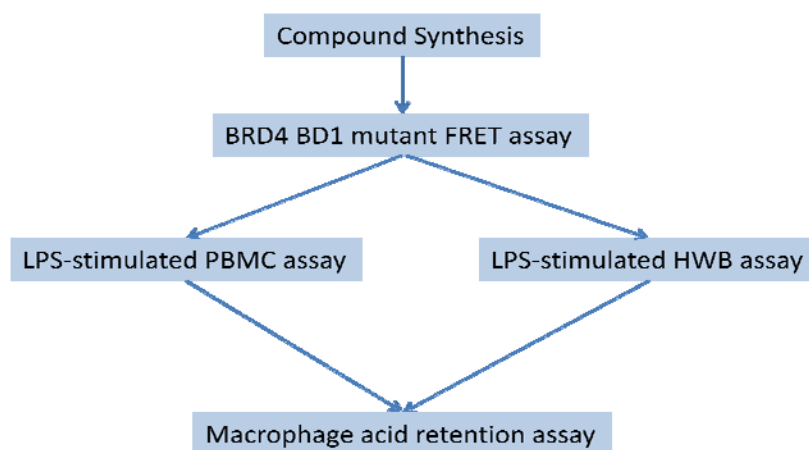


Figure 3.09: Screening cascade displaying the assays used to profile the ESM-containing compounds synthesised in Section 3.4.2.

Initially, the potency of the compounds at the first bromodomain (BD1) of BRD4 was measured using fluorescence resonance energy transfer (FRET) assays.^{A8} This assay measures binding of the compounds to a mutated BRD4 protein, where the mutation prevents binding to the second bromodomain (BD2) of BRD4. The protein–protein interaction is detected through binding of a fluorescently-labelled small molecule BET bromodomain inhibitor. The theoretical tight binding limit^{3,19} of the BRD4-BD1 FRET assay is a pIC₅₀ of 8.3.

If the compounds showed some potency in the biochemical assay, their effect on the production of MCP-1 in LPS-stimulated PBMCs or HWB would be determined. Potency in these cellular assays for ESM-containing esters is not solely a result of biochemical potency, cellular penetration, and (for the HWB assay) extent of protein binding. Intracellular hydrolysis by hCE-1 of the ESM-containing esters to the acids, and reduced permeability of the acid with respect to the ester, may lead to higher localised concentration of the BET-active acid molecules and therefore to an increased level of potency in cellular assays. The protocols for the LPS-

stimulated PBMC^{A5} and HWB^{A1} assays were as described previously in Section 2.5, with the only difference in this case that the effect on MCP-1 was measured rather than IL-6. This was due to a change in assay format which reduced the variability of the data. It was found, by comparison of historical assay data (data not shown), that the MCP-1 readout gave an increase in pIC₅₀ of approximately half a log unit over the IL-6 readout.

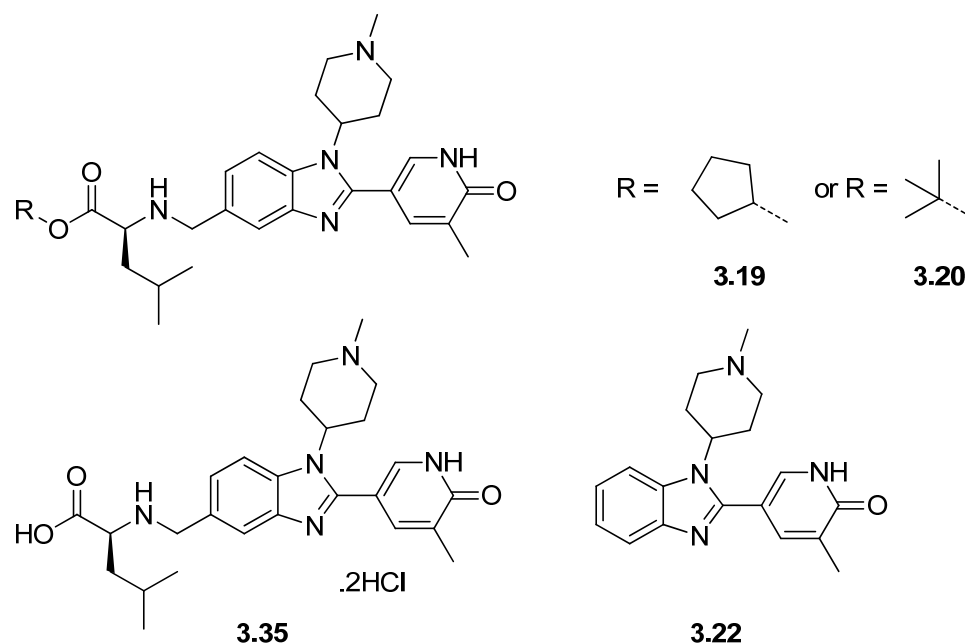
The final biological assay run on the ESM-containing compounds was the macrophage acid retention assay.^{A9} In this assay, the ESM-containing esters were incubated with isolated human M1 macrophages over a time-course of six or 48 hours. The supernatant and the cellular material were separated using centrifugation, and the cells within the cellular fraction lysed. The concentration of both the ESM-ester parent and the acid hydrolysis product were then determined in both the supernatant and the cellular portion by mass spectrometry. This indicates the extent of ester hydrolysis, as well as the amount of acid which is retained within the cell rather than expelled into the supernatant.

3.4.3.1 Primary Screening Data

The data generated in the biochemical and cellular assays for the ESM-containing compounds, as well as the measured lipophilicity, is shown below (Table 3.05).

Both the cyclopentyl and *tert*-butyl esters **3.19** and **3.20** maintained a good level of potency in the BRD4-BD1 biochemical assay. The parent molecule without an ESM attached, compound **3.22**, also has similar biochemical potency. Therefore, as predicted when these ESM-containing compounds were designed, incorporation of the amino acid ester ESM has no significant detrimental effect on biochemical activity.

Pleasingly, the ESM-containing cyclopentyl ester **3.19** had a higher potency in the HWB assay than the non-hydrolysable *tert*-butyl control **3.20**, and the data was consistent on repeated runs of the assay. However, despite this very promising data, we did not have the level of increase from compound **3.20** to **3.19** that we would have liked. Nonetheless, the good biochemical and PBMC potency of compound **3.19** are very encouraging for the potential of this series going forward as they show the pyridone–ESM series is both potent, cell permeable, and likely to be hydrolysed to some extent within the cell.



	BRD4-BD1 pIC ₅₀ (n)	HWB (MCP-1) pIC ₅₀ (n)	mChromlogD _{pH7.4}	cChromlogD _{pH7.4}
3.19	5.3 (7)	5.6 (3), < 6.9 (1)	4.2	4.1
3.20	5.0 (2)	< 5.0 (2)	4.0	3.8
3.35	4.6 (2)	N/A	0.0	-0.7
3.22	5.4 (3)	< 5.0 (4)	0.9	2.2

Table 3.05: Biological assay results for the parent molecule **3.22**, ESM-containing cyclopentyl ester **3.19**, *t*-butyl ester control **3.20**, and acid hydrolysis product **3.35**. Also shown are the measured^{A7} and calculated^{B2} ChromlogD_{pH7.4}.

3.4.3.2 Secondary Screening Data

To determine the level of hydrolysis of the ESM-containing ester **3.19**, the compound was profiled in the macrophage acid retention assay.^{A9} Initially, this assay was run over six hours, and the amount of ESM ester **3.19**, and acid hydrolysis product **3.21**, measured in both the supernatant and cell lysate samples (Figure 3.10).

It can be seen that over the first four hours of the experiment, the ester **3.19** is moving towards a steady state between the extracellular (blue) and intracellular (green) compartments. This indicates that compound **3.19** is able to permeate into the macrophages. The total amount of acid **3.21** within the cell lysate (red) and supernatant (purple) is increasing with time. This

indicates that the acid is being produced, and then permeating out of the cell. The ester was shown to be stable in the extracellular assay media over the time course of this experiment, therefore any acid seen was produced intracellularly within the macrophages.

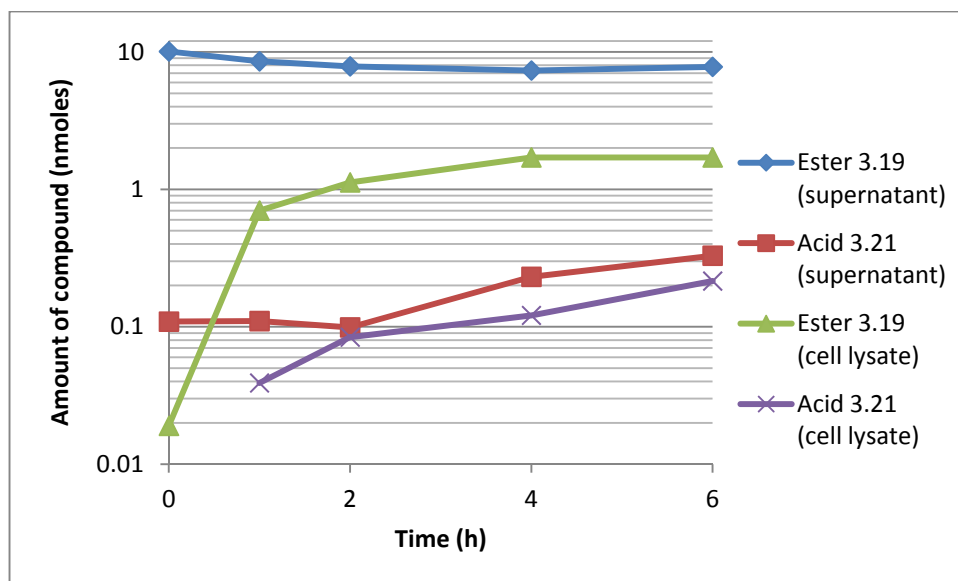


Figure 3.10: The concentration in supernatant and cell lysate of both ester 3.19 and acid 3.21 after incubation of compound 3.19 with M1 macrophages over a time course of six hours.

As the amount of acid 3.20 still appeared to be increasing at the six hour time point, the experiment was repeated over a 48-hour time course (Figure 3.11).

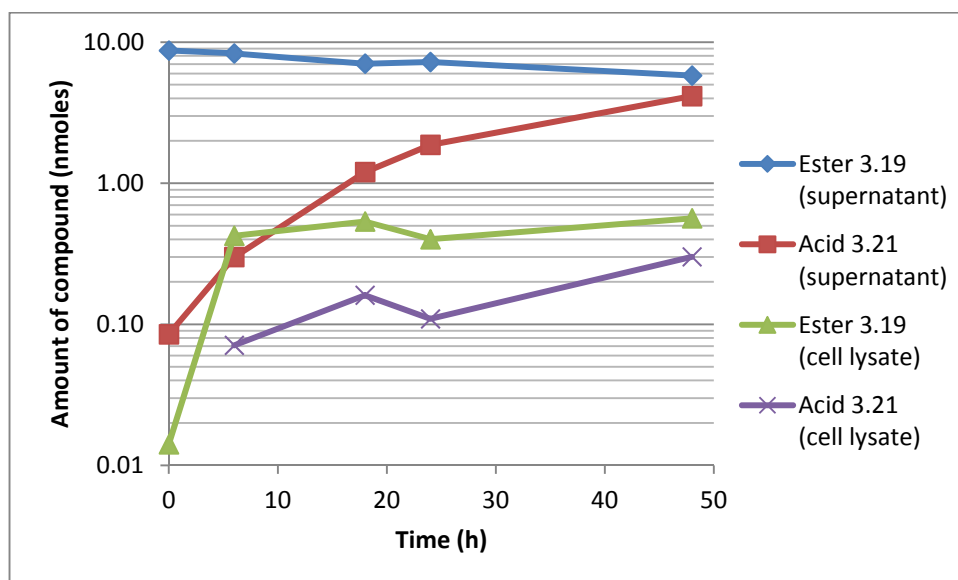


Figure 3.11: The concentration in supernatant and cell lysate of both ester 3.19 and acid 3.21 after incubation of compound 3.19 with M1 macrophages over a time course of 48 hours.

This longer time course shows that ester hydrolysis within the macrophages is still occurring after 48 hours, as the amount of both intracellular and extracellular acid is still being produced at this point. Whilst it is encouraging that the acid is being produced, the rate of hydrolysis is slower than would be desired in a final drug molecule. This is because *in vivo* the ester would be likely to have been cleared from the bloodstream within a few hours after dosing.

To understand the cellular data generated, the rate of hydrolysis of the ESM-containing compound **3.19** was measured in the two isoforms of human carboxyesterase 1, hCE-1b and hCE-1c.^{3.22} The data generated are shown below (Figure 3.12).^{3.23}

Encouragingly, the hCE-1 isoforms found in cells of the monocyte-macrophage lineage both showed reduction in the amount of ester **3.19** present after 45 minutes. These data are very encouraging as they show the compounds are turned over by the desired hCE-1 isoforms. With further optimisation of the molecule there is potential to improve the rate of turnover by the hCE1 enzymes, thereby improving cell specificity.

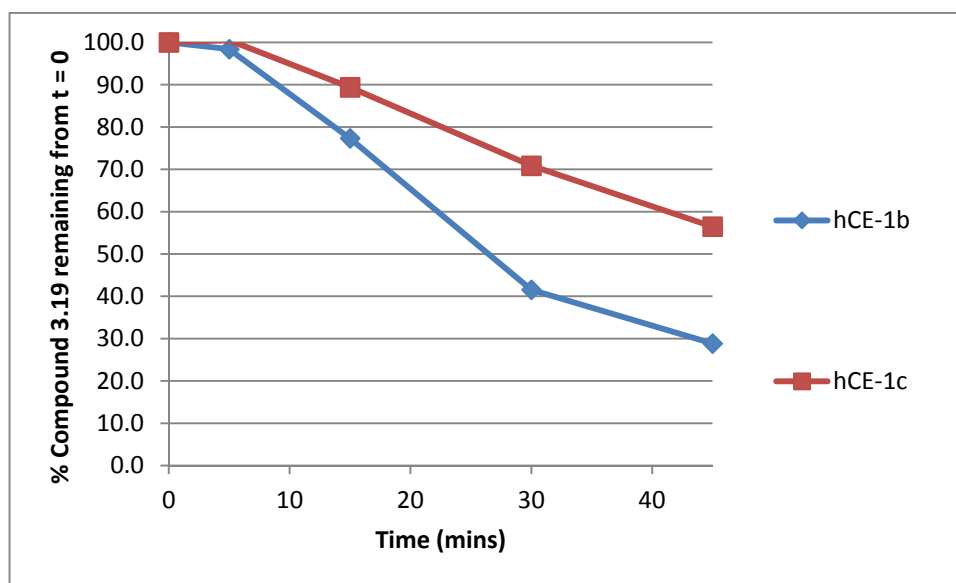


Figure 3.12: The amount of ESM ester **3.19** remaining after incubation with human carboxyesterases hCE-1b and hCE-1c over a 45 minute time course. The data is normalised for the esterase free control samples.

3.5 Summary of Proof of Concept Studies

As a result of the work described, an *in vitro* tool molecule **3.19** was identified, which was used in proof of concept experiments to validate the use of ESM technology within BET bromodomain inhibitors. At the outset of this chapter, there were three criteria identified which would support the use of ESMs within the BET area (Figure 3.04). These criteria have largely been met by the design and synthesis of the ESM-containing compound **3.19**.

Firstly, it has been shown that the ESM portion of the molecule could be appended to the template in such a way that the BET bromodomain activity was retained (Table 3.05). This was achieved using structure-aided design, as well as an understanding of ELT technology. Secondly, incubation of the ESM-containing ester **3.18** in human macrophages indicated that the compound was hydrolysed to the acid within macrophages over at least a 48-hour time course (Figure 3.11). Ideally, the hydrolysis rate would be significantly quicker as by a 48-hour time point *in vivo* the compound would be likely to have been cleared from the bloodstream. The initial data are encouraging in that there is cellular penetration, as well as evidence of hydrolysis by hCE-1. To progress this series, the rate of hydrolysis by hCE-1 would require further investigation.

Thirdly, it was desired to show that the acid hydrolysis product of the ESM-containing compound was being retained within the cell, rather than being excreted either passively or actively. The data generated in the macrophage assay (Figure 3.11) do show an increase in acid levels within cells. However, the acid **3.21** is also seen in the supernatant at a much higher level, indicating that the acid is being excreted from the cell once it is formed from the ester. It is not possible to extrapolate the rate of acid expulsion from the cell from the data generated on compound **3.19**, as the acid is still being formed from the ester at the 48 hour time point. To establish whether ESM-containing compounds within this series could be better retained within the cell would require the design of compounds which are hydrolysed by hCE-1 at a faster rate.

The data generated during the work described within this chapter suggests that the pyridone template is an excellent starting point for designing ESM-containing BET inhibitors. Compound **3.19** has established that an ESM strategy has potential within the BET bromodomain area. The design and synthesis of compound **3.19** has allowed us to show that an ESM can be incorporated into the BET pharmacophore without significant loss of affinity for the BET protein, that compounds containing the ESM were cell penetrant, and that the ester was hydrolysed within human macrophages.

Chapter 4

The Identification of a Molecule to Probe the *in Vitro* Biology of BET Bromodomain Inhibitors Containing an Esterase Sensitive Motif

“You can’t make an omelette without breaking a few eggs.”

Peter Ludwig von der Pahlen

Synopsis

The identification of compound **3.19** as a BET-ESM tool molecule supported initial proof of concept studies which established that ESM technology was applicable to the BET bromodomain area. To better understand whether ESM technology can be used within BET to produce a drug molecule with an increased therapeutic index, an *in vitro* probe molecule was required which had an increased rate of hydrolysis by hCE-1 over compound **3.19**. This chapter describes a programme of work which was undertaken to understand the SAR within the pyridone template, and the subsequent incorporation of ESMs into these compounds. This work led to the identification of an *in vitro* BET-ESM probe molecule, which was used to elucidate BET-ESM biology.

4.1 Criteria for BET–ESM *In Vitro* Probe Molecule

To progress understanding of the viability of using ESM technology to target BET bromodomain inhibitors to macrophages, a suitable *in vitro* probe molecule was required. The initial tool molecule **3.19** was not an appropriate probe molecule, as it was not hydrolysed quickly enough within macrophages and did not show sufficient HWB potency. The criteria required for the *in vitro* probe molecule are shown below (Figure 4.01).

- The ESM is incorporated with minimal effect on BET-bromodomain activity in biochemical assays.
- The pIC₅₀ shift between the biochemical and HWB assays is > 1.
- The ester of the ESM is hydrolysed to the acid within macrophages, but not within cell types negative to hCE-1.
- The acid is retained within the cell over a time-course of six hours.

Figure 4.01: The in vitro probe criteria for a BET–ESM molecule.

The initial BET-ESM tool compound **3.19** (Chapter 3) had established that within the pyridone-benzimidazole template it is possible to incorporate the ESM with minimal effect on BRD4-BD1 potency. Therefore this chemical series was identified as a good starting point for optimisation towards an *in vitro* probe molecule. This chemical series had not been significantly investigated prior to this programme of work, and not at all with the ultimate aim of incorporation of an ESM. To allow a wider range of ESM-containing compounds to be synthesised, it was therefore necessary to first establish a deeper understanding of the SAR within the template. To this end, a range of compounds were designed and synthesised to investigate a number of areas of the template. Initially, compounds were synthesised without the ESM attached to allow a wider variety of changes to be rapidly investigated. However, with the ultimate aim being ESM incorporation, physicochemical profiling was performed on the analogous ESM-containing molecules during medicinal chemistry design.

Initially, two areas of the pyridone-benzimidazole series were selected for investigation as the most likely areas to allow modulation of potency, as well as physicochemical properties. These were the benzimidazole *N*-substituent, and the benzimidazole ring itself. Modulation of the physicochemical properties was identified as important as these would be expected to affect the cell permeability of subsequent BET–ESM acids.

4.2 Medicinal Chemistry Design of Changes to the Benzimidazole Core

A number of changes to the benzimidazole core were designed to establish the contribution of the benzimidazole ring system to BRD4-BD1 potency, as well as to access compounds with a lower lipophilicity. The first changes planned (Table 4.01) involved replacement of the biaryl benzimidazole with monoaryl aromatic and heteroaromatic ring systems. The rationale for these changes was a reduction in aromatic ring count, which correlates with a lower risk of attrition.^{4.01} It was also important, at this early stage in investigation of the template, to increase the knowledge of the SAR around the benzimidazole portion of the molecule. Initially, a number of these mono aryl compounds were synthesised without a ‘WPF-shelf’ group (Section 1.3.2, Figure 1.13) in place. This could be designed in later to any compounds of interest.

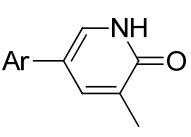
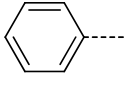
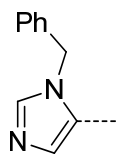
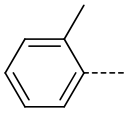
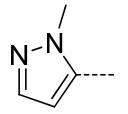
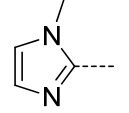
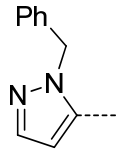
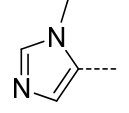
	Ar	cChromlogD _{pH7.4}		Ar	cChromlogD _{pH7.4}
4.01		4.2	4.05		3.5
4.02		4.6	4.06		2.5
4.03		2.3	4.07		4.0
4.04		2.9			

Table 4.01: Replacements of the benzimidazole core with mono-aryl and mono-heteroaryl ring systems. The cChromlogD_{pH7.4}^{B2} is shown.

The simple phenyl compound **4.01** was designed to give an understanding of the baseline potency of a monoaryl system, and the *ortho*-tolyl **4.02** in case a twist in the ring systems is preferred. The 5-membered heterocycle **4.03** was designed to be a direct monoaryl truncate of the benzimidazole core. This compound has a lower lipophilicity than compounds **4.01** and

4.02, and also allows *N*-substitution with the same angle as the benzimidazole *N*-substituent. This would be expected to allow access to the WPF shelf, and therefore gives potential for increasing potency. Compounds **4.04** and **4.06** were designed to investigate alternative nitrogen atom positions. To test the hypothesis of accessing the WPF shelf, compounds **4.05** and **4.07** were included for synthesis as they would be expected to have increased potency over the *N*-methyl compounds.

Once the biochemical profiles of these compounds were established, it would be necessary to investigate whether an ESM could be incorporated within these analogues. Where benzimidazole core changes were successful, analogous compounds containing an ESM would be synthesised, as shown below (Figure 4.02). It would be necessary to identify an appropriate position for substitution onto the aryl ring to allow incorporation of the ESM without loss in BRD4-BD1 potency.

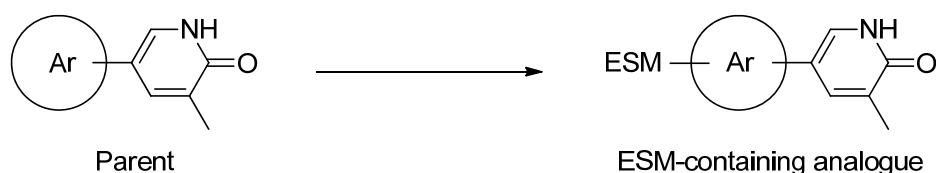


Figure 4.02: Strategy for the introduction of ESM into monoaryl benzimidazole cores.

The second set of changes planned made to the core benzimidazole involved the introduction of additional nitrogen atoms to reduce lipophilicity. Single carbon to nitrogen point changes in all positions, except that where the ESM was attached in compound **3.16**, were considered. For each analogue the predicted physicochemical profiles of the parent, as well as that of the ESM-containing compound and its acid hydrolysis product, were calculated *in silico* (Table 4.02).

Introduction of an additional nitrogen atom into the core is predicted to reduce the lipophilicity by 0.5–0.8 log units in all cases, for both the ESM-containing esters and acids. This translates to a slightly lower predicted passive permeability,^{B3} reflected in some of the non-ESM parent molecules being predicted to have low permeability. Although the ESM-containing acids are predicted to have low passive permeability irrespective of the core, these compounds are of interest in investigating whether reducing the lipophilicity further increases the amount of cellular retention of the acid. The strategy for investigating these core changes was to first synthesise the parent molecules to ascertain the affect of the extra nitrogen atom on BRD4-BD1 potency. If the resulting data were promising, the relevant ESM-containing molecules would then be synthesised.

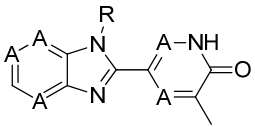
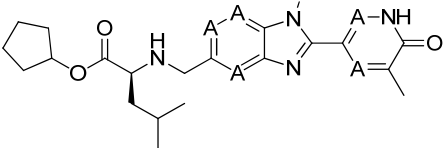
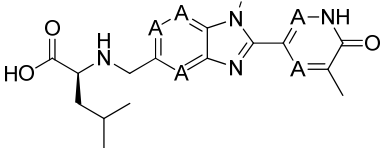
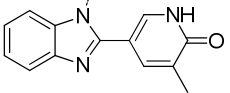
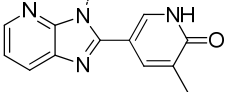
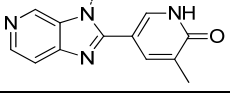
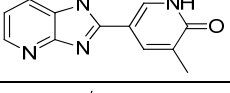
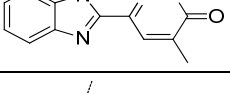
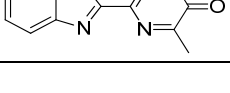
Core Structure	 Parent	 ESM-containing Ester	 ESM-containing acid
 3.22 2.2, Medium	3.19 4.1, Medium	3.21 -0.7, Low	
 4.08 1.4, Low	4.09 3.4, Medium	4.10 -1.4, Low	
 4.11 1.2, Low	4.12 3.3, Medium	4.13 -1.5, Low	
 4.14 1.4, Low	4.15 3.4, Medium	4.16 -1.4, Low	
 4.17 1.7, Medium	4.18 3.6, Medium	4.19 -1.2, Low	
 4.20 1.6, Medium	4.21 3.5, Medium	4.22 -1.3, Low	

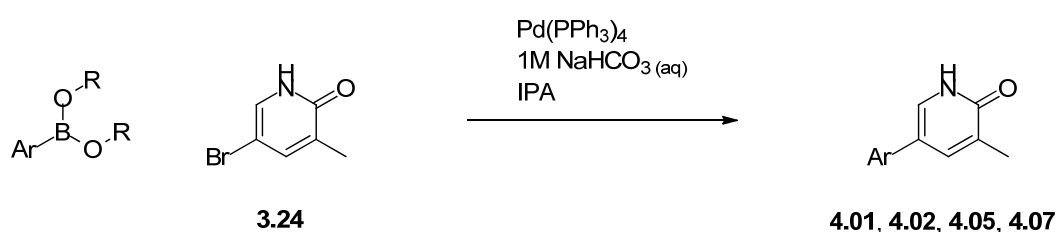
Table 4.02: Comparison of the predicted physicochemical properties of compounds containing single point carbon to nitrogen changes, with the previously synthesised **3.19** and **3.21**. The predicted physicochemical properties of the parent, ESM-containing ester and ESM-containing acid are shown. The calculated $\text{ChromlogD}_{\text{pH}7.4}^{\text{B}2}$ is in blue and predicted passive permeability^{B3} is in green. R is a 4-N-methylpiperidine substituent.

4.3 Synthesis of Compounds with Benzimidazole Core Changes

The compounds designed (Section 4.2) were synthesised in sufficient quantity for biological screening.

4.3.1 Synthesis of Compounds with Benzimidazole Core Replacements

The compounds containing simple mono-aryl benzimidazole replacements **4.01** and **4.02**, as well as the benzyl imidazole **4.05** and benzyl pyrazole **4.07**, were synthesised from the previously described aryl bromide **3.24** (Scheme 3.01). This was done using the commercially available boronic acid or ester, under standard Suzuki coupling conditions (Scheme 4.01).^{4.02}



*Scheme 4.01: Synthesis of biaryl compounds **4.01**, **4.02**, **4.05** and **4.07** using a Suzuki coupling reaction. The aryl boronic acids or esters used are shown in Table 4.03.*

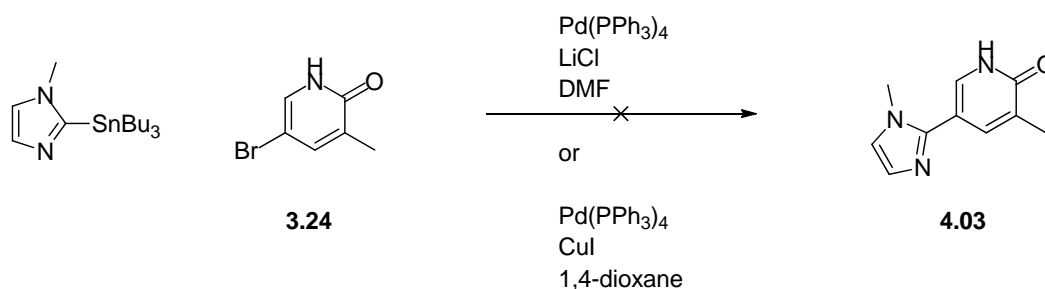
The compounds synthesised using this chemistry, and the isolated yield of the Suzuki coupling reaction, are summarised below (Table 4.03).

	Aryl boronate or boronic acid	Yield		Aryl boronate or boronic acid	Yield
4.01		33%	4.05		6%
4.02		47%	4.07		10%

Table 4.03: Boronic esters or acids used in Scheme 4.01, and isolated yields of the reactions.

The isolated yields of the reactions were low to moderate, and especially poor in the case of the heteroaromatic **4.05** and **4.07**. However, sufficient material was produced for biological screening, therefore the reaction conditions were not optimised further at this stage.

As it was not possible to access the required boronic acid or ester, the synthesis of compound **4.03** was attempted using Stille chemistry, as shown below (Scheme 4.02). Using either lithium chloride^{4.03} or copper iodide^{4.04} as the additive in the Stille reaction led to no evidence of product formation by LCMS after microwave heating.

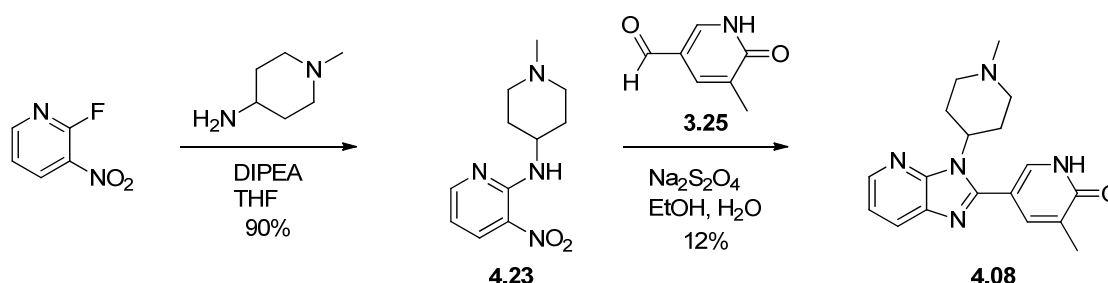


*Scheme 4.02: Attempted synthesis of compound **4.03** using the Stille reaction.*

The decision was subsequently undertaken not to investigate the synthesis of compound **4.03** further, and the syntheses of compounds **4.04** and **4.06** have not been attempted. This is due to data being available for the phenyl examples **4.05** and **4.07**, as well as positive data generated in other areas of this programme of work which led to reprioritisation of targets.

4.3.2 Synthesis of Aza-benzimidazole Templates

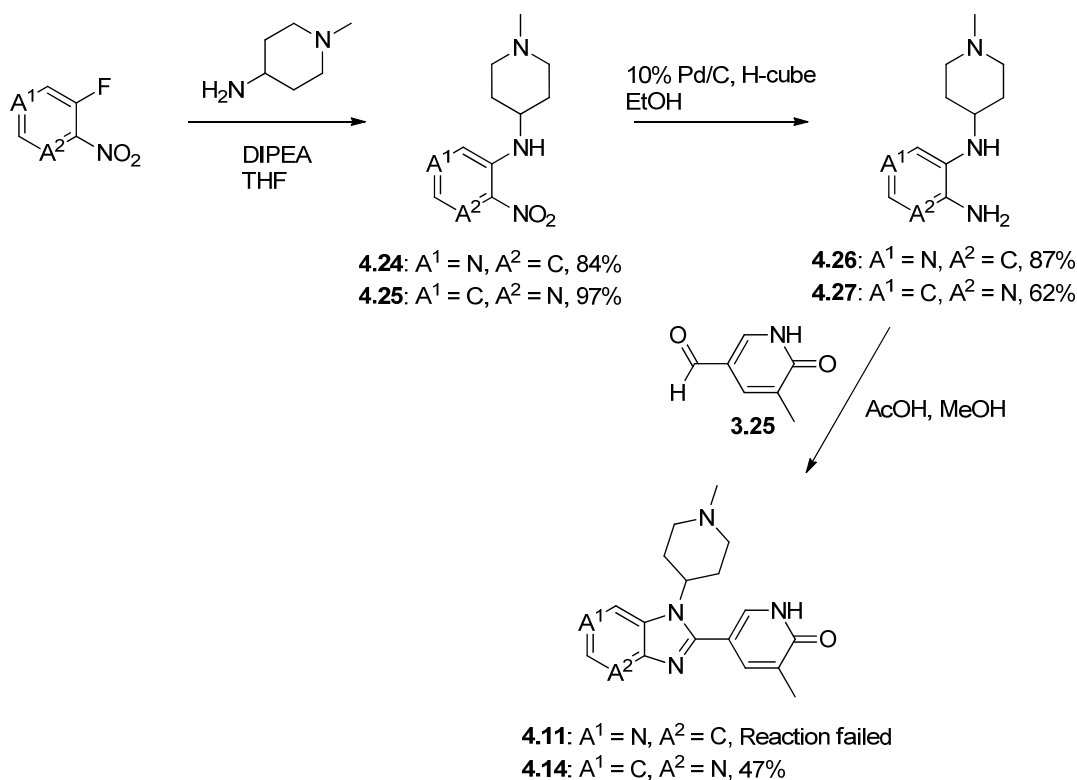
The synthesis of the three azabenzimidazoles **4.08**, **4.11** and **4.14** was initially attempted using the standard reductive cyclisation conditions employed for the benzimidazole exemplar **3.22** (Scheme 3.02). Interestingly, this approach was only successful in the case of compound **4.08** (Scheme 4.03).



*Scheme 4.03: Synthetic route used to prepare azabenzimidazole **4.08**.*

Compound **4.23** was prepared from the commercially available 2-fluoro-3-nitropyridine, under standard S_NAr conditions, in 90% yield. The azabenzimidazole was then synthesised using the pyridone aldehyde **3.25**, via reductive cyclisation, in 12% yield. The introduction of the pyridine nitrogen significantly reduced the yield in comparison to the 48% seen in the case of the analogous phenyl example **3.22** (Scheme 3.02).

To attempt to access compounds **4.11** and **4.14**, an alternative strategy was used, in which the nitro-group reduction was performed prior to the benzimidazole cyclisation (Scheme 4.04).

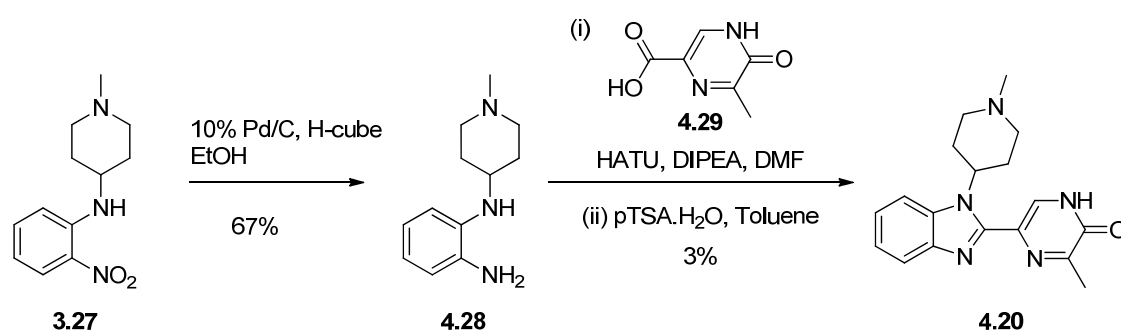


Scheme 4.04: Synthetic route used to prepare azabenzimidazoles **4.11** and **4.14**.

Compounds **4.24** and **4.25** were prepared using S_NAr chemistry from commercially available fluoronitropyridines in 84% and 97% yield, respectively. These were converted to the diamino compounds **4.26** and **4.27** by hydrogenation with 10% palladium on carbon as the catalyst. The hydrogenation was performed using H-cube apparatus,^{4.05} and gave the products in 87% and 62% yield. The bis-arylamines were reacted with the pyridone aldehyde **3.25**, with acetic acid present to aid in formation of the benzimidazole ring system after imine formation.^{4.06} Despite the one-pot reductive cyclisation (Scheme 4.03) having been unsuccessful, this two-step benzimidazole-formation procedure was successful in the synthesis of **4.14**. This was despite

the low nucleophilicity of the pyridyl amine involved in imine formation. The cyclisation proceeded in 47% yield to give compound **4.14**. This gave an overall yield from the fluoronitropyridine for the synthesis of compound **4.14** of 28%. In the case of **4.11**, there was no product formation seen in the benzimidazole cyclisation reaction. Due to the lack of success in other aza-benzimidazoles synthesised in reducing the lipophilicity and retaining potency (Table 4.05), the synthesis of compound **4.11** was not pursued further.

To synthesise the pyrazinone compound **4.20**, the acid **4.29** was used rather than the analogous aldehyde as the acid was commercially available (Scheme 4.05). Therefore, a route was designed analogous to that used successfully in earlier work within this thesis (Scheme 2.11).



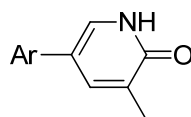
Scheme 4.05: Synthetic route used to prepare pyrazinone **4.20**.

Intermediate **3.27**, which had previously been prepared (Scheme 3.02), was reduced under similar conditions to those used previously (Scheme 4.04) to give bis-aniline **4.28** in 67% isolated yield. Compound **4.28** was subsequently reacted with the commercially available pyrazinone acid **4.29**, using HATU to activate the acid. After isolation, the crude material was cyclised using tosic acid to aid dehydration to give compound **4.20** in 3% isolated yield. The low yield was as a direct result of poor conversion during the cyclisation which appeared to be due to low solubility. Increased reaction time, or use of acetic acid to increase solubility (Section 2, Scheme 2.03), could be applied in future to increase the yield of this reaction.

The final nitrogen-containing compound **4.17** was not readily accessible using any of the synthetic routes described above. This is due to the relevant aldehyde or acid analogue of the pyridazinone portion not being readily available. Due to poor BRD4-BD1 potency seen using the pyridazinone as the acetyl lysine mimetic in a similar chemical series elsewhere within our laboratories,^{4.08} the synthesis of compound **4.17** was not pursued at this stage.

4.4 Primary Data for Compounds with Benzimidazole Core Replacements

The compounds designed to replace the benzimidazole substituent were profiled in the BRD4-BD1 FRET assay,^{A8} and the ChromlogD_{pH7.4} was also measured.^{A7} The data for compounds where the benzimidazole was replaced with a mono-aryl system is shown below (Table 4.04).



	Ar	BRD4-BD1 pIC ₅₀ (n)	mChromlogD _{pH7.4}	cChromlogD _{pH7.4}
4.01		4.8 (2)	2.7	4.2
4.02		4.6 (2)	3.3	4.6
4.05		5.4 (2)	1.7	3.5
4.07		5.8 (2)	2.5	4.0

Table 4.04: Data generated on mono-aryl compounds. Potency at BRD4-BD1 was assessed using a FRET assay,^{A8} and measured^{A7} and calculated^{B2} ChromlogD_{pH7.4} are shown.

The data generated on compounds **4.01** and **4.02** shows that the benzimidazole ring system can be replaced with a phenyl ring, albeit with some reduction in potency. Comparison of compound **4.02** with the *N*-methylbenzimidazole **4.36** (Table 4.09) indicates that this change results in loss of approximately half a log unit in potency. This observation can be rationalised by the loss of lipophilic surface contact with Leu92 of BRD4-BD1, which is close to the 6-membered aryl of the benzimidazole ring system.

The *N*-benzylimidazole **4.05** and *N*-benzylpyrazole **4.07** showed a good level of activity for BRD4-BD1, which was rationalised by the reduction in potency due to the loss of interaction

with Leu92 being offset by an increase in potency derived from interaction of the phenyl of the benzyl substituent with the WPF shelf. Despite compound **4.05** having the same aromatic ring count, and indeed similar properties, as the *N*-methylbenzimidazole **4.36**, it is potentially of interest for further investigation as it would allow different vectors for ESM incorporation due to the different bond angles in five and six-membered aromatic ring systems. It should be noted in all cases that the calculated $\text{ChromlogD}_{\text{pH}7.4}$ underestimated the measured value significantly.

The compounds with an additional nitrogen atom introduced into the core benzimidazole ring system were also profiled in the BRD4-BD1 FRET assay,^{A8} as well their $\text{ChromlogD}_{\text{pH}7.4}$ being measured,^{A7} to establish the impact of these changes (Table 4.05).

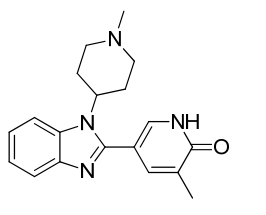
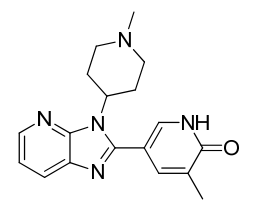
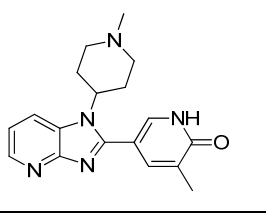
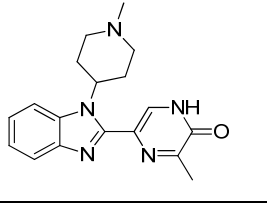
	Structure	BRD4-BD1 pIC_{50} (n)	mChromlogD _{pH7.4}	cChromlogD _{pH7.4}
3.22		5.4 (3)	0.9	2.2
4.08		4.9 (2)	0.6	1.4
4.14		4.4 (1), < 4.3 (1)	0.2	1.4
4.20		4.4 (1), < 4.3 (1)	0.8	1.6

Table 4.05: Data generated on compounds made to assess the impact of introduction of additional nitrogen atoms. Potency at BRD4-BD1 was assessed using a FRET assay.^{A8} Both measured^{A7} and calculated^{B2} $\text{ChromlogD}_{\text{pH}7.4}$ are shown.

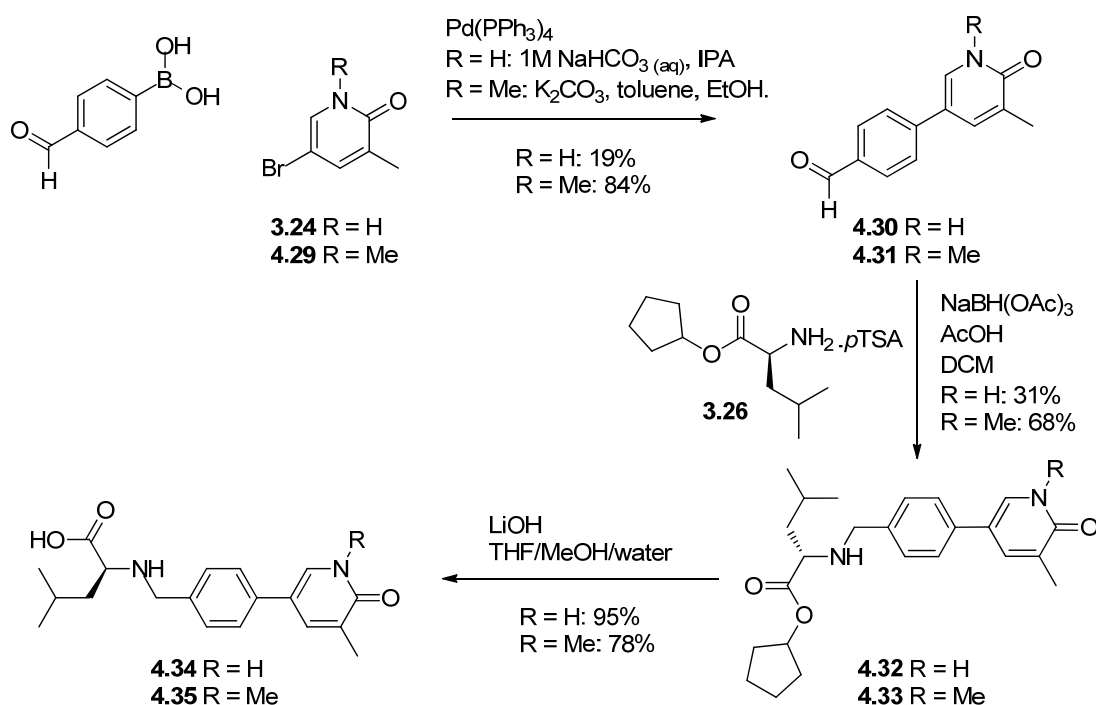
The most potent of the aza-analogues was compound **4.08**, which showed approximately a 0.5 log unit drop in potency over the benzimidazole analogue **3.22**. Unfortunately, there is no significant impact on the measured $\text{ChromlogD}_{\text{pH}7.4}$ on introduction of the heteroatom into any position despite this being predicted *in silico*. This suggests that there were no, or few, azabenzimidazoles in the test set used to build the *in silico* model. Introduction of an additional nitrogen atom into the core of compound **3.22** to give compounds **4.14** and **4.23** led to at least a log unit loss in potency. The incorporation of nitrogen atoms into the benzimidazole core therefore does not appear to give any advantage. It was therefore decided not to incorporate ESMs into the aza-benzimidazole compounds at this stage.

4.5 ESM-containing Compounds with Monoaryl Cores

The phenyl compounds **4.01** and **4.02** maintained sufficient potency at BRD4-BD1 that incorporation of an ESM into this series was initiated as previously described (Section 4.2, Figure 4.02). This was also a desirable structural change due to the corresponding reduction in aromatic ring count over the benzimidazole giving this series better potential for development in the longer term.^{4.01} Due to the *ortho*-methyl of compound **4.02** not conveying any additional potency, the ESM was incorporated into compound **4.01**. The *para*-position of the phenyl ring was selected for ESM incorporation, as it appeared the most likely to place the ESM within the BRD4 protein in a similar position to that of compound **3.19**, where it has already been shown to be tolerated. Due to the relatively low potency of compound **4.01**, the ESM-containing compound was also synthesised with the more potent *N*-methyl pyridone group present (cf. compound **3.15**, Table 3.03).

4.5.1 Synthesis of ESM-containing Compounds with Monoaryl Cores

To synthesise the phenyl ESM analogues based on compound **4.01**, a route was designed (Scheme 4.06) where the aldehyde required for reductive amination of the amino ester was taken through a Suzuki reaction using commercially available starting material.



Scheme 4.06: Synthesis of ESM-containing analogues of the parent molecule **4.01**.

Compound **4.30** was synthesised using Suzuki coupling conditions in an unoptimised 19% isolated yield from the intermediate aryl bromide **3.24** (Scheme 3.01) and the commercially available (4-formylphenyl)boronic acid. Compound **4.31** was also prepared using Suzuki coupling conditions elsewhere within our laboratory.^{4,07} In this case either the non-aqueous Suzuki conditions, or the methylation of the pyridone nitrogen, led to a significantly increased yield of 84%. The aldehydes **4.30** and **4.31** were then reacted with the *L*-leucine cyclopentyl ester **3.26** under standard reductive amination conditions to give the ESM-containing esters **4.32** and **4.33** in 31% and 68% yield, respectively. The esters were subsequently hydrolysed using lithium hydroxide to the acids **4.34** and **4.35** in 95% and 78% yield.

4.5.2 Biological Data on ESM-containing Compounds with Monoaryl Cores

Compounds **4.32** to **4.35** were initially profiled in the BRD4-BD1 FRET assay,^{A8} and the ChromlogD_{pH7.4} was also measured.^{A7} The data generated is shown below (Table 4.06).

Comparison of the biochemical potency of the ESM-containing compound **4.32** with the parent molecule **4.02** (Table 4.04, BRD4-BD1 pIC₅₀ = 4.6) showed no significant impact on biochemical potency on incorporation of the ESM ester. The *N*-methyl pyridone analogue **4.33** showed an increase in potency of approximately 0.5 log units compared with compound **4.32**, which is consistent with data seen previously (Table 3.03).

The ester hydrolysis products **4.34** and **4.35** both showed potencies which were around the lower limit of the BRD4-BD1 biochemical assay. The level of activity of these compounds is therefore difficult to assess, although the data indicates a significant decrease in potency compared to the ester analogues. It was noted that the measured ChromlogD_{pH7.4} of the ESM-containing compounds **4.32** and **4.33** is, in contrast to the ESM-containing benzimidazole **3.19**, approximately ten-fold higher than the predicted value, and puts the compounds into a very poor physicochemical space. This difference is not seen for the acid hydrolysis products **4.34** and **4.35**.

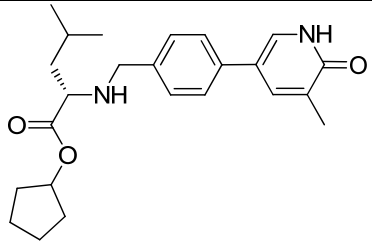
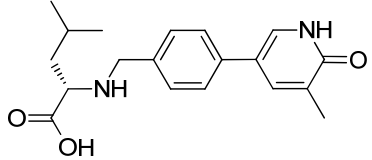
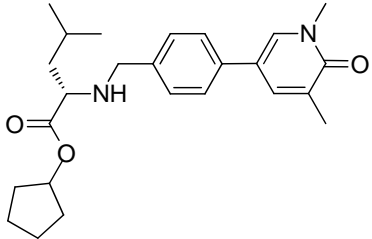
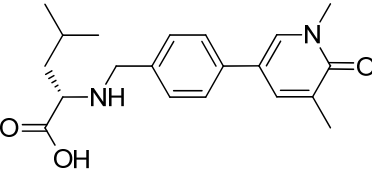
	Structure	BRD4-BD1 pIC ₅₀ (n)	mChromlogD _{pH7.4}	cChromlogD _{pH7.4}
4.32		4.9 (3)	6.7	5.7
4.34		4.5 (1), < 4.3 (1)	0.4	0.4
4.33		5.5 (4)	7.5	6.3
4.35		4.5 (1), < 4.3 (2)	0.9	1.1

Table 4.06: Biological data generated on ESM-containing analogues of compound **4.01**. Potency at BRD4-BD1 was assessed using a FRET assay.^{A8} Both measured ChromlogD_{pH7.4}^{A7} and calculated ChromlogD_{pH7.4}^{B2} are shown.

To assess this new series within a cellular environment, the more potent ESM-containing compound **4.33** was taken forward into the human whole blood (HWB) assay^{A1} (Table 4.07).

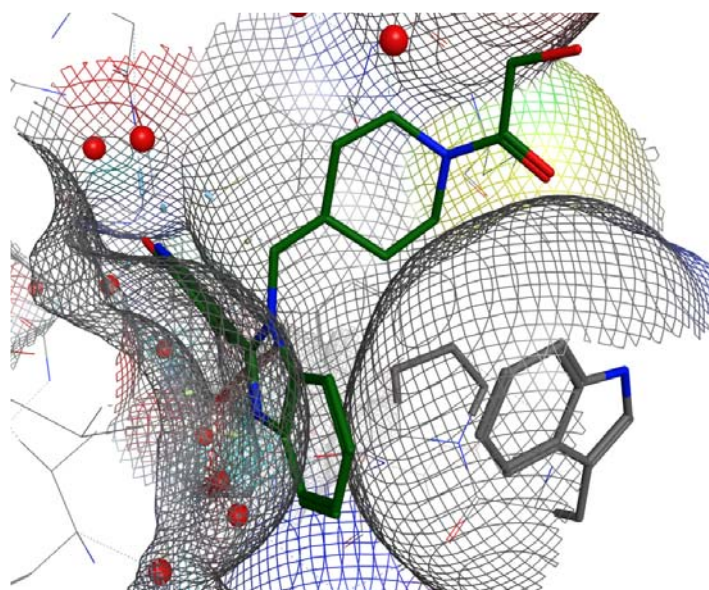
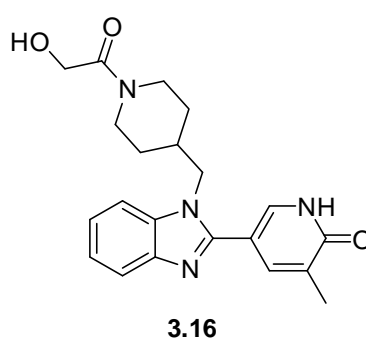
	BRD4-BD1 pIC₅₀ (n)	HWB (MCP-1) pIC₅₀ (n)	Permeability nm/s (n)	HSA binding
4.33	5.5 (4)	5.8 (2), < 5.5 (1)	590 (1)	96%

*Table 4.07: Biological assay results for the ESM-containing cyclopentyl ester **4.33**. Also shown is the artificial membrane permeability at pH7.4,^{A10} and human serum albumin (HSA) binding.^{A11}*

Encouragingly, for two of the test occasions in the human whole blood assay, a pIC₅₀ of 5.8 was measured. On the third occasion the pIC₅₀ was measured as less than 5.5. Nonetheless, given the low potency, high lipophilicity, and relatively high HSA binding of this compound, this was an encouraging hint of cellular activity. The data generated on this compound supports further work in this monoaryl core series. Compound **4.33** was therefore used as a hit molecule for a new pyridone subseries, and a new programme of work was initiated elsewhere within our laboratories.^{4.08}

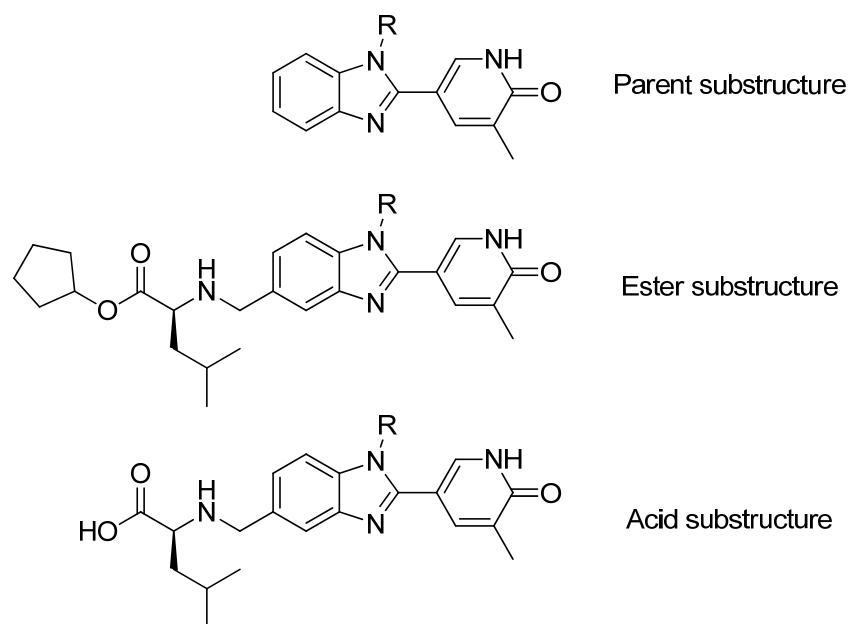
4.6 Design of Compounds to Investigate the Benzimidazole *N*-Substituent

In addition to investigation of alterations to the benzimidazole core of the initial tool BET-ESM molecule **3.19**, the benzimidazole *N*-substituent of compound **3.19** was also optimised. Inspection of the X-ray crystal structure of compound **3.16** (Figure 4.03) established that the benzimidazole *N*-substituent occupies the WPF-shelf region of the BRD4 protein. Experience from previous work in this area (Chapter 2) has shown that the WPF shelf is a key region for modulating potency. This observation indicates that a wider investigation of the SAR of the benzimidazole *N*-substituent has a good chance of increasing potency at BRD4-BD1. It also indicates that the use of known SAR from earlier programmes of work within our laboratories, in particular that reported earlier within this thesis (Chapter 2), will be of particular relevance.



*Figure 4.03: X-ray crystal structure of compound **3.16** bound to BRD4-BD1. Compound **3.16** is shown in green, the protein structure in grey. A molecular surface is added to the protein. The Trp and Pro WPF-shelf residue side-chains are highlighted with increased bond thickness.*

A series of compounds was designed for synthesis to probe the SAR of the benzimidazole *N*-substituent. These compounds were selected to reveal the contribution of the *N*-substituent to potency, and to introduce a variety of non-aromatic groups which would lead to final BET-ESM compounds with acceptable physicochemical properties. A representative subset of the compounds designed, intended to show the range of functional groups to be incorporated, is shown below (Table 4.08). General structures are shown prior to the table. The full list of compounds for synthesis is shown in Appendix 2 (Table 1).



Substructures for table shown overleaf.

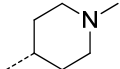
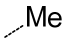
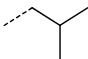
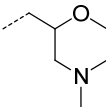
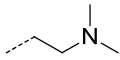
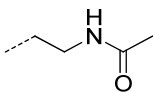
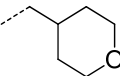
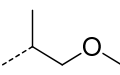
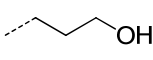
Substituent type	R	Parent	Ester	Acid
Cyclic amine		3.22 2.2, Medium	3.19 4.1, Medium	3.21 -0.7, Low
Alkyl		4.36 3.5, High	4.37 5.3, Medium	4.38 0.0, Low
Alkyl		4.39 4.8, High	4.40 6.4, Medium	4.41 1.2, Low
Cyclic amine		4.42 2.7, Medium	4.43 4.5, Medium	4.44 -0.5, Low
Acyclic amine		4.45 2.2, Medium	4.46 4.1, Medium	4.47 -0.6, Low
Acyclic amide		4.48 2.5, Medium	4.49 4.3, Medium	4.50 -1.0, Low
Cyclic ether		4.51 3.9, High	4.52 5.6, Medium	4.53 0.3, Low
Acyclic ether		4.54 3.8, High	4.55 5.6, Medium	4.56 0.3, Low
Acyclic alcohol		4.57 2.6, Medium	4.58 4.4, Medium	4.59 -0.2, Low

Table 4.08: A subset of the list of changes to be made to the benzimidazole N-substituent, and the predicted physicochemical properties of the parent benzimidazole, ESM-containing ester and acid hydrolysis product. The $c\text{Chromlog}D_{\text{pH}7.4}^{\text{B}2}$ is shown in blue, and predicted passive permeability^{B3} is shown in green. The full list of compounds for synthesis is shown in Appendix 2 (Table 1). Compounds 3.19, 3.21 and 3.22 are shown for comparison.

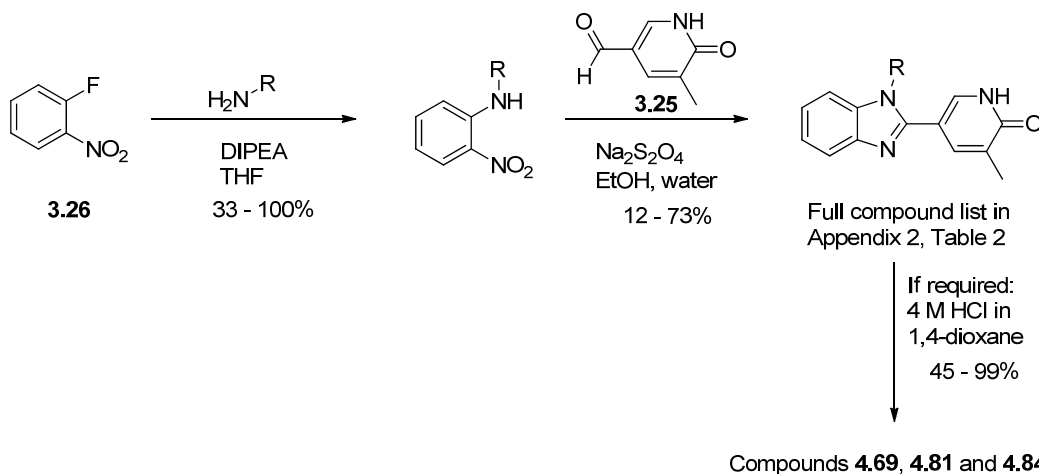
A range of small alkyl benzimidazole *N*-substituents, such as the isobutyl of compound **4.39**, were designed as the WPF-shelf region of the BRD4-BD1 protein is known to accept these groups and maintain a good level of potency, such as in the cyclopropylmethyl substituted compound **2.49** (Table 2.07). Knowledge from this previous work also inspired the design of cyclic and acyclic ether compounds, such as compounds **4.51** and **4.54**. These two examples were of particular interest for this programme of work. The tetrahydropyran of compound **4.51** is found in molecule **2.12** (Table 2.09), which was one of the furthest progressed compounds in the work described earlier within this thesis. The acyclic ether **4.54** was the component of the lead molecule **2.67** (Table 2.09) which interacted with the WPF-shelf of BRD4-BD1, and therefore would be expected to convey a very good balance between potency and physicochemical properties.

It was noted from the *in silico* profiling performed that incorporation of the ESM motif adds a significant amount to the lipophilicity of the molecule, predicted at approximately two log units. To move the ESM-containing compounds into a more desirable physicochemical space, a number of *N*-substituents which lowered the calculated $\text{ChromlogD}_{\text{pH}7.4}^{\text{B}2}$ further than the ether compounds were also designed. These included polar groups such as cyclic and acyclic amines, alcohols, and amides.

The *in silico* profiling performed showed that the majority of the ESM esters would be predicted to be close to, or slightly above, the desired lipophilicity (Table 3.04). However, the compounds were still of interest at this early stage of the programme as changes elsewhere in the molecule, combined with these changes to the benzimidazole *N*-substituent may then be used to reduce overall lipophilicity to the desired value. The esters were all predicted to have medium passive permeability,^{B3} which should ensure sufficient compound is able to enter the cell. All acids were predicted to have low passive permeability, which would be necessary to see retention of the acid within the cell.

4.7 Synthesis of Benzimidazole *N*-Substituent Analogues

The synthetic route used to access the compounds designed to investigate the SAR of the benzimidazole *N*-substituent was the same as that described previously in the synthesis of compound **3.22** (Scheme 3.02). In addition, a small number of compounds required an additional BOC-deprotection step to be performed to yield the final compound. The synthetic route used is shown below (Scheme 4.07).

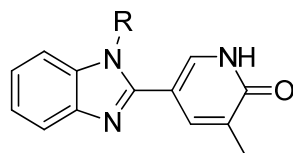


Scheme 4.07: Preparation of the parent pyridone-benzimidazole compounds designed above (Section 4.6). The compound numbers and isolated yields of each reaction are shown in Appendix 2 (Table 2).

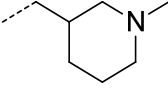
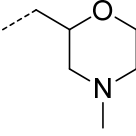
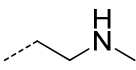
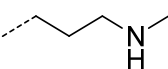
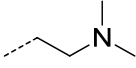
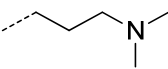
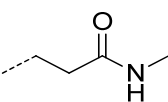
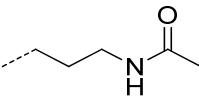
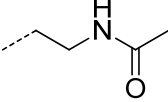
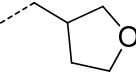
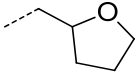
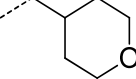
The commercially available 1-fluoro-2-nitrobenzene **3.26** was reacted with the appropriate amine in an S_NAr reaction to give the intermediates in 33–100% yield, with the majority of reactions proceeding in over 80% isolated yield. These intermediates were reacted with aldehyde **3.25** in a reductive cyclisation reaction using reaction conditions previously described (Section 3.4.2.2).^{4,09} The products were isolated in 12–73% yield, with the majority of reactions proceeding in over 40% yield. The subsequent BOC-deprotection to give compounds **4.69**, **4.81** and **4.84** was performed with hydrochloric acid, and provided these final compounds as the hydrochloride salts. The isolated yields of each reaction, as well as the intermediate compound numbers are shown in Appendix 2 (Table 2).

4.8 Primary Data for Benzimidazole *N*-Substituent Changes

The compounds described above (full compound list in Appendix 2, Table 2) were profiled in a range of biochemical and physicochemical assays, as described previously (Section 3.4.3). As the compounds did not contain an ESM group, the key data generated was the BRD4-BD1 potency and the mChromlogD_{pH7.4} (Table 4.09). This data would be used to prioritise which molecules would be of interest for ESM incorporation.



	R type	R	BRD4-BD1 pIC₅₀ (n)	mChromlogD (pH7.4)	cChromlogD (pH7.4)
3.22	Cyclic amine		5.4 (3)	0.9	2.2
4.36	Alkyl	Me	5.0 (3)	1.8	3.5
4.60	Alkyl		5.2 (2)	2.2	3.9
4.63	Alkyl		5.5 (1)	2.7	4.3
4.39	Alkyl		5.9 (2)	3.4	4.8
4.66	Alkyl		6.0 (2)	3.0	4.3
4.69	Cyclic amine		4.8 (2)	0.3	1.1
4.72	Cyclic amine		5.7 (2)	2.3	2.6
4.75	Cyclic amine		5.2 (2)	0.6	2.6

	R type	R	BRD4-BD1 pIC ₅₀ (n)	mChromlogD (pH7.4)	cChromlogD (pH7.4)
4.78	Cyclic amine		5.7 (2)	0.9	2.7
4.42	Cyclic amine		5.8 (2)	1.8	2.7
4.81	Acyclic amine		4.7 (2)	0.6	1.5
4.84	Acyclic amine		4.6 (2)	0.3	1.6
4.45	Acyclic amine		5.6 (2)	1.9	2.2
4.87	Acyclic amine		4.7 (2)	0.8	2.2
4.90	Acyclic amide		4.6 (2)	1.0	2.5
4.93	Acyclic amide		4.7 (2)	1.2	2.7
4.48	Acyclic amide		4.4 (1), < 4.3 (1)	1.0	2.5
4.96	Cyclic ether		5.8 (3)	2.0	3.5
4.99	Cyclic ether		5.5 (2)	2.5	3.8
4.51	Cyclic ether		6.4 (2)	2.2	3.9

	R type	R	BRD4-BD1 pIC ₅₀ (n)	mChromlogD (pH7.4)	cChromlogD (pH7.4)
4.102	Cyclic ether		6.7 (3)	2.7	3.9
4.105	Cyclic ether		6.3 (2)	3.6	4.2
4.108	Cyclic ether		5.4 (1)	2.1	3.4
4.111	Acyclic ether		5.5 (2)	2.1	3.5
4.54	Acyclic ether		5.9 (2)	2.5	3.8
4.57	Acyclic alcohol		5.3 (2)	1.3	2.6
4.114	Acyclic alcohol		4.8 (2)	1.1	2.3
4.117	Acyclic alcohol		5.4 (4)	1.5	2.7

Table 4.09: Data generated on compounds with benzimidazole N-substituent changes. Potency at BRD4-BD1 was assessed using a FRET assay.^{A8} Measured^{A7} and calculated^{B2} ChromlogD are shown. Compounds **4.69**, **4.81** and **4.84** were synthesised as hydrochloride salts.

The biochemical data generated showed that the potency of the molecules at the BRD4-BD1 bromodomain can be significantly altered by modification of the *N*-substituent, as would be expected. The compounds synthesised showed a wide range of potencies at BRD4-BD1 (pIC₅₀ from < 4.4 to 6.7). The most potent examples are the 3-methylenetetrahydropyran **4.102**, as well as the 4-methylenetetrahydropyran **4.51**, both substituents which were designed as they were very potent in previous work reported (Table 2.07, Compounds **2.07** and **2.08**).

The alkyl examples, such as **4.39** and **4.66**, indicate that lipophilicity is well tolerated in this region of the molecule, and as expected potency increases with increasing size of the substituents. A number of cyclic amine examples also show good potency, especially those with an amine in the heterocyclic 3-position such as compounds **4.78** and **4.42**. These examples show a significantly lower measured $\text{ChromlogD}_{\text{pH}7.4}$ than the alkyl, and indeed ether, substituents.

Data generated on the secondary acyclic amines **4.81** and **4.84** suggests that the protein will not tolerate a hydrogen bond donor in this region. The methylated analogue of **4.81**, compound **4.45**, showed a ten-fold increase in potency to support this hypothesis. However, this was not consistent in the methylated analogue of **4.84**, compound **4.87**, which did not show a corresponding increase in potency. These data are surprising given the relative potency of a wide range of cyclic tertiary amines in this region of the molecule. In contrast to the amines, none of the acyclic amide-containing substituents synthesised showed good potency at BRD4-BD1. Again, these compounds also contain hydrogen bond donors.

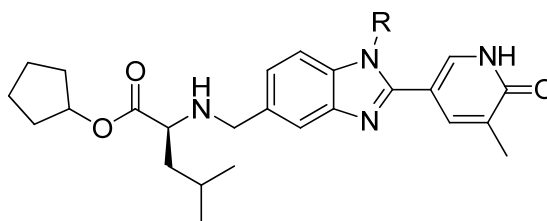
All cyclic and acyclic ethers show good potency at BRD4-BD1, ranging from pIC_{50} of 5.4 to 6.7. This type of substituent showed the most consistently good potency in the biochemical assays. However, the measured $\text{ChromlogD}_{\text{pH}7.4}$ of these compounds is significantly higher of that of the amines, which needs to be considered when selecting which compounds would be synthesised with ESM groups incorporated. It appears from the tetrahydrofuran and tetrahydropyran compounds that the position of the oxygen in the heterocyclic ring makes little difference in potency. An increased number of test occasions would be required to identify whether there are any small but significant differences between these compounds.

Finally, in contrast to the data seen for the secondary amines and amides, it appears that a hydrogen bond donor can be accommodated in the WPF-shelf region of the protein when present in alcohol examples **4.57** and **4.117**. The slightly less lipophilic alcohol **4.114** shows a corresponding reduction in potency.

In summary, cyclic and acyclic ethers were identified as the most promising benzimidazole *N*-substituents to balance potency and lipophilicity. However, the potency levels of the alcohol and amine substituents were also encouraging given their lower lipophilicities. The range of potencies and lipophilicities measured is particularly useful for any future ESM incorporation, as this will allow ESM-containing compounds to be made with a range of biochemical and physicochemical properties. This would provide increased understanding of which properties are most important in optimising the HWB potency of ESM-containing compounds.

4.9 Incorporation of ESMs into Pyridone Benzimidazole Template

Using the data generated on the compounds made to investigate the benzimidazole *N*-substituent (Table 4.09), a number of ESM-containing compounds were designed to probe whether modifications to the *N*-substituent gave compounds with an improved profile over the initial tool molecule **3.19**. The key data used to design these compounds was the potency and lipophilicity of the parent benzimidazoles (Table 4.09). The most potent substituents were incorporated into the structure of compound **3.19**, and in addition a range of functional groups and lipophilicities were targeted. The final list of compounds is shown below (Table 4.10).



	R	cChromlogD _{pH7.4}	Parent molecule
3.19		4.1	3.22
4.37	Me	5.3	4.36
4.76		4.4	4.75
4.46		4.1	4.45
4.58		4.4	4.57
4.43		4.5	4.42
4.52		5.6	4.51
4.112		5.3	4.111

Table 4.10: List of compounds for synthesis where the piperidine *N*-substituent of compound **3.19** has been replaced, with their cChromlogD_{pH7.4}.^{B2} Compound **3.19** is shown for comparison.

Hydrolysis by hCE-1 may be affected by the shape of the molecule due to differing efficiency of binding of the compound to hCE-1. Therefore, as well as selecting compounds with a parent molecule which maintains potency, a range of functional groups within the *N*-substituent were selected. The changes to the benzimidazole *N*-substituent reflect a range of conformational changes such as complete truncation of the piperidine to a methyl group in compound **4.37**, or increased flexibility by insertion of a methylene linker between the benzimidazole and piperidine of the tool molecule **3.19**, such as in compound **4.76**. More polar substituents, such as the dimethylamino group of compound **4.46** and the alcohol of compound **4.58** were also selected, as these were the most potent acyclic amine and alcohol substituents identified previously (Table 4.09). The morpholine of compound **4.43** gives a final molecule with a predicted lipophilicity close to that of the piperidine analogues, but with a lower basicity.

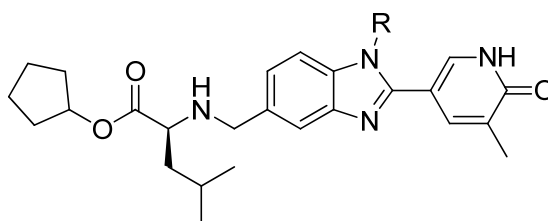
To ensure that the most potent *N*-substituents were represented, the tetrahydropyran of compound **4.52** was included, and this was supplemented by the more flexible ether **4.112**. Although these analogues had a predicted lipophilicity higher than was desired, if these compounds were of interest further optimisation in other areas of the molecule could be initiated to move them into a more drug-like physicochemical space.

4.10 Biological Data on ESM-containing Compounds from Pyridone Benzimidazole Template

To aid the speed of progression of the BET-ESM programme at this critical juncture, the compounds designed to investigate the benzimidazole *N*-substituent (Table 4.10) were synthesised by final compounds and intermediate preparation being spread between myself and a number of other synthetic chemists within our laboratories.^{4,10} The route used to access these compounds was directly analogous to that used successfully to prepare the initial ESM-containing compound **3.19** (Scheme 3.03). Once synthesised, the compounds were then profiled in the BRD4-BD1 FRET assay^{A8} and the LPS-stimulated human whole blood (HWB) assay.^{A1} The ChromlogD_{pH7.4} was also measured.^{A7} The data generated is shown below (Table 4.11).

The impact on biochemical potency at BRD4-BD1 of the benzimidazole *N*-substituent was consistent between the previously described parent molecules (Table 4.09) and their ESM-containing analogues (Table 4.11). In all cases, the incorporation of the ESM had no significant impact on biochemical potency. In contrast, the potency in the LPS-stimulated HWB assay was significantly impacted by the nature of the benzimidazole *N*-substituent. In the case of a number of the compounds, such as the amines **4.76** and **4.43**, and the alcohol **4.58**, there was little difference between the biochemical and HWB potency. This was consistent with the data for the initial tool molecule **3.19**. This implies that the ESM is not contributing significantly to the HWB potency. This may be due to a number of factors such as a lack of hCE-1 hydrolysis, or poor retention of the subsequent acid by the cell.

However, for a number of compounds there was over a ten-fold increase in pIC₅₀ between the biochemical and HWB assays. This was seen in the truncated *N*-methyl analogue **4.37**, the dimethylaminoethyl **4.46**, the tetrahydropyranyl **4.52** and the methoxyethyl **4.112**. Due to the similarity in physicochemical properties of acids generated by the compounds which show variable HWB potency, it was hypothesised that higher HWB potency is a result of a higher turnover of the ester by hCE-1.



Substructure of compounds in table overleaf.

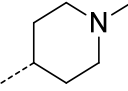
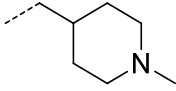
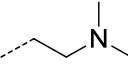
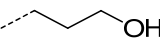
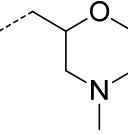
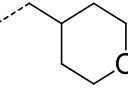
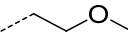
	R	BRD4-BD1 pIC ₅₀ (n)	HWB (MCP-1) pIC ₅₀ (n)	ΔpIC ₅₀ (HWB - BRD4)	cChromlogD _{pH7.4} / mChromlogD _{pH7.4}
3.19		5.3 (7)	5.6 (3), < 6.9 (1)	n.d.	4.1 / 4.2
4.37	Me	5.2 (2)	6.8 (2)	1.6	5.3 / 5.5
4.76		5.4 (2)	5.8 (4)	0.4	4.4 / 3.9
4.46		5.4 (3)	6.5 (2)	1.1	4.1 / 5.5
4.58		5.5 (2)	5.8 (2)	0.3	4.4 / 4.7
4.43		5.9 (3)	6.1 (2)	0.2	4.5 / 5.1
4.52		6.1 (10)	7.7 (33)	1.6	5.6 / 5.4
4.112		5.7 (3)	7.2 (2)	1.5	5.3 / 5.7

Table 4.11: Data generated on benzimidazole N-substituent analogues of compound **3.19**. Potency at BRD4-BD1,^{A8} and HWB potency^{A1} were measured. Both measured^{A7} and calculated^{B2} ChromlogD_{pH7.4} are shown. Compound **3.19** is shown for comparison.

Due to its high shift from biochemical to HWB potency, combined with the high absolute HWB potency as a result of its higher biochemical activity, the tetrahydropyranyl analogue **4.52** was selected for progression into the macrophage acid retention assay (Figure 4.04).^{A9} This assay was performed as previously (Section 3.4.3.2), except with a 24 hour time course. The amount of ester **4.52** and acid hydrolysis product **4.151** in cell lysates and supernatants were measured.

Over the 24-hour time course of the macrophage acid retention assay, the majority of the ester **4.52** had been converted into the acid hydrolysis product **4.151**. In this assay, 10 nmoles of the ester was incubated with the isolated macrophages at the outset. After 24 hours, only 2.6 nmoles of the ester **4.52** was detected; this is in contrast to the experiment where the tool molecule ester

3.19 was incubated and 7.3 nmoles of the ester was detected at 24 hours. In both experiments the esters were shown to be stable under the assay conditions. This supported the hypothesis that an increased hydrolysis rate for compound **4.52** is the cause of the increased shift between the biochemical and HWB assays for compound **4.52** over **3.19**.

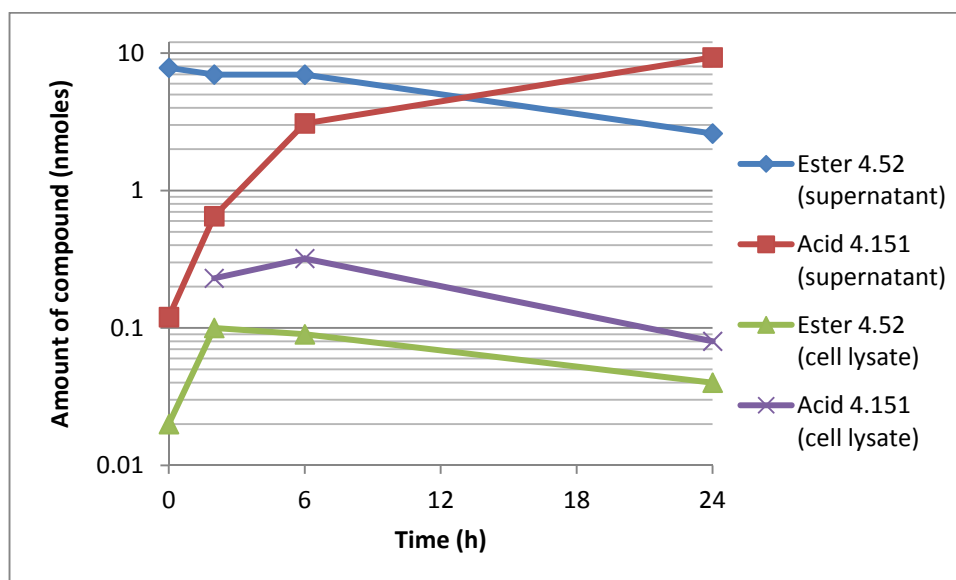
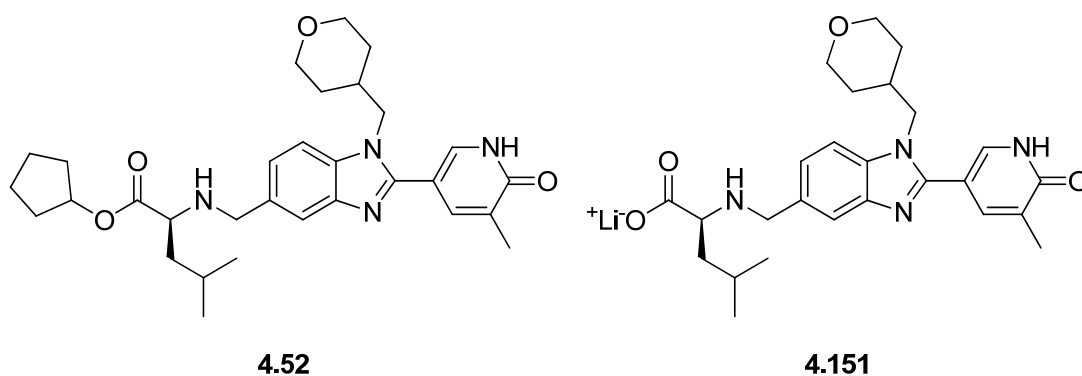


Figure 4.04: The concentration in supernatant and cell lysate of both ester **4.52** and its corresponding acid **4.151** after incubation of compound **4.52** with M1 macrophages over a time course of 24 hours. Structures of the compounds are shown above the table.

Although compound **4.52** showed an increased rate of hydrolysis, the acid was still not retained within the cell over an extended time course. It can be seen from the data above (Figure 4.04) that the acid **4.151** is expelled into the supernatant. The amount of acid within the cell at six hours, a time-point believed to be biologically relevant, was compared after incubation of the macrophages with ester **4.52** (acid **4.151**), ester **3.19** (acid **3.21**) and the standard non-ESM BET inhibitor I-BET151 **1.06** (Figure 1.16). This data is shown below (Figure 4.05).

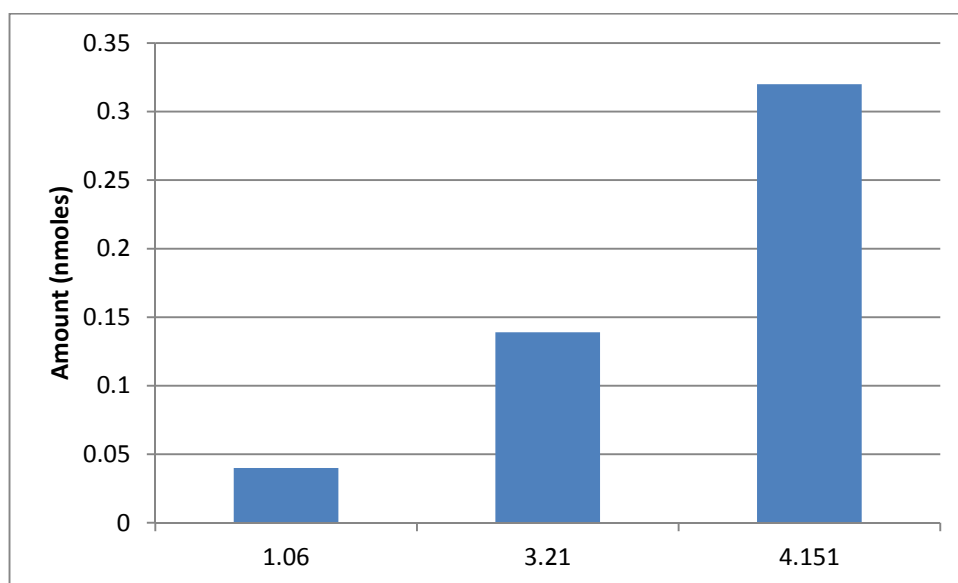
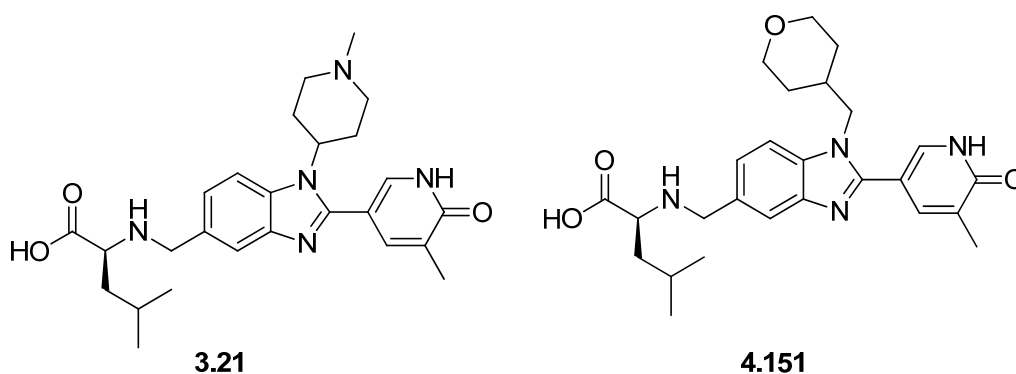


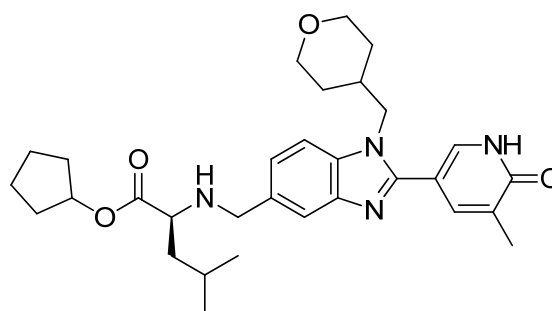
Figure 4.05: The amount of compound (**1.06**) or ester hydrolysis product **3.21** (ester **3.19**) and **4.151** (ester **4.52**) within the cell lysate at 6 hours in the macrophage acid retention assay.^{A9}

At six hours, the amount of acid **4.151** measured in the macrophage cell lysates was approximately 10-fold higher than the concentration of **1.06**, and over two fold higher than that of acid **3.21**. This shows the effect of the ESM in altering cellular concentration of BET inhibitor within the macrophages, and is evidence for why it is having such a profound effect on the HWB potency (Table 4.11).

Analysis of the complete data set generated on compound **4.52** shows that this compound meets the *in vitro* probe criteria set out at the beginning of this programme of work (Figure 4.01). In particular, the shift of pIC₅₀ between the HWB and biochemical assays means that this compound can be used as an *in vitro* probe molecule.

4.11 Conclusions and Future Work within the ESM Programme

The generation of a wide range of biochemical and physicochemical SAR on the pyridone template has established that there are multiple areas which will allow optimisation of the pyridone-benzimidazole series. In particular, the optimisation of the benzimidazole *N*-substituent reported within this thesis, led to the identification of the first known example of a BET–ESM *in vitro* probe molecule **4.52** (Table 4.12).



4.52

	Desired Profile	4.52
BRD4-BD1 pIC₅₀ (n)	Minimal loss of activity from non-ESM parent	6.1 (10)
HWB (MCP-1) pIC₅₀ (n)	N/A	7.7 (33)
ΔpIC₅₀ (HWB – BRD4-BD1)	> 1	1.6
Macrophage cell retention assay	ESM hydrolysed in macrophages	Yes
	Acid present in cell at 6 hours	Yes

Table 4.12: Comparison of compound **4.52** with desired *in vitro* probe molecule profile.

The *in vitro* probe molecule **4.52** has been used extensively within our laboratories to perform the biological profiling of a BET–ESM compound. These studies have increased our understanding of ESM technology, and support our original hypothesis that the use of ESM technology has potential to increase the therapeutic index of compounds over the currently established BET bromodomain inhibitors.

As a result of these encouraging data, the focus of the BET-ESM programme subsequently progressed from probe identification into a full lead optimisation programme. This required optimisation of the compounds towards a new set of criteria, which reflect the biological and physicochemical profile required to produce a molecule suitable for progression into pre-clinical development. The SAR generated on the pyridone-benzimidazole template within this reported work indicates that modification of the structure can impact a range of developability criteria including biochemical and cellular potency, lipophilicity, and solubility. The template was therefore declared as a lead series which could be optimised towards these goals.

In addition to the successful work on the pyridone-benzimidazole series, the work reported has identified an alternative starting point for optimisation of compounds towards a pre-clinical candidate profile within the BET-ESM area. This biaryl pyridone series was exemplified by the ESM-containing compound **4.33**. A new programme of work was required to follow up the encouraging data generated on this compound. This series was an encouraging starting point for development as reduction in the aromatic ring count, as well as reduction in size of the molecule, makes it possible to more easily design compounds within a drug-like physicochemical space. A programme of work is currently underway elsewhere within our laboratories to capitalise on the initial findings in this area.^{4.08}

Chapter 5

Discovery of an *In Vivo* Tool BET Bromodomain Inhibitor Containing an Esterase Sensitive Motif

“The line between good and evil is permeable and almost anyone can be induced to cross it when pressured by situational forces.”

Philip Zimbardo.

Synopsis

As a result of positive data reported on the *in vitro* probe molecule **4.52**, the use of esterase sensitive motifs to increase the therapeutic index of BET bromodomain inhibitors was validated as a viable medicinal chemistry strategy. To progress this area of research further, the pyridone benzimidazole series was optimised towards criteria consistent with the discovery of a pre-clinical candidate molecule. This chapter describes the medicinal chemistry design and synthesis undertaken to optimise compound **4.52** in light of these criteria, and the progress towards a molecule with properties which would allow its use as an *in vivo* tool. The lead compound is currently undergoing further profiling to assess its suitability as a pre-clinical candidate molecule.

development. These are designed to maximise solubility whilst minimising dose and property forecast index (PFI).^{5.01} Thirdly, the compound must have an *in vivo* pharmacokinetic profile in cynomolgus monkey suitable for oral dosing in a pre-clinical safety study. In light of these criteria a desired compound profile was established (Figure 5.02).

- Human whole blood (HWB) pIC₅₀ > 7.0
- > 10-fold shift in pIC₅₀ from biochemical to HWB assay
- PFI < 7, ideally PFI < 6.
- Solubility in FaSSIF media > 100 µg/ml.
- *In vitro* intrinsic clearance (cynomolgus S9 fraction) < 10 ml/min/g

Figure 5.02: The criteria established for a BET–ESM *in vivo* probe molecule.

Due to there being no high throughput hCE-1 hydrolysis assay, or macrophage retention assay, available for SAR generation, the HWB assay was used to measure the contribution of the ESM technology to potency. We aimed to identify a compound with comparable potency in the HWB assay to the pre-clinical non-ESM BET bromodomain inhibitor **2.67**, driven from a biochemical potency at least 10-fold lower than its HWB potency. This would imply that the HWB potency had been enhanced by the hydrolysis and retention of the ESM ester.

GSK's candidate quality criteria were officially adopted in late 2012 for the assessment of all molecules considered for candidate selection. Low risk compounds are identified as those with a PFI ≤ 6,^{5.01} FaSSIF solubility of ≥ 100 µg/ml,^{5.02} and a predicted human dose of ≤ 100 mg. For each of the criteria not fulfilled, the risk is considered to have increased. The successful use of ESM technology would be expected to provide a low-dose compound, so the desired compound criteria were focussed on reducing the PFI and increasing the FaSSIF solubility of compounds.

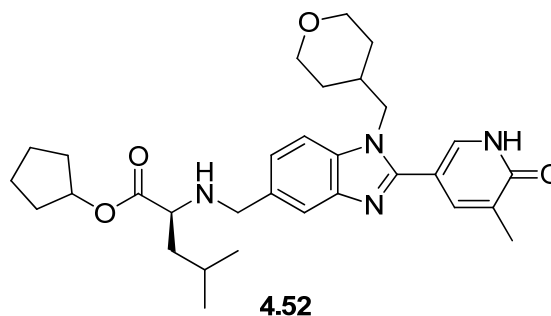
Due to the low sequence homology between rodent, dog, and human esterases, it was planned to carry out pre-clinical toxicity studies of compounds using ESM technology using cynomolgus monkeys, where the sequence homology is greater.^{5.03} Ethical considerations make running routine DMPK studies using monkeys impossible,^{5.04} and therefore *in vitro* clearance was used to drive the DMPK-related optimisation of compounds. For this, an intrinsic clearance assay^{A12} using cynomolgus monkey liver S9 fraction^{5.05} was used.

This chapter describes the work undertaken to identify a compound which met these *in vivo* probe molecule criteria (Figure 5.02). This molecule could then be progressed into an *in vivo*

DMPK study in cynomolgus monkey to establish its suitability for pre-clinical safety and efficacy studies.

5.2 Medicinal Chemistry Design of Compounds for Synthesis

As a starting point for optimisation, the *in vitro* probe molecule **4.52**, identified in Chapter 4, was assessed in relation to the desired compound profile for further progression (Figure 5.02). The data for compound **4.52** in comparison with this profile is shown below (Table 5.01).



	Desired	4.52
BRD4-BD1 pIC ₅₀ (n)	N/A	6.1 (10)
HWB (MCP-1) pIC ₅₀ (n)	> 7.0	7.7 (33)
ΔpIC ₅₀ (HWB – BRD4-BD1)	> 1	+ 1.6
mChromlogD _{pH7.4}	< 4	5.4
PFI	< 7	8.4
FaSSIF Solubility (μg/ml)	> 100	165
Cyno S9 clearance (ml/min/g)	< 10	25.6

Table 5.01: Profile of compound **4.52** in comparison with the desired compound profile. Included are data from the BRD4-BD1 mutant FRET assay,^{A8} the HWB assay,^{A1} and the ΔpIC₅₀ between these assays. The measured ChromlogD_{pH7.4}^{A7} is shown. In vitro clearance is measured in cynomolgus liver S9 fraction,^{A12} and solubility in FaSSIF media.^{A13} Data which meets the criteria is highlighted in green, data which does not is highlighted in red.

Unsurprisingly, given its profile in the macrophage cell retention assay (Section 4.10), compound **4.52** meets the HWB potency criteria, as well as having the desired biochemical to HWB potency shift. The compound also shows a reasonable level of solubility. However, due to its high lipophilicity, the PFI is well above that desired in a molecule for progression towards *in vivo* studies. This would be likely to negatively impact developability criteria such as the PK

profile, solubility and toxicity.^{5.01} For example, the high lipophilicity is likely to be contributing to the high *in vitro* clearance of the compound.

By comparison of compound **4.52** to the desired compound profile, the strategy to optimise compound **4.52** was tailored to reducing lipophilicity whilst maintaining the desirable HWB potency. As already shown within this thesis (Section 4.10), the nature of the substituent on the benzimidazole has a limited impact on the overall lipophilicity of the molecule, and initial optimisation of this area of the molecule did not deliver a compound which met the desired compound criteria. In contrast, *in silico* profiling showed that small modifications of the ESM portion of the molecule are predicted to have a dramatic effect on lipophilicity. Therefore, it was decided that the priority for the medicinal chemistry was to focus on optimisation of the ESM.

The design of amino ester ESMs to be synthesised was inspired by a number of sources. Firstly, known ESM groups within the literature were researched, and in addition to these a set of amino acid cyclopentyl esters of naturally occurring amino acids that were under synthesis elsewhere within our laboratories^{5.06} were also considered. Secondly, *in silico* profiling was used to analyse all commercially available starting materials, and then bias the set of amino esters towards those which would be predicted to give compounds with good physicochemical properties. Lastly, a docking of compound **4.52** to hCE-1 was performed (Figure 5.03) which was used as an aid when visually inspecting possible amino esters for synthesis.

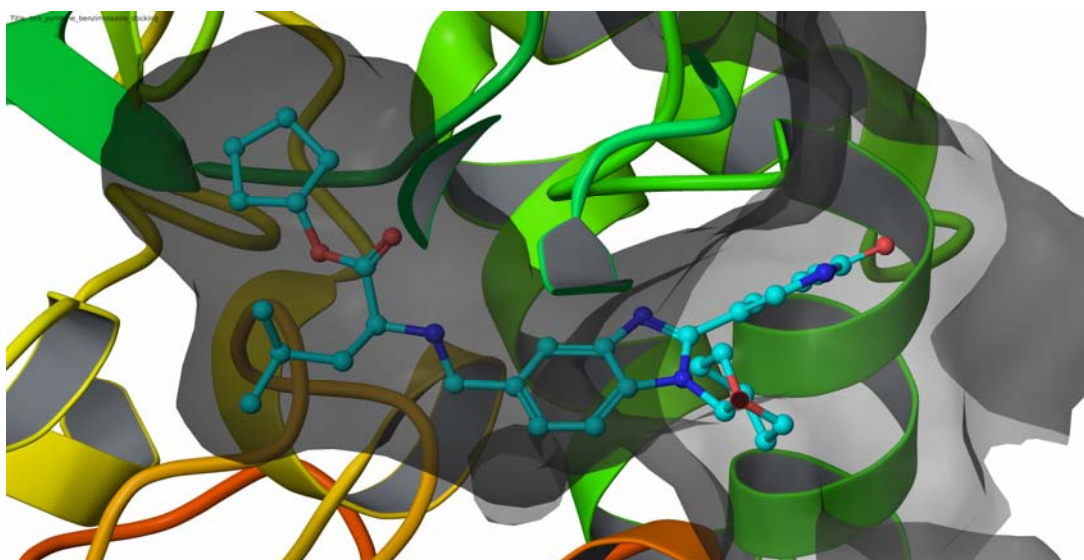


Figure 5.03: Compound **4.52** (blue) docked into hCE-1 (loops in green, yellow and orange). The molecular surface of the protein is shown with a transparent grey surface. The amino ester and benzimidazole are sat within the enzyme, the THP and pyridone exit out of the pocket.

An *in silico* profiling process, followed by rational medicinal chemistry design, was used to generate a final list of amino esters for synthesis. This process was performed in two stages; firstly on amino acids which would be synthesised as cyclopentyl amino esters, and secondly on alcohols which would be used to make various amino esters of leucine. The process used to select the amino acid monomers is outlined below (Figure 5.04).

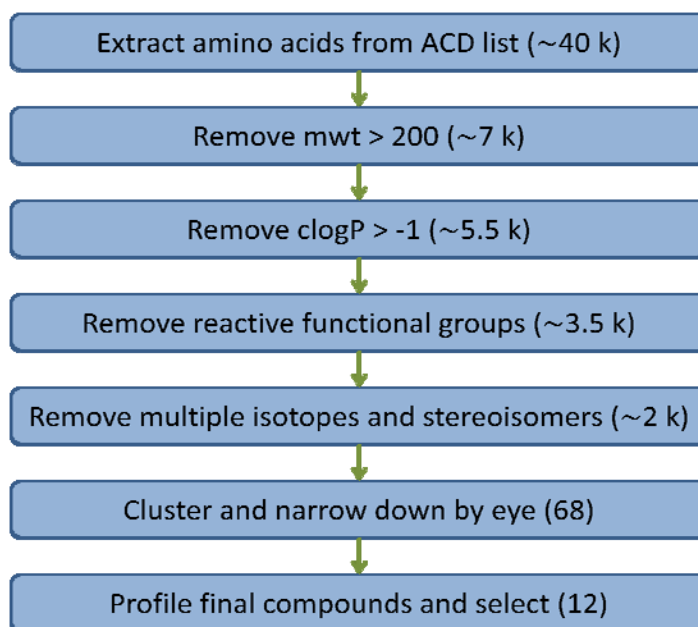


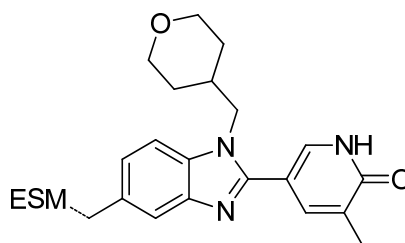
Figure 5.04: The process used to select amino acid starting materials for incorporation into final ESM-containing molecules. The ACD list used is the Accelrys Available Chemicals Directory.^{5.07} The number of amino acids remaining after each stage is shown in brackets.

The initial list of amino acids was taken from the Accelrys ‘Available Chemicals Directory’. This was converted into a SMILES format^{5.08} and manipulated using GSK’s in-house Helium software^{5.09} within Microsoft Excel. The amino acids were then filtered on the physical properties of molecular weight and clogP, with the aim of keeping both of these as low as possible. The filters used were slightly less restrictive than those of leucine (mwt of 131, clogP of -1.3) as improvements may be made by further optimisation elsewhere in the molecule. The list was also filtered by removing amino acids with reactive functional groups, as well as rationalising into one single isotope and stereoisomer in each case.

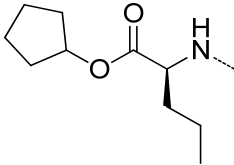
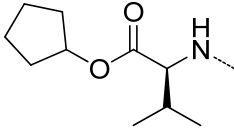
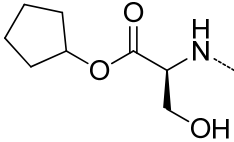
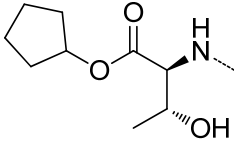
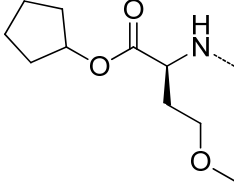
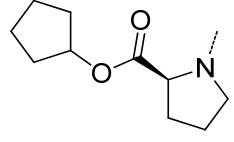
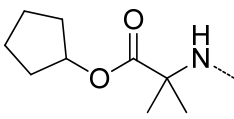
These filters led to a list of approximately two thousand amino acids, which was clustered into groups of structural similarity using Ward’s clustering.^{5.10} The use of the clustering algorithm allowed all two thousand amino acids to be inspected by eye within a workable timeframe. This

inspection was used to select compounds which looked plausible substrates for binding to hCE-1, contained sensible drug-like functional groups, and retained a variety of structural diversity.

The resulting 68 amino acids were each incorporated *in silico* into the full molecule which would be synthesised. In order to accurately establish the effect of the newly incorporated ESM groups on HWB potency and lipophilicity, all modifications were made to the ESM of compound **4.52**, with the rest of the molecule remaining constant. This gave 68 analogues of **4.52**, where the isobutyl side-chain of leucine had been replaced. These full structures were profiled *in silico* and compounds with a higher $c\text{ChromlogD}_{\text{pH}7.4}^{\text{B}2}$ than **4.52** (4.9) removed. Each compound was then considered individually in terms of the rationale for synthesis and synthetic tractability, and a final list of 12 compounds to be synthesised was generated. These are shown, along with their rationale for synthesis, below (Table 5.02).



	Amino Ester ESM	$c\text{ChromlogD}_{\text{pH}7.4}$	Design rationale
4.52		4.9	- <i>In vitro</i> probe molecule 4.52 , included in table for comparison.
5.01		3.5	- Smallest possible substituent, much lowered lipophilicity. - ESM known in literature. ^{5.11}
5.02		4.4	- Slightly more hindered than 5.01 , may reduce hydrolysis rate but may be more specific for hCE-1. - Not known in literature so will enhance ESM SAR.

	Amino Ester ESM	cChromlogD _{pH7.4}	Design rationale
5.03		4.4	<ul style="list-style-type: none"> - Most simple change to 4.52 whilst lowering lipophilicity. - Not known in literature so will enhance ESM SAR.
5.04		4.0	<ul style="list-style-type: none"> - Lowered lipophilicity over 4.52. - Does more hindered amino ester reduce hydrolysis rate? - ESM known in literature.^{5.12}
5.05		2.8	<ul style="list-style-type: none"> - Large reduction in lipophilicity. - Is hydroxyl tolerated in hCE-1? - Is there an effect of altered electronics on ester hydrolysis? - ESM known in literature.^{5.12}
5.06		3.1	<ul style="list-style-type: none"> - Similar rationale to 5.05, but with more hindered amino ester. - ESM known in literature.^{5.13}
5.07		3.5	<ul style="list-style-type: none"> - Reduction of lipophilicity without introducing hydroxyl functionality. - Commercially available amino acid. - Not known in literature so will enhance ESM SAR.
5.08		3.7	<ul style="list-style-type: none"> - Is tertiary amine ESM hydrolysed by hCE-1? - Lowered lipophilicity over 4.52. - Not known in literature so will enhance ESM SAR.
5.09		4.0	<ul style="list-style-type: none"> - Quaternary centre on amino ester, more hindered than 5.01. - Reduced lipophilicity over 4.52. - Known in literature.^{5.14}

	Amino Ester ESM	cChromlogD _{pH7.4}	Design rationale
5.10		3.1	<ul style="list-style-type: none"> - Is basic group tolerated by hCE-1? - Reduced lipophilicity over 4.52. - Not known in literature so will enhance ESM SAR.
5.11		3.7	<ul style="list-style-type: none"> - A less lipophilic analogue of the cyclohexyl ESM of key HDAC compound 3.02 (Figure 3.01).^{5.15} - Not known in literature so will enhance ESM SAR.
5.12		3.7	<ul style="list-style-type: none"> - Constrained analogue of 5.09, less hindered ester. - ESM known in literature.^{5.14}

Table 5.02: Compounds for synthesis, with their cChromlogD_{pH7.4}^{B2} and their design rationale.

A similar *in silico* profiling process, followed by rational design, was undertaken to design a set of alcohols to be incorporated into amino acid esters (Figure 5.04).

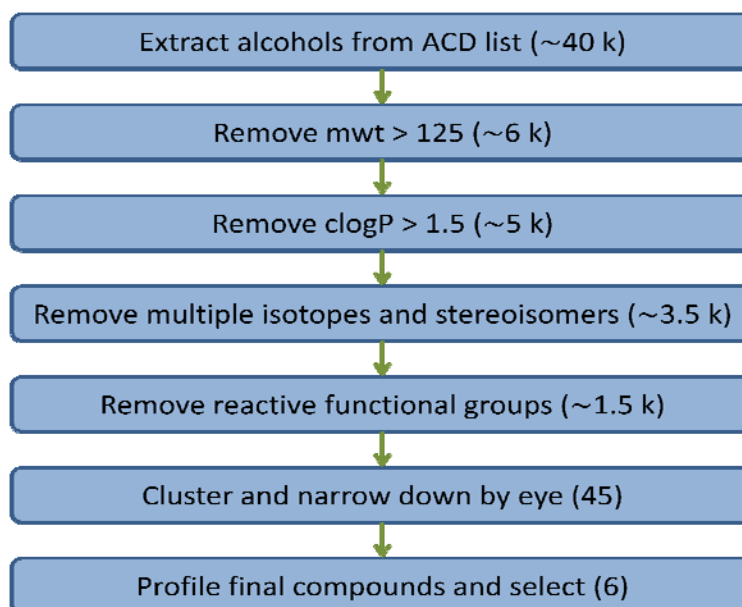
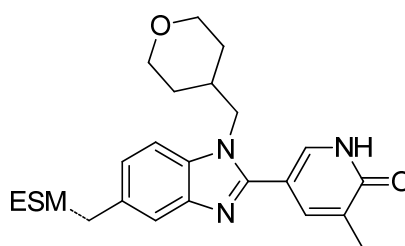


Figure 5.04: Process used to identify alcohol starting materials for incorporation into final ESM-containing molecules. The ACD list is the Accelrys Available Chemicals Directory.^{5.07} The number of alcohols remaining after each stage is shown in brackets.

The full list of commercially available alcohols was taken from the Accelrys ‘Available Chemicals Directory’. This was, as with the previous amino acid list, converted into a SMILES format^{5,08} and manipulated using Helium^{5,09} within Microsoft Excel. The list was filtered on the physical properties of molecular weight and clogP, with the aim of keeping both of these as low as possible. The filters used were slightly less restrictive than those of cyclopentanol (mwt of 125, clogP of 1.5) as improvements may again be made by further optimisation elsewhere in the molecule. The list was also simplified by rationalising into one single isotope and stereoisomer in each case, followed by the removal of reactive functional groups.

At this point, a list of approximately 1500 alcohols remained. This was clustered into groups of structural similarity using Ward’s clustering,^{4,10} and then inspected by eye to retain both sensible drug-like functional groups and a variety of structural diversity. The remaining 45 alcohols were each incorporated *in silico* into the full molecule which would be synthesised. This gave 45 analogues of **4.52**, where the cyclopentanol ester substituent had been replaced. These structures were profiled *in silico* and compounds with a higher cChromlogD_{pH7.4}^{B2} than **4.52** (4.9) removed. The remaining compounds were considered in terms of the medicinal chemistry rationale for synthesis, as well as their synthetic tractability. Using these criteria, a final list of six compounds for synthesis was generated (Table 5.03). In all cases, the amino ester ESMs were not known in the literature, so their synthesis will also increase the knowledge of ESM SAR. The *in silico* profiling process described led to a list of 18 modifications in total to the ESM of compound **4.52** which required preparation. The synthesis of these compounds is described in the subsequent section (Section 5.3).



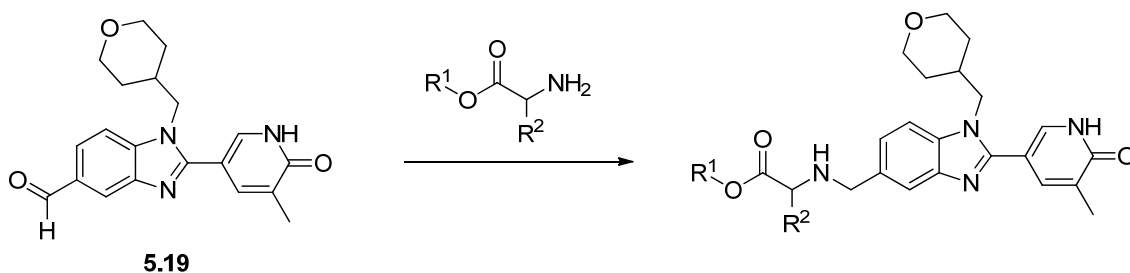
Substructure of compounds in table overleaf.

	Amino Ester ESM	cChromlogD _{pH7.4}	Design rationale
4.52		4.9	- <i>In vitro</i> probe molecule 4.52 , included in table for comparison.
5.13		3.9	- Truncation of cyclopentyl, maintains secondary centre next to ester. - Reduced lipophilicity over 4.52 .
5.14		4.7	- Less hindered ester than cyclopentyl would be expected to be less stable to hydrolysis. - Does this affect hCE-1 turnover?
5.15		4.7	- No secondary centre next to ester. - Sterics of <i>tert</i> -butyl should mean neopentyl ester more stable than other primary esters.
5.16		3.8	- Introduction of heteroatom significantly reduces lipophilicity over 4.52 . - How does introduction of oxygen atom impact hCE-1 binding and ester stability?
5.17		3.6	- Open chain analogue of 5.16 , also reduces lipophilicity over 4.52 . - Secondary centre next to ester maintained.
5.18		4.0	- Ring expansion of 5.16 , still has reduced lipophilicity over 4.52 .

Table 5.03: Compounds for synthesis, with their cChromlogD_{pH7.4} and rationale for synthesis.

5.3 Synthesis of Initial Target Molecules

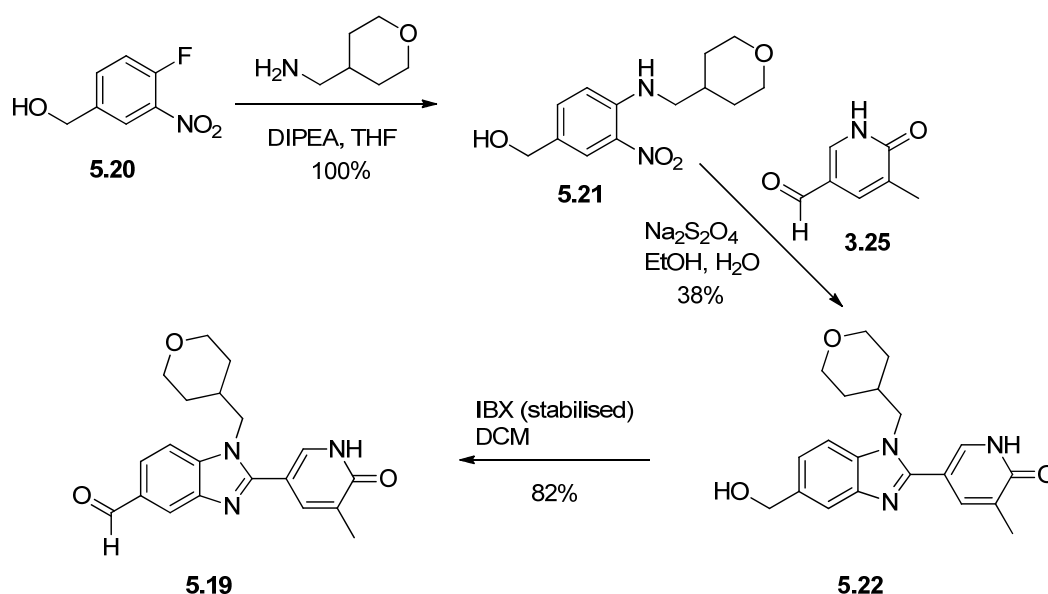
To synthesise the compounds described above (Section 5.2, Tables 5.02 and 5.03), a new synthetic route was designed. This enabled coupling of the amino ester ESM monomer to the benzimidazole core as the final step in the synthesis using a reductive amination reaction (Scheme 5.01), and significantly reduced the total number of reactions required.



Scheme 5.01: General route used to synthesise the BET-ESM compounds designed in Section 5.2.

A number of key intermediates were required to implement this synthetic strategy. Route optimisation of the method used previously to synthesise compound **3.19** (Scheme 3.03) led to a robust synthetic route to the required aldehyde **5.19**.^{5,16} The order of reactions was altered, and an additional oxidation reaction was incorporated. This allowed the aldehyde to be introduced after the benzimidazole cyclisation reaction was complete, to avoid any competing processes from occurring. After optimisation, this synthetic route was performed on a multi-gram scale to allow the synthesis of the desired final compounds (Scheme 5.02).

The commercially available fluoro-nitro benzyl alcohol **5.20** was reacted under standard nucleophilic aromatic substitution (S_NAr) conditions to give the aromatic amine **5.21** in quantitative yield. This amine was reacted with the previously prepared pyridone aldehyde **3.25** (Scheme 3.02), using the now standard reductive cyclisation reaction^{4,09} to give benzimidazole **5.22** in 38% isolated yield. The benzylic alcohol of **5.22** was oxidised to give the aldehyde **5.19** in 82% isolated yield. The oxidation was performed using stabilised 2-iodoxybenzoic acid (IBX)^{5,18} due to the clean reaction profile observed. Although it required an extended reaction time of 72 hours, due to the limited solubility of IBX, dichloromethane was used as the reaction solvent in preference to the more commonly used dimethylsulfoxide. This was due to the simplification of the reaction workup on a large scale. This synthetic route gave an overall yield of 12% from the commercially available **5.20**, and was used routinely to deliver multi-gram quantities of aldehyde **5.19**.



Scheme 5.02: The synthesis of key aldehyde intermediate 5.19.

In order to allow the reductive amination as the final step, as described above (Scheme 5.01), the required amino ester building blocks were also synthesised. As synthetic tractability had been taken into consideration during the design process, the amino acid and alcohol building blocks required were all commercially available. In addition, a number of amino esters were already under synthesis for a programme of work ongoing elsewhere within our laboratories.^{5.06} As a result, it was not necessary to synthesise amino esters 5.23–5.28 (Figure 5.06), which were available in multi-gram quantities as *p*-toluenesulfonic acid salts.

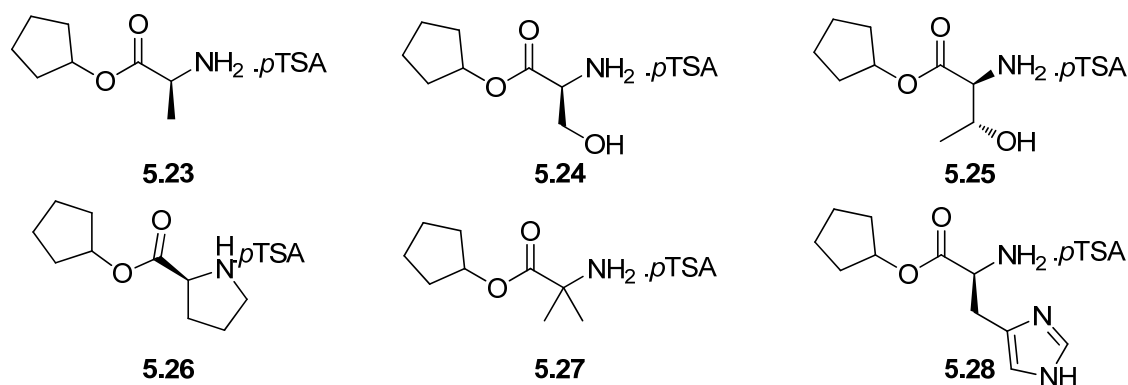
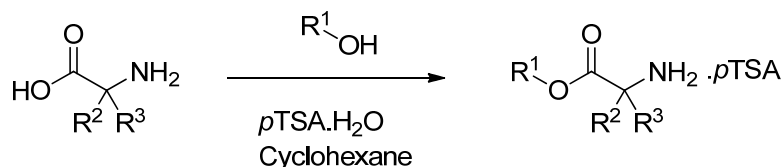


Figure 5.06: Structures of the available amino esters 5.23–5.28.

The majority of the remaining amino esters were synthesised using classic acid-catalysed esterification methodology (Scheme 5.03).^{5.19} This method was attractive as it was a one-step reaction from commercially available starting materials, with no protecting groups required.



Scheme 5.03: The general route used to synthesise the amino esters listed below (Table 5.04)

The relevant amino acids were heated with an excess of the relevant alcohols and *p*-toluenesulfonic acid, under reflux, with a Dean–Stark apparatus attached to remove water. The reactions were heated overnight, or over a weekend. In some cases the reaction had not progressed sufficiently, and heating was continued for a longer time. The isolation of the final amino esters as *p*-toluenesulfonic acid salts was achieved either by collecting the solid from the cooled reaction mixture by filtration, or by evaporation of volatile components followed by recrystallisation. The amino esters **5.29–5.39** obtained by this method, and their isolated yields, are listed below (Table 5.04).

The isolated yield of the majority of the esterification reactions was between 60% and 90%, although in a small number of cases the yield was lower. This appeared to be due to not optimising the recrystallisation solvent in each specific case, rather than poor reaction progression.

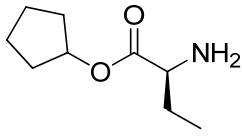
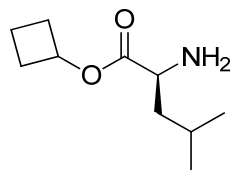
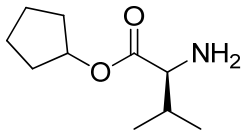
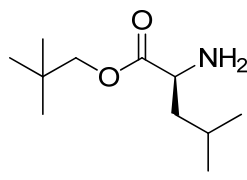
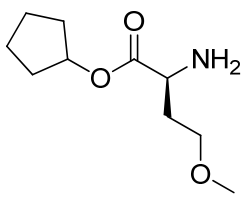
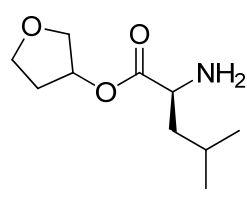
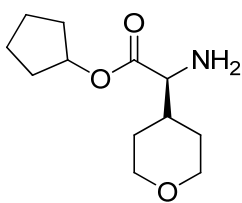
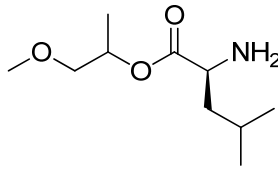
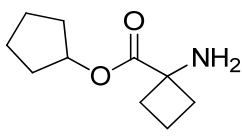
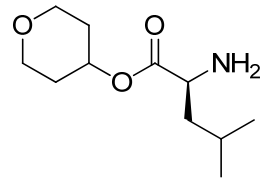
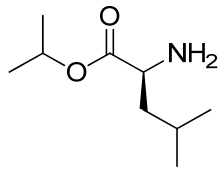
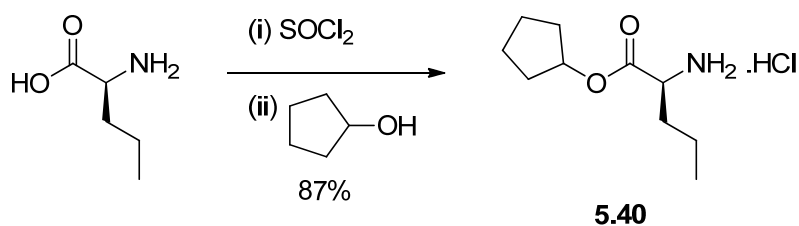
	Structure	Yield		Structure	Yield
5.29		63%	5.35		92%
5.30		77%	5.36		86%
5.31		56%	5.37		59%
5.32		35%	5.38		15%
5.33		65%	5.39		63%
5.34		70%			

Table 5.04: The isolated yields of amino esters 5.29–5.39, synthesised using the synthetic route described above (Scheme 4.03). All amino esters were synthesised as the pTSA salts.

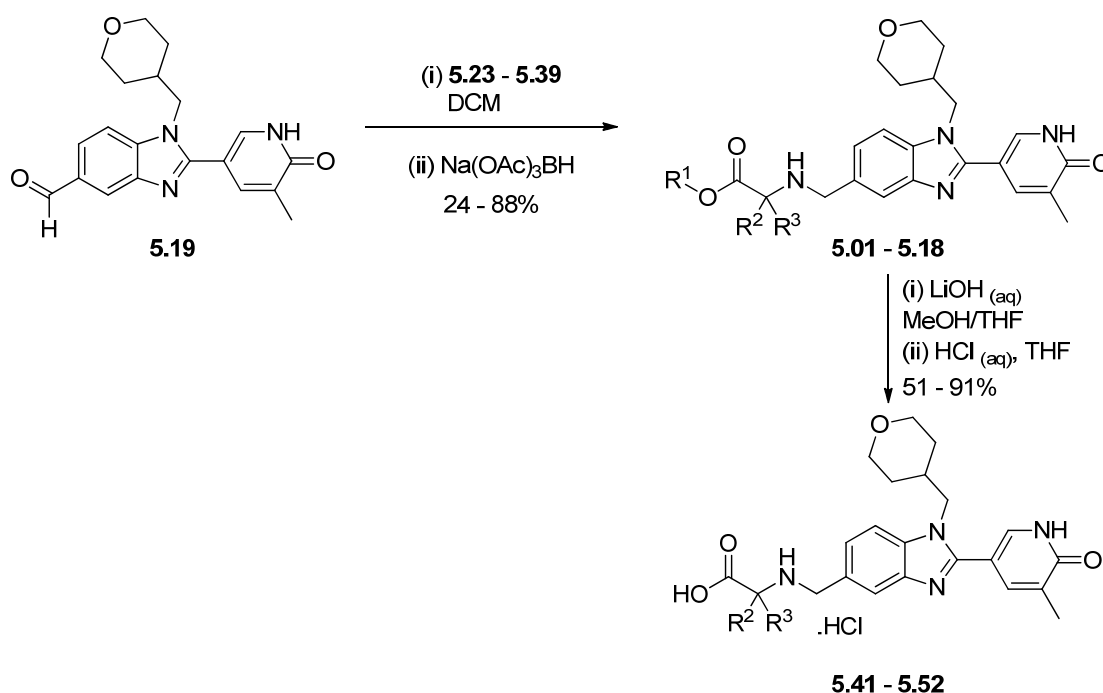
During the initial synthetic method development, alternative reaction conditions were attempted in addition to the acid-catalysed esterification described above. The most successful of these was the formation of the acid chloride using thionyl chloride, followed by the subsequent reaction with the cyclopentyl alcohol to form the ester (Scheme 5.04).^{5.20}



Scheme 5.04: The synthesis of amino ester **5.40** via the formation of the acid chloride.

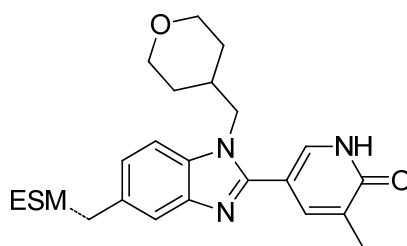
The amino ester **5.40** was synthesised as the hydrochloride salt using this methodology in 87% isolated yield. Although the acid-catalysed esterification was preferred for the synthesis of the majority of the amino esters, as it was a one-step process, this is an alternative method which may also be used in future to synthesise further amino esters if the acid-catalysed esterification was found to be unsuitable.

Once the synthesis of both aldehyde **5.19** and the amino esters were complete, they were reacted under standard reductive amination conditions to give the final ESM-containing esters **5.01** to **5.18** (Scheme 5.05). These final compounds were also hydrolysed to form the acids **5.41** to **5.52**, which were also required for biological screening to establish their biochemical potency.



Scheme 5.05: The synthesis of the final BET-ESM esters **5.01–5.18**, and their corresponding acids **5.41–5.52**. Triethylamine was added in the formation of **5.03**, and sodium hydroxide in the formation of **5.44**. Methanol was added to the salt formations in the case of **5.41**, **5.45** and **5.46**.

The reductive amination reactions proceeded in good isolated yields, with the majority over 50%. The major impurity seen in these reactions was the benzyl alcohol **5.22** (Scheme 5.02), presumably formed by reduction of the aldehyde starting material **5.19** prior to imine formation. All reactions were completed using the same reagents, with the exception of that to form **5.03**, where triethylamine was added to neutralise the hydrochloride salt. The isolated yields of the esters **5.01–5.18** are summarised below (Table 5.05).



	ESM-substituent	Yield		ESM-substituent	Yield
5.01		63%	5.10		24%
5.02		60%	5.11		64%
5.03		80%	5.12		44%
5.04		66%	5.13		55%

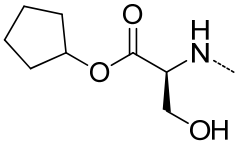
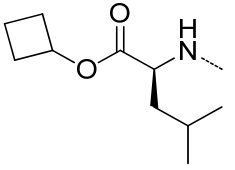
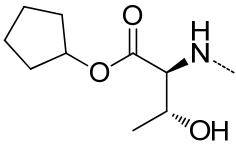
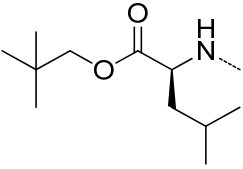
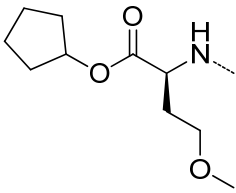
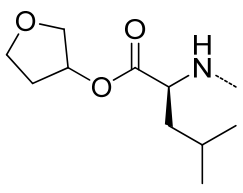
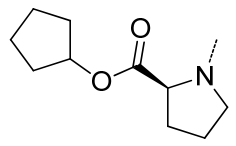
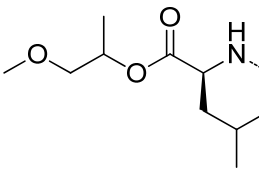
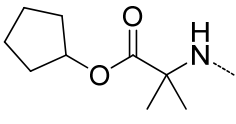
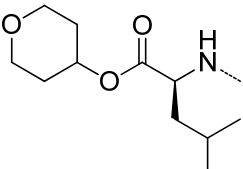
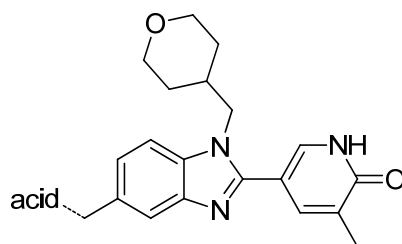
	ESM-substituent	Yield		ESM-substituent	Yield
5.05		81%	5.14		28%
5.06		88%	5.15		69%
5.07		52%	5.16		80%
5.08		47%	5.17		40%
5.09		49%	5.18		52%

Table 5.05: The BET–ESM esters **5.01–5.18** synthesised using the route described above (Scheme 5.04). The isolated yield of each reaction is shown.

Esters **5.01–5.12** were hydrolysed to acids **5.41–5.52** using lithium hydroxide in 51 to 91% isolated yield (Table 5.06). It was not necessary to hydrolyse esters **5.13–5.18**, as they all have the same acid substructure, **4.151**, which had previously been synthesised (Section 4.10). The hydrolysis of ester **5.04** proceeded particularly slowly, and sodium hydroxide was added to increase the reaction rate. The slow hydrolysis rate was presumed to be due to the hindered nature of the ester. After ester hydrolysis and purification, the substituted amino acids were converted to their hydrochloride salts using aqueous hydrochloric acid in tetrahydrofuran. In the first few salt formations performed (**5.41**, **5.45** and **5.46**), methanol was added to the reaction suspension to aid solubility. However, this led to some methyl ester formation and re-

purification was required, therefore the remaining salt formations were performed without methanol present.



Product	Acid-substituent	Parent ester	Isolated yield
5.41		5.01	91%
5.42		5.02	73%
5.43		5.03	85%
5.44		5.04	60%
5.45		5.05	70%
5.46		5.06	86%

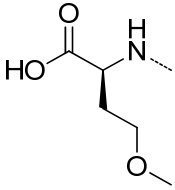
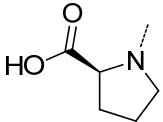
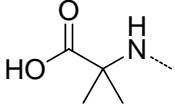
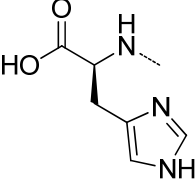
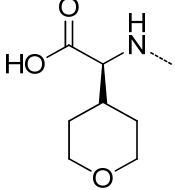
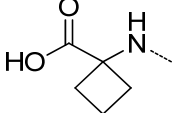
Product	Acid-substituent	Parent ester	Isolated yield
5.47		5.07	65%
5.48		5.08	73%
5.49		5.09	82%
5.50		5.10	76%
5.51		5.11	51%
5.52		5.12	58%

Table 5.06: The acid hydrolysis products **5.41–5.52** of esters **5.01–5.12**, synthesised using the route described above (Scheme 5.04). The isolated yield of each reaction is shown.

Using the synthetic strategy described above all of the desired ESM-containing esters **5.01–5.18**, and their corresponding ester hydrolysis products **5.41 – 5.52** were produced. The reaction conditions described tolerated a range of functional groups within the amino ester portion of the molecule with little or no optimisation. If a larger scale preparation of any of the final compounds were later required, optimisation of the reaction conditions for that specific compound may allow for an increased yield.

5.4 Biological Results and Analysis

The initial biological assays run on the compounds designed and synthesised above (Section 4.2 and 4.3) were used to understand the contribution of the various ESM substituents to the human whole blood (HWB) potency of the molecules. Compounds of interest were then further profiled to understand their potential as *in vivo* tool molecules. The screening cascade utilised is shown below (Figure 5.07).

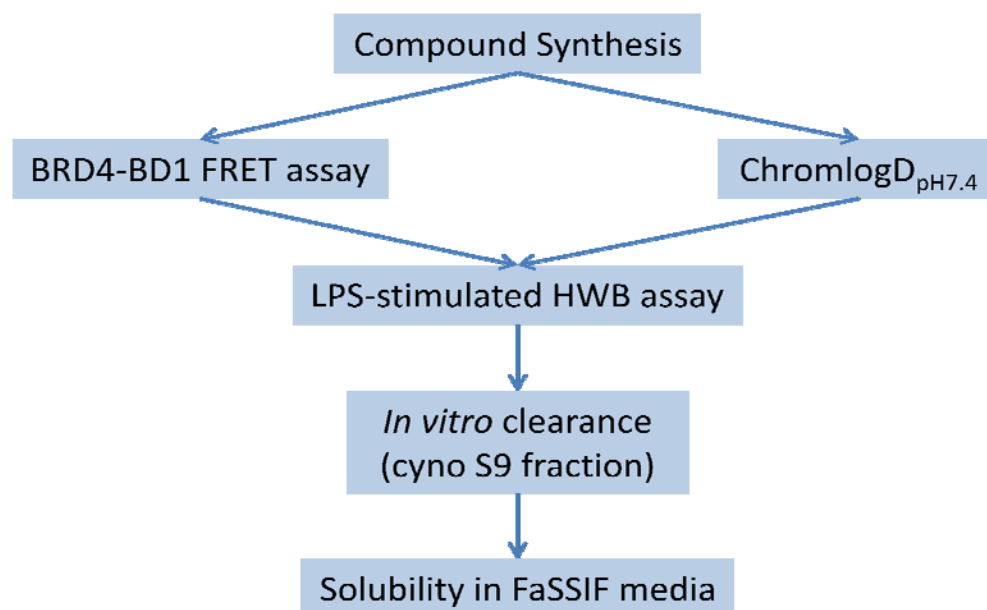


Figure 5.07: Screening cascade used to profile BET-ESM compounds.

Initially, the biochemical potency of both the ESM-containing esters, and their acid hydrolysis products, were established. The potencies were measured at the BD1 bromodomain of BRD4, using the FRET assay described previously (Section 3.4.3).^{A8} This established whether the ESM had been incorporated into the molecule without having an adverse effect on biochemical potency. In parallel, the measured ChromlogD_{pH7.4}^{A7} was established to determine the lipophilicity of the compounds, as well as to enable calculation of their PFI.

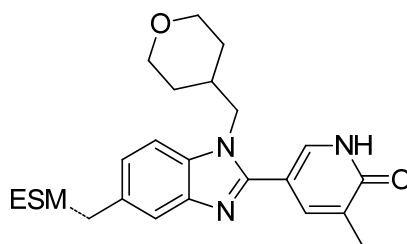
Where the ESM-containing esters showed a biochemical potency which was at least comparable with that of the previously-described *in vitro* probe molecule **4.52** (pIC₅₀ = 6.1), the compounds were progressed into the LPS-stimulated human whole blood (HWB) assay.^{A1} This assay was in the same format as that described previously (Section 3.4.3), where the effect of the compound on the production of MCP-1 was measured. The potency of compounds in a whole blood assay is classically affected by a number of factors. Key amongst these are biochemical potency,

cellular penetration, and plasma protein binding. Additionally, for compounds containing an ESM, the efficiency of turnover of the ester by hCE-1, as well as the retention of the resulting acid by the cell, may both lead to a higher local concentration of compound at the site of action and thereby an increased HWB activity. The shift between the pIC_{50} of the biochemical and HWB assays was therefore used to understand the effect of the different ESM's which had been incorporated into the compounds.

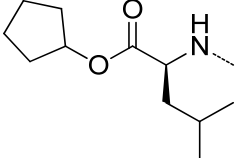
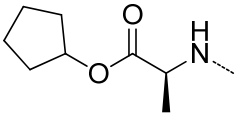
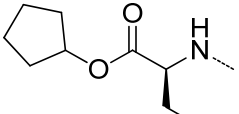
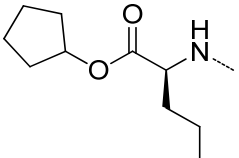
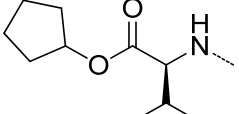
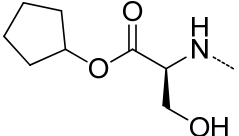
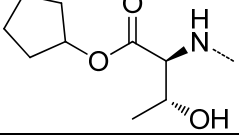
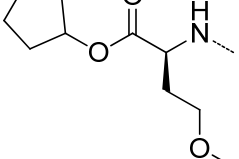
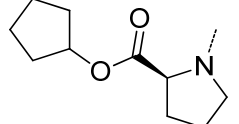
Once compounds were identified that met the potency criteria established at the outset of this programme of work (Figure 5.02: HWB $pIC_{50} > 7.0$, with a 10-fold increase in HWB potency over biochemical potency), they were considered for progression into an *in vitro* clearance assay.^{A12} In this assay, the stability of compounds in the hepatic S9 (post-mitochondrial supernatant) fraction^{5.05} of the cynomolgus monkey was measured. This fraction contains a mixture of Phase I and Phase II enzymes, and therefore gives a good prediction of overall metabolic stability. Compounds with lower $mChromlogD_{pH7.4}$ were prioritised for this experiment, as reduced lipophilicity is known to correlate with reduced clearance.^{5.21} A small number of compounds also had their solubility measured in a high-throughput solubility assay. In this assay, the solubility of the compounds at four hours in fasted stated simulated intestinal fluid (FaSSIF)^{5.02} was determined to establish whether the compounds were sufficiently soluble to support their further development.^{A13}

5.4.1 Primary Screening Data

The data generated in the biochemical and HWB assays for the ESM-containing esters, where the amino ester side chain had been modified (as designed in Section 5.2, Table 5.02) is shown below (Table 5.07). Their measured lipophilicity ($mChromlogD_{pH7.4}$) is also given.



Substructure of compounds in table overleaf.

	ESM Substituent	BRD4- BD1 pIC ₅₀ (n)	HWB (MCP-1) pIC ₅₀ (n)	ΔpIC ₅₀ (HWB - BRD4-BD1)	cChromlogD _{pH7.4} / mChromlogD _{pH7.4}
4.52		6.1 (10)	7.7 (33)	1.6	4.9 / 5.4
5.01		6.4 (3)	7.4 (4)	1.0	3.5 / 3.8
5.02		6.6 (3)	8.4 (4)	1.8	4.4 / 4.5
5.03		6.3 (2)	8.1 (2)	1.8	4.4 / 5.0
5.04		6.4 (3)	6.4 (4)	0	4.0 / 5.3
5.05		6.3 (3)	5.5 (1), < 5.5 (1)	n.d.	2.8 / 2.8
5.06		6.5 (5)	6.3 (2)	-0.2	3.1 / 3.4
5.07		6.0 (2)	7.2 (6), < 5.0 (2)	n.d.	3.5 / 4.0
5.08		6.2 (2)	7.0 (2)	0.8	3.7 / 4.6

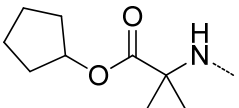
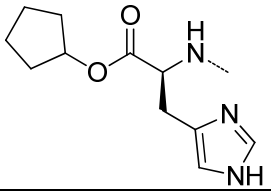
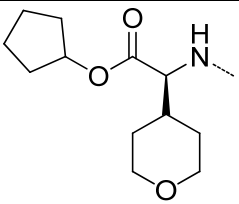
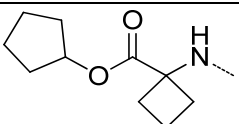
	ESM Substituent	BRD4-BD1 pIC ₅₀ (n)	HWB (MCP-1) pIC ₅₀ (n)	ΔpIC ₅₀ (HWB – BRD4-BD1)	cChromlogD _{pH7.4} / mChromlogD _{pH7.4}
5.09		6.3 (3)	6.7 (2)	0.4	4.0 / 4.4
5.10		6.3 (2)	5.6 (2)	-0.7	3.1 / 2.7
5.11		6.0 (2)	5.8 (2)	-0.2	3.7 / 4.1
5.12		6.4 (2)	6.3 (2)	-0.1	3.7 / 4.8

Table 5.07: Data for the ESM-containing esters **5.01–5.12**, compared to those of in vitro probe molecule **4.52**, in the BRD4-BD1 FRET assay,^{A8} and the HWB assay.^{A1} The ΔpIC₅₀ between these two assays is also given. Also shown are the measured^{A7} (m) and calculated^{B2} (c) ChromlogD_{pH7.4}. Where the HWB potency could not be accurately established, the ΔpIC₅₀ was not determined (n.d.). The substructure of the compounds is shown above the table.

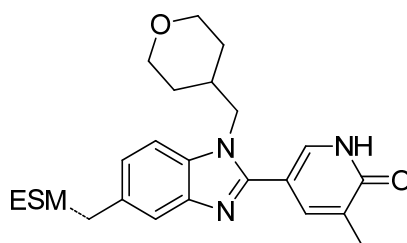
The biochemical activity of the ESM-containing esters **5.01–5.12** was consistent across the amino ester side-chain changes, within the expected variation of the assay. This was also the case for the corresponding acids **5.41–5.52**, which showed approximately a 0.5 log unit reduction in potency from the esters (Appendix 2, Table 3). The HWB assay data was therefore used to understand the SAR around the amino ester side-chain, as well as to prioritise compounds for further screening assays.

Compounds **5.01–5.03** show the impact of increasing the chain-length of the amino ester side-chain, and can also be compared to the leucine-containing **4.52**. The shift between the biochemical and HWB assays was consistent across the ethyl **5.02**, *n*-propyl **5.03**, and the leucine-containing **4.52**. These side-chains are therefore potential replacements for the isobutyl of **4.52**, in particular the ethyl **5.02** which has a ten-fold reduction in mChromlogD_{pH7.4}. The

methyl **5.01** gave a lower, but still significant, shift between the two assays. Potential explanations for this include a lower shape complementarity for the hCE-1 enzyme reducing the hydrolysis rate, or poorer stability to blood esterases due to lower steric hindrance around the ester leading to instability of the compound in human blood over the timescale of the assay.

The branched valine-containing ESM-ester **5.04** showed no shift between the biochemical and HWB assays. This was hypothesised to be due to the steric hindrance of the isopropyl side chain reducing the ester hydrolysis rate by hCE-1. This hypothesis is supported by the longer-than-expected reaction time required to chemically hydrolyse **5.04** to the corresponding acid **5.44**. Compound **5.04** also did not show the expected reduction in lipophilicity from **4.52**, with the measured $\text{ChromlogD}_{\text{pH}7.4}$ over 10-fold higher than the calculated value. For these reasons, the valine amino ester side-chain was not pursued further.

For both of the esters with an alcohol-containing side chain, the serine-containing **5.05** and the threonine-containing **5.06**, there was no positive shift between the biochemical and HWB assays. In the case of the threonine **5.06**, this may be due to the same steric hindrance hypothesised for the analogous valine **5.04**. However, this explanation is not consistent with the difference in potency between the serine-containing **4.05** and the ethyl amino ester **4.02**. One hypothesis considered was that the hydroxyl side-chain is not well tolerated within the active site of hCE-1. This is plausible due to the serine side-chain of hCE-1 that is present in this region as part of the catalytic machinery of the protein. A second hypothesis for the poor HWB activity of esters **5.05** and **5.06** was made using data from a high-throughput artificial membrane permeability (AMP) assay^{A10} which is summarised below for key examples (Table 5.08).



Substructure of compounds in table overleaf.

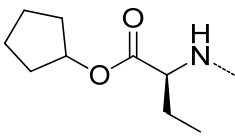
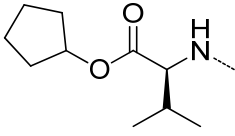
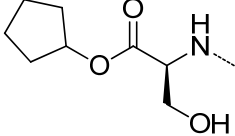
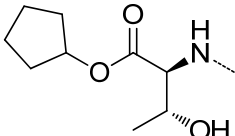
	ESM Substituent	HWB (MCP-1) pIC ₅₀ (n)	ΔpIC ₅₀ (HWB – BRD4-BD1)	AMP (nm/s)
5.02		8.4 (4)	1.8	100
5.04		6.4 (4)	0	220
5.05		5.5 (1), < 5.5 (1)	n.d.	< 3.0
5.06		6.3 (2)	-0.2	< 3.0, 16

Table 5.08: Artificial membrane permeability assay^{A10} results for the ESM-containing esters **5.02** and **5.04–5.06**. The data from the HWB assay,^{A1} and the ΔpIC₅₀ between this and the BRD4-BD1 FRET assay^{A8} is also given.

The permeability data generated on the hydroxyl-containing ESM esters **5.05** and **5.06** showed a very significant reduction in permeability compared to the analogous carbon-chain esters **5.02** and **5.03** to the extent where their permeability was not always measurable under the standard assay conditions. It was hypothesised that the poor HWB activity of these two compounds was at least in part due to poor permeability into cells. It is therefore not possible, on the basis of the HWB data, to conclude whether the serine- and threonine-containing esters **5.05** and **5.06** are hydrolysed by hCE-1.

Considering the potency of the remaining compounds which had been prepared (Table 5.07), compound **5.07**, with an ether-containing side-chain, had inconsistent results within the HWB assay, with a pIC₅₀ < 5 on the first two occasions it was screened, in duplicate, within the assay.

As this data was unexpected, a fresh sample was dispensed and the subsequent data showed an average pIC₅₀ of 7.2 across three duplicate test occasions. This suggests a shift of approximately ten fold between the biochemical and HWB assays. With a mChromlogD_{pH7.4} of 4.0, there is potential to investigate other ether side-chains within the amino ester. However, compound **5.07** was not progressed further due to the variability seen in the HWB data.

The only tertiary amine-containing ESM was that of the proline-containing **5.08**. This compound gave a lower, but still significant, shift between the biochemical and HWB assays. Compound **5.08** showed a ten-fold reduction in mChromlogD_{pH7.4} over the initial leucine-containing **4.52**, although it was noted that this was ten-fold higher than was predicted. Tertiary-amine-containing ESMs may be worthy of further investigation in the future, but due to the larger assay shift seen with the ethyl-containing **5.02**, which has a similar mChromlogD_{pH7.4}, further profiling of the proline-containing **5.08** was not carried out.

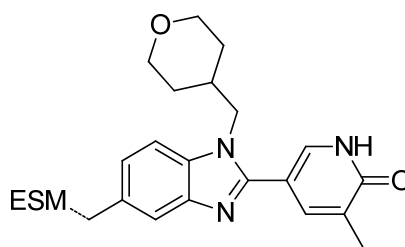
The addition of a second methyl group onto the amino-ester of **5.01** to give the *gem*-dimethyl ester **5.09** resulted in a compound that showed little shift between the biochemical and HWB assays. A similar lack of HWB potency was seen in the *spiro*-cyclobutyl analogue **5.12**. This may be as a result of poor complementarity to hCE-1, or increased steric hindrance around the ester. As a result of the poor HWB data for these compounds, geminal and spiro, substituents were not added onto other ESM esters.

The lowest HWB potency of the compounds synthesised was that of the histidine-containing ester **5.10**. This compound was comparable to that of the serine-containing ester **5.05** in having a significantly lower HWB activity than biochemical potency. The lack of permeability seen for ester **5.05** was also seen with ester **5.10**, which showed an artificial membrane permeability of < 3 nm/s. It was therefore hypothesised that the lack of potency in the HWB assay was due to poor cellular permeability, and that the turnover of the ester by hCE-1 could not be determined.

The tetrahydropyran analogue **5.11**, which had been designed as a lower lipophilicity analogue of the cyclohexyl-containing ESM within the literature ESM-HDAC analogue **3.02**, showed no shift between the biochemical and HWB assays. The lack of permeability seen for esters **5.05**, **5.06** and **5.10** was not mirrored by compound **5.11**, which had an artificial membrane permeability of 48 nm/s. It was therefore hypothesised that the lack of potency in the HWB assay was due to poor turnover of the ester by hCE-1. This was a surprising result due to the similarity of the ESM ester to that of the ESM-HDAC analogue **3.02**,^{5,15} and may be due to a lack of tolerance for polarity in the region of the protein that the tetrahydropyran oxygen sits.

Of all the compounds designed with alternative amino ester side chains, the most encouraging data in terms of shift between the HWB and biochemical assays, in conjunction with a lowered $mChromlogD_{pH7.4}$, were compounds **5.02** and **5.07**. The ethyl amino ester side-chains are therefore of further interest, as are ether-containing side-chains, although the inconsistency of the data for compound **5.07** must be kept in mind and ideally different ethers designed. A number of ester side-chains which resulted in a significantly reduced $mChromlogD_{pH7.4}$, such as the serine **5.05** and the threonine **5.06**, also have potential for further investigation. Increasing the cellular permeability of these molecules may provide compounds where the ability of hCE-1 to hydrolyse these amino esters can be determined.

A similar set of data was generated in the biochemical and HWB assays for the ESM-containing esters where the ester substituent had been modified (as designed in Section 5.2, Table 5.03). These data are shown below (Table 5.09), alongside the measured lipophilicity ($mChromlogD_{pH7.4}$) of the compounds.



	Substructure	BRD4-BD1 pIC_{50} (n)	HWB (MCP-1) pIC_{50} (n)	ΔpIC_{50} (HWB - BRD4-BD1)	$cChromlogD_{pH7.4}$ / $mChromlogD_{pH7.4}$
4.52		6.1 (10)	7.7 (33)	1.6	4.9 / 5.4
5.13		6.2 (2)	8.2 (2)	2.0	3.9 / 5.0

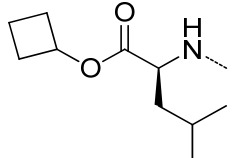
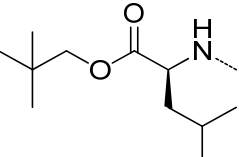
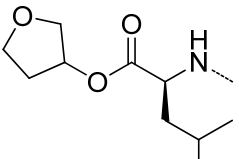
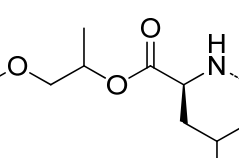
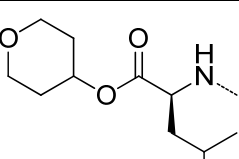
	Substructure	BRD4-BD1 pIC ₅₀ (n)	HWB (MCP-1) pIC ₅₀ (n)	ΔpIC ₅₀ (HWB - BRD4-BD1)	cChromlogD _{pH7.4} / mChromlogD _{pH7.4}
5.14		6.2 (4)	8.4 (4)	2.2	4.7 / 5.2
5.15		6.2 (4)	8.1 (1), > 8.8 (1)	n.d.	4.7 / 6.2
5.16		6.1 (6)	7.5 (2)	1.4	3.8 / 3.8
5.17		6.3 (2)	7.6 (2)	1.3	3.6 / 4.5
5.18		6.3 (4)	7.7 (2)	1.4	4.0 / 4.0

Table 5.09: Data for the ESM-containing esters **5.13–5.18**, compared to compound **4.52**, in the BRD4-BD1 FRET assay,^{A8} and the HWB assay.^{A1} The ΔpIC₅₀ between these two assays is also given. Also shown are the measured^{A7} (m) and calculated^{B2} (c) ChromlogD_{pH7.4}. Where the HWB potency could not be accurately established, the ΔpIC₅₀ was not determined (n.d.). The substructure of the compounds is shown above the table.

The BRD4-BD1 biochemical potency of all six esters **5.13–5.18** was similar to that measured for compound **4.52**. This was as a result of the ester portion of the molecules being positioned away from the bromodomain of the protein and exposed to solvent.

Where the size of the ester had been reduced over the cyclopentyl **4.52**, such as in the isopropyl ester **5.13** and the cyclobutyl ester **5.14**, the shift between the biochemical and HWB assays was around 100-fold. This was significantly higher than the shift seen for compound **4.52**. This was attributed to the increased ability of these esters to be hydrolysed by hCE-1. These esters would be expected to also be more labile to other blood esterases, but they maintain sufficient blood stability over the time course of the HWB assay. The reduction in size of the cyclopentyl ester to the isopropyl of **5.13** and the cyclobutyl of **5.14** did not have however the expected impact on lowering lipophilicity. This was particularly the case for the isopropyl ester **5.13**, where the $m\text{ChromlogD}_{\text{pH}7.4}$, was over ten-fold higher than predicted.

Replacing the cyclopentyl ester of **4.52** with the neopentyl of compound **5.15** led to a high HWB potency. On two test occasions, the pIC_{50} was higher than 8.8, which was the maximum that was able to be determined using this assay format. It was therefore not possible to accurately define the shift between the biochemical and HWB assays, but this shift was at the least 100-fold. Unfortunately, the calculated $\text{ChromlogD}_{\text{pH}7.4}$ was a particularly poor prediction in the case of compound **5.15**, being around 30-fold too low. The $m\text{ChromlogD}_{\text{pH}7.4}$ was much higher than compound **4.52**, and therefore compound **5.15** was not suitable for further progression. However, due to the high shift between HWB and biochemical assays, the neopentyl ester may still be of interest if it were combined with amino ester side-chains which would lower the overall lipophilicity of the molecule.

A single atom change in the cyclopentyl ester of compound **4.52** to give the tetrahydrofuryl ester **5.16** produced a compound with comparable HWB potency. This implied that the tetrahydrofuryl substituent was tolerated within the hCE-1 enzyme, and did not reduce the turnover rate of the ester. The benefit of the tetrahydrofuryl **5.16** over the cyclopentyl analogue **4.52** is a vastly reduced lipophilicity. The $m\text{ChromlogD}_{\text{pH}7.4}$ of **5.16** is 3.7, the lowest of any of the analogues which maintain a comparable HWB potency to **4.52**. As compound **5.16** met the criteria for progression in terms of HWB potency and PFI (Figure 5.02), it was progressed into further assays to determine its *in vitro* clearance and FaSSIF solubility (Section 5.4.2).

As for the tetrahydrofuryl **5.16**, the acyclic ether analogue **5.17** also showed comparable HWB potency to compound **4.52**. However, despite the similar calculated $\text{ChromlogD}_{\text{pH}7.4}$ for esters **5.16** and **5.17**, the measured value was around 10-fold higher in the case of **5.17**. The open-chain ether analogue **5.17** was therefore not progressed further.

The tetrahydropyranyl ester **5.18** again showed comparable HWB potency to compound **4.52**. In this case the measured $\text{ChromlogD}_{\text{pH}7.4}$ was slightly higher than that of the tetrahydrofuryl analogue **5.16**, but still significantly lowered over **4.52**. In case of unfavourable data on compound **5.16**, the tetrahydropyranyl analogue **5.18** would still be of interest.

The complete data set generated on the analogues where the ESM of the *in vitro* probe **4.52** has been modified (Tables 5.06 and 5.08) showed that despite all compounds having comparable biochemical potencies, the HWB potency of the molecules ranged from a pIC_{50} from the lower to the upper limit of the assay, a range in potencies of over 1000-fold. This was due to the impact on HWB potency of factors such as the cellular permeability of the compounds as well as hydrolysis of the amino ester by hCE-1. The most promising compound identified was the tetrahydrofuryl ester **5.16** which maintained a HWB potency comparable with the *in vitro* probe molecule **4.52** whilst reducing the $\text{mChromlogD}_{\text{pH}7.4}$ by approximately 100-fold, bringing the molecule into a drug-like physicochemical space.

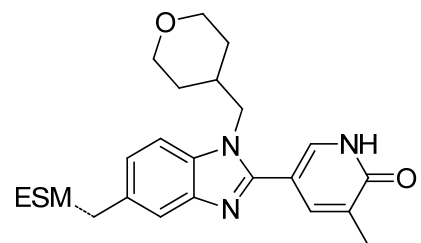
5.4.2 Secondary Screening Data for Compounds of Interest

As a result of the promising HWB assay data (Section 5.4.1), two compounds were selected for progression into *in vitro* metabolic clearance studies, using cynomolgus monkey S9 liver fraction.^{A12} These compounds also had their solubility measured in FaSSIF media.^{A13}

The first compound selected for progression was the threonine cyclopentyl ester **5.06**. This ester had the lowest lipophilicity ($\text{mChromlogD}_{\text{pH}7.4} = 3.3$) of the compounds which maintained measurable HWB activity. Whilst there was no significant shift from the biochemical to HWB assay for this compound, this may be explained by its low permeability (Table 5.08). The impact of lowering lipophilicity on *in vitro* clearance could be better understood by profiling this compound, and permeability may then be optimised in future work. As the cells in the *in vitro* clearance assay are homogenised, the lack of cellular permeability of the compound had no impact on the data generated.

The second compound selected for progression was the leucine tetrahydrofuryl ester **5.16**. This compound also has an acceptable lipophilicity ($\text{mChromlogD}_{\text{pH}7.4} = 3.7$), and was used to understand the impact of the tetrahydrofuryl ester on *in vitro* clearance. As ester **5.16** meets the other criteria set out at the outset of this programme of work (Figure 5.02), further profiling this compound will also identify whether it is suitable for progression into *in vivo* studies.

The data generated on compounds **5.06** and **5.16** is shown below (Table 5.10).



	Substructure	mChromlogD _{pH7.4}	BRD4-BD1 pIC ₅₀ (n)	HWB (MCP-1) pIC ₅₀ (n)	ΔpIC ₅₀ (HWB – BRD4-BD1)	Cyno S9 clearance (ml/min/g)	FaSSIF solubility (μg/ml)
4.52		5.4	6.1 (10)	7.7 (33)	1.6	25.6	165
5.06		3.4	6.5 (3)	6.3 (2)	-0.2	6.6	> 1000
5.16		3.7	6.1 (4)	7.5 (4)	1.4	19.2	> 908

Table 5.10: In vitro clearance of esters **5.06** and **5.16** in cynomolgus S9 fraction,^{A12} and their solubility in FaSSIF media,^{A13} in comparison with ester **4.52**. Included are data from the BRD4-BD1 mutant FRET assay,^{A8} the MCP-1 readout of the LPS-stimulated HWB assay,^{A1} and the ΔpIC₅₀ between these two assays. The measured ChromlogD_{pH7.4}^{A7} is also shown. The substructure of the compounds is shown above the table.

Pleasingly, in the case of both esters **5.06** and **5.16**, the solubility in FASSIF media was significantly improved over compound **4.52**. This is likely to be due to the significantly lower lipophilicity of these two compounds.^{5.22}

Despite its much lower lipophilicity, the tetrahydrofuranlyl ester **5.16** has only a slightly lower *in vitro* clearance compared to its cyclopentyl analogue **4.52**. It was hypothesised that this was due to lower metabolic stability of the tetrahydrofuranlyl ester negating any positive effect on metabolic stability due to its reduced lipophilicity. This was supported by a more detailed study of the *in vitro* clearance data, where the amount of compound present at 45 mins was measured when the cofactors NADPH (reduced nicotinamide adenine dinucleotide phosphate) and UDPGA (uridine diphosphate glucuronic acid) were not added to the S9 fraction. Measurement with NADPH absent gives a measurement of non-CYP450 mediated metabolism only, as the CYP450 enzymes require NADPH to be activated. In addition, removal of UDPGA does not allow glucuronidation, one method of Phase II metabolism, to be carried out. For compound **4.52** only 8% of the compound remained with NADPH and UDPGA absent at 45 minutes, and for compound **5.16** only 2% of the compound remained. This indicated that non-CYP450 mediated metabolism was the primary route of metabolism for both these compounds; it was hypothesised that this was as a result of ester hydrolysis. The established correlation of metabolism with lipophilicity is a result of the rate of metabolism by CYP450 enzymes, which have high affinity for lipophilic substrates.^{5.23} Therefore the reduction of lipophilicity from compound **4.52** to compound **5.16** does not impact the *in vitro* clearance.

In contrast to the *in vitro* clearance data generated for compound **5.16**, the threonine cyclopentyl ester **5.06** showed a significantly reduced *in vitro* clearance compared with compound **4.52**. In this case, the *in vitro* clearance was appropriate for progression into *in vivo* DMPK studies. The amount of compound **5.06** present after 45 mins in the absence of the cofactor NADPH was 76%, whereas with NADPH present only 11% remained. The difference between the two values indicates a combination of processes are involved in the metabolism of this compound. It was hypothesised that the reduced non-CYP450 mediated metabolism in this case was as a result of increased stability of the ester due to the greater steric bulk of the threonine side-chain.

Although compound **5.06** met the *in vitro* clearance criteria for *in vivo* DMPK studies to be initiated, it was not progressed due to its poor HWB potency. Nonetheless, the positive HWB and *in vitro* clearance data for compounds **5.16** and **5.06** respectively gave encouragement that further medicinal chemistry could yield a single compound which met all of the *in vivo* probe molecule criteria outlined previously (Figure 5.02).

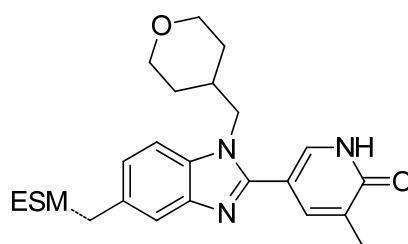
5.5 Further Medicinal Chemistry Design

To optimise the previously identified compounds **5.06** and **5.16** towards an *in vivo* probe molecule which met the initial compound criteria (Figure 5.02), further medicinal chemistry was required. The areas for focus were identified as the optimisation of cellular permeability and hCE-1 hydrolysis rate, whilst maintaining lipophilicity as low as possible. Given the positive *in vitro* clearance data for compound **5.06** in comparison with **4.52** (Table 5.10), all compounds were designed to have a calculated ChromlogD_{pH7.4} < 4. This was to reduce the risk of a high *in vitro* clearance driven by high CYP450 mediated metabolism.

Use of *in silico* modelling tools to design compounds within the pyridone benzimidazole chemical series with improved permeability was not successful, as all lower lipophilicity compounds profiled within this series were predicted to have low permeability. This was hypothesised to be due to the high size to lipophilicity ratio of compounds within this series where the cChromlogD_{pH7.4} was < 4. Although programmes of work were established elsewhere within our laboratories to redress this by looking at smaller chemical templates, the encouraging data within this chemical series meant that an alternative design strategy to increase permeability was required to build on this promising area.

It has been suggested that as well as lipophilicity, the hydrogen bonding ability of a compound has some influence in the cellular permeability of compounds, and that a lower hydrogen bond donor count can result in increased permeability.^{5,24} Modifications to compound **5.06** were therefore designed which reduced hydrogen bond donor count.

As discussed previously, the low permeability of compound **5.06** precludes understanding of whether the lack of biochemical to HWB assay potency shift is due to its low permeability alone. Low turnover of compound **5.06** by hCE-1 may also be a contributing factor. To understand the ability of hCE-1 to hydrolyse the amino esters, compounds were profiled in an hCE-1 enzyme assay, which was newly accessible within our laboratories. This measured the specific activity of the compounds with isolated hCE-1 protein.^{A14} The assay was low throughput, and therefore data for all compounds could not be generated. However, a subset of the compounds were profiled and the data is shown below (Table 5.11).

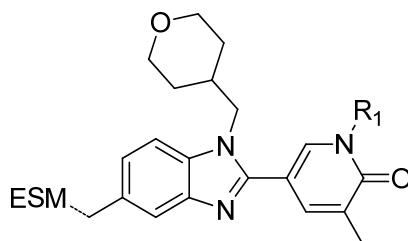


	Substructure	BRD4-BD1 pIC ₅₀ (n)	HWB (MCP-1) pIC ₅₀ (n)	ΔpIC ₅₀ (HWB – BRD4-BD1)	hCE-1 Activity (n) (μM/min/μM)
4.52		6.1 (10)	7.7 (33)	1.6	6.5 (4)
5.04		6.4 (3)	6.4 (6)	0	0.0 (1)
5.06		6.5 (5)	6.3 (2)	-0.2	0.0 (2)
5.15		6.2 (4)	8.1 (2), > 8.8 (2)	n.d.	30.9 (1)

Table 5.11: Specific activity of esters **4.52**, **5.04**, **5.06**, **5.15** at hCE-1, measured in μM/min/μM protein.^{A14} Included are BRD4-BD1,^{A8} and HWB assay data,^{A1} and the ΔpIC₅₀ between these assays. Where HWB potency could not be established, ΔpIC₅₀ was not determined (n.d.).

For the small set of compounds profiled, the rank order of the hCE-1 activity was consistent with the shift between the biochemical and HWB assays. Comparison of cyclopentyl ester **4.52** with its neopentyl analogue **5.15** showed that the neopentyl ester was more easily hydrolysed by hCE-1, and there was a corresponding increase in HWB activity. The valine and threonine cyclopentyl ester analogues **5.04** and **5.06** showed no detectable hydrolysis by hCE-1 under the assay conditions than the leucine analogue **4.52**, and significantly lower HWB activity. This is

likely to be due to a combination of poorer shape complementarity with the hCE-1 enzyme, as well as increased steric bulk around the ester. To increase the hydrolysis rate of compounds **5.04** and **5.06**, both of these factors would be investigated. Based on the strategy of reducing the hydrogen bond donor count, controlling lipophilicity, and modifying the steric bulk around the amino ester, six compounds were designed (Table 5.12).



	Amino Ester (ESM)	R ¹	cChromlogD _{pH7.4}	HBD
5.06		H	3.1	3
5.53		Me	3.8	2
5.54		H	3.9	2
5.55		H	2.9	3
5.56		Me	3.6	2
5.57		Me	3.7	2
5.58		H	3.8	2

Table 5.12: Compounds for synthesis, their cChromlogD_{pH7.4}^{B2} and the number of hydrogen bond donors (HBD). Compound **5.06** is included in the table for comparison.

To reduce the hydrogen bond donor count of compound **5.06**, the *N*-methyl pyridone analogue **5.53** was designed. This change was expected to increase the biochemical potency at BRD4-BD1, based on the potency difference of compounds **4.32** and **4.33** described previously (Chapter 4, Table 4.06). Despite the lipophilicity increase, expected from the addition of a methyl group, compound **5.53** was predicted to have a ChromlogD_{pH7.4} below 4.

The valine-containing compound **5.04** had a lower hydrogen bond count than its threonine-containing analogue **5.06**. To increase hydrolysis by hCE-1, the cyclopentyl ester of compound **5.04** was replaced by the neopentyl ester to give compound **5.54**. This compound was predicted to have a ChromlogD_{pH7.4} below 4, although the poor prediction for **5.04** suggested that this may be an underestimate. However, the compound would be made to interrogate this hypothesis.

To increase the ester hydrolysis rate, an ESM containing the neopentyl ester of threonine was also designed. The threonine neopentyl ester **5.55** was the direct analogue of cyclopentyl ester **5.06**, which would enable the increase in hydrolysis by hCE-1 to be measured. The pyridone *N*-methyl analogue **5.56** was also included, as it had a lower hydrogen bond donor count.

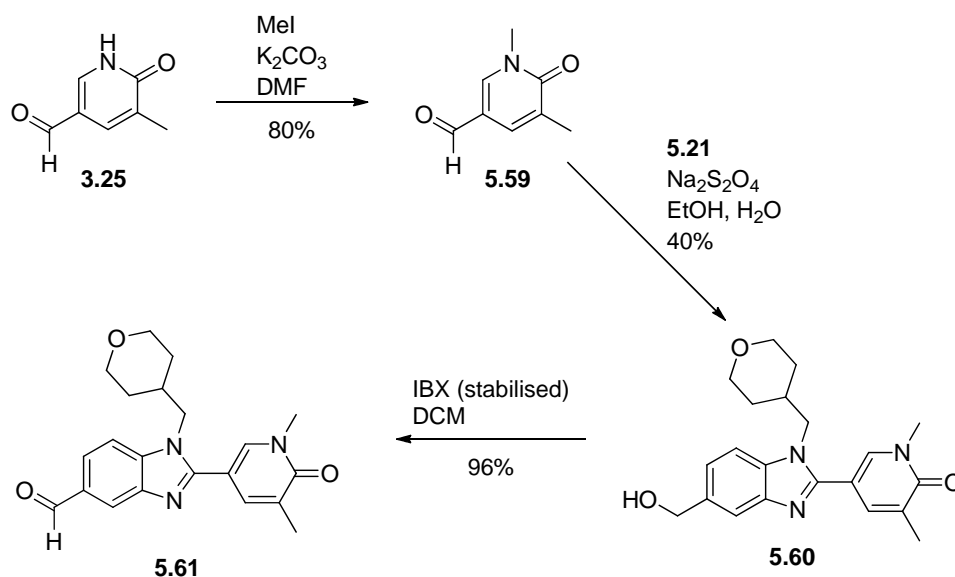
Due to the difference in the rate of hydrolysis by hCE-1 between the threonine-containing ester **5.06** and the leucine-containing **4.52**, it was hypothesised that the replacement of the cyclopentyl ester by the neopentyl ester may not sufficiently increase the rate of hydrolysis by hCE-1. The isobutyl ester analogue **5.57**, where the ester was less sterically hindered, was designed to increase the ester hydrolysis rate further. The pyridone *N*-methyl template with lower hydrogen bond donor count was selected for this ESM, due to its lower predicted lipophilicity, to give the best chance of cellular permeability.

The final analogue designed was compound **5.58**, a direct analogue of the serine-containing **5.05** where the hydroxyl of the serine side-chain had been methylated. As for the *N*-methyl pyridone analogues, this compound was designed to reduce the hydrogen bond count over compound **5.06**. This compound was also designed to address the low hydrolysis rate by hCE-1 of compound **5.06** as the tertiary centre of the amino acid side-chain has been removed.

5.6 Further Synthesis of Target Molecules

Synthesis of the compounds designed above (Section 5.5) was performed using synthetic routes as described for the previous ESM-BET compounds (Section 5.3). The aldehyde intermediate **5.19** (Scheme 5.02) was used for the reductive amination reactions to form *NH*-pyridones **5.54**, **5.55** and **5.58**. The route used previously to synthesise aldehyde **5.19** (Scheme 5.02) was

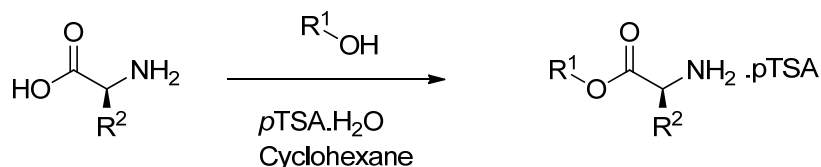
adapted to synthesise its *N*-methyl pyridone aldehyde analogue **5.61**, as shown below (Scheme 5.06).



Scheme 5.06: The synthesis of the key *N*-methyl pyridone aldehyde intermediate **5.61**.

Methylation of the previously described pyridone aldehyde intermediate **3.25** (Scheme 3.01) with methyl iodide gave its *N*-methyl pyridone analogue **5.59** in 80% yield. This was reacted with the aminophenyl intermediate **5.21** (Scheme 5.02) under standard reductive cyclisation conditions to give the benzimidazole **5.60**. The alcohol was oxidised using stabilised IBX to provide aldehyde **5.61** in 98% isolated yield. This synthetic route was used to produce aldehyde **5.61** in 31% yield over three steps from aldehyde **3.25**.

The novel amino esters required to synthesise compounds **5.54** to **5.57** were prepared using the acid-catalysed esterification methodology used for previous amino esters (Scheme 5.03). The reactions to form amino esters **5.54** to **5.57** are shown below (Scheme 5.07).



Scheme 5.07: The general route used to synthesise the amino esters listed below (Table 5.13)

Amino esters **5.62**, **5.63** and **5.64** were synthesised using these reaction conditions (Table 5.13), with a Dean–Stark apparatus again used to push the equilibrium towards ester formation.

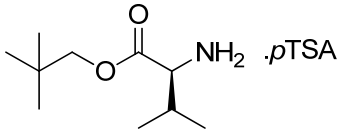
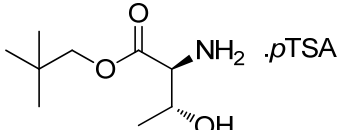
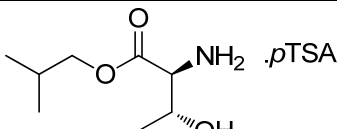
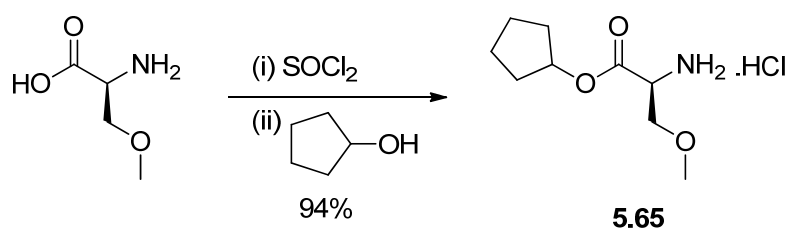
Amino ester	Structure	Isolated yield
5.62	 .pTSA	56%
5.63	 .pTSA	87%
5.64	 .pTSA	30%

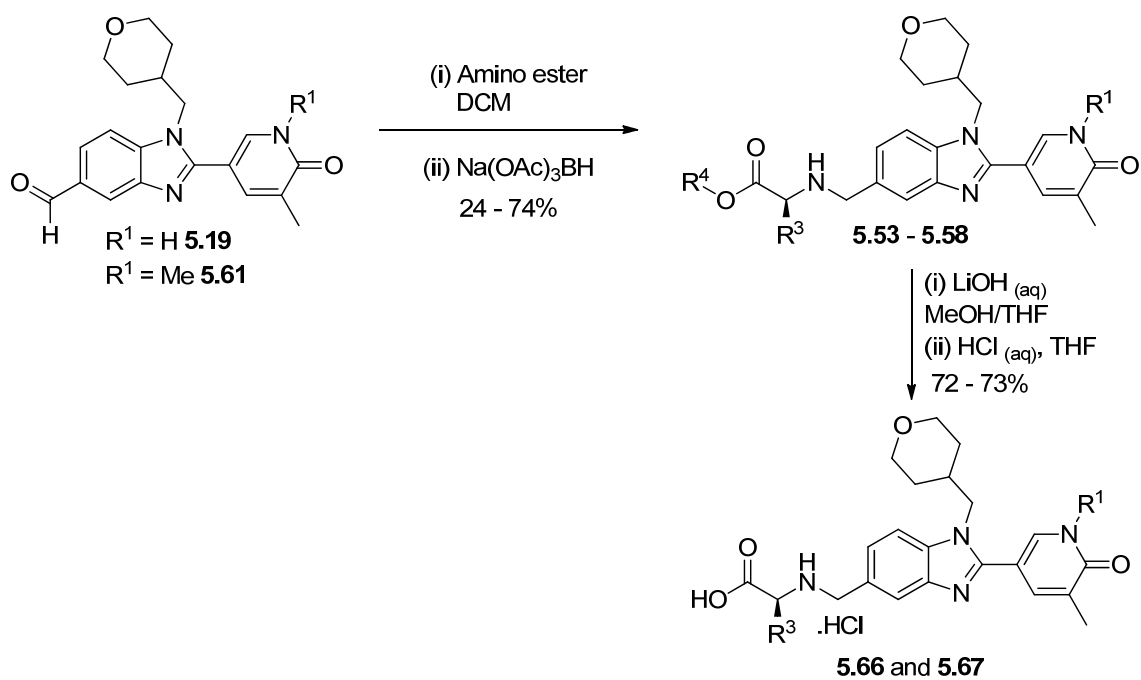
Table 5.13: The amino esters synthesised using the synthetic route described in Scheme 5.07.

The reaction to form amino ester **5.65** was also attempted using acid-catalysed esterification conditions, but on this occasion there was no evidence of ester formation. The amino ester **5.65** was instead accessed via the acid chloride, as previously described for amino ester **5.40** (Scheme 5.04), as shown below (Scheme 5.08).

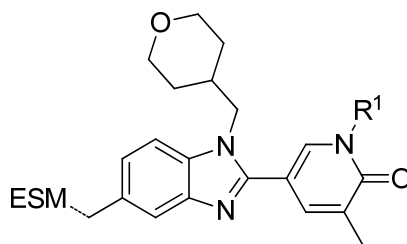


Scheme 5.08: The synthesis of **5.65** via the formation of the acid chloride.

The reductive amination reactions proceeded in acceptable isolated yields, ranging from 24–74%. The isolated yields of the BET–ESM esters **5.53** to **5.58** are shown below (Table 5.14).



Scheme 5.09: The synthesis of BET-ESM esters **5.53** to **5.58**, and acids **5.66**–**5.67**. Triethylamine was added to form **5.56**–**5.58**. The full ESM structures are listed in Table 5.14.



	ESM	R ¹	Yield		ESM	R ¹	Yield
5.53		Me	63%	5.56		Me	74%
5.54		H	50%	5.57		Me	24%
5.55		H	31%	5.58		H	71%

Table 5.14: The BET-ESM esters synthesised using the synthetic route in Scheme 5.09.

The corresponding ester hydrolysis products for compounds **5.54** (acid **5.44**) and **5.55** (acid **5.46**) have already been synthesised (Section 5.4). Only two further ester hydrolysis reactions were required to produce the remaining acids. Esters **5.53**, **5.56** and **5.57** are all hydrolysed to the parent acid **5.66**, and ester **5.58** is hydrolysed to the parent acid **5.67**. Esters **5.53** and **5.58** were hydrolysed using aqueous lithium hydroxide, as shown below (Table 5.15).

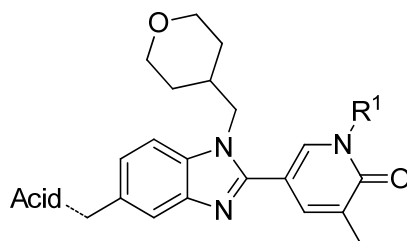
Product	Starting material	R ¹	Isolated yield
5.66	5.53	Me	73%
5.67	5.58	H	72%

Table 5.15: The acid hydrolysis products **5.66** and **5.67**, synthesised using the route described in Scheme 5.09. The starting material ester used in each reaction is shown.

As previously (Section 5.3), the synthetic route was tolerant of the required range of functional groups, allowing synthesis of all compounds (Table 5.12) in sufficient quantity and purity for biological testing.

5.7 Further Biological Results and Analysis

The compounds synthesised above (Section 5.6) were profiled using the standard screening cascade for BET-ESM compounds (Figure 5.06). This includes measurement of biochemical potency using the BRD4-BD1 FRET assay^{A8} and measurement of HWB potency using the MCP-1 readout of the LPS-stimulated HWB assay.^{A1} In addition, the artificial membrane permeability^{A10} and activity at hCE-1^{A14} were also measured (Table 5.16).



Substructure of compounds in table overleaf.

As hypothesised during compound design, the reduction in hydrogen bond donors on addition of the *N*-methyl pyridone substituent led to an increase in artificial membrane permeability of compound **5.53** compared to its *NH*-pyridone analogue **5.06**. However, this did not lead to the desired shift in potency between the biochemical and HWB assays for this compound, which can be rationalised by the hydrolysis of the ester by hCE-1 being undetectable.

The valine-containing neopentyl ester **5.54** showed a significantly increased HWB potency ($pIC_{50} = 7.2$) over its cyclopentyl analogue **5.04** ($pIC_{50} = 6.4$), which is likely to be due to an increased turnover by hCE-1. However, due to its very high measured lipophilicity this compound was not progressed further, and the hCE-1 assay data was not generated.

The threonine-containing neopentyl ester **5.55** showed little shift between the biochemical and HWB assays ($\Delta pIC_{50} = 0.3$), and as was the case for its cyclopentyl analogue **5.06**, the permeability of compound **5.55** was poor. However, incorporation of the *N*-methyl pyridone to give compound **5.56** again increased the permeability of the compound. This, in combination with an expected increased activity at hCE-1 due to the more labile neopentyl ester, led to a 10-fold shift between the biochemical and HWB assay. Unfortunately, the measured $ChromlogD_{pH7.4}$ was again significantly higher than predicted and therefore this compound was not progressed further.

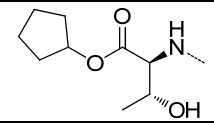
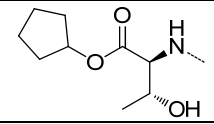
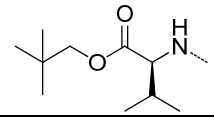
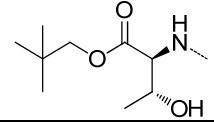
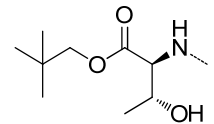
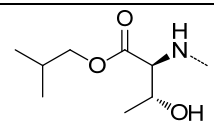
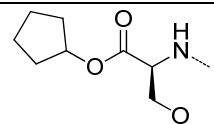
	Substructure	R ¹	BRD4-BD1 pIC ₅₀ (n)	HWB (MCP-1) pIC ₅₀ (n)	ΔpIC ₅₀ (HWB – BRD4-BD1)	cChromlogD _{pH7.4} / mChromlogD _{pH7.4}	AMP (nm/s)	hCE-1 Activity (μM/min/μM)
5.06		H	6.5 (5)	6.3 (2)	-0.2	3.1 / 3.4	< 3, 16	0.0 (2)
5.53		Me	7.3 (5)	7.8 (8)	0.5	3.8 / 3.7	93	0.0 (1)
5.54		H	6.6 (2)	7.2 (2)	0.6	3.9 / 5.9	300	N/A
5.55		H	6.6 (2)	7.0 (2)	0.4	2.9 / 3.9	13	0.1 (1)
5.56		Me	7.3 (4)	8.6 (2)	1.3	3.6 / 4.4	175	N/A
5.57		Me	7.2 (6)	8.3 (8), >8.8 (2)	1.0	3.7 / 3.6	122	0.4 (1)
5.58		H	6.2 (3)	7.3 (4)	1.1	3.8 / 3.8	40	0.5 (1)

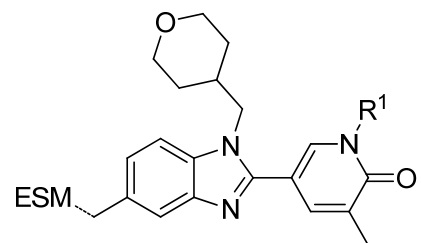
Table 5.16: Biological assay results for ESM-containing esters 5.53 – 5.58, compared to compound 5.06, in the BRD4-BD1 FRET assay,^{A8} and the HWB assay.^{A1} The ΔpIC₅₀ between these two assays is given. Also shown are the measured^{A7} and calculated^{B2} ChromlogD_{pH7.4}, artificial membrane permeability (AMP),^{A10} and hCE-1 specific activity.^{A14} The substructure of the compounds is shown on the previous page.

In contrast, the threonine-containing isobutyl ester **5.57** had a measured $\text{ChromlogD}_{\text{pH}7.4}$ of 3.6, and maintained the encouraging HWB profile of compound **5.56**. This compound was hydrolysed by hCE-1, and the presence of the pyridone *N*-methyl substituent conferred sufficient permeability. These combined properties resulted in a 10-fold shift between the biochemical and HWB assays. Compound **5.57** was therefore progressed into *in vitro* clearance studies.

The methoxymethyl analogue **5.58**, which used methylation of the hydroxyl of the serine-containing **5.05** to reduce hydrogen bond donor count, also showed increased permeability. This compound was also hydrolysed by hCE-1, leading to a 10-fold shift between the biochemical and HWB assays. This compound had a measured $\text{ChromlogD}_{\text{pH}7.4}$ of 3.8, was therefore also progressed into *in vitro* clearance studies.

The *in vitro* clearance of compounds **5.57** and **5.58** were measured in the previously described cynomolgus monkey liver S9 fraction,^{A12} and their solubility in FaSSIF media^{A13} was also determined (Table 5.17).

As was seen for previous examples (Table 5.10), the reasonably low lipophilicity of compounds **5.57** and **5.58** results in a high solubility in FaSSIF media, consistent with that set out for further progression. Both compounds also show reduced *in vitro* clearance over the initial leucine-containing *in vitro* probe **4.52** (26 ml/min/g). The clearance of the threonine-containing isobutyl ester analogue **5.57** is particularly low, and compatible with the criteria set out at the outset of this programme of work for progression into *in vivo* studies (Figure 5.02). It was hypothesised that compound **5.57** provided a balance between good-enough ester hydrolysis to confer an increased HWB activity, and a stable-enough ester to confer a low *in vitro* clearance. Compound **5.57** was the first example of a BET–ESM compound which met all of the criteria for progression (Figure 5.02), and was considered a candidate for *in vivo* DMPK studies.

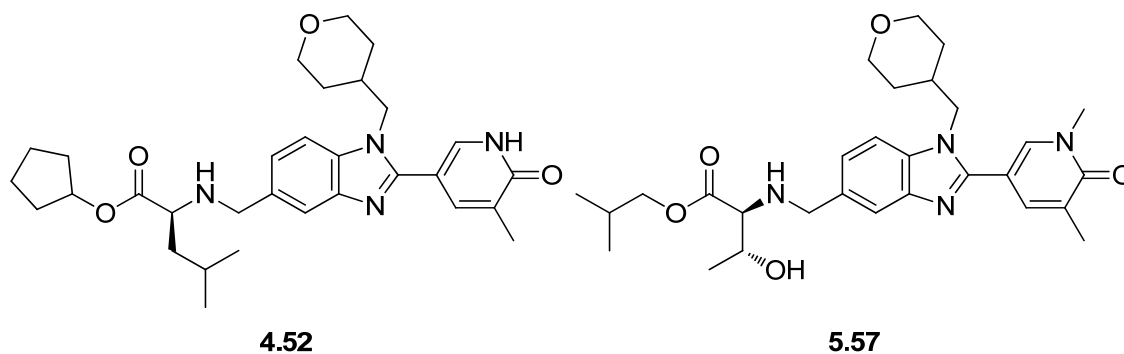


	Substructure	R ¹	mChromlogD _{pH7.4}	BRD4-BD1 pIC ₅₀ (n)	HWB (MCP-1) pIC ₅₀ (n)	ΔpIC ₅₀ (HWB – BRD4-BD1)	hCE-1 Activity (μM/min/μM)	Cyno S9 clearance (ml/min/g)	FaSSIF solubility (μg/ml)
5.06		H	3.4	6.5 (5)	6.3 (2)	-0.2	0.0 (2)	6.6	> 1000
5.57		Me	3.6	7.2 (6)	8.3 (8), > 8.8 (2)	1.1	0.44	6.6	> 1000, 950
5.58		H	3.8	6.2 (3)	7.3 (4)	1.1	0.52	13.7	> 1000

Table 5.17: In vitro clearance of esters 5.57 and 5.58 in cyno liver S9 fraction,^{A12} and solubility in FaSSIF media,^{A13} compared with ester 5.06. BRD4-BD1 FRET assay data,^{A8} HWB assay data,^{A1} and the ΔpIC₅₀ between these assays are shown. The mChromlogD_{pH7.4}^{A7} and the hCE-1 activity^{A14} are also shown. The substructure of the compounds is shown above the table.

5.8 Conclusions and Further Work

Comparison of the desired compound profile of an *in vivo* tool molecule (Figure 5.02) with the profile of compound **5.57** indicates that this compound meets the criteria set out for further progression (Table 5.18).



	Desired Compound	4.52	5.57
BRD4-BD1 pIC₅₀ (n)	N/A	6.1 (10)	7.2 (4)
HWB (MCP-1) pIC₅₀ (n)	> 7.0	7.7 (33)	8.3 (8), > 8.8 (2)
ΔpIC₅₀ (HWB – BRD4-BD1)	> 1	+ 1.6	+ 1.1
mChromlogD_{pH7.4}	< 4	5.4	3.6
PFI	< 7	8.4	6.6
FaSSIF Solubility (μg/ml)	> 100	165	>1000, 950
Cyno S9 clearance (ml/min/g)	< 10	25.6	6.6

Table 5.18: Profile of compound **5.57** in comparison to *in vitro* probe molecule **4.52** and the desired *in vivo* tool compound profile (Figure 5.02). Included are data from the BRD4-BD1 FRET assay,^{A8} the HWB assay,^{A1} and the ΔpIC₅₀ between these two assays. The measured^{A7} ChromlogD_{pH7.4} is also shown. *In vitro* clearance is measured in cynomolgus monkey liver S9 fraction,^{A12} and solubility is measured in FaSSIF media.^{A13} Data which meets the criteria is highlighted in green, data which does not meet the criteria is highlighted in red. The structure the compounds are shown above the table.

Compound **5.57** had HWB potency approximately 10-fold higher than the non-ESM containing oral pre-clinical candidate **2.67**, driven from the same level of biochemical potency. This indicated that an increased therapeutic index might be expected for compound **5.57** in pre-clinical safety studies.

Comparison of compound **5.57** with the criteria set out to ensure the good developability characteristics of compounds ($mChromlogD_{pH7.4} < 4$ and $PFI < 7$; FaSSIF solubility $> 100 \mu\text{g/ml}$), indicated that it has good drug-like physicochemical properties. Ideally the PFI would be reduced further to below six, but due to the three aromatic rings present in the pyridone-benzimidazole core this would be unlikely to be possible without reducing cellular permeability.

Most pleasingly, compound **5.57** is the first example of a BET-ESM molecule where it has been possible to combine the desired HWB properties with low *in vitro* clearance. This was achieved by the medicinal chemistry design reported within this chapter, by balancing sufficient hCE-1 activity to confer good HWB potency, with low enough hCE-1 activity to reduce esterase mediated metabolism. As a result of the data presented, compound **5.57** was declared as an *in vivo* tool molecule, which could be used to evaluate ESM technology in an *in vivo* setting. Additionally, compound **5.57** is currently being evaluated in a wide range of *in vitro* and *in vivo* studies within our laboratories. These will be used to establish whether it has the appropriate profile for progression into preclinical safety and efficacy studies to support its further progression.

Chapter 6

Epilogue

“Still round the corner there may wait, a new road or a secret gate...”

The Return of the King, J.R.R. Tolkien

Conclusions

The work described within this thesis has resulted in the identification of an oral BET bromodomain inhibitor which has progressed into pre-clinical studies as a potential treatment for a number of oncology indications. In addition, *in vitro* and *in vivo* tool molecules have been designed which have enabled a significant advancement in the understanding of the use of ESM technology within the BET bromodomain area.

In Chapter 2, an orally bioavailable BET bromodomain inhibitor **2.67** (Figure 6.01), suitable for clinical progression, was designed and synthesised. This compound met the efficacy, pharmacokinetic, and safety criteria required to progress into pre-clinical safety studies. Compound **2.67** provided a compound from a structurally distinct chemical series to I-BET762, which is in ongoing clinical development in the oncology area for cancers with a high unmet medical need. This therefore mitigates structurally-related attrition of this molecule.

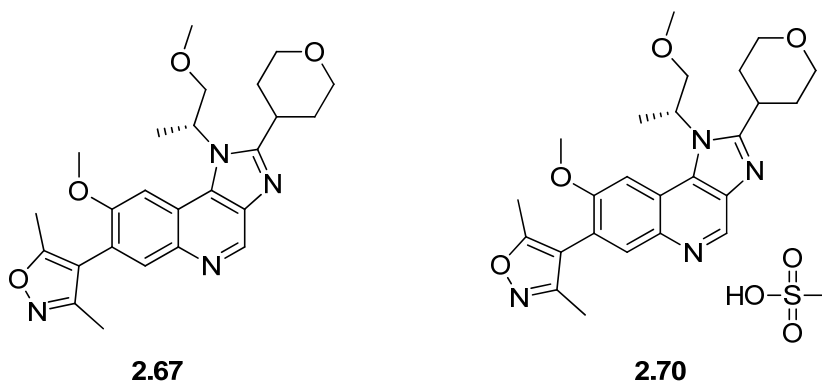


Figure 6.01: The oral BET bromodomain inhibitor **2.67** and its mesylate salt **2.70**.

The medicinal chemistry reported in Chapter 2 showed the value of thorough examination of available SAR, as well as the use of *in silico* profiling to design molecules which are more likely to have the desired physicochemical properties. The requirement for single known enantiomers for progression into *in vivo* studies was highlighted, and it was noted that accessing these molecules as quickly and efficiently as possible reduced the timelines required to progress the ongoing science.

Although a challenging structural series to work on, due to the high aromatic ring count, it was shown that by stringent control of physicochemical properties it is nonetheless possible to identify compounds with a good oral pharmacokinetic profile. However, these overall physicochemical properties of the molecule were likely to have contributed to the low and variable solubility of the compound, and therefore future work in this area should look to reduce

aromatic ring count further if possible. For compound **2.67**, the risk of low solubility was mitigated by the formation of a number of salts of the parent molecule. After measurement of their physicochemical properties, the mesylate salt **2.70** (Figure 6.01) was identified as the preferred form for pre-clinical progression.

The final chapters of these PhD studies describe the progression of BET bromodomain inhibitors containing esterase sensitive motifs (ESMs), from the first compound synthesis through to an *in vivo* tool molecule which is currently being profiled with a view to progression into pre-clinical safety and efficacy studies in immune diseases.

Initial work focussed on the establishment of a proof of principle that ESMs could be incorporated into BET bromodomain inhibitors, and retain their ability to be hydrolysed by hCE-1. This was shown by the design and synthesis of compound **3.19**, where understanding of encoded library technology (ELT) was used to incorporate the ESM on the vector previously used to attach the DNA tag (Figure 6.02). This resulted in a molecule which retained both BET bromodomain and hCE-1 activity.

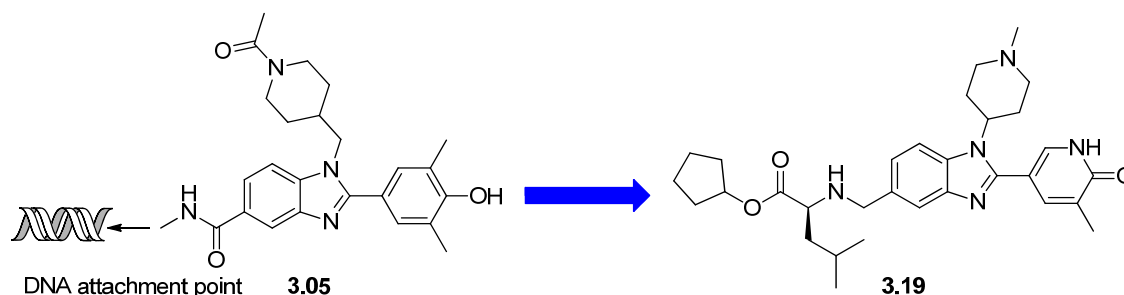
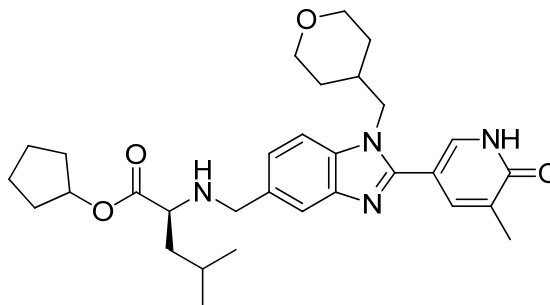


Figure 6.02: The identification of the *in vitro* tool molecule **3.19** from a hit which had been identified using an ELT screen.

These encouraging initial results led to continuation of work in the BET–ESM area, as reported in Chapter 4, where the SAR of the pyridone-benzimidazole series was developed to provide alternative starting points for ESM incorporation. As a result of the conclusions from Chapter 2, compounds were designed with a reduced aromatic ring count, such as compound **4.33**, and this led to the initiation of a new programme of work elsewhere within our laboratories to follow up the encouraging initial findings. The major focus of the work reported in Chapter 4 was the identification of a set of benzimidazole *N*-substituents, with a variety of lipophilicities and functional groups, which maintained BET bromodomain activity. These were successfully designed using known SAR from Chapter 2, as well as *in silico* physicochemical profiling prior to synthesis. As a result, a set of ESM-containing compounds were designed and synthesised

which led to the identification of the *in vitro* tool molecule **4.52** (Figure 6.03). By studying this molecule, it was established that ESM technology can be used to increase the pharmacological effect of BET bromodomain inhibitors, by targeting the molecules to compounds of the monocyte/macrophage lineage.

**4.52**

BRD4-BD1 pIC₅₀ (n) = 6.1 (10)

HWB (MCP-1) pIC₅₀ (n) = 7.7 (33)

Δ pIC₅₀ (HWB - BRD4-BD1) = 1.6

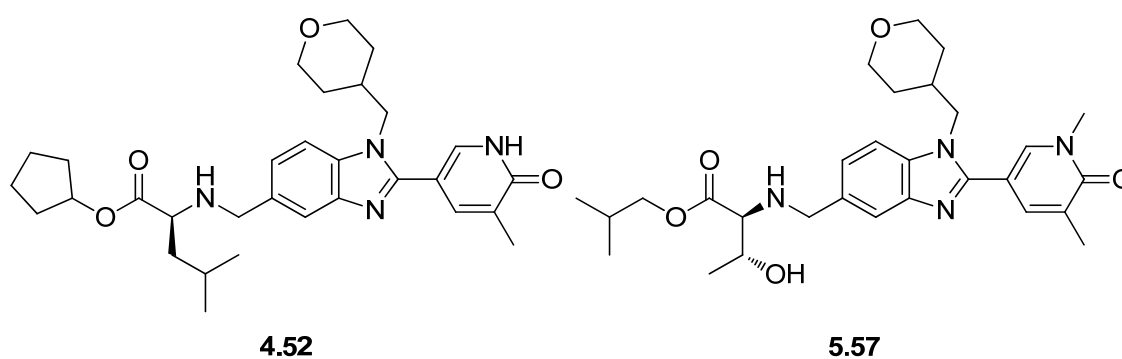
Macrophage cell retention assay:

ESM hydrolysed in macrophages

Acid present in cell at 6 hours

Figure 6.03: Profile of the BET-ESM in vitro probe molecule 4.52.

In Chapter 5, the focus of the work moved to the identification of a molecule with an improved *in vitro* clearance profile whilst maintaining good HWB potency. To do this, the steric and electronic properties of the ESM were systematically modified. This allowed modulation of the hCE-1 activity, and balanced sufficient esterase-driven hydrolysis to show the pharmacological effects with low enough esterase-driven clearance by the liver to suggest *in vivo* dosing would be possible. Finding the correct balance between these two factors led to the identification of the *in vivo* tool molecule **5.58** (Figure 6.04).



	4.52	5.57
BRD4-BD1 pIC₅₀ (n)	6.1 (10)	7.2 (4)
HWB (MCP-1) pIC₅₀ (n)	7.7 (33)	8.3 (8), > 8.8 (2)
ΔpIC₅₀ (HWB – BRD4-BD1)	+ 1.6	+ 1.1
mChromlogD_{pH7.4}	5.4	3.6
PFI	8.4	6.6
FaSSiF Solubility (μg/ml)	165	>1000, 950
Cyno S9 clearance (ml/min/g)	25.6	6.6

Figure 6.04: Profile of *in vivo* tool compound **5.57** in comparison to *in vitro* probe molecule **4.52**.

Compound **5.58** is currently being extensively profiled to understand its potential for progression into pre-clinical safety and efficacy studies. The successful strategy of balancing the whole blood potency and hepatic clearance by modulating the esterase activity is the key outcome of the work described within this chapter. This strategy is currently being used within our laboratories to identify further ESM-containing BET bromodomain inhibitors in alternative chemical series which also have potential for progression into *in vivo* studies.

Experimental

“Double, double toil and trouble; Fire burn, and cauldron bubble.”

William Shakespeare, Macbeth

General Experimental Details

The names of the following compounds have been obtained using ChemDraw Ultra 12.0.

LCMS Methodology

Method using formic acid modifier: “LCMS (formic acid)”

LC conditions: The UPLC analysis was conducted on an Acquity UPLC BEH C₁₈ column (50 mm x 2.1 mm, i.d. 1.7 µm packing diameter) at 40 °C. The solvents employed were: A = 0.1% v/v solution of formic acid in water; B = 0.1% v/v solution of formic acid in acetonitrile. The gradient (A:B) employed was from 97:3 to 3:97 over 2 min. The UV detection was a summed signal from wavelength of 210 nm to 350 nm.

MS conditions: The mass spectrometry was conducted on a Waters ZQ mass spectrometer, with an ionisation mode of alternate-scan positive and negative electrospray. The scan range was 100 to 1000 AMU, the scan time was 0.27 sec and the inter-scan delay was 0.10 sec.

Method using trifluoroacetic acid modifier: “LCMS (TFA)”

The method was as for LCMS (formic acid), except the solvents employed were: A = 0.1% v/v solution of trifluoroacetic acid in water; B = 0.1% v/v solution of trifluoroacetic acid in acetonitrile.

Method using ammonium bicarbonate modifier: “LCMS (high pH)”

The method was as for LCMS (formic acid), except the solvents employed were: A = ammonium hydrogen carbonate in water adjusted to pH 10 with ammonia solution; B = acetonitrile.

High Resolution Mass Spectrometry

Chromatography and analysis conditions: An Agilent 1100 Liquid Chromatograph equipped with a model G1367A autosampler, a model G1312A binary pump and a HP1100 model G1315B diode array detector was used. The method used was generic for all experiments. All separations were achieved using a C₁₈ reversed phase column (100 x 2.1 mm, 3 µm particle size) or equivalent. Gradient elution was carried out with the mobile phases as (A) water containing 0.1% (v/v) TFA and (B) acetonitrile containing 0.1% (v/v) TFA. The conditions for the gradient elution were initially 0% B, increasing linearly to 95% B over 8 min, remaining at 95% B for 0.5 min then decreasing linearly to 0% B over 0.1 min followed by an equilibration

period of 1.49 min prior to the next injection. The flow rate was 1 ml/min, split to source and the temperature controlled at 40 °C with an injection volume of between 2 to 5 µl.

Mass Spectrometry conditions: Positive ion mass spectra were acquired using a Thermo LTQ–Orbitrap FT mass spectrometer, equipped with an ESI interface, over a mass range of 100 – 1100 Da, with a scan time of 1 sec. The elemental composition was calculated using Xcalibur software and processed using RemoteAnalyzer (Spectral Works Ltd) for the [M+H]⁺ and the mass error quoted as ppm.

MDAP Methodology

Method using formic acid modifier: “MDAP (formic acid)”

LC conditions: The HPLC analysis was conducted on either a Sunfire C₁₈ column (100 mm x 19 mm, i.d 5 µm packing diameter) or a Sunfire C₁₈ column (150 mm x 30 mm, i.d. 5 µm packing diameter) at ambient temperature. The solvents employed were: A = 0.1% v/v solution of formic acid in water; B = 0.1% v/v solution of formic acid in acetonitrile. The purification was run as a gradient (A:B) over either 15 min or 25 min, with a flow rate of 20 ml/min (100 mm x 19 mm, i.d 5 µm packing diameter) or 40 ml/min (150 mm x 30 mm, i.d. 5 µm packing diameter). The UV detection was a summed signal from wavelength of 210 nm to 350 nm.

MS conditions: The mass spectrometry was conducted on a Waters ZQ mass spectrometer, with an ionisation mode of alternate-scan positive and negative electrospray. The scan range was 100 to 1000 AMU, the scan time was 0.50 secs and the inter-scan delay was 0.20 sec.

Method using ammonium bicarbonate modifier: “MDAP (high pH)”

The method was as for MDAP (formic acid), except the solvents employed were: A = 10 mM ammonium bicarbonate in water, adjusted to pH 10 with ammonia solution; B = acetonitrile.

NMR Spectroscopy

Unless otherwise specified, ¹H and ¹³C NMR spectra were recorded at 400 MHz and 101 MHz respectively, and chemical shifts are given in ppm (δ) relative to tetramethylsilane (TMS) as an internal standard. Spectra were analysed using ACD/SpecManager version 11. Chemical shifts are given to the nearest 0.01 ppm (¹H NMR) or 0.1 ppm (¹³C NMR) and coupling constants are given to the nearest 0.1 Hz. NMR spectra were recorded at room temperature unless otherwise stated.

IR Spectroscopy

Infra-red (IR) spectra were recorded using a Perkin Elmer Spectrum One FT-IR spectrometer, and key well-defined peaks were recorded in cm^{-1} .

Optical Rotation

Optical rotation measurements were recorded using a Jasco P-1030 polarimeter. The concentration was recorded in g/ml, path length in mm, and temperature in °C.

H-cube™

Where compounds were hydrogenated using an H-cube, a Thales H-cube continuous-flow hydrogenation reactor was used, where hydrogen is generated *in situ*. Thales disposable catalyst cartridges were used, either the CatCart 30 (30 mm cartridge, containing 140 mg of 10% Pd/C catalyst) or the CatCart 70 (70 mm cartridge, containing 350 mg of 10% Pd/C catalyst).

Microwave Reactor

Reactions heated under microwave conditions were heated in a Biotage Initiator microwave. Unless otherwise stated, the initial absorption was set as 'high' and 15 sec of pre-stirring was applied before heating commenced.

Compound Purity

The purity of compounds tested in *in vitro* and *in vivo* assays was of greater than 95% using interpretation of a combination of LCMS and ^1H NMR data, unless stated otherwise.

Chapter 2

4-(8-Methoxy-1-(1-methoxypropan-2-yl)-2-(tetrahydro-2H-pyran-4-yl)-1H-imidazo[4,5-c]quinoline-7-yl)-3,5-dimethylisoxazole, **2.02**, Preparation A:

A suspension of *N*-(7-(3,5-dimethylisoxazol-4-yl)-6-methoxy-4-((1-methoxypropan-2-yl)amino)quinolin-3-yl)tetrahydro-2H-pyran-4-carboxamide **2.69** (29.4 g, 62.7 mmol) in acetic acid (250 ml, 62.7 mmol) was heated at 120 °C for 2 hours. LCMS showed no significant conversion to product. 3 Å molecular sieves (20 g) were added and heating continued for 3.5 hours. Further 3 Å molecular sieves (20 g, oven dried) were added and heating was continued overnight. Further 3 Å molecular sieves (20 g, oven dried) were added and heating continued for a further 24 hours. The reaction mixture was allowed to cool to room temperature, and the solid removed by filtration. The solid and solution were analysed by LCMS, and found to have similar profiles. The two were therefore combined and evaporated under reduced pressure. Water (3000 ml) was added, and the resultant slurry was neutralised via the slow addition of solid sodium bicarbonate. The aqueous slurry was extracted using DCM (3 x 1000 l), and the organic layers were combined, dried using a hydrophobic frit and evaporated under reduced pressure to give a brown gum (22.1 g) which solidified on standing. The material was dissolved, with warming and the use of an ultrasonic bath, in a minimal quantity of DCM. The solution was applied to an SPE column (silica, 750 g) which had been pre-wetted with DCM. The column was eluted with a gradient of 0 – 8% (0.5 M ammonia in MeOH) in DCM. The pure product fractions were combined and evaporated to dryness under reduced pressure to give a cream glassy foam. The sample was dried *in vacuo* to give impure material (13.0 g). The mixed product fractions from the SPE column were combined and evaporated to dryness under reduced pressure to give a deep yellow oil. The oil was dissolved in diethyl ether and the volatiles evaporated under reduced pressure to give a yellow solid. The solid was triturated with diethyl ether and the solid isolated by filtration and washed twice with diethyl ether to give an off-white solid. The impure material (13.0 g) was triturated with a mixture of diethyl ether and EtOAc. The mixture was evaporated to dryness under reduced pressure and the trituration was repeated with pure diethyl ether. The pure off-white solid previously isolated was added to the suspension and the mixture aged overnight. The resulting solid was isolated by filtration and washed with diethyl ether to give a cream solid. The sample was again triturated with diethyl ether, with stirring over approximately 30 min. The solid was isolated by filtration and washed with diethyl ether. The solid was dried in a vacuum oven to give 4-(8-methoxy-1-(1-methoxypropan-2-yl)-2-(tetrahydro-2H-pyran-4-yl)-1H-imidazo[4,5-c]quinoline-7-yl)-3,5-dimethylisoxazole **2.02** (11.73 g, 26.05 mmol, 42% yield) as a white solid.

LCMS (formic acid): *rt* = 0.76 min, *MH*⁺ = 451

¹H NMR (*d*₆-DMSO, 393 K): δ 1.83 (d, *J* = 7.3 Hz, 3 H), 1.86 – 2.00 (m, 2 H), 2.03 – 2.14 (m, 2 H), 2.17 (s, 3 H), 2.35 (s, 3 H), 3.28 (s, 3 H), 3.42 – 3.51 (m, 1 H), 3.56 – 3.68 (m, 2 H), 4.00 – 4.08 (m, 6 H), 4.09 – 4.18 (m, 1 H), 5.36 – 5.53 (m, 1 H), 7.74 (s, 1 H), 7.99 (s, 1 H), 9.04 (s, 1 H).

4-(8-Methoxy-1-(1-methoxypropan-2-yl)-2-(tetrahydro-2*H*-pyran-4-yl)-1*H*-imidazo[4,5-*c*]quinoline-7-yl)-3,5-dimethylisoxazole, **2.02**, Preparation B:

A mixture of *N*-(7-(3,5-dimethylisoxazol-4-yl)-6-methoxy-4-((1-methoxypropan-2-yl)amino)quinoline-3-yl)tetrahydro-2*H*-pyran-4-carboxamide **2.69** (11.95 g, 25.5 mmol) and *p*-toluenesulfonic acid (1.2 g, 25.5 mmol) in toluene (250 ml) was heated at reflux, under nitrogen, using Dean–Stark apparatus for 3 days. Further *p*-toluenesulfonic acid (0.2 g, 4.3 mmol) was added and heating continued overnight. On inspection the reaction mixture had boiled dry, due to one of the glass joints having a small gap allowing solvent to escape. Water (750 ml) was added, followed by saturated aqueous sodium bicarbonate solution until the pH reached 8. The aqueous layer was extracted with EtOAc (3 x 750 ml). The organic layers were combined, dried using a hydrophobic frit, and evaporated under reduced pressure to give a light brown solid, ~ 11 g. The solid was triturated in ether (~200 ml), placed briefly in an ultrasonic bath, and the majority of the solid appeared to be a fine powder. The fine powder suspended in the ether was decanted, the solid isolated by filtration, and dried in a vacuum oven to give 6.3 g of material. This material was triturated in ether (~100 ml), placed briefly in an ultrasonic bath, and stood overnight at room temperature. The solid was isolated by filtration and dried in a vacuum oven (at this point some of the material was spilt and lost) to give 4-(8-methoxy-1-(1-methoxypropan-2-yl)-2-(tetrahydro-2*H*-pyran-4-yl)-1*H*-imidazo[4,5-*c*]quinoline-7-yl)-3,5-dimethylisoxazole **2.02** (4.9 g, 10.88 mmol, 43% yield). The clumped solid left over from the decanting was triturated in ether (100 ml), placed in an ultrasonic bath for 15 min, and stood at room temperature for 3 days. The solid was isolated by filtration and dried in a vacuum oven to give 4-(8-methoxy-1-(1-methoxypropan-2-yl)-2-(tetrahydro-2*H*-pyran-4-yl)-1*H*-imidazo[4,5-*c*]quinoline-7-yl)-3,5-dimethylisoxazole **2.02** (3.6 g, 7.99 mmol, 31% yield).

The total amount of material obtained over the two batches was 8.5 g, 74% yield.

LCMS (formic acid): *rt* = 0.76 min, *MH*⁺ = 451

¹H NMR (*d*₆-DMSO, 393 K): δ 1.80 (d, *J* = 7.3 Hz, 3 H), 1.83 – 1.96 (m, 2 H), 2.01 – 2.10 (m, 2 H), 2.13 (s, 3 H), 2.32 (s, 3 H), 3.25 (s, 3 H), 3.38 – 3.48 (m, 1 H), 3.54 – 3.63 (m, 2 H), 3.95 – 4.05 (m, 6 H), 4.08 – 4.14 (m, 1 H), 5.32 – 5.52 (m, 1 H), 7.71 (s, 1 H), 7.96 (s, 1H), 9.01 (s, 1H).

7-(3,5-Dimethylisoxazol-4-yl)-8-methoxy-N-(2-methoxyethyl)-1-(pyridine-2-ylmethyl)-1H-imidazo[4,5-c]quinoline-2-amine, **2.06**:

To a solution of 7-(3,5-dimethylisoxazol-4-yl)-6-methoxy-N4-(pyridine-2-ylmethyl)quinoline-3,4-diamine **2.64** (875 mg, 2.331 mmol) in EtOH (50 ml) was added 1-isothiocyanato-2-methoxyethane (0.506 ml, 4.66 mmol) and the reaction mixture heated at 60 °C for 6 hours. The solvent was evaporated under reduced pressure. EDC (894 mg, 4.66 mmol) and THF (50 ml) were added and the reaction mixture stirred at 60 °C for 1 hour, followed by stirring at room temperature overnight. The solvent was removed under reduced pressure. The sample was loaded in MeOH/DCM (and the column dried in a vacuum oven) and purified by SPE (silica, 100 g) using a gradient of 0–10% (2 M ammonia in MeOH) in DCM. The appropriate fractions were combined and evaporated under reduced pressure to give a brown gum (310 mg). A portion (40 mg) of this gum was dissolved in DMSO (1 ml) and purified by MDAP (high pH). The solvent was blown down a stream of nitrogen to give the required product 7-(3,5-dimethylisoxazol-4-yl)-8-methoxy-N-(2-methoxyethyl)-1-(pyridine-2-ylmethyl)-1H-imidazo[4,5-c]quinoline-2-amine **2.06** (23 mg, 0.050 mmol, 2% yield) as a white solid. The remaining crude material was kept in case further material was required.

LCMS (formic acid): rt = 0.68 min, MH⁺ = 459

¹H NMR (d₆-DMSO, 393 K): δ 2.08 (s, 3 H), 2.27 (s, 3 H), 3.35 (s, 3 H), 3.63 – 3.71 (m, 4 H), 3.73 (s, 3 H), 5.83 (s, 2 H), 6.77 – 6.88 (br m, 1 H), 7.24 (d, *J* = 7.8 Hz, 1 H), 7.27 – 7.35 (m, 1 H), 7.45 (s, 1 H), 7.72 – 7.83 (m, 2 H), 8.58 (d, *J* = 4.3 Hz, 1 H), 8.81 (s, 1 H).

¹³C NMR (d₆-DMSO, 303 K): δ 10.3, 11.3, 42.5, 55.4, 58.0, 70.5, 98.8, 112.5, 116.8, 118.5, 120.8, 123.0, 131.7, 132.5, 131.7, 132.5, 136.7, 138.8, 139.5, 149.5, 154.3, 155.5, 156.5, 159.1, 165.7.

IR (neat): 3233 (imine NH), 1611 (aryl), 1572 (aryl), 1221 (aryl ether), 777 (aryl C-H) cm⁻¹

M.pt.: 245–252 °C

HRMS: (C₂₅H₂₇N₆O₃) requires MH⁺ 459.2145, found MH⁺ 459.2151.

7-(3,5-Dimethylisoxazol-4-yl)-8-methoxy-1-((tetrahydro-2H-pyran-4-yl)methyl)-1H-imidazo[4,5-c]quinoline-2(3H)-one, **2.07**:

To a suspension of 7-(3,5-dimethylisoxazol-4-yl)-6-methoxy-4-(((tetrahydro-2H-pyran-4-yl)methyl)amino)quinoline-3-carboxamide **2.35** (1.7 g, 4.14 mmol) in MeOH (15 ml) was added potassium hydroxide (0.349 g, 6.21 mmol), and the reaction mixture stirred at room temperature for 20 min. The reaction mixture was cooled in an ice/water bath, iodobenzene diacetate (1.734 g, 5.38 mmol) added, and the reaction mixture stirred at 0 °C for 2 hours. The reaction mixture was blown down under a stream of nitrogen. The residue was loaded as a suspension in MeOH

and DCM (and the column dried in a vacuum oven) and purified by SPE (silica, 100 g) using 0 – 20% MeOH in DCM. The appropriate fractions were combined and dried under a stream of nitrogen to give the required product 7-(3,5-dimethylisoxazol-4-yl)-8-methoxy-1-((tetrahydro-2H-pyran-4-yl)methyl)-1H-imidazo[4,5-c]quinoline-2(3H)-one **2.07** (1.50 g, 3.67 mmol, 89% yield) as a pale brown foam.

LCMS (formic acid): $rt = 0.66$ min, $MH^+ = 409$

1H NMR (d_6 -DMSO): δ 1.34 – 1.48 (m, 2 H), 1.60 (d, $J = 11.1$ Hz, 2 H), 2.14 (s, 3 H), 2.17 – 2.25 (m, 1 H), 2.33 (s, 3 H), 3.22 – 3.28 (m, 2 H), 3.84 (dd, $J = 11.4, 2.0$ Hz, 2 H), 3.97 (s, 3 H), 4.23 (d, $J = 7.3$ Hz, 2 H), 7.46 (s, 1 H), 7.87 (s, 1 H), 8.57 (s, 1 H), 11.45 – 11.58 (br s, 1 H).

^{13}C NMR (d_6 -DMSO, 300 K): δ 10.4, 11.4, 30.2, 36.7, 46.9, 55.6, 66.4, 99.0, 112.2, 115.6, 120.6, 122.0, 128.3, 132.1, 133.0, 139.7, 154.3, 155.0, 159.1, 166.1.

IR (neat): 1694 (urea), 1597 (aryl), 1228 (aryl ether), 841 (aryl C-H) cm^{-1}

M.pt.: 233–238 °C

HRMS: $C_{22}H_{25}N_4O_4$ MH^+ requires 409.1870, found MH^+ 409.1870

7-(3,5-Dimethylisoxazol-4-yl)-8-methoxy-1-((tetrahydro-2H-pyran-3-yl)methyl)-1H-imidazo[4,5-c]quinoline-2(3H)-one, **2.08**:

Method as for **2.07**, using the following reagents: 7-(3,5-dimethylisoxazol-4-yl)-6-methoxy-4-(((tetrahydro-2H-pyran-3-yl)methyl)amino)quinoline-3-carboxamide **2.36** (610 mg, 1.486 mmol), potassium hydroxide (125 mg, 2.229 mmol), iodobenzene diacetate (622 mg, 1.932 mmol) and MeOH (5 ml). LCMS (formic acid) of the reaction mixture showed 91% product by UV, $rt = 0.68$ min, $MH^+ = 409$. The silica column was eluted using 0 – 100% EtOAc in cyclohexane followed by 0 – 10% MeOH in DCM. The final product was: 7-(3,5-dimethylisoxazol-4-yl)-8-methoxy-1-((tetrahydro-2H-pyran-3-yl)methyl)-1H-imidazo[4,5-c]quinoline-2(3H)-one **2.08** (407 mg, 0.996 mmol, 67% yield) as a pale brown foam.

LCMS (formic acid): $rt = 0.69$ min, $MH^+ = 409$

1H NMR (d_6 -DMSO, 393 K): δ 1.43 – 1.53 (m, 2 H), 1.65 – 1.75 (m, 1 H), 1.79 – 1.87 (m, 1 H), 2.12 (s, 3 H), 2.14 – 2.26 (m, 1 H), 2.31 (s, 3 H), 3.37 – 3.48 (m, 2 H), 3.64 – 3.79 (m, 2 H), 3.96 (s, 3 H), 4.23 (m, 2 H), 7.50 (s, 1 H), 7.82 (s, 1 H), 8.55 (s, 1 H), 10.91 – 11.24 (br s, 1 H).

7-(3,5-Dimethylisoxazol-4-yl)-8-methoxy-1-((tetrahydrofuran-3-yl)methyl)-1H-imidazo[4,5-c]quinoline-2(3H)-one, **2.09**:

Method as for **2.07**, using the following reagents: 7-(3,5-dimethylisoxazol-4-yl)-6-methoxy-4-(((tetrahydrofuran-3-yl)methyl)amino)quinoline-3-carboxamide **2.37** (667 mg, 1.682 mmol), potassium hydroxide (142 mg, 2.52 mmol), iodobenzene diacetate (704 mg, 2.187 mmol) and MeOH (5 ml). LCMS (formic acid) of the reaction mixture showed 90% product by UV, $rt =$

0.63 min, $MH^+ = 395$. The silica column was eluted using 0 – 10% MeOH in DCM. The final product was: 7-(3,5-dimethylisoxazol-4-yl)-8-methoxy-1-((tetrahydrofuran-3-yl)methyl)-1*H*-imidazo[4,5-*c*]quinoline-2(3*H*)-one **2.09** (558 mg, 1.415 mmol, 84% yield) as a pale brown foam.

LCMS (formic acid): $rt = 0.65$ min, $MH^+ = 395$

1H NMR (d_6 -DMSO, 393 K): δ 1.80 – 1.90 (m, 1 H), 2.01 – 2.11 (m, 1 H), 2.14 (s, 3 H), 2.33 (s, 3 H), 2.85 – 2.98 (m, 1 H), 3.66 – 3.77 (m, 3 H), 3.87 – 3.93 (m, 1 H), 3.99 (s, 3 H), 4.29 – 4.40 (m, 2 H), 7.57 (s, 1 H), 7.84 (s, 1 H), 8.58 (s, 1 H), 10.90 – 11.31 (br s, 1 H).

1-(Cyclopropylmethyl)-7-(3,5-dimethylisoxazol-4-yl)-8-methoxy-1*H*-imidazo[4,5-*c*]quinoline-2(3*H*)-one, **2.11**:

To a suspension of 4-((cyclopropylmethyl)amino)-7-(3,5-dimethylisoxazol-4-yl)-6-methoxyquinoline-3-carboxamide **2.39** (365 mg, 0.996 mmol) in MeOH (4 ml) was added potassium hydroxide (84 mg, 1.494 mmol), and the reaction mixture stirred at room temperature for 20 min. The reaction mixture was cooled to 0 °C (ice/water bath), iodobenzene diacetate (417 mg, 1.295 mmol) added, and the reaction mixture stirred at 0 °C for a further 2 hours. The reaction mixture was blown down under a stream of nitrogen. LCMS (formic acid) of the reaction mixture showed 90% product by UV, $rt = 0.72$ min, $MH^+ = 365$. A portion (100 mg) of the crude material was dissolved in DMSO (1 ml) and purified by MDAP (high pH). The solvent was blown down a stream of nitrogen to give the required product 1-(cyclopropylmethyl)-7-(3,5-dimethylisoxazol-4-yl)-8-methoxy-1*H*-imidazo[4,5-*c*]quinoline-2(3*H*)-one **2.11** (22 mg, 0.060 mmol, 6% yield). The remaining crude material (902 mg) was kept for further purification if required.

LCMS (formic acid): $rt = 0.73$ min, $MH^+ = 365$

1H NMR (d_6 -DMSO, 393 K): δ 0.46 – 0.51 (m, 2 H), 0.55 – 0.61 (m, 2 H), 1.36 – 1.46 (m, 1 H), 2.14 (s, 3 H), 2.33 (s, 3 H), 3.99 (s, 3 H), 4.29 (d, $J = 6.3$ Hz, 2 H), 7.67 (s, 1 H), 7.84 (s, 1 H), 8.58 (s, 1 H), 10.87 – 10.99 (br s, 1 H).

4-(8-Methoxy-2-(tetrahydro-2*H*-pyran-4-yl)-1-((tetrahydro-2*H*-pyran-4-yl)methyl)-1*H*-imidazo[4,5-*c*]quinoline-7-yl)-3,5-dimethylisoxazole, **2.12**:

A solution of *N*-(7-(3,5-dimethylisoxazol-4-yl)-6-methoxy-4-(((tetrahydro-2*H*-pyran-4-yl)methyl)amino)quinoline-3-yl)tetrahydro-2*H*-pyran-4-carboxamide (10 mg, 0.020 mmol) in glacial acetic acid (0.5 ml, 0.020 mmol) was heated under microwave conditions at 110 °C for a total of 2 hours. The reaction mixture was blown down under a stream of nitrogen and the residue dissolved in DMSO (1 ml) and purified by MDAP (formic acid). The solvent was blown down under a stream of nitrogen to give the required product 4-(8-methoxy-2-

(tetrahydro-2*H*-pyran-4-yl)-1-((tetrahydro-2*H*-pyran-4-yl)methyl)-1*H*-imidazo[4,5-*c*]quinoline-7-yl)-3,5-dimethylisoxazole **2.12** (9.4 mg, 0.020 mmol, 98% yield).

LCMS (formic acid): *rt* = 0.71 min, MH^+ = 477

1H NMR (d_6 -DMSO, 393 K): δ 1.47 – 1.66 (m, 4 H), 1.87 – 1.93 (m, 2 H), 1.99 – 2.12 (m, 2 H), 2.16 (s, 3 H), 2.26 – 2.33 (m, 4 H), 2.52 – 2.56 (m, 1 H), 3.25 – 3.31 (m, 2 H), 3.39 – 3.47 (m, 1 H), 3.60 – 3.67 (m, 2 H), 3.85 – 3.93 (m, 2 H), 4.00 – 4.07 (m, 5 H), 4.64 (d, *J* = 7.6 Hz, 2 H), 7.69 (s, 1 H), 7.97 (s, 1 H), 9.03 (s, 1 H).

4-(8-Methoxy-2-(tetrahydro-2*H*-pyran-4-yl)-1-(1-(tetrahydro-2*H*-pyran-4-yl)ethyl)-1*H*-imidazo[4,5-*c*]quinoline-7-yl)-3,5-dimethylisoxazole, **2.13**:

To a suspension of tetrahydro-2*H*-pyran-4-carboxylic acid (50.7 mg, 0.390 mmol) and HATU (168 mg, 0.442 mmol) in DMF (2 ml) was added DIPEA (0.136 ml, 0.779 mmol) and the resulting solution stirred at room temperature for 15 min. 7-(3,5-Dimethylisoxazol-4-yl)-6-methoxy-*N*4-(1-(tetrahydro-2*H*-pyran-4-yl)ethyl)quinoline-3,4-diamine **2.47** (103 mg, 0.260 mmol) was added and the reaction mixture stirred at room temperature overnight. The reaction mixture was blown down under a stream of nitrogen and the residue loaded in DCM and purified by SPE (aminopropyl, 5 g), eluted using 10% MeOH in DCM. The appropriate fractions were combined and dried under a stream of nitrogen to give a brown gum. The gum was dissolved in DMSO (2 x 1 ml) and purified by MDAP (formic acid). The solvent was dried under a stream of nitrogen to give a light brown solid (45 mg). To the solid was added glacial acetic acid (1 ml, 0.088 mmol) and the reaction mixture was heated under microwave conditions at 120 °C for a total of 29 hours. The reaction mixture was blown down under a stream of nitrogen. The resulting gum was dissolved in DMSO (1 ml) and purified by MDAP (high pH). The solvent was blown down a stream of nitrogen to give the required product 4-(8-methoxy-2-(tetrahydro-2*H*-pyran-4-yl)-1-(1-(tetrahydro-2*H*-pyran-4-yl)ethyl)-1*H*-imidazo[4,5-*c*]quinoline-7-yl)-3,5-dimethylisoxazole **2.13** (18.7 mg, 0.038 mmol, 15% yield) as a light pink solid.

LCMS (formic acid): *rt* = 0.75 min, MH^+ = 491

1H NMR (d_6 -DMSO, 393 K): δ 0.83 – 0.96 (m, 1 H), 1.19 – 1.34 (m, 1 H), 1.55 – 1.70 (m, 1 H), 1.80 – 1.97 (m, 6 H), 2.01 – 2.11 (m, 2 H), 2.17 (s, 3 H), 2.35 (s, 3 H), 2.55 – 2.70 (m, 1 H), 3.06 – 3.19 (m, 1 H), 3.39 – 3.53 (m, 2 H) 3.58 – 3.76 (m, 2 H), 3.94 – 4.13 (m, 7 H), 4.69 – 5.12 (m, 1 H), 7.75 (s, 1 H), 7.99 (s, 1 H), 9.04 (s, 1 H).

4-(8-Methoxy-2-(methoxymethyl)-1-((tetrahydro-2*H*-pyran-4-yl)methyl)-1*H*-imidazo[4,5-*c*]quinoline-7-yl)-3,5-dimethylisoxazole, **2.14**:

A solution of 2-methoxyacetic acid (0.015 ml, 0.193 mmol), HATU (81 mg, 0.213 mmol) and DIPEA (0.084 ml, 0.484 mmol) in DMF (2 ml) was stirred at room temperature for 15 min. 7-

(3,5-dimethylisoxazol-4-yl)-6-methoxy-*N*4-((tetrahydro-2*H*-pyran-4-yl)methyl)quinoline-3,4-diamine **2.46** (37 mg, 0.097 mmol) was added and the reaction mixture stirred at room temperature for 3 hours. The reaction mixture was blown down under a stream of nitrogen. The sample was loaded in DCM and purified by SPE (aminopropyl, 2 g), eluted using 10% MeOH in DCM. The appropriate fractions were combined and blown down a stream of nitrogen to give a brown gum. The gum was dissolved in DMSO (1 ml) and purified by MDAP (high pH). The solvent was blown down a stream of nitrogen to give a colourless gum (22 mg). To this was added acetonitrile (1.5 ml) and 10 mM aqueous ammonium bicarbonate solution, adjusted to pH 10 using ammonia (1.5 ml), and the reaction mixture stood at room temperature for 4 days. The reaction mixture was blown down under a stream of nitrogen to give the required product 4-(8-methoxy-2-(methoxymethyl)-1-((tetrahydro-2*H*-pyran-4-yl)methyl)-1*H*-imidazo[4,5-*c*]quinoline-7-yl)-3,5-dimethylisoxazole **2.14** (22 mg, 0.050 mmol, 52% yield) as a colourless glass.

LCMS (formic acid): *rt* = 0.70 min, MH^+ = 437

1H NMR (d_6 -DMSO, 393 K): δ 1.51 – 1.64 (m, 4 H), 2.16 (s, 3 H), 2.35 – 2.43 (m, 4 H), 3.26 – 3.32 (m, 2 H), 3.45 (s, 3 H), 3.85 – 3.90 (m, 2 H), 4.02 (s, 3 H), 4.69 (d, J = 7.6 Hz, 2 H), 4.84 (s, 2 H), 7.73 (s, 1 H), 8.00 (s, 1 H), 9.06 (s, 1 H).

4-(8-Methoxy-2-(methoxymethyl)-1-(1-methoxypropan-2-yl)-1*H*-imidazo[4,5-*c*]quinoline-7-yl)-3,5-dimethylisoxazole, **2.16**:

A solution of 2-methoxyacetic acid (0.043 ml, 0.556 mmol), HATU (229 mg, 0.602 mmol) and DIPEA (0.243 ml, 1.389 mmol) in DMF (2 ml) was stirred at room temperature for 15 min. 7-(3,5-Dimethylisoxazol-4-yl)-6-methoxy-*N*4-(1-methoxypropan-2-yl)quinoline-3,4-diamine **2.48** (165 mg, 0.463 mmol) was added and the reaction mixture stirred at room temperature over the weekend. A solution of 2-methoxyacetic acid (0.022 ml, 0.278 mmol), HATU (115 mg, 0.302 mmol) and DIPEA (0.121 ml, 0.693 mmol) in DMF (1 ml) was stirred at room temperature for 15 min. This was added to the reaction mixture, which was then stirred at room temperature for 6 hours. The reaction mixture was blown down under a stream of nitrogen. The sample was loaded in DCM and purified by SPE (aminopropyl, 2 g), eluted using 10% MeOH in DCM. The appropriate fractions were combined and blown down under a stream of nitrogen to give a brown gum. The gum was dissolved in DMSO (2 x 1 ml) and purified by MDAP (high pH). The solvent was blown down under a stream of nitrogen to give a colourless gum. The gum was dissolved in acetic acid (1.5 ml, 0.336 mmol) and the reaction mixture heated under microwave conditions at 120 °C for 1 hour. The reaction mixture was blown down under a stream of nitrogen. The resulting gum was dissolved in DMSO (2 x 1 ml) and purified by MDAP (high

pH). The solvent was blown down under a stream of nitrogen to give the required product 4-(8-methoxy-2-(methoxymethyl)-1-(1-methoxypropan-2-yl)-1*H*-imidazo[4,5-*c*]quinoline-7-yl)-3,5-dimethylisoxazole **2.16** (40 mg, 0.097 mmol, 21% yield) colourless glass.

LCMS (formic acid): *rt* = 0.75 min, MH^+ = 491

¹H NMR (*d*₆-DMSO, 393 K): δ 1.81 (d, *J* = 7.1 Hz, 3 H), 2.16 (s, 3 H), 2.35 (s, 3 H), 3.31 (s, 2 H), 3.43 (s, 2 H), 3.94 – 4.05 (m, 4 H), 4.79 – 4.92 (m, 2 H), 5.42 – 5.56 (m, 1 H), 7.83 (s, 1 H), 8.00 (s, 1 H), 9.06 (s, 1 H).

4-(2-Cyclopropyl-8-methoxy-1-((tetrahydro-2*H*-pyran-4-yl)methyl)-1*H*-imidazo[4,5-*c*]quinoline-7-yl)-3,5-dimethylisoxazole, **2.17**:

To a solution of 7-(3,5-dimethylisoxazol-4-yl)-6-methoxy-*N*4-((tetrahydro-2*H*-pyran-4-yl)methyl)quinoline-3,4-diamine **2.46** (136 mg, 0.356 mmol) in DCM (2 ml) was added pyridine (0.144 ml, 1.778 mmol) and cyclopropanecarbonyl chloride (0.039 ml, 0.427 mmol), and the reaction mixture stirred at room temperature for 3 days. The reaction mixture was blown down under a stream of nitrogen and the residue dissolved in DMSO (2 x 1 ml) and purified by MDAP (high pH). The solvent was blown down a stream of nitrogen to give an off-white gum. The gum was dissolved in acetic acid (1.5 ml, 0.193 mmol) and the reaction mixture heated under microwave conditions at 110 °C for a total of 3 hours. The reaction mixture was blown down under a stream of nitrogen and dissolved in DMSO (2 x 1 ml) and purified by MDAP (high pH). The solvent was blown down under a stream of nitrogen to give the required product 4-(2-cyclopropyl-8-methoxy-1-((tetrahydro-2*H*-pyran-4-yl)methyl)-1*H*-imidazo[4,5-*c*]quinoline-7-yl)-3,5-dimethylisoxazole **2.17** (55 mg, 0.127 mmol, 37% yield) as an off-white gum.

LCMS (formic acid): *rt* = 0.73 min, MH^+ = 433

¹H NMR (*d*₆-DMSO, 393 K): δ 1.11 – 1.26 (m, 4 H), 1.53 – 1.69 (m, 4 H), 2.16 (s, 3 H), 2.29 – 2.46 (m, 5 H), 3.24 – 3.41 (m, 2 H), 3.89 – 3.92 (m, 2 H), 4.01 (s, 3 H), 4.73 (d, *J* = 7.6 Hz, 2 H), 7.70 (s, 1 H), 7.95 (s, 1 H), 8.94 (s, 1 H).

4-(2-Cyclopropyl-8-methoxy-1-(1-methoxypropan-2-yl)-1*H*-imidazo[4,5-*c*]quinoline-7-yl)-3,5-dimethylisoxazole, **2.19**:

To a solution of 7-(3,5-dimethylisoxazol-4-yl)-6-methoxy-*N*4-(1-methoxypropan-2-yl)quinoline-3,4-diamine **2.48** (200 mg, 0.561 mmol) in DCM (2 ml) was added pyridine (0.227 ml, 2.81 mmol) and cyclopropanecarbonyl chloride (0.062 ml, 0.673 mmol), and the reaction mixture stirred at room temperature for 2 hours. The reaction mixture was blown down under a stream of nitrogen. The residue was dissolved in DMSO (3 x 1 ml) and purified by MDAP (high pH). The solvent was blown down under a stream of nitrogen to give an off-white gum. The

gum was dissolved in acetic acid (1.5 ml, 0.304 mmol) and the reaction mixture heated under microwave conditions at 110 °C for 10 hours. The reaction mixture was blown down under a stream of nitrogen and the residue dissolved in DMSO (2 x 1 ml) and purified by MDAP (high pH). The solvent was blown down under a stream of nitrogen to give the required product 4-(2-cyclopropyl-8-methoxy-1-(1-methoxypropan-2-yl)-1*H*-imidazo[4,5-*c*]quinoline-7-yl)-3,5-dimethylisoxazole **2.19** (116 mg, 0.285 mmol, 69% yield) as an off-white solid.

LCMS (formic acid): *rt* = 0.79 min, MH^+ = 407

¹H NMR (d₆-DMSO, 393 K): δ 1.10 – 1.31 (m, 4 H), 1.85 (d, *J* = 7.3 Hz, 3 H), 2.16 (s, 3 H), 2.29 – 2.41 (m, 4 H), 3.32 (s, 3 H), 3.98 – 4.09 (m, 4 H), 4.21 (dd, *J* = 10.6, 8.1 Hz, 1 H), 5.59 – 5.68 (m, 1 H), 7.80 (s, 1 H), 7.95 (s, 1 H), 8.94 (s, 1 H).

7-(3,5-Dimethylisoxazol-4-yl)-8-methoxy-*N,N*-dimethyl-1-((tetrahydro-2*H*-pyran-4-yl)methyl)-1*H*-imidazo[4,5-*c*]quinoline-2-amine, **2.20**:

7-(3,5-Dimethylisoxazol-4-yl)-6-methoxy-*N*4-((tetrahydro-2*H*-pyran-4-yl)methyl)quinoline-3,4-diamine **2.46** (50 mg, 0.131 mmol) and *N*-(dichloromethylene)-*N*-methylmethanaminium chloride (42.5 mg, 0.261 mmol) were combined in dry acetonitrile (0.5 ml) and heated under microwave conditions at 120 °C for 10 min. The reaction mixture was blown down under a stream of nitrogen and the residue dissolved in DMSO (1 ml) and purified by MDAP (high pH). The solvent was blown down under a stream of nitrogen to give the required product 7-(3,5-dimethylisoxazol-4-yl)-8-methoxy-*N,N*-dimethyl-1-((tetrahydro-2*H*-pyran-4-yl)methyl)-1*H*-imidazo[4,5-*c*]quinoline-2-amine **2.20** (44 mg, 0.101 mmol, 77% yield) as a yellow gum.

LCMS (formic acid): *rt* = 0.70 min, MH^+ = 436

¹H NMR (d₆-DMSO, 393 K): δ 1.31 – 1.37 (m, 4 H), 2.15 (s, 3 H), 2.17 – 2.25 (m, 1H), 2.34 (s, 3 H), 2.99 (s, 6 H), 3.13 – 3.26 (m, 2 H), 3.74 – 3.84 (m, 2 H), 3.99 (s, 3 H), 4.51 (d, *J* = 7.3 Hz, 2 H), 7.60 (s, 1 H) 7.91 (s, 1 H) 8.90 (s, 1 H).

¹³C NMR (d₆-DMSO, 300 K): δ 10.4, 11.4, 29.6, 35.0, 42.7, 50.8, 55.8, 66.2, 99.4, 112.4, 117.9, 119.6, 131.9, 132.9, 135.8, 138.9, 141.0, 155.0, 159.2, 160.6, 165.9.

IR (neat): 2944 (NCH₃), 2911 (NCH₃), 2853 (NCH₃), 1574 (aryl), 1531 (aryl), 1216 (aryl ether), 845 (aryl C-H) cm⁻¹

M.pt.: 205–207 °C

HRMS: (C₂₄H₃₀N₅O₃) MH^+ requires 436.2343, found MH^+ 436.2335

Ethyl 7-(3,5-dimethylisoxazol-4-yl)-4-hydroxy-6-methoxyquinoline-3-carboxylate, **2.29**:

To refluxing diphenyl ether (50 ml) was added portionwise diethyl 2-(((3-(3,5-dimethylisoxazol-4-yl)-4-methoxyphenyl)amino)methylene)malonate **2.28** (9.5 g, 48.9 mmol). Vigorous effervescence occurred. Heating was continued for a further 16 min, at which point

the heating was stopped and the reaction mixture allowed to cool to room temperature over two hours. Diethyl ether (50 ml) was added and the mixture stood at room temperature for 60 min. The resulting solid was removed by filtration, washed on the filter with diethyl ether (2 x 50 ml), and dried in a vacuum oven overnight to give ethyl 7-(3,5-dimethylisoxazol-4-yl)-4-hydroxy-6-methoxyquinoline-3-carboxylate **2.29** (8.0 g, 23.37 mmol, 96% yield) as a crunchy light brown solid.

LCMS (formic acid): rt = 0.73 min, MH^+ = 343

1H NMR (d_6 -DMSO): δ 1.29 (t, J = 7.1 Hz, 3 H), 2.12 (s, 3 H), 2.32 (s, 3 H), 3.88 (s, 3 H), 4.23 (q, J = 7.1 Hz, 2 H), 7.52 (s, 1 H), 7.70 (s, 1 H), 8.55 (s, 1 H), 12.25 (br s, 1H).

7-(3,5-Dimethylisoxazol-4-yl)-4-hydroxy-6-methoxyquinoline-3-carboxylic acid, **2.30**:

To a suspension of ethyl 7-(3,5-dimethylisoxazol-4-yl)-4-hydroxy-6-methoxyquinoline-3-carboxylate **2.29** (11.2 g, 32.7 mmol) in EtOH (50 ml) was added 2 M aqueous sodium hydroxide solution (50 ml, 100 mmol) and the reaction mixture heated at 100 °C for 3 hours. The reaction mixture was concentrated to approximately half volume under reduced pressure, and water (50 ml) added. The solution was washed with EtOAc (100 ml) and the aqueous layer acidified to pH 3 using 2 M aqueous hydrochloric acid solution. The resulting thick suspension was stood for 20 min. The solid was removed by filtration and washed on the filter with water (50 ml), followed by diethyl ether (50 ml), and dried in a vacuum oven overnight to give 7-(3,5-dimethylisoxazol-4-yl)-4-hydroxy-6-methoxyquinoline-3-carboxylic acid **2.30** (10.1 g, 32.1 mmol, 98% yield) as a pale brown crunchy solid.

LCMS (formic acid): rt = 0.77 min, MH^+ = 315

1H NMR (d_6 -DMSO): δ 2.14 (s, 3 H), 2.34 (s, 3 H), 3.95 (s, 3 H), 7.75 (s, 1 H), 7.77 (s, 2 H), 8.86 (d, J = 5.1 Hz, 1 H), 13.49 (br s, 1H), 15.35 – 15.61 (br s, 1 H).

7-(3,5-Dimethylisoxazol-4-yl)-6-methoxyquinolin-4-ol, **2.31**:

To refluxing diphenyl ether (120 ml) was added 7-(3,5-dimethylisoxazol-4-yl)-4-hydroxy-6-methoxyquinoline-3-carboxylic acid **2.30** (6.05 g, 19.3 mmol) in small portions over eight minutes. Vigorous bubbling was seen on addition. The reaction mixture was heated at reflux for 16 min, and then allowed to cool to room temperature over 2 hours. Diethyl ether (100 ml) was added and the mixture stood at room temperature for 2 hours. The solid was removed by filtration, washed on the filter with diethyl ether (2 x 50 ml), and dried in a vacuum oven overnight to give 7-(3,5-dimethylisoxazol-4-yl)-6-methoxyquinolin-4-ol **2.31** (4.6 g, 17.02 mmol, 88% yield) as a pale brown powder.

LCMS (formic acid): rt = 0.62 min, MH^+ = 271

^1H NMR (d_6 -DMSO): δ 2.12 (s, 3 H), 2.32 (s, 3 H), 3.31 (s, 3 H), 6.03 (d, $J = 7.3$ Hz, 1 H), 7.43 (s, 1 H), 7.62 (s, 1 H), 7.86 – 7.91 (m, 1 H), 11.66 – 11.76 (br s, 1 H).

7-(3,5-Dimethylisoxazol-4-yl)-6-methoxy-3-nitroquinolin-4-ol, **2.32**:

To a stirred solution of 7-(3,5-dimethylisoxazol-4-yl)-6-methoxyquinolin-4-ol **2.31** (8.7 g, 32.2 mmol) in propionic acid (88 ml) was added, dropwise, fuming nitric acid (3.16 ml, 70.8 mmol). After addition was complete, the reaction mixture was stirred at 100 °C for 1 hour. The reaction mixture was allowed to cool to room temperature. The solid was removed by filtration, washed on the filter with diethyl ether (100 ml), and dried in a vacuum oven to give 7-(3,5-dimethylisoxazol-4-yl)-6-methoxy-3-nitroquinolin-4-ol **2.32** (7.3 g, 23.15 mmol, 72% yield) as a mustard yellow solid.

LCMS (formic acid): rt = 0.70 min, $\text{MH}^+ = 316$

^1H NMR (d_6 -DMSO): δ 2.13 (s, 3 H), 2.33 (s, 3 H), 3.92 (s, 3 H), 7.61 (s, 1 H), 7.78 (s, 1 H), 9.17 (br s, 1 H), 12.88 – 13.01 (br s, 1 H).

^{13}C NMR (d_6 -DMSO, 303 K): δ 10.3, 11.4, 55.9, 105.6, 111.7, 122.3, 125.2, 129.2, 130.4, 132.4, 141.3, 155.1, 158.8, 166.6, 166.8.

IR: 1613 (aryl), 1536 (aryl), 1536 (NO_2), 1361 (NO_2), 1221 (aryl ether), 786 (aryl C-H) cm^{-1}

M.pt.: 257–267 (decomposition)

HRMS: ($\text{C}_{15}\text{H}_{15}\text{N}_3\text{O}_5$) MH^+ requires 316.0933, found MH^+ 316.0937

4-(4-Chloro-6-methoxy-3-nitroquinolin-7-yl)-3,5-dimethylisoxazole, **2.33**:

A solution of 7-(3,5-dimethylisoxazol-4-yl)-6-methoxy-3-nitroquinolin-4-ol **2.32** (3.5 g, 11.10 mmol) in phosphorus oxychloride (35 ml, 375 mmol) was heated at 120 °C for 2 hours. The reaction mixture was allowed to cool to room temperature and evaporated under reduced pressure. Twice, toluene (50 ml) was added and the mixture evaporated under reduced pressure. The residual brown liquid was dissolved in DCM (250 ml) and the organic layer was washed with saturated aqueous sodium bicarbonate solution (3 x 150 ml), until the aqueous layer removed was neutral. The organic layer was dried using a hydrophobic frit and evaporated under reduced pressure. The sample was loaded in DCM and purified by SPE (silica, 100 g) using 0 – 50% EtOAc in cyclohexane. The appropriate fractions were combined and evaporated under reduced pressure to give the required product 4-(4-chloro-6-methoxy-3-nitroquinolin-7-yl)-3,5-dimethylisoxazole **2.33** (2.76 g, 8.27 mmol, 75% yield) as a yellow solid.

LCMS (formic acid): rt = 1.13 min, $\text{MH}^+ = 334$

^1H NMR (d_6 -DMSO): δ 2.16 (s, 3 H), 2.36 (s, 3 H), 4.05 (s, 3 H), 7.74 (s, 1 H), 8.15 (s, 1 H), 9.27 (s, 1 H).

^{13}C NMR (d_6 -DMSO, 303 K): δ 10.3, 11.4, 55.9, 105.6, 111.7, 122.3, 125.2, 129.2, 130.4, 132.4, 141.3, 155.1, 158.8, 166.6, 166.8.

IR (neat): 1612 (aryl), 1589 (aryl), 1535 (NO_2), 1361 (NO_2), 1223 (aryl ether), 784 (aryl C-H) cm^{-1}

M.pt.: 279–>300 °C (decomposition)

HRMS: ($\text{C}_{15}\text{H}_{14}\text{N}_3\text{O}_5$ - consistent with hydroxyl replacement of chloro) MH^+ requires 316.0928, found MH^+ : 316.0926

7-(3,5-Dimethylisoxazol-4-yl)-6-methoxy-4-(((tetrahydro-2H-pyran-4-yl)methyl)amino)quinoline-3-carboxamide, 2.35:

To a suspension of 4-chloro-7-(3,5-dimethylisoxazol-4-yl)-6-methoxyquinoline-3-carboxamide **2.34** (2 g, 6.03 mmol) in *N*-methyl-2-pyrrolidinone (5 ml) was added DIPEA (2.63 ml, 15.07 mmol) and (tetrahydro-2H-pyran-4-yl)methanamine (0.868 g, 7.54 mmol), and the reaction mixture heated at 120 °C for 2 hours. LCMS (formic acid) of the reaction mixture showed 92% product by UV, $rt = 0.63$ min, $\text{MH}^+ = 411$. The reaction mixture was loaded directly onto and purified by SPE (70 g, SCX) washed with 20% MeOH in DCM and eluted using (2 M ammonia in MeOH). The appropriate fractions were combined and evaporated under reduced pressure. The resulting gum was triturated using EtOAc to give the required product 7-(3,5-dimethylisoxazol-4-yl)-6-methoxy-4-(((tetrahydro-2H-pyran-4-yl)methyl)amino)quinoline-3-carboxamide **2.35** (1.76 g, 4.29 mmol, 71% yield) as a pale brown solid.

LCMS (formic acid): $rt = 0.64$ min, $\text{MH}^+ = 411$

^1H NMR (d_6 -DMSO): δ 1.20 – 1.30 (m, 2 H), 1.60 – 1.72 (m, 2 H), 1.84 – 1.96 (m, 1 H), 2.13 (s, 3 H), 2.32 (s, 3 H), 3.22 – 3.33 (m, 2 H), 3.53 (d, $J = 6.1$ Hz, 2 H), 3.86 (dd, $J = 11.2, 3.2$ Hz, 2 H), 3.92 (s, 3 H), 7.39 – 7.51 (m, 1 H), 7.66 – 7.67 (m, 2 H), 7.98 – 8.09 (br s, 1 H), 8.58 (s, 1 H), 8.61 (t, $J = 5.3$ Hz, 1 H).

7-(3,5-Dimethylisoxazol-4-yl)-6-methoxy-4-(((tetrahydro-2H-pyran-3-yl)methyl)amino)quinoline-3-carboxamide, 2.36:

To a suspension of 4-chloro-7-(3,5-dimethylisoxazol-4-yl)-6-methoxyquinoline-3-carboxamide **2.34** (1 g, 3.01 mmol) in dry *N*-methyl-2-pyrrolidinone (2.5 ml) was added DIPEA (1.316 ml, 7.54 mmol) and (tetrahydro-2H-pyran-3-yl)methanamine (0.434 g, 3.77 mmol). The reaction mixture was heated under nitrogen at 100 °C for 2 hours, and then stood at room temperature overnight. LCMS (formic acid) of the reaction mixture showed 81% product by UV, $rt = 0.63$ min, $\text{MH}^+ = 411$. The solution was added directly onto, and purified by, SPE (50 g, SCX). The column was washed with 10% MeOH in DCM and eluted with 50% (2 M ammonia in MeOH) in DCM. The appropriate fractions were combined and evaporated under reduced pressure to

give a brown gum. The gum was triturated in EtOAc (~ 15 ml); the solid was removed by filtration and dried in a vacuum oven overnight to give 7-(3,5-dimethylisoxazol-4-yl)-6-methoxy-4-(((tetrahydro-2*H*-pyran-3-yl)methyl)amino)quinoline-3-carboxamide **2.36** (614 mg, 1.496 mmol, 50% yield) as a pale brown solid.

LCMS (formic acid): $rt = 0.66$ min, $MH^+ = 411$

1H NMR (d_6 -DMSO): δ 1.23 – 1.35 (m, 1 H), 1.42 – 1.53 (m, 1 H), 1.54 – 1.63 (m, 1 H), 1.81 – 1.97 (m, 2 H), 2.13 (s, 3 H), 2.33 (s, 3 H), 3.18 (dd, $J = 11.1, 9.1$ Hz, 1 H), 3.49 (t, $J = 6.2$ Hz, 1 H), 3.67 – 3.75 (m, 1 H), 3.79 – 3.86 (m, 1 H), 3.93 (s, 3 H), 7.44 – 7.51 (br s, 1 H), 7.67 (s, 2 H), 8.02 – 8.09 (br s, 1 H), 8.36 (br t, 1 H), 8.55 (s, 1 H).

7-(3,5-Dimethylisoxazol-4-yl)-6-methoxy-4-(((tetrahydrofuran-3-yl)methyl)amino)quinoline-3-carboxamide, **2.37**:

To a suspension of 4-chloro-7-(3,5-dimethylisoxazol-4-yl)-6-methoxyquinoline-3-carboxamide **2.34** (1 g, 3.01 mmol) in dry *N*-methyl-2-pyrrolidone (2.5 ml) was added DIPEA (1.316 ml, 7.54 mmol) and (tetrahydrofuran-3-yl)methanamine (0.381 g, 3.77 mmol). The reaction mixture was heated under nitrogen at 100 °C for 2 hours, and then stood at room temperature overnight. LCMS (formic acid) of the reaction mixture showed 91% product by UV, $rt = 0.59$ min, $MH^+ = 397$. The solution was added directly onto, and purified by, SPE (50 g, SCX). The column was washed with 10% MeOH in DCM and eluted with 50% (2 M ammonia in MeOH) in DCM. The appropriate fractions were combined and evaporated under reduced pressure to give a brown gum. The gum was triturated in EtOAc (~ 15 ml); the solid was removed by filtration and dried in a vacuum oven for 2 hours to give 7-(3,5-dimethylisoxazol-4-yl)-6-methoxy-4-(((tetrahydrofuran-3-yl)methyl)amino)quinoline-3-carboxamide **2.37** (671 mg, 1.693 mmol, 56% yield) as a pale brown solid.

LCMS (formic acid): $rt = 0.61$ min, $MH^+ = 397$

1H NMR (d_6 -DMSO): δ 1.55 – 1.65 (m, 1 H), 1.96 – 2.05 (m, 1H), 2.13 (s, 3 H), 2.32 (s, 3 H), 2.55 – 2.64 (m, 1 H), 3.47 (dd, $J = 9.0, 6.0$ Hz, 1 H) 3.56 – 3.66 (m, 3 H) 3.71 – 3.80 (m, 2 H), 3.92 (s, 3 H), 7.42 – 7.51 (br s, 1 H), 7.66 (s, 1 H), 7.67 (s, 1 H), 8.00 – 8.08 (br s, 1 H), 8.45 (br t, 1 H), 8.57 (s, 1 H).

7-(3,5-dimethylisoxazol-4-yl)-6-methoxy-4-((oxetan-3-ylmethyl)amino)quinoline-3-carboxamide, **2.38**:

To a suspension of 4-chloro-7-(3,5-dimethylisoxazol-4-yl)-6-methoxyquinoline-3-carboxamide **2.34** (1 g, 3.01 mmol) in dry *N*-methyl-2-pyrrolidone (2.5 ml) was added DIPEA (1.316 ml, 7.54 mmol) and oxetan-3-ylmethanamine (0.328 g, 3.77 mmol) and the reaction mixture heated under nitrogen at 100 °C for 2 hours and then stood at room temperature overnight. LCMS

(formic acid) showed only production of the 7-(3,5-dimethylisoxazol-4-yl)-4-hydroxy-6-methoxyquinoline-3-carboxamide side-product, and none of the desired product. The reaction was therefore abandoned.

4-((Cyclopropylmethyl)amino)-7-(3,5-dimethylisoxazol-4-yl)-6-methoxyquinoline-3-carboxamide, **2.39**:

To a suspension of 4-chloro-7-(3,5-dimethylisoxazol-4-yl)-6-methoxyquinoline-3-carboxamide **2.34** (500 mg, 1.507 mmol) in dry *N*-methyl-2-pyrrolidinone (2.5 ml) was added DIPEA (0.658 ml, 3.77 mmol) and cyclopropylmethanamine (0.163 ml, 1.884 mmol). The reaction mixture was heated under nitrogen at 100 °C for 3.5 hours. Further cyclopropylmethanamine (0.163 ml, 1.884 mmol) was added and the reaction mixture heated under nitrogen at 100 °C overnight. LCMS (formic acid) of the reaction mixture showed 80% product by UV, *rt* = 0.70 min, *MH*⁺ = 367. The sample was loaded directly onto, and purified by, SPE (50 g, SCX). The column was washed with 10% MeOH in DCM and eluted using (2 M ammonia in MeOH). The appropriate fractions were combined and evaporated under reduced pressure to give a brown gum. The compound was triturated in EtOAc; the solid was removed and dried in a vacuum oven overnight to give 4-((cyclopropylmethyl)amino)-7-(3,5-dimethylisoxazol-4-yl)-6-methoxyquinoline-3-carboxamide **2.39** (371 mg, 1.013 mmol, 67% yield) as a yellow solid.

LCMS (formic acid): *rt* = 0.70 min, *MH*⁺ = 367

¹H NMR (d₆-DMSO): δ 0.27 – 0.34 (m, 2 H), 0.48 – 0.56 (m, 2 H), 1.12 – 1.23 (m, 1 H), 2.13 (s, 3 H) 2.32 (s, 3 H), 3.50 – 3.56 (m, 2 H) 3.91 (s, 3 H), 7.33 – 7.44 (br s, 1 H), 7.64 – 7.67 (m, 2 H), 7.97 – 8.07 (br s, 1 H), 8.60 (s, 1 H) 8.75 (t, *J* = 5.3 Hz, 1 H).

7-(3,5-Dimethylisoxazol-4-yl)-6-methoxy-4-((1-(tetrahydro-2*H*-pyran-4-yl)ethyl)amino)quinoline-3-carboxamide, **2.40**:

4-Chloro-7-(3,5-dimethylisoxazol-4-yl)-6-methoxyquinoline-3-carboxamide **2.34** (1 g, 3.01 mmol) was suspended in *N*-methyl-2-pyrrolidinone (5 ml), 1-(tetrahydro-2*H*-pyran-4-yl)ethanamine **2.55** (0.487 g, 3.77 mmol) and DIPEA (1.316 ml, 7.54 mmol) added, and the reaction mixture heated at 100 °C for 3.5 hours. LCMS (formic acid) of the reaction mixture showed 21% product by UV, *rt* = 0.67 min, *MH*⁺ = 425. The sample was loaded directly, and purified by, SPE (50g, SCX), washed with 50% MeOH in DCM and eluted using (2 M ammonia in MeOH). The appropriate fractions were combined and evaporated under reduced pressure to give a brown gum. The gum was loaded in MeOH/DCM (and the column dried in a vacuum oven) and purified by SPE (100 g, silica) using a gradient of 0 – 100% EtOAc in cyclohexane followed by 0–10% (2 M ammonia in MeOH) in DCM. The appropriate fractions were combined and evaporated under reduced pressure to give the required product 7-(3,5-

dimethylisoxazol-4-yl)-6-methoxy-4-((1-(tetrahydro-2*H*-pyran-4-yl)ethyl)amino)quinoline-3-carboxamide **2.40** (173 mg, 0.408 mmol, 14% yield) as a brown gum.

LCMS (formic acid): *rt* = 0.68 min, MH^+ = 425, 77% pure by UV.

1H NMR (d_6 -DMSO): δ 1.23 – 1.29 (m, 5 H) 1.27 (d, J = 6.6 Hz, 3 H) 1.52 – 1.62 (m, 1 H) 1.62 – 1.74 (m, 2 H) 2.14 (s, 3 H) 2.34 (s, 3 H) 3.22 – 3.30 (m, 3 H) 3.82 – 3.90 (m, 2 H) 3.93 (s, 3 H) 7.54 (s, 1 H) 7.70 (s, 1 H) 8.38 (d, J = 9.9 Hz, 1 H) 8.65 (s, 1 H). Compound > 70% pure by NMR.

7-(3,5-Dimethylisoxazol-4-yl)-8-methoxy-1-(1-(tetrahydro-2*H*-pyran-4-yl)ethyl)-1*H*-imidazo[4,5-*c*]quinoline-2(3*H*)-one, **2.41**:

To a suspension of 7-(3,5-dimethylisoxazol-4-yl)-6-methoxy-4-((1-(tetrahydro-2*H*-pyran-4-yl)ethyl)amino)quinoline-3-carboxamide **2.40** (169 mg, 0.398 mmol) in MeOH (2 ml) was added potassium hydroxide (33.5 mg, 0.597 mmol), and the reaction mixture stirred at room temperature for 20 min. The reaction mixture was cooled to 0 °C (ice/water bath), iodobenzene diacetate (167 mg, 0.518 mmol) added, and the reaction mixture stirred at 0 °C for a further 2 hours. LCMS (formic acid) of the reaction mixture showed 65% product by UV, *rt* = 0.70 min, MH^+ = 423. The reaction mixture was blown down under a stream of nitrogen and the residue dissolved in DMSO (4 x 1 ml) and purified by MDAP (1 x formic acid, 3 x high pH). The solvent was dried under a stream of nitrogen to give the required product 7-(3,5-dimethylisoxazol-4-yl)-8-methoxy-1-(1-(tetrahydro-2*H*-pyran-4-yl)ethyl)-1*H*-imidazo[4,5-*c*]quinoline-2(3*H*)-one **2.41** (41 mg, 0.097 mmol, 24% yield).

LCMS (formic acid): *rt* = 0.71 min, MH^+ = 423

1H NMR (d_6 -DMSO, 393 K): δ 1.20 – 1.31 (m, 1 H), 1.31 – 1.38 (m, 1 H), 1.39 – 1.52 (m, 1 H), 1.66 (d, J = 7.1 Hz, 3 H), 1.85 – 1.94 (m, 1 H), 2.12 (s, 3 H), 2.30 (s, 3 H), 2.55 – 2.68 (m, 1 H), 3.21 (dt, J = 11.6, 2.5 Hz, 1 H), 3.37 (dt, J = 11.4, 2.8 Hz, 1 H), 3.72 – 3.79 (m, 1 H), 3.92 – 3.96 (m, 4 H), 4.66 – 4.76 (m, 1 H), 7.53 (s, 1 H), 7.82 (s, 1 H), 8.11 – 8.14 (br s, 1 H) 8.54 (s, 1 H).

7-(3,5-Dimethylisoxazol-4-yl)-6-methoxy-3-nitro-*N*-((tetrahydro-2*H*-pyran-4-yl)methyl)quinoline-4-amine, **2.42**:

To a suspension of 4-(4-chloro-6-methoxy-3-nitroquinolin-7-yl)-3,5-dimethylisoxazole **2.33** (2 g, 5.99 mmol) in *N*-methyl-2-pyrrolidone (5 ml) was added DIPEA (1.047 ml, 5.99 mmol) and (tetrahydro-2*H*-pyran-4-yl)methanamine (1.035 g, 8.99 mmol) and the reaction mixture heated at 100 °C overnight. LCMS (formic acid) of the reaction mixture showed 79% product by UV, *rt* = 0.88 min, MH^+ = 413. The resulting solid was triturated in EtOAc to give a 7-(3,5-

dimethylisoxazol-4-yl)-6-methoxy-3-nitro-*N*-((tetrahydro-2*H*-pyran-4-yl)methyl)quinoline-4-amine **2.42** (2.1 g, 5.09 mmol, 85% yield) as a yellow solid.

LCMS (formic acid): *rt* = 0.87 min, MH^+ = 413

1H NMR (d_6 -DMSO): δ 1.18 – 1.29 (m, 2 H), 1.56 – 1.65 (m, 2 H), 1.91 – 2.04 (m, 1 H), 2.14 (s, 3 H), 2.33 (s, 3 H), 3.23 – 3.28 (m, 2 H), 3.29 (s, 3 H), 3.47 (t, J = 6.0 Hz, 2 H), 3.85 (dd, J = 11.2, 3.2 Hz, 2 H), 3.97 (s, 3 H), 7.79 (s, 1 H) 7.92 (s, 1 H) 8.67 – 8.72 (m, 1 H) 8.93 (s, 1 H).

7-(3,5-Dimethylisoxazol-4-yl)-6-methoxy-3-nitro-*N*-(1-(tetrahydro-2*H*-pyran-4-yl)ethyl)quinoline-4-amine, **2.43**:

4-(4-Chloro-6-methoxy-3-nitroquinolin-7-yl)-3,5-dimethylisoxazole **2.33** (520 mg, 1.558 mmol) was dissolved in *N*-methyl-2-pyrrolidinone (5 ml), DIPEA (0.272 ml, 1.558 mmol) and 1-(tetrahydro-2*H*-pyran-4-yl)ethanamine **2.55** (302 mg, 2.337 mmol) added, and the reaction mixture heated at 100 °C for 3.5 hours. LCMS (formic acid) of the reaction mixture after 2.5 hours showed 35% product by UV, *rt* = 0.98 min, MH^+ = 427; also present is 31% by UV of a side-product at *rt* = 0.70 min, MH^+ = 316, consistent with 7-(3,5-dimethylisoxazol-4-yl)-6-methoxy-3-nitroquinolin-4-ol. The sample was loaded directly, and purified by, SPE (SCX, 50 g). The column was washed with 50% MeOH in DCM and eluted using (2 M ammonia in MeOH). The appropriate fractions were combined and evaporated under reduced pressure to give a brown gum. The gum was loaded in MeOH/DCM (and the column dried in a vacuum oven) and purified by SPE (silica, 25 g) using 0 – 20% (2 M ammonia in MeOH) in DCM. The appropriate fractions were combined and dried under a stream of nitrogen to give the required product 7-(3,5-dimethylisoxazol-4-yl)-6-methoxy-3-nitro-*N*-(1-(tetrahydro-2*H*-pyran-4-yl)ethyl)quinoline-4-amine **2.43** (124 mg, 0.291 mmol, 19% yield) as a brown gum.

LCMS (formic acid): *rt* = 0.97 min, MH^+ = 427, 68% pure by UV.

1H NMR (d_6 -DMSO): δ 1.46 (d, J = 6.3 Hz, 3 H) 1.53 – 1.61 (m, 2 H) 2.16 (s, 3 H) 2.16 – 2.22 (m, 3 H) 2.35 (s, 3 H) 3.19 – 3.29 (m, 1 H) 3.81 – 3.90 (m, 4 H) 3.99 (s, 3 H) 7.75 (s, 1 H) 7.81 (s, 1 H) 8.45 – 8.53 (m, 1 H) 8.99 (s, 1 H). Compound > 60% by NMR.

7-(3,5-Dimethylisoxazol-4-yl)-6-methoxy-*N*-(1-methoxypropan-2-yl)-3-nitroquinolin-4-amine, **2.44**, Preparation A:

4-(4-Chloro-6-methoxy-3-nitroquinolin-7-yl)-3,5-dimethylisoxazole **2.33** (1 g, 3.00 mmol) was dissolved in *N*-methyl-2-pyrrolidinone (4 ml), DIPEA (0.523 ml, 3.00 mmol) and 1-methoxypropan-2-amine (0.474 ml, 4.49 mmol) added, and the reaction mixture heated at 100 °C for 2.5 hours. LCMS (formic acid) of the reaction mixture showed 93% product by UV, *rt* = 0.98 min, MH^+ = 387. The sample was loaded directly, and purified by, SPE (SCX, 50 g). The column was washed with 50% MeOH in DCM and eluted using (2 M ammonia in MeOH). The

appropriate fractions were combined and evaporated under reduced pressure to give a brown gum. The sample was loaded in DCM and purified by SPE (silica, 50 g) using 0 – 20% (2 M ammonia in MeOH) in DCM. The appropriate fractions were combined and blown down a stream of nitrogen to give the required product 7-(3,5-dimethylisoxazol-4-yl)-6-methoxy-*N*-(1-methoxypropan-2-yl)-3-nitroquinolin-4-amine **2.44** (715 mg, 1.850 mmol, 62% yield) as a brown gum.

LCMS (formic acid): rt = 0.97 min, MH⁺ = 387

¹H NMR (d₆-DMSO): δ 1.41 (d, *J* = 6.6 Hz, 3 H), 2.15 (s, 3 H), 2.34 (s, 3 H), 3.27 (s, 3 H), 3.50 – 3.58 (m, 2 H), 3.98 (s, 3 H), 4.33 – 4.43 (m, 1 H), 7.82 (s, 1 H), 7.83 (s, 1 H), 8.64 (d, *J* = 9.4 Hz, 1 H), 9.03 (s, 1 H).

7-(3,5-Dimethylisoxazol-4-yl)-6-methoxy-*N*-(1-methoxypropan-2-yl)-3-nitroquinolin-4-amine,

2.44, Preparation B:

To a solution of 4-(4-chloro-6-methoxy-3-nitroquinolin-7-yl)-3,5-dimethylisoxazole **2.33** (20 g, 59.9 mmol) in 1,4-dioxane (200 ml) was added 1-methoxypropan-2-amine (31.6 ml, 300 mmol) and the reaction mixture heated at 70 °C for 1.5 hours. The solvent was removed under reduced pressure and the resulting solid partitioned between EtOAc (3 x 750 ml) and water (750 ml). The organic layers were combined, dried using a hydrophobic frit and evaporated under reduced pressure to give 7-(3,5-dimethylisoxazol-4-yl)-6-methoxy-*N*-(1-methoxypropan-2-yl)-3-nitroquinolin-4-amine **2.44** (25.8 g). The yield is 98 % when the EtOAc seen in the NMR is taken into account.

LCMS (formic acid): rt = 0.97 min, MH⁺ = 387

¹H NMR (d₆-DMSO): δ 1.41 (d, *J* = 6.6 Hz, 3 H), 2.15 (s, 3 H), 2.34 (s, 3 H), 3.29 (s, 3 H), 3.55 – 3.58 (m, 2 H), 3.97 (s, 3 H), 4.34 – 4.44 (m, 1 H), 7.79 (s, 1 H), 7.83 (s, 1 H), 8.63 (d, *J* = 9.1 Hz, 1 H), 9.04 (s, 1 H).

N-(Cyclopropylmethyl)-7-(3,5-dimethylisoxazol-4-yl)-6-methoxy-3-nitroquinolin-4-amine,

2.45:

4-(4-Chloro-6-methoxy-3-nitroquinolin-7-yl)-3,5-dimethylisoxazole **2.33** (1 g, 3.00 mmol) was dissolved in *N*-methyl-2-pyrrolidinone (4 ml), DIPEA (0.523 ml, 3.00 mmol) and cyclopropylmethanamine (0.378 ml, 4.49 mmol) added, and the reaction mixture heated at 100 °C for 3.5 hours. LCMS (formic acid) of the reaction mixture showed 92% product by UV, rt = 0.98 min, MH⁺ = 369. The sample was loaded directly, and purified by, SPE (SCX, 20 g), washed with 50% MeOH in DCM and eluted using (2 M ammonia in MeOH). The appropriate fractions were combined and evaporated under reduced pressure to give a brownish yellow solid. The solid was triturated in EtOAc, filtered, and dried in a vacuum oven to leave *N*-

(cyclopropylmethyl)-7-(3,5-dimethylisoxazol-4-yl)-6-methoxy-3-nitroquinolin-4-amine **2.45**
(259 mg, 0.703 mmol, 23% yield) as a yellow solid.

LCMS (formic acid): $rt = 0.97$ min, $MH^+ = 369$

1H NMR (d_6 -DMSO): δ 0.33 – 0.39 (m, 2 H), 0.53 – 0.61 (m, 2 H), 1.14 – 1.26 (m, 1 H), 2.14 (s, 3 H), 2.33 (s, 3 H), 3.58 (dd, $J = 6.2, 4.9$ Hz, 2 H), 3.97 (s, 3 H), 7.78 (s, 1 H), 7.88 (s, 1 H), 8.97 (s, 1 H), 9.00 – 9.04 (m, 1 H).

7-(3,5-Dimethylisoxazol-4-yl)-6-methoxy-N4-((tetrahydro-2H-pyran-4-yl)methyl)quinoline-3,4-diamine, **2.46**, Preparation A:

To a suspension of 7-(3,5-dimethylisoxazol-4-yl)-6-methoxy-3-nitro-*N*-((tetrahydro-2*H*-pyran-4-yl)methyl)quinoline-4-amine **2.42** (270 mg, 0.655 mmol) in EtOAc (6 ml) and EtOH (2 ml) was added MeOH (20 ml). The reaction flask was placed in an ultrasonic bath until the suspended material had dissolved. The resulting solution was hydrogenated using an H-cube (20 °C, 1 bar, 1ml/min flow rate) with a 10% Pd/C CatCart 30. Part way through the hydrogenation, the H-cube became blocked. This was presumably due to material coming out of solution. The material in the product flask that had passed through the H-cube was blown down under a stream of nitrogen and the residue dissolved in DMSO (1 ml) and purified by MDAP (high pH). The solvent was blown down under a stream of nitrogen to give the required product 7-(3,5-dimethylisoxazol-4-yl)-6-methoxy-*N*4-((tetrahydro-2*H*-pyran-4-yl)methyl)quinoline-3,4-diamine **2.46** (41 mg, 0.107 mmol, 16% yield) as a pale yellow solid.

LCMS (formic acid): $rt = 0.68$ min, $MH^+ = 383$

1H NMR (d_6 -DMSO): δ 1.20 – 1.31 (m, 2 H), 1.72 – 1.83 (m, 3 H), 2.10 (s, 3 H), 2.29 (s, 3 H), 3.05 (t, $J = 6.6$ Hz, 2 H), 3.21 – 3.29 (m, 2 H), 3.79 – 3.94 (m, 5 H), 4.74 (t, $J = 7.1$ Hz, 1 H), 5.08 (s, 2 H), 7.39 (s, 1 H), 7.55 (s, 1 H), 8.27 (s, 1 H).

7-(3,5-Dimethylisoxazol-4-yl)-6-methoxy-N4-((tetrahydro-2H-pyran-4-yl)methyl)quinoline-3,4-diamine, **2.46**, Preparation B:

To a suspension of 7-(3,5-dimethylisoxazol-4-yl)-6-methoxy-3-nitro-*N*-((tetrahydro-2*H*-pyran-4-yl)methyl)quinoline-4-amine **2.42** (1.1 g, 2.67 mmol) in EtOH (20 ml) was added tin (II) chloride (1.770 g, 9.33 mmol) and the reaction mixture stirred at 40 °C for 1.5 hours. The reaction mixture was basified to pH 12 using 2 M aqueous sodium hydroxide solution. Water (50 ml) was added and the aqueous suspension extracted with DCM (3 x 50 ml). The organic layers were combined, dried using a hydrophobic frit and blown down under a stream of nitrogen. The sample was loaded in DCM and purified by SPE (silica, 100 g) using a gradient of 0 – 10% (2 M ammonia in MeOH) in DCM. The appropriate fractions were combined and blown down under a stream of nitrogen to give the required product 7-(3,5-dimethylisoxazol-4-

yl)-6-methoxy-*N*4-((tetrahydro-2*H*-pyran-4-yl)methyl)quinoline-3,4-diamine **2.46** (984 mg, 2.57 mmol, 96% yield) as a brown gum.

LCMS (formic acid): *rt* = 0.69 min, MH^+ = 383

1H NMR (d_6 -DMSO): δ 1.20 – 1.31 (m, 2 H), 1.72 – 1.80 (m, 3 H), 2.10 (s, 3 H), 2.29 (s, 3 H), 3.05 (t, *J* = 6.6 Hz, 2 H), 3.22 – 3.28 (m, 2 H), 3.82 – 3.93 (m, 5 H), 4.74 (t, *J* = 7.1 Hz, 1 H), 5.07 (br s, 2 H), 7.39 (s, 1 H), 7.55 (s, 1 H), 8.27 (s, 1 H).

7-(3,5-Dimethylisoxazol-4-yl)-6-methoxy-*N*4-(1-(tetrahydro-2*H*-pyran-4-yl)ethyl)quinoline-3,4-diamine, **2.47**:

7-(3,5-Dimethylisoxazol-4-yl)-6-methoxy-3-nitro-*N*-(1-(tetrahydro-2*H*-pyran-4-yl)ethyl)quinoline-4-amine **2.43** (120 mg, 0.281 mmol) was dissolved in EtOAc (4.5 ml) and EtOH (1.5 ml) and the reaction mixture was hydrogenated using an H-cube (20 °C, 1 bar, 1 ml/min flow rate) with a 10% Pd/C CatCart 30. After the first pass through the H-cube the reaction mixture was re-circulated for 60 min. The reaction mixture was blown down under a stream of nitrogen to give 7-(3,5-dimethylisoxazol-4-yl)-6-methoxy-*N*4-(1-(tetrahydro-2*H*-pyran-4-yl)ethyl)quinoline-3,4-diamine **2.47** (104 mg, 0.262 mmol, 93% yield) as a brown gum.

LCMS (formic acid): *rt* = 0.74 min, MH^+ = 397, 69% pure by LCMS

1H NMR not performed due to low purity.

7-(3,5-Dimethylisoxazol-4-yl)-6-methoxy-*N*4-(1-methoxypropan-2-yl)quinoline-3,4-diamine, **2.48**, Preparation A:

7-(3,5-Dimethylisoxazol-4-yl)-6-methoxy-*N*-(1-methoxypropan-2-yl)-3-nitroquinolin-4-amine **2.44** (715 mg, 1.850 mmol) was dissolved in EtOAc (15 ml) and EtOH (5 ml), and the reaction mixture was hydrogenated using an H-cube (20 °C, 1 bar, 1 ml/min flow rate) with a 10% Pd/C CatCart 30. The material was passed through the H-cube twice, after which time the reaction mixture was blown down under a stream of nitrogen to give 7-(3,5-dimethylisoxazol-4-yl)-6-methoxy-*N*4-(1-methoxypropan-2-yl)quinoline-3,4-diamine **2.48** (633 mg, 1.776 mmol, 96% yield) as a brown gum.

LCMS (formic acid): *rt* = 0.74 min, MH^+ = 357

1H NMR (d_6 -DMSO): δ 1.18 (d, *J* = 6.6 Hz, 3 H), 2.10 (s, 3 H), 2.30 (s, 3 H), 3.31 – 3.39 (m, 2 H), 3.49 – 3.63 (m, 1 H), 3.88 (s, 3 H), 4.51 (d, *J* = 10.4 Hz, 1 H), 5.13 (br s, 2 H), 7.45 (s, 1 H) 7.55 (s, 1 H) 8.29 (s, 1 H).

7-(3,5-Dimethylisoxazol-4-yl)-6-methoxy-N4-(1-methoxypropan-2-yl)quinoline-3,4-diamine,**2.48, Preparation B:**

7-(3,5-Dimethylisoxazol-4-yl)-6-methoxy-N-(1-methoxypropan-2-yl)-3-nitroquinolin-4-amine **2.44** (25.8 g, 66.8 mmol) was dissolved in a mixture of EtOAc (1000 ml) and dimethyl sulfoxide (50 ml) and the solution was hydrogenated using an H-cube (settings: 20 °C, 1 bar, 1ml/min flow rate) using 10% Pd/C CatCart 70 cartridges containing the catalyst. The catalyst cartridge was changed whenever it became blocked. The reaction mixture was evaporated under reduced pressure and partitioned between EtOAc (750 ml) and water (3 x 750 ml). The aqueous layers were combined and extracted with EtOAc (750 ml). Both organic layers were combined, dried using a hydrophobic frit, and evaporated under reduced pressure. The residue was loaded in DCM and purified by SPE (silica, 8 x 100 g) using a gradient of 0 – 4% (2 M ammonia in MeOH) in DCM. The appropriate fractions were combined and evaporated under reduced pressure to give batches of product (13.6 g) and recovered starting material (6.5 g).

The recovered starting material was dissolved in EtOAc (250 ml) and the reaction was hydrogenated using an H-cube (settings: 20 °C, 1 bar, 1ml/min flow rate) using a 10% Pd/C CatCart 70 as the catalyst. The reaction mixture was evaporated under reduced pressure and the residue was loaded in DCM and purified by SPE (silica, 2 x 100 g) using a gradient of 0–4% (2 M ammonia in MeOH) in DCM. The appropriate fractions were combined and evaporated under reduced pressure to give a second batch of product.

Both batches of product were combined to give 7-(3,5-dimethylisoxazol-4-yl)-6-methoxy-N4-(1-methoxypropan-2-yl)quinoline-3,4-diamine **2.48** (15.6 g, 43.8 mmol, 66% yield) as a sticky dark brown gum.

LCMS (formic acid): $rt = 0.73$ min, $MH^+ = 357$

1H NMR (d_6 -DMSO, 393 K): δ 1.20 (d, $J = 6.6$ Hz, 2 H), 2.11 (s, 3 H), 2.30 (s, 3 H), 3.32 (s, 3 H), 3.35 – 3.43 (m, 2 H) 3.52 – 3.65 (m, 1 H), 3.89 (s, 3 H), 4.31 (d, $J = 10.1$ Hz, 1 H), 4.96 (s, 1 H), 7.45 (s, 1 H), 7.55 (s, 1 H), 8.32 (s, 1 H).

4-(1-(Cyclopropylmethyl)-8-methoxy-2-(tetrahydro-2H-pyran-4-yl)-1H-imidazo[4,5-c]quinoline-7-yl)-3,5-dimethylisoxazole, 2.49:

To a suspension of N-(cyclopropylmethyl)-7-(3,5-dimethylisoxazol-4-yl)-6-methoxy-3-nitroquinolin-4-amine **2.45** (100 mg, 0.271 mmol) and sodium hydrosulfite (142 mg, 0.814 mmol) in EtOH (0.8 ml) and water (0.4 ml) was added tetrahydro-2H-pyran-4-carbaldehyde (62.0 mg, 0.543 mmol), and the reaction mixture heated in under microwave conditions at 100 °C for 1 hour. The reaction mixture was blown down under a stream of nitrogen and the residue dissolved in DMSO (3 x 1 ml) and purified by MDAP (high pH). One of these runs failed and

the material was lost. The solvent was blown down under a stream of nitrogen to give the required product 4-(1-(cyclopropylmethyl)-8-methoxy-2-(tetrahydro-2*H*-pyran-4-yl)-1*H*-imidazo[4,5-*c*]quinoline-7-yl)-3,5-dimethylisoxazole **2.49** (32 mg, 0.074 mmol, 27% yield) as a colourless gum.

LCMS (formic acid): *rt* = 0.78 min, MH^+ = 433

¹H NMR (*d*₆-DMSO, 393 K): δ 0.48 – 0.55 (m, 2 H) 0.64 – 0.68 (m, 2 H), 1.38 – 1.52 (m, 1 H), 1.89 – 1.92 (m, 2 H), 2.01 – 2.10 (m, 2H), 2.15 (s, 3 H), 2.34 (s, 3 H), 3.30 – 3.43 (m, 1 H), 3.56 – 3.68 (m, 2 H), 3.99 – 4.09 (m, 5 H), 4.71 (d, *J* = 6.0 Hz, 2 H), 7.89 (s, 1 H), 7.97 (s, 1 H), 9.04 (s, 1 H).

4-(2-Cyclopropyl-1-(cyclopropylmethyl)-8-methoxy-1*H*-imidazo[4,5-*c*]quinoline-7-yl)-3,5-dimethylisoxazole, **2.50**:

To a suspension of *N*-(cyclopropylmethyl)-7-(3,5-dimethylisoxazol-4-yl)-6-methoxy-3-nitroquinolin-4-amine **2.45** (30 mg, 0.081 mmol) and sodium hydrosulfite (42.5 mg, 0.244 mmol) in EtOH (0.4 ml) and water (0.2 ml) was added cyclopropanecarbaldehyde (0.012 ml, 0.163 mmol), and the reaction mixture heated under microwave conditions at 100 °C for a total of 2 hours. The reaction mixture was blown down under a stream of nitrogen and the residue dissolved in DMSO (1 ml) and purified by MDAP (high pH). The solvent was blown down under a stream of nitrogen to give the required product 4-(2-cyclopropyl-1-(cyclopropylmethyl)-8-methoxy-1*H*-imidazo[4,5-*c*]quinoline-7-yl)-3,5-dimethylisoxazole **2.50** (9.5 mg, 0.024 mmol, 30% yield) as a colourless gum.

LCMS (formic acid): *rt* = 0.80 min, MH^+ = 389

¹H NMR (*d*₆-DMSO, 393 K): δ 0.50 – 0.55 (m, 2 H), 0.56 – 0.63 (m, 2 H), 1.11 – 1.17 (m, 4 H), 1.44 – 1.57 (m, 1 H), 2.15 (s, 3 H), 2.34 (s, 3 H), 2.36 – 2.42 (m, 1 H), 4.03 (s, 3 H), 4.80 (d, *J* = 6.3 Hz, 2 H), 7.84 (s, 1 H), 7.96 (s, 1 H), 8.96 (s, 1 H).

(*S,E*)-2-Methyl-*N*-((tetrahydro-2*H*-pyran-4-yl)methylene)propane-2-sulfonamide, **2.57-R**:

To a mixture of (*S*)-2-methylpropane-2-sulfonamide **2.56-S** (1.327 g, 10.95 mmol), pyridinium *p*-toluenesulfonate (0.138 g, 0.548 mmol) and magnesium sulfate (6.59 g, 54.8 mmol) in dichloroethane (16 ml) was added tetrahydro-2*H*-pyran-4-carbaldehyde **2.51** (2.5 g, 21.90 mmol) and the reaction mixture stirred under nitrogen at room temperature overnight. The reaction mixture was filtered, the solid washed with DCM and discarded. The filtrate was blown down under a stream of nitrogen. The sample was loaded in DCM and purified by SPE (silica, 100 g) using a gradient of 0 – 50% EtOAc in cyclohexane. The appropriate fractions were combined and evaporated under reduced pressure to give the required product (*S,E*)-2-methyl-*N*-((tetrahydro-2*H*-pyran-4-yl)methylene)propane-2-sulfonamide **2.57-R** (2.1 g, 9.66 mmol, 44%

yield) as a white crystalline solid.

LCMS (formic acid): rt = 0.78 min, MH⁺ = 218

¹H NMR (CDCl₃): δ 1.20 (s, 9 H), 1.60 – 1.78 (m, 2 H), 1.79 – 1.90 (m, 2 H), 2.65 – 2.77 (m, 1 H), 3.44 – 3.56 (m, 2 H), 3.95 – 4.06 (m, 2 H), 8.01 (d, *J* = 3.8 Hz, 1H).

(*R,E*)-2-Methyl-*N*-((tetrahydro-2*H*-pyran-4-yl)methylene)propane-2-sulfinamide, **2.57-S**:

Method as for **2.57-R**, using the following reagents: (*R*)-2-methylpropane-2-sulfinamide **2.56-R** (1.207 ml, 10.95 mmol), pyridinium *p*-toluenesulfonate (0.138 g, 0.548 mmol), magnesium sulfate (6.59 g, 54.8 mmol), tetrahydro-2*H*-pyran-4-carbaldehyde **2.51** (2.5 g, 21.90 mmol) and dichloroethane (16 ml). The final product was: (*R,E*)-2-methyl-*N*-((tetrahydro-2*H*-pyran-4-yl)methylene)propane-2-sulfinamide **2.57-S** (1.74 g, 8.01 mmol, 36% yield) as a white crystalline solid.

LCMS (formic acid): rt = 0.78 min, MH⁺ = 218

¹H NMR (CDCl₃): δ 1.20 (s, 9 H) 1.62 – 1.79 (m, 2 H) 1.79 – 1.89 (m, 2 H) 2.61 – 2.78 (m, 1 H) 3.40 – 3.56 (m, 2 H) 3.92 – 4.07 (m, 2 H) 8.0 (d, *J* = 3.8 Hz, 1 H)

(*S*)-2-Methyl-*N*-((*R*)-1-(tetrahydro-2*H*-pyran-4-yl)ethyl)propane-2-sulfinamide, **2.58-R**:

A solution of (*S,E*)-2-methyl-*N*-((tetrahydro-2*H*-pyran-4-yl)methylene)propane-2-sulfinamide **2.57-R** (2.1 g, 9.66 mmol) in dry DCM (50 ml) under nitrogen was cooled to 0 °C (ice/water bath), and 2 M methylmagnesium bromide in THF (9.66 ml, 19.33 mmol) added dropwise. The reaction mixture was allowed to warm to room temperature and stirred for a further 3 hours. Saturated aqueous ammonium chloride solution (10 ml) was added, and the aqueous layer removed. The organic layer was washed with water (40 ml), brine (40 ml), dried using a hydrophobic frit and evaporated under reduced pressure. The sample was loaded in DCM and purified by SPE (silica, 100 g) using a gradient of 0 – 100% EtOAc in cyclohexane. The appropriate fractions were combined and evaporated under reduced pressure to give the required product (*S*)-2-methyl-*N*-((*R*)-1-(tetrahydro-2*H*-pyran-4-yl)ethyl)propane-2-sulfinamide **2.58-R** (1.19 g, 5.10 mmol, 53% yield) as a colourless liquid.

LCMS (formic acid): no UV chromophore

¹H NMR (CDCl₃): δ 1.22 (s, 9 H), 1.28 (d, *J* = 6.6 Hz, 3 H), 1.30 – 1.48 (m, 2 H), 1.50 – 1.57 (m, 1 H), 1.65 – 1.74 (m, 1 H), 2.81 (d, *J* = 7.6 Hz, 1 H), 3.14 – 3.24 (m, 1 H), 3.33 – 3.38 (m, 2 H), 3.94 – 4.05 (m, 2 H).

(*R*)-2-Methyl-*N*-((*S*)-1-(tetrahydro-2*H*-pyran-4-yl)ethyl)propane-2-sulfinamide, **2.58-S**:

Method as for **2.58-R**, using the following reagents: (*R,E*)-2-methyl-*N*-((tetrahydro-2*H*-pyran-4-yl)methylene)propane-2-sulfinamide **2.57-S** (1.74 g, 8.01 mmol), 2 M methylmagnesium

bromide in THF (8.01 ml, 16.01 mmol) and DCM (40 ml). The final product was: (*R*)-2-methyl-*N*-((*S*)-1-(tetrahydro-2*H*-pyran-4-yl)ethyl)propane-2-sulfonamide **2.58-S** (1.47 g, 6.30 mmol, 79% yield) as a colourless liquid.

LCMS (formic acid): no UV chromophore

¹H NMR (CDCl₃): δ 1.22 (s, 9 H) 1.28 (d, *J* = 6.6 Hz, 3 H) 1.31 – 1.49 (m, 2 H) 1.50 – 1.57 (m, 1 H) 1.66 – 1.75 (m, 1 H) 2.82 (d, *J* = 7.8 Hz, 1 H) 3.14 – 3.24 (m, 1 H) 3.31 – 3.43 (m, 2 H) 3.96 – 4.04 (m, 2 H)

(*R*)-1-(Tetrahydro-2*H*-pyran-4-yl)ethanamine hydrochloride, **2.59-R**:

To a solution of (*S*)-2-methyl-*N*-((*R*)-1-(tetrahydro-2*H*-pyran-4-yl)ethyl)propane-2-sulfonamide **2.58-R** (1.19 g, 5.10 mmol) in MeOH (15 ml) was added 4 M hydrochloric acid in 1,4-dioxane (12.75 ml, 51.0 mmol) and the reaction mixture stirred at room temperature for 1 hour. The reaction mixture was evaporated under reduced pressure and triturated in diethyl ether to give (*R*)-1-(tetrahydro-2*H*-pyran-4-yl)ethanamine hydrochloride **2.59-R** (855 mg, 5.16 mmol, 101% yield) as an off-white solid. The yield is 96% when the 1,4-dioxane in the NMR is taken into account.

LCMS (formic acid): rt = 0.22 min, MH⁺ = 130, no UV chromophore

¹H NMR (CDCl₃): δ 1.40 (d, *J* = 6.6 Hz, 3 H) 1.42 – 1.57 (m, 2 H), 1.68 (d, *J* = 12.9 Hz, 1 H), 1.76 – 1.96 (m, 2 H), 3.08 – 3.23 (m, 1 H), 3.38 (m, 2 H), 4.02 (d, *J* = 11.6 Hz, 2 H), 8.43 (br s, 3 H).

(*S*)-1-(Tetrahydro-2*H*-pyran-4-yl)ethanamine hydrochloride, **2.59-S**:

To a solution of (*R*)-2-methyl-*N*-((*S*)-1-(tetrahydro-2*H*-pyran-4-yl)ethyl)propane-2-sulfonamide **2.58-S** (1.47 g, 6.30 mmol) in MeOH (15 ml) was added 4 M hydrochloric acid in 1,4-dioxane (15.75 ml, 63.0 mmol) and the reaction mixture stirred at room temperature for 1 hour. The reaction mixture was evaporated under reduced pressure and triturated in ether to give (*S*)-1-(tetrahydro-2*H*-pyran-4-yl)ethanamine hydrochloride **2.59-S** (984 mg, 5.94 mmol, 94% yield) as an off-white solid.

LCMS (formic acid): rt = 0.22 min, MH⁺ = 130, no UV chromophore

¹H NMR (CDCl₃): δ 1.40 (d, *J* = 6.8 Hz, 3 H) 1.41 – 1.53 (m, 2 H) 1.67 (d, *J* = 12.6 Hz, 1 H) 1.77 – 1.95 (m, 2 H) 3.07 – 3.24 (m, 1 H) 3.30 – 3.46 (m, 2 H) 4.02 (d, *J* = 11.6 Hz, 2 H) 8.43 (br s, 3 H)

7-(3,5-Dimethylisoxazol-4-yl)-6-methoxy-3-nitro-*N*-((*R*)-1-(tetrahydro-2*H*-pyran-4-yl)ethyl)quinoline-4-amine, **2.60-R**:

4-(4-Chloro-6-methoxy-3-nitroquinolin-7-yl)-3,5-dimethylisoxazole **2.33** (1.5 g, 4.49 mmol)

was dissolved in *N*-methyl-2-pyrrolidone (5 ml), (*R*)-1-(tetrahydro-2*H*-pyran-4-yl)ethanamine **2.59-R** (855 mg, 6.62 mmol) and DIPEA (2.355 ml, 13.48 mmol) added, and the reaction mixture heated at 100 °C for 3 hours. The sample was loaded directly, and purified by, SPE (SCX, 70 g), washed with 50% MeOH in DCM and eluted using (2 M ammonia in MeOH). The MeOH/DCM fractions were combined and evaporated under reduced pressure to give a brown liquid (~ 6 ml) which contained NMP. The liquid was purified, without further dilution, by MDAP (high pH). The solvent was blown down a stream of nitrogen to give the required product 7-(3,5-dimethylisoxazol-4-yl)-6-methoxy-3-nitro-*N*-((*R*)-1-(tetrahydro-2*H*-pyran-4-yl)ethyl)quinoline-4-amine **2.60-R** (1.17 g, 2.74 mmol, 61% yield) as a yellow solid.

LCMS (formic acid): rt = 0.97 min, MH⁺ = 427

¹H NMR (d₆-DMSO): δ 1.11 – 1.33 (m, 2 H), 1.45 (d, *J* = 6.3 Hz, 3 H), 1.57 (d, *J* = 11.4 Hz, 2 H), 1.80 – 1.93 (m, 1 H), 2.15 (s, 3 H), 2.34 (s, 3 H), 3.21 – 3.28 (m, 2 H), 3.79 – 3.96 (m, 3 H), 3.98 (s, 3 H), 7.74 (s, 1 H), 7.81 (s, 1 H), 8.42 – 8.54 (m, 1 H), 8.98 (s, 1 H).

Chiral HPLC (25 cm Chiralpak IA, column no. IA00CE-MC024, 60% EtOH in heptane, 1 ml/min flow rate, UV detection at 215 nm): 12.34 min, 99.9% by UV; 6.23 min, 0.1% by UV, consistent with **2.60-S**.

7-(3,5-Dimethylisoxazol-4-yl)-6-methoxy-3-nitro-*N*-((*S*)-1-(tetrahydro-2*H*-pyran-4-yl)ethyl)quinolin-4-amine, **2.60-S**:

4-(4-Chloro-6-methoxy-3-nitroquinolin-7-yl)-3,5-dimethylisoxazole **2.33** (1.5 g, 4.49 mmol) was dissolved in *N*-methyl-2-pyrrolidone (10 ml), (*S*)-1-(tetrahydro-2*H*-pyran-4-yl)ethanamine **2.59-S** (980 mg, 7.59 mmol) and DIPEA (2.59 ml, 14.83 mmol) added, and the reaction mixture heated at 100 °C for 4 hours. The sample was loaded directly, and purified by, SPE (SCX, 70 g), washed with 50% MeOH in DCM and eluted using 2 M ammonia in MeOH. The appropriate basic fractions were combined and evaporated under reduced pressure to give a brown gum. The gum was loaded in DCM and purified by SPE (silica, 100 g) using 0 – 10% (2 M ammonia in MeOH) in DCM. The appropriate fractions were combined and dried under a stream of nitrogen to give a first batch of the required product 7-(3,5-dimethylisoxazol-4-yl)-6-methoxy-3-nitro-*N*-((*S*)-1-(tetrahydro-2*H*-pyran-4-yl)ethyl)quinolin-4-amine **2.60-S** (486 mg, 1.140 mmol, 25% yield) as a brown gum. The 50 % MeOH in DCM fractions from the SCX column were combined and evaporated under reduced pressure to give a brown liquid (~ 10 ml) which contained *N*-methyl-2-pyrrolidone. The liquid was purified, without further dilution, by MDAP (high pH). The solvent was evaporated under reduced pressure to give a second batch of the required product 7-(3,5-dimethylisoxazol-4-yl)-6-methoxy-3-nitro-*N*-((*S*)-1-(tetrahydro-2*H*-pyran-4-yl)ethyl)quinolin-4-amine **2.60-S** (1.18 g, 2.77 mmol, 62 % yield) as a yellow solid.

The total yield of the reaction was 87%.

Batch 1:

LCMS (formic acid): $rt = 0.97$ min, $MH^+ = 427$

1H NMR (d_6 -DMSO): δ 1.25 – 1.37 (m, 2 H), 1.41 (d, $J = 6.3$ Hz, 3 H), 1.56 – 1.68 (m, 2 H), 1.84 – 1.95 (m, expected as 1 H, impurity partially obscured peak), 2.11 – 2.18 (m, expected as s, 3 H, impurity partially obscured peak), 2.32 (s, 3 H), 2.69 (s, 3 H), 2.82 (s, 3 H), 3.25 – 3.32 (m, 2 H), 3.79 – 3.96 (m, 2 H), 3.96 (s, 3 H), 7.71 (s, 1 H), 7.75 (s, 1 H), 8.32 – 8.39 (m, 1 H), 8.99 (s, 1 H). Sample approximately 80% pure by NMR.

Chiral HPLC (25 cm Chiralpak IA, column no. IA00CE-MC024, 60% EtOH in heptane, 1 ml/min flow rate, UV detection at 215 nm): 6.21 min, 100% by UV, no evidence of **2.60-R** at 12.34 min.

Batch 2:

LCMS (formic acid): $rt = 0.97$ min, $MH^+ = 427$

1H NMR (d_6 -DMSO): δ 1.12 – 1.32 (m, 2 H), 1.45 (d, $J = 6.6$ Hz, 3 H), 1.57 (d, $J = 11.6$ Hz, 2 H), 1.82 – 1.93 (m, 1 H), 2.15 (s, 3 H), 2.34 (s, 3 H), 3.21 – 3.29 (m, 2 H), 3.80 – 3.90 (m, 3 H), 3.98 (s, 3 H), 7.74 (s, 1 H), 7.81 (s, 1 H), 8.48 (d, $J = 9.1$ Hz, 1 H), 8.98 (s, 1 H). Sample > 95% pure by NMR.

4-(8-Methoxy-2-(tetrahydro-2H-pyran-4-yl)-1-((R)-1-(tetrahydro-2H-pyran-4-yl)ethyl)-1H-imidazo[4,5-c]quinoline-7-yl)-3,5-dimethylisoxazole, **2.61-R**:

To a suspension of 7-(3,5-dimethylisoxazol-4-yl)-6-methoxy-3-nitro-*N*-((*R*)-1-(tetrahydro-2H-pyran-4-yl)ethyl)quinoline-4-amine **2.60-R** (106 mg, 0.249 mmol) and sodium hydrosulfite (130 mg, 0.746 mmol) in EtOH (1 ml) and water (0.4 ml) was added tetrahydro-2H-pyran-4-carbaldehyde (142 mg, 1.243 mmol), and the reaction mixture heated under microwave conditions to 100 °C for 3 hours. The reaction mixture was blown down under a stream of nitrogen and the residue dissolved in DMSO (4 x 1 ml) and purified by MDAP (high pH). The solvent was blown down under a stream of nitrogen to give 4-(8-methoxy-2-(tetrahydro-2H-pyran-4-yl)-1-((*R*)-1-(tetrahydro-2H-pyran-4-yl)ethyl)-1H-imidazo[4,5-c]quinoline-7-yl)-3,5-dimethylisoxazole **2.61-R** (2.4 mg, 4.89 μ mol, 2% yield).

LCMS (formic acid): $rt = 0.78$ min, $MH^+ = 491$

1H NMR (d_6 -DMSO): δ 0.78 – 0.92 (m, 1 H), 1.15 – 1.36 (m, 1 H), 1.54 – 1.69 (m, 1 H), 1.78 – 1.93 (m, 6 H), 1.98 – 2.08 (m, 2 H), 2.14 (s, 3 H) 2.33 (s, 3 H), 3.01 – 3.18 (m, 1 H), 3.36 – 3.49 (m, 2 H), 3.58 – 3.70 (m, 4 H), 3.94 – 4.10 (m, 7 H), 7.72 (br s, 1 H) 7.97 (s, 1 H) 9.02 (s, 1 H).

4-(8-Methoxy-2-(tetrahydro-2H-pyran-4-yl)-1-((S)-1-(tetrahydro-2H-pyran-4-yl)ethyl)-1H-imidazo[4,5-c]quinolin-7-yl)-3,5-dimethylisoxazole, **2.61-S**:

To a suspension of 7-(3,5-dimethylisoxazol-4-yl)-6-methoxy-3-nitro-*N*-((S)-1-(tetrahydro-2H-pyran-4-yl)ethyl)quinolin-4-amine **2.60-S** (75 mg, 0.176 mmol) and sodium hydrosulfite (92 mg, 0.528 mmol) in EtOH (1 ml) and water (0.4 ml) was added tetrahydro-2H-pyran-4-carbaldehyde (100 mg, 0.879 mmol) and the reaction mixture heated under microwave conditions at 100 °C for 4 hours. The reaction mixture was blown down under a stream of nitrogen and the residue dissolved in DMSO (2 x 1 ml) and purified by MDAP (high pH). The solvent was blown down under a stream of nitrogen to give crude material (14 mg). LCMS (formic acid) indicated 96 % product by UV at 0.76 min, MH⁺ 491. However, analysis indicated major impurities. The reaction was therefore abandoned.

7-(3,5-Dimethylisoxazol-4-yl)-6-methoxy-3-nitro-*N*-(pyridine-2-ylmethyl)quinoline-4-amine, **2.62**:

To a suspension of 4-(4-chloro-6-methoxy-3-nitroquinolin-7-yl)-3,5-dimethylisoxazole **2.33** (3 g, 8.99 mmol) in 1,4-dioxane (20 ml) was added pyridine-2-ylmethanamine (1.402 ml, 13.48 mmol), and the reaction mixture stirred at room temperature for 5 hours. Further pyridine-2-ylmethanamine (0.7 ml, 6.74 mmol) was added and the reaction mixture stirred at room temperature overnight. The solvent was removed under reduced pressure and the residue loaded in MeOH/DCM (and the column dried in a vacuum oven) and purified by SPE (silica, 2 x 100 g) using a gradient of 50 – 100% EtOAc in cyclohexane. The appropriate fractions were combined and evaporated under reduced pressure to give the required product 7-(3,5-dimethylisoxazol-4-yl)-6-methoxy-3-nitro-*N*-(pyridine-2-ylmethyl)quinoline-4-amine **2.62** (2.67 g, 6.59 mmol, 73% yield) as a yellow solid.

LCMS (formic acid): rt = 0.87 min, MH⁺ = 406

¹H NMR (d₆-DMSO, 393 K): δ 2.14 (s, 3 H), 2.34 (s, 3 H), 3.90 (s, 3 H), 5.17 (d, *J* = 4.8 Hz, 2 H), 7.29 – 7.39 (m, 1 H), 7.51 (d, *J* = 7.8 Hz, 1 H), 7.77 (s, 1H), 7.80 – 7.84 (m, 1 H), 7.96 (s, 1 H), 8.60 (d, *J* = 4.5 Hz, 1 H), 9.02 (s, 1 H), 9.47 – 9.66 (br s, 1 H).

7-(3,5-Dimethylisoxazol-4-yl)-6-methoxy-3-nitro-*N*-((R)-1-(pyridine-2-yl)ethyl)quinoline-4-amine, **2.63**:

Method as for **2.62**, using the following reagents: 4-(4-chloro-6-methoxy-3-nitroquinolin-7-yl)-3,5-dimethylisoxazole **2.33** (1 g, 3.00 mmol), (*R*)-1-(pyridine-2-yl)ethanamine (0.549 g, 4.49 mmol) and 1,4-dioxane (6.5 ml). After 5 hours, further (*R*)-1-(pyridine-2-yl)ethanamine (0.255 g, 2.25 mmol) was added. The final product was: 7-(3,5-dimethylisoxazol-4-yl)-6-methoxy-3-nitro-*N*-((*R*)-1-(pyridine-2-yl)ethyl)quinoline-4-amine **2.63** (1.15 g, 2.74 mmol, 92% yield) as

an orange solid.

LCMS (formic acid): $rt = 0.98$ min, $MH^+ = 420$

1H NMR (d_6 -DMSO, 393 K): δ 1.74 (d, $J = 6.6$ Hz, 3 H), 2.13 (s, 3H), 2.32 (s, 3H), 3.86 (s, 3 H), 5.51 – 5.58 (m, 1 H), 7.29 – 7.33 (m, 1 H), 7.56 (d, $J = 7.8$ Hz, 1 H), 7.77 (s, 1H), 7.78 (s, 1H), 7.79 – 7.82 (m, 1H), 8.58 (d, $J = 4.8$ Hz, 1 H), 9.05 (s, 1 H) 9.24 (d, $J = 7.6$ Hz, 1 H).

7-(3,5-Dimethylisoxazol-4-yl)-6-methoxy-N4-(pyridine-2-ylmethyl)quinoline-3,4-diamine,

2.64:

To a suspension of 7-(3,5-dimethylisoxazol-4-yl)-6-methoxy-3-nitro-N-(pyridine-2-ylmethyl)quinoline-4-amine **2.62** (2.67 g, 6.59 mmol) in EtOH (50 ml) was added tin (II) chloride (4.37 g, 23.05 mmol) and the reaction mixture stirred at 40 °C for 2.5 hours. The reaction mixture was basified to pH 12 using 2 M aqueous sodium hydroxide solution. Water (100 ml) was added and the aqueous suspension extracted with DCM (3 x 100 ml). The organic layers were combined, dried using a hydrophobic frit and blown down a stream of nitrogen. The sample was loaded in DCM and purified by SPE (silica, 100 g) using a gradient of 0 – 10% (2 M ammonia in MeOH) in DCM. The appropriate fractions were combined and blown down a stream of nitrogen to give the required product 7-(3,5-dimethylisoxazol-4-yl)-6-methoxy-N4-(pyridine-2-ylmethyl)quinoline-3,4-diamine **2.64** (879 mg, 2.341 mmol, 36% yield) as a dark brown gum.

LCMS (formic acid): $rt = 0.63$ min, $MH^+ = 376$

1H NMR (d_6 -DMSO, 393 K): δ 2.10 (s, 3 H), 2.29 (s, 3 H), 3.82 (s, 3 H), 4.52 (d, $J = 3.8$ Hz, 2 H), 4.82 – 5.01 (br s, 2 H) 5.12 – 5.25 (br s, 1 H), 7.24 – 7.27 (m, 1 H), 7.47 (s, 1 H), 7.49 (d, $J = 7.8$ Hz, 1 H), 7.55 (s, 1 H), 7.72 – 7.76 (m, 1 H), 8.33 (s, 1 H), 8.57 (d, $J = 4.3$ Hz, 1 H).

7-(3,5-Dimethylisoxazol-4-yl)-6-methoxy-N4-((R)-1-(pyridine-2-yl)ethyl)quinoline-3,4-diamine, **2.65:**

Method as for **2.64**, using the following reagents: 7-(3,5-dimethylisoxazol-4-yl)-6-methoxy-3-nitro-N-((R)-1-(pyridine-2-yl)ethyl)quinoline-4-amine **2.63** (1.05 g, 2.503 mmol), tin (II) chloride (1.661 g, 8.76 mmol) and EtOH (20 ml). The final product was: 7-(3,5-dimethylisoxazol-4-yl)-6-methoxy-N4-((R)-1-(pyridine-2-yl)ethyl)quinoline-3,4-diamine **2.65** (543 mg, 1.394 mmol, 56% yield) as a dark brown gum.

LCMS (formic acid): $rt = 0.70$ min, $MH^+ = 390$

1H NMR (d_6 -DMSO, 393 K): δ 1.58 (d, $J = 6.8$ Hz, 3 H), 2.09 (s, 3 H), 2.28 (s, 3 H), 3.83 (s, 3 H), 4.66 – 4.80 (m, 1 H), 4.80 – 4.97 (m, 2 H), 7.18 – 7.27 (m, 1 H), 7.38 (s, 1 H), 7.45 (d, $J = 7.8$ Hz, 1 H), 7.53 (s, 1 H), 7.67 – 7.73 (m, 1 H), 8.33 (s, 1 H), 8.56 (d, $J = 4.8$ Hz, 1 H).

7-(3,5-Dimethylisoxazol-4-yl)-8-methoxy-*N*-(2-methoxyethyl)-1-((*R*)-1-(pyridine-2-yl)ethyl)-1*H*-imidazo[4,5-*c*]quinoline-2-amine, **2.66**:

To a solution of 7-(3,5-dimethylisoxazol-4-yl)-6-methoxy-*N*4-((*R*)-1-(pyridine-2-yl)ethyl)quinoline-3,4-diamine **2.65** (538 mg, 1.381 mmol) in EtOH (40 ml) was added 1-isothiocyanato-2-methoxyethane (0.300 ml, 2.76 mmol) and the reaction mixture heated at 60 °C for 5.5 hours. Further 1-isothiocyanato-2-methoxyethane (0.150 ml, 1.38 mmol) was added and the reaction mixture heated at 60 °C overnight. The solvent was removed under reduced pressure, and the residue dissolved in THF (40 ml), EDC (530 mg, 2.76 mmol) added, and the mixture heated at 60 °C for 4 hours. The solvent was removed under reduced pressure and the sample was loaded in MeOH/DCM (and the column dried in a vacuum oven) and purified by SPE (silica, 100 g) using a gradient of 0 – 10% (2 M ammonia in MeOH) in DCM. The appropriate fractions were combined and evaporated under reduced pressure to give crude product (~600 mg). The crude product was dissolved in DMSO (5 x 1 ml) and purified by MDAP (high pH). For three of the five injections the machine leaked and the product was lost. The samples from the successful injections were blown down under a stream of nitrogen to give the required product 7-(3,5-dimethylisoxazol-4-yl)-8-methoxy-*N*-(2-methoxyethyl)-1-((*R*)-1-(pyridine-2-yl)ethyl)-1*H*-imidazo[4,5-*c*]quinoline-2-amine **2.66** (122 mg, 0.258 mmol, 19% yield) as a white solid.

LCMS (formic acid): rt = 0.73 min, MH⁺ = 473

¹H NMR (d₆-DMSO, 393 K): δ 2.06 – 2.11 (m, 6 H), 2.27 (s, 3 H), 3.35 (s, 3 H), 3.59 (s, 3 H), 3.62 – 3.73 (m, 4 H), 6.32 (q, *J* = 7.1 Hz, 1 H), 6.77 – 6.85 (br m, 1 H), 6.96 (s, 1 H), 7.30 (d, *J* = 7.8 Hz, 1 H), 7.33 – 7.39 (m, 1 H), 7.75 – 7.81 (m, 2 H), 8.68 (d, *J* = 4.0 Hz, 1 H), 8.82 (s, 1 H).

¹³C NMR (d₆-DMSO, 303 K): δ 10.3, 11.3, 17.7, 42.8, 55.3, 58.1 (br, 2 C), 70.5, 112.3, 113.9, 116.7, 118.3, 121.1, 121.2, 122.9, 132.7, 137.8, 138.5, 139.9, 149.5, 149.6, 154.0, 155.7, 158.9, 159.1, 165.8.

IR (neat): 3239 (imine NH), 1591 (aryl), 1556 (aryl), 1219 (aryl ether), 772 (aryl C-H) cm⁻¹

M.pt.: 109–111 °C

HRMS: (C₂₆H₂₉N₆O₃) MH⁺ requires 473.2296, found MH⁺ 473.2284

[α_D]^{23.1°C} (c 1.0, MeOH): +118.7°

4-(8-Methoxy-1-((*R*)-1-methoxypropan-2-yl)-2-(tetrahydro-2*H*-pyran-4-yl)-1*H*-imidazo[4,5-*c*]quinoline-7-yl)-3,5-dimethylisoxazole, **2.67**:

The racemic 4-(1-(1-methoxypropan-2-yl)-2-(tetrahydro-2*H*-pyran-4-yl)-1*H*-imidazo[4,5-*c*]quinoline-7-yl)-3,5-dimethylisoxazole **2.02** (85 mg, 0.189 mmol) was separated by chiral

HPLC. The HPLC analysis was carried out on a Chiralpak AD-H column “ADH10029-01” (250 x 30 mm, i.d. 5 μ m packing diameter). The purification was run using 15% EtOH in heptane over 35 min, with a flow rate of 45 ml/min. The UV detection was at a wavelength of 300 nm. The second eluting enantiomer was collected, between 28 min and 31 min. Combined fraction solutions were evaporated to dryness under reduced pressure, the residue transferred to a vial using EtOH, and the solvent was dried under a stream of nitrogen to leave 4-(8-methoxy-1-((*R*)-1-methoxypropan-2-yl)-2-(tetrahydro-2*H*-pyran-4-yl)-1*H*-imidazo[4,5-*c*]quinoline-7-yl)-3,5-dimethylisoxazole **2.67** (39 mg, 0.087 mmol, 46% yield).

LCMS (formic acid): rt = 0.73 min, MH⁺ = 451

¹H NMR (d₆-DMSO, 393 K): δ 1.80 (d, *J* = 7.3 Hz, 3 H), 1.83 – 1.98 (m, 2 H), 2.00 – 2.10 (m, 2 H), 2.13 (s, 3 H), 2.32 (s, 3 H), 3.26 (s, 3 H), 3.39 – 3.49 (m, 1 H), 3.54 – 3.62 (m, 2 H), 3.95 – 4.05 (m, 6 H), 4.08 – 4.12 (m, 1 H) 5.35 – 5.47 (m, 1 H), 7.72 (s, 1 H), 7.95 (s, 1 H), 9.00 (s, 1 H).

Chiral HPLC (conditions as for preparative HPLC, except column diameter of 4.6 mm): 97% ee.

Additional analytical information was generated on subsequent batches of material after the separation was performed using identical methodology on a larger scale:

¹³C NMR (d₆-DMSO, 303 K): δ 10.3, 11.3, 17.6, 31.3, 31.7, 33.2, 51.3, 55.6, 58.5, 66.6, 74.0, 101.2, 102.6, 112.1, 117.4, 119.4, 132.1, 133.1, 137.5, 139.5, 142.7, 154.7, 159.1, 166.0.

IR: 2963 (saturated CH₂), 2940 (saturated CH₂), 2852 (ether COCH₃), 1618 (aryl), 1583 (aryl), 1221 (aryl ether), 839 (aryl C-H) cm⁻¹

M.pt.: 190–192 °C

HRMS: (C₂₅H₃₁N₄O₄) MH⁺ requires 451.2340, found MH⁺ 451.2331

[α _D]^{23.1 °C} (c 1.0, MeOH): +2.9°

4-(8-Methoxy-1-((*S*)-1-methoxypropan-2-yl)-2-(tetrahydro-2*H*-pyran-4-yl)-1*H*-imidazo[4,5-*c*]quinoline-7-yl)-3,5-dimethylisoxazole, **2.68**:

The racemic 4-(1-(1-methoxypropan-2-yl)-2-(tetrahydro-2*H*-pyran-4-yl)-1*H*-imidazo[4,5-*c*]quinolin-7-yl)-3,5-dimethylisoxazole **2.02** (85 mg, 0.189 mmol) was purified by chiral HPLC. The HPLC analysis was carried out on a Chiralpak AD-H column “ADH10029-01” (250 x 30 mm, i.d. 5 μ m packing diameter). The purification was run using 15% EtOH in heptane over 35 min, with a flow rate of 45 ml/min. The UV detection was at a wavelength of 300 nm. The first eluting enantiomer was collected, between 24 min and 26.5 min. Combined fraction solutions were evaporated to dryness under reduced pressure, the residue transferred to a vial using EtOH, and the solvent was dried under a stream of nitrogen to leave 4-(8-methoxy-1-((*S*)-

1-methoxypropan-2-yl)-2-(tetrahydro-2*H*-pyran-4-yl)-1*H*-imidazo[4,5-*c*]quinolin-7-yl)-3,5-dimethylisoxazole **2.68** (38 mg, 0.084 mmol, 44% yield).

LCMS (formic acid): *rt* = 0.73 min, MH^+ = 451

¹H NMR (*d*₆-DMSO, 393 K): δ 1.80 (d, *J* = 7.3 Hz, 3 H), 1.82 – 1.98 (m, 2 H), 2.00 – 2.10 (m, 1 H), 2.13 (s, 3 H), 2.32 (s, 3 H), 3.26 (s, 3 H), 3.54 – 3.63 (m, 2 H), 3.96 – 4.05 (m, 7 H), 5.34 – 5.49 (br m, 1 H), 7.72 (s, 1 H), 7.95 (s, 1 H), 9.00 (s, 1 H).

Chiral HPLC (conditions as for preparative HPLC, except column diameter of 4.6 mm): > 99% ee.

N-(7-(3,5-Dimethylisoxazol-4-yl)-6-methoxy-4-((1-methoxypropan-2-yl)amino)quinoline-3-yl)tetrahydro-2*H*-pyran-4-carboxamide, **2.69**:

A solution of 7-(3,5-dimethylisoxazol-4-yl)-6-methoxy-*N*4-(1-methoxypropan-2-yl)quinoline-3,4-diamine **2.48** (9.1 g, 25.5 mmol) in DCM (300 ml) was treated with pyridine (30 ml) and tetrahydro-2*H*-pyran-4-carbonyl chloride (5.0 ml, 41.1 mmol). The solution was stirred under nitrogen at room temperature for 3.5 hours, and then left standing overnight. The reaction mixture was concentrated under reduced pressure, and the residue partitioned between DCM and water. The organic phase was washed with water (x 2) and the combined aqueous layers extracted with DCM. The combined organic layers were washed with brine, dried using a hydrophobic frit, and evaporated under reduced pressure. The combined aqueous layers, including the brine wash, were basified with solid sodium bicarbonate and the aqueous layer twice extracted with DCM. The organic fractions were dried using a hydrophobic frit, combined with the previously extracted material, and evaporated to dryness under reduced pressure to give a brown foam. This foam was further dried *in vacuo* to give 13.5 g of material. The material was triturated with diethyl ether, the suspension chilled (ice/water bath), and the solid isolated by filtration. The solid was washed with a little diethyl ether and air-dried to give *N*-(7-(3,5-dimethylisoxazol-4-yl)-6-methoxy-4-((1-methoxypropan-2-yl)amino)quinoline-3-yl)tetrahydro-2*H*-pyran-4-carboxamide **2.69** as a beige solid (11.95 g, 25.5 mmol, 100% yield).

LCMS (formic acid): *rt* = 0.68 min, MH^+ = 469

¹H NMR (*d*₆-DMSO, 393 K): δ 1.19 (d, *J* = 6.6 Hz, 3 H), 1.65 – 1.86 (m, 4 H), 2.13 (s, 3 H), 2.32 (s, 3 H), 2.65 – 2.75 (m, 1H), 3.25 – 3.46 (broad water peak, other peaks below), 3.88 – 4.02 (m, 6 H), 5.33 (d, *J* = 9.9 Hz, 1 H), 7.64 (s, 1 H), 7.70 (s, 1 H), 8.38 (s, 1 H), 9.50 (s, 1 H).

4-(8-Methoxy-1-((*R*)-1-methoxypropan-2-yl)-2-(tetrahydro-2*H*-pyran-4-yl)-1*H*-imidazo[4,5-*c*]quinolin-7-yl)-3,5-dimethylisoxazole, methanesulfonic acid salt, **2.70**:

4-(8-Methoxy-1-((*R*)-1-methoxypropan-2-yl)-2-(tetrahydro-2*H*-pyran-4-yl)-1*H*-imidazo[4,5-*c*]quinolin-7-yl)-3,5-dimethylisoxazole **2.67** (1.016 g, 2.255 mmol) was dissolved in the

minimum amount of hot MeOH, and methanesulfonic acid, 70% weight in water, (0.209 ml, 2.255 mmol) added. The solution was blown down under a stream of nitrogen to leave a white gum. The gum was triturated in diethyl ether and then dried in a vacuum oven to give 4-(8-methoxy-1-((*R*)-1-methoxypropan-2-yl)-2-(tetrahydro-2*H*-pyran-4-yl)-1*H*-imidazo[4,5-*c*]quinolin-7-yl)-3,5-dimethylisoxazole, methanesulfonic acid salt **2.70** (1.18 g, 2.159 mmol, 96 % yield).

LCMS (formic acid): rt = 0.73 min, MH⁺ = 451

¹H NMR (d₆-DMSO, 393 K): δ 1.83 (d, *J* = 7.3 Hz, 3 H), 1.86 – 2.01 (m, 2 H), 2.03 – 2.13 (m, 2 H), 2.16 (s, 3 H), 2.35 (s, 3 H), 2.40 (s, 3 H), 3.26 (s, 3 H), 3.50 – 3.65 (m, 3 H), 3.98 – 4.08 (m, 6 H), 4.11 – 4.16 (m, 1 H), 5.48 – 5.63 (m, 1 H), 7.87 (s, 1 H), 8.12 (s, 1 H), 9.36 (s, 1 H).

¹³C NMR: unable to obtain sample of sufficient strength to analyse.

IR (neat): 2849 (ether COCH₃), 1610 (aryl), 1389 (OSO₂), 1223 (aryl ether), 1163 (OSO₂) 841 (aryl C-H) cm⁻¹

M.pt.: 256–259 °C

HRMS: (C₂₅H₃₁N₄O₄) MH⁺ requires 451.2340, found MH⁺ 451.2338

[α_D]^{23.1 °C} (c 1.0, MeOH): +22.4 °

4-(8-Methoxy-1-((*R*)-1-methoxypropan-2-yl)-2-(tetrahydro-2*H*-pyran-4-yl)-1*H*-imidazo[4,5-*c*]quinolin-7-yl)-3,5-dimethylisoxazole, maleic acid salt, **2.71**:

4-(8-Methoxy-1-((*R*)-1-methoxypropan-2-yl)-2-(tetrahydro-2*H*-pyran-4-yl)-1*H*-imidazo[4,5-*c*]quinolin-7-yl)-3,5-dimethylisoxazole **2.67** (932 mg, 2.069 mmol) was dissolved in the minimum amount of hot MeOH, maleic acid (240 mg, 2.069 mmol) added, and the solution allowed to cool to room temperature. Cyclohexane (20 ml) was added to the solution, followed by cooling in an ice-water bath. A white gum was produced, which re-dissolved when the ice/water bath was removed. The solution was blown down under a stream of nitrogen to give an off-white gum. This was triturated in diethyl ether, whereupon a white suspension formed. The suspension was allowed to settle and the clear solution portion decanted. Twice more, further diethyl ether was added, the suspension allowed to settle, and the clear solution decanted. The thick white suspension that remained was dried under a stream of nitrogen, and then in a vacuum oven, to leave 4-(8-methoxy-1-((*R*)-1-methoxypropan-2-yl)-2-(tetrahydro-2*H*-pyran-4-yl)-1*H*-imidazo[4,5-*c*]quinolin-7-yl)-3,5-dimethylisoxazole, maleic acid salt **2.71** (1.120 g, 1.977 mmol, 96 % yield).

LCMS (formic acid): rt = 0.73 min, MH⁺ = 451

¹H NMR (d₆-DMSO, 393 K): δ 1.80 (d, J = 7.1 Hz, 3 H), 1.85 – 1.96 (m, 2 H), 1.99 – 2.09 (m, 2 H), 2.14 (s, 3 H), 2.33 (s, 3 H), 3.25 (s, 3 H), 3.38 – 3.49 (m, 1 H), 3.55 – 3.63 (m, 2 H), 3.94 – 4.05 (m, 6 H), 4.10 (dd, J = 10.6, 8.3 Hz, 1 H), 5.39 – 5.48 (m, 1 H), 6.17 (s, 2 H), 7.74 (s, 1 H), 7.98 (s, 1 H), 9.08 (s, 1 H).

4-(8-Methoxy-1-((R)-1-methoxypropan-2-yl)-2-(tetrahydro-2H-pyran-4-yl)-1H-imidazo[4,5-c]quinolin-7-yl)-3,5-dimethylisoxazole, 4-methylbenzenesulfonic acid salt, 2.72:

4-(8-Methoxy-1-((R)-1-methoxypropan-2-yl)-2-(tetrahydro-2H-pyran-4-yl)-1H-imidazo[4,5-c]quinolin-7-yl)-3,5-dimethylisoxazole **2.67** (1.018 g, 2.260 mmol) was dissolved in the minimum amount of hot MeOH, and *p*-toluenesulfonic acid monohydrate (0.430 g, 2.260 mmol) added. The solution was blown down under a stream of nitrogen to leave a white gum which contained some solid particles. The gum was triturated in diethyl ether and then dried in a vacuum oven to give 4-(8-methoxy-1-((R)-1-methoxypropan-2-yl)-2-(tetrahydro-2H-pyran-4-yl)-1H-imidazo[4,5-c]quinolin-7-yl)-3,5-dimethylisoxazole, 4-methylbenzenesulfonic acid salt **2.72** (1.29 g, 2.072 mmol, 92 % yield).

LCMS (formic acid): rt = 0.74 min, MH^+ = 451

¹H NMR (d₆-DMSO, 393 K): δ 1.83 (d, J = 7.1 Hz, 3 H), 1.87 – 2.00 (m, 2 H), 2.01 – 2.11 (m, 2 H), 2.16 (s, 3 H), 2.28 (s, 3 H), 2.35 (s, 3 H), 3.26 (s, 3 H), 3.48 – 3.67 (m, 3 H), 3.97 – 4.07 (m, 6 H), 4.13 (dd, J = 10.6, 8.6 Hz, 1 H), 5.51 – 5.59 (m, 1 H), 7.06 (d, J = 7.8 Hz, 2 H), 7.52 (d, J = 8.1 Hz, 2 H), 7.87 (s, 1 H), 8.10 (s, 1 H), 9.36 (s, 1 H).

4-(8-Methoxy-1-((R)-1-methoxypropan-2-yl)-2-(tetrahydro-2H-pyran-4-yl)-1H-imidazo[4,5-c]quinolin-7-yl)-3,5-dimethylisoxazole, citric acid salt, 2.73:

4-(8-Methoxy-1-((R)-1-methoxypropan-2-yl)-2-(tetrahydro-2H-pyran-4-yl)-1H-imidazo[4,5-c]quinolin-7-yl)-3,5-dimethylisoxazole **2.67** (924 mg, 2.051 mmol) was dissolved in the minimum amount of hot MeOH, and 2-hydroxypropane-1,2,3-tricarboxylic acid monohydrate (431 mg, 2.051 mmol) added. The solution was blown down under a stream of nitrogen to leave a colourless gum. The gum was triturated in diethyl ether and then dried in a vacuum oven to give 4-(8-methoxy-1-((R)-1-methoxypropan-2-yl)-2-(tetrahydro-2H-pyran-4-yl)-1H-imidazo[4,5-c]quinolin-7-yl)-3,5-dimethylisoxazole, citric acid salt **2.73** (1.39 g, 2.163 mmol, 95 % yield, yield corrected for diethyl ether in NMR).

LCMS (formic acid): rt = 0.73 min, MH^+ = 451

¹H NMR (d₆-DMSO, 393 K): δ 1.80 (d, J = 7.3 Hz, 3 H), 1.84 – 1.96 (m, 2 H), 1.99 – 2.09 (m, 2 H), 2.14 (s, 3 H), 2.32 (s, 3 H), 2.69 (d, J = 15.4 Hz, 2 H), 2.77 (d, J = 15.4 Hz, 2 H), 3.25 (s, 3 H), 3.42 – 3.48 (m, 1 H), 3.54 – 3.62 (m, 2 H), 3.97 – 4.04 (m, 6 H), 4.11 (dd, J = 10.6, 8.3 Hz, 1 H), 5.37 – 5.46 (m, 1 H), 7.72 (s, 1 H), 7.96 (s, 1 H), 9.02 (s, 1 H).

4-(8-Methoxy-1-((R)-1-methoxypropan-2-yl)-2-(tetrahydro-2H-pyran-4-yl)-1H-imidazo[4,5-c]quinolin-7-yl)-3,5-dimethylisoxazole, sulfuric acid salt, **2.74**:

4-(8-Methoxy-1-((R)-1-methoxypropan-2-yl)-2-(tetrahydro-2H-pyran-4-yl)-1H-imidazo[4,5-c]quinolin-7-yl)-3,5-dimethylisoxazole **2.67** (1.004 g, 2.228 mmol) was dissolved in the minimum amount of hot MeOH, and fuming sulfuric acid (0.119 ml, 2.228 mmol) added. The solution was blown down under a stream of nitrogen to leave a white gum which contained some solid particles. The gum was triturated in diethyl ether and then dried in a vacuum oven to give 4-(8-methoxy-1-((R)-1-methoxypropan-2-yl)-2-(tetrahydro-2H-pyran-4-yl)-1H-imidazo[4,5-c]quinolin-7-yl)-3,5-dimethylisoxazole, sulfuric acid salt **2.74** (1.20 g, 2.187 mmol, 98 % yield).

LCMS (formic acid): rt = 0.74 min, MH⁺ = 451

¹H NMR (d₆-DMSO, 393 K): δ 1.84 (d, *J* = 7.3 Hz, 3 H), 1.87 – 2.01 (m, 2 H), 2.01 – 2.11 (m, 2 H), 2.16 (s, 3 H), 2.36 (s, 3 H), 3.27 (s, 3 H), 3.50 – 3.67 (m, 3 H), 3.97 – 4.09 (m, 6 H), 4.12 – 4.16 (m, 1 H) 5.46 – 5.66 (m, 1 H), 7.90 (s, 1 H), 8.14 (s, 1 H), 9.41 (s, 1 H).

Chapter 3(S)-Cyclopentyl 4-methyl-2-(((2-(5-methyl-6-oxo-1,6-dihydropyridin-3-yl)-1-(1-methylpiperidin-4-yl)-1H-benzo[d]imidazol-5-yl)methyl)amino)pentanoate, **3.19**:

To a mixture of 5-methyl-6-oxo-1,6-dihydropyridine-3-carbaldehyde **3.25** (54.4 mg, 0.396 mmol) and sodium hydrosulfite (207 mg, 1.189 mmol) was added a solution of (S)-cyclopentyl 4-methyl-2-(((4-((1-methylpiperidin-4-yl)amino)-3-nitrobenzyl)amino)pentanoate **3.33** (177 mg, 0.396 mmol) in ethanol (1.5 ml), followed by water (0.75 ml). The reaction mixture was heated under microwave conditions at 100 °C for 5 hours. The reaction mixture was partitioned between saturated aqueous sodium bicarbonate solution (10 ml) and DCM (3 x 10 ml). The organic layers were combined, dried using a hydrophobic frit and blown down under a stream of nitrogen. The sample was dissolved in DMSO and purified by MDAP (high pH). The solvent was blown down under a stream of nitrogen to give the required product (S)-cyclopentyl 4-methyl-2-(((2-(5-methyl-6-oxo-1,6-dihydropyridin-3-yl)-1-(1-methylpiperidin-4-yl)-1H-benzo[d]imidazol-5-yl)methyl)amino)pentanoate **3.19** (72 mg, 0.135 mmol, 34% yield) as an off-white gum.

LCMS (high pH): rt = 1.08 min, MH⁺ = 534

¹H NMR (d₆-DMSO): δ 0.80 (d, *J* = 6.6 Hz, 3 H) 0.86 (d, *J* = 6.6 Hz, 3 H) 1.28 – 1.48 (m, 2 H) 1.48 – 1.75 (m, 8 H) 1.75 – 1.93 (m, 4 H) 2.03 – 2.12 (m, 5 H) 2.26 (s, 3 H) 2.43 – 2.55 (m, partially obscured by solvent peak) 2.95 (d, *J* = 10.8 Hz, 2 H) 3.11 (t, *J* = 7.3 Hz, 1 H) 3.62 (d, *J* = 13.2 Hz, 1 H) 3.82 (d, *J* = 13.2 Hz, 1 H) 4.19 – 4.25 (m, 1 H) 5.06 – 5.16 (m, 1 H) 7.16 – 7.19 (m, 1 H) 7.51 (s, 1 H) 7.56 (s, 2 H) 7.64 (d, *J* = 8.6 Hz, 1 H)

Additional analytical information was generated on subsequent batches of material after the separation was performed using identical methodology on a larger scale:

¹³C NMR (d₆-DMSO, 303 K): δ 16.9, 22.7, 23.1, 23.7, 24.9, 30.3, 32.7, 32.7, 42.5, 46.2, 51.6, 55.1 (DCM), 58.8, 76.9, 108.8, 112.5, 119.0, 123.0, 129.2, 133.0, 134.3, 134.4, 138.4, 143.8, 151.1, 162.7, 175.4

IR (neat): 2955 (amine NH), 1727 (ester), 1658 (pyridone), 1439 (NH bending) cm⁻¹

M.pt.: 97–98 °C

HRMS: (C₃₁H₄₄N₅O₃) MH⁺ requires 534.3439, found MH⁺ 534.3419

[α_D]^{23.9 °C} (c 1.0, methanol): -8.3 °

(S)-tert-Butyl 4-methyl-2-(((2-(5-methyl-6-oxo-1,6-dihydropyridin-3-yl)-1-(1-methylpiperidin-4-yl)-1H-benzo[d]imidazol-5-yl)methyl)amino)pentanoate, **3.20**:

Method as for **3.19**, using the following reagents: 5-methyl-6-oxo-1,6-dihydropyridine-3-carbaldehyde **3.25** (38.2 mg, 0.278 mmol), sodium hydrosulfite (145 mg, 0.835 mmol), (S)-tert-

butyl 4-methyl-2-((4-((1-methylpiperidin-4-yl)amino)-3-nitrobenzyl)amino)pentanoate **3.34** (121 mg, 0.278 mmol), ethanol (2 ml), and water (1 ml). The final product was: (*S*)-*tert*-butyl 4-methyl-2-(((2-(5-methyl-6-oxo-1,6-dihydropyridin-3-yl)-1-(1-methylpiperidin-4-yl)-1*H*-benzo[*d*]imidazol-5-yl)methyl)amino)pentanoate **3.20** (36 mg, 0.069 mmol, 25% yield) as a colourless gum.

LCMS (high pH): *rt* = 1.07 min, MH^+ = 522

¹H NMR (*d*₆-DMSO): δ 0.80 (d, *J* = 6.6 Hz, 3 H) 0.86 (d, *J* = 6.6 Hz, 3 H) 1.29 – 1.46 (m, 11 H) 1.70 – 1.78 (m, 1 H) 1.85 (d, *J* = 11.1 Hz, 2 H) 1.94 – 2.03 (m, 2 H) 2.07 (s, 3 H) 2.22 (s, 3 H) 2.45 – 2.52 (m, peak partially obscured by solvent) 2.90 (d, *J* = 11.1 Hz, 2 H) 3.02 – 3.05 (m, 1 H) 3.63 (d, *J* = 13.1 Hz, 1 H) 3.83 (d, *J* = 13.1 Hz, 1 H) 4.16 – 4.24 (m, 1 H) 7.18 (d, *J* = 8.3 Hz, 1 H) 7.51 (s, 1 H) 7.53 – 7.57 (m, 2 H) 7.63 (d, *J* = 8.3 Hz, 1 H)

(*S*)-4-Methyl-2-(((2-(5-methyl-6-oxo-1,6-dihydropyridin-3-yl)-1-(1-methylpiperidin-4-yl)-1*H*-benzo[*d*]imidazol-5-yl)methyl)amino)pentanoic acid, **3.21**:

To a solution of (*S*)-cyclopentyl 4-methyl-2-(((2-(5-methyl-6-oxo-1,6-dihydropyridin-3-yl)-1-(1-methylpiperidin-4-yl)-1*H*-benzo[*d*]imidazol-5-yl)methyl)amino)pentanoate **3.19** (42 mg, 0.079 mmol) in MeOH (2.5 ml) and THF (2.5 ml) was added 1 M aqueous lithium hydroxide solution (0.236 ml, 0.236 mmol) and the reaction mixture stirred at 50 °C overnight. The sample was blown down under a stream of nitrogen. The residue was dissolved in DMSO (1 ml), the solid removed by filtration, and the solution purified by MDAP (formic acid). The solvent was blown down under a stream of nitrogen to give the required product (*S*)-4-methyl-2-(((2-(5-methyl-6-oxo-1,6-dihydropyridin-3-yl)-1-(1-methylpiperidin-4-yl)-1*H*-benzo[*d*]imidazol-5-yl)methyl)amino)pentanoic acid **3.21** (8.8 mg, 0.019 mmol, 24% yield) as a yellow gum.

LCMS (high pH): *rt* = 0.56 min, MH^+ = 466

¹H NMR (*d*₆-DMSO): δ 0.80 (d, *J* = 6.4 Hz, 3 H) 0.86 (d, *J* = 6.6 Hz, 3 H) 1.39 – 1.56 (m, 2 H) 1.74 – 1.94 (m, 3 H) 2.04 – 2.14 (m, 5 H) 2.26 (s, 3 H) 2.43 – 2.48 (m, peak partially obscured by solvent) 2.89 – 3.02 (m, 2 H) 3.07 – 3.15 (m, 1 H) 3.90 (d, *J* = 13.2 Hz, 1 H) 4.03 (d, *J* = 13.0 Hz, 1 H) 4.16 – 4.33 (m, 1 H) 7.27 (d, *J* = 8.3 Hz, 1 H) 7.54 – 7.60 (m, 2 H) 7.65 (s, 1 H) 7.71 (d, *J* = 8.3 Hz, 1 H) 8.26 (s, 1 H)

3-Methyl-5-(1-(1-methylpiperidin-4-yl)-1*H*-benzo[*d*]imidazol-2-yl)pyridin-2(1*H*)-one, **3.22**:

To a mixture of 5-methyl-6-oxo-1,6-dihydropyridine-3-carbaldehyde **3.25** (75 mg, 0.548 mmol) and sodium hydrosulfite (286 mg, 1.645 mmol) was added a solution of 1-methyl-*N*-(2-nitrophenyl)piperidin-4-amine **3.27** (129 mg, 0.548 mmol) in ethanol (1.5 ml), followed by water (0.75 ml). The reaction mixture was heated under microwave at 100 °C for 5 hours. The reaction mixture was partitioned between saturated aqueous sodium bicarbonate solution (10

ml) and DCM (2 x 10 ml). The organic layers were combined, dried using a hydrophobic frit and blown down under a stream of nitrogen. The residue was dissolved in DMSO (2 x 1 ml) and purified by MDAP (high pH). The solvent was blown down under a stream of nitrogen to give the required product 3-methyl-5-(1-(1-methylpiperidin-4-yl)-1*H*-benzo[*d*]imidazol-2-yl)pyridin-2(1*H*)-one **3.22** (84 mg, 0.261 mmol, 48% yield) as an off-white solid.

LCMS (formic acid): *rt* = 0.36 min, MH^+ = 323

1H NMR (d_6 -DMSO): δ 1.88 (d, *J* = 11.5 Hz, 2 H) 2.00 – 2.13 (br. m., 5 H) 2.26 (s, 3 H) 2.43 – 2.56 (m, partially obscured by solvent peak) 2.89 – 3.01 (m, 2 H) 2.87 – 3.03 (m, 2 H) 4.17 – 4.36 (m, 1 H) 7.19 – 7.25 (m, 2 H) 7.57 (s, 2 H) 7.60 – 7.67 (m, 1 H) 7.72 (d, *J* = 7.1 Hz, 1 H) 11.89 (br. s., 1 H).

^{13}C NMR (d_6 -DMSO, 303 K): δ 16.4, 29.5, 45.5, 54.5, 108.3, 112.5, 119.4, 121.6, 122.0, 128.8, 133.5, 134.0, 138.0, 143.2, 150.6, 162.2. One carbon atom is likely to be hidden under the solvent peak.

IR (neat): 2944 (amine NH), 1665 (pyridone), 1567 (aryl), 754 (aryl C-H) cm^{-1}

M.pt.: 257–264 °C

HRMS: ($C_{19}H_{25}N_4O$) MH^+ requires 323.1866, found MH^+ 323.1863

5-Bromo-3-methylpyridin-2(1*H*)-one, **3.24**:

To a suspension of 5-bromo-3-methylpyridin-2-amine **3.23** (15 g, 80 mmol) in water (270 ml) was added 1 M aqueous sulfuric acid solution (44.9 ml, 44.9 mmol) and the reaction mixture cooled to 3 °C internal temperature using an ice/water bath with added ammonium chloride. A solution of sodium nitrite (8.85 g, 128 mmol) in water (60 ml) was added dropwise over approximately 30 minutes, maintaining an internal temperature of between 0–5 °C. Foam was being formed at this point. The reaction was left stirring in the cooling bath for 30 min, and then it was allowed to warm to room temperature and stirred overnight. The resulting suspension, which had a large amount of foam on top, was filtered and the solid washed on the filter with water. The solid was collected and dried in a vacuum oven to give a white solid. To a suspension of this crude material in water (270 ml) was added 1 M aqueous sulfuric acid solution (44.9 ml, 44.9 mmol) and the reaction mixture cooled to 8 °C internal temperature using an ice/water bath. A solution of sodium nitrite (8.85 g, 128 mmol) in water (60 ml) was added dropwise over approximately 30 minutes, maintaining an internal temperature of 5–10 °C. Foam was again being formed at this point. The reaction mixture was left stirring in the cooling bath for 2 hours, allowed to warm to room temperature, and stirred overnight. The resulting suspension, which again had a large amount of foam on top, was filtered and the solid washed

on the filter with water. The solid was collected and dried in a vacuum oven to give a white solid, 5-bromo-3-methylpyridin-2(1*H*)-one **3.24** (10.1 g, 53.7 mmol, 67% yield).

LCMS (formic acid): *rt* = 0.59 min, MH^+ = 188/190

1H NMR (d_6 -DMSO): δ 1.97 (s, 3 H) 7.38 - 7.55 (m, 2 H) 11.69 (br. s., 1 H).

5-Methyl-6-oxo-1,6-dihydropyridine-3-carbaldehyde, Preparation A, **3.25**:

To a flask which had been purged with nitrogen was added 5-bromo-3-methylpyridin-2(1*H*)-one **3.24** (1.5 g, 7.98 mmol) in dry THF (75 ml). The solution was stirred in a dry ice/acetone bath for 20 minutes. 1.6 M *n*-butyllithium in hexanes (14.96 ml, 23.93 mmol) was added dropwise over ten minutes, whereupon the reaction mixture became bright yellow. The reaction mixture was stirred under nitrogen in the dry ice/acetone bath for 3 hours. Dry DMF (14.83 ml, 191 mmol) was added dropwise over approximately 5 minutes, and the reaction mixture stirred under nitrogen in the dry ice/acetone bath for 1 hour. The reaction mixture was quenched using saturated aqueous ammonium chloride solution (~ 30 ml), and then allowed to warm to room temperature. The resulting slurry was partitioned between EtOAc (100 ml) and water (100 ml). The organic layer was washed with brine (50 ml), dried using a hydrophobic frit, and evaporated under reduced pressure to give a dark purple solid. The solid was triturated in diethyl ether, the solid removed by filtration and dried in a vacuum oven, to give 5-methyl-6-oxo-1,6-dihydropyridine-3-carbaldehyde **3.25** (151 mg, 1.101 mmol, 14% yield) as an off-white solid. The aqueous layers were combined and re-extracted with DCM (2 x 75 ml). These organic layers were combined, dried using a hydrophobic frit and evaporated under reduced pressure to give a yellow solid. The solid was triturated in diethyl ether, the solid removed by filtration and dried in a vacuum oven to give a second batch of 5-methyl-6-oxo-1,6-dihydropyridine-3-carbaldehyde **3.25** (308 mg, 2.246 mmol, 28% yield) as a pale yellow solid. The overall yield of the reaction was 42%.

Batch 1:

LCMS (formic acid): *rt* = 0.40 min, MH^+ = 138

1H NMR (d_6 -DMSO): δ 2.01 (s, 3 H) 7.63 – 7.64 (m, 1 H) 8.13 (d, *J* = 2.5 Hz, 1 H) 9.56 (s, 1 H) 12.21 (br. s., 1 H).

Batch 2:

LCMS (formic acid): *rt* = 0.40 min, MH^+ = 138

1H NMR (d_6 -DMSO): δ 2.01 (s, 3 H) 7.63 (s, 1 H) 8.13 (d, *J* = 2.2 Hz, 1 H) 9.56 (s, 1 H) 12.21 (br. s., 1 H).

Further analysis performed on subsequent batch prepared using identical methodology:

^{13}C NMR (d_6 -DMSO, 303 K): δ 16.2, 117.4, 129.2, 132.1, 144.1, 163.3, 187.6.

IR (neat): 1701 (aldehyde), 1647 (pyridone), 1589 (aryl), 859 (aryl C-H) cm^{-1}

M.pt.: 222–223 °C

HRMS: ($\text{C}_7\text{H}_9\text{NO}_2$) MH^+ requires 138.0550, found MH^+ 138.0546

5-Methyl-6-oxo-1,6-dihydropyridine-3-carbaldehyde, Preparation B, 3.25:

5-Bromo-3-methylpyridin-2(1*H*)-one **3.24** (1.5 g, 7.98 mmol) was added to a flask which was purged with nitrogen. Anhydrous THF (75 ml) was added and the solution was stirred under nitrogen, in dry-ice/acetone bath for 20 min. 1.6 M *n*-Butyllithium in hexanes (14.96 ml, 23.93 mmol) was added dropwise to the mixture and the reaction mixture was stirred under nitrogen in dry-ice/acetone bath for 3 hours. Anhydrous DMF (14.83 ml, 191 mmol) was added dropwise and the reaction mixture was stirred under nitrogen in dry-ice/acetone bath for 1 hour. It was quenched using saturated aqueous ammonium chloride solution (30 ml) and allowed to warm to room temperature. The resulting slurry was partitioned between EtOAc (100 ml) and water (100 ml) and the layers were separated. The organic layer was washed with brine (50 ml), dried, and evaporated under reduced pressure to give a pale yellow solid. The solid was triturated with diethyl ether and the solid filtered was collected as the required product 5-methyl-6-oxo-1,6-dihydropyridine-3-carbaldehyde (Batch 1) **3.25** (210.8 mg, 1.537 mmol, 19% yield). The aqueous layers from the previous extractions were combined and re-extracted with DCM (4 x 75 ml and 4 x 100 ml). The combined organic layers were dried and evaporated under reduced pressure to give a pale yellow liquid. The liquid residue was azeotroped with toluene (2 x 30 ml) and the solvents were removed under reduced pressure to give a yellow solid. The solid was triturated with diethyl ether, and the solid filtered was collected as the required product 5-methyl-6-oxo-1,6-dihydropyridine-3-carbaldehyde (Batch 2) **3.25** (452.4 mg, 3.30 mmol, 41% yield). The total yield of the reaction was 61%.

Batch 1:

LCMS (formic acid): $\text{rt} = 0.41$ min, $\text{MH}^+ = 138$

^1H NMR (d_6 -DMSO): δ 2.01 (s, 3 H) 7.63 – 7.64 (m, 1 H) 8.13 (d, $J = 2.5$ Hz, 1 H) 9.56 (s, 1 H) 12.05 – 12.37 (br. s., 1 H).

Batch 2:

LCMS (formic acid): $\text{rt} = 0.41$ min, $\text{MH}^+ = 138$

^1H NMR (d_6 -DMSO): δ 2.01 (s, 3 H) 7.63 – 7.64 (s, 1 H) 8.13 (d, $J = 2.2$ Hz, 1 H) 9.56 (s, 1 H) 12.18 (br. s., 1 H).

1-Methyl-*N*-(2-nitrophenyl)piperidin-4-amine, **3.27**:

To a solution of 1-fluoro-2-nitrobenzene **3.26** (0.075 ml, 0.709 mmol) in THF (1.5 ml) was added 1-methylpiperidin-4-amine (243 mg, 2.126 mmol) and DIPEA (0.371 ml, 2.126 mmol), and the reaction mixture heated under microwave conditions at 120 °C for 30 minutes. The reaction mixture was partitioned between DCM (3 x 10 ml) and saturated aqueous sodium bicarbonate solution (10 ml). The organic layers were combined, dried using a hydrophobic frit and blown down under a stream of nitrogen to give an orange gum. The sample was loaded in DCM and purified by SPE (silica, 10 g) using a gradient of 0 – 10 % (2 M ammonia in MeOH) in DCM. The appropriate fractions were combined and blown down under a stream of nitrogen to give the required product 1-methyl-*N*-(2-nitrophenyl)piperidin-4-amine **3.27** (132 mg, 0.561 mmol, 79% yield) as an orange gum.

LCMS (formic acid): rt = 0.56 min, MH⁺ = 236

¹H NMR (d₆-DMSO): δ 1.50 – 1.74 (m, 2 H) 1.92 – 1.99 (m, 2 H) 2.06 – 2.27 (m, 5 H) 2.66 (d, *J* = 11.5 Hz, 2 H) 3.59 – 3.68 (m, 1 H) 6.65 – 6.81 (m, 1 H) 7.12 (d, *J* = 8.6 Hz, 1 H) 7.51 – 7.56 (m, 1 H) 7.94 (d, *J* = 7.6 Hz, 1 H) 8.07 (dd, *J* = 8.6, 1.5 Hz, 1 H).

(*S*)-Cyclopentyl 2-((4-fluoro-3-nitrobenzyl)amino)-4-methylpentanoate, **3.31**:

To a solution of 4-fluoro-3-nitrobenzaldehyde **3.30** (2 g, 11.83 mmol) and (*S*)-cyclopentyl 2-amino-4-methylpentanoate 4-methylbenzenesulfonate **3.28** (4.83 g, 13.01 mmol) in DCM (50 ml) was added acetic acid (2.031 ml, 35.5 mmol) and the reaction mixture stirred under nitrogen for 1.5 hours. Sodium triacetoxyborohydride (5.01 g, 23.65 mmol) was added portion-wise, and the reaction mixture stirred at room temperature overnight. Saturated aqueous sodium bicarbonate solution (100 ml) was added slowly, and stirring continued until fizzing had stopped. The resulting suspension was extracted with DCM (3 x 100 ml). The organic layers were combined, dried using a hydrophobic frit and evaporated under reduced pressure. The sample was loaded in DCM and purified by SPE (silica, 100 g) using a gradient of 0 – 50% EtOAc in cyclohexane. The appropriate fractions were combined and evaporated under reduced pressure to give the required product (*S*)-cyclopentyl 2-((4-fluoro-3-nitrobenzyl)amino)-4-methylpentanoate **3.31** (3.5 g, 9.93 mmol, 84% yield) as a yellow gum.

LCMS (formic acid): rt = 1.00 min, MH⁺ = 353

¹H NMR (d₆-DMSO): δ 0.81 (d, *J* = 6.6 Hz, 3 H), 0.87 (d, *J* = 6.9 Hz, 3 H) 1.32 – 1.48 (m, 2 H) 1.52 – 1.75 (m, 7 H) 1.76 – 1.85 (m, 2 H) 2.52 – 2.77 (m, 1 H) 3.04 – 3.17 (m, 1 H) 3.59 – 3.86 (m, 2 H) 5.05 – 5.20 (m, 1 H) 7.53 (dd, *J* = 11.3, 8.6 Hz, 1 H) 7.74 (ddd, *J* = 8.5, 4.5, 2.2 Hz, 1 H) 8.09 (dd, *J* = 7.5, 2.1 Hz, 1 H).

(S)-Tert-butyl 2-((4-fluoro-3-nitrobenzyl)amino)-4-methylpentanoate, 3.32:

To a solution of 4-fluoro-3-nitrobenzaldehyde **3.30** (1 g, 5.91 mmol) and (S)-tert-butyl 2-amino-4-methylpentanoate hydrochloride **3.29** (1.455 g, 6.50 mmol) in DCM (25 ml) was added acetic acid (1.016 ml, 17.74 mmol) and the reaction mixture stirred under nitrogen for 1 hour. Sodium triacetoxyborohydride (2.507 g, 11.83 mmol) was added portion-wise, and the reaction mixture stirred at room temperature overnight. Saturated aqueous sodium bicarbonate solution (50 ml) was added slowly, and stirring continued until fizzing had stopped. The resulting suspension was extracted with DCM (3 x 50 ml). The organic layers were combined, dried using a hydrophobic frit and evaporated under reduced pressure. The sample was loaded in DCM and purified by SPE (silica, 100 g) using a gradient of 0 – 50 % EtOAc in cyclohexane. The appropriate fractions were combined and evaporated under reduced pressure to give the required product (S)-tert-butyl 2-((4-fluoro-3-nitrobenzyl)amino)-4-methylpentanoate **3.32** (1.66 g, 4.88 mmol, 82% yield) as a yellow gum.

LCMS (formic acid): rt = 0.95 min, MH⁺ = 341

¹H NMR (d₆-DMSO): δ 0.82 (d, J = 6.6 Hz, 3 H) 0.87 (d, J = 6.6 Hz, 3 H) 1.34 – 1.39 (m, 2 H) 1.39 – 1.46 (m, 9 H) 1.68 – 1.80 (m, 1 H) 2.53 – 2.64 (m, 1 H) 2.96 – 3.06 (m, 1 H) 3.64 (dd, J = 14.4, 5.9 Hz, 1 H) 3.82 (dd, J = 14.4, 5.1 Hz, 1 H) 7.54 (dd, J = 11.5, 8.6 Hz, 1 H) 7.71 – 7.78 (m, 1 H) 8.09 (d, J = 7.5, 2.1 Hz, 1 H).

(S)-Cyclopentyl 4-methyl-2-((4-((1-methylpiperidin-4-yl)amino)-3-nitrobenzyl)amino)pentanoate, 3.33:

To a solution of (S)-cyclopentyl 2-((4-fluoro-3-nitrobenzyl)amino)-4-methylpentanoate **3.31** (500 mg, 1.419 mmol) in THF (9 ml) was added 1-methylpiperidin-4-amine (486 mg, 4.26 mmol) and DIPEA (0.743 ml, 4.26 mmol), and the reaction mixture heated under microwave conditions at 120 °C for a total of 90 min. Further 1-methylpiperidin-4-amine (486 mg, 4.26 mmol) was added and the reaction mixture heated for a further 30 min at 120 °C. The reaction mixture was partitioned between DCM (2 x 100 ml) and saturated aqueous sodium bicarbonate solution (100 ml). The organic layers were combined, dried using a hydrophobic frit and evaporated under reduced pressure. The sample was loaded in DCM and purified by SPE (silica, 100 g) using a gradient of 0 – 5 % (2 M ammonia in MeOH) in DCM. The appropriate fractions were combined and evaporated under reduced pressure to give the required product (S)-cyclopentyl 4-methyl-2-((4-((1-methylpiperidin-4-yl)amino)-3-nitrobenzyl)amino)pentanoate **3.33** (456 mg, 1.021 mmol, 72% yield) as an orange gum.

LCMS (formic acid): rt = 0.70 min, MH⁺ = 447

¹H NMR (d₆-DMSO): δ 0.79 (d, *J* = 6.6 Hz, 3 H) 0.85 (d, *J* = 6.6 Hz, 3 H) 1.30 – 1.43 (m, 2 H) 1.51 – 1.72 (m, 10 H) 1.74 – 1.88 (m, 2 H) 1.89 – 2.00 (m, 2 H) 2.09 – 2.23 (m, 5 H) 2.65 (d, *J* = 11.3 Hz, 2 H) 3.00 – 3.12 (m, 1 H) 3.47 (d, *J* = 13.7 Hz, 1 H) 3.60 – 3.68 (m, 2 H) 5.04 – 5.08 (m, 1 H) 7.10 (d, *J* = 9.1 Hz, 1 H) 7.47 (dd, *J* = 8.8, 2.0 Hz, 1 H) 7.94 (d, *J* = 7.6 Hz, 1 H) 7.97 (d, *J* = 1.7 Hz, 1 H).

(*S*)-tert-Butyl 4-methyl-2-(((4-((1-methylpiperidin-4-yl)amino)-3-nitrobenzyl)amino)pentanoate, **3.34**:

To a solution of (*S*)-tert-butyl 2-((4-fluoro-3-nitrobenzyl)amino)-4-methylpentanoate **3.32** (250 mg, 0.734 mmol) in THF (3.5 ml) was added 1-methylpiperidin-4-amine (252 mg, 2.203 mmol) and DIPEA (0.385 ml, 2.203 mmol), and the reaction mixture heated under microwave conditions to 120 °C for 30 min. The reaction mixture was partitioned between DCM (2 x 20 ml) and saturated aqueous sodium bicarbonate solution (20 ml). The organic layers were combined, dried using a hydrophobic frit and blown down under a stream of nitrogen. The sample was loaded in DCM and purified by SPE (silica, 25 g) using a gradient of 0 – 10 % (2 M ammonia in MeOH) in DCM. The appropriate fractions were combined and evaporated under reduced pressure to give (*S*)-tert-butyl 4-methyl-2-(((4-((1-methylpiperidin-4-yl)amino)-3-nitrobenzyl)amino)pentanoate **3.34** (127 mg, 0.292 mmol, 40% yield).

LCMS (high pH): rt = 1.09 min, MH⁺ = 435

¹H NMR (d₆-DMSO): δ 0.80 (d, *J* = 6.6 Hz, 3 H) 0.86 (d, *J* = 6.6 Hz, 3 H) 1.31 – 1.37 (m, 2 H) 1.40 (s, 9 H) 1.47 – 1.63 (m, 2 H) 1.64 – 1.79 (m, 1 H) 1.88 – 2.10 (m, 2 H) 2.11 – 2.18 (m, 5 H) 2.26 – 2.37 (m, 1 H) 2.59 – 2.71 (m, 2 H) 2.92 – 3.04 (m, 1 H) 3.46 (d, *J* = 13.6 Hz, 1 H) 3.58 – 3.70 (m, 2 H) 7.10 (d, *J* = 9.1 Hz, 1 H) 7.48 (dd, *J* = 8.8, 1.8 Hz, 1 H) 7.93 (d, *J* = 7.6 Hz, 1 H) 7.97 (d, *J* = 1.8 Hz, 1 H)

(*S*)-4-Methyl-2-(((2-(5-methyl-6-oxo-1,6-dihydropyridin-3-yl)-1-(1-methylpiperidin-4-yl)-1*H*-benzo[*d*]imidazol-5-yl)methyl)amino)pentanoic acid bis-hydrochloride, **3.35**:

To a solution of (*S*)-cyclopentyl 4-methyl-2-(((2-(5-methyl-6-oxo-1,6-dihydropyridin-3-yl)-1-(1-methylpiperidin-4-yl)-1*H*-benzo[*d*]imidazol-5-yl)methyl)amino)pentanoate **3.19** (34 mg, 0.064 mmol) in MeOH (2 ml) and THF (2 ml) was added 1 M aqueous lithium hydroxide solution (0.191 ml, 0.191 mmol) and the reaction mixture stirred at 50 °C for two nights. The reaction mixture was blown down under a stream of nitrogen. The sample was dissolved in 2 M hydrochloric acid (0.1 ml) and MeOH (0.9 ml) and purified by MDAP (high pH). The appropriate fractions were combined, blown down under a stream of nitrogen, and dried in a vacuum oven overnight. The sample was suspended in THF (1 ml), 2 M aqueous hydrochloric acid (0.5 ml) added, and the resulting solution blown down under a stream of nitrogen to give

the required product (*S*)-4-methyl-2-(((2-(5-methyl-6-oxo-1,6-dihydropyridin-3-yl)-1-(1-methylpiperidin-4-yl)-1*H*-benzo[*d*]imidazol-5-yl)methyl)amino)pentanoic acid bis-hydrochloride **3.35** (26 mg, 0.048 mmol, 76 % yield) as an off-white solid.

LCMS (high pH): rt = 0.56 min, MH⁺ = 466

¹H NMR (d₆-DMSO): δ 0.92 (d, *J* = 6.1 Hz, 6 H) 1.71 – 1.94 (m, 3 H) 2.10 (s, 3 H) 2.29 (d, *J* = 11.9 Hz, 2 H) 2.75 (d, *J* = 4.6 Hz, 3 H) 3.03 – 3.18 (m, 2 H) 3.18 – 3.33 (m, 2 H) 3.55 (d, *J* = 10.9 Hz, 2 H) 3.79 – 3.86 (m, 1 H) 4.28 – 4.38 (m, 1 H) 4.38 – 4.48 (m, 1 H) 4.74 – 4.87 (m, 1 H) 7.66 (s, 1 H) 7.72 (d, *J* = 8.6 Hz, 1 H) 7.96 (d, *J* = 2.3 Hz, 1 H) 8.14 (s, 1 H) 8.79 (d, *J* = 8.9 Hz, 1 H) 9.66 (br. s., 1 H) 10.16 (br. s., 1 H) 11.88 (br. s., 1 H)

Chapter 4**3-Methyl-5-phenylpyridin-2(1H)-one, 4.01:**

5-Bromo-3-methylpyridin-2(1H)-one **3.24** (50 mg, 0.266 mmol), phenylboronic acid (38.9 mg, 0.319 mmol), and tetrakis(triphenylphosphine)palladium(0) (30.7 mg, 0.027 mmol) were combined in isopropanol (2.4 ml), 1 M aqueous sodium bicarbonate solution (0.798 ml, 0.798 mmol) added, and the reaction mixture heated under microwave conditions at 120 °C for 10 min. The reaction mixture was partitioned between DCM (2 x 10 ml) and water (10 ml). The organic layers were combined, dried using a hydrophobic frit and blown down a stream of nitrogen. The residue was dissolved in DMSO (1 ml) and purified by MDAP (formic acid). The solvent was blown down under a stream of nitrogen to give the required product 3-methyl-5-phenylpyridin-2(1H)-one **4.01** (16 mg, 0.086 mmol, 33% yield) as an off-white solid.

LCMS (formic acid): rt = 0.77 min, MH⁺ = 186

¹H NMR (d₆-DMSO): δ 2.05 (s, 3 H) 7.27 (t, *J* = 7.3 Hz, 1 H) 7.39 (t, *J* = 7.7 Hz, 2 H) 7.50 – 7.60 (m, 3 H) 7.73 (dd, *J* = 2.7, 1.2 Hz, 1 H) 11.70 (br. s., 1 H)

¹³C NMR (d₆-DMSO, 303 K): δ 16.6, 117.6, 125.2, 126.6, 128.7, 128.9, 129.5, 136.5, 136.9, 162.1.

IR (neat): 1646 (pyridone), 1594 (aryl). 1565 (aryl), 877 (aryl, isolated C-H), 772 (CH of monosubstituted aryl), 695 (CH of monosubstituted aryl) cm⁻¹

M.pt.: 206–219 °C

HRMS: (C₁₂H₁₂NO) MH⁺ requires 186.0913, found MH⁺ 186.0910

3-Methyl-5-(*o*-tolyl)pyridin-2(1H)-one, 4.02:

Method as for **4.01**, using the following reagents: 5-bromo-3-methylpyridin-2(1H)-one **3.24** (50 mg, 0.266 mmol), *o*-tolylboronic acid (43.4 mg, 0.319 mmol), and tetrakis(triphenylphosphine)palladium(0) (30.7 mg, 0.027 mmol), 1 M aqueous sodium bicarbonate solution (0.798 ml, 0.798 mmol) and isopropanol (2.4 ml). The final product was: 3-methyl-5-(*o*-tolyl)pyridin-2(1H)-one **4.02** (25 mg, 0.125 mmol, 47% yield) as an off-white solid.

LCMS (formic acid): rt = 0.83 min, MH⁺ = 200

¹H NMR (d₆-DMSO): δ 2.02 (s, 3 H) 2.25 (s, 3 H) 7.11 - 7.30 (m, 5 H) 7.36 (s, 1 H) 11.60 (br. s., 1 H).

3-Methyl-5-(1-methyl-1H-imidazol-2-yl)pyridin-2(1H)-one, 4.03 (Method A):

A mixture of 5-bromo-3-methylpyridin-2(1H)-one **3.24** (50 mg, 0.266 mol) and tetrakis(triphenylphosphine)palladium(0) (30.7 mg, 0.027 mmol) were combined in DMF (1

ml), 1-methyl-2-(tributylstannyl)-1*H*-imidazole (0.102 ml, 0.319 mmol) was added, and the reaction mixture heated under microwave conditions at 120 °C for 15 min. LCMS (formic acid) showed no evidence of product, 56% starting material (aryl bromide) remained. Lithium chloride (11.27 mg, 0.266 mmol) was added and the reaction mixture heated for a further 120 °C for 15 min. LCMS (formic acid) showed little change and no evidence of product formation. The reaction was therefore abandoned.

3-Methyl-5-(1-methyl-1*H*-imidazol-2-yl)pyridin-2(1*H*)-one, **4.03** (Method B):

A mixture of 5-bromo-3-methylpyridin-2(1*H*)-one **3.24** (50 mg, 0.266 mmol), tetrakis(triphenylphosphine)palladium(0) (30.7 mg, 0.027 mmol) and copper (I) iodide (10.13 mg, 0.053 mmol) were combined in 1,4-dioxane (1 ml), 1-methyl-2-(tributylstannyl)-1*H*-imidazole (0.102 ml, 0.319 mmol) added, and the reaction mixture heated under microwave conditions to 120 °C for 15 min. LCMS (formic acid) showed no evidence of product formation. The reaction was therefore abandoned.

5-(1-Benzyl-1*H*-imidazol-5-yl)-3-methylpyridin-2(1*H*)-one, **4.05**:

5-Bromo-3-methylpyridin-2(1*H*)-one **3.24** (50 mg, 0.266 mmol), 1-benzyl-5-(4,4,5,5-tetramethyl-1,3,2-dioxaborolan-2-yl)-1*H*-imidazole (64.5 mg, 0.227 mmol), and tetrakis(triphenylphosphine)palladium(0) (30.7 mg, 0.027 mmol) were combined in isopropanol (2.4 ml), 1 M aqueous sodium bicarbonate solution (0.798 ml, 0.798 mmol) added, and the reaction mixture heated under microwave conditions at 120 °C for 10 min. Further 1-benzyl-5-(4,4,5,5-tetramethyl-1,3,2-dioxaborolan-2-yl)-1*H*-imidazole (64.5 mg, 0.227 mmol) and tetrakis(triphenylphosphine)palladium(0) (30.7 mg, 0.027 mmol) were added, and heating continued for a further 10 min at 120 °C. The reaction mixture was partitioned between DCM (2 x 10 ml) and water (10 ml). The organic layers were combined, dried using a hydrophobic frit and blown down under a stream of nitrogen. The residue was dissolved in DMSO (2 x 1 ml) and purified by MDAP (high pH). One of the two samples was lost due to machine failure. The solvent was blown down a stream of nitrogen to give the required product 5-(1-benzyl-1*H*-imidazol-5-yl)-3-methylpyridin-2(1*H*)-one **4.05** (4.5 mg, 0.017 mmol, 6% yield) as a colourless gum.

LCMS (formic acid): *rt* = 0.45 min, MH^+ = 266

¹H NMR (d₆-DMSO): δ 1.91 (s, 3 H) 5.21 (s, 2 H) 6.89 - 7.06 (m, 3 H) 7.12 (d, *J* = 2.2 Hz, 1 H) 7.16 - 7.20 (m, 1 H) 7.23 - 7.33 (m, 2 H) 7.81 (s, 1 H) 8.39 (s, 1 H)

5-(1-Benzyl-1*H*-pyrazol-5-yl)-3-methylpyridin-2(1*H*)-one, **4.07**:

Method as for **4.01**, using the following reagents: 5-bromo-3-methylpyridin-2(1*H*)-one **3.24** (50 mg, 0.266 mmol), 1-benzyl-5-(4,4,5,5-tetramethyl-1,3,2-dioxaborolan-2-yl)-1*H*-pyrazole (91 mg, 0.319 mmol), tetrakis(triphenylphosphine)palladium(0) (30.7 mg, 0.027 mmol), 1 M aqueous sodium bicarbonate solution (0.798 ml, 0.798 mmol) and isopropanol (2.4 ml). The reaction mixture was heated for 20 min. The final product was: 5-(1-benzyl-1*H*-pyrazol-5-yl)-3-methylpyridin-2(1*H*)-one **4.07** (6.7 mg, 0.025 mmol, 10% yield) as an off-white gum.

LCMS (formic acid): *rt* = 0.74 min, MH^+ = 266

¹H NMR (*d*₆-DMSO): δ 1.95 (s, 3 H) 5.34 (s, 2 H) 6.37 (d, *J* = 1.8 Hz, 1 H) 6.99 (d, *J* = 7.1 Hz, 2 H) 7.16 – 7.36 (m, 5 H) 7.53 (d, *J* = 1.8 Hz, 1 H) 11.36 – 11.95 (m, 1 H)

3-Methyl-5-(3-(1-methylpiperidin-4-yl)-3*H*-imidazo[4,5-*b*]pyridin-2-yl)pyridin-2(1*H*)-one, **4.08**:

To a mixture of 5-methyl-6-oxo-1,6-dihydropyridine-3-carbaldehyde **3.25** (59.2 mg, 0.432 mmol) and sodium hydrosulfite (225 mg, 1.295 mmol) was added a solution of *N*-(1-methylpiperidin-4-yl)-3-nitropyridin-2-amine **4.23** (102 mg, 0.432 mmol) in ethanol (1.2 ml), followed by water (0.6 ml). The reaction mixture was heated under microwave conditions at 100 °C for 5 hours. The reaction mixture was partitioned between saturated aqueous sodium bicarbonate solution (10 ml) and DCM (3 x 10 ml). The organic layers were combined, dried using a hydrophobic frit and blown down under a stream of nitrogen. The residue was dissolved in DMSO (1 ml) and purified by MDAP (high pH). The solvent was blown down under a stream of nitrogen to give the required product 3-methyl-5-(3-(1-methylpiperidin-4-yl)-3*H*-imidazo[4,5-*b*]pyridin-2-yl)pyridin-2(1*H*)-one **4.08** (17 mg, 0.053 mmol, 12% yield) as a yellow gum.

LCMS (high pH): *rt* = 0.63 min, MH^+ = 324

¹H NMR (*d*₆-DMSO): δ 1.80 (d, *J* = 11.0 Hz, 2 H) 1.96 (t, *J* = 11.6 Hz, 2 H) 2.07 (s, 3 H) 2.20 (s, 3 H) 2.83 – 3.02 (m, 4 H) 4.22 (m, 1 H) 7.27 (dd, *J* = 8.0, 4.8 Hz, 1 H) 7.57 – 7.67 (m, 2 H) 8.02 (dd, *J* = 7.8, 1.5 Hz, 1 H) 8.32 (dd, *J* = 4.9, 1.5 Hz, 1 H) 11.94 (br. s., 1 H)

3-Methyl-5-(1-(1-methylpiperidin-4-yl)-1*H*-imidazo[4,5-*b*]pyridin-2-yl)pyridin-2(1*H*)-one, **4.14**:

To a mixture of *N*3-(1-methylpiperidin-4-yl)pyridine-2,3-diamine **4.27** (60 mg, 0.291 mmol) and 5-methyl-6-oxo-1,6-dihydropyridine-3-carbaldehyde **3.24** (39.9 mg, 0.291 mmol) was added MeOH (0.375 ml) followed by acetic acid (0.125 ml). The reaction mixture was heated under microwave conditions at 120 °C for a total of 8 hours. The reaction mixture was blown down under a stream of nitrogen and the residue dissolved in DMSO (1 ml) and purified by

MDAP (high pH). The solvent was blown down under a stream of nitrogen to give the required product 3-methyl-5-(1-(1-methylpiperidin-4-yl)-1*H*-imidazo[4,5-*b*]pyridin-2-yl)pyridin-2(1*H*)-one **4.14** (44 mg, 0.136 mmol, 47% yield) as a pale brown solid.

LCMS (high pH): rt = 0.57 min, MH⁺ = 324

¹H NMR (d₆-DMSO): δ 1.87 – 1.95 (m, 2 H) 1.95 – 2.15 (m, 5 H) 2.22 (s, 3 H) 2.37 – 2.47 (m, 2 H) 2.91 (d, *J* = 11.4 Hz, 2 H) 4.22 – 4.30 (m, 1 H) 7.23 (dd, *J* = 8.2, 4.7 Hz, 1 H) 7.58 – 7.63 (m, 1 H) 7.64 (d, *J* = 2.5 Hz, 1 H) 8.15 (dd, *J* = 8.1, 1.3 Hz, 1 H) 8.40 (dd, *J* = 4.6, 1.3 Hz, 1 H) 11.94 (br.s., 1 H)

3-Methyl-5-(1-(1-methylpiperidin-4-yl)-1*H*-benzo[*d*]imidazol-2-yl)pyrazin-2(1*H*)-one, **4.20**:

To a mixture of 6-methyl-5-oxo-4,5-dihydropyrazine-2-carboxylic acid **4.29** (95 mg, 0.616 mmol) and HATU (256 mg, 0.672 mmol) in DMF (2 ml) was added DIPEA (0.293 ml, 1.680 mmol) and the reaction mixture stirred at room temperature for 15 min. *N*1-(1-methylpiperidin-4-yl)benzene-1,2-diamine **4.28** (115 mg, 0.560 mmol) was added and the reaction mixture stirred at room temperature for 4 hours. The reaction mixture was blown down under a stream of nitrogen and the residue loaded in DCM and purified by SPE (5 g, aminopropyl), eluted using 10% MeOH in DCM. The appropriate fractions were combined and blown down under a stream of nitrogen to give a brown solid. The sample was loaded in DCM and purified by SPE (silica, 10 g) using a gradient of 0 – 10 % (2 M ammonia in MeOH) in DCM. The appropriate fractions were combined and blown down under a stream of nitrogen to give a brown solid (35 mg). A portion of this material (32 mg) and *p*-toluenesulfonic acid monohydrate (17.83 mg, 0.094 mmol) in toluene (3 ml) was stirred at 110 °C overnight. The reaction mixture was blown down under a stream of nitrogen and the residue dissolved in DMSO (1 ml) and purified by MDAP (high pH). The solvent was blown down under a stream of nitrogen to give the required product 3-methyl-5-(1-(1-methylpiperidin-4-yl)-1*H*-benzo[*d*]imidazol-2-yl)pyrazin-2(1*H*)-one **4.20** (5.6 mg, 0.017 mmol, 3% yield) as an off-white gum.

LCMS (formic acid): rt = 0.64 min, MH⁺ = 324

¹H NMR (d₆-DMSO): δ 1.84 – 1.94 (m, 2 H) 2.08 (td, *J* = 11.9, 2.5 Hz, 2 H) 2.28 (s, 3 H) 2.40 (s, 3 H) 2.52 – 2.63 (m, 2 H) 2.90 – 3.03 (m, 2 H) 5.06 – 5.14 (m, 1 H) 7.15 – 7.27 (m, 2 H) 7.62 (dd, *J* = 7.1, 1.5 Hz, 1 H) 7.67 – 7.74 (m, 1 H) 7.94 (s, 1 H)

N-(1-Methylpiperidin-4-yl)-3-nitropyridin-2-amine, **4.23**:

To a solution of 2-fluoro-3-nitropyridine (0.080 ml, 0.732 mmol) in THF (1.5 ml) was added 1-methylpiperidin-4-amine (251 mg, 2.196 mmol) and DIPEA (0.384 ml, 2.196 mmol), and the reaction mixture heated under microwave conditions at 120 °C for 30 min. The reaction mixture was partitioned between DCM (3 x 10 ml) and saturated aqueous sodium bicarbonate solution

(10 ml). The organic layers were combined, dried using a hydrophobic frit and blown down under a stream of nitrogen to give an orange gum. The sample was loaded in DCM and purified by SPE (silica, 10 g) using a gradient of 0 – 10 % (2 M ammonia in MeOH) in DCM. The appropriate fractions were combined and blown down under a stream of nitrogen to give the required product *N*-(1-methylpiperidin-4-yl)-3-nitropyridin-2-amine **4.23** (155 mg, 0.656 mmol, 90% yield) as an orange gum.

LCMS (high pH): *rt* = 0.86 min, MH^+ = 237

1H NMR (d_6 -DMSO): δ 1.59 – 1.69 (m, 2 H) 1.88 – 1.95 (m, 2 H) 2.00 – 2.15 (m, 2 H) 2.18 (s, 3 H) 2.70 (d, J = 11.7 Hz, 2 H) 4.02 – 4.23 (m, 1 H) 6.78 (dd, J = 8.4, 4.5 Hz, 1 H) 8.10 (d, J = 7.3 Hz, 1 H), 8.43 (dd, J = 8.4, 1.8 Hz, 1 H) 8.49 (dd, J = 4.4, 1.7 Hz, 1 H)

N-(1-Methylpiperidin-4-yl)-4-nitropyridin-3-amine, **4.24**:

To a solution of 3-fluoro-4-nitropyridine (1.05 g, 7.39 mmol) in THF (15 ml) was added 1-methylpiperidin-4-amine (2.53 g, 22.17 mmol) and DIPEA (3.87 ml, 22.17 mmol), and the reaction mixture heated under microwave conditions at 120 °C for 90 min. The reaction mixture was partitioned between DCM (3 x 100 ml) and saturated aqueous sodium bicarbonate solution (100 ml). The organic layers were combined, dried using a hydrophobic frit, and evaporated under reduced pressure to give an orange solid. The sample was loaded in DCM and purified by SPE (silica, 100 g) using a gradient of 0 – 10 % (2 M ammonia in MeOH) in DCM. The appropriate fractions were combined and evaporated under reduced pressure to give the required product *N*-(1-methylpiperidin-4-yl)-4-nitropyridin-3-amine **4.24** (1.47 g, 6.22 mmol, 84% yield) as a yellow solid.

LCMS (high pH): *rt* = 0.69 min, MH^+ = 237

1H NMR (d_6 -DMSO): δ 1.41 – 1.51 (m, 2 H) 1.88 (d, J = 12.0 Hz, 2 H) 1.97 – 2.11 (m, 2 H) 2.18 (s, 3 H) 2.70 – 2.76 (m, 2 H) 3.35 – 3.44 (m, 1 H) 7.09 (dd, J = 9.1, 3.0 Hz, 1 H) 7.32 (d, J = 7.8 Hz, 1 H) 7.90 (d, J = 2.7 Hz, 1 H) 8.09 (d, J = 9.1 Hz, 1 H).

N-(1-Methylpiperidin-4-yl)-2-nitropyridin-3-amine, **4.25**:

To a solution of 3-fluoro-2-nitropyridine (896 mg, 6.31 mmol) in THF (8 ml) was added 1-methylpiperidin-4-amine (2.160 g, 18.92 mmol) and DIPEA (3.30 ml, 18.92 mmol), and the reaction mixture was heated under microwave conditions at 120 °C for 30 min. The reaction mixture was partitioned between DCM (3 x 100 ml) and saturated aqueous sodium bicarbonate solution (100 ml). The organic layers were combined, dried using a hydrophobic frit, and blown down under a stream of nitrogen to give an orange solid. The sample was loaded in DCM and purified by SPE (silica, 100 g) using a gradient of 0 – 10 % (2 M ammonia in MeOH) in DCM. The appropriate fractions were combined and blown down under a stream of nitrogen to give

the required product *N*-(1-methylpiperidin-4-yl)-2-nitropyridin-3-amine **4.25** (1.45 g, 6.14 mmol, 97% yield) as an orange solid.

LCMS (high pH): *rt* = 0.67 min, MH^+ = 237

1H NMR (d_6 -DMSO): δ 1.54 – 1.64 (m, 2 H) 1.90 – 1.97 (m, 2 H) 2.06 – 2.17 (m, 2 H) 2.19 (s, 3 H) 2.61 – 2.76 (m, 2 H) 3.63 (d, J = 7.8 Hz, 1 H) 7.53 (d, J = 7.3 Hz, 1 H) 7.60 (dd, J = 8.7, 3.9 Hz, 1 H) 7.71 (d, J = 8.6 Hz, 1 H) 7.83 (dd, J = 3.9, 1.4 Hz, 1 H).

*N*3-(1-Methylpiperidin-4-yl)pyridine-3,4-diamine, **4.26**:

N-(1-Methylpiperidin-4-yl)-4-nitropyridin-3-amine **4.24** (400 mg, 1.693 mmol) was dissolved in ethanol (20 ml) and the reaction mixture was hydrogenated using an H-cube (20 °C, 1 bar, 1 ml/min flow rate) with 10% Pd/C CatCart 30. The reaction mixture was circulated through the H-cube apparatus for 30 min. The reaction mixture was blown down under a stream of nitrogen and the residue loaded in DCM and purified SPE (silica, 50 g) using a gradient of 0 – 10 % (2 M ammonia in MeOH) in DCM. The appropriate fractions were combined and evaporated under reduced pressure to give the required product *N*3-(1-methylpiperidin-4-yl)pyridine-3,4-diamine **4.26** (304 mg, 1.474 mmol, 87% yield) as a purple gum.

LCMS (high pH): *rt* = 0.49 min, MH^+ = 207

1H NMR (d_6 -DMSO): δ 1.26 – 1.36 (m, 2 H) 1.76 – 1.87 (m, 2 H) 1.89 – 2.02 (m, 2 H) 2.15 (s, 3 H) 2.66 – 2.74 (m, 2 H) 2.91 – 3.06 (br. s., 1 H) 4.42 – 4.54 (m, 1 H) 4.97 (br. s., 2 H) 6.32 (d, J = 8.6 Hz, 1 H) 6.83 (dd, J = 8.7, 2.8 Hz, 1 H) 7.39 (d, J = 2.7 Hz, 1 H)

*N*3-(1-Methylpiperidin-4-yl)pyridine-2,3-diamine, **4.27**:

N-(1-Methylpiperidin-4-yl)-2-nitropyridin-3-amine **4.25** (1.45 g, 6.14 mmol) was dissolved in ethanol (75 ml) and the solution was hydrogenated using an H-cube (20 °C, 1 bar, 1 ml/min flow rate) with a 10% Pd/C CatCart 30. The reaction mixture was circulated through the H-cube for 30 min. The reaction mixture was evaporated under reduced pressure to give a dark purple solid. The sample was loaded in DCM and purified by SPE (silica, 100 g) using a gradient of 0 – 10 % (2 M ammonia in MeOH) in DCM. The appropriate fractions were combined and evaporated under reduced pressure to give the required product *N*3-(1-methylpiperidin-4-yl)pyridine-2,3-diamine **4.27** (790 mg, 3.83 mmol, 62% yield) as a purple solid.

LCMS (high pH): *rt* = 0.61 min, MH^+ = 207

1H NMR (d_6 -DMSO): δ 1.35 – 1.45 (m, 2 H) 1.83 – 1.94 (m, 2 H) 1.94 – 2.07 (m, 2 H) 2.17 (s, 3 H) 2.74 (d, J = 11.9 Hz, 1 H) 3.09 – 3.18 (m, 1 H) 4.43 (d, J = 7.1 Hz, 1 H) 5.42 (s, 2 H) 6.42 (dd, J = 7.6, 4.8 Hz, 1 H) 6.59 (d, J = 7.6 Hz, 1 H) 7.24 (dd, J = 4.9, 1.4 Hz, 1 H)

*N*1-(1-Methylpiperidin-4-yl)benzene-1,2-diamine, **4.28**:

1-Methyl-*N*-(2-nitrophenyl)piperidin-4-amine **3.27** (400 mg, 1.700 mmol) was dissolved in ethanol (34 ml) and the reaction was hydrogenated using an H-cube (settings: 20 °C, 1 bar, 1 ml/min flow rate) with a 10% Pd/C CatCart 30. The reaction mixture was blown down under a stream of nitrogen to give a pale orange solid. The material was hydrogenated a second time, under identical conditions, and then the resulting solution blown down under a stream of nitrogen to give a light brown solid (284 mg). The sample was dried in a vacuum pistol at 40 °C for 1.5 hours to give *N*1-(1-methylpiperidin-4-yl)benzene-1,2-diamine **4.28** (232 mg, 1.130 mmol, 67% yield).

LCMS (high pH): *rt* = 0.73 min, MH^+ = 206

¹H NMR (*d*₆-DMSO): δ 1.36 – 1.46 (m, 2 H) 1.90 (d, *J* = 11.4 Hz, 2 H) 2.00 (t, *J* = 11.5 Hz, 2 H) 2.17 (s, 3 H) 2.74 (d, *J* = 11.6 Hz, 2 H) 3.09 – 3.18 (m, 1 H) 4.09 (br. s., 1 H) 4.48 (br. s., 1 H) 6.35 – 6.41 (m, 1 H) 6.42 – 6.50 (m, 2 H) 6.53 (d, *J* = 7.6 Hz, 1 H)

4-(5-Methyl-6-oxo-1,6-dihydropyridin-3-yl)benzaldehyde, **4.30**:

5-Bromo-3-methylpyridin-2(1*H*)-one **3.24** (100 mg, 0.532 mmol), (4-formylphenyl)boronic acid (96 mg, 0.638 mmol), and tetrakis(triphenylphosphine)palladium(0) (61.5 mg, 0.053 mmol) were combined in isopropanol (3 ml), 1 M aqueous sodium bicarbonate solution (1.596 ml, 1.596 mmol) added, and the reaction mixture heated under microwave conditions at 120 °C for 10 min. The reaction mixture was partitioned between DCM (2 x 10 ml) and water (10 ml). The organic layers were combined, dried using a hydrophobic frit and blown down under a stream of nitrogen. The residue was dissolved in DMSO (3 ml). The first 1 ml was purified by MDAP (formic acid) and was lost due to machine failure. The remaining 2 ml purified by MDAP (as standard conditions, except column: Waters BEH C18, 150 x 19 mm, 5 μ m packing diameter; gradient solvent A: 0.1% v/v solution of formic acid in water, gradient solvent B: MeOH). The samples were blown down under a stream of nitrogen to give 4-(5-methyl-6-oxo-1,6-dihydropyridin-3-yl)benzaldehyde **4.30** (21 mg, 0.098 mmol, 19% yield).

LCMS (formic acid): *rt* = 0.66 min, MH^+ = 214

¹H NMR not performed due to low mass available for subsequent reactions.

(*S*)-Cyclopentyl _____ 4-methyl-2-((4-(5-methyl-6-oxo-1,6-dihydropyridin-3-yl)benzyl)amino)pentanoate, **4.32**:

To a mixture of 4-(5-methyl-6-oxo-1,6-dihydropyridin-3-yl)benzaldehyde **4.30** (21 mg, 0.098 mmol) and (*S*)-cyclopentyl 2-amino-4-methylpentanoate 4-methylbenzenesulfonate **3.26** (40.2 mg, 0.108 mmol) in DCM (2 ml) was added acetic acid (0.017 ml, 0.295 mmol) and the reaction mixture was stirred at room temperature for 15 min. Sodium triacetoxyborohydride

(41.7 mg, 0.197 mmol) was added, and the reaction mixture stirred at room temperature for 1.5 hours. The reaction mixture was partitioned between DCM (3 x 10 ml) and saturated sodium bicarbonate solution (10 ml). The organic layers were combined, dried using a hydrophobic frit and blown down under a stream of nitrogen. The residue was dissolved in DMSO (1 ml) and purified by MDAP (high pH). The solvent was blown down under a stream of nitrogen to give two batches of material: batch 1, (*S*)-cyclopentyl 4-methyl-2-((4-(5-methyl-6-oxo-1,6-dihydropyridin-3-yl)benzyl)amino)pentanoate **4.32** (12 mg, 0.030 mmol, 31% yield), as a yellow solid; and batch 2, (*S*)-cyclopentyl 4-methyl-2-((4-(5-methyl-6-oxo-1,6-dihydropyridin-3-yl)benzyl)amino)pentanoate **4.32** (12 mg, 0.030 mmol, 31% yield), as a yellow solid.

Batch 1:

LCMS (high pH): rt = 1.24 min, MH⁺ = 397

¹H NMR (d₆-DMSO): δ 0.80 (d, *J* = 6.6 Hz, 3 H) 0.86 (d, *J* = 6.6 Hz, 3 H) 1.32 – 1.45 (m, 2 H) 1.50 – 1.74 (m, 7 H) 1.74 – 1.96 (m, 2 H) 2.05 (s, 3 H) 2.21 – 2.42 (m, 1 H) 3.06 – 3.13 (m, 1 H) 3.53 (d, *J* = 13.7, 1 H) 3.74 (d, *J* = 13.5 Hz, 1 H) 5.02 – 5.18 (m, 1 H) 7.30 (d, *J* = 8.3 Hz, 2 H) 7.49 (d, *J* = 8.3 Hz, 2 H) 7.53 (d, *J* = 2.5 Hz, 1 H) 7.68 – 7.78 (m, 1 H).

Batch 2:

LCMS (formic acid): rt = 0.82 min, MH⁺ = 397, 92% pure by UV. Also contains at rt = 0.66 min, MH⁺ = 214, 8% by UV, consistent with starting material aldehyde.

¹H NMR not done due to low purity.

(*S*)-Cyclopentyl 2-((4-(1,5-dimethyl-6-oxo-1,6-dihydropyridin-3-yl)benzyl)amino)-4-methylpentanoate, **4.33**:

To a mixture of 4-(1,5-dimethyl-6-oxo-1,6-dihydropyridin-3-yl)benzaldehyde **4.31** (203 mg, 0.893 mmol) and (*S*)-cyclopentyl 2-amino-4-methylpentanoate 4-methylbenzenesulfonate **3.26** (365 mg, 0.983 mmol) in DCM (10 ml) was added acetic acid (0.153 ml, 2.68 mmol) and the reaction mixture was stirred at room temperature for 15 min under nitrogen. Sodium triacetoxyborohydride (379 mg, 1.787 mmol) was added, and the reaction mixture stirred at room temperature for 1.5 hours. The reaction mixture was partitioned between DCM (3 x 50 ml) and saturated sodium bicarbonate solution (50 ml). The organic layers were combined, dried using a hydrophobic frit, and evaporated under reduced pressure. The sample was loaded in DCM and purified by SPE (silica, 25 g) using a gradient of 0 – 10 % (2 M ammonia in MeOH) in DCM. The appropriate fractions were combined and blown down under a stream of nitrogen. The sample was loaded in DCM and purified by SPE (silica, 25 g) using a gradient of 0 – 6% (2 M ammonia in MeOH) in DCM. The appropriate fractions were combined and blown down under a stream of nitrogen to give two batches of product, batch 1, (*S*)-cyclopentyl 2-((4-(1,5-

dimethyl-6-oxo-1,6-dihydropyridin-3-yl)benzyl)amino)-4-methylpentanoate **4.33** (171 mg, 0.418 mmol, 47% yield), and batch 2, crude material which was not pure (126 mg, 34% yield). Batch 2 was dissolved in DMSO (2 x 1 ml) and purified by MDAP (high pH). The solvent was blown down under a stream of nitrogen to give the required product, batch 3, (*S*)-cyclopentyl 2-((4-(1,5-dimethyl-6-oxo-1,6-dihydropyridin-3-yl)benzyl)amino)-4-methylpentanoate **4.33** (77 mg, 0.188 mmol, 21% yield) as a yellow solid. The total yield of the reaction was 68%.

Batch 1:

LCMS (formic acid): $rt = 0.86$ min, $MH^+ = 411$

1H NMR (d_6 -DMSO): δ 0.80 (d, $J = 6.6$ Hz, 2 H) 0.86 (d, $J = 6.6$ Hz, 2 H) 1.33 – 1.45 (m, 2 H) 1.49 – 1.75 (m, 7 H) 1.75 – 1.91 (m, 2 H) 2.08 (s, 3 H) 2.28 – 2.43 (m, 1 H) 3.00 – 3.15 (m, 1 H) 3.33 (s, 3 H) 3.55 (m, partially obscured by water peak) 3.73 (d, $J = 13.5$ Hz, 1 H) 5.08 – 5.13 (m, 1 H) 7.32 (d, $J = 8.3$ Hz, 2 H) 7.51 (d, $J = 8.3$ Hz, 2 H) 7.72 – 7.74 (m, 1 H) 7.97 (d, $J = 2.5$ Hz, 1 H)

^{13}C NMR (d_6 -DMSO, 303 K): δ 17.1, 22.2, 22.6, 23.2, 24.4, 32.3, 37.2, 42.0, 50.5, 58.4, 76.5, 117.0, 124.9, 127.7, 128.5, 134.2, 134.8, 135.8, 138.8, 161.6, 174.8.

IR (neat): 2953 (amine N-H), 1726 (ester), 1654 (pyridone), 1594 (aryl), 1516 (aryl), 816 (aryl C-H), 767 (aryl C-H) cm^{-1}

M.pt.: 88–90 °C

HRMS: ($C_{25}H_{35}N_2O_3$) MH^+ requires 411.2639, found MH^+ 411.2642

$[\alpha_D]^{23.9^\circ C}$ (c 1.0, methanol): -22.3 °

Batch 2:

LCMS (formic acid): $rt = 0.86$ min, $MH^+ = 411$

1H NMR (d_6 -DMSO): δ 0.80 (d, $J = 6.6$ Hz, 2 H) 0.86 (d, $J = 6.6$ Hz, 2 H) 1.32 – 1.45 (m, 2 H) 1.48 – 1.75 (m, 7 H) 1.78 – 1.86 (m, 2 H) 2.08 (s, 3 H) 3.09 (t, $J = 7.3$ Hz, 1 H) 3.54 (d, $J = 13.7$ Hz, 1 H) 3.75 (d, $J = 13.7$ Hz, 1 H) 5.09 – 5.12 (m, 1 H) 7.32 (d, $J = 8.3$ Hz, 2 H) 7.51 (d, $J = 8.3$ Hz, 2 H) 7.72 – 7.74 (m, 1 H) 7.97 (d, $J = 2.5$ Hz, 1 H).

(*S*)-4-Methyl-2-((4-(5-methyl-6-oxo-1,6-dihydropyridin-3-yl)benzyl)amino)pentanoic acid, hydrochloride, **4.34**:

To a solution of (*S*)-cyclopentyl 4-methyl-2-((4-(5-methyl-6-oxo-1,6-dihydropyridin-3-yl)benzyl)amino)pentanoate **4.32** (12 mg, 0.030 mmol) in MeOH (1 ml) and THF (1 ml) was added 1M aqueous lithium hydroxide solution (0.091 ml, 0.091 mmol), and the reaction mixture stirred at room temperature for 11 days. The sample was blown down under a stream of nitrogen and the residue suspended in DMSO (1 ml). The sample was filtered and the solution purified by MDAP (formic acid). The solvent was blown down under a stream of nitrogen to give the

required product (*S*)-4-methyl-2-((4-(5-methyl-6-oxo-1,6-dihydropyridin-3-yl)benzyl)amino)pentanoic acid, hydrochloride **4.34** (10.5 mg, 0.029 mmol, 95% yield) as an off-white solid.

LCMS (high pH): rt = 0.54 min, MH⁺ = 327

¹H NMR (d₆-DMSO): δ 0.89 – 0.91 (m, 6 H) 1.70 – 1.81 (m, 3 H) 2.06 (s, 3 H) 3.78 – 3.92 (m, 1 H) 4.12 – 4.23 (m, 2 H) 7.54 (d, *J* = 8.3 Hz, 2 H) 7.60 – 7.69 (m, 3 H) 7.77 – 7.79 (m, 1 H) 9.29 – 9.53 (m, 1 H) 9.53 – 9.73 (m, 1 H) 11.64 – 11.97 (m, 1 H) 13.37 – 14.65 (m, 1 H).

(*S*)-2-((4-(1,5-Dimethyl-6-oxo-1,6-dihydropyridin-3-yl)benzyl)amino)-4-methylpentanoic acid, **4.35**:

To a solution of (*S*)-cyclopentyl 2-((4-(1,5-dimethyl-6-oxo-1,6-dihydropyridin-3-yl)benzyl)amino)-4-methylpentanoate **4.33** (100 mg, 0.244 mmol) in MeOH (2.5 ml) and THF (2.5 ml) was added 1 M aqueous lithium hydroxide solution (0.731 ml, 0.731 mmol) and the reaction mixture stirred at 50 °C overnight. The sample was blown down under a stream of nitrogen, DMSO (3 x 1 ml) added, the solid removed by filtration and the solution purified by MDAP (formic acid). The solvent was blown down under a stream of nitrogen to give the required product (*S*)-2-((4-(1,5-dimethyl-6-oxo-1,6-dihydropyridin-3-yl)benzyl)amino)-4-methylpentanoic acid **4.35** (65 mg, 0.190 mmol, 78% yield) as an off-white solid.

LCMS (formic acid): rt = 0.55 min, MH⁺ = 343

¹H NMR (d₆-DMSO): δ 0.80 (d, *J* = 6.6 Hz, 3 H) 0.86 (d, *J* = 6.6 Hz, 3 H) 1.39 – 1.50 (m, 2 H) 1.75 – 1.84 (m, 1 H) 2.08 (s, 3 H) 3.09 (t, *J* = 7.1 Hz, 1 H) 3.51 (s, 3 H) 3.73 (d, *J* = 13.7 Hz, 1 H) 3.90 (d, *J* = 13.5 Hz, 1 H) 7.40 (d, *J* = 8.1 Hz, 2 H) 7.55 (d, *J* = 8.1 Hz, 2 H) 7.70 – 7.78 (m, 1 H) 7.99 (d, *J* = 2.2 Hz, 1 H).

3-Methyl-5-(1-methyl-1*H*-benzo[*d*]imidazol-2-yl)pyridin-2(1*H*)-one, **4.36**:

N-Methyl-2-nitroaniline **4.120** (54.4 mg, 0.357 mmol) in ethanol (1.5 ml) and water (0.75 ml) was added to a mixture of 5-methyl-6-oxo-1,6-dihydropyridine-3-carbaldehyde **3.25** (49 mg, 0.357 mmol) and sodium hydrosulfite (187 mg, 1.072 mmol). The reaction mixture was heated under microwave conditions at 100 °C for 5 hours. The reaction mixture was partitioned between DCM and saturated aqueous sodium bicarbonate solution. The combined organic layers were dried and evaporated. The crude sample was dissolved in DMSO and purified by MDAP (formic acid). The solvent was evaporated to give the required product 3-methyl-5-(1-methyl-1*H*-benzo[*d*]imidazol-2-yl)pyridin-2(1*H*)-one **4.36** (35 mg, 0.146 mmol, 41% yield) as a white solid.

LCMS (formic acid): rt = 0.44 min, MH⁺ = 240

¹H NMR (d₆-DMSO): δ 2.08 (s, 3 H) 3.86 (s, 3 H) 7.16 – 7.31 (m, 2 H) 7.56 (d, *J* = 7.3 Hz, 1 H) 7.59 – 7.64 (m, 1 H) 7.78 (d, *J* = 2.2 Hz, 1 H) 7.81 – 7.87 (m, 1 H) 11.47 – 12.36 (br.s., 1 H)

5-(1-Isobutyl-1*H*-benzo[*d*]imidazol-2-yl)-3-methylpyridin-2(1*H*)-one, **4.39**:

N-Isobutyl-2-nitroaniline **4.123** (65 mg, 0.335 mmol), 5-methyl-6-oxo-1,6-dihydropyridine-3-carbaldehyde **3.25** (45.9 mg, 0.335 mmol) and sodium hydrosulfite (175 mg, 1.004 mmol) were dissolved in ethanol (1.5 ml) and water (0.75 ml) and heated under microwave conditions at 100 °C for 5 hours. Saturated aqueous sodium bicarbonate solution was added, followed by DCM. The layers were separated and the aqueous phase extracted using DCM. The organic layers were combined, dried over magnesium sulfate, and the solvent removed. The yellow residue was then purified by SPE (silica) using a gradient of 0 – 10 % MeOH in DCM. The appropriate fractions were combined and the solvent removed to give 5-(1-isobutyl-1*H*-benzo[*d*]imidazol-2-yl)-3-methylpyridin-2(1*H*)-one **4.39** (46 mg, 0.163 mmol, 50 % yield) as a white solid.

LCMS (formic acid): rt = 0.64 min, MH⁺ = 282

¹H NMR (CDCl₃): δ 0.80 (d, *J* = 6.8 Hz, 6 H) 2.15 – 2.22 (m, 1 H) 4.05 (d, *J* = 7.3 Hz, 2 H) 7.25 – 7.31 (m, 2 H) 7.34 – 7.40 (m, 1 H) 7.74 (s, 2 H) 7.76 – 7.80 (m, 1 H)

3-Methyl-5-(1-((4-methylmorpholin-2-yl)methyl)-1*H*-benzo[*d*]imidazol-2-yl)pyridin-2(1*H*)-one, **4.42**:

Method as for **4.36**, using the following reagents: *N*-((4-Methylmorpholin-2-yl)methyl)-2-nitroaniline **4.130** (84 mg, 0.335 mmol), 5-methyl-6-oxo-1,6-dihydropyridine-3-carbaldehyde **3.25** (46 mg, 0.335 mmol), sodium hydrosulfite (175 mg, 1.006 mmol), ethanol (1.5 ml) and water (0.75 ml). MDAP (high pH) was used. The final product was: 3-methyl-5-(1-((4-methylmorpholin-2-yl)methyl)-1*H*-benzo[*d*]imidazol-2-yl)pyridin-2(1*H*)-one **4.42** (56 mg, 0.165 mmol, 49% yield) as a colourless gum.

LCMS (formic acid): rt = 0.37 min, MH⁺ = 339

¹H NMR (d₆-DMSO): δ 1.78 (t, *J* = 10.6 Hz, 1 H) 1.95 – 2.02 (m, 1 H) 2.06 (s, 3 H) 2.17 (s, 3 H) 2.57 (d, *J* = 11.7 Hz, 1 H) 2.78 (d, *J* = 11.3 Hz, 1 H) 3.32 – 3.38 (m, 1 H) 3.66 – 3.76 (m, 1 H) 3.84 – 3.91 (m, 1 H) 4.22 – 4.38 (m, 2 H) 7.20 – 7.27 (m, 2 H) 7.58 – 7.67 (m, 2 H) 7.79 – 7.81 (m, 1 H) 7.90 (d, *J* = 2.2 Hz, 1 H)

5-(1-(2-(Dimethylamino)ethyl)-1*H*-benzo[*d*]imidazol-2-yl)-3-methylpyridin-2(1*H*)-one, **4.45**:

Method as for **4.39**, using the following reagents: *N*1,*N*1-Dimethyl-*N*2-(2-nitrophenyl)ethane-1,2-diamine **4.135** (75 mg, 0.358 mmol), 5-methyl-6-oxo-1,6-dihydropyridine-3-carbaldehyde **3.25** (49.2 mg, 0.358 mmol), sodium hydrosulfite (187 mg, 1.075 mmol), ethanol (1.5 ml) and water (0.75 ml). The final product was: 5-(1-(2-(dimethylamino)ethyl)-1*H*-benzo[*d*]imidazol-2-

yl)-3-methylpyridin-2(1*H*)-one **4.45** (49 mg, 0.165 mmol, 46% yield) as a colourless oil.

LCMS (formic acid): *rt* = 0.37 min, MH^+ = 297

1H NMR ($CDCl_3$): δ 2.26 (s, 9 H) 2.72 – 2.79 (m, 2 H) 4.28 – 4.33 (m, 2 H) 7.29 – 7.35 (m, 2 H) 7.38 – 7.44 (m, 1 H) 7.76 – 7.82 (m, 1 H) 7.86 – 7.87 (m, 1 H) 8.01 (d, *J* = 2.2 Hz, 1 H)

N-(2-(2-(5-Methyl-6-oxo-1,6-dihydropyridin-3-yl)-1*H*-benzo[*d*]imidazol-1-yl)ethyl)acetamide, **4.48**:

Method as for **4.90**, using the following reagents: *N*-(2-((2-Nitrophenyl)amino)ethyl)acetamide **4.139** (68 mg, 0.305 mmol), 5-methyl-6-oxo-1,6-dihydropyridine-3-carbaldehyde **3.25** (41.8 mg, 0.305 mmol), sodium hydrosulfite (159 mg, 0.914 mmol), ethanol (1.5 ml) and water (0.75 ml). The final product was: *N*-(2-(2-(5-methyl-6-oxo-1,6-dihydropyridin-3-yl)-1*H*-benzo[*d*]imidazol-1-yl)ethyl)acetamide **4.48** (11 mg, 0.035 mmol, 12% yield) as a colourless oil.

LCMS (formic acid): *rt* = 0.41 min, MH^+ = 311

1H NMR (d_3 MeOD): δ 1.70 (s, 3 H) 2.20 (s, 3 H) 3.48 (t, *J* = 6.2 Hz, 2 H) 4.44 (t, *J* = 6.2 Hz, 2 H) 7.27 – 7.37 (m, 2 H) 7.60 (d, *J* = 7.6 Hz, 1 H) 7.66 (d, *J* = 7.6 Hz, 1 H) 7.77 – 7.80 (m, 2 H)

3-Methyl-5-(1-((tetrahydro-2*H*-pyran-4-yl)methyl)-1*H*-benzo[*d*]imidazol-2-yl)pyridin-2(1*H*)-one, **4.51**:

Method as for **4.36**, using the following reagents: 2-Nitro-*N*-((tetrahydro-2*H*-pyran-4-yl)methyl)aniline **4.142** (86 mg, 0.365 mmol), 5-methyl-6-oxo-1,6-dihydropyridine-3-carbaldehyde **3.25** (50 mg, 0.365 mmol), sodium hydrosulfite (190 mg, 1.094 mmol), ethanol (1.5 ml) and water (0.75 ml). The final product was: 3-methyl-5-(1-((tetrahydro-2*H*-pyran-4-yl)methyl)-1*H*-benzo[*d*]imidazol-2-yl)pyridin-2(1*H*)-one **4.51** (53.4 mg, 0.165 mmol, 45% yield) as an off-white gum.

LCMS (formic acid): *rt* = 0.54 min, MH^+ = 324

1H NMR (d_3 -MeOD): δ 1.17 – 1.37 (m, 4 H) 2.01 – 2.16 (m, 1 H) 2.21 (s, 3 H) 3.20 – 3.27 (m, 2 H) 3.76 – 3.88 (m, 2 H) 4.26 (d, *J* = 7.6 Hz, 2 H) 7.28 – 7.37 (m, 2 H) 7.61 (d, *J* = 7.6 Hz, 1 H) 7.66 (d, *J* = 7.3 Hz, 1 H) 7.75 (d, *J* = 2.2 Hz, 1 H) 7.77 – 7.79 (m, 1 H)

^{13}C NMR (d_6 -DMSO, 303 K): δ 16.9, 30.5, 35.6, 49.8, 66.8, 109.1, 111.5, 119.2, 122.3, 122.6, 129.4, 134.2, 136.5, 138.3, 142.8, 151.1, 162.6.

IR (neat): 2934 (saturated CH_2), 2908 (saturated CH_2), 2838 (saturated CH_2), 1656 (pyridone), 744 (aryl C-H) cm^{-1}

M.pt.: 259–261 °C

HRMS: ($C_{19}H_{22}N_3O_2$) MH^+ requires 324.1712, found MH^+ 324.1704

5-(1-(1-Methoxypropan-2-yl)-1*H*-benzo[*d*]imidazol-2-yl)-3-methylpyridin-2(1*H*)-one, 4.54:

Method as for **4.36**, using the following reagents: *N*-(1-Methoxypropan-2-yl)-2-nitroaniline **4.147** (77 mg, 0.365 mmol), 5-methyl-6-oxo-1,6-dihydropyridine-3-carbaldehyde **3.25** (50 mg, 0.365 mmol), sodium hydrosulfite (190 mg, 1.094 mmol), ethanol (1.5 ml) and water (0.75 ml).

The final product was: 5-(1-(1-methoxypropan-2-yl)-1*H*-benzo[*d*]imidazol-2-yl)-3-methylpyridin-2(1*H*)-one **4.54** (64.6 mg, 0.217 mmol, 60% yield) as a colourless gum.

LCMS (formic acid): *rt* = 0.57 min, MH^+ = 298

¹H NMR (*d*₆-DMSO): δ 1.52 (d, *J* = 7.1 Hz, 3 H) 2.06 (s, 3 H) 3.15 (s, 3 H) 3.69 (dd, *J* = 10.3, 4.4 Hz, 1 H) 4.02 (t, *J* = 9.9 Hz, 1 H) 4.70 – 4.82 (m, 1 H) 7.15 – 7.27 (m, 2 H) 7.58 – 7.70 (m, 3 H) 7.72 – 7.80 (m, 1 H)

5-(1-(3-Hydroxypropyl)-1*H*-benzo[*d*]imidazol-2-yl)-3-methylpyridin-2(1*H*)-one, 4.57:

3-((2-Nitrophenyl)amino)propan-1-ol **4.148** (61 mg, 0.311 mmol), 5-methyl-6-oxo-1,6-dihydropyridine-3-carbaldehyde **3.25** (42.6 mg, 0.311 mmol) and sodium hydrosulfite (162 mg, 0.933 mmol) were dissolved in ethanol (1.5 ml) and water (0.75 ml) and heated under microwave conditions at 100 °C for 5 hours. Saturated aqueous sodium bicarbonate solution (15 ml) was added, followed by EtOAc (15 ml). The layers were separated and the aqueous phase further extracted using EtOAc (2 x 15 ml). The organic layers were combined, dried over magnesium sulfate, and the solvent removed. The residue was purified by SPE (silica) using a gradient of 0 – 10% MeOH in DCM. The appropriate fractions were combined and the solvent removed to give 5-(1-(3-hydroxypropyl)-1*H*-benzo[*d*]imidazol-2-yl)-3-methylpyridin-2(1*H*)-one **4.57** (23 mg, 0.081 mmol, 26% yield) as a colourless oil.

LCMS (formic acid): *rt* = 0.43 min, MH^+ = 284

¹H NMR (*d*₃-MeOD): δ 1.94 – 2.07 (m, 2 H) 2.19 (s, 3 H) 3.54 (t, *J* = 5.8 Hz, 2 H) 4.37 – 4.45 (m, 2 H) 7.24 – 7.37 (m, 2 H) 7.57 – 7.61 (m, 1 H) 7.62 – 7.70 (m, 1 H) 7.81 (d, *J* = 1.2 Hz, 1 H) 7.80 – 7.82 (m, 1 H)

5-(1-Ethyl-1*H*-benzo[*d*]imidazol-2-yl)-3-methylpyridin-2(1*H*)-one, 4.60:

Method as for **4.36**, using the following reagents: *N*-ethyl-2-nitroaniline **4.121** (60.6 mg, 0.365 mmol), 5-methyl-6-oxo-1,6-dihydropyridine-3-carbaldehyde **3.25** (50 mg, 0.365 mmol), sodium hydrosulfite (190 mg, 1.094 mmol), ethanol (1.5 ml) and water (0.75 ml). The final product was: 5-(1-ethyl-1*H*-benzo[*d*]imidazol-2-yl)-3-methylpyridin-2(1*H*)-one **4.60** (67.8 mg, 0.268 mmol, 73% yield) as a white gum.

LCMS (formic acid): *rt* = 0.50 min, MH^+ = 254

¹H NMR (*d*₆-DMSO): δ 1.33 (t, *J* = 7.1 Hz, 3 H) 2.08 (s, 3 H) 4.30 (q, *J* = 7.1 Hz, 2 H) 7.18 – 7.29 (m, 2 H) 7.58 – 7.65 (m, 2 H) 7.68 (d, *J* = 2.2 Hz, 1 H) 7.72 – 7.76 (m, 1 H)

5-(1-isopropyl-1H-benzo[d]imidazol-2-yl)-3-methylpyridin-2(1H)-one, 4.63:

Method as for **4.36**, using the following reagents: *N*-isopropyl-2-nitroaniline **4.122** (65.7 mg, 0.365 mmol), 5-methyl-6-oxo-1,6-dihydropyridine-3-carbaldehyde (50 mg, 0.365 mmol), sodium dithionite (190 mg, 1.094 mmol), in ethanol (1.5 ml) and water (0.75 ml). The final product was 5-(1-isopropyl-1H-benzo[d]imidazol-2-yl)-3-methylpyridin-2(1H)-one **4.63** (61.5 mg, 0.230 mmol, 63% yield) as a colourless gum.

LCMS (formic acid): rt = 0.56 min, MH⁺ = 268

¹H NMR (d₆-DMSO): δ 1.59 (d, *J* = 6.8 Hz, 6 H) 2.07 (s, 3 H) 4.61 – 4.83 (m, 1 H) 7.12 – 7.31 (m, 2 H) 7.54 – 7.59 (m, 2 H) 7.59 – 7.65 (m, 1 H) 7.70 – 7.84 (m, 1 H)

5-(1-(Cyclopropylmethyl)-1H-benzo[d]imidazol-2-yl)-3-methylpyridin-2(1H)-one, 4.66:

Method as for **4.39**, using the following reagents: *N*-(cyclopropylmethyl)-2-nitroaniline **4.124** (68 mg, 0.354 mmol), 5-methyl-6-oxo-1,6-dihydropyridine-3-carbaldehyde **3.25** (48.5 mg, 0.354 mmol), sodium hydrosulfite (185 mg, 1.061 mmol), ethanol (1.5 ml) and water (0.75 ml). The final product was: 5-(1-(cyclopropylmethyl)-1H-benzo[d]imidazol-2-yl)-3-methylpyridin-2(1H)-one **4.66** (49 mg, 0.175 mmol, 50% yield) as a white solid.

LCMS (formic acid): rt = 0.60 min, MH⁺ = 280

¹H NMR (CDCl₃): δ 0.24 – 0.32 (m, 2 H) 0.53 – 0.61 (m, 2 H) 1.12 – 1.22 (m, 1 H) 2.26 (s, 3 H) 4.14 (d, *J* = 6.4 Hz, 3 H) 7.27 – 7.34 (m, 3 H) 7.42 – 7.46 (m, 1 H) 7.77 – 7.81 (m, 3 H)

5-(1-(Azetidin-3-yl)-1H-benzo[d]imidazol-2-yl)-3-methylpyridin-2(1H)-one, 4.69:

tert-Butyl 3-(2-(5-methyl-6-oxo-1,6-dihydropyridin-3-yl)-1H-benzo[d]imidazol-1-yl)azetidine-1-carboxylate **4.126** (62 mg, 0.163 mmol) was dissolved in 1,4-dioxane (3 ml), then 4 M hydrochloric acid in 1,4-dioxane (1 ml) was added to the reaction mixture. The mixture was left stirring at room temperature for 72 hours. Diethyl ether (2 x 10 ml) was added, and each time the supernatant collected. The solvent was removed under reduced pressure and the residue purified by MDAP (high pH). The appropriate fractions were combined and the solvent removed to give 5-(1-(azetidin-3-yl)-1H-benzo[d]imidazol-2-yl)-3-methylpyridin-2(1H)-one **4.69** (45 mg, 0.161 mmol, 99% yield) as a white powder.

LCMS (formic acid): rt = 0.37 min, MH⁺ = 281

¹H NMR (d₆-DMSO): δ 2.06 (s, 3 H) 3.89 – 3.96 (m, 4 H) 5.38 – 5.46 (m, 1 H) 7.18 – 7.36 (m, 2 H) 7.58 (br. s., 2 H) 7.65 (d, *J* = 7.3 Hz, 1 H) 8.03 (d, *J* = 7.3 Hz, 1 H)

3-Methyl-5-(1-(1-methylpiperidin-3-yl)-1H-benzo[d]imidazol-2-yl)pyridin-2(1H)-one, 4.72:

Method as for **4.36**, using the following reagents: 1-methyl-*N*-(2-nitrophenyl)piperidin-3-amine **4.127** (54.9 mg, 0.233 mmol), 5-methyl-6-oxo-1,6-dihydropyridine-3-carbaldehyde **3.25** (32

mg, 0.233 mmol), sodium hydrosulfite (122 mg, 0.700 mmol), ethanol (1.5 ml) and water (0.75 ml). The final product was: 3-methyl-5-(1-(1-methylpiperidin-3-yl)-1*H*-benzo[*d*]imidazol-2-yl)pyridin-2(1*H*)-one **4.72** (35.5 mg, 0.110 mmol, 47% yield) as a colourless gum.

LCMS (formic acid): *rt* = 0.44 min, MH^+ = 323

¹H NMR (*d*₆-DMSO): δ 1.50 – 1.65 (m, 1 H) 1.76 – 1.79 (br.d., 1 H) 1.89 – 1.99 (m, 1 H) 2.00 – 2.05 (m, 1 H) 2.07 (s, 3 H) 2.16 – 2.28 (m, 4 H) 2.70 (t, *J* = 11.0 Hz, 1 H) 2.76 (d, *J* = 11.3 Hz, 1 H) 2.91 – 3.00 (m, 1 H) 4.34 – 4.43 (m, 1 H) 7.17 – 7.25 (m, 2 H) 7.57 (s, 2 H) 7.60 – 7.65 (m, 1 H) 7.78 – 7.83 (m, 1 H) 11.92 (br.s., 1 H)

3-Methyl-5-(1-((1-methylpiperidin-4-yl)methyl)-1*H*-benzo[*d*]imidazol-2-yl)pyridin-2(1*H*)-one, **4.75:**

5-Methyl-6-oxo-1,6-dihydropyridine-3-carbaldehyde **3.25** (50 mg, 0.365 mmol) and sodium hydrosulfite (190 mg, 1.094 mmol) were added to a solution of *N*-((1-methylpiperidin-4-yl)methyl)-2-nitroaniline **4.128** (91 mg, 0.365 mmol) in ethanol (1.5 ml) and water (0.75 ml), and the reaction mixture was heated under microwave conditions at 100 °C for 5 hours. The reaction mixture was partitioned between DCM (15 ml) and saturated aqueous sodium bicarbonate solution (15 ml). The aqueous layer was further extracted with DCM (3 x 15 ml) and the combined organic layers were dried through a hydrophobic frit and evaporated under reduced pressure. The sample was loaded in DCM and purified by SPE (silica, 10 g) using a gradient of 0 – 16% (2 M ammonia in MeOH) in DCM. The appropriate fractions were combined and evaporated under reduced pressure to give a colourless gum. The compound was loaded in DCM and again purified by SPE (silica, 10 g) using a gradient of 8 – 18% (2 M ammonia in MeOH) in DCM. The appropriate fractions were combined and evaporated under reduced pressure to give the required product 3-methyl-5-(1-((1-methylpiperidin-4-yl)methyl)-1*H*-benzo[*d*]imidazol-2-yl)pyridin-2(1*H*)-one **4.75** (39.5 mg, 0.117 mmol, 32 % yield) as a colourless gum.

LCMS (formic acid): *rt* = 0.37 min, MH^+ = 337

¹H NMR (*d*₆-DMSO): δ 1.08 – 1.18 (m, 2 H) 1.29 (d, *J* = 11.0 Hz, 2 H) 1.59 – 1.76 (m, 3 H) 2.08 (s, 3 H) 2.07 (s, 3 H) 2.65 (d, *J* = 11.3 Hz, 2 H) 4.21 (d, *J* = 7.1 Hz, 2 H) 7.15 – 7.31 (m, 2 H) 7.57 – 7.67 (m, 2 H) 7.70 – 7.77 (m, 2 H) 11.88 (br. s., 1 H)

3-Methyl-5-(1-((1-methylpiperidin-3-yl)methyl)-1*H*-benzo[*d*]imidazol-2-yl)pyridin-2(1*H*)-one, **4.78:**

Method as for **4.36**, using the following reagents: 5-methyl-6-oxo-1,6-dihydropyridine-3-carbaldehyde **3.25** (47 mg, 0.343 mmol), sodium hydrosulfite (179 mg, 1.028 mmol), *N*-((1-methylpiperidin-3-yl)methyl)-2-nitroaniline **4.129** (85 mg, 0.343 mmol), ethanol (1.5 ml) and

water (0.75 ml). MDAP (high pH) was used. The final product was: 3-methyl-5-(1-((1-methylpiperidin-3-yl)methyl)-1*H*-benzo[*d*]imidazol-2-yl)pyridin-2(1*H*)-one **4.78** (65.1 mg, 0.194 mmol, 57 % yield) as an off-white gum.

LCMS (formic acid): *rt* = 0.39 min, MH^+ = 337

¹H NMR (d₆-DMSO): δ 0.87 – 1.03 (m, 1 H) 1.23 – 1.42 (m, 2 H) 1.45 – 1.58 (m, 1 H) 1.63 – 1.73 (m, 1 H) 1.89 – 2.00 (m, 2 H) 2.01 (s, 3 H) 2.07 (s, 3 H) 2.21 – 2.29 (m, 1 H) 2.36 – 2.46 (m, 1 H) 4.18 – 4.32 (m, 2 H) 7.17 – 7.31 (m, 2 H) 7.58 – 7.65 (m, 2 H) 7.79 (d, *J* = 2.2 Hz, 1 H) 7.77 (d, *J* = 1.2 Hz, 1 H) 11.76 – 12.05 (br.s., 1 H)

3-Methyl-5-(1-(2-(methylamino)ethyl)-1*H*-benzo[*d*]imidazol-2-yl)pyridin-2(1*H*)-one hydrochloride, **4.81**:

tert-Butyl methyl(2-(2-(5-methyl-6-oxo-1,6-dihydropyridin-3-yl)-1*H*-benzo[*d*]imidazol-1-yl)ethyl)carbamate **4.132** (101 mg, 0.264 mmol) was dissolved in 1,4-dioxane (3 ml), and then 4 M hydrochloric acid in 1,4-dioxane (1 ml) was added to the reaction mixture which was stirred at room temperature overnight. Further 4 M hydrochloric acid in 1,4-dioxane (0.5 ml) was added to the reaction mixture, which was stirred at room temperature for 4 hours. Diethyl ether (2 x 10 ml) was added, and each time the supernatant removed. The supernatants were combined and the solvent was removed under reduced pressure to give 3-methyl-5-(1-(2-(methylamino)ethyl)-1*H*-benzo[*d*]imidazol-2-yl)pyridin-2(1*H*)-one hydrochloride **4.81** (38 mg, 0.119 mmol, 45% yield) as a pale yellow solid.

LCMS (formic acid): *rt* = 0.35 min, MH^+ = 283

¹H NMR (d₆-DMSO): δ 2.10 (s, 3 H) 3.26 – 3.36 (m, 2 H) 4.82 (t, *J* = 6.6 Hz, 2 H) 7.55 – 7.63 (m, 2 H) 7.74 – 7.77 (m, 1 H) 7.78 – 7.87 (m, 1 H) 8.00 – 8.08 (m, 1 H) 8.16 (d, *J* = 7.3 Hz, 1 H) 9.36 (br.s., 2 H) 12.27 – 12.54 (br.s., 1 H). One proton singlet (3 H) is likely to be hidden under the solvent peak at ~2.52 ppm.

3-Methyl-5-(1-(3-(methylamino)propyl)-1*H*-benzo[*d*]imidazol-2-yl)pyridin-2(1*H*)-one hydrochloride, **4.84**:

tert-Butyl methyl(3-(2-(5-methyl-6-oxo-1,6-dihydropyridin-3-yl)-1*H*-benzo[*d*]imidazol-1-yl)propyl)carbamate **4.134** (150 mg, 0.378 mmol) was dissolved in 1,4-dioxane (3 ml), then 4 M hydrochloric acid in 1,4-dioxane (1 ml) was added to the reaction mixture and left stirring for 72 hours at room temperature. Diethyl ether (2 x 10 ml) was added, and the supernatant removed each time and combined. The solvent was removed under reduced pressure to give 3-methyl-5-(1-(3-(methylamino)propyl)-1*H*-benzo[*d*]imidazol-2-yl)pyridin-2(1*H*)-one hydrochloride **4.84** (95 mg, 0.285 mmol, 75% yield) as a white powder.

LCMS (formic acid): *rt* = 0.35 min, MH^+ = 297

¹H NMR (d₆-DMSO): δ 2.06 – 2.19 (m, 5 H) 2.46 – 2.49 (m, 2 H) 2.88 – 2.97 (m, 2 H) 4.56 (t, *J* = 7.6 Hz, 2 H) 7.51 – 7.61 (m, 2 H) 7.75 (d, *J* = 1.2 Hz, 1 H) 7.78 – 7.85 (m, 1 H) 7.98 (br.s., 1 H) 8.03 – 8.12 (m, 1 H) 8.95 – 9.10 (br.s., 2 H) 12.17 – 12.54 (br.s., 1 H). One proton singlet (3 H) is likely to be hidden under the solvent peak at ~2.50 ppm.

5-(1-(3-(Dimethylamino)propyl)-1*H*-benzo[*d*]imidazol-2-yl)-3-methylpyridin-2(1*H*)-one, **4.87**:
N,*N*-Dimethyl-*N*3-(2-nitrophenyl)propane-1,3-diamine **4.136** (78 mg, 0.349 mmol), 5-methyl-6-oxo-1,6-dihydropyridine-3-carbaldehyde **3.25** (47.9 mg, 0.349 mmol) and sodium hydrosulfite (182 mg, 1.048 mmol) were dissolved in ethanol (1.5 ml) and water (0.75 ml), and heated under microwave conditions at 100 °C for 5 hours. Saturated aqueous sodium bicarbonate solution (15 ml) was added, followed by EtOAc (15 ml). The layers were separated and the aqueous phase further extracted using EtOAc (2 x 15 ml). The organic layers were combined, dried over magnesium sulfate, and the solvent removed. The residue was purified by SPE (SCX), which was washed with MeOH (25 ml) and then eluted with 2 M ammonia in MeOH (25 ml). The ammonia in MeOH fractions were evaporated, and the residue purified by MDAP (high pH). The appropriate fractions were combined and the solvent removed to give 5-(1-(3-(dimethylamino)propyl)-1*H*-benzo[*d*]imidazol-2-yl)-3-methylpyridin-2(1*H*)-one **4.87** (28 mg, 0.090 mmol, 26% yield) as a white solid.

LCMS (formic acid): rt = 0.36 min, MH⁺ = 311

¹H NMR (CDCl₃): δ 1.97 – 2.05 (m, 2 H) 2.25 (s, 6 H) 2.26 (s, 3 H) 2.33 (t, *J* = 6.6 Hz, 2 H) 4.34 (t, *J* = 7.3 Hz, 2 H) 7.28 – 7.34 (m, 2 H) 7.41 – 7.47 (m, 1 H) 7.77 – 7.82 (m, 1 H) 7.86 – 7.88 (m, 1 H) 7.92 (d, *J* = 2.3 Hz, 1 H)

N-Methyl-3-(2-(5-methyl-6-oxo-1,6-dihydropyridin-3-yl)-1*H*-benzo[*d*]imidazol-1-yl)propanamide, **4.90**:

N-Methyl-3-((2-nitrophenyl)amino)propanamide **4.137** (53 mg, 0.237 mmol), 5-methyl-6-oxo-1,6-dihydropyridine-3-carbaldehyde **3.25** (32.6 mg, 0.237 mmol), and sodium hydrosulfite (124 mg, 0.712 mmol) were dissolved in ethanol (1.5 ml), water (0.75 ml) and heated under microwave conditions at 100 °C for 5 hours. Saturated aqueous sodium bicarbonate solution (15 ml) was added, followed by EtOAc (15 ml). The layers were separated and the aqueous phase further extracted using EtOAc (2 x 15 ml). The organic layers were combined, dried over magnesium sulfate, and the solvent removed. The residue was purified by SPE (silica) using a gradient of 5 – 20% MeOH in DCM. The appropriate fractions were combined and the solvent removed to give *N*-methyl-3-(2-(5-methyl-6-oxo-1,6-dihydropyridin-3-yl)-1*H*-benzo[*d*]imidazol-1-yl)propanamide **4.90** (31 mg, 0.100 mmol, 42% yield) as a white solid.

LCMS (formic acid): rt = 0.41 min, MH⁺ = 311

¹H NMR (d₃-MeOD): δ 2.20 (s, 3 H) 2.57 (s, 3 H) 2.65 (t, *J* = 6.9 Hz, 2 H) 4.60 (t, *J* = 6.9 Hz, 2 H) 7.26 – 7.36 (m, 2 H) 7.59 (d, *J* = 7.3 Hz, 1 H) 7.63 – 7.66 (m, 1 H) 7.77 (s, 2 H)

N-(3-(2-(5-Methyl-6-oxo-1,6-dihydropyridin-3-yl)-1*H*-benzo[*d*]imidazol-1-yl)propyl)acetamide, **4.93**:

Method as for **4.90**, using the following reagents: *N*-(3-((2-nitrophenyl)amino)propyl)acetamide **4.138** (74 mg, 0.312 mmol), 5-methyl-6-oxo-1,6-dihydropyridine-3-carbaldehyde **3.25** (42.8 mg, 0.312 mmol), sodium hydrosulfite (163 mg, 0.936 mmol), ethanol (1.5 ml) and water (0.75 ml). The final product was: *N*-(3-(2-(5-methyl-6-oxo-1,6-dihydropyridin-3-yl)-1*H*-benzo[*d*]imidazol-1-yl)propyl)acetamide **4.93** (14 mg, 0.043 mmol, 14 % yield) as a white solid. LCMS (formic acid): *rt* = 0.42 min, *MH*⁺ = 325

¹H NMR (d₃-MeOD): δ 1.86 (s, 3 H) 1.94 – 2.03 (m, 2 H) 2.21 (s, 3 H) 3.11 (t, *J* = 6.9 Hz, 2 H) 4.34 (t, *J* = 7.6 Hz, 2 H) 7.26 – 7.39 (m, 2 H) 7.58 (d, *J* = 7.6 Hz, 1 H) 7.66 (d, *J* = 7.3 Hz, 1 H) 7.73 (d, *J* = 2.2 Hz, 1 H) 7.74 – 7.76 (m, 1 H)

3-Methyl-5-(1-((tetrahydrofuran-3-yl)methyl)-1*H*-benzo[*d*]imidazol-2-yl)pyridin-2(1*H*)-one, **4.96**:

2-Nitro-*N*-((tetrahydrofuran-3-yl)methyl)aniline **4.124** (70 mg, 0.315 mmol), 5-methyl-6-oxo-1,6-dihydropyridine-3-carbaldehyde **3.25** (43.2 mg, 0.315 mmol) and sodium hydrosulfite (165 mg, 0.945 mmol) were dissolved in ethanol (1.5 ml) and water (0.75 ml) and heated under microwave conditions at 100 °C for 5 hours. Saturated aqueous sodium bicarbonate solution (15 ml) was added, followed by EtOAc (15 ml). The layers were separated and the aqueous phase further extracted using EtOAc (2 x 15 ml). The organic layers were combined, dried over magnesium sulfate, and the solvent removed. The residue was purified by SPE (silica) using a gradient of 0 – 10% MeOH in DCM. The appropriate fractions were combined and the solvent removed to give 3-methyl-5-(1-((tetrahydrofuran-3-yl)methyl)-1*H*-benzo[*d*]imidazol-2-yl)pyridin-2(1*H*)-one **4.96** (58 mg, 0.187 mmol, 60% yield) as a colourless oil.

LCMS (formic acid): *rt* = 0.52 min, *MH*⁺ = 310

¹H NMR (CDCl₃): δ 1.52 – 1.61 (m, signal partially obscured under solvent peak) 1.90 – 2.02 (m, 1 H) 2.27 (s, 3 H) 2.77 – 2.91 (m, 1 H) 3.48 – 3.55 (m, 1 H) 3.56 – 3.62 (m, 1 H) 3.69 – 3.77 (m, 1 H) 3.86 – 3.94 (m, 1 H) 4.26 (d, *J* = 8.3 Hz, 2 H) 7.30 – 7.37 (m, 2 H) 7.41 – 7.47 (m, 1 H) 7.74 – 7.76 (m, 1 H) 7.76 – 7.78 (m, 1 H) 7.79 – 7.83 (m, 1 H) 12.00 – 12.23 (br.s., 1 H)

3-Methyl-5-(1-((tetrahydrofuran-2-yl)methyl)-1*H*-benzo[*d*]imidazol-2-yl)pyridin-2(1*H*)-one, **4.99**:

2-Nitro-*N*-((tetrahydrofuran-2-yl)methyl)aniline **4.141** (77 mg, 0.346 mmol), 5-methyl-6-oxo-

1,6-dihydropyridine-3-carbaldehyde **3.25** (47.5 mg, 0.346 mmol) and sodium hydrosulfite (181 mg, 1.039 mmol) were dissolved in ethanol (1.5 ml) and water (0.75 ml) and heated under microwave conditions at 100 °C for 5 hours. Saturated aqueous sodium bicarbonate solution (15 ml) was added, followed by EtOAc (15 ml). The layers were separated and the aqueous phase further extracted using EtOAc (2 x 15 ml). The organic layers were combined, dried over magnesium sulfate, and the solvent removed. The residue was then purified by SPE (silica) using a gradient of 5 – 10% MeOH in DCM. The appropriate fractions were combined and the solvent removed to give 3-methyl-5-(1-((tetrahydrofuran-2-yl)methyl)-1*H*-benzo[*d*]imidazol-2-yl)pyridin-2(1*H*)-one **4.99** (44 mg, 0.142 mmol, 41% yield) as a colourless oil.

LCMS (formic acid): *rt* = 0.57 min, MH^+ = 310

¹H NMR (CDCl₃): δ 1.57 – 1.68 (m, 1 H) 1.89 – 1.99 (m, 2 H) 2.06 – 2.16 (m, 1 H) 2.25 (s, 3 H) 3.73 – 3.81 (m, 1 H) 3.85 – 3.92 (m, 1 H) 4.27 – 4.30 (m, 2 H) 4.34 – 4.43 (m, 1 H) 7.29 – 7.34 (m, 2 H) 7.41 – 7.46 (m, 1 H) 7.77 – 7.82 (m, 1 H) 7.87 – 7.90 (m, 1 H) 7.99 (d, *J* = 2.0 Hz, 1 H) 11.26 – 11.52 (br.s., 1 H)

3-Methyl-5-(1-((tetrahydro-2*H*-pyran-3-yl)methyl)-1*H*-benzo[*d*]imidazol-2-yl)pyridin-2(1*H*)-one, **4.102**:

To a mixture of 5-methyl-6-oxo-1,6-dihydropyridine-3-carbaldehyde **3.25** (31.9 mg, 0.233 mmol) and sodium hydrosulfite (122 mg, 0.698 mmol) was added a solution of 2-nitro-*N*-((tetrahydro-2*H*-pyran-3-yl)methyl)aniline **4.143** (55 mg, 0.233 mmol) in ethanol (0.8 ml), followed by water (0.4 ml). The reaction mixture was heated under microwave conditions at 100 °C for 5 hours. The reaction mixture was partitioned between saturated aqueous sodium bicarbonate solution (10 ml) and DCM (2 x 10 ml). The organic layers were combined, dried using a hydrophobic frit, and blown down under a stream of nitrogen. The residue was dissolved in DMSO (1 ml) and purified by MDAP (formic acid). The solvent was blown down under a stream of nitrogen to give crude material (45 mg). The sample was dissolved in DMSO (1 ml) and purified by MDAP (high pH). The solvent was blown down under a stream of nitrogen to give the required product 3-methyl-5-(1-((tetrahydro-2*H*-pyran-3-yl)methyl)-1*H*-benzo[*d*]imidazol-2-yl)pyridin-2(1*H*)-one **4.102** (22 mg, 0.068 mmol, 29% yield) as a colourless glass.

LCMS (high pH): *rt* = 0.77 min, MH^+ = 324

¹H NMR (d₆-DMSO): δ 1.11 – 1.20 (m, 1 H) 1.22 – 1.39 (m, 1 H) 1.40 – 1.58 (m, 2 H) 1.91 – 2.01 (m, 1 H) 2.07 (s, 3 H) 3.09 (dd, *J* = 11.1, 8.3 Hz, 1 H) 3.25 – 3.37 (m, partially obscured by water peak) 3.44 (dd, *J* = 11.2, 3.4 Hz, 1 H) 3.56 – 3.63 (m, 1 H) 4.17 – 4.29 (m, 2 H) 7.12 – 7.35 (m, 2 H) 7.55 – 7.70 (m, 2 H) 7.75 (s, 2 H) 11.74 (br. s., 1 H).

3-Methyl-5-(1-((tetrahydro-2H-pyran-2-yl)methyl)-1H-benzo[d]imidazol-2-yl)pyridin-2(1H)-one, 4.105:

To a mixture of 5-methyl-6-oxo-1,6-dihydropyridine-3-carbaldehyde **3.25** (36.6 mg, 0.267 mmol) and sodium hydrosulfite (139 mg, 0.800 mmol) was added a solution of 2-nitro-*N*-((tetrahydro-2H-pyran-2-yl)methyl)aniline **4.144** (63 mg, 0.267 mmol) in ethanol (0.8 ml), followed by water (0.4 ml). The reaction mixture was heated under microwave conditions at 100 °C for 5 hours. The reaction mixture was partitioned between saturated aqueous sodium bicarbonate solution (10 ml) and DCM (2 x 10 ml). The organic layers were combined, dried using a hydrophobic frit and blown down under a stream of nitrogen. The residue was dissolved in DMSO (2 x 1 ml) and purified by MDAP (high pH). The solvent was blown down under a stream of nitrogen to give the required product 3-methyl-5-(1-((tetrahydro-2H-pyran-2-yl)methyl)-1H-benzo[d]imidazol-2-yl)pyridin-2(1H)-one **4.105** (45 mg, 0.139 mmol, 52% yield) as an off-white solid.

LCMS (high pH): $rt = 0.67$ min, $MH^+ = 324$

1H NMR (d_6 -DMSO): δ 1.19 – 1.30 (m, 1 H) 1.39 – 1.53 (m, 3 H) 1.70 (d, $J = 12.1$ Hz, 1 H) 1.76 – 1.86 (m, 1 H) 2.06 (s, 3 H) 3.14 – 3.26 (m, 1 H) 3.71 – 3.84 (m, 2 H) 4.17 – 4.30 (m, 2 H) 7.18 – 7.27 (m, 2 H) 7.59 – 7.62 (m, 2 H) 7.79 – 7.84 (m, 1 H) 7.93 (d, $J = 2.3$ Hz, 1 H) 11.85 (br. s., 1 H).

3-Methyl-5-(1-(tetrahydro-2H-pyran-4-yl)-1H-benzo[d]imidazol-2-yl)pyridin-2(1H)-one, 4.108:

Method as for **4.36**, using the following reagents: *N*-(2-nitrophenyl)tetrahydro-2H-pyran-4-amine **4.145** (81 mg, 0.365 mmol), 5-methyl-6-oxo-1,6-dihydropyridine-3-carbaldehyde **3.25** (50 mg, 0.365 mmol), sodium hydrosulfite (190 mg, 1.094 mmol), ethanol (1.5 ml) and water (0.75 ml). The final product was: 3-methyl-5-(1-(tetrahydro-2H-pyran-4-yl)-1H-benzo[d]imidazol-2-yl)pyridin-2(1H)-one **4.108** (73.4 mg, 0.237 mmol, 65% yield) as a white solid.

LCMS (formic acid): $rt = 0.53$ min, $MH^+ = 310$

1H NMR (d_6 -DMSO): δ 1.88 (dd, $J = 12.4, 2.8$ Hz, 2 H) 2.07 (s, 3 H) 2.42 – 2.53 (m, partially obscured by solvent peak) 3.45 (t, $J = 11.1$ Hz, 2 H) 4.00 (dd, $J = 11.5, 4.2$ Hz, 2 H) 4.49 – 4.58 (m, 1 H) 7.18 – 7.27 (m, 2 H) 7.59 (s, 2 H) 7.61 – 7.67 (m, 1 H) 7.70 – 7.77 (m, 1 H)

5-(1-(2-Methoxyethyl)-1H-benzo[d]imidazol-2-yl)-3-methylpyridin-2(1H)-one, 4.111:

Method as for **4.36**, using the following reagents: 5-methyl-6-oxo-1,6-dihydropyridine-3-carbaldehyde **3.25** (84 mg, 0.612 mmol), sodium hydrosulfite (319 mg, 1.835 mmol), *N*-(2-methoxyethyl)-2-nitroaniline **4.146** (120 mg, 0.612 mmol), ethanol (1.5 ml), and water (0.75

ml). The final product was: 5-(1-(2-methoxyethyl)-1*H*-benzo[*d*]imidazol-2-yl)-3-methylpyridin-2(1*H*)-one **4.111** (83 mg, 0.293 mmol, 48% yield) as an off-white solid.

LCMS (formic acid): *rt* = 0.51 min, MH^+ = 284

¹H NMR (*d*₆-DMSO): δ 2.06 (s, 3 H) 3.18 (s, 3 H) 3.74 (t, *J* = 5.1 Hz, 2 H) 4.42 (t, *J* = 5.1 Hz, 2 H) 7.19 – 7.28 (m, 2 H) 7.59 – 7.64 (m, 2 H) 7.78 – 7.79 (m, 1 H) 7.87 (d, *J* = 2.2 Hz, 1 H) 11.89 (br.s., 1 H).

5-(1-(2-Hydroxyethyl)-1*H*-benzo[*d*]imidazol-2-yl)-3-methylpyridin-2(1*H*)-one, **4.114**:

2-((2-Nitrophenyl)amino)ethanol (64 mg, 0.351 mmol), 5-methyl-6-oxo-1,6-dihydropyridine-3-carbaldehyde **3.25** (48.2 mg, 0.351 mmol) and sodium hydrosulfite (183 mg, 1.054 mmol) were dissolved in ethanol (1.5 ml) and water (0.75 ml) and heated under microwave conditions at 100 °C for 5 hours. Saturated aqueous sodium bicarbonate solution was added, followed by EtOAc (15 ml). The layers were separated and the aqueous phase further extracted using EtOAc (2 x 15 ml). The organic layers were combined, dried over magnesium sulfate, and the solvent removed. The residue was then purified by SPE (silica) using 0 – 10% MeOH in DCM. The appropriate fractions were combined and the solvent removed to give 5-(1-(2-hydroxyethyl)-1*H*-benzo[*d*]imidazol-2-yl)-3-methylpyridin-2(1*H*)-one **4.114** (31 mg, 0.115 mmol, 33% yield) as a white solid.

LCMS (formic acid): *rt* = 0.41 min, MH^+ = 270

¹H NMR (CDCl₃): δ 2.27 (s, 3 H) 4.16 – 4.28 (m, 2 H) 4.28 – 4.40 (m, 2 H) 6.80 – 6.88 (m, 1 H) 6.96 – 7.06 (m, 2 H) 7.06 – 7.12 (m, 1 H) 7.82 – 7.90 (m, 1 H) 8.19 – 8.26 (m, 1 H) 13.07 – 13.58 (m, 1 H)

5-(1-(1-Hydroxypropan-2-yl)-1*H*-benzo[*d*]imidazol-2-yl)-3-methylpyridin-2(1*H*)-one, **4.117**:

2-((2-Nitrophenyl)amino)propan-1-ol **4.150** (58 mg, 0.296 mmol), 5-methyl-6-oxo-1,6-dihydropyridine-3-carbaldehyde **3.25** (40.5 mg, 0.296 mmol) and sodium hydrosulfite (154 mg, 0.887 mmol) were dissolved in ethanol (1.5 ml) and water (0.75 ml) and heated under microwave conditions at 100 °C for 5 hours. Saturated aqueous sodium bicarbonate solution (15 ml) was added, followed by EtOAc (15 ml). The layers were separated and the aqueous phase extracted using EtOAc (2 x 15 ml). The organic layers were combined, dried over magnesium sulfate, and the solvent removed. The residue was purified by SPE (silica) using 0 – 10% MeOH in DCM. The appropriate fractions were combined and the solvent removed to give 5-(1-(1-hydroxypropan-2-yl)-1*H*-benzo[*d*]imidazol-2-yl)-3-methylpyridin-2(1*H*)-one **4.117** (43 mg, 0.152 mmol, 51% yield) as a colourless oil.

LCMS (formic acid): *rt* = 0.46 min, MH^+ = 284

^1H NMR ($\text{d}_3\text{-MeOD}$): δ 1.59 (d, $J = 7.1$ Hz, 3 H) 2.19 (s, 3 H) 3.83 – 3.90 (m, 1 H) 4.22 – 4.33 (m, 1 H) 4.64 – 4.77 (m, 1 H) 7.26 – 7.32 (m, 2 H) 7.64 – 7.70 (m, 1 H) 7.70 – 7.76 (m, 1 H) 7.80 – 7.84 (m, 2 H)

N-Methyl-2-nitroaniline, **4.120**:

2 M Methanamine in THF (1.595 ml, 3.19 mmol) and DIPEA (0.557 ml, 3.19 mmol) were added to a solution of 1-fluoro-2-nitrobenzene **3.26** (0.112 ml, 1.063 mmol) in THF (2 ml). The reaction mixture was heated under microwave conditions at 120 °C for 30 min. The reaction mixture was partitioned between DCM and saturated aqueous sodium bicarbonate solution. The combined organic layers were dried and evaporated under reduced pressure. The sample was loaded in cyclohexane/EtOAc and purified by SPE (silica, 10 g) using a gradient of 0 – 7% EtOAc in cyclohexane. The appropriate fractions were combined and evaporated under reduced pressure to give the required product *N*-methyl-2-nitroaniline **4.120** (155.8 mg, 1.024 mmol, 96% yield) as an orange solid.

LCMS (formic acid): $r_t = 0.91$ min, $\text{MH}^+ = 153$

^1H NMR ($\text{d}_6\text{-DMSO}$): δ 2.96 (d, $J = 5.1$ Hz, 3 H) 6.66 – 6.70 (m, 1 H) 6.99 (d, $J = 8.8$ Hz, 1 H) 7.50 – 7.60 (m, 1 H) 8.06 (dd, $J = 8.6, 1.5$ Hz, 1 H) 8.15 (br.s., 1 H)

N-Ethyl-2-nitroaniline, **4.121**:

Method as for **4.120**, using the following reagents: 2 M ethanamine in THF (1.595 ml, 3.19 mmol), DIPEA (0.557 ml, 3.19 mmol), 1-fluoro-2-nitrobenzene **3.26** (0.112 ml, 1.063 mmol) and THF (2 ml). The final product was: *N*-ethyl-2-nitroaniline **4.121** (155.8 mg, 0.938 mmol, 88 % yield) as an orange oil.

LCMS (formic acid): $r_t = 1.04$ min, $\text{MH}^+ = 167$

^1H NMR ($\text{d}_6\text{-DMSO}$): δ 1.24 (t, $J = 7.1$ Hz, 3 H) 3.33 – 3.45 (m, 2 H) 6.66 – 6.70 (m, 1 H) 7.04 (d, $J = 8.6$ Hz, 1 H) 7.48 – 7.60 (m, 1 H) 8.06 (dd, $J = 8.6, 1.7$ Hz, 2 H)

N-Isopropyl-2-nitroaniline, **4.122**:

Method as for **4.120**, using the following reagents: 1-fluoro-2-nitrobenzene **3.26** (0.112 ml, 1.063 mmol), propan-2-amine (0.272 ml, 3.19 mmol), DIPEA (0.557 ml, 3.19 mmol) and THF (2 ml) and to this solution. The final product was: *N*-isopropyl-2-nitroaniline **4.122** (137.3 mg, 0.762 mmol, 72% yield) as an orange oil.

LCMS (formic acid): $r_t = 1.12$ min, $\text{MH}^+ = 181$

^1H NMR ($\text{d}_6\text{-DMSO}$): δ 1.27 (d, $J = 6.4$ Hz, 6 H) 3.85 – 4.02 (m, 1 H) 6.66 – 6.70 (m, 1 H) 7.09 (d, $J = 8.6$ Hz, 1 H) 7.52 – 7.56 (m, 1 H) 7.88 (d, $J = 7.3$ Hz, 1 H) 8.07 (dd, $J = 8.7, 1.6$ Hz, 1 H)

N-Isobutyl-2-nitroaniline, **4.123**:

1-Fluoro-2-nitrobenzene **3.26** (74.7 μ l, 0.709 mmol), 2-methylpropan-1-amine (211 μ l, 2.123 mmol) and DIPEA (371 μ l, 2.126 mmol) were dissolved in THF (2 ml) and heated under microwave conditions at 120 °C for 30 min. Saturated aqueous sodium bicarbonate solution was added, followed by DCM. The layers were separated and the aqueous phase extracted using DCM. The organic layers were combined, dried over magnesium sulfate, and the solvent removed. The yellow residue was then purified by SPE (silica) using a gradient of 10 – 40% EtOAc in cyclohexane. The appropriate fractions were combined and the solvent removed to give *N*-isobutyl-2-nitroaniline **4.123** (129 mg, 0.664 mmol, 94% yield) as a yellow oil.

LCMS (formic acid): rt = 1.23 min, MH⁺ = 195

¹H NMR (CDCl₃): δ 1.04 (d, J = 6.6 Hz, 6 H) 1.91 – 2.08 (m, 1 H) 3.07 – 3.17 (m, 2 H) 6.60 (t, J = 7.7 Hz, 1 H) 6.83 (d, J = 8.8 Hz, 1 H) 7.38 – 7.43 (m, 1 H) 8.13 – 8.15 (m, 2 H)

N-(Cyclopropylmethyl)-2-nitroaniline, **4.124**:

1-Fluoro-2-nitrobenzene **3.26** (75 μ l, 0.711 mmol), cyclopropylmethanamine (183 μ l, 2.134 mmol) and DIPEA (373 μ l, 2.134 mmol) were dissolved in THF (2 ml) and heated under microwave conditions at 120 °C for 30 min. Saturated aqueous sodium carbonate solution (15 ml) was added, followed by DCM (15 ml). The layers were separated and the aqueous phase extracted using DCM (2 x 15 ml). The organic layers were combined, dried over magnesium sulfate, and the solvent removed. The yellow residue was then purified by SPE (silica) using 10 – 40% EtOAc in cyclohexane. The appropriate fractions were combined and the solvent removed to give *N*-(cyclopropylmethyl)-2-nitroaniline **4.124** (136 mg, 0.708 mmol, 99% yield) as a yellow oil.

LCMS (formic acid): rt = 1.15 min, MH⁺ = 193

¹H NMR (CDCl₃): δ 0.27 – 0.36 (m, 2 H) 0.54 – 0.68 (m, 2 H) 1.10 – 1.21 (m, 1 H) 3.12 – 3.15 (m, 2 H) 6.54 – 6.67 (m, 1 H) 6.80 (d, J = 8.6 Hz, 1 H) 7.39 (t, J = 7.6 Hz, 1 H) 7.96 – 8.26 (m, 2 H)

tert-Butyl 3-((2-nitrophenyl)amino)azetidine-1-carboxylate, **4.125**:

Method as for **4.123**, using the following reagents: 1-fluoro-2-nitrobenzene **3.26** (0.187 ml, 1.772 mmol), *tert*-butyl 3-aminoazetidine-1-carboxylate (0.834 ml, 5.32 mmol), DIPEA (0.928 ml, 5.32 mmol) and THF (2 ml). The final product was: *tert*-butyl 3-((2-nitrophenyl)amino)azetidine-1-carboxylate **4.125** (269 mg, 0.917 mmol, 52% yield) as a yellow oil.

LCMS (formic acid): rt = 1.14 min, (M-*t*Bu)H⁺ = 238

^1H NMR (CDCl_3): δ 1.47 (s, 9 H) 3.85 – 3.94 (m, 2 H) 4.29 – 4.44 (m, 3 H) 6.50 – 6.58 (m, 1 H) 6.73 – 6.81 (m, 1 H) 7.44 – 7.50 (m, 1 H) 8.15 – 8.24 (m, 2 H)

tert-Butyl 3-(2-(5-methyl-6-oxo-1,6-dihydropyridin-3-yl)-1*H*-benzo[*d*]imidazol-1-yl)azetidine-1-carboxylate, **4.126**:

tert-Butyl 3-((2-nitrophenyl)amino)azetidine-1-carboxylate **4.125** (135 mg, 0.460 mmol), 5-methyl-6-oxo-1,6-dihydropyridine-3-carbaldehyde **3.25** (63.1 mg, 0.460 mmol) and sodium hydrosulfite (240 mg, 1.381 mmol) were dissolved in ethanol (3 ml) and water (1.5 ml), and heated under microwave conditions at 100 °C for 5 hours. Saturated aqueous sodium bicarbonate solution (30 ml) was added, followed by EtOAc (30 ml). The layers were separated and the aqueous phase extracted using EtOAc (2 x 30 ml). The organic layers were combined, dried over magnesium sulfate, and the solvent removed. The residue was then purified by SPE (silica) using 0 – 10% MeOH in DCM. The appropriate fractions were combined and the solvent removed to give *tert*-butyl 3-(2-(5-methyl-6-oxo-1,6-dihydropyridin-3-yl)-1*H*-benzo[*d*]imidazol-1-yl)azetidine-1-carboxylate **4.126** (84 mg, 0.221 mmol, 48% yield) as a colourless oil.

LCMS (formic acid): $rt = 0.80$ min, $MH^+ = 381$

^1H NMR (CDCl_3): δ 1.53 (s, 9 H) 2.26 (s, 3 H) 4.47 – 4.52 (m, 2 H) 4.62 – 4.66 (m, 2 H) 5.29 – 5.41 (m, 1 H) 7.36 – 7.38 (m, 2 H) 7.44 – 7.66 (m, 2 H) 7.75 – 7.92 (m, 2 H)

1-Methyl-*N*-(2-nitrophenyl)piperidin-3-amine, **4.127**:

1-Fluoro-2-nitrobenzene **3.26** (0.075 ml, 0.709 mmol) was added to a mixture of 1-methylpiperidin-3-amine dihydrochloride (398 mg, 2.126 mmol) and DIPEA (0.371 ml, 2.126 mmol) in THF (2 ml). The reaction mixture was heated under microwave conditions at 120 °C for a total of 5.5 hours, followed by 130 °C for 5 hours. THF (1 ml) was added to the reaction mixture and it was heated under microwave conditions at 130 °C for 10 hours. The reaction mixture was partitioned between DCM (15 ml) and saturated aqueous sodium bicarbonate solution (15 ml) and the layers were separated. The aqueous layer was further extracted with DCM (2 x 15 ml) and the combined organic layers were dried and evaporated under reduced pressure. The sample was loaded in DCM and purified by SPE (silica, 10 g) using a gradient of 0 – 7% MeOH in DCM. The appropriate fractions were combined and evaporated under reduced pressure to give the required product 1-methyl-*N*-(2-nitrophenyl)piperidin-3-amine **4.127** (54.3 mg, 0.231 mmol, 33% yield) as an orange oil.

LCMS (formic acid): $rt = 0.56$ min, $MH^+ = 236$

¹H NMR (d₆-DMSO): δ 1.44 – 1.56 (m, 1 H) 1.57 – 1.66 (m, 3 H) 2.07 – 2.19 (m, 1 H) 2.21 (s, 3 H) 2.43 – 2.49 (m, 3 H) 3.85 – 3.99 (m, 1 H) 6.67 (ddd, *J* = 8.5, 7.0, 1.1 Hz, 1 H) 7.09 (d, *J* = 8.6 Hz, 1 H) 7.50 – 7.55 (m, 1 H) 8.07 (dd, *J* = 8.6, 1.5 Hz, 1 H) 8.29 – 8.45 (m, 1 H)

N-((1-Methylpiperidin-4-yl)methyl)-2-nitroaniline, **4.128**:

(1-Methylpiperidin-4-yl)methanamine (273 mg, 2.126 mmol) and DIPEA (0.371 ml, 2.126 mmol) were added to a solution of 1-fluoro-2-nitrobenzene **3.26** (0.075 ml, 0.709 mmol) in THF (3 ml) and the reaction mixture was heated under microwave conditions to 120 °C for 30 min. The reaction mixture was partitioned between DCM (15 ml) and saturated aqueous sodium bicarbonate solution (15 ml) and the layers were separated. The aqueous layer was extracted with DCM (3 x 15 ml) and the combined organic layers were dried and evaporated under reduced pressure to give an orange solid. The sample was loaded in DCM and purified by SPE (silica, 10 g) using a gradient of 2 – 12% MeOH in DCM. The appropriate fractions were combined and evaporated under reduced pressure to give the required product *N*-((1-methylpiperidin-4-yl)methyl)-2-nitroaniline **4.128** (170.2 mg, 0.683 mmol, 96% yield) as an orange solid.

LCMS (formic acid): *rt* = 0.61 min, MH⁺ = 250

¹H NMR (d₆-DMSO): δ 1.20 – 1.31 (m, 2 H) 1.52 – 1.64 (m, 1 H) 1.68 (d, *J* = 13.2 Hz, 2 H) 1.78 – 1.90 (m, 2 H) 2.15 (s, 3 H) 2.78 (d, *J* = 11.5 Hz, 2 H) 3.26 (t, *J* = 6.2 Hz, 2 H) 6.67 (ddd, *J* = 8.5, 7.0, 1.1 Hz, 1 H) 7.07 (d, *J* = 8.6 Hz, 1 H) 7.49 – 7.56 (m, 1 H) 8.05 (dd, *J* = 8.6, 1.7 Hz, 1 H) 8.15 – 8.19 (m, 1 H)

N-((1-Methylpiperidin-3-yl)methyl)-2-nitroaniline, **4.129**:

(1-Methylpiperidin-3-yl)methanamine (273 mg, 2.126 mmol) and DIPEA (0.371 ml, 2.126 mmol) were added to a solution of 1-fluoro-2-nitrobenzene **3.26** (0.075 ml, 0.709 mmol) in THF (2 ml) and the reaction mixture was heated under microwave conditions at 120 °C for 30 min. The reaction mixture was partitioned between DCM and saturated aqueous sodium bicarbonate solution and the layers were separated. The aqueous layer was further extracted with DCM and the combined organic layers were dried and evaporated under reduced pressure. The sample was loaded in cyclohexane and purified by SPE (silica, 10 g) using a gradient of 0 – 7% MeOH in DCM. The appropriate fractions were combined and evaporated under reduced pressure to give the crude product *N*-((1-methylpiperidin-3-yl)methyl)-2-nitroaniline **4.129** (159.7 mg, 0.641 mmol, 90% yield) as an orange oil.

LCMS (formic acid): *rt* = 0.59 min, MH⁺ = 250

¹H NMR (d₃-MeOD): δ 1.02 – 1.16 (m, 1 H) 1.54 – 1.69 (m, 1 H) 1.71 – 1.80 (m, 1 H) 1.83 – 1.91 (m, 2 H) 1.97 – 2.07 (m, 2 H) 2.28 (s, 3 H) 2.77 – 2.87 (m, 1 H) 2.89 – 2.97 (m, 1 H) 3.26 – 3.29 (m, 2 H) 6.63 – 6.69 (m, 1 H) 7.01 (d, *J* = 8.8 Hz, 1 H) 7.46 – 7.51 (m, 1 H) 8.12 (dd, *J* = 8.6, 1.5 Hz, 1 H), 8.16 (br.s, 1 H)

N-((4-Methylmorpholin-2-yl)methyl)-2-nitroaniline, **4.130**:

Method as for **4.129**, using the following reagents: (4-methylmorpholin-2-yl)methanamine (277 mg, 2.126 mmol), DIPEA (0.371 ml, 2.126 mmol), 1-fluoro-2-nitrobenzene **3.26** (0.075 ml, 0.709 mmol) and THF (2 ml). The final product was: *N*-((4-methylmorpholin-2-yl)methyl)-2-nitroaniline **4.130** (169.1 mg, 0.673 mmol, 95% yield) as an orange oil.

LCMS (formic acid): *rt* = 0.57 min, *MH*⁺ = 252

¹H NMR (d₆-DMSO): δ 1.83 (dd, *J* = 11.0, 10.0 Hz, 1 H) 1.96 – 2.03 (m, 1 H) 2.18 (s, 3 H) 2.57 – 2.62 (m, 1 H) 2.74 (d, *J* = 11.3 Hz, 1 H) 3.33 – 3.40 (m, 1 H) 3.45 – 3.58 (m, 2 H) 3.67 – 3.76 (m, 1 H) 3.81 – 3.86 (m, 1 H) 6.70 (ddd, *J* = 8.5, 7.0, 1.1 Hz, 1 H) 7.08 (d, *J* = 8.1 Hz, 1 H) 7.51 – 7.57 (m, 1 H) 8.06 (dd, *J* = 8.6, 1.7 Hz, 1 H) 8.19 (t, *J* = 5.1 Hz, 1 H)

tert-Butyl methyl(2-((2-nitrophenyl)amino)ethyl)carbamate, **4.131**:

Method as for **4.123**, using the following reagents: 1-fluoro-2-nitrobenzene **3.26** (187 μl, 1.773 mmol), *tert*-butyl (2-aminoethyl)(methyl)carbamate (951 μl, 5.32 mmol), DIPEA (929 μl, 5.32 mmol) and THF (2 ml). The final product was: *tert*-butyl methyl(2-((2-nitrophenyl)amino)ethyl)carbamate **4.131** (491 mg, 1.663 mmol, 94% yield) as a yellow oil.

LCMS (formic acid): *rt* = 1.16 min, *MH*⁺ = 296

¹H NMR (CDCl₃): δ 1.48 (s, 9 H) 2.93 (s, 3 H) 3.43 – 3.53 (m, 2 H) 3.53 – 3.59 (m, 2 H) 6.61 – 6.72 (m, 1 H) 6.88 – 7.00 (m, 1 H) 7.41 – 7.50 (m, 1 H) 8.08 – 8.26 (m, 2 H)

tert-Butyl methyl(2-(2-(5-methyl-6-oxo-1,6-dihydropyridin-3-yl)-1*H*-benzo[*d*]imidazol-1-yl)ethyl)carbamate, **4.132**:

Method as for **4.39**, using the following reagents: *tert*-butyl methyl(2-((2-nitrophenyl)amino)ethyl)carbamate **4.131** (246 mg, 0.833 mmol), 5-methyl-6-oxo-1,6-dihydropyridine-3-carbaldehyde **3.25** (114 mg, 0.833 mmol), sodium hydrosulfite (435 mg, 2.499 mmol), ethanol (3 ml) and water (1.5 ml). The final product was: *tert*-butyl methyl(2-(2-(5-methyl-6-oxo-1,6-dihydropyridin-3-yl)-1*H*-benzo[*d*]imidazol-1-yl)ethyl)carbamate **4.132** (182 mg, 0.476 mmol, 57% yield) as a colourless oil.

LCMS (formic acid): *rt* = 0.70 min, *MH*⁺ = 383

^1H NMR (d_6 -DMSO, 393 K): δ 1.15 (s, 9 H) 2.08 (s, 3 H) 2.51 (s, 3 H) 3.48 (t, J = 6.1 Hz, 2 H) 4.38 (t, J = 6.1 Hz, 2 H) 7.17 – 7.25 (m, 2 H) 7.51 (d, J = 7.3 Hz, 1 H) 7.58 – 7.64 (m, 3 H) 11.26 – 11.55 (br.s, 1 H)

tert-Butyl methyl(3-((2-nitrophenyl)amino)propyl)carbamate, 4.133:

Method as for **4.123**, using the following reagents: 1-fluoro-2-nitrobenzene **3.26** (0.187 ml, 1.772 mmol), *tert*-butyl (3-aminopropyl)(methyl)carbamate (1001 mg, 5.32 mmol), DIPEA (0.928 ml, 5.32 mmol) and THF (2 ml). The final product was: *tert*-butyl methyl(3-((2-nitrophenyl)amino)propyl)carbamate **4.133** (504 mg, 1.629 mmol, 92% yield) as a yellow oil.

LCMS (formic acid): rt = 1.21 min, MH^+ = 310

^1H NMR (CDCl_3): δ 1.45 (s, 9 H) 1.95 (quin, J = 7.0 Hz, 2 H) 2.89 (s, 3 H) 3.31 – 3.43 (m, 4 H) 6.62 – 6.69 (m, 1 H) 6.84 (d, J = 8.8 Hz, 1 H) 7.41 – 7.47 (m, 1 H) 7.97 – 8.14 (m, 1 H) 8.18 (dd, J = 8.7, 1.3 Hz, 1 H)

tert-Butyl methyl(3-(2-(5-methyl-6-oxo-1,6-dihydropyridin-3-yl)-1*H*-benzo[*d*]imidazol-1-yl)propyl)carbamate, 4.134:

tert-Butyl methyl(3-((2-nitrophenyl)amino)propyl)carbamate **4.133** (252 mg, 0.815 mmol), 5-methyl-6-oxo-1,6-dihydropyridine-3-carbaldehyde **3.25** (112 mg, 0.815 mmol) and sodium hydrosulfite (425 mg, 2.444 mmol) were dissolved in ethanol (3 ml), water (1.5 ml) and heated under microwave conditions at 100 °C for 5 hours. Saturated aqueous sodium bicarbonate solution (30 ml) was added, followed by EtOAc (30 ml). The layers were separated and the aqueous phase further extracted using EtOAc (2 x 30 ml). The organic layers were combined, dried over magnesium sulfate and the solvent removed. The residue was purified by SPE (silica) using a gradient of 0 – 10% MeOH in DCM. The appropriate fractions were combined and the solvent removed to give *tert*-butyl methyl(3-(2-(5-methyl-6-oxo-1,6-dihydropyridin-3-yl)-1*H*-benzo[*d*]imidazol-1-yl)propyl)carbamate **4.134** (174 mg, 0.439 mmol, 54% yield) as a colourless oil.

LCMS (formic acid): rt = 0.75 min, MH^+ = 397

^1H NMR (CDCl_3): δ 1.43 (s, 9 H) 2.00 – 2.11 (m, 2 H) 2.27 (s, 3 H) 2.86 (s, 3 H) 3.30 (br. s., 2 H) 4.20 – 4.33 (m, 2 H) 7.29 – 7.42 (m, 3 H) 7.69 – 7.85 (m, 3 H) 12.47 – 12.94 (br.s, 1 H)

*N*1,*N*1-Dimethyl-*N*2-(2-nitrophenyl)ethane-1,2-diamine, 4.135:

*N*1,*N*1-Dimethylethane-1,2-diamine (233 μl , 2.134 mmol), 1-fluoro-2-nitrobenzene **3.26** (75 μl , 0.711 mmol) and DIPEA (373 μl , 2.134 mmol) were dissolved in THF (2 ml) and heated under microwave conditions at 120 °C for 30 min. Saturated aqueous sodium bicarbonate solution was added, followed by DCM. The layers were separated and the aqueous phase extracted using

DCM. The organic layers were combined, dried over magnesium sulfate, and the solvent removed. The yellow residue was then purified by SPE (silica) using a gradient of 0 – 10% MeOH in DCM. The appropriate fractions were combined and the solvent removed to give *N1,N1*-dimethyl-*N2*-(2-nitrophenyl)ethane-1,2-diamine **4.135** (149 mg, 0.712 mmol, 100% yield) as a yellow oil.

LCMS (formic acid): *rt* = 0.45 min, MH^+ = 210

1H NMR ($CDCl_3$): δ 2.29 (s, 6 H) 2.61 (t, J = 6.2 Hz, 2 H) 3.30 – 3.35 (m, 2 H) 6.57 – 6.63 (m, 1 H) 6.81 (d, J = 8.8 Hz, 1 H) 7.36 – 7.46 (m, 1 H) 8.13 (dd, J = 8.6, 1.5 Hz, 1 H) 8.23 – 8.37 (br.s., 1 H)

N1,N1-Dimethyl-*N3*-(2-nitrophenyl)propane-1,3-diamine, **4.136**:

Method as for **4.135**, using the following reagents: 1-fluoro-2-nitrobenzene **3.26** (75 μ l, 0.711 mmol), *N1,N1*-dimethylpropane-1,3-diamine (268 μ l, 2.134 mmol), DIPEA (373 μ l, 2.134 mmol) and THF (2 ml). The final product was: *N1,N1*-dimethyl-*N3*-(2-nitrophenyl)propane-1,3-diamine **4.136** (156 mg, 0.699 mmol, 98% yield) as a yellow oil.

LCMS (formic acid): *rt* = 0.53 min, MH^+ = 224

1H NMR ($CDCl_3$): δ 1.84 – 1.92 (m, 2 H) 2.27 (s, 6 H) 2.44 (t, J = 6.7 Hz, 2 H) 3.36 – 3.42 (m, 2 H) 6.59 – 6.65 (m, 1 H) 6.88 (d, J = 8.6 Hz, 1 H) 7.37 – 7.48 (m, 1 H) 8.17 (d, J = 8.6 Hz, 1 H) 8.35 – 8.52 (br.s., 1 H)

N-Methyl-3-((2-nitrophenyl)amino)propanamide, **4.137**:

1-Fluoro-2-nitrobenzene **3.26** (75 μ l, 0.711 mmol), 3-amino-*N*-methylpropanamide (515 μ l, 2.134 mmol) and DIPEA (373 μ l, 2.134 mmol) were dissolved in THF (2 ml) and heated under microwave conditions at 120 °C for 30 min. Saturated aqueous sodium bicarbonate solution (15 ml) was added, followed by EtOAc (15 ml). The layers were separated and the aqueous phase further extracted using EtOAc (2 x 15 ml). The organic layers were combined, dried over magnesium sulfate, and the solvent removed. The yellow residue was then purified by SPE (silica) using a gradient of 0 – 5% MeOH in DCM. The appropriate fractions were combined and the solvent removed to give *N*-methyl-3-((2-nitrophenyl)amino)propanamide **4.137** (106 mg, 0.475 mmol, 67 % yield) as a yellow oil.

LCMS (formic acid): *rt* = 0.69 min, MH^+ = 224

1H NMR ($CDCl_3$): δ 2.56 (t, J = 6.6 Hz, 2 H) 2.85 (d, J = 4.7 Hz, 3 H) 3.70 (q, J = 6.6 Hz, 1 H) 5.45 – 5.64 (br.s., 1 H) 6.62 – 6.73 (m, 1 H) 6.93 (d, J = 8.1 Hz, 1 H) 7.43 – 7.49 (m, 1 H) 8.12 – 8.21 (m, 2 H)

N-(3-((2-Nitrophenyl)amino)propyl)acetamide, **4.138**:

Method as for **4.137**, using the following reagents: 1-fluoro-2-nitrobenzene **3.26** (75 μ l, 0.711 mmol), *N*-(3-aminopropyl)acetamide (105 μ l, 2.134 mmol), DIPEA (373 μ l, 2.134 mmol) and THF (2 ml). The final product was: *N*-(3-((2-nitrophenyl)amino)propyl)acetamide **4.138** (148 mg, 0.624 mmol, 88% yield) as a yellow oil.

LCMS (formic acid): rt = 0.74 min, MH⁺ = 238

¹H NMR (CDCl₃): δ 1.92 – 1.99 (m, 2 H) 2.01 (s, 3 H) 3.35 – 3.46 (m, 4 H) 5.63 – 5.77 (br.s., 1 H) 6.63 – 6.69 (m, 1 H) 6.85 (d, *J* = 8.8 Hz, 1 H) 7.42 – 7.47 (m, 1 H) 8.05 – 8.13 (br.s., 1 H) 8.18 (dd, *J* = 8.6, 1.5 Hz, 1 H)

N-(2-((2-Nitrophenyl)amino)ethyl)acetamide, **4.139**:

Method as for **4.137**, using the following reagents: 1-fluoro-2-nitrobenzene **3.26** (75 μ l, 0.711 mmol), *N*-(2-aminoethyl)acetamide (204 μ l, 2.134 mmol), DIPEA (373 μ l, 2.134 mmol) and THF (2 ml). The final product was: *N*-(2-((2-nitrophenyl)amino)ethyl)acetamide **4.139** (68 mg, 0.305 mmol, 43% yield) as a yellow oil.

LCMS (high pH): rt = 0.72 min, MH⁺ = 224

¹H NMR (CDCl₃): δ 2.01 (s, 3 H) 3.47 – 3.601 (m, 4 H) 5.73 – 5.91 (m, 1 H) 6.63 – 6.72 (m, 1 H) 6.98 (d, *J* = 8.6 Hz, 1 H) 7.43 – 7.49 (m, 1 H) 8.10 – 8.20 (m, 2 H)

2-Nitro-*N*-((tetrahydrofuran-3-yl)methyl)aniline, **4.140**:

1-Fluoro-2-nitrobenzene **3.26** (0.075 ml, 0.709 mmol), (tetrahydrofuran-3-yl)methanamine (215 mg, 2.126 mmol) and DIPEA (0.371 ml, 2.126 mmol) were dissolved in tetrahydrofuran (2 ml) and heated under microwave conditions at 120 °C for 30 min. Saturated aqueous sodium bicarbonate solution (15 ml) was added, followed by EtOAc (15 ml). The layers were separated and the aqueous phase further extracted using EtOAc (2 x 15 ml). The organic layers were combined, dried over magnesium sulfate, and the solvent removed. The orange residue was then purified by SPE (silica) using a gradient of 5 – 40% EtOAc in cyclohexane. The appropriate fractions were combined and the solvent removed to give 2-nitro-*N*-((tetrahydrofuran-3-yl)methyl)aniline **4.140** (139 mg, 0.625 mmol, 88% yield) as an orange oil.

LCMS (formic acid): rt = 0.94 min, MH⁺ = 223

¹H NMR (CDCl₃): δ 1.70 – 1.79 (m, 1 H) 2.13 – 2.24 (m, 1 H) 2.63 – 2.73 (m, 1 H) 3.27 – 3.39 (m, 2 H) 3.67 (dd, *J* = 8.9, 5.0 Hz, 1 H) 3.77 – 3.85 (m, 1 H) 3.88 – 4.01 (m, 2 H) 6.68 (ddd, *J* = 8.4, 7.0, 1.2 Hz, 1 H) 6.87 (d, *J* = 8.8 Hz, 1 H) 7.42 – 7.50 (m, 1 H) 8.05 – 8.17 (br.s., 1 H) 8.20 (dd, *J* = 8.7, 1.6 Hz, 1 H)

2-Nitro-*N*-((tetrahydrofuran-2-yl)methyl)aniline, 4.141:

1-Fluoro-2-nitrobenzene **3.26** (0.075 ml, 0.709 mmol), (tetrahydrofuran-2-yl)methanamine (0.217 ml, 2.126 mmol) and DIPEA (0.371 ml, 2.126 mmol) were dissolved in THF (2 ml) and heated under microwave conditions at 120 °C for 30 min. Saturated aqueous sodium bicarbonate solution (15 ml) was added, followed by EtOAc (15 ml). The layers were separated and the aqueous phase further extracted using EtOAc (2 x 15 ml). The organic layers were combined, dried over magnesium sulfate, and the solvent removed. The orange residue was then purified by SPE (silica) using a gradient of 0 – 50% EtOAc in cyclohexane. The appropriate fractions were combined and the solvent removed to give 2-nitro-*N*-((tetrahydrofuran-2-yl)methyl)aniline **4.141** (154 mg, 0.693 mmol, 98% yield) as an orange oil.

LCMS (formic acid): rt = 1.02 min, MH⁺ = 223

¹H NMR (CDCl₃): δ 1.67 – 1.78 (m, 1 H) 1.91 – 2.03 (m, 2 H) 2.04 – 2.14 (m, 1 H) 3.33 – 3.41 (m, 1 H) 3.43 – 3.50 (m, 1 H) 3.78 – 3.87 (m, 1 H) 3.93 – 4.01 (m, 1 H) 4.17 – 4.25 (m, 1 H) 6.65 (ddd, *J* = 8.5, 7.2, 1.2 Hz, 1 H) 6.89 (d, *J* = 8.1 Hz, 1 H) 7.39 – 7.47 (m, 1 H) 8.18 (dd, *J* = 8.7, 1.6 Hz, 1 H) 8.23 (br.s., 1 H)

2-Nitro-*N*-((tetrahydro-2*H*-pyran-4-yl)methyl)aniline, 4.142:

To a solution of 1-fluoro-2-nitrobenzene **3.26** (0.075 ml, 0.709 mmol) in THF (1.5 ml) was added (tetrahydro-2*H*-pyran-4-yl)methanamine (245 mg, 2.126 mmol) and DIPEA (0.371 ml, 2.126 mmol). The reaction mixture was heated under microwave conditions to 120 °C for 20 min. The reaction mixture was partitioned between DCM (2 x 10 ml) and saturated aqueous sodium bicarbonate solution (10 ml). The organic layers were combined, dried using a hydrophobic frit and blown down under a stream of nitrogen. The sample was loaded in DCM and purified by SPE (silica, 10 g) using a gradient of 0 – 15% EtOAc in cyclohexane. The appropriate fractions were combined and blown down under a stream of nitrogen to give the required product 2-nitro-*N*-((tetrahydro-2*H*-pyran-4-yl)methyl)aniline **4.142** (154 mg, 0.652 mmol, 92% yield) as an orange oil.

LCMS (high pH): rt = 1.05 min, MH⁺ = 237

¹H NMR (d₆-DMSO): δ 1.20 – 1.34 (m, 2 H) 1.63 (dd, *J* = 12.9, 1.8 Hz, 2 H) 1.83 – 1.97 (m, 1 H) 3.23 – 3.30 (m, 4 H) 3.86 (dd, *J* = 11.2, 2.9 Hz, 2 H) 6.68 (ddd, *J* = 8.5, 7.0, 1.1 Hz, 1 H) 7.10 (d, *J* = 8.1 Hz, 1 H) 7.46 – 7.58 (m, 1 H) 8.06 (dd, *J* = 8.6, 1.5 Hz, 1 H) 8.18 (t, *J* = 5.4 Hz, 1 H)

2-Nitro-*N*-((tetrahydro-2*H*-pyran-3-yl)methyl)aniline, 4.143:

To a solution of 1-fluoro-2-nitrobenzene **3.26** (0.037 ml, 0.354 mmol) in THF (0.5 ml) was added (tetrahydro-2*H*-pyran-3-yl)methanamine (122 mg, 1.063 mmol) and DIPEA (0.186 ml,

1.063 mmol), and the reaction mixture heated under microwave conditions at 120 °C for 30 min. The reaction mixture was partitioned between DCM (3 x 10 ml) and saturated aqueous sodium bicarbonate solution (10 ml). The organic layers were combined, dried using a hydrophobic frit and blown down under a stream of nitrogen to give an orange solid. The sample was loaded in DCM and purified by SPE (silica, 10 g) using a gradient of 0 – 10 % (2 M ammonia in MeOH) in DCM. The appropriate fractions were combined and blown down a stream of nitrogen to give the required product 2-nitro-*N*-((tetrahydro-2*H*-pyran-3-yl)methyl)aniline **4.143** (69 mg, 0.292 mmol, 82% yield) as an orange solid.

LCMS (high pH): *rt* = 1.08 min, MH^+ = 237

¹H NMR (*d*₆-DMSO): δ 1.26 – 1.35 (m, 1 H) 1.42 – 1.53 (m, 1 H) 1.55 – 1.66 (m, 1 H) 1.77 – 1.99 (m, 2 H) 3.1. – 3.41 (m, partially obscured by solvent peak) 3.66 – 3.75 (m, 1 H) 3.75 – 3.86 (m, 1 H) 6.68 (dd, *J* = 8.3, 7.1 Hz, 1 H) 7.07 (d, *J* = 8.6 Hz, 1 H) 7.46 – 7.58 (m, 1 H) 8.06 (dd, *J* = 8.6, 1.5 Hz, 1 H) 8.10 – 8.16 (m, 1 H).

2-Nitro-*N*-((tetrahydro-2*H*-pyran-2-yl)methyl)aniline, **4.144**:

Method as for **4.143**, using the following reagents: 1-fluoro-2-nitrobenzene **3.26** (0.037 ml, 0.354 mmol), (tetrahydro-2*H*-pyran-2-yl)methanamine (122 mg, 1.063 mmol), DIPEA (0.186 ml, 1.063 mmol), and THF (0.5 ml). The final product was: 2-nitro-*N*-((tetrahydro-2*H*-pyran-2-yl)methyl)aniline **4.144** (67 mg, 0.284 mmol, 80% yield) as an orange gum.

LCMS (high pH): *rt* = 1.18 min, MH^+ = 237

¹H NMR (*d*₆-DMSO): δ 1.23 – 1.37 (m, 1 H) 1.42 – 1.56 (m, 3 H) 1.60 – 1.70 (m, 1 H) 1.78 – 1.84 (m, 1 H) 3.23 – 3.29 (m, 1 H) 3.35 – 3.50 (m, 2 H) 3.52 – 3.59 (m, 1 H) 3.85 – 4.00 (m, 1 H) 6.69 (ddd, *J* = 8.5, 7.1, 1.1 Hz, 1 H) 7.07 (dd, *J* = 7.8, 1.0 Hz, 1 H) 7.46 – 7.59 (m, 1 H) 8.06 (dd, *J* = 8.6, 1.5 Hz, 1 H) 8.20 (t, *J* = 4.7 Hz, 1 H).

N-(2-Nitrophenyl)tetrahydro-2*H*-pyran-4-amine, **4.145**:

1-Fluoro-2-nitrobenzene **3.26** (0.075 ml, 0.709 mmol) was added to THF (2 ml), and to this solution tetrahydro-2*H*-pyran-4-amine (0.310 ml, 2.126 mmol) and DIPEA (0.371 ml, 2.126 mmol) were added. The reaction mixture was heated under microwave conditions at 120 °C for a total of 45 min. DCM (10 ml) and saturated aqueous sodium bicarbonate solution (10 ml) were added and the layers were separated. The aqueous layer was further extracted with DCM (2 x 10 ml) and the organic layers were combined, dried and evaporated under reduced pressure. The sample was purified by SPE (silica, 10 g) using a gradient of 10 – 20% EtOAc in cyclohexane. The appropriate fractions were combined and evaporated under reduced pressure to give the required product *N*-(2-nitrophenyl)tetrahydro-2*H*-pyran-4-amine **4.145** (156.7 mg, 0.705 mmol, 99 % yield) as an orange solid.

LCMS (formic acid): rt = 0.96 min, MH⁺ = 223

¹H NMR (d₆-DMSO): δ 1.46 – 1.66 (m, 2 H) 1.90 – 2.03 (m, 2 H) 3.49 (td, *J* = 11.5, 2.2 Hz, 2 H) 3.83 – 3.92 (m, 3 H) 6.70 (ddd, *J* = 8.5, 7.2, 1.2 Hz, 1 H) 7.18 (d, *J* = 8.6 Hz, 1 H) 7.47 – 7.59 (m, 1 H) 7.92 (d, *J* = 7.3 Hz, 1 H) 8.08 (dd, *J* = 8.6, 1.5 Hz, 1 H)

N-(2-Methoxyethyl)-2-nitroaniline, 4.146:

Method as for **4.143**, using the following reagents: 1-fluoro-2-nitrobenzene **3.26** (0.075 ml, 0.709 mmol), 2-methoxyethanamine (0.185 ml, 2.126 mmol), DIPEA (0.371 ml, 2.126 mmol), and THF (1 ml). The final product was: *N*-(2-methoxyethyl)-2-nitroaniline **4.146** (126 mg, 0.642 mmol, 91% yield) as an orange gum.

LCMS (high pH): rt = 0.97 min, MH⁺ = 296

¹H NMR (d₆-DMSO): δ 3.31 (s, 3 H) 3.47 – 3.56 (m, 2 H) 3.55 – 3.65 (m, 2 H) 6.67 – 6.72 (m, 1 H) 7.09 (d, *J* = 8.8 Hz, 1 H) 7.52 – 7.57 (m, 1 H) 8.07 (dd, *J* = 8.6, 1.5 Hz, 1 H) 8.11 – 8.22 (m, 1 H).

N-(1-Methoxypropan-2-yl)-2-nitroaniline, 4.147:

1-Fluoro-2-nitrobenzene **3.26** (0.075 ml, 0.709 mmol) was added to THF (2 ml) and to this solution 1-methoxypropan-2-amine (0.224 ml, 2.126 mmol) and DIPEA (0.371 ml, 2.126 mmol) were added. The mixture was heated under microwave conditions at 120 °C for a total of 2 hours 10 min. DCM (10 ml) and saturated aqueous sodium bicarbonate solution (10 ml) were added and the layers were separated. The aqueous layer was further extracted with DCM (2 x 10 ml) and the organic layers were combined, dried, and evaporated under reduced pressure. The sample was purified by SPE (silica, 10 g) using a gradient of 0 – 10% EtOAc in cyclohexane. The appropriate fractions were combined and evaporated under reduced pressure to give the required product *N*-(1-methoxypropan-2-yl)-2-nitroaniline **4.147** (141.8 mg, 0.675 mmol, 95% yield) as an orange oil.

LCMS (formic acid): rt = 1.05 min, MH⁺ = 211

¹H NMR (d₆-DMSO): δ 1.23 (d, *J* = 6.6 Hz, 3 H) 3.32 (s, 3 H) 3.48 (d, *J* = 4.6 Hz, 2 H) 3.97 – 4.10 (m, 1 H) 6.66 – 6.72 (m, 1 H) 7.13 (d, *J* = 8.6 Hz, 1 H) 7.51 – 7.57 (m, 1 H) 8.05 – 8.12 (m, 2 H)

3-((2-Nitrophenyl)amino)propan-1-ol, 4.148:

1-Fluoro-2-nitrobenzene **3.26** (0.075 ml, 0.709 mmol), 3-aminopropan-1-ol (0.163 ml, 2.126 mmol) and DIPEA (0.371 ml, 2.126 mmol) were dissolved in THF (2 ml) and heated under microwave conditions at 120 °C for 30 min. Saturated aqueous sodium bicarbonate (15 ml) was added, followed by EtOAc (15 ml). The layers were separated and the aqueous phase further

extracted using EtOAc (2 x 15 ml). The organic layers were combined, dried over magnesium sulfate, and the solvent removed. The orange residue was then purified by SPE (silica) using a gradient of 15 – 60% EtOAc in cyclohexane. The appropriate fractions were combined and the solvent removed to give 3-((2-nitrophenyl)amino)propan-1-ol **4.148** (116 mg, 0.591 mmol, 83% yield) as an orange oil.

LCMS (formic acid): $rt = 0.77$ min, $MH^+ = 197$

1H NMR ($CDCl_3$): δ 1.99 (quin, $J = 6.4$ Hz, 2 H) 3.41 – 3.52 (m, 2 H) 3.79 – 3.90 (m, 2 H) 6.64 (ddd, $J = 8.5, 7.2, 1.2$ Hz, 1 H) 6.89 (d, $J = 8.6$ Hz, 1 H) 7.40 – 7.48 (m, 1 H) 8.16 – 8.23 (m, 2H)

2-((2-Nitrophenyl)amino)ethanol, **4.149**:

Method as for **4.148**, using the following reagents: 1-fluoro-2-nitrobenzene **3.26** (74.7 μ l, 0.709 mmol), 2-aminoethanol (127 μ l, 2.121 mmol), DIPEA (371 μ l, 2.126 mmol) and THF (2 ml). The final product was: 2-((2-nitrophenyl)amino)ethanol **4.149** (127 mg, 0.697 mmol, 98 % yield) as an orange solid.

LCMS (formic acid): $rt = 0.71$ min, $MH^+ = 183$

1H NMR ($CDCl_3$): δ 1.67 (t, $J = 5.3$ Hz, 1 H) 3.53 (q, $J = 5.5$ Hz, 2 H) 3.96 (q, $J = 5.3$ Hz, 2 H) 6.69 (ddd, $J = 8.6, 7.1, 1.2$ Hz, 1 H) 6.91 (d, $J = 8.6$ Hz, 1 H) 7.43 – 7.48 (m, 1 H) 8.18 – 8.27 (m, 2 H)

2-((2-Nitrophenyl)amino)propan-1-ol, **4.150**:

Method as for **4.148**, using the following reagents: 1-fluoro-2-nitrobenzene **3.26** (0.075 ml, 0.709 mmol), 2-aminopropan-1-ol (160 mg, 2.126 mmol), DIPEA (0.371 ml, 2.126 mmol) and THF (2 ml). The final product was: 2-((2-nitrophenyl)amino)propan-1-ol **4.150** (122 mg, 0.622 mmol, 88% yield) as an orange oil.

LCMS (formic acid): $rt = 0.81$ min, $MH^+ = 197$

1H NMR ($CDCl_3$): δ 1.34 (d, $J = 6.6$ Hz, 3 H) 1.70 (dd, $J = 6.1, 5.1$ Hz, 1 H) 3.66 – 3.82 (m, 2 H) 3.82 – 3.98 (m, 1 H) 6.65 (ddd, $J = 8.4, 7.0, 1.2$ Hz, 1 H) 6.95 (d, $J = 8.6$ Hz, 1 H) 7.37 – 7.47 (m, 1 H) 8.00 – 8.12 (m, 1 H) 8.19 (dd, $J = 8.7, 1.6$ Hz, 1 H)

Chapter 5

(S)-Cyclopentyl 2-(((2-(5-methyl-6-oxo-1,6-dihydropyridin-3-yl)-1-((tetrahydro-2H-pyran-4-yl)methyl)-1H-benzo[d]imidazol-5-yl)methyl)amino)propanoate, **5.01**:

2-(5-Methyl-6-oxo-1,6-dihydropyridin-3-yl)-1-((tetrahydro-2H-pyran-4-yl)methyl)-1H-benzo[d]imidazole-5-carbaldehyde **5.19** (200 mg, 0.569 mmol), and (S)-cyclopentyl 2-aminopropanoate 4-methylbenzenesulfonate **5.23** (375 mg, 1.138 mmol) were stirred together in DCM (10 ml) under nitrogen for 15 minutes. Sodium triacetoxyborohydride (241 mg, 1.138 mmol) was added and the reaction mixture was stirred under nitrogen overnight. The reaction mixture was partitioned between DCM and saturated aqueous sodium bicarbonate solution. The combined organic layers were dried using a hydrophobic frit, and evaporated under reduced pressure. The crude sample was dissolved in DMSO and purified by MDAP (high pH). The solvent was evaporated to give the required product (S)-cyclopentyl 2-(((2-(5-methyl-6-oxo-1,6-dihydropyridin-3-yl)-1-((tetrahydro-2H-pyran-4-yl)methyl)-1H-benzo[d]imidazol-5-yl)methyl)amino)propanoate **5.01** (175.8 mg, 0.357 mmol, 63% yield) as a white solid.

LCMS (high pH): rt = 0.94 min, MH⁺ = 493

¹H NMR (d₆-DMSO, 293 K): δ 1.08 – 1.29 (m, 7 H) 1.49 – 1.73 (m, 6 H) 1.75 – 1.89 (m, 2 H) 1.89 – 2.01 (m, 1 H) 2.07 (s, 3 H) 2.23 – 2.45 (m, 1 H) 3.06 – 3.15 (m, 2 H) 3.17 – 3.26 (m, 1 H) 3.64 – 3.77 (m, 3 H) 3.82 (d, J = 13.0 Hz, 1 H) 4.20 (d, J = 7.3 Hz, 2 H) 5.04 – 5.14 (m, 1 H) 7.20 (dd, J = 8.3, 1.5 Hz, 1 H) 7.50 (s, 1 H) 7.58 (d, J = 8.3 Hz, 1 H) 7.70 – 7.75 (m, 2 H) 11.68 – 12.22 (br.s., 1 H)

(S)-Cyclopentyl 2-(((2-(5-methyl-6-oxo-1,6-dihydropyridin-3-yl)-1-((tetrahydro-2H-pyran-4-yl)methyl)-1H-benzo[d]imidazol-5-yl)methyl)amino)butanoate, **5.02**:

Method as for **5.01**, using the following reagents: 2-(5-methyl-6-oxo-1,6-dihydropyridin-3-yl)-1-((tetrahydro-2H-pyran-4-yl)methyl)-1H-benzo[d]imidazole-5-carbaldehyde **5.19** (130 mg, 0.370 mmol), (S)-cyclopentyl 2-aminobutanoate 4-methylbenzenesulfonate **5.29** (254 mg, 0.740 mmol), sodium triacetoxyborohydride (157 mg, 0.740 mmol) and DCM (5 ml). The reaction time was 5 hours. The final product was: (S)-cyclopentyl 2-(((2-(5-methyl-6-oxo-1,6-dihydropyridin-3-yl)-1-((tetrahydro-2H-pyran-4-yl)methyl)-1H-benzo[d]imidazol-5-yl)methyl)amino)butanoate **5.02** (112.2 mg, 0.221 mmol, 60% yield) as a white solid.

LCMS (high pH): rt = 1.02 min, MH⁺ = 507

¹H NMR (d₆-DMSO, 293 K): δ 0.86 (t, *J* = 7.3 Hz, 3 H) 1.09 – 1.28 (m, 4 H) 1.50 – 1.71 (m, 8 H) 1.76 – 1.89 (m, 2 H) 1.90 – 2.00 (m, 1 H) 2.07 (s, 3 H) 3.05 (t, *J* = 6.6 Hz, 1 H) 3.07 – 3.16 (m, 2 H) 3.66 (d, *J* = 13.2 Hz, 1 H) 3.69 – 3.78 (m, 2 H) 3.83 (d, *J* = 13.2 Hz, 1 H) 4.20 (d, *J* = 7.3 Hz, 2 H) 5.07 – 5.14 (m, 1 H) 7.20 (dd, *J* = 8.3, 1.2 Hz, 1 H) 7.50 (s, 1 H) 7.58 (d, *J* = 8.3 Hz, 1 H) 7.67 – 7.79 (m, 2 H) 11.71 – 12.03 (br.s., 1 H)

(*S*)-Cyclopentyl 2-(((2-(5-methyl-6-oxo-1,6-dihydropyridin-3-yl)-1-((tetrahydro-2*H*-pyran-4-yl)methyl)-1*H*-benzo[*d*]imidazol-5-yl)methyl)amino)pentanoate, **5.03**:

2-(5-Methyl-6-oxo-1,6-dihydropyridin-3-yl)-1-((tetrahydro-2*H*-pyran-4-yl)methyl)-1*H*-benzo[*d*]imidazole-5-carbaldehyde **5.19** (120 mg, 0.341 mmol) and (*S*)-cyclopentyl 2-aminopentanoate hydrochloride **5.40** (151 mg, 0.683 mmol) were dissolved in DCM (5 ml) and triethylamine (0.119 ml, 0.854 mmol) was added. The mixture was stirred under nitrogen for 15 minutes before adding sodium triacetoxyborohydride (145 mg, 0.683 mmol). The reaction mixture was stirred under nitrogen for 18 hours. The reaction mixture was partitioned between DCM (15 ml) and saturated aqueous sodium bicarbonate solution (15 ml). The layers were separated and the aqueous layer was extracted with DCM (3 x 15 ml). The combined organic layers were dried using a hydrophobic frit. The solvent was removed under reduced pressure and the crude material was dissolved in DMSO (2 x 1 ml) and purified by MDAP (high pH). The solvent was evaporated under reduced pressure to give the required product (*S*)-cyclopentyl 2-(((2-(5-methyl-6-oxo-1,6-dihydropyridin-3-yl)-1-((tetrahydro-2*H*-pyran-4-yl)methyl)-1*H*-benzo[*d*]imidazol-5-yl)methyl)amino)pentanoate **5.03** (141.7 mg, 0.272 mmol, 80% yield) as a white solid.

LCMS (high pH): *rt* = 1.09 min, *MH*⁺ = 521

¹H NMR (d₆-DMSO, 293 K): δ 0.83 (t, *J* = 7.2 Hz, 3 H) 1.09 – 1.27 (m, 4 H) 1.32 – 1.39 (m, 2 H) 1.45 – 1.70 (m, 8 H) 1.75 – 1.89 (m, 2 H) 1.89 – 2.02 (m, 1 H) 2.07 (s, 3 H) 3.05 – 3.17 (m, 3 H) 3.64 (d, *J* = 13.2 Hz, 1 H) 3.72 (d, *J* = 11.0 Hz, 2 H) 3.83 (d, *J* = 13.2 Hz, 1 H) 4.20 (d, *J* = 7.3 Hz, 2 H) 5.07 – 5.12 (m, 1 H) 7.20 (d, *J* = 8.6 Hz, 1 H) 7.50 (s, 1 H) 7.58 (d, *J* = 8.3 Hz, 1 H) 7.71 – 7.74 (m, 2 H) 11.74 – 12.02 (br.s., 1 H)

(*S*)-Cyclopentyl 3-methyl-2-(((2-(5-methyl-6-oxo-1,6-dihydropyridin-3-yl)-1-((tetrahydro-2*H*-pyran-4-yl)methyl)-1*H*-benzo[*d*]imidazol-5-yl)methyl)amino)butanoate, **5.04**:

Method as for **5.01**, using the following reagents: 2-(5-methyl-6-oxo-1,6-dihydropyridin-3-yl)-1-((tetrahydro-2*H*-pyran-4-yl)methyl)-1*H*-benzo[*d*]imidazole-5-carbaldehyde **5.19** (200 mg, 0.569 mmol), (*S*)-cyclopentyl 2-amino-3-methylbutanoate 4-methylbenzenesulfonate **5.30** (407 mg, 1.138 mmol), sodium triacetoxyborohydride (241 mg, 1.138 mmol) and DCM (10 ml). The reaction time was 2 hours. The final product was: (*S*)-cyclopentyl 3-methyl-2-(((2-(5-methyl-6-

oxo-1,6-dihydropyridin-3-yl)-1-((tetrahydro-2*H*-pyran-4-yl)methyl)-1*H*-benzo[*d*]imidazol-5-yl)methyl)amino)butanoate **5.04** (196.1 mg, 0.377 mmol, 66% yield) as a white solid.

LCMS (high pH): rt = 1.11 min, MH⁺ = 521

¹H NMR (d₆-DMSO, 293 K): δ 0.86 (d, *J* = 6.6 Hz, 3 H) 0.90 (d, *J* = 6.6 Hz, 3 H) 1.08 – 1.29 (m, 4 H) 1.49 – 1.71 (m, 6 H) 1.76 – 1.87 (m, 3 H) 1.89 – 2.01 (m, 1 H) 2.07 (s, 3 H) 2.18 – 2.36 (m, 1 H) 2.81 – 2.90 (m, 1 H) 3.07 – 3.15 (m, 2 H) 3.62 (d, *J* = 13.2 Hz, 1 H) 3.67 – 3.77 (m, 2 H) 3.85 (d, *J* = 13.5 Hz, 1 H) 4.20 (d, *J* = 7.1 Hz, 2 H) 5.03 – 5.17 (m, 1 H) 7.19 (dd, *J* = 8.3, 1.2 Hz, 1 H) 7.50 (s, 1 H) 7.58 (d, *J* = 8.3 Hz, 1 H) 7.70 – 7.74 (m, 2 H) 11.72 – 12.02 (br.s., 1 H)

(*S*)-Cyclopentyl 3-hydroxy-2-(((2-(5-methyl-6-oxo-1,6-dihydropyridin-3-yl)-1-((tetrahydro-2*H*-pyran-4-yl)methyl)-1*H*-benzo[*d*]imidazol-5-yl)methyl)amino)propanoate, **5.05**:

Method as for **5.01**, using the following reagents: 2-(5-methyl-6-oxo-1,6-dihydropyridin-3-yl)-1-((tetrahydro-2*H*-pyran-4-yl)methyl)-1*H*-benzo[*d*]imidazole-5-carbaldehyde **5.19** (200 mg, 0.569 mmol), (*S*)-cyclopentyl 2-amino-3-hydroxypropanoate 4-methylbenzenesulfonate **5.24** (393 mg, 1.138 mmol), sodium triacetoxyborohydride (241 mg, 1.138 mmol) and DCM (10 ml). The reaction time was 2 hours. The final product was: (*S*)-cyclopentyl 3-hydroxy-2-(((2-(5-methyl-6-oxo-1,6-dihydropyridin-3-yl)-1-((tetrahydro-2*H*-pyran-4-yl)methyl)-1*H*-benzo[*d*]imidazol-5-yl)methyl)amino)propanoate **5.05** (233.7 mg, 0.459 mmol, 81% yield) as a white solid.

LCMS (high pH): rt = 0.81 min, MH⁺ = 509

¹H NMR (d₆-DMSO, 293 K): δ 1.09 – 1.27 (m, 4 H) 1.49 – 1.70 (m, 6 H) 1.74 – 1.89 (m, 2 H) 1.89 – 2.02 (m, 1 H) 2.07 (s, 3 H) 2.26 – 2.43 (m, 1 H) 3.05 – 3.16 (m, 3 H) 3.16 – 3.25 (m, 1 H) 3.54 – 3.59 (m, 2 H) 3.67 – 3.75 (m, 3 H) 3.86 (d, *J* = 13.0 Hz, 1 H) 4.20 (d, *J* = 7.1 Hz, 2 H) 4.76 (t, *J* = 5.4 Hz, 1 H) 5.06 – 5.15 (m, 1 H) 7.20 (dd, *J* = 8.3, 1.2 Hz, 1 H) 7.51 (s, 1 H) 7.59 (d, *J* = 8.6 Hz, 1 H) 7.71 – 7.74 (m, 2 H) 11.65 – 12.02 (br.s., 1 H)

(2*S*,3*R*)-Cyclopentyl 3-hydroxy-2-(((2-(5-methyl-6-oxo-1,6-dihydropyridin-3-yl)-1-((tetrahydro-2*H*-pyran-4-yl)methyl)-1*H*-benzo[*d*]imidazol-5-yl)methyl)amino)butanoate, **5.06**:

Method as for **5.01**, using the following reagents: 2-(5-methyl-6-oxo-1,6-dihydropyridin-3-yl)-1-((tetrahydro-2*H*-pyran-4-yl)methyl)-1*H*-benzo[*d*]imidazole-5-carbaldehyde **5.19** (200 mg, 0.569 mmol), (2*S*,3*R*)-cyclopentyl 2-amino-3-hydroxybutanoate 4-methylbenzenesulfonate **5.25** (409 mg, 1.138 mmol), sodium triacetoxyborohydride (241 mg, 1.138 mmol) and DCM (10 ml). The final product was: (2*S*,3*R*)-cyclopentyl 3-hydroxy-2-(((2-(5-methyl-6-oxo-1,6-dihydropyridin-3-yl)-1-((tetrahydro-2*H*-pyran-4-yl)methyl)-1*H*-benzo[*d*]imidazol-5-yl)methyl)amino)butanoate **5.06** (260.5 mg, 0.498 mmol, 88% yield) as an off-white solid.

LCMS (high pH): rt = 0.88 min, MH⁺ = 523

¹H NMR (d₆-DMSO, 293 K): δ 1.11 (d, *J* = 6.4 Hz, 3 H) 1.12 – 1.29 (m, 4 H) 1.48 – 1.70 (m, 6 H) 1.74 – 1.85 (m, 2 H) 1.89 – 2.02 (m, 1 H) 2.07 (s, 3 H) 2.22 – 2.37 (m, 1 H) 3.00 (br. s., 1 H) 3.05 – 3.18 (m, 2 H) 3.66 (d, *J* = 13.0 Hz, 1 H) 3.69 – 3.76 (m, 2 H) 3.80 (br. s., 1 H) 3.89 (d, *J* = 13.0 Hz, 1 H) 4.20 (d, *J* = 7.3 Hz, 2 H) 4.59 – 4.73 (m, 1 H) 5.07 – 5.12 (m, 1 H) 7.21 (dd, *J* = 8.3, 1.0 Hz, 1 H) 7.52 (s, 1 H) 7.59 (d, *J* = 8.3 Hz, 1 H) 7.71 – 7.74 (m, 2 H) 11.58 – 12.09 (br.s., 1 H)

¹³C NMR (d₆-DMSO, 300 K): δ 16.9, 20.6, 23.7, 23.8, 30.5, 32.7, 35.6, 49.9, 52.2, 66.6, 66.8, 68.0, 77.0, 109.1, 111.1, 118.5, 123.2, 129.3, 134.2, 134.5, 135.6, 138.3, 142.9, 151.1, 162.6, 173.4.

IR (neat): 2962 (amine NH), 1727 (ester), 1658 (pyridone) cm⁻¹

M.pt.: 82–83 °C

HRMS: (C₂₉H₃₉N₄O₅) MH⁺ requires 523.2920, found MH⁺ 523.2922

[α_D]^{21.1 °C} (c 0.25, MeOH): +20.0 °

(S)-Cyclopentyl 4-methoxy-2-(((2-(5-methyl-6-oxo-1,6-dihydropyridin-3-yl)-1-((tetrahydro-2H-pyran-4-yl)methyl)-1H-benzo[*d*]imidazol-5-yl)methyl)amino)butanoate, **5.07**:

Method as for **5.01**, using the following reagents: 2-(5-methyl-6-oxo-1,6-dihydropyridin-3-yl)-1-((tetrahydro-2H-pyran-4-yl)methyl)-1H-benzo[*d*]imidazole-5-carbaldehyde **5.19** (120 mg, 0.341 mmol), (S)-cyclopentyl 2-amino-4-methoxybutanoate 4-methylbenzenesulfonate **5.31** (255 mg, 0.683 mmol), sodium triacetoxyborohydride (145 mg, 0.683 mmol) and DCM (5 ml). The reaction time was 5 hours. The final product was (S)-cyclopentyl 4-methoxy-2-(((2-(5-methyl-6-oxo-1,6-dihydropyridin-3-yl)-1-((tetrahydro-2H-pyran-4-yl)methyl)-1H-benzo[*d*]imidazol-5-yl)methyl)amino)butanoate **5.07** (95.8 mg, 0.179 mmol, 52% yield) as a white solid.

LCMS (high pH): rt = 0.96 min, MH⁺ = 537

¹H NMR (d₆-DMSO, 293 K): δ 1.08 – 1.31 (m, 4 H) 1.50 – 1.88 (m, 10 H) 1.88 – 2.03 (m, 1 H) 2.07 (s, 3 H) 3.05 – 3.15 (m, 2 H) 3.15 – 3.22 (m, 4 H) 3.32 – 3.38 (m, 1 H) 3.39 – 3.46 (m, 1 H) 3.64 (d, *J* = 13.5 Hz, 1 H) 3.68 – 3.76 (m, 2 H) 3.84 (d, *J* = 13.2 Hz, 1 H) 4.20 (d, *J* = 7.3 Hz, 2 H) 5.07 – 5.12 (m, 1 H) 7.19 (dd, *J* = 8.3, 1.2 Hz, 1 H) 7.49 (s, 1 H) 7.58 (d, *J* = 8.3 Hz, 1 H) 7.70 – 7.74 (m, 2 H) 11.76 – 11.98 (br.s., 1 H)

(S)-Cyclopentyl 1-(((2-(5-methyl-6-oxo-1,6-dihydropyridin-3-yl)-1-((tetrahydro-2H-pyran-4-yl)methyl)-1H-benzo[*d*]imidazol-5-yl)methyl)pyrrolidine-2-carboxylate, **5.08**:

Method as for **5.01**, using the following reagents: 2-(5-methyl-6-oxo-1,6-dihydropyridin-3-yl)-1-((tetrahydro-2H-pyran-4-yl)methyl)-1H-benzo[*d*]imidazole-5-carbaldehyde **5.19** (150 mg,

0.427 mmol), (*S*)-cyclopentyl pyrrolidine-2-carboxylate 4-methylbenzenesulfonate **5.26** (303 mg, 0.854 mmol), sodium triacetoxyborohydride (181 mg, 0.854 mmol) and DCM (10 ml). The final product was: (*S*)-cyclopentyl 1-((2-(5-methyl-6-oxo-1,6-dihydropyridin-3-yl)-1-((tetrahydro-2*H*-pyran-4-yl)methyl)-1*H*-benzo[*d*]imidazol-5-yl)methyl)pyrrolidine-2-carboxylate **5.08** (103 mg, 0.199 mmol, 47% yield) as a colourless gum.

LCMS (high pH): *rt* = 0.96 min, MH^+ = 537

¹H NMR (*d*₆-DMSO, 293 K): δ 1.07 – 1.29 (m, 4 H) 1.47 – 1.67 (m, 6 H) 1.67 – 1.87 (m, 5 H) 1.89 – 2.14 (m, 5 H) 2.40 (d, *J* = 8.3 Hz, 1 H) 2.80 – 2.91 (m, 1 H) 3.11 (t, *J* = 11.0 Hz, 2 H) 3.19 – 3.25 (m, 1 H) 3.61 (d, *J* = 12.9 Hz, 1 H) 3.68 – 3.78 (m, 2 H) 3.95 (d, *J* = 12.6 Hz, 1 H) 4.20 (d, *J* = 7.1 Hz, 2 H) 4.99 – 5.09 (m, 1 H) 7.19 (dd, *J* = 8.1, 0.9 Hz, 1 H) 7.48 (s, 1 H) 7.57 (d, *J* = 8.3 Hz, 1 H) 7.70 – 7.74 (m, 2 H) 11.66 – 12.09 (br.s., 1 H)

Cyclopentyl 2-methyl-2-(((2-(5-methyl-6-oxo-1,6-dihydropyridin-3-yl)-1-((tetrahydro-2*H*-pyran-4-yl)methyl)-1*H*-benzo[*d*]imidazol-5-yl)methyl)amino)propanoate, **5.09**:

Method as for **5.01**, using the following reagents: 2-(5-methyl-6-oxo-1,6-dihydropyridin-3-yl)-1-((tetrahydro-2*H*-pyran-4-yl)methyl)-1*H*-benzo[*d*]imidazole-5-carbaldehyde **5.19** (200 mg, 0.569 mmol), cyclopentyl 2-amino-2-methylpropanoate 4-methylbenzenesulfonate **5.27** (391 mg, 1.138 mmol), sodium triacetoxyborohydride (241 mg, 1.138 mmol) and DCM (10 ml). The final product was: cyclopentyl 2-methyl-2-(((2-(5-methyl-6-oxo-1,6-dihydropyridin-3-yl)-1-((tetrahydro-2*H*-pyran-4-yl)methyl)-1*H*-benzo[*d*]imidazol-5-yl)methyl)amino)propanoate **5.09** (139.9 mg, 0.276 mmol, 49% yield) as a white solid.

LCMS (high pH): *rt* = 1.01 min, MH^+ = 507

¹H NMR (*d*₆-DMSO, 293 K): δ 1.08 – 1.21 (m, 4 H) 1.26 (s, 6 H) 1.54 – 1.74 (m, 6 H) 1.78 – 2.01 (m, 2 H) 2.07 (s, 3 H) 2.13 – 2.29 (m, 1 H) 3.04 – 3.16 (m, 2 H) 3.66 (s, 2 H) 3.68 – 3.77 (m, 2 H) 4.21 (d, *J* = 7.3 Hz, 2 H) 5.06 – 5.14 (m, 1 H) 7.21 (dd, *J* = 8.3, 1.2 Hz, 1 H) 7.51 (s, 1 H) 7.58 (d, *J* = 8.3 Hz, 1 H) 7.70 – 7.75 (m, 2 H) 11.67 – 12.06 (br.s., 1 H)

(*S*)-Cyclopentyl 3-(1*H*-imidazol-5-yl)-2-(((2-(5-methyl-6-oxo-1,6-dihydropyridin-3-yl)-1-((tetrahydro-2*H*-pyran-4-yl)methyl)-1*H*-benzo[*d*]imidazol-5-yl)methyl)amino)propanoate, **5.10**:

To a mixture of 2-(5-methyl-6-oxo-1,6-dihydropyridin-3-yl)-1-((tetrahydro-2*H*-pyran-4-yl)methyl)-1*H*-benzo[*d*]imidazole-5-carbaldehyde **5.19** (150 mg, 0.427 mmol) in DCM (10 ml) was added (*S*)-cyclopentyl 2-amino-3-(1*H*-imidazol-4-yl)propanoate dihydrochloride **5.28** (253 mg, 0.854 mmol) and the reaction mixture stirred at room temperature for 15 min. Sodium triacetoxyborohydride (181 mg, 0.854 mmol) was added and the reaction mixture stirred at room temperature overnight. Further sodium triacetoxyborohydride (181 mg, 0.854 mmol) was added and the reaction mixture stirred at room temperature for three hours. Again, further

sodium triacetoxyborohydride (181 mg, 0.854 mmol) was added and the reaction mixture stirred at room temperature for 2 nights. Saturated sodium bicarbonate solution (10 ml) was added and the organic layer separated. The aqueous layer was extracted with further DCM (10 ml), and the organic layers were combined, dried using a hydrophobic frit, and blown down under a stream of nitrogen. The sample was dissolved in dissolved in DMSO (2 x 1 ml) and purified by MDAP (high pH). The solvent was blown down under a stream of nitrogen to give the required product (*S*)-cyclopentyl 3-(1*H*-imidazol-5-yl)-2-(((2-(5-methyl-6-oxo-1,6-dihydropyridin-3-yl)-1-((tetrahydro-2*H*-pyran-4-yl)methyl)-1*H*-benzo[*d*]imidazol-5-yl)methyl)amino)propanoate **5.10** (57 mg, 0.102 mmol, 24% yield) as a colourless gum.

LCMS (high pH): rt = 0.79 min, MH⁺ = 559

¹H NMR (d₆-DMSO, 293 K): δ 1.10 – 1.28 (m, 4 H) 1.41 – 1.61 (m, 6 H) 1.67 – 1.79 (m, 2 H) 1.92 – 2.02 (m, 1 H) 2.07 (s, 3 H) 2.75 – 2.84 (m, 2 H) 3.11 (t, *J* = 10.7 Hz, 2 H) 3.41 (t, *J* = 6.8 Hz, 1 H) 3.64 – 3.77 (m, 3 H) 3.83 (d, *J* = 13.1 Hz, 1 H) 4.20 (d, *J* = 7.3 Hz, 2 H) 5.00 – 5.04 (m, 1 H) 6.61 – 6.80 (m, 1 H) 7.17 (d, *J* = 8.3 Hz, 1 H) 7.46 – 7.50 (m, 2 H) 7.57 (d, *J* = 8.3 Hz, 1 H) 7.70 – 7.74 (m, 2 H) 10.93 – 12.36 (br.s., 1 H)

(*S*)-Cyclopentyl 2-(((2-(5-methyl-6-oxo-1,6-dihydropyridin-3-yl)-1-((tetrahydro-2*H*-pyran-4-yl)methyl)-1*H*-benzo[*d*]imidazol-5-yl)methyl)amino)-2-(tetrahydro-2*H*-pyran-4-yl)acetate,

5.11:

Method as for **5.01**, using the following reagents: 2-(5-methyl-6-oxo-1,6-dihydropyridin-3-yl)-1-((tetrahydro-2*H*-pyran-4-yl)methyl)-1*H*-benzo[*d*]imidazole-5-carbaldehyde **5.19** (120 mg, 0.341 mmol), (*S*)-cyclopentyl 2-amino-2-(tetrahydro-2*H*-pyran-4-yl)acetate 4-methylbenzenesulfonate **5.32** (273 mg, 0.683 mmol), sodium triacetoxyborohydride (145 mg, 0.683 mmol) and DCM (5 ml) The reaction time was 5 hours. The final product was: (*S*)-cyclopentyl 2-(((2-(5-methyl-6-oxo-1,6-dihydropyridin-3-yl)-1-((tetrahydro-2*H*-pyran-4-yl)methyl)-1*H*-benzo[*d*]imidazol-5-yl)methyl)amino)-2-(tetrahydro-2*H*-pyran-4-yl)acetate **5.11** (122.3 mg, 0.217 mmol, 64% yield) as a white solid.

LCMS (high pH): rt = 0.98 min, MH⁺ = 563

¹H NMR (d₆-DMSO, 293 K): δ 1.09 – 1.38 (m, 7 H) 1.50 – 1.88 (m, 10 H) 1.88 – 2.01 (m, 1 H) 2.07 (s, 3 H) 2.91 (d, *J* = 6.9 Hz, 1 H) 3.07 – 3.16 (m, 2 H) 3.19 – 3.28 (m, 2 H) 3.62 (d, *J* = 13.5 Hz, 1 H) 3.68 – 3.77 (m, 2 H) 3.78 – 3.87 (m, 3 H) 4.20 (d, *J* = 7.3 Hz, 2 H) 5.05 – 5.14 (m, 1 H) 7.19 (dd, *J* = 8.3, 1.0 Hz, 1 H) 7.50 (s, 1 H) 7.58 (d, *J* = 8.3 Hz, 1 H) 7.70 – 7.74 (m, 2 H) 11.80 – 11.96 (br.s., 1 H)

Cyclopentyl 1-(((2-(5-methyl-6-oxo-1,6-dihydropyridin-3-yl)-1-((tetrahydro-2H-pyran-4-yl)methyl)-1H-benzo[d]imidazol-5-yl)methyl)amino)cyclobutanecarboxylate, 5.12:

Method as for **5.01**, using the following reagents: 2-(5-methyl-6-oxo-1,6-dihydropyridin-3-yl)-1-((tetrahydro-2H-pyran-4-yl)methyl)-1H-benzo[d]imidazole-5-carbaldehyde **5.19** (125 mg, 0.356 mmol), cyclopentyl 1-aminocyclobutanecarboxylate 4-methylbenzenesulfonate **5.33** (253 mg, 0.711 mmol), sodium triacetoxyborohydride (151 mg, 0.711 mmol) and DCM (5 ml). The final product was: cyclopentyl 1-(((2-(5-methyl-6-oxo-1,6-dihydropyridin-3-yl)-1-((tetrahydro-2H-pyran-4-yl)methyl)-1H-benzo[d]imidazol-5-yl)methyl)amino) cyclobutanecarboxylate **5.12** (81 mg, 0.156 mmol, 44% yield) as a off-white gum.

LCMS (high pH): rt = 1.04 min, MH⁺ = 519

¹H NMR (d₆-DMSO, 293 K): δ 1.06 – 1.30 (m, 4 H) 1.52 – 1.75 (m, 6 H) 1.75 – 1.89 (m, 3 H) 1.89 – 1.99 (m, 2 H) 1.99 – 2.12 (m, 5 H) 2.24 – 2.39 (m, 2 H) 3.03 – 3.17 (m, 2 H) 3.63 – 3.76 (m, 4 H) 4.21 (d, *J* = 7.3 Hz, 2 H) 5.04 – 5.18 (m, 1 H) 7.23 (dd, *J* = 8.3, 1.0 Hz, 1 H) 7.54 (s, 1 H) 7.59 (d, *J* = 8.3 Hz, 1 H) 7.70 – 7.76 (m, 2 H) 11.74 – 12.02 (br.s., 1 H)

(S)-Isopropyl 4-methyl-2-(((2-(5-methyl-6-oxo-1,6-dihydropyridin-3-yl)-1-((tetrahydro-2H-pyran-4-yl)methyl)-1H-benzo[d]imidazol-5-yl)methyl)amino)pentanoate, 5.13:

Method as for **5.01**, using the following reagents: 2-(5-methyl-6-oxo-1,6-dihydropyridin-3-yl)-1-((tetrahydro-2H-pyran-4-yl)methyl)-1H-benzo[d]imidazole-5-carbaldehyde **5.19** (75 mg, 0.213 mmol) (*S*)-isopropyl 2-amino-4-methylpentanoate 4-methylbenzenesulfonate **5.34** (147 mg, 0.427 mmol), sodium triacetoxyborohydride (90 mg, 0.427 mmol) and DCM (5 ml). The final product was: (*S*)-isopropyl 4-methyl-2-(((2-(5-methyl-6-oxo-1,6-dihydropyridin-3-yl)-1-((tetrahydro-2H-pyran-4-yl)methyl)-1H-benzo[d]imidazol-5-yl)methyl)amino)pentanoate **5.13** (60 mg, 0.118 mmol, 55% yield) as a colourless gum.

LCMS (high pH): rt = 1.07 min, MH⁺ = 509

¹H NMR (d₆-DMSO, 293 K): δ 0.77 (d, *J* = 6.6 Hz, 3 H) 0.85 (d, *J* = 6.6 Hz, 3 H) 1.07 – 1.28 (m, 11 H) 1.31 – 1.46 (m, 2 H) 1.66 – 1.80 (m, 1 H) 1.87 – 2.01 (m, 1 H) 2.07 (s, 3 H) 3.04 – 3.16 (m, 3 H) 3.63 (d, *J* = 13.1 Hz, 1 H) 3.72 (d, *J* = 10.9 Hz, 2 H) 3.84 (d, *J* = 13.1 Hz, 1 H) 4.20 (d, *J* = 7.3 Hz, 2 H) 4.87 – 5.01 (m, 1 H) 7.20 (d, *J* = 8.3 Hz, 1 H) 7.49 (s, 1 H) 7.58 (d, *J* = 8.3 Hz, 1 H) 7.71 – 7.74 (m, 2 H) 11.72 – 12.02 (br.s., 1 H)

(S)-Cyclobutyl 4-methyl-2-(((2-(5-methyl-6-oxo-1,6-dihydropyridin-3-yl)-1-((tetrahydro-2H-pyran-4-yl)methyl)-1H-benzo[d]imidazol-5-yl)methyl)amino)pentanoate, 5.14:

Method as for **5.01**, using the following reagents: 2-(5-methyl-6-oxo-1,6-dihydropyridin-3-yl)-1-((tetrahydro-2H-pyran-4-yl)methyl)-1H-benzo[d]imidazole-5-carbaldehyde **5.19** (75 mg, 0.213 mmol), (*S*)-cyclobutyl 2-amino-4-methylpentanoate 4-methylbenzenesulfonate **5.35** (153

mg, 0.427 mmol), sodium triacetoxyborohydride (90 mg, 0.427 mmol) and DCM (5 ml). The final product was: (*S*)-cyclobutyl 4-methyl-2-(((2-(5-methyl-6-oxo-1,6-dihydropyridin-3-yl)-1-((tetrahydro-2*H*-pyran-4-yl)methyl)-1*H*-benzo[*d*]imidazol-5-yl)methyl)amino)pentanoate **5.14** (31 mg, 0.060 mmol, 28% yield) as a white solid.

LCMS (high pH): *rt* = 1.08 min, MH^+ = 521

¹H NMR (d₆-DMSO, 293 K): δ 0.77 (d, *J* = 6.3 Hz, 3 H) 0.86 (d, *J* = 6.6 Hz, 3 H) 1.08 – 1.26 (m, 4 H) 1.33 – 1.47 (m, 2 H) 1.53 – 1.67 (m, 1 H) 1.68 – 1.81 (m, 2 H) 1.90 – 2.04 (m, 3 H) 2.07 (s, 3 H) 2.23 – 2.35 (m, 2 H) 3.03 – 3.20 (m, 3 H) 3.63 (d, *J* = 13.1 Hz, 1 H) 3.72 (d, *J* = 10.4 Hz, 2 H) 3.84 (d, *J* = 13.1 Hz, 1 H) 4.21 (d, *J* = 7.1 Hz, 2 H) 4.89 – 4.96 (m, 1 H) 7.20 (d, *J* = 8.3 Hz, 1 H) 7.50 (s, 1 H) 7.58 (d, *J* = 8.3 Hz, 1 H) 7.70 – 7.75 (dm, 2 H) 11.68 – 12.00 (br.s., 1 H)

(*S*)-Neopentyl 4-methyl-2-(((2-(5-methyl-6-oxo-1,6-dihydropyridin-3-yl)-1-((tetrahydro-2*H*-pyran-4-yl)methyl)-1*H*-benzo[*d*]imidazol-5-yl)methyl)amino)pentanoate, **5.15**:

Method as for **5.01**, using the following reagents: 2-(5-methyl-6-oxo-1,6-dihydropyridin-3-yl)-1-((tetrahydro-2*H*-pyran-4-yl)methyl)-1*H*-benzo[*d*]imidazole-5-carbaldehyde **5.19** (200 mg, 0.569 mmol), (*S*)-neopentyl 2-amino-4-methylpentanoate 4-methylbenzenesulfonate **5.36** (425 mg, 1.138 mmol), sodium triacetoxyborohydride (241 mg, 1.138 mmol) and DCM (10 ml). The final product was: (*S*)-neopentyl 4-methyl-2-(((2-(5-methyl-6-oxo-1,6-dihydropyridin-3-yl)-1-((tetrahydro-2*H*-pyran-4-yl)methyl)-1*H*-benzo[*d*]imidazol-5-yl)methyl)amino)pentanoate **5.15** (209.2 mg, 0.390 mmol, 69% yield) as a white solid.

LCMS (high pH): *rt* = 1.20 min, MH^+ = 537

¹H NMR (d₆-DMSO, 293 K): δ 0.78 (d, *J* = 6.6 Hz, 3 H) 0.86 (d, *J* = 6.6 Hz, 3 H) 0.92 (s, 9 H) 1.07 – 1.25 (m, 4 H) 1.36 – 1.52 (m, 2 H) 1.67 – 1.79 (m, 1 H) 1.87 – 1.99 (m, 1 H) 2.07 (s, 3 H) 2.24 – 2.45 (m, 1 H) 3.05 – 3.15 (m, 2 H) 3.17 – 3.25 (m, 1 H) 3.64 (d, *J* = 13.2 Hz, 1 H) 3.68 – 3.74 (m, 2 H) 3.76 (s, 2 H) 3.86 (d, *J* = 13.2 Hz, 1 H) 4.21 (d, *J* = 7.3 Hz, 2 H) 7.20 (d, *J* = 8.3, 1.2 Hz, 1 H) 7.50 (s, 1 H) 7.58 (d, *J* = 8.3 Hz, 1 H) 7.71 – 7.75 (m, 2 H)

(2*S*)-Tetrahydrofuran-3-yl 4-methyl-2-(((2-(5-methyl-6-oxo-1,6-dihydropyridin-3-yl)-1-((tetrahydro-2*H*-pyran-4-yl)methyl)-1*H*-benzo[*d*]imidazol-5-yl)methyl)amino)pentanoate, **5.16**:

Method as for **5.01**, using the following reagents: 2-(5-methyl-6-oxo-1,6-dihydropyridin-3-yl)-1-((tetrahydro-2*H*-pyran-4-yl)methyl)-1*H*-benzo[*d*]imidazole-5-carbaldehyde **5.19** (200 mg, 0.569 mmol), (2*S*)-tetrahydrofuran-3-yl 2-amino-4-methylpentanoate 4-methylbenzenesulfonate **5.37** (425 mg, 1.138 mmol), sodium triacetoxyborohydride (241 mg, 1.138 mmol) and DCM (10 ml). The final product was: (2*S*)-tetrahydrofuran-3-yl 4-methyl-2-(((2-(5-methyl-6-oxo-1,6-dihydropyridin-3-yl)-1-((tetrahydro-2*H*-pyran-4-yl)methyl)-1*H*-benzo[*d*]imidazol-5-

yl)methyl)amino)pentanoate **5.16** (243.1 mg, 0.453 mmol, 80% yield) as a white solid.

LCMS (high pH): $rt = 0.93$ min, $MH^+ = 537$

1H NMR (d_6 -DMSO, 293 K): δ 0.77 (d, $J = 6.6$ Hz, 3 H) 0.85 (d, $J = 6.9$ Hz, 3 H) 1.08 – 1.27 (m, 4 H) 1.31 – 1.49 (m, 2 H) 1.65 – 1.80 (m, 1 H) 1.80 – 1.99 (m, 2 H) 2.07 (s, 3 H) 2.09 – 2.20 (m, 1 H) 2.27 – 2.45 (m, 1 H) 3.05 – 3.20 (m, 3 H) 3.59 – 3.89 (m, 8 H) 4.20 (d, $J = 7.3$ Hz, 2 H) 5.21 – 5.26 (m, 1 H) 7.20 (dd, $J = 8.3, 1.2$ Hz, 1 H) 7.50 (s, 1 H) 7.58 (d, $J = 8.3$ Hz, 1 H) 7.70 – 7.76 (m, 2 H) 11.59 – 12.05 (br.s., 1 H)

^{13}C NMR (d_6 -DMSO, 300 K): δ 16.9, 22.5, 23.1, 24.9, 30.4, 32.8, 35.6, 42.3, 51.7, 58.6, 66.7, 66.8, 72.8, 75.1, 109.1, 111.1, 118.6, 123.2, 134.5, 135.6, 138.3, 142.8, 162.6, 175.5. (Two signals of insufficient strength to be visible)

IR (neat): 2954 (amine NH), 1730 (ester), 1657 (pyridone) cm^{-1}

M.pt.: 84–86 °C

HRMS: ($C_{30}H_{41}N_4O_5$) MH^+ requires 537.3077, found MH^+ 537.3038 – error 6.2 pmm, above desired value of 5 ppm, possible degradation of target compound during experiment.

$[\alpha_D]^{21.3^\circ C}$ (c 0.5, MeOH): -3.3 °

(2S)-1-Methoxypropan-2-yl 4-methyl-2-(((2-(5-methyl-6-oxo-1,6-dihydropyridin-3-yl)-1-((tetrahydro-2H-pyran-4-yl)methyl)-1H-benzo[d]imidazol-5-yl)methyl)amino)pentanoate, **5.17**:

A mixture of 2-(5-methyl-6-oxo-1,6-dihydropyridin-3-yl)-1-((tetrahydro-2H-pyran-4-yl)methyl)-1H-benzo[d]imidazole-5-carbaldehyde **5.19** (75 mg, 0.213 mmol) and (2S)-1-methoxypropan-2-yl 2-amino-4-methylpentanoate 4-methylbenzenesulfonate **5.38** (160 mg, 0.427 mmol) in DCM (5 ml) was stirred at room temperature for 10 min. Sodium triacetoxyborohydride (90 mg, 0.427 mmol) was added and the reaction mixture stirred at room temperature overnight. Further sodium triacetoxyborohydride (30 mg, 0.142 mmol) was added and the reaction mixture stirred at room temperature for 2 hours. Saturated sodium bicarbonate solution (10 ml) was added and the organic layer separated. The aqueous layer was extracted with DCM, and the organic layers were combined, dried using a hydrophobic frit and blown down under a stream of nitrogen. The sample was dissolved in DMSO (1 ml) and purified by MDAP (high pH). The solvent was blown down under a stream of nitrogen to give the required product (2S)-1-methoxypropan-2-yl 4-methyl-2-(((2-(5-methyl-6-oxo-1,6-dihydropyridin-3-yl)-1-((tetrahydro-2H-pyran-4-yl)methyl)-1H-benzo[d]imidazol-5-yl)methyl)amino)pentanoate **5.17** (46 mg, 0.085 mmol, 40% yield) as an off-white gum. The diastereomeric ratio could not be determined by NMR.

LCMS (high pH): $rt = 1.00$ min, $MH^+ = 539$

¹H NMR (d₆-DMSO, 293 K): δ 0.72 – 0.81 (m, 3 H) 0.85 (d, *J* = 6.6 Hz, 3 H) 1.08 – 1.28 (m, 6 H) 1.31 – 1.48 (m, 2 H) 1.68 – 1.80 (m, 1 H) 1.87 – 2.01 (m, 1 H) 2.07 (s, 3 H) 3.04 – 3.19 (m, 3 H) 3.26 (s, 3 H) 3.27 – 3.36 (m, 2 H) 3.36 – 3.46 (m, 2 H) 3.59 – 3.68 (m, 1 H) 3.72 (d, *J* = 10.1 Hz, 2 H) 3.85 (d, *J* = 13.1 Hz, 1 H) 4.20 (d, *J* = 7.3 Hz, 2 H) 4.97 – 5.10 (m, 1 H) 7.20 (d, *J* = 8.3 Hz, 1 H) 7.50 (s, 1 H) 7.58 (d, *J* = 8.3 Hz, 1 H) 7.71 – 7.75 (m, 2 H) 11.86 (br.s., 1 H)

(S)-Tetrahydro-2H-pyran-4-yl 4-methyl-2-(((2-(5-methyl-6-oxo-1,6-dihydropyridin-3-yl)-1-((tetrahydro-2H-pyran-4-yl)methyl)-1H-benzo[*d*]imidazol-5-yl)methyl)amino)pentanoate, **5.18**:

A mixture of 2-(5-methyl-6-oxo-1,6-dihydropyridin-3-yl)-1-((tetrahydro-2H-pyran-4-yl)methyl)-1H-benzo[*d*]imidazole-5-carbaldehyde **5.19** (75 mg, 0.213 mmol) and (S)-tetrahydro-2H-pyran-4-yl 2-amino-4-methylpentanoate 4-methylbenzenesulfonate **5.39** (165 mg, 0.427 mmol) in DCM (5 ml) was stirred at room temperature for 10 min. Sodium triacetoxyborohydride (90 mg, 0.427 mmol) was added and the reaction mixture stirred at room temperature overnight. Further sodium triacetoxyborohydride (30 mg, 0.142 mmol) was added and the reaction mixture stirred at room temperature for 2 hours. Saturated sodium bicarbonate solution (10 ml) was added and the organic layer separated. The aqueous layer was extracted with DCM, and the organic layers were combined, dried using a hydrophobic frit, and blown down under a stream of nitrogen. The sample was dissolved in DMSO (2 x 1 ml) and purified by MDAP (high pH). The solvent was blown down under a stream of nitrogen to give the required product (S)-tetrahydro-2H-pyran-4-yl 4-methyl-2-(((2-(5-methyl-6-oxo-1,6-dihydropyridin-3-yl)-1-((tetrahydro-2H-pyran-4-yl)methyl)-1H-benzo[*d*]imidazol-5-yl)methyl)amino)pentanoate **5.18** (61 mg, 0.111 mmol, 52% yield) as a yellow gum.

LCMS (high pH): rt = 0.96 min, MH⁺ = 551

¹H NMR (d₆-DMSO, 293 K): δ 0.78 (d, *J* = 6.6 Hz, 3 H) 0.86 (d, *J* = 6.6 Hz, 3 H) 1.07 – 1.27 (m, 4 H) 1.35 – 1.47 (m, 2 H) 1.49 – 1.60 (m, 2 H) 1.66 – 1.79 (m, 1 H) 1.80 – 1.88 (m, 2 H) 1.91 – 1.99 (m, 1 H) 2.07 (s, 3 H) 3.04 – 3.22 (m, 3 H) 3.43 – 3.50 (m, 2 H) 3.65 (d, *J* = 13.1 Hz, 1 H) 3.68 – 3.82 (m, 4 H) 3.85 (d, *J* = 13.1 Hz, 1 H) 4.21 (d, *J* = 7.3 Hz, 2 H) 4.87 – 4.94 (m, 1 H) 7.20 (dd, *J* = 8.3, 1.3 Hz, 1 H) 7.50 (s, 1 H) 7.58 (d, *J* = 8.3 Hz, 1 H) 7.71 – 7.75 (m, 2 H) 11.87 (br.s., 1 H)

2-(5-Methyl-6-oxo-1,6-dihydropyridin-3-yl)-1-((tetrahydro-2H-pyran-4-yl)methyl)-1H-benzo[*d*]imidazole-5-carbaldehyde, **5.19**:

2-Iodoxybenzoic acid (9.78 g, 15.72 mmol, 45% by weight: stabilised by benzoic acid and isophthalic acid) was added portion-wise to a suspension of 5-(5-(hydroxymethyl)-1-((tetrahydro-2H-pyran-4-yl)methyl)-1H-benzo[*d*]imidazol-2-yl)-3-methylpyridin-2(1H)-one **5.22** (5.05 g, 14.29 mmol) in DCM (500 ml). The reaction mixture was stirred under nitrogen

for 72 hours. The reaction mixture was split into three equal portions. Saturated aqueous sodium bicarbonate solution (200 ml) was added to each portion and the layers were separated. The aqueous layer in each case was further extracted with DCM (2 x 200 ml) and all the organic layers were combined and dried over a hydrophobic frit. The solvent was removed under reduced pressure to give a white solid. The solid compound was split into three equal portions. Each portion was redissolved in DCM (200 ml) and saturated aqueous sodium bicarbonate solution (200 ml) was added. The layers were separated and the aqueous layer was extracted with DCM (2 x 200 ml). All the organic layers were combined and solvent was evaporated under reduced pressure to give the required product 2-(5-methyl-6-oxo-1,6-dihydropyridin-3-yl)-1-((tetrahydro-2*H*-pyran-4-yl)methyl)-1*H*-benzo[*d*]imidazole-5-carbaldehyde **5.19** (4.57 g, 11.70 mmol, 82% yield) as a white solid.

LCMS (high pH): *rt* = 0.67 min, MH^+ = 352

1H NMR (d_6 -DMSO, 293 K): δ 1.09 – 1.31 (m, 4 H) 1.86 – 2.02 (m, 1 H) 2.08 (s, 3 H) 3.05 – 3.16 (m, 2 H) 3.72 (d, J = 11.0 Hz, 2 H) 4.31 (d, J = 7.1 Hz, 1 H) 7.75 – 7.85 (m, 3 H) 7.90 (d, J = 8.6 Hz, 1 H) 8.20 (s, 1 H) 10.06 (s, 1 H) 11.96 (br.s, 1 H)

^{13}C NMR (d_6 -DMSO, 300 K): δ 16.9, 30.3, 35.6, 50.1, 66.8, 108.4, 112.3, 122.7, 123.2, 129.5, 131.8, 134.8, 138.1, 141.0, 142.6, 153.5, 162.7, 193.0.

IR (neat): 2914 (aldehyde CH), 2713 (aldehyde CH), 1698 (aldehyde CO), 1653 (pyridone), 798 (aryl CH), 746 (aryl CH) cm^{-1}

M.pt.: 229–233 °C

HRMS: ($C_{20}H_{22}N_3O_3$) MH^+ requires 352.1661, found MH^+ 352.1667

(3-Nitro-4-(((tetrahydro-2*H*-pyran-4-yl)methyl)amino)phenyl)methanol, **5.21**:

A mixture of (4-fluoro-3-nitrophenyl)methanol **5.20** (3 g, 17.53 mmol), (tetrahydro-2*H*-pyran-4-yl)methanamine (3 g, 26.0 mmol) and DIPEA (9 ml, 51.5 mmol) in THF (30 ml) was heated in three equal portions under microwave conditions at 120 °C for 1.5 hours. The reaction mixtures were combined and partitioned between saturated aqueous sodium bicarbonate solution (100 ml) and DCM (3 x 100 ml). The organic layers were combined, dried using a hydrophobic frit, and evaporated under reduced pressure to give an orange oil. The sample was loaded in DCM and purified by SPE (silica, 2 x 100 g) using a gradient of 0 – 7% (2 M ammonia in MeOH) in DCM. The appropriate fractions were combined and evaporated under reduced pressure to give the required product (3-nitro-4-(((tetrahydro-2*H*-pyran-4-yl)methyl)amino)phenyl)methanol **5.21** (4.66 g, 17.49 mmol, 100% yield) as an orange oil.

LCMS (formic acid): *rt* = 0.76 min, MH^+ = 267

¹H NMR (d₆-DMSO, 293 K): δ 1.17 – 1.35 (m, 2 H) 1.55 – 1.77 (m, 2 H) 1.83 – 1.95 (m, 1 H) 3.20 – 3.37 (m, 5 H) 3.86 (dd, *J* = 11.2, 3.2 Hz, 1 H) 4.40 (d, *J* = 5.8 Hz, 1 H) 5.18 (t, *J* = 5.8 Hz, 1 H) 7.09 (d, *J* = 9.1 Hz, 1 H) 7.46 – 7.50 (m, 1 H) 8.00 (s, 1 H) 8.18 (t, *J* = 5.7 Hz, 1 H)

5-(5-(Hydroxymethyl)-1-((tetrahydro-2*H*-pyran-4-yl)methyl)-1*H*-benzo[*d*]imidazol-2-yl)-3-methylpyridin-2(1*H*)-one, **5.22**:

(3-Nitro-4-(((tetrahydro-2*H*-pyran-4-yl)methyl)amino)phenyl)methanol **5.21** (10 g, 37.6 mmol) was dissolved in a solution of EtOH (100 ml) and water (50 ml), before adding 5-methyl-6-oxo-1,6-dihydropyridine-3-carbaldehyde **3.25** (5.15 g, 37.6 mmol) and sodium hydrosulfite (19.61 g, 113 mmol). The reaction mixture was heated at 100 °C for 3 hours. The reaction mixture was partitioned between saturated aqueous sodium bicarbonate solution (100 ml) and 25% propan-2-ol in DCM solution (100 ml). The layers were separated and the aqueous layer was further extracted with 25% propan-2-ol in DCM solution (2 x 100 ml). The organic layer from the first partition was washed with saturated aqueous sodium bicarbonate solution (100 ml). All organic layers were combined and the solvent was evaporated under reduced pressure. The sample was loaded in DCM/MeOH and purified by SPE (silica, 340g) using a gradient of 0 – 15% (2 M ammonia in MeOH) in DCM. The appropriate fractions were combined and evaporated under reduced pressure to give the required product 5-(5-(hydroxymethyl)-1-((tetrahydro-2*H*-pyran-4-yl)methyl)-1*H*-benzo[*d*]imidazol-2-yl)-3-methylpyridin-2(1*H*)-one **5.22** (5.06 g, 14.31 mmol, 38% yield) as a white solid.

LCMS (high pH): rt = 0.60 min, MH⁺ = 354

¹H NMR (d₆-DMSO, 293 K): δ 1.09 – 1.27 (m, 4 H) 1.86 – 2.02 (m, 1 H) 2.07 (s, 3 H) 3.04 – 3.15 (m, 2 H) 3.65 – 3.81 (m, 2 H) 4.21 (d, *J* = 7.1 Hz, 2 H) 4.58 (d, *J* = 5.6 Hz, 1 H) 5.12 (t, *J* = 5.8 Hz, 1 H) 7.22 (dd, *J* = 8.3, 1.2 Hz, 1 H) 7.54 (s, 1 H) 7.60 (d, *J* = 8.3 Hz, 1 H) 7.71 – 7.73 (m, 1 H) 7.74 (d, *J* = 1.2 Hz, 1 H) 11.88 (br. s., 1 H)

(*S*)-Cyclopentyl 2-aminobutanoate 4-methylbenzenesulfonate, **5.29**:

(*S*)-2-Aminobutanoic acid (3.0 g, 29.1 mmol), cyclopentanol (20.5 g, 238 mmol) and 4-methylbenzenesulfonic acid monohydrate (7.19 g, 37.8 mmol) were added to cyclohexane (100 ml) and the reaction mixture was heated to 125 °C, whereupon complete dissolution was achieved. It was then heated at this temperature for 24 hours. After cooling to room temperature, the volatile components were removed from the slurry under reduced pressure to give a white solid. The solid was recrystallised from the minimum amount of hot EtOAc. The resulting crystals were filtered and washed with a little cold EtOAc to give the required product (*S*)-cyclopentyl 2-aminobutanoate 4-methylbenzenesulfonate **5.29** (6.30 g, 18.35 mmol, 63% yield) as a white solid.

^1H NMR (d_6 -DMSO, 293 K): δ 0.92 (t, $J = 7.5$ Hz, 3 H) 1.52 – 1.73 (m, 6 H) 1.73 – 1.95 (m, 4 H) 2.29 (s, 3 H) 3.90 – 4.01 (m, 1 H) 5.18 – 5.22 (m, 1 H) 7.11 (d, $J = 7.8$ Hz, 2 H) 7.48 (d, $J = 8.1$ Hz, 1 H) 8.26 (br.s., 3 H)

(S)-Cyclopentyl 2-amino-3-methylbutanoate 4-methylbenzenesulfonate, 5.30:

(S)-2-Amino-3-methylbutanoic acid (800 mg, 6.83 mmol), cyclopentanol (5.07 ml, 55.9 mmol) and 4-methylbenzenesulfonic acid monohydrate (1.689 g, 8.88 mmol) were suspended in cyclohexane (15 ml) and the reaction mixture was heated to 95 °C with a Dean-Stark condenser attached. Complete dissolution was achieved, and the reaction mixture was heated at 95 °C overnight. No water had been collected in the Dean–Stark apparatus. The temperature of the reaction mixture was raised to 110 °C, and the reaction mixture was heated at 110 °C overnight. The reaction mixture was cooled to room temperature to give a white slurry. The solvent was removed under reduced pressure to give a white solid. This crude material was dissolved in a minimum volume of hot EtOAc and the solution was allowed to cool. The resulting white solid was filtered, washed with a small amount of EtOAc, and dried to give the required product (S)-cyclopentyl 2-amino-3-methylbutanoate 4-methylbenzenesulfonate **5.30** (1.89 g, 5.28 mmol, 77% yield) as an off-white solid.

^1H NMR (d_6 -DMSO, 293 K): δ 0.94 (d, $J = 7.1$ Hz, 3 H) 0.96 (d, $J = 7.1$ Hz, 3 H) 1.54 – 1.76 (m, 6 H) 1.81 – 1.95 (m, 2 H) 2.05 – 2.20 (m, 1 H) 2.29 (s, 3 H) 3.85 – 3.90 (m, 1 H) 5.20 – 5.24 (m, 1 H) 7.11 (d, $J = 7.8$ Hz, 2 H) 7.47 (d, $J = 8.1$ Hz, 2 H) 8.23 (br.s., 3 H)

(S)-Cyclopentyl 2-amino-4-methoxybutanoate 4-methylbenzenesulfonate, 5.31:

Method as for **5.29**, using the following reagents: (S)-2-amino-4-methoxybutanoic acid (3 g, 22.53 mmol), cyclopentanol (15.87 g, 184 mmol), 4-methylbenzenesulfonic acid monohydrate (5.57 g, 29.3 mmol) and cyclohexane (100 ml). The final product was: (S)-cyclopentyl 2-amino-4-methoxybutanoate 4-methylbenzenesulfonate **5.31** (4.70 g, 12.58 mmol, 56% yield) as a white solid.

^1H NMR (d_6 -DMSO, 293 K): δ 1.49 – 1.62 (m, 2 H) 1.62 – 1.77 (m, 4 H) 1.76 – 1.92 (m, 2 H) 2.00 (q, $J = 6.1$ Hz, 2 H) 2.29 (s, 3 H) 3.22 (s, 3 H) 3.40 – 3.43 (m, partially obscured by solvent peak) 3.92 – 4.09 (m, 1 H) 5.16 – 5.20 (m, 1 H) 7.11 (d, $J = 7.8$ Hz, 2 H) 7.48 (d, $J = 8.1$ Hz, 2 H) 8.24 (br.s., 3 H)

(S)-Cyclopentyl 2-amino-2-(tetrahydro-2H-pyran-4-yl)acetate 4-methylbenzenesulfonate, 5.32:

Method as for **5.29**, using the following reagents: (S)-2-amino-2-(tetrahydro-2H-pyran-4-yl)acetic acid (2.0 g, 12.56 mmol), cyclopentanol (8.85 g, 103 mmol), 4-methylbenzenesulfonic acid monohydrate (3.11 g, 16.33 mmol) and cyclohexane (60 ml). After 24 hours heating.

cyclohexane (40 ml) was added, and the reaction mixture was heated at 125 °C overnight. The final product was: (*S*)-cyclopentyl 2-amino-2-(tetrahydro-2*H*-pyran-4-yl)acetate 4-methylbenzenesulfonate **5.32** (1.77 g, 4.42 mmol, 35% yield) as a white solid.

¹H NMR (d₆-DMSO, 293 K): δ 1.19 – 1.36 (m, 1 H) 1.40 – 1.53 (m, 2 H) 1.53 – 1.74 (m, 7 H) 1.82 – 1.92 (m, 2 H) 1.97 – 2.11 (m, 1 H) 2.29 (s, 3 H) 3.20 – 3.31 (m, 2 H) 3.81 – 3.96 (m, 3 H) 5.19 – 5.24 (s, 1 H) 7.11 (d, *J* = 7.8 Hz, 2 H) 7.48 (d, *J* = 8.1 Hz, 2 H) 8.30 (br.s., 3 H)

Cyclopentyl 1-aminocyclobutanecarboxylate 4-methylbenzenesulfonate, **5.33**:

1-Aminocyclobutanecarboxylic acid (1.66 g, 14.42 mmol), 4-methylbenzenesulfonic acid monohydrate (3.57 g, 18.74 mmol) and cyclopentanol (10.16 g, 118 mmol) were added to cyclohexane (100 ml) and the reaction mixture was heated to 130 °C. Full dissolution was achieved, and the reaction mixture was heated at this temperature for 3 days. The solvent had evaporated due to the condenser not being fitted properly. The resulting pale brown solid was recrystallised from EtOAc, filtered, washed, and dried to give the tosic acid salt of the starting material amino acid. This recovered starting material (3.7726 g, 13.13 mmol), cyclopentanol (10.16 g, 118 mmol) and 4-methylbenzenesulfonic acid monohydrate (0.823 g, 4.33 mmol) were added to cyclohexane (100 ml) and the reaction mixture was heated at 130 °C for 5 days. The resulting slurry was evaporated under reduced pressure and dried in a vacuum oven. The solid was recrystallised from hot EtOAc, filtered, washed, and dried to give the required product cyclopentyl 1-aminocyclobutanecarboxylate 4-methylbenzenesulfonate **5.33** (3.31 g, 9.31 mmol, 65% yield) as a white solid.

¹H NMR (d₆-DMSO, 293 K): δ 1.55 – 1.65 (m, 2 H) 1.65 – 1.77 (m, 4 H) 1.81 – 1.93 (m, 2 H) 1.97 – 2.05 (m, 2 H) 2.29 (s, 3 H) 2.30 – 2.39 (m, 2 H) 2.39 – 2.49 (m, 2 H) 5.21 – 5.25 (m, 1 H) 7.12 (d, *J* = 8.3 Hz, 2 H) 7.48 (d, *J* = 8.1 Hz, 2 H) 8.50 (br.s., 3 H)

(*S*)-Isopropyl 2-amino-4-methylpentanoate 4-methylbenzenesulfonate, **5.34**:

Method as for **5.29**, using the following reagents: (*S*)-2-amino-4-methylpentanoic acid (2.27 g, 17.31 mmol), propan-2-ol (10.58 ml, 138 mmol), 4-methylbenzenesulfonic acid monohydrate (4.28 g, 22.50 mmol) and cyclohexane (100 ml). The reaction mixture was heated at 130 °C for 4 nights. The final product was: a white solid, (*S*)-isopropyl 2-amino-4-methylpentanoate 4-methylbenzenesulfonate **5.34** (4.2 g, 12.16 mmol, 70% yield).

¹H NMR (d₆-DMSO, 293 K): δ 0.89 (d, *J* = 2.0 Hz, 3 H) 0.91 (d, *J* = 2.3 Hz, 3 H) 1.22 – 1.26 (m, 6 H) 1.54 – 1.66 (m, 2 H) 1.67 – 1.81 (m, 1 H) 2.29 (s, 3 H) 3.93 (t, *J* = 7.1 Hz, 1 H) 4.91 – 5.10 (m, 1 H) 7.12 (m, *J* = 8.1 Hz, 2 H) 7.48 (m, *J* = 8.1 Hz, 2 H) 8.27 (br.s., 3 H)

(S)-Cyclobutyl 2-amino-4-methylpentanoate 4-methylbenzenesulfonate, 5.35:

Method as for **5.29**, using the following reagents: (*S*)-2-amino-4-methylpentanoic acid (2.27 g, 17.31 mmol), cyclobutanol (9.98 g, 138 mmol), 4-methylbenzenesulfonic acid monohydrate (4.28 g, 22.50 mmol) and cyclohexane (100 ml). The reaction mixture was heated at 130 °C overnight. The final product was: a white solid, (*S*)-cyclobutyl 2-amino-4-methylpentanoate 4-methylbenzenesulfonate **5.35** (5.7 g, 15.95 mmol, 92% yield).

¹H NMR (d₆-DMSO, 293 K): δ 0.90 (d, *J* = 2.0 Hz, 3 H) 0.91 (d, *J* = 2.0 Hz, 3 H) 1.54 – 1.84 (m, 5 H) 1.96 – 2.15 (m, 2 H) 2.23 – 2.39 (m, 5 H) 3.97 (t, *J* = 7.1 Hz, 1 H) 4.98 – 5.06 (m, 1 H) 7.11 (m, *J* = 7.8 Hz, 2 H) 7.48 (m, *J* = 8.1 Hz, 2 H) 8.27 (br.s., 3 H)

(S)-Neopentyl 2-amino-4-methylpentanoate 4-methylbenzenesulfonate, 5.36:

Method as for **5.29**, using the following reagents: 2,2-dimethylpropan-1-ol (10.99 g, 125 mmol), (*S*)-2-amino-4-methylpentanoic acid (2 g, 15.25 mmol), 4-methylbenzenesulfonic acid monohydrate (3.77 g, 19.82 mmol) and cyclohexane (100 ml). The reaction mixture was heated under reflux for three days. The final product was: (*S*)-neopentyl 2-amino-4-methylpentanoate 4-methylbenzenesulfonate **5.36** (4.91 g, 13.16 mmol, 86% yield) as a white solid.

¹H NMR (d₆-DMSO, 293 K): δ 0.90 (d, *J* = 3.7 Hz, 2 H) 0.91 – 0.94 (m, 12 H) 1.54 – 1.81 (m, 3 H) 2.29 (s, 3 H) 3.84 (d, *J* = 10.5 Hz, 1 H) 3.89 (d, *J* = 10.5 Hz, 1 H) 3.98 – 4.08 (m, 1 H) 7.11 (d, *J* = 7.8 Hz, 2 H) 7.48 (d, *J* = 8.1 Hz, 2 H) 8.20 – 8.41 (br.s., 3 H)

(2S)-Tetrahydrofuran-3-yl 2-amino-4-methylpentanoate 4-methylbenzenesulfonate, 5.37:

Method as for **5.29**, using the following reagents: (*S*)-2-amino-4-methylpentanoic acid (2 g, 15.25 mmol), tetrahydrofuran-3-ol (10.99 g, 125 mmol), 4-methylbenzenesulfonic acid monohydrate (3.77 g, 19.82 mmol) and cyclohexane (50 ml). The reaction mixture was heated at 110 °C for two nights. The final product was: (2*S*)-tetrahydrofuran-3-yl 2-amino-4-methylpentanoate 4-methylbenzenesulfonate **5.37** (3.37 g, 9.03 mmol, 59% yield) as a white solid.

¹H NMR (d₆-DMSO, 293 K): δ 0.90 (d, *J* = 2.2 Hz, 2 H) 0.91 (d, *J* = 2.2 Hz, 2 H) 1.54 – 1.77 (m, 3 H) 1.86 – 2.00 (m, 1 H) 2.13 – 2.25 (m, 1 H) 2.29 (s, 3 H) 3.69 – 3.87 (m, 4 H) 3.95 – 4.02 (m, 1 H) 5.33 – 5.39 (m, 1 H) 7.11 (d, *J* = 8.1 Hz, 2 H) 7.47 (d, *J* = 8.1 Hz, 2 H) 8.28 (br.s., 3 H)

(2S)-1-Methoxypropan-2-yl 2-amino-4-methylpentanoate 4-methylbenzenesulfonate (mixture of diastereomers), 5.38:

Method as for **5.29**, using the following reagents: (*S*)-2-amino-4-methylpentanoic acid (2.27 g, 17.31 mmol), 1-methoxypropan-2-ol (12.48 g, 138 mmol), 4-methylbenzenesulfonic acid

monohydrate (4.28 g, 22.50 mmol) and cyclohexane (100 ml). The reaction mixture was heated at 130 °C overnight. The final product was: (2*S*)-1-methoxypropan-2-yl 2-amino-4-methylpentanoate 4-methylbenzenesulfonate **5.38** (950 mg, 2.53 mmol, 15% yield) as a white solid. The ratio of diastereomers was ~1.5:1 by NMR, the absolute stereochemistry of the major diastereomer was unassigned.

¹H NMR (d₆-DMSO, 293 K): δ 0.85 – 1.01 (m, 6 H) 1.19 (d, *J* = 4.7 Hz, 1.3 H) 1.21 (d, *J* = 4.9 Hz, 1.8 H) 1.50 – 1.68 (m, 2 H) 1.68 – 1.85 (m, 1 H) 2.29 (s, 3 H) 3.25 (s, 1.7 H) 3.27 (s, 1.2 H) 3.36 – 3.51 (m, 2 H) 3.93 – 4.02 (m, 1 H) 5.03 – 5.17 (m, 1 H) 7.11 (d, *J* = 7.8 Hz, 2 H) 7.48 (d, *J* = 8.1 Hz, 2 H) 8.29 (br.s., 3 H)

(*S*)-Tetrahydro-2*H*-pyran-4-yl 2-amino-4-methylpentanoate 4-methylbenzenesulfonate, **5.39**:

Method as for **5.29**, using the following reagents: tetrahydro-2*H*-pyran-4-ol (9.34 g, 91 mmol), (*S*)-2-amino-4-methylpentanoic acid (1.5 g, 11.44 mmol), 4-methylbenzenesulfonic acid monohydrate (2.83 g, 14.87 mmol) and cyclohexane (100 ml). The reaction mixture was heated at 130 °C overnight. The final product was: (*S*)-tetrahydro-2*H*-pyran-4-yl 2-amino-4-methylpentanoate 4-methylbenzenesulfonate **5.39** (2.8 g, 7.23 mmol, 63% yield) as a white solid.

¹H NMR (d₆-DMSO, 293 K): δ 0.90 (d, *J* = 2.9 Hz, 3 H) 0.92 (d, *J* = 2.9 Hz, 3 H) 1.49 – 1.78 (m, 5 H) 1.84 – 1.93 (m, 1 H) 2.29 (s, 3 H) 3.46 – 3.54 (m, 2 H) 3.76 – 3.82 (m, 2 H) 3.89 – 4.18 (m, 1 H) 4.98 – 5.05 (m, 1 H) 5.75 (s, 1 H) 7.11 (m, *J* = 8.1 Hz, 2 H) 7.48 (m, *J* = 8.1 Hz, 2 H) 8.29 (br.s., 3 H)

(*S*)-Cyclopentyl 2-aminopentanoate hydrochloride, **5.40**:

(*S*)-2-Aminopentanoic acid (2.5 g, 21.34 mmol) was added to cyclopentanol (30 ml) and the suspension was brought to -5 °C using a dry ice/acetone bath. After stirring at this temperature for ten minutes, thionyl chloride (3.58 ml, 49.1 mmol) was added dropwise. The suspension was left stirring and allowed to warm to room temperature. It was stirred at this temperature for 18 hours. The reaction mixture was warmed to 60 °C and stirred at this temperature for 24 hours. The volatile components were removed by evaporating under reduced pressure, and the crude material was dried in a vacuum oven. The product was recrystallised from EtOAc, filtered, washed, and dried to give a first batch of material (2.62 g) as a white solid. The filtrate from the recrystallisation was concentrated under reduced pressure and dried in a vacuum oven to give a brown solid. The solid was recrystallised from EtOAc, filtered, washed, and dried to give a second batch of material (1.48 g) as an off-white solid. Both batches were combined to give the required product (*S*)-cyclopentyl 2-aminopentanoate hydrochloride **5.40** (4.10 g, 18.48 mmol, 87% yield) as a white solid.

¹H NMR (d₆-DMSO, 293 K): δ 0.89 (t, *J* = 7.3 Hz, 3 H) 1.20 – 1.50 (m, 2 H) 1.50 – 1.79 (m, 8 H) 1.79 – 1.96 (m, 2 H) 3.91 (t, *J* = 6.2 Hz, 1 H) 5.16 – 5.22 (m, 1 H) 8.49 (br.s., 3 H)

(*S*)-2-(((2-(5-Methyl-6-oxo-1,6-dihydropyridin-3-yl)-1-((tetrahydro-2*H*-pyran-4-yl)methyl)-1*H*-benzo[*d*]imidazol-5-yl)methyl)amino)propanoic acid hydrochloride, **5.41**:

1 M Aqueous lithium hydroxide solution (0.305 ml, 0.305 mmol) was added to a solution of (*S*)-cyclopentyl 2-(((2-(5-methyl-6-oxo-1,6-dihydropyridin-3-yl)-1-((tetrahydro-2*H*-pyran-4-yl)methyl)-1*H*-benzo[*d*]imidazol-5-yl)methyl)amino)propanoate **5.01** (50 mg, 0.102 mmol) in MeOH (2 ml) and THF (2 ml). The reaction mixture was heated at 60 °C overnight. The reaction mixture was blown down under a stream of nitrogen to give a white solid. The solid was dissolved in MeOH (1.65 ml) and 2 M aqueous hydrochloric acid (0.15 ml, 0.305 mmol) and purified by MDAP (high pH). The solvent was evaporated under reduced pressure and the crude product was dried in a vacuum oven to give a white solid. The crude sample was suspended in MeOH and 2 M aqueous hydrochloric acid (1 ml) was added. The clear solution was blown down under a stream of nitrogen to give the required product (*S*)-2-(((2-(5-methyl-6-oxo-1,6-dihydropyridin-3-yl)-1-((tetrahydro-2*H*-pyran-4-yl)methyl)-1*H*-benzo[*d*]imidazol-5-yl)methyl)amino)propanoic acid hydrochloride **5.41** (42.6 mg, 0.092 mmol, 91% yield) as a white solid.

LCMS (high pH): rt = 0.49 min, MH⁺ = 425

¹H NMR (d₆-DMSO, 293 K): δ 1.14 – 1.27 (m, 2 H) 1.28 – 1.36 (m, 2 H) 1.55 (d, *J* = 7.1 Hz, 2 H) 1.93 – 2.06 (m, 1 H) 2.09 (s, 3 H) 3.08 – 3.19 (m, 3 H) 3.69 – 3.80 (m, 2 H) 3.95 – 4.08 (m, 1 H) 4.29 – 4.44 (m, 3 H) 7.69 (d, *J* = 8.3 Hz, 1 H) 7.82 (d, *J* = 1.2 Hz, 1 H) 7.98 – 8.13 (m, 3 H) 9.39 – 9.70 (br.s., 1 H) 9.85 – 10.17 (br.s., 1 H) 12.08 – 12.60 (br.s., 1 H)

(*S*)-2-(((2-(5-Methyl-6-oxo-1,6-dihydropyridin-3-yl)-1-((tetrahydro-2*H*-pyran-4-yl)methyl)-1*H*-benzo[*d*]imidazol-5-yl)methyl)amino)butanoic acid hydrochloride, **5.42**:

(*S*)-Cyclopentyl 2-(((2-(5-methyl-6-oxo-1,6-dihydropyridin-3-yl)-1-((tetrahydro-2*H*-pyran-4-yl)methyl)-1*H*-benzo[*d*]imidazol-5-yl)methyl)amino)butanoate **5.02** (57.8 mg, 0.114 mmol) was dissolved in MeOH (2 ml) and THF (2 ml), and 1 M aqueous lithium hydroxide solution (0.342 ml, 0.342 mmol) was added. The reaction mixture was stirred at 60 °C under nitrogen overnight. The reaction mixture was blown down under a stream of nitrogen. The crude sample was suspended in MeOH (1.63 ml) and 2 M aqueous hydrochloric acid (0.17 ml, 0.34 mmol) and purified by MDAP (high pH). The solvent was evaporated under reduced pressure to give a white solid. The solid was suspended in THF (2 ml) and 2 M aqueous hydrochloric acid (1 ml) was added. The clear solution was blown down under a stream of nitrogen to give the crude product as a white solid. NMR analysis showed significant presence of ammonium salt. The

sample was repurified by MDAP (high pH). The solvent was evaporated under reduced pressure to give a white solid, which was dried in a vacuum oven overnight. The solid was suspended in THF (2 ml) and 2 M aqueous hydrochloric acid (1 ml) was added. The clear solution was blown down under a stream of nitrogen to give the required product (*S*)-2-(((2-(5-methyl-6-oxo-1,6-dihydropyridin-3-yl)-1-((tetrahydro-2*H*-pyran-4-yl)methyl)-1*H*-benzo[*d*]imidazol-5-yl)methyl)amino)butanoic acid hydrochloride **5.42** (39.6 mg, 0.083 mmol, 73% yield) as a white solid.

LCMS (high pH): *rt* = 0.50 min, MH^+ = 439

¹H NMR (*d*₆-DMSO, 293 K): δ 0.96 (t, *J* = 7.5 Hz, 3 H) 1.14 – 1.35 (m, 4 H) 1.87 – 2.06 (m, 3 H) 2.09 (s, 3 H) 3.08 – 3.15 (m, 2 H) 3.73 – 3.76 (m, 2 H) 3.88 (br.s., 1 H) 4.30 – 4.44 (m, 4 H) 7.66 (d, *J* = 8.3 Hz, 1 H) 7.82 (s, 1 H) 8.01 – 8.08 (m, 3 H) 9.40 – 9.70 (br.s., 1 H) 9.70 – 9.99 (br.s., 1 H) 12.17 – 12.50 (br.s., 1 H)

(*S*)-2-(((2-(5-Methyl-6-oxo-1,6-dihydropyridin-3-yl)-1-((tetrahydro-2*H*-pyran-4-yl)methyl)-1*H*-benzo[*d*]imidazol-5-yl)methyl)amino)pentanoic acid hydrochloride, **5.43**:

(*S*)-Cyclopentyl 2-(((2-(5-methyl-6-oxo-1,6-dihydropyridin-3-yl)-1-((tetrahydro-2*H*-pyran-4-yl)methyl)-1*H*-benzo[*d*]imidazol-5-yl)methyl)amino)pentanoate **5.03** (47 mg, 0.090 mmol) was dissolved in MeOH (2 ml) and THF (2 ml), and 1 M aqueous lithium hydroxide solution (0.271 ml, 0.271 mmol) was added. The reaction mixture was stirred at 60 °C for 36 hours. The reaction mixture was blown down under a stream of nitrogen. The crude sample was suspended in MeOH (1.65 ml) and 2 M aqueous hydrochloric acid (0.15 ml, 0.27 mmol) and purified by MDAP (high pH). The solvent was evaporated under reduced pressure to give a white solid, which was dried in a vacuum oven. The solid was suspended in THF (2 ml) and 2 M aqueous hydrochloric acid (1 ml) was added. The clear solution was blown down under a stream of nitrogen to give the required product (*S*)-2-(((2-(5-methyl-6-oxo-1,6-dihydropyridin-3-yl)-1-((tetrahydro-2*H*-pyran-4-yl)methyl)-1*H*-benzo[*d*]imidazol-5-yl)methyl)amino)pentanoic acid hydrochloride **5.43** (37.7 mg, 0.077 mmol, 85% yield) as a white solid.

LCMS (high pH): *rt* = 0.54 min, MH^+ = 453

¹H NMR (*d*₆-DMSO, 293 K): δ 0.90 (t, *J* = 7.3 Hz, 3 H) 1.13 – 1.39 (m, 5 H) 1.42 – 1.58 (m, 1 H) 1.82 – 2.05 (m, 2 H) 2.09 (s, 3 H) 3.05 – 3.17 (m, 2 H) 3.67 – 3.81 (m, 2 H) 3.83 – 3.93 (m, 1 H) 4.29 – 4.45 (m, 4 H) 7.70 (d, *J* = 8.6 Hz, 1 H) 7.83 (d, *J* = 1.2 Hz, 1 H) 8.04 – 8.10 (m, 3 H) 9.44 – 9.73 (br.s., 1 H) 9.85 – 10.19 (br.s., 1 H) 12.19 – 12.54 (br.s., 1 H)

(*S*)-3-Methyl-2-(((2-(5-methyl-6-oxo-1,6-dihydropyridin-3-yl)-1-((tetrahydro-2*H*-pyran-4-yl)methyl)-1*H*-benzo[*d*]imidazol-5-yl)methyl)amino)butanoic acid hydrochloride, **5.44**:

1 M Aqueous lithium hydroxide solution (0.288 ml, 0.288 mmol) was added to a solution of (*S*)-

cyclopentyl 3-methyl-2-(((2-(5-methyl-6-oxo-1,6-dihydropyridin-3-yl)-1-((tetrahydro-2H-pyran-4-yl)methyl)-1H-benzo[d]imidazol-5-yl)methyl)amino)butanoate **5.04** (50 mg, 0.096 mmol) in MeOH (2 ml) and THF (2 ml). The reaction mixture was heated under nitrogen at 50 °C overnight. Further 1 M aqueous lithium hydroxide solution (0.288 ml, 0.288 mmol) was added to the reaction mixture, which was stirred at 60 °C overnight. The reaction mixture was blown down under a stream of nitrogen to give a white solid. The crude material was dissolved in MeOH (1.5 ml) and 2 M aqueous hydrochloric acid (0.566 mmol, 0.3 ml), and purified by MDAP (high pH). The solvent was evaporated under reduced pressure, and the crude material was dried in a vacuum oven to give a white solid (16.8mg). The sample was suspended in a mixture of DCM (2ml) MeOH (2 ml) and THF (2 ml), and 1 M aqueous sodium hydroxide solution (37 µl, 0.037mmol) was added. After stirring for 5 min, the solution was blown down under a stream of nitrogen to give a white solid (29.3 mg) which was found to be not very soluble in DMSO. The sample was suspended in MeOH (1 ml) and 2 M aqueous hydrochloric acid was added dropwise until dissolution was achieved, and the solution purified by MDAP (high pH). The solvent was evaporated under reduced pressure and the crude sample was dried in a vacuum oven to give a white solid. The crude product was suspended in MeOH and 2 M aqueous hydrochloric acid (1 ml) was added. The clear solution was blown down under a stream of nitrogen to give the required product (*S*)-3-methyl-2-(((2-(5-methyl-6-oxo-1,6-dihydropyridin-3-yl)-1-((tetrahydro-2H-pyran-4-yl)methyl)-1H-benzo[d]imidazol-5-yl)methyl)amino)butanoic acid hydrochloride **5.44** (28.2 mg, 0.058 mmol, 60% yield) as a white solid.

LCMS (high pH): rt = 0.53 min, MH⁺ = 453

¹H NMR (d₆-DMSO, 293 K): δ 0.97 (d, *J* = 6.9 Hz, 3 H) 1.05 (d, *J* = 7.1 Hz, 3 H) 1.16 – 1.26 (m, 2 H) 1.28 – 1.37 (m, 2 H) 1.93 – 2.06 (m, 1 H) 2.09 (s, 3 H) 2.41 – 2.49 (m, 1 H) 3.08 – 3.16 (m, 2 H) 3.69 – 3.79 (m, 3 H) 4.32 – 4.39 (m, 2 H) 4.42 (d, *J* = 7.1 Hz, 2 H) 7.73 (d, *J* = 8.6 Hz, 1 H) 7.84 (d, *J* = 1.2 Hz, 1 H) 8.04 – 8.13 (m, 3 H) 9.27 – 9.62 (br.s., 1 H) 9.77 – 10.11 (br.s., 1 H) 12.16 – 12.71 (br.s., 1 H)

(*S*)-3-Hydroxy-2-(((2-(5-methyl-6-oxo-1,6-dihydropyridin-3-yl)-1-((tetrahydro-2H-pyran-4-yl)methyl)-1H-benzo[d]imidazol-5-yl)methyl)amino)propanoic acid hydrochloride, **5.45**:

1 M Aqueous lithium hydroxide solution (0.295 ml, 0.295 mmol) was added to a solution of (*S*)-cyclopentyl 3-hydroxy-2-(((2-(5-methyl-6-oxo-1,6-dihydropyridin-3-yl)-1-((tetrahydro-2H-pyran-4-yl)methyl)-1H-benzo[d]imidazol-5-yl)methyl)amino)propanoate **5.05** (50 mg, 0.098 mmol) in MeOH (2 ml) and THF (2 ml). The reaction mixture was heated at 50 °C for 5 hours. The reaction mixture was blown down under a stream of nitrogen to give a white solid. The

crude material was dissolved in MeOH (1.65 ml) and 2 M aqueous hydrochloric acid (0.30 mmol, 0.15 ml) and purified by MDAP (high pH). The solvent was evaporated under reduced pressure and the crude sample was dried in a vacuum oven to give a white solid (34.4 mg). The sample was suspended in a mixture of DCM (3 ml), MeOH (3 ml) and THF (3 ml), and 1 M aqueous sodium hydroxide solution (98 μ l, 0.098 mmol) was added. After stirring for 5 minutes, the solution was blown down under a stream of nitrogen. Excess sodium hydroxide was present in the sample. The sample was dissolved in DMSO (2 x 1 ml) and repurified by MDAP (high pH). The solvent was evaporated under reduced pressure, and the crude sample was dried in a vacuum oven to give a white solid (18.4 mg). The sample was suspended in MeOH and 2 M aqueous hydrochloric acid (1 ml) was added. The clear solution was blown down under a stream of nitrogen to give the crude product as a white solid. The sample was redissolved in 1:1 MeOH:DMSO (1 ml) and purified by MDAP (high pH). The solvent was evaporated under reduced pressure and the crude sample was dried in a vacuum oven to give a white solid. The crude product was suspended in MeOH and 2 M hydrochloric acid (1 ml) was added. The clear solution was blown down under a stream of nitrogen to give the required product (*S*)-3-hydroxy-2-(((2-(5-methyl-6-oxo-1,6-dihydropyridin-3-yl)-1-((tetrahydro-2*H*-pyran-4-yl)methyl)-1*H*-benzo[*d*]imidazol-5-yl)methyl)amino)propanoic acid hydrochloride **5.45** (32.8 mg, 0.069 mmol, 70% yield) as a white solid.

LCMS (high pH): *rt* = 0.48 min, MH^+ = 441

¹H NMR (*d*₆-DMSO, 293 K): δ 1.14 – 1.29 (m, 2 H) 1.30 – 1.39 (m, 2 H) 1.93 – 2.06 (m, 1 H) 2.09 (s, 3 H) 3.08 – 3.14 (m, 2 H) 3.70 – 3.79 (m, 2 H) 3.88 – 3.96 (m, 1 H) 3.96 – 4.00 (br.s., 1 H) 4.00 – 4.07 (m, 1 H) 4.38 – 4.48 (m, 5 H) 7.74 (d, *J* = 8.6 Hz, 1 H) 7.83 – 7.85 (m, 1 H) 8.08 – 8.13 (m, 3 H) 9.45 – 9.73 (br.s., 1 H) 9.73 – 10.04 (br.s., 1 H) 12.24 – 12.63 (br.s., 1 H)

(2*S*,3*R*)-3-Hydroxy-2-(((2-(5-methyl-6-oxo-1,6-dihydropyridin-3-yl)-1-((tetrahydro-2*H*-pyran-4-yl)methyl)-1*H*-benzo[*d*]imidazol-5-yl)methyl)amino)butanoic acid hydrochloride, **5.46**:

1 M Aqueous lithium hydroxide solution (0.287 ml, 0.287 mmol) was added to a solution of (2*S*,3*R*)-cyclopentyl 3-hydroxy-2-(((2-(5-methyl-6-oxo-1,6-dihydropyridin-3-yl)-1-((tetrahydro-2*H*-pyran-4-yl)methyl)-1*H*-benzo[*d*]imidazol-5-yl)methyl)amino)butanoate **5.06** (50 mg, 0.096 mmol) in MeOH (2 ml) and THF (2 ml). The reaction mixture was heated at 50 °C for 5 hours. The reaction mixture was blown down under a stream of nitrogen to give an off-white solid. The crude material was dissolved in MeOH (1.66 ml) and 2 M aqueous hydrochloric acid (0.29 mmol, 0.14 ml) and purified by MDAP (high pH). The solvent was evaporated under reduced pressure, and the crude material was dried in a vacuum oven to give a white solid (31.4 mg). The sample was suspended in a mixture of DCM (3 ml), MeOH (3 ml) and THF (3 ml), and 1

M aqueous sodium hydroxide solution (96 μ l, 0.096mmol) was added. After stirring for 5 minutes, the solution was blown down under a stream of nitrogen. Excess sodium hydroxide was present in the sample. The crude sample was dissolved in DMSO (2 x 1 ml) and repurified by MDAP (high pH). The solvent was evaporated under reduced pressure and the crude sample was dried in a vacuum oven to give a white solid. The crude product was suspended in MeOH and 2 M aqueous hydrochloric acid (1 ml) was added. The clear solution was blown down a stream of nitrogen to give the required product (2*S*,3*R*)-3-hydroxy-2-(((2-(5-methyl-6-oxo-1,6-dihydropyridin-3-yl)-1-((tetrahydro-2*H*-pyran-4-yl)methyl)-1*H*-benzo[*d*]imidazol-5-yl)methyl)amino)butanoic acid hydrochloride **5.46** (40.3 mg, 0.082 mmol, 86% yield) as a white solid.

LCMS (high pH): rt = 0.49 min, MH^+ = 455

1H NMR (d_6 -DMSO, 293 K): δ 1.15 – 1.27 (m, 5 H) 1.29 – 1.38 (m, 1 H) 1.94 – 2.07 (m, 1 H) 2.09 (s, 3 H) 3.09 – 3.16 (m, 2 H) 3.56 – 3.63 (m, 1 H) 3.70 – 3.79 (m, 2 H) 4.10 – 4.18 (m, 1 H) 4.38 – 4.47 (m, 4 H) 7.71 (d, J = 8.8 Hz, 1 H) 7.84 (d, J = 1.2 Hz, 1 H) 8.06 – 8.13 (m, 3 H) 9.44 – 9.71 (br.s., 1 H)

(*S*)-4-Methoxy-2-(((2-(5-methyl-6-oxo-1,6-dihydropyridin-3-yl)-1-((tetrahydro-2*H*-pyran-4-yl)methyl)-1*H*-benzo[*d*]imidazol-5-yl)methyl)amino)butanoic acid hydrochloride, **5.47**:

(*S*)-Cyclopentyl 4-methoxy-2-(((2-(5-methyl-6-oxo-1,6-dihydropyridin-3-yl)-1-((tetrahydro-2*H*-pyran-4-yl)methyl)-1*H*-benzo[*d*]imidazol-5-yl)methyl)amino)butanoate **5.07** (55.5 mg, 0.103 mmol) was dissolved in MeOH (2 ml) and THF (2 ml), and 1 M aqueous lithium hydroxide solution (0.310 ml, 0.310 mmol) was added. The reaction mixture was stirred at 60 °C under nitrogen overnight. The reaction mixture was blown down under a stream of nitrogen. The crude sample was suspended in MeOH (1.65 ml) and 2 M aqueous hydrochloric acid (0.15 ml, 0.3 mmol) and purified by MDAP (high pH). The solvent was evaporated under reduced pressure to give a white solid. The solid was suspended in THF (2 ml) and 2 M aqueous hydrochloric acid (1 ml) was added. The clear solution was blown down under a stream of nitrogen to give the crude product as a white solid. The sample was repurified by MDAP (high pH). The solvent was evaporated under reduced pressure to give a white solid, which was dried in a vacuum oven overnight. The sample was suspended in THF (2 ml) and 2 M aqueous hydrochloric acid (1 ml) was added. The clear solution was blown down under a stream of nitrogen to give the required product (*S*)-4-methoxy-2-(((2-(5-methyl-6-oxo-1,6-dihydropyridin-3-yl)-1-((tetrahydro-2*H*-pyran-4-yl)methyl)-1*H*-benzo[*d*]imidazol-5-yl)methyl)amino)butanoic acid hydrochloride **5.47** (33.8 mg, 0.067 mmol, 65% yield) as a white solid.

LCMS (high pH): rt = 0.51 min, MH⁺ = 469

¹H NMR (d₆-DMSO, 293 K): δ 1.13 – 1.33 (m, 4 H) 1.92 – 2.03 (m, 1 H) 2.09 (s, 3 H) 3.06 – 3.17 (m, 2 H) 3.23 (s, 3 H) 3.89 – 3.97 (m, 2 H) 4.31 – 4.41 (m, 4 H) 7.54 – 7.60 (m, 1 H) 7.79 (s, 1 H) 7.89 – 8.02 (m, 3 H) 9.38 – 9.69 (br.s., 2 H) Three protons are obscured by a broad water peak at 3.44 – 3.79 ppm.

(S)-1-((2-(5-Methyl-6-oxo-1,6-dihydropyridin-3-yl)-1-((tetrahydro-2H-pyran-4-yl)methyl)-1H-benzo[d]imidazol-5-yl)methyl)pyrrolidine-2-carboxylic acid hydrochloride, 5.48:

To a solution of (S)-cyclopentyl 1-((2-(5-methyl-6-oxo-1,6-dihydropyridin-3-yl)-1-((tetrahydro-2H-pyran-4-yl)methyl)-1H-benzo[d]imidazol-5-yl)methyl)pyrrolidine-2-carboxylate **5.08** (35 mg, 0.067 mmol) in MeOH (2 ml) and THF (2 ml) was added 1 M aqueous lithium hydroxide solution (0.202 ml, 0.202 mmol), and the reaction mixture heated at 50 °C overnight. The reaction mixture was blown down under a stream of nitrogen. The sample was dissolved in 2 M aqueous hydrochloric acid (0.1 ml) and MeOH (0.9 ml) and purified by MDAP (high pH). The solvent was blown down under a stream of nitrogen and the residue suspended in THF (1 ml). 2 M aqueous hydrochloric acid (0.5 ml) was added and the resulting solution blown down under a stream of nitrogen to give the required product (S)-1-((2-(5-methyl-6-oxo-1,6-dihydropyridin-3-yl)-1-((tetrahydro-2H-pyran-4-yl)methyl)-1H-benzo[d]imidazol-5-yl)methyl)pyrrolidine-2-carboxylic acid hydrochloride **5.48** (24 mg, 0.049 mmol, 73% yield) as an off-white solid.

LCMS (high pH): rt = 0.52 min, MH⁺ = 451

¹H NMR (d₆-DMSO, 293 K): δ 1.17 – 1.28 (m, 2 H) 1.35 (d, J = 11.9 Hz, 2 H) 1.83 – 1.95 (m, 1 H) 1.96 – 2.16 (m, 6 H) 3.13 (t, J = 10.9 Hz, 2 H) 3.27 – 3.40 (m, 1 H) 3.40 – 3.52 (m, 1 H) 3.69 – 3.80 (m, 2 H) 4.40 – 4.49 (m, 3 H) 4.57 (d, J = 12.6 Hz, 1 H) 4.73 (d, J = 12.6 Hz, 1 H) 7.75 (d, J = 8.6 Hz, 1 H) 7.85 (s, 1 H) 8.08 – 8.11 (m, 2 H) 8.14 (d, J = 8.6 Hz, 1 H) 10.32 – 10.57 (br.s., 1 H) 12.18 – 12.67 (br.s., 1 H)

2-Methyl-2-(((2-(5-methyl-6-oxo-1,6-dihydropyridin-3-yl)-1-((tetrahydro-2H-pyran-4-yl)methyl)-1H-benzo[d]imidazol-5-yl)methyl)amino)propanoic acid hydrochloride, 5.49:

1 M Aqueous lithium hydroxide solution (0.237 ml, 0.237 mmol) was added to a solution of cyclopentyl 2-methyl-2-(((2-(5-methyl-6-oxo-1,6-dihydropyridin-3-yl)-1-((tetrahydro-2H-pyran-4-yl)methyl)-1H-benzo[d]imidazol-5-yl)methyl)amino)propanoate **5.09** (40 mg, 0.079 mmol) in MeOH (2 ml) and THF (2 ml). The reaction mixture was heated at 60 °C for two nights. The reaction mixture was blown down under a stream of nitrogen to give a white solid. The crude sample was dissolved in MeOH (1.68 ml) and 2 M aqueous hydrochloric acid (0.12 ml) and purified by MDAP (high pH). The solvent was evaporated under reduced pressure, and the crude sample was dried in a vacuum oven to give a white solid. The sample was suspended

in THF and 2 M aqueous hydrochloric acid (1 ml) was added. The clear solution was blown down under a stream of nitrogen to give the required product 2-methyl-2-(((2-(5-methyl-6-oxo-1,6-dihydropyridin-3-yl)-1-((tetrahydro-2*H*-pyran-4-yl)methyl)-1*H*-benzo[*d*]imidazol-5-yl)methyl)amino)propanoic acid hydrochloride **5.49** (30.6 mg, 0.064 mmol, 82% yield) as a white solid.

LCMS (high pH): *rt* = 0.51 min, MH^+ = 439

¹H NMR (*d*₆-DMSO, 293 K): δ 1.15 – 1.26 (m, 2 H) 1.27 – 1.33 (m, 2 H) 1.64 (s, 6 H) 1.94 – 2.06 (m, 1 H) 2.09 (s, 3 H) 3.07 – 3.16 (m, 2 H) 3.71 – 3.80 (m, 2 H) 4.25 – 4.34 (m, 2 H) 4.41 (d, *J* = 7.1 Hz, 2 H) 7.68 (d, *J* = 8.3 Hz, 1 H) 7.81 – 7.85 (m, 1 H) 8.01 – 8.09 (m, 3 H) 9.79 (br. s., 2 H) 12.25 – 12.47 (m, 1 H)

(*S*)-3-(1*H*-Imidazol-5-yl)-2-(((2-(5-methyl-6-oxo-1,6-dihydropyridin-3-yl)-1-((tetrahydro-2*H*-pyran-4-yl)methyl)-1*H*-benzo[*d*]imidazol-5-yl)methyl)amino)propanoic acid bis-hydrochloride. **5.50**:

To a solution of (*S*)-cyclopentyl 3-(1*H*-imidazol-5-yl)-2-(((2-(5-methyl-6-oxo-1,6-dihydropyridin-3-yl)-1-((tetrahydro-2*H*-pyran-4-yl)methyl)-1*H*-benzo[*d*]imidazol-5-yl)methyl)amino)propanoate **5.10** (35 mg, 0.063 mmol) in MeOH (2 ml) and THF (2 ml) was added 1 M aqueous lithium hydroxide (0.188 ml, 0.188 mmol), and the reaction mixture heated at 50 °C overnight. The reaction mixture had at this point evaporated to dryness. The reaction mixture was blown down under a stream of nitrogen. The sample was dissolved in 2 M aqueous hydrochloric acid (0.1 ml) and MeOH (0.9 ml) and purified by MDAP (high pH). The solvent was blown down under a stream of nitrogen to give a white gum. The sample was suspended in THF (1 ml) and 2 M aqueous hydrochloric acid (0.5 ml) added to give a clear solution. The sample was blown down under a stream of nitrogen to give the required product (*S*)-3-(1*H*-imidazol-5-yl)-2-(((2-(5-methyl-6-oxo-1,6-dihydropyridin-3-yl)-1-((tetrahydro-2*H*-pyran-4-yl)methyl)-1*H*-benzo[*d*]imidazol-5-yl)methyl)amino)propanoic acid bis-hydrochloride **5.50** (27 mg, 0.048 mmol, 76% yield) as an off-white solid.

LCMS (high pH): *rt* = 0.48 min, MH^+ = 491

¹H NMR (*d*₆-DMSO, 293 K): δ 1.14 – 1.30 (m, 2 H) 1.33 – 1.39 (m, 2 H) 1.95 – 2.07 (m, 1 H) 2.09 (s, 3 H) 3.15 (d, *J* = 12.6 Hz, 2 H) 3.45 (dd, *J* = 15.7, 8.3 Hz, 1 H) 3.61 (dd, *J* = 15.7, 4.9 Hz, 1 H) 3.68 – 3.82 (m, 2 H) 4.38 – 4.61 (m, 5 H) 7.56 (s, 1 H) 7.76 – 7.94 (m, 2 H) 8.14 – 8.22 (m, 3 H) 9.08 (d, *J* = 1.0 Hz, 1 H) 14.44 – 14.78 (br.s., 1 H)

(S)-2-(((2-(5-Methyl-6-oxo-1,6-dihydropyridin-3-yl)-1-((tetrahydro-2H-pyran-4-yl)methyl)-1H-benzo[d]imidazol-5-yl)methyl)amino)-2-(tetrahydro-2H-pyran-4-yl)acetic acid hydrochloride, 5.51:

(S)-Cyclopentyl 2-(((2-(5-methyl-6-oxo-1,6-dihydropyridin-3-yl)-1-((tetrahydro-2H-pyran-4-yl)methyl)-1H-benzo[d]imidazol-5-yl)methyl)amino)-2-(tetrahydro-2H-pyran-4-yl)acetate **5.11** (61.1 mg, 0.109 mmol) was dissolved in MeOH (2 ml) and THF (2 ml), and 1 M aqueous lithium hydroxide solution (1 ml, 1.000 mmol) was added. The reaction mixture was stirred at 60 °C under nitrogen overnight. The reaction mixture was blown down under a stream of nitrogen. The crude sample was suspended in MeOH (1.3 ml) and 2 M aqueous hydrochloride solution (0.5 ml) and purified by MDAP (high pH). The solvent was evaporated under reduced pressure to give a white solid. The sample was suspended in THF (2 ml), and 2 M aqueous hydrochloric acid (1 ml) was added. The clear solution was blown down under a stream of nitrogen to give the crude product as a white solid. The sample was repurified by MDAP (high pH). The solvent was evaporated under reduced pressure to give a white solid, which was dried in a vacuum oven overnight. The sample was suspended in THF (2 ml) and 2 M aqueous hydrochloric acid (1 ml) was added. The clear solution was blown down under a stream of nitrogen to give the required product (S)-2-(((2-(5-methyl-6-oxo-1,6-dihydropyridin-3-yl)-1-((tetrahydro-2H-pyran-4-yl)methyl)-1H-benzo[d]imidazol-5-yl)methyl)amino)-2-(tetrahydro-2H-pyran-4-yl)acetic acid hydrochloride **5.51** (29.6 mg, 0.056 mmol, 51% yield) as a white solid.

LCMS (high pH): $rt = 0.51$ min, $MH^+ = 495$

1H NMR (d_6 -DMSO, 293 K): δ 1.17 – 1.28 (m, 3 H) 1.28 – 1.37 (m, 2 H) 1.53 – 1.63 (m, 2 H) 1.70 – 1.78 (m, 1 H) 1.95 – 2.05 (m, 1 H) 2.09 (s, 3 H) 2.31 – 2.44 (m, 1 H) 3.12 (t, $J = 10.9$ Hz, 2 H) 3.21 – 3.31 (m, 2 H) 3.71 – 3.78 (m, 2 H) 3.85 – 3.93 (m, 2 H) 4.32 – 4.46 (m, 4 H) 7.71 (d, $J = 8.6$ Hz, 1 H) 7.83 (s, 1 H) 8.04 – 8.12 (m, 3 H) 9.40 – 9.66 (br.s., 1 H) 9.81 – 10.07 (br.s., 1 H) 12.22 – 12.55 (br.s., 1 H)

1-(((2-(5-Methyl-6-oxo-1,6-dihydropyridin-3-yl)-1-((tetrahydro-2H-pyran-4-yl)methyl)-1H-benzo[d]imidazol-5-yl)methyl)amino)cyclobutanecarboxylic acid hydrochloride, 5.52:

To a solution of cyclopentyl 1-(((2-(5-methyl-6-oxo-1,6-dihydropyridin-3-yl)-1-((tetrahydro-2H-pyran-4-yl)methyl)-1H-benzo[d]imidazol-5-yl)methyl)amino)cyclobutanecarboxylate **5.12** (35 mg, 0.067 mmol) in MeOH (2 ml) and THF (2 ml) was added 1 M aqueous lithium hydroxide solution (0.202 ml, 0.202 mmol), and the reaction mixture heated at 50 °C under nitrogen overnight. The reaction mixture was blown down under a stream of nitrogen. The sample was dissolved in 2 M aqueous hydrochloric acid (0.1 ml) and MeOH (0.9 ml) and

purified by MDAP (high pH). The solvent was blown down under a stream of nitrogen to give a white gum. The sample was suspended in THF (1 ml) and 2 M aqueous hydrochloric acid (0.5 ml) added to give a clear solution. The mixture was blown down under a stream of nitrogen to give the required product 1-(((2-(5-methyl-6-oxo-1,6-dihydropyridin-3-yl)-1-((tetrahydro-2H-pyran-4-yl)methyl)-1H-benzo[d]imidazol-5-yl)methyl)amino)cyclobutanecarboxylic acid hydrochloride **5.52** (19 mg, 0.039 mmol, 58% yield) as an off-white solid.

LCMS (high pH): $rt = 0.52$ min, $MH^+ = 451$

1H NMR (d_6 -DMSO, 293 K): δ 1.13 – 1.29 (m, 2 H) 1.34 (d, $J = 11.1$ Hz, 2 H) 1.97 – 2.14 (m, 6 H) 2.40 – 2.48 (m, 2 H) 2.72 – 2.82 (m, 2 H) 3.09 – 3.17 (m, 2 H) 3.75 (dd, $J = 11.2, 2.7$ Hz, 2 H) 4.25 – 4.30 (m, 2 H) 4.45 (d, $J = 7.3$ Hz, 3 H) 7.76 (dd, $J = 8.6, 1.0$ Hz, 1 H) 7.85 (d, $J = 1.3$ Hz, 1 H) 8.08 (s, 1 H) 8.14 (d, $J = 2.3$ Hz, 1 H) 8.17 (d, $J = 8.6$ Hz, 1 H) 10.21 – 10.41 (br.s., 2 H)

(2S,3R)-Cyclopentyl 2-(((2-(1,5-dimethyl-6-oxo-1,6-dihydropyridin-3-yl)-1-((tetrahydro-2H-pyran-4-yl)methyl)-1H-benzo[d]imidazol-5-yl)methyl)amino)-3-hydroxybutanoate, **5.53**:

Method as for **5.01**, using the following reagents: 2-(1,5-dimethyl-6-oxo-1,6-dihydropyridin-3-yl)-1-((tetrahydro-2H-pyran-4-yl)methyl)-1H-benzo[d]imidazole-5-carbaldehyde **5.61** (150 mg, 0.410 mmol), (2S,3R)-cyclopentyl 2-amino-3-hydroxybutanoate 4-methylbenzenesulfonate **5.25** (295 mg, 0.821 mmol), sodium triacetoxyborohydride (174 mg, 0.821 mmol) and DCM (10 ml). The final product was: (2S,3R)-cyclopentyl 2-(((2-(1,5-dimethyl-6-oxo-1,6-dihydropyridin-3-yl)-1-((tetrahydro-2H-pyran-4-yl)methyl)-1H-benzo[d]imidazol-5-yl)methyl)amino)-3-hydroxybutanoate **5.53** (138 mg, 0.257 mmol, 63% yield) as a colourless gum.

LCMS (high pH): $rt = 0.91$ min, $MH^+ = 537$

1H NMR (d_6 -DMSO, 293 K): δ 1.06 – 1.27 (m, 7 H) 1.50 – 1.69 (m, 6 H) 1.75 – 1.87 (m, 2 H) 1.90 – 2.01 (m, 1 H) 2.11 (s, 3 H) 3.01 (d, $J = 4.8$ Hz, 1 H) 3.11 (t, $J = 11.1$ Hz, 2 H) 3.56 (s, 3 H) 3.66 (d, $J = 13.1$ Hz, 1 H) 3.68 – 3.77 (m, 2 H) 3.77 – 3.86 (m, 1 H) 3.90 (d, $J = 13.1$ Hz, 1 H) 4.26 (d, $J = 7.3$ Hz, 2 H) 4.63 – 4.70 (m, 1 H) 5.06 – 5.15 (m, 1 H) 7.22 (d, $J = 8.3$ Hz, 1 H) 7.53 (s, 1 H) 7.60 (d, $J = 8.3$ Hz, 1 H) 7.73 (s, 1 H) 8.11 (s, 1 H)

(S)-Neopentyl 3-methyl-2-(((2-(5-methyl-6-oxo-1,6-dihydropyridin-3-yl)-1-((tetrahydro-2H-pyran-4-yl)methyl)-1H-benzo[d]imidazol-5-yl)methyl)amino)butanoate, **5.54**:

Method as for **5.01**, using the following reagents: 2-(5-methyl-6-oxo-1,6-dihydropyridin-3-yl)-1-((tetrahydro-2H-pyran-4-yl)methyl)-1H-benzo[d]imidazole-5-carbaldehyde **5.19** (75 mg, 0.213 mmol), (S)-neopentyl 2-amino-3-methylbutanoate 4-methylbenzenesulfonate **5.62** (153 mg, 0.427 mmol), sodium triacetoxyborohydride (90 mg, 0.427 mmol) and DCM (5 ml). The final product was: (S)-neopentyl 3-methyl-2-(((2-(5-methyl-6-oxo-1,6-dihydropyridin-3-yl)-1-

((tetrahydro-2*H*-pyran-4-yl)methyl)-1*H*-benzo[*d*]imidazol-5-yl)methyl)amino)butanoate **5.54**
(56 mg, 0.107 mmol, 50% yield) as a yellow gum.

LCMS (high pH): *rt* = 1.16 min, MH^+ = 523

¹H NMR (*d*₆-DMSO, 293 K): δ 0.84 – 0.95 (m, 15 H) 1.12 – 1.28 (m, 4 H) 1.82 – 2.02 (m, 2 H) 2.07 (s, 3 H) 2.96 (d, *J* = 5.8 Hz, 1 H) 3.06 – 3.16 (m, 2 H) 3.63 (d, *J* = 13.1 Hz, 1 H) 3.69 – 3.73 (m, 1 H) 3.88 (d, *J* = 13.4 Hz, 1 H) 4.20 (d, *J* = 7.1 Hz, 2 H) 7.20 (d, *J* = 8.3 Hz, 1 H) 7.52 (s, 1 H) 7.58 (d, *J* = 8.3 Hz, 1 H) 7.70 – 7.74 (m, 2 H) 11.90 (br.s., 1 H)

(2*S*,3*R*)-Neopentyl 3-hydroxy-2-(((2-(5-methyl-6-oxo-1,6-dihydropyridin-3-yl)-1-((tetrahydro-2*H*-pyran-4-yl)methyl)-1*H*-benzo[*d*]imidazol-5-yl)methyl)amino)butanoate, **5.55**:

Method as for **5.01**, using the following reagents: 2-(5-methyl-6-oxo-1,6-dihydropyridin-3-yl)-1-((tetrahydro-2*H*-pyran-4-yl)methyl)-1*H*-benzo[*d*]imidazole-5-carbaldehyde **5.19** (75 mg, 0.213 mmol), (2*S*,3*R*)-neopentyl 2-amino-3-hydroxybutanoate 4-methylbenzenesulfonate **5.63** (154 mg, 0.427 mmol), sodium triacetoxyborohydride (90 mg, 0.427 mmol) and DCM (5 ml). The final product was: (2*S*,3*R*)-neopentyl 3-hydroxy-2-(((2-(5-methyl-6-oxo-1,6-dihydropyridin-3-yl)-1-((tetrahydro-2*H*-pyran-4-yl)methyl)-1*H*-benzo[*d*]imidazol-5-yl)methyl)amino)butanoate **5.55** (35 mg, 0.067 mmol, 31% yield) as a yellow gum.

LCMS (high pH): *rt* = 0.93 min, MH^+ = 524

¹H NMR (*d*₆-DMSO, 293 K): δ 0.92 (s, 9 H) 1.11 – 1.27 (m, 7 H) 1.88 – 2.04 (m, 1 H) 2.07 (s, 3 H) 3.07 – 3.19 (m, 4 H) 3.67 (d, *J* = 13.1 Hz, 1 H) 3.69 – 3.75 (m, 2 H) 3.79 (d, *J* = 10.4 Hz, 1 H) 3.82 – 3.90 (m, 1 H) 3.94 (m, *J* = 13.1 Hz, 1 H) 4.20 (d, *J* = 7.3 Hz, 1 H) 4.63 – 4.74 (m, 1 H) 7.07 (dd, *J* = 8.3, 1.3 Hz, 1 H) 7.53 (s, 1 H) 7.59 (d, *J* = 8.3 Hz, 1 H) 7.71 – 7.75 (m, 2 H)

(2*S*,3*R*)-Neopentyl 2-(((2-(1,5-dimethyl-6-oxo-1,6-dihydropyridin-3-yl)-1-((tetrahydro-2*H*-pyran-4-yl)methyl)-1*H*-benzo[*d*]imidazol-5-yl)methyl)amino)-3-hydroxybutanoate, **5.56**:

Method as for **5.01**, using the following reagents: 2-(1,5-dimethyl-6-oxo-1,6-dihydropyridin-3-yl)-1-((tetrahydro-2*H*-pyran-4-yl)methyl)-1*H*-benzo[*d*]imidazole-5-carbaldehyde **5.61** (75 mg, 0.205 mmol), (2*S*,3*R*)-neopentyl 2-amino-3-hydroxybutanoate 4-methylbenzenesulfonate **5.63** (148 mg, 0.410 mmol), sodium triacetoxyborohydride (87 mg, 0.410 mmol) and DCM (5 ml). The final product was: (2*S*,3*R*)-neopentyl 2-(((2-(1,5-dimethyl-6-oxo-1,6-dihydropyridin-3-yl)-1-((tetrahydro-2*H*-pyran-4-yl)methyl)-1*H*-benzo[*d*]imidazol-5-yl)methyl)amino)-3-hydroxybutanoate **5.56** (30 mg, 0.056 mmol, 27% yield) as a colourless gum.

LCMS (high pH): *rt* = 0.98 min, MH^+ = 539

¹H NMR (d₆-DMSO, 293 K): δ 0.92 (s, 9 H) 1.10 – 1.24 (m, 7 H) 1.88 – 2.03 (m, 1 H) 2.10 (s, 3 H) 2.26 – 2.41 (m, 1 H) 3.05 – 3.15 (m, 3 H) 3.56 (s, 3 H) 3.63 – 3.83 (m, 5 H) 3.94 (d, *J* = 13.1 Hz, 1 H) 4.25 (d, *J* = 7.1 Hz, 2 H) 4.69 (d, *J* = 5.3 Hz, 1 H) 7.23 (dd, *J* = 8.3, 1.0 Hz, 1 H) 7.54 (s, 1 H) 7.61 (d, *J* = 8.3 Hz, 1 H) 7.73 (d, *J* = 1.0 Hz, 1 H) 8.11 (d, *J* = 2.3 Hz, 1 H)

(2*S*,3*R*)-Isobutyl 2-(((2-(1,5-dimethyl-6-oxo-1,6-dihydropyridin-3-yl)-1-((tetrahydro-2*H*-pyran-4-yl)methyl)-1*H*-benzo[*d*]imidazol-5-yl)methyl)amino)-3-hydroxybutanoate, **5.57**:

To a mixture of 2-(1,5-dimethyl-6-oxo-1,6-dihydropyridin-3-yl)-1-((tetrahydro-2*H*-pyran-4-yl)methyl)-1*H*-benzo[*d*]imidazole-5-carbaldehyde **5.61** (75 mg, 0.205 mmol) in DCM (5 ml) was added (2*S*,3*R*)-isobutyl 2-amino-3-hydroxybutanoate 4-methylbenzenesulfonate **5.64** (143 mg, 0.410 mmol) and triethylamine (0.072 ml, 0.513 mmol), and the reaction mixture stirred at room temperature for 1 hour. Sodium triacetoxyborohydride (87 mg, 0.410 mmol) was added, and the reaction mixture stirred at room temperature overnight. Saturated sodium bicarbonate solution (10 ml) was added and the organic layer separated. The aqueous layer was extracted with further DCM (10 ml), and the organic layers were combined, dried using a hydrophobic frit, and blown down under a stream of nitrogen. The sample was dissolved in DMSO (1 ml) and purified by MDAP (high pH). The solvent was blown down under a stream of nitrogen to give crude product of insufficient purity. The sample was again dissolved in DMSO (1 ml) and purified by MDAP (high pH). The solvent was blown down under a stream of nitrogen and dried in a vacuum oven to give the required product (2*S*,3*R*)-isobutyl 2-(((2-(1,5-dimethyl-6-oxo-1,6-dihydropyridin-3-yl)-1-((tetrahydro-2*H*-pyran-4-yl)methyl)-1*H*-benzo[*d*]imidazol-5-yl)methyl)amino)-3-hydroxybutanoate **5.57** (26 mg, 0.050 mmol, 24% yield) as an off-white foam.

LCMS (high pH): *rt* = 0.91 min, *MH*⁺ = 525

¹H NMR (d₆-DMSO, 293 K): δ 0.92 (d, *J* = 6.6 Hz, 6 H) 1.06 – 1.26 (m, 7 H) 1.82 – 2.02 (m, 2 H) 2.10 (s, 3 H) 3.05 – 3.19 (m, 3 H) 3.56 (s, 3 H) 3.64 – 3.76 (m, 3 H) 3.81 – 3.90 (m, 3 H) 3.93 (d, *J* = 13.1 Hz, 1 H) 4.26 (d, *J* = 7.1 Hz, 2 H) 4.61 – 4.79 (m, 1 H) 7.22 (dd, *J* = 8.3, 1.3 Hz, 1 H) 7.54 (s, 1 H) 7.61 (d, *J* = 8.3 Hz, 1 H) 7.71 – 7.75 (m, 1 H) 8.11 (d, *J* = 2.3 Hz, 1 H)

Remaining analysis performed on subsequent batch synthesised using similar conditions.

¹³C NMR (d₆-DMSO, 300 K): δ 17.4, 19.4, 20.7, 27.8, 30.4, 35.6, 37.9, 49.9, 52.2, 66.7, 66.8, 68.0, 70.3, 108.9, 111.2, 118.4, 123.2, 128.3, 134.6, 135.6, 137.3, 138.7, 142.9, 151.0, 162.3, 173.7.

M.pt.: 78–80 °C

HRMS: (C₂₉H₄₁N₄O₅) *MH*⁺ requires 525.3077, found *MH*⁺ 525.3070

[α_D]^{21.4 °C} (c 1.0, MeOH): -27.6 °

(S)-Cyclopentyl 3-methoxy-2-(((2-(5-methyl-6-oxo-1,6-dihydropyridin-3-yl)-1-((tetrahydro-2H-pyran-4-yl)methyl)-1H-benzo[d]imidazol-5-yl)methyl)amino)propanoate, 5.58:

Method as for **5.01**, using the following reagents: 2-(5-methyl-6-oxo-1,6-dihydropyridin-3-yl)-1-((tetrahydro-2H-pyran-4-yl)methyl)-1H-benzo[d]imidazole-5-carbaldehyde **5.19** (120 mg, 0.341 mmol), (S)-cyclopentyl 2-amino-3-methoxypropanoate hydrochloride **5.65** (153 mg, 0.683 mmol), triethylamine (0.119 ml, 0.854 mmol), sodium triacetoxyborohydride (145 mg, 0.683 mmol) and DCM (5 ml). The final product was: (S)-cyclopentyl 3-methoxy-2-(((2-(5-methyl-6-oxo-1,6-dihydropyridin-3-yl)-1-((tetrahydro-2H-pyran-4-yl)methyl)-1H-benzo[d]imidazol-5-yl)methyl)amino)propanoate **5.58** (127 mg, 0.243 mmol, 71% yield) as a white solid.

LCMS (high pH): rt = 0.92 min, MH⁺ = 523

¹H NMR (d₆-DMSO, 293 K): δ 1.10 – 1.26 (m, 4 H) 1.49 – 1.72 (m, 6 H) 1.74 – 1.87 (m, 2 H) 1.88 – 2.03 (m, 1 H) 2.07 (s, 3 H) 3.05 – 3.16 (m, 2 H) 3.21 (s, 3 H) 3.32 – 3.38 (m, 1 H) 3.49 (dd, *J* = 5.5, 1.3 Hz, 2 H) 3.66 – 3.77 (m, 3 H) 3.86 (d, *J* = 13.2 Hz, 1 H) 4.20 (d, *J* = 7.3 Hz, 2 H) 5.07 – 5.13 (m, 1 H) 7.20 (dd, *J* = 8.3, 1.2 Hz, 1 H) 7.50 (s, 1 H) 7.59 (d, *J* = 8.3 Hz, 1 H) 7.70 – 7.75 (m, 2 H) 11.65 – 12.01 (br.s., 1 H)

1,5-Dimethyl-6-oxo-1,6-dihydropyridine-3-carbaldehyde, 5.59:

A mixture of 5-methyl-6-oxo-1,6-dihydropyridine-3-carbaldehyde **3.25** (5 g, 36.5 mmol) and potassium carbonate (10.08 g, 72.9 mmol) in DMF (50 ml) was cooled in an ice/water bath, and methyl iodide (5.70 ml, 91 mmol) added dropwise. The reaction mixture was stirred for 15 min under nitrogen and then allowed to warm to room temperature and stirred for a further 2.5 hours. The solid was removed by filtration and the resulting solution evaporated under reduced pressure. The residue was partitioned between EtOAc (2 x 150 ml) and 1:1 water:saturated brine solution (150 ml). The organic layers were combined, dried using a hydrophobic frit, and evaporated under reduced pressure. The sample was loaded in DCM and purified by SPE (silica, 100 g) using a gradient of 0 – 50 % EtOAc in cyclohexane. The appropriate fractions were combined and evaporated under reduced pressure to give the required product 1,5-dimethyl-6-oxo-1,6-dihydropyridine-3-carbaldehyde **5.59** (4.4 g, 29.1 mmol, 80% yield) as an off-white solid.

LCMS (formic acid): rt = 0.46 min, MH⁺ = 152

¹H NMR (d₆-DMSO, 293 K): δ 2.04 (s, 3 H) 3.54 (s, 3 H) 7.59 – 7.73 (m, 1 H) 8.46 (d, *J* = 2.3 Hz, 1 H) 9.54 (s, 1 H)

Further analysis performed on subsequent batch prepared using similar conditions.

¹³C NMR (d₆-DMSO, 300 K): δ 12.4, 33.7, 113.1, 125.4, 127.7, 140.3, 159.0, 181.6.

IR (neat): 1695 (aldehyde), 1645 (pyridone), 1569 (aryl) cm^{-1}

M.pt.: 110–112 °C

HRMS: ($\text{C}_8\text{H}_{10}\text{NO}_2$) MH^+ requires 152.0712, found MH^+ 152.0708

5-(5-(Hydroxymethyl)-1-((tetrahydro-2H-pyran-4-yl)methyl)-1H-benzo[d]imidazol-2-yl)-1,3-dimethylpyridin-2(1H)-one, **5.60**:

To a mixture of 1,5-dimethyl-6-oxo-1,6-dihydropyridine-3-carbaldehyde **5.59** (1.135 g, 7.51 mmol) and sodium hydrosulfite (3.92 g, 22.53 mmol) was added a solution of (3-nitro-4-(((tetrahydro-2H-pyran-4-yl)methyl)amino)phenyl)methanol **5.21** (2 g, 7.51 mmol) in EtOH (12 ml), followed by water (6 ml). The reaction mixture was heated under microwave conditions at 100 °C for 5 hours. The reaction mixture was partitioned between saturated aqueous sodium bicarbonate solution (100 ml) and 3:1 chloroform:isopropanol (3 x 75 ml). The organic layers were combined, dried using a hydrophobic frit, and evaporated under reduced pressure. The sample was loaded in DCM and purified by SPE (silica, 100 g) using a gradient of 0 – 12% (2 M ammonia in MeOH) in DCM. The appropriate fractions were combined and evaporated under reduced pressure to give the required product 5-(5-(hydroxymethyl)-1-((tetrahydro-2H-pyran-4-yl)methyl)-1H-benzo[d]imidazol-2-yl)-1,3-dimethylpyridin-2(1H)-one **5.60** (1.1 g, 2.99 mmol, 40% yield) as an off-white foam.

LCMS (high pH): rt = 0.63 min, MH^+ = 368

^1H NMR (d_6 -DMSO, 293 K): δ 1.07 – 1.24 (m, 4 H) 1.90 – 2.01 (m, 1 H) 2.11 (s, 3 H) 3.06 – 3.14 (m, 2 H) 3.56 (s, 3 H) 3.66 – 3.77 (m, 2 H) 4.26 (d, J = 7.1 Hz, 2 H) 4.59 (d, J = 5.6 Hz, 2 H) 5.12 (t, J = 5.7 Hz, 1 H) 7.22 (d, J = 8.3 Hz, 1 H) 7.54 (s, 1 H) 7.62 (d, J = 8.3 Hz, 1 H) 7.74 (s, 1 H) 8.12 (d, J = 2.3 Hz, 1 H)

2-(1,5-Dimethyl-6-oxo-1,6-dihydropyridin-3-yl)-1-((tetrahydro-2H-pyran-4-yl)methyl)-1H-benzo[d]imidazole-5-carbaldehyde, **5.61**:

To a solution of 5-(5-(hydroxymethyl)-1-((tetrahydro-2H-pyran-4-yl)methyl)-1H-benzo[d]imidazol-2-yl)-1,3-dimethylpyridin-2(1H)-one **5.60** (1.1 g, 2.99 mmol) in DCM (50 ml) was added 45% iodoxybenzoic acid (stabilised by benzoic acid and isophthalic acid) (2.049 g, 3.29 mmol), portionwise. The reaction mixture was stirred at room temperature for 3 nights. The reaction mixture was partitioned between DCM (3 x 100 ml) and saturated aqueous sodium bicarbonate solution (100 ml). The organic layers were combined, dried using a hydrophobic frit, and evaporated under reduced pressure to give 2-(1,5-dimethyl-6-oxo-1,6-dihydropyridin-3-yl)-1-((tetrahydro-2H-pyran-4-yl)methyl)-1H-benzo[d]imidazole-5-carbaldehyde **5.61** (1.05 g, 2.87 mmol, 96% yield) as a pale yellow foam.

LCMS (high pH): rt = 0.71 min, MH^+ = 366

¹H NMR (d₆-DMSO, 293 K): δ 1.09 – 1.29 (m, 4 H) 1.90 – 2.01 (m, 1 H) 2.11 (s, 3 H) 3.11 (td, *J* = 10.9, 3.2 Hz, 2 H) 3.31 (s, 2 H) 3.72 (d, *J* = 11.1 Hz, 2 H) 4.36 (d, *J* = 7.3 Hz, 2 H) 7.78 (s, 1 H) 7.83 (d, *J* = 8.6 Hz, 1 H) 7.91 (d, *J* = 8.3 Hz, 1 H) 8.20 (s, 2 H) 10.06 (s, 1 H)

¹³C NMR (d₆-DMSO, 300 K): δ 17.3, 30.3, 35.6, 38.0, 50.1, 66.8, 108.1, 112.4, 122.7, 123.2, 128.4, 131.8, 137.0, 139.3, 141.0, 142.6, 153.4, 162.3, 193.0.

IR (neat): 2917 (saturated CH₂), 2842 (saturated CH₂), 1681 (aldehyde), 1654 (pyridone), 1604 (aryl), cm⁻¹

HRMS: (C₂₁H₂₄N₃O₃) MH⁺ requires 366.1818, found MH⁺ 366.1813

(S)-Neopentyl 2-amino-3-methylbutanoate 4-methylbenzenesulfonate, 5.62:

Method as for **5.29**, using the following reagents: (*S*)-2-amino-3-methylbutanoic acid (2.27 g, 19.38 mmol), 2,2-dimethylpropan-1-ol (13.66 g, 155 mmol), 4-methylbenzenesulfonic acid monohydrate (4.79 g, 25.2 mmol) and cyclohexane (100 ml). The reaction mixture was heated at 130 °C overnight. The final product was: (*S*)-neopentyl 2-amino-3-methylbutanoate 4-methylbenzenesulfonate **5.62** (3.9 g, 10.85 mmol, 56% yield) as a white solid.

¹H NMR (d₆-DMSO, 293 K): δ 0.94 (s, 9 H), 0.97 (d, *J* = 7.1 Hz, 3 H), 1.01 (d, *J* = 6.9 Hz, 3 H) 2.02 – 2.24 (m, 1 H) 2.29 (s, 3 H) 3.86 (d, *J* = 10.3 Hz, 1 H), 3.90 (d, *J* = 10.3 Hz, 1 H) 3.98 (d, *J* = 4.7 Hz, 1 H) 7.11 (d, *J* = 7.8 Hz, 2 H) 7.48 (d, *J* = 8.1 Hz, 2 H) 8.03 – 8.46 (br.s., 3 H)

(2*S*,3*R*)-Neopentyl 2-amino-3-hydroxybutanoate 4-methylbenzenesulfonate, 5.63:

To a suspension of (2*S*,3*R*)-2-amino-3-hydroxybutanoic acid (2.27 g, 19.06 mmol) and 4-methylbenzenesulfonic acid monohydrate (4.71 g, 24.77 mmol) in cyclohexane (100 ml) was added 2,2-dimethylpropan-1-ol (13.44 g, 152 mmol). The reaction mixture was fitted with a Dean–Stark condenser and heated at 130 °C overnight. A white slurry was formed upon cooling to room temperature, and it was evaporated under reduced pressure to remove the solvent. The white solid was dissolved in minimum amount of hot EtOAc and the clear solution was allowed to cool and then placed in an ice/water bath. No crystallisation occurred. The solution was evaporated under reduced pressure and dried in a vacuum oven for four nights. The resultant solid was recrystallised from EtOAc and allowed to cool, whereupon a white solid was formed. The resulting white solid was removed by filtration, washed with a little cold EtOAc, and dried in a vacuum oven to give the required product (2*S*,3*R*)-neopentyl 2-amino-3-hydroxybutanoate 4-methylbenzenesulfonate **5.63** (6.0 g, 16.60 mmol, 87% yield) as a white solid.

¹H NMR (d₆-DMSO, 293 K): δ 0.94 (s, 9 H) 1.22 (d, *J* = 6.3 Hz, 3 H) 2.29 (s, 3 H) 3.84 (d, *J* = 10.4 Hz, 1 H) 3.92 (d, *J* = 10.6 Hz, 1 H) 3.99 (d, *J* = 3.8 Hz, 1 H) 4.13 – 4.20 (m, 1 H) 5.61 (d, *J* = 4.3 Hz, 1 H) 7.11 (m, *J* = 7.8 Hz, 2 H) 7.48 (m, *J* = 8.1 Hz, 2 H) 8.22 (br.s., 3 H)

(2*S*,3*R*)-Isobutyl 2-amino-3-hydroxybutanoate 4-methylbenzenesulfonate, 5.64:

To a suspension of (2*S*,3*R*)-2-amino-3-hydroxybutanoic acid (2.5 g, 20.99 mmol) and 4-methylbenzenesulfonic acid monohydrate (5.19 g, 27.3 mmol) in cyclohexane (100 ml) was added 2-methylpropan-1-ol (15.50 ml, 168 mmol). The reaction mixture was fitted with a Dean–Stark condenser and heated at 130 °C overnight. The reaction mixture was allowed to cool to room temperature and the solvent removed under reduced pressure. The resulting colourless liquid was dried in a vacuum oven for three nights. Initially, recrystallisation was attempted using EtOAc, but the sample remained in solution and therefore the solvent was removed under reduced pressure. Trituration in diethyl ether was again unsuccessful, so the sample (with ether still present) was stood overnight open to the air, with a pasteur pipette and spatula left in the gum to attempt to induce crystallisation. A small amount of solid had formed around the spatula and pipette, so trituration in diethyl ether was again attempted, and was this time successful. The resulting white solid was removed by filtration and dried in a vacuum oven to give (2*S*,3*R*)-isobutyl 2-amino-3-hydroxybutanoate 4-methylbenzenesulfonate **5.64** (2.2 g, 6.33 mmol, 30% yield) as a white solid.

¹H NMR (d₆-DMSO, 293 K): δ 0.92 (d, *J* = 6.6 Hz, 6 H) 1.21 (d, *J* = 6.6 Hz, 3 H) 1.82 – 1.99 (m, 1 H) 2.29 (s, 3 H) 3.92 – 4.00 (m, 3 H) 4.11 – 4.17 (m, 1 H) 7.11 (d, *J* = 7.8 Hz, 2 H) 7.48 (d, *J* = 8.1 Hz, 2 H) 8.23 (br.s., 3 H)

¹³C NMR (d₆-DMSO, 300 K): δ 19.2, 20.6, 21.3, 27.7, 58.3, 65.5, 71.8, 126.0, 128.5, 138.1, 146.2, 168.7.

IR (neat): 1739 (ester), 1602 (secondary amine salt), 1405 (OSO₂), 1161 (OSO₂) cm⁻¹

M.pt.: amorphous solid

HRMS: (C₈H₁₈NO₃) MH⁺ requires 176.1287, found MH⁺ 176.1289

[α_D]^{21.4 °C} (c 1.0, MeOH): -3.2 °

(*S*)-Cyclopentyl 2-amino-3-methoxypropanoate hydrochloride, 5.65:

(*S*)-2-Amino-3-methoxypropanoic acid hydrochloride (3.3131 g, 21.30 mmol) was added to cyclopentanol (30 ml) and the suspension was brought to -5 °C using a dry ice/acetone bath. After stirring at this temperature for ten minutes, thionyl chloride (3.57 ml, 49.0 mmol) was added dropwise. The suspension was left stirring and allowed to warm to room temperature. The reaction mixture was warmed to 60 °C and stirred at this temperature for 24 hours. The volatile components were removed from the reaction mixture under reduced pressure. Hot EtOAc was added with the intention of performing a recrystallisation. The material did not dissolve so the suspension was filtered off, washed on the filter, and dried in a vacuum oven to give (*S*)-cyclopentyl 2-amino-3-methoxypropanoate hydrochloride **5.65** (4.49 g, 0.24 mmol,

94% yield) as a white solid.

¹H NMR (d₆-DMSO, 293 K): δ 1.51 – 1.76 (m, 6 H) 1.76 – 1.92 (m, 2 H) 3.29 (s, 3 H) 3.75 (d, *J* = 3.4 Hz, 2 H) 4.21 (t, *J* = 3.4 Hz, 1 H) 5.17 – 5.21 (m, 1 H) 8.64 (br.s., 3 H)

(2*S*,3*R*)-2-(((2-(1,5-Dimethyl-6-oxo-1,6-dihydropyridin-3-yl)-1-((tetrahydro-2*H*-pyran-4-yl)methyl)-1*H*-benzo[*d*]imidazol-5-yl)methyl)amino)-3-hydroxybutanoic acid hydrochloride,

5.66:

To a solution of (2*S*,3*R*)-cyclopentyl 2-(((2-(1,5-dimethyl-6-oxo-1,6-dihydropyridin-3-yl)-1-((tetrahydro-2*H*-pyran-4-yl)methyl)-1*H*-benzo[*d*]imidazol-5-yl)methyl)amino)-3-hydroxybutanoate **5.53** (35 mg, 0.065 mmol) in MeOH (2 ml) and THF (2 ml) was added 1 M aqueous lithium hydroxide solution (0.196 ml, 0.196 mmol), and the reaction mixture heated at 50 °C overnight. The reaction mixture was blown down under a stream of nitrogen. The sample was dissolved in 2 M aqueous hydrochloric acid (0.1 ml) and MeOH (0.9 ml) and purified by MDAP (high pH). The solvent was blown down under a stream of nitrogen and the residue suspended in THF (1 ml). 2 M aqueous hydrochloric acid (0.5 ml) was added and the resulting solution blown down under a stream of nitrogen to give the required product (2*S*,3*R*)-2-(((2-(1,5-dimethyl-6-oxo-1,6-dihydropyridin-3-yl)-1-((tetrahydro-2*H*-pyran-4-yl)methyl)-1*H*-benzo[*d*]imidazol-5-yl)methyl)amino)-3-hydroxybutanoic acid hydrochloride **5.66** (24 mg, 0.048 mmol, 73% yield) as an off-white solid.

LCMS (high pH): *rt* = 0.51 min, *MH*⁺ = 469

¹H NMR (d₆-DMSO, 293 K): δ 1.13 – 1.27 (m, 5 H) 1.27 – 1.35 (m, 2 H) 1.94 – 2.08 (m, 1 H) 2.13 (s, 3 H) 3.07 – 3.18 (m, 2 H) 3.55 – 3.65 (m, 4 H) 3.69 – 3.79 (m, 2 H) 4.11 – 4.17 (m, 1 H) 4.42 (br. s., 2 H) 4.49 (d, *J* = 7.1 Hz, 2 H) 7.72 (d, *J* = 8.8 Hz, 1 H) 7.85 (d, *J* = 1.3 Hz, 1 H) 8.08 (s, 1 H) 8.12 (d, *J* = 8.6 Hz, 1 H) 8.46 – 8.51 (m, 1 H) 9.47 – 9.72 (m, 1 H)

(*S*)-3-Methoxy-2-(((2-(5-methyl-6-oxo-1,6-dihydropyridin-3-yl)-1-((tetrahydro-2*H*-pyran-4-yl)methyl)-1*H*-benzo[*d*]imidazol-5-yl)methyl)amino)propanoic acid hydrochloride, **5.67:**

(*S*)-Cyclopentyl 3-methoxy-2-(((2-(5-methyl-6-oxo-1,6-dihydropyridin-3-yl)-1-((tetrahydro-2*H*-pyran-4-yl)methyl)-1*H*-benzo[*d*]imidazol-5-yl)methyl)amino)propanoate **5.58** (50 mg, 0.096 mmol) was dissolved in MeOH (2 ml) and THF (2 ml), and 1 M aqueous lithium hydroxide solution (0.287 ml, 0.287 mmol) was added. The reaction mixture was stirred at 60 °C for 18 hours. The reaction mixture was blown down under a stream of nitrogen. The crude sample was then suspended in MeOH (1.64 ml) and 2 M aqueous hydrochloric acid (0.16 ml, 0.28 mmol), and purified by MDAP (high pH). The solvent was evaporated under reduced pressure to give a white solid which was dried in a vacuum oven. The sample was suspended in THF (2 ml) and 2 M aqueous hydrochloric acid (1 ml) was added. The clear solution was blown down under a

stream of nitrogen to give the required product (*S*)-3-methoxy-2-(((2-(5-methyl-6-oxo-1,6-dihydropyridin-3-yl)-1-((tetrahydro-2*H*-pyran-4-yl)methyl)-1*H*-benzo[*d*]imidazol-5-yl)methyl)amino)propanoic acid hydrochloride **5.67** (33.7 mg, 0.069 mmol, 72% yield) as an off-white solid.

LCMS (high pH): *rt* = 0.50 min, MH^+ = 455

1H NMR (d_6 -DMSO, 293 K): δ 1.14 – 1.27 (m, 2 H) 1.28 – 1.35 (m, 2 H) 1.94 – 2.05 (m, 1 H) 2.09 (s, 3 H) 3.08 – 3.17 (m, 2 H) 3.32 (s, 3 H) 3.71 – 3.79 (m, 2 H) 3.85 – 3.95 (m, 2 H) 4.13 – 4.19 (m, 1 H) 4.34 – 4.45 (m, 4 H) 7.68 (d, J = 8.3 Hz, 1 H) 7.79 – 7.87 (m, 1 H) 8.02 – 8.08 (m, 3 H) 9.50 – 10.13 (br.s., 2 H) 12.18 – 12.55 (m, 1 H)

Appendix 1

Assay details

“Don't know much biology”

Sam Cooke, Wonderful World

In Vitro Assay Protocols

A1. HWB (IL-6 and MCP-1) assay

Human whole blood (HWB) was incubated with compounds in 96-well plates and then stimulated with LPS overnight. Supernatants were removed and the IL-6 and MCP-1 levels analysed by MSD assay to measure the effect of the compounds on the production of IL-6 and MCP-1.

15 µl of compounds in 10 mM DMSO were serially diluted (1:3) and added to IL-6 alpha-coated 96-well plates (MSD MA6000 96-well plate). 130 µl of human whole blood (with added sodium heparin, 10 µl/ml) was added to the compound wells, the plates incubated (37 °C, 5% CO₂) for 30 min, and 10 µl of 2.8 µg/ml LPS (diluted in 1% BSA) was added. The plates were incubated (37 °C, 5% CO₂) for 24 hours. 140 µl of either PBS or saline was added, and the plate shaken for 10 min. The plates were centrifuged at either 2000 or 2500 rpm for 10 min, and 100 µl of supernatant removed. To MSD plates were added 25 µl of diluted (MSD diluent) 1 in 40 supernatant and the plates were shaken for two hours. 25 µl of Sulfo-tag anti-IL-6/MCP-1 antibody (1 mg/ml dilution in MSD antibody diluent for IL-6 sample only) was added and the plates shaken for two hours. 150 µl MSD read buffer T (diluted 1:1 in distilled water) was added and the plates read on an MSD Specter 6000 reader.

A2. hERG FP assay

The hERG fluorescence polarization (FP) assay relies upon the binding of a fluorescent ligand to hERG membranes. When excited with polarized light, unbound ligand emits largely depolarized light during the fluorescence lifetime due to rapid rotation of the molecule in solution. Bound ligand is immobilized enough to emit more of the light in the same plane in which it was excited. The increase in FP is calculated from a weighted average of fluorescence intensity in the parallel and perpendicular planes. Potential hERG ligands will compete with the fluorescent compound and cause a decrease in FP signal.

0.1 µl of 10 mM astemizole solution was dispensed into a 384 well assay plate and 0.1 µl of compound in DMSO was added. An assay mixture was then made up as follows: 9654 µl hERG Assay Buffer (25 mM HEPES, 1.2 mM MgCl₂, 100 mM KCl, pH7.4), 50 µL pluronic acid, hERG membranes to a final concentration of 0.06 mg/ml, 10 µL Cy3B dofetilide ligand. 5 µl per well of assay mixture was added to the assay plate. The plates were covered and incubated for 60 min. The plates were read on an Envision Reader.

A3. CYP450 isoform assays

The CYP450 1A2 assay is described as an example; assays to identify inhibition of other CYP450 isoforms were performed in a similar manner.

The assay was performed with automation using Nanodrop/ThermoCRS/Envision or manually using a combination of Cybi and Multidrop Combi and was intended for detecting inhibition of cytochrome P450 (CYP450) 1A2 activity for drug developability purposes. This assay format utilizes the dealkylation of ethoxyresorufin to yield fluorescent resorufin.

Compounds were serially diluted (1:3) and added to Greiner 384 well plates. 2.5 µl of cofactor solution (2.02 µM ethoxyresorufin and 33.9 nM CYP450 1A2 bacosomes in 500 mM potassium phosphate, adjusted to pH 8.0) was added and the plates incubated at room temperature for 30 min. The fluorescence intensity was read immediately using an Envision plate reader (excitation: 431 nm, emission: 595 nm)

A4. BRD2/3/4 HTRF assay

The BRD4 HTRF assay is described, the protocol is similar for the BRD2 and BRD3 assays.

Homogenous time resolved fluorescence (HTRF) was used to measure binding of the tetraacetylated histone H4 peptide to BRD4 protein. The protein:protein interaction was detected through binding of the APC labelled anti-6His antibody to His-tagged BRD4 protein. Europium cryptate-labelled streptavidin binds the biotin in the H4 peptide, resulting in FRET between the two fluorophores when in close proximity upon excitation at 317 nm. Fluorescent emission by APC at 665 nm correlates with the amount of protein:protein binding.

50 nl of test compounds (serially diluted 1:3) were added to a black 384 Greiner plate. 8 µl of the assay reagent: 125 nM BRD4 in assay buffer (50 mM HEPES, pH7.4, 50 mM NaCl, 0.5 mM CHAPS) with added 375 nM biotinylated H4 peptide was added. Plates were spun at 1000 rpm, covered, and incubated in the dark for 1 hour at room temperature. 10 minutes before the end of the assay 2 µl incubation detection buffer containing 50 nM Monoclonal anti-6His antibody, labelled with XL665, and 10 nM Streptavidin, labelled with europium cryptate were added. Plates were read on an appropriate HTRF reader.

A5. PBMC (IL-6 and MCP-1) assay

Peripheral blood mononuclear cells (PBMCs) are a heterogeneous cell population that includes monocytes, T-cells and B-cells. Monocytes migrate to sites of inflammation and secrete

inflammatory cytokines, thereby activating other cell types such as T-cells. Stimulation of monocytes with LPS leads to downstream signalling events via its Toll-like receptor 4 (TLR4). Inhibition of LPS-induced activation of signal pathways is an important target for the treatment of many inflammatory diseases. In this assay, the activation of human primary monocytes following stimulation with LPS was monitored by the secretion of the cytokines IL-6 and MCP-1.

Previously frozen PBMCs were thawed using a water bath (37 °C), and the contents transferred into a 50 ml Falcon tube. 20 ml of assay media (DMEM with 10% FCS, 200 mM L-glutamine and 1% penicillin/streptomycin solution) was added dropwise. The cells were spun down in a centrifuge at 1000 rpm for 5 min and the supernatant decanted. The cells were resuspended in the above assay media to a dilution of 2×10^5 cells/ml. LPS was added to give a final concentration of 1 ng/ml, and 50 µl of this stimulated PBMC solution added immediately to Greiner 384 well assay plates containing 500 nl of test compound (serially diluted 1:3, top concentration 10 mM). The plates were incubated (37 °C, 5% CO₂, high humidity) for 24 hours. 5 µl of supernatants from the assay plates were transferred to white low-volume Greiner 384 well plates. 2 µl detection mixture (10.5 µg/ml M620 capture antibody conjugated AlphaLisa acceptor beads in FAC 3 µg/ml, and 210 ng/ml M621B biotinylated anti IL-6 antibody in FAC 60 ng/ml in the assay buffer described above) were added and the plates were incubated for 1 hour at room temperature. 2 µl of donor beads (54 µg/ml AlphaScreen Streptavidin–Donor beads in FAC 12 µg/ml, in the assay buffer described above). The plates were read on an Envision Reader using standard AlphaLisa protocols.

A6. Solubility by CLND assay

The aqueous solubility of compounds was determined using chemiluminescent nitrogen detection (CLND) as a quantification method. Stock solutions of 10 mM compounds in DMSO were serially diluted in phosphate buffered saline (pH7.4) and analysed by HPLC (Agilent 1100 HPLC system; mobile phase 90% methanol, 10% water; flow rate 0.2 ml/min) using CLND (Antek 8060C chemiluminescent nitrogen detector).

A7. CHIlogD determination

Chromatographic Hydrophobicity Index (CHI) is a high throughput way to measure the lipophilicity of a compound. The gradient retention time was transformed to an index, and can be expressed on a logD or logP scale (CHIlogD/CHIlogP). As both ChromlogD and CHIlogD are derived from the CHI scale they can be converted to each other: $\text{CHIlogD} = 0.613 \times$

ChromlogD - 0.242. The CHIlogD was measured at three pHs (2, 7.4 and 10.5) on a 4-way HPLC system (Agilent). The mobile phase at pH7.4 is 50 mM ammonium acetate adjusted to pH7.4, using concentrated ammonia solution.

A8. BRD4-BD1/2 FRET Assays

The BRD4-BD1 FRET assay is described. The protocol is similar for the BRD4-BD2 assay, except the protein used is a BRD4-Y97A mutant.

This assay is in a time-resolved Forster resonance energy transfer (TR-FRET) format, using a fluorescent ligand which is tagged with AlexaFluor647 and binds to both bromodomains of BRD4 with equal affinity. This acts as the acceptor in the FRET pair. To detect binding, the 6His purification tag at the *N*-terminal of BRD4 was utilised. This acted as the epitope for anti-6His europium chelate allowing binding of the europium to BRD4, which acted as the donor in the FRET pair. The protein utilised was a mutant of BRD4, which is BRD4-Y390A. This site-directed mutant (SDM) was unable to bind the fluorescent ligand at BD2 with the same affinity as BD1 (at least a 1000-fold decrease in affinity). This biased the assay to monitor binding at only the non-mutated domain, which in this case was BD1. When mixed with compounds, if the interaction was disrupted then there was a decrease in FRET.

50 nl of test compounds (serially diluted 1:3) were added to a Greiner 384 well low-volume assay plate. 5 µl of protein/ligand solution (to an assay buffer of 50 mM HEPES, 150 mM NaCl, 1 mM CHAPS pH7.4, 5% glycerol and 1 mM DTT pH7.4 (using NaOH) was added the fluoroprobe and BRD4-Y390A protein) was added. Plates were centrifuged at 1000 rpm for 60 seconds, and then incubated at room temperature for 30 min. Assay plates were read using an Envision Reader (emission 1: 665 nm, emission 2: 615 nm).

A9. Macrophage Acid Retention Assay

M1 macrophages were differentiated from CD14-positive monocytes. The monocytes were diluted to 1 million/ml and then treated with 5 ng/ml GM-CSF, plated at 1 million/well of a 24 well plate and allowed to differentiate for 5 days at 37 °C, 5% CO₂. After 5 days the plate was centrifuged and the medium carefully removed. The cells were treated with 10 µM of the relevant compound for a variety of time points. Additionally, medium containing compound (as above) was added to wells that did not contain any cells (no cell control; NCC) to determine the stability of the compound over time in cell culture medium. The NCC was also set up in lysis buffer (Mammalian Protein Extraction Reagent (MPER)). After the desired amount of time, the supernatant was removed and stored at -20 °C, the cells were washed twice with 500 µl PBS

each (which was also stored at -20 °C) and then 100 µl of MPER was added to lyse the cells and the lysate was also then stored at -20 °C. NCC wells were not washed but the supernatant/MPER buffer was removed and stored as above.

The samples were then analysed by mass spectrometry. 10 µM supernatants and no cell control samples were diluted 1/10 by adding 10 µl of sample to 90 µl of blank media. To 25 µl of all samples, 25 µl acetonitrile:water was added and all vials were capped and mechanically shaken for 20 min. An aliquot of the supernatant was analysed by LCMS/MS (API4000, SN: J1390111 (Demolishor)).

A10. Artificial Membrane Permeability Assay

The permeability of compounds through an artificial cell membrane was measured in a high-throughput assay.

3.5 µl of lipid solution (1.8% phosphatidylcholine in 1% cholesterol decane solution) was added to the filter plate (Millicell 96-well culture plate, 0.4 µm, PCF, 0.11 cm², non sterile), the plate was shaken for 12 seconds, and then 250 µl of buffer was added to the donor side and 100 µl to the receiver side. The assay plate was shaken for 45 min before adding the compounds. The test compounds (2.5 µl) were added to the donor side and the plates were then incubated at room temperature for 3 hours. The donor and receiver solution were then analysed by HPLC.

A11. Human Serum Albumin Binding Assay

The assay was designed to measure human serum albumin (HSA) binding. The basic principle of the assay was the determination of gradient retention times of compounds on immobilised HSA column, and converting these retention times to the appropriate property values using calibration. The peaks were detected and identified by UV. Calibration sets of compounds were measured before each run, for which the HSA binding values are known.

10 µl of 10 mM samples were diluted to 100 µl using 50% IPA and 50% water. The samples were analysed by HPLC (column: Chiral Technologies HSA column 50 x 3.0 mm (5 micron), flow rate: 1.8 ml/min, temperature: 30 °C, gradient: 0 to 3.0 minutes 0 to 30% mobile phase B, 3.0 to 5.0 minutes 30 % B, 5.0 to 5.1 minutes 30 to 0 % B, 5.1 to 6 min 0% B, detection: 254, 210 and 230 nm). The mobile phases were A: ammonium acetate solution in water, 50 mM, adjusted to pH7.4. B: IPA.

A12. Metabolism by Liver S9 Fraction Assay

The objective of the liver S9 metabolism assay was to measure the stability of the test compound in the presence of liver S9 fraction. The test compound was incubated over the course of a 45 min experiment, and analysed by LC-MS/MS.

Liver S9 fraction (1 mg/ml), 0.1 M phosphate buffer (pH7.4) and test compound (final substrate concentration 0.5 μ M) were incubated at 37 °C, and NADPH and UDGPA (final concentrations 1 mM) added to initiate the reaction. A control incubation was also tested without NADPH and UDGPA. Each compound was incubated for 45 min and the reaction stopped by the addition of methanol (100 μ l). The samples were centrifuged at 2500 rpm for 20 min at 4 °C to precipitate the protein, and then analysed by LC-MS/MS.

A13. FaSSIF Solubility Assay

This assay was designed as a high-throughput method to measure the solubility of compounds, from solid, in fasted state simulated intestinal fluid (FaSSIF).

FaSSIF solution (2.24 mg/ml, pH 6.5) was prepared by the addition of 2.24 mg SIF powder to 0.5 ml assay buffer (3.437 g sodium dihydrogen phosphate, 6.186 g sodium chloride and 0.42 g sodium hydroxide pellets in 500 ml distilled water) and 0.5 ml distilled water. This solution was added to a vial containing compound (1 mg), which was capped, inverted three times, and shaken at 900 rpm for 4 hours. 175 μ l was transferred to a filter plate (0.4 μ pore size), which was centrifuged for 5 min at 2000 rpm to capture the filtrate. The filtrate was analysed by HPLC, and the solubility generated by comparison with HPLC data generated by analysing the compound when fully dissolved in DMSO.

A14. Human Carboxyesterase-1 (hCE-1) Assay

The human carboxyesterase-1 (hCE-1) assay was designed to measure the specific activity of hCE-1 to cleave compounds containing an ESM. The reactions were run at fixed concentration of compound and enzyme at room temperature, over a number of time points. The reactions were stopped at low pH and analysed by reverse-phase HPLC. The percentage of product formed was used to determine the initial rate of the reaction, from which the specific activity of the enzyme under these conditions was obtained.

An enzyme solution (hCE-1 enzyme diluted to 100 nM in aqueous assay buffer: 50 mM sodium phosphate pH 7.5 and 100 mM sodium chloride) was added to wells of test compound solution (10 mM DMSO solutions of test compounds diluted to 100 μ M in aqueous assay buffer: 50 mM

sodium phosphate pH 7.5 and 100 mM sodium chloride). Individual wells were stopped in sequence by the addition of 20 μ l 5% v/v aqueous formic acid. The plate was analysed by HPLC (Agilent HPLC system, UV detection, Phenomenex Gemini 5 μ C18 column, mobile phase A: water + 0.1% formic acid, B: acetonitrile + 0.1% formic acid) and the percentage product formed at each time point obtained from the integrated chromatograms. Time courses for product concentration were plotted and the initial rate of the reaction obtained from the linear portion of the reaction. The resulting rate was divided by the enzyme concentration to give the specific activity (μ M/min/ μ M).

In Silico Modelling Details

B1. ACD clogP model, version 11.0

This model predicts the log (octanol/water partition coefficient). This is a measure of the lipophilicity of the unionised form of the compound and is independent of pH. The logP values are derived from an internal ACD/logP database containing over 5000 experimental logP values. All the logD octanol/water measures available at the time of this study (11 September 2008) were downloaded from GSK proprietary databases. After removing compounds with odd values the final set had 50445 unique compound measures.

B2. Calculated ChromlogD at pH7.4 Model.

This model predicts the chromatographic logD, which is a measure of the ionised form of the compound and is therefore dependent on pH. The model was initially generated using all the current results (8 August 2008) of the measured ChromlogD assay. It was regularly updated as new data became available to improve its predictive capability.^{A7} Using SIMCA-P v11.5 software, an orthogonal partial least squares model of ChromlogD was developed.

B3. Passive permeability in MDCK2 cells model

In order to build *in silico* models for passive permeability through MDCK2 cells at pH 6.5 and pH7.4, the physicochemical properties of 1362 compounds were calculated. These properties included the calculated ACD logP and logD, total polar surface area, molecular weight, the Abraham descriptors Alpha, Betah, V_x, R₂ and Pi, CMR, number of hydrogen bond acceptors, number of hydrogen bond donors, acid and base classes (an in-house scale based on the pK_a of the compounds) and numbers of positive ionisable centres, negative ionisable centres, aromatic rings, non aromatic rings and rotatable bonds. In addition, an additional set of descriptors based on a PCA analysis of the three-dimensional structure of the compounds was also included. Compounds were classified as 'high permeability' (> 200 nm/s), 'medium permeability' (from 50 nm/s to 200 nm/s) and 'low permeability' (<50nm/s) and split up randomly in a training and validation set. The training set consisted of 600 compounds, while the remaining compounds made up the validation set. The number of high permeability compounds in the validation set was bigger at pH7.4, and the number of low permeability compounds almost negligible.

Appendix 2

Benzimidazole *N*-Substituent Changes

“I don't expect you will really understand the beauty of the softly simmering cauldron with its shimmering fumes, the delicate power of liquids that creep through human veins, bewitching the mind, ensnaring the senses.”

Severus Snape, Harry Potter and the Philosopher's Stone, JK Rowling.

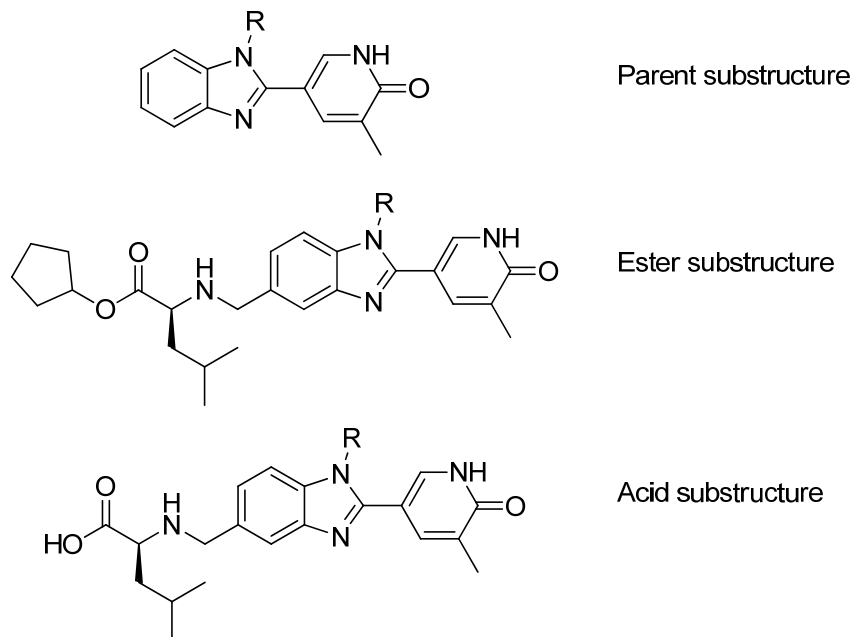
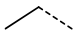
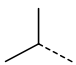
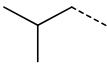
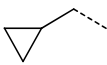

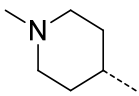
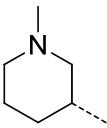
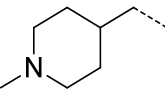
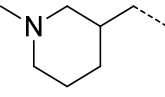
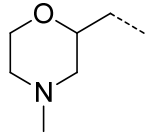
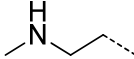
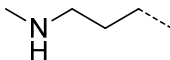
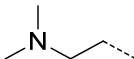
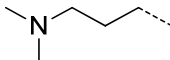
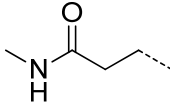
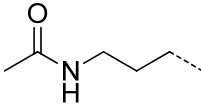
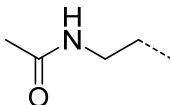
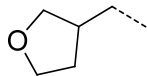
Table 1: Full List of Compounds for Synthesis

Table 1 (Below): List of changes to be made to the benzimidazole N-substituent, and the predicted physicochemical properties of the parent benzimidazole, ESM-containing ester and ESM-containing acid. Calculated ChromlogD^{B2} is shown in blue, and predicted passive permeability^{B3} is shown in green. The substructures are shown above the table.

Substituent type	R	Profile of parent	Profile of ester	Profile of acid
Alkyl	Me	4.36, 3.5, High	4.37, 5.3, Medium	4.38, 0.0, Low
Alkyl		4.60, 3.9, High	4.61, 5.7, Medium	4.62, 0.4, Low
Alkyl		4.63, 4.3, High	4.64, 6.0, Medium	4.65, 0.7, Low
Alkyl		4.39, 4.8, High	4.40, 6.4, Medium	4.41, 1.2, Low
Alkyl		4.66, 4.3, High	4.67, 6.1, Medium	4.68, 0.8, Low
Cyclic amine		4.69, 1.1, Low	4.70, 3.1, Low	4.71, -1.7, Low
Cyclic amine		3.22, 2.2, Medium	3.19, 4.1, Medium	3.21, -0.7, Low
Cyclic amine		4.72, 2.6, Medium	4.73, 4.5, Medium	4.74, -0.3, Low
Cyclic amine		4.75, 2.6, Medium	4.75, 4.4, Medium	4.77, -0.3, Low
Cyclic amine		4.78, 2.7, Medium	4.79, 4.4, Medium	4.80, -0.3, Low

Cyclic amine		4.42, 2.7, Medium	4.43, 4.5, Medium	4.44, -0.5, Low
Acyclic amine		4.81, 1.5, Low	4.82, 3.5, Low	4.83, -1.2, Low
Acyclic amine		4.84, 1.6, Low	4.85, 3.6, Low	4.86, -1.1, Low
Acyclic amine		4.45, 2.2, Medium	4.46, 4.1, Medium	4.47, -0.6, Low
Acyclic amine		4.87, 2.2, Medium	4.88, 4.1, Medium	4.89, -0.6, Low
Acyclic amide		4.90, 2.5, Medium	4.91, 4.3, Medium	4.92, -1.0, Low
Acyclic amide		4.93, 2.7, Medium	4.94, 4.5, Medium	4.95, -0.8, Low
Acyclic amide		4.48, 2.5, Medium	4.49, 4.3, Medium	4.50, -1.0, Low
Cyclic ether		4.96, 3.5, High	4.97, 5.9, Medium	4.98, 0.0, Low

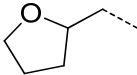
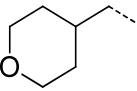
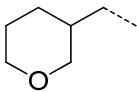
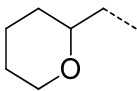
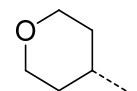
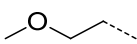
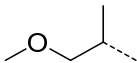
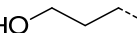

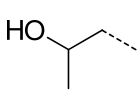
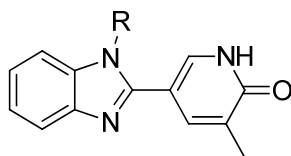
Cyclic ether		4.99, 3.8, High	4.100, 5.5, Medium	4.101, 0.3, Low
Cyclic ether		4.51, 3.9, High	4.52, 5.6, Medium	4.53, 0.3, Low
Cyclic ether		4.102, 3.9, High	4.103, 5.6, Medium	4.104, 0.4, Low
Cyclic ether		4.105, 4.2, High	4.106, 5.6, Medium	4.107, 0.6, Low
Cyclic ether		4.108, 3.4, High	4.109, 5.2, Medium	4.110, -0.1, Low
Acyclic ether		4.111, 3.5, High	4.112, 5.3, Medium	4.113, 0.0, Low
Acyclic ether		4.54, 3.8, High	4.55, 5.6, Medium	4.56, 0.3, Low
Acyclic alcohol		4.57, 2.6, Medium	4.58, 4.4, Medium	4.59, -0.2, Low
Acyclic alcohol		4.114, 2.3, Medium	4.115, 4.2, Medium	4.116, -0.5, Low
Acyclic alcohol		4.117, 2.6, Medium	4.118, 4.5, Medium	4.119, -0.1, Low

Table 2: Yields of Reactions in Chapter 4, Scheme 4.07

	R	S_NAr yield	Cyclisation yield
4.36	Me	96%, 4.120	41%, 4.36
4.60		88%, 4.121	73%, 4.60
4.63		72%, 4.122	63%, 4.63
4.39		94%, 4.123	50%, 4.39
4.66		99%, 4.124	50%, 4.66
4.69		52%, 4.125	48%, 4.126, 4.69
4.72		33%, 4.127	47%, 4.72
4.75		96%, 4.128	32%, 4.75
4.78		90%, 4.129	57%, 4.78
4.42		95%, 4.130	49%, 4.42
4.81		94%, 4.131	26%, 4.132, 4.81
4.84		92%, 4.133	41%, 4.134, 4.84
4.45		100%, 4.135	46%, 4.45

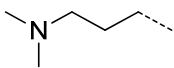
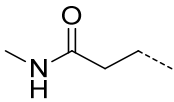
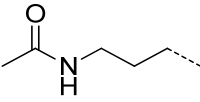
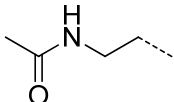
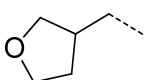
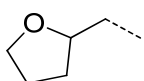
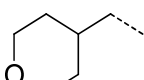
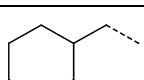
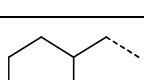
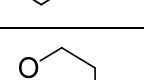
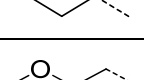
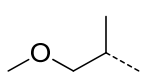
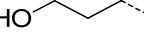
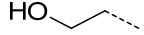

4.87		98%, 4.136	26%, 4.87
4.90		67%, 4.137	42%, 4.90
4.93		88%, 4.138	14%, 4.93
4.48		43%, 4.139	12%, 4.48
4.96		88%, 4.140	60%, 4.96
4.99		98%, 4.141	41%, 4.99
4.51		92%, 4.142	45%, 4.51
4.102		82%, 4.143	29%, 4.102
4.105		80%, 4.144	52%, 4.105
4.108		99%, 4.145	65%, 4.108
4.111		91%, 4.146	48%, 4.111
4.54		95%, 4.147	60%, 4.54
4.57		83%, 4.148	26%, 4.57
4.114		98%, 4.149	33%, 4.114
4.117		88%, 4.150	51%, 4.117

Table 2: Isolated yield for the S_NAr and benzimidazole cyclisation reactions shown in Scheme 4.07. For compounds 4.69, 4.81 and 4.84 the cyclisation yield also includes a BOC-deprotection. Underneath the yield is shown the compound number for each intermediate.

Table 3: Assay Data for Ester Hydrolysis Products for Compounds 5.01 – 5.12

Acid	BRD4-BD1 pIC₅₀ (n)	mChromlogD_{pH7.4}	Parent Ester
4.151	5.8 (5)	0.6	4.52
5.41	6.0 (2)	0.0	5.01
5.42	5.9 (2)	0.2	5.02
5.43	5.8 (2)	0.4	5.03
5.44	6.1 (3)	0.3	5.04
5.45	5.9 (3)	0.0	5.05
5.46	5.8 (3)	0.0	5.06
5.47	5.7 (2)	0.4	5.07
5.48	5.7 (2)	0.2	5.08
5.49	5.8 (2)	0.2	5.09
5.50	5.6 (2)	0.1	5.10
5.51	5.6 (2)	0.2	5.11
5.52	5.5 (2)	0.1	5.12

Table 3: Biological assay results for the acid hydrolysis products 5.41 – 5.52 for the ESM-containing esters 5.01 – 5.12, compared to the acid 4.151 of in vitro probe molecule 4.52, in the BRD4-BD1 mutant FRET assay,^{A8} and the mChromlogD_{pH7.4}.^{A7} The substructure of the compounds is shown above the table. The compounds are all hydrochloride salts, apart from 4.151 which is the lithium salt.

Appendix 3

Abbreviations

“itsl”

“Interesting to say the least”, www.cricketweb.net/forum (colloquial).

#Ar	Number of aromatic rings
Ac	Acetyl
ACD	Advanced Chemistry Development
ADC	Antibody drug conjugate
ADMET	Absorption, distribution, metabolism, excretion and toxicity
AIMS	Amplification of intermethylated sites
Alu-SP	SP subfamily of the Alu element of DNA
AMU	Atomic mass unit
APC	Allophycocyanin
ApoA1	Apolipoprotein A1
Ar	Aromatic ring
Asn	Asparagine
Asp	Aspartic acid
AUC	Area under the curve
BD1	Bromodomain 1
BD2	Bromodomain 2
BEH	Ethylene bridged hybrid
BET	Bromodomain and extra-terminal
Bn	Benzyl
BOC	<i>tert</i> -Butyloxycarbonyl
BRD2	Bromodomain-containing protein 2
BRD3	Bromodomain-containing protein 3
BRD4	Bromodomain-containing protein 4
BRD4-BD1	First bromodomain of bromodomain-containing protein 4
BRD4-BD2	Second bromodomain of bromodomain-containing protein 4
BRDt	Bromodomain testis-specific protein
BSA	Bovine serum albumin
cChromlogD	Calculated chromatographic distribution coefficient
CCL-2	Chemokine (C-C motif) ligand 2 (also known as MCP-1)
CES-1	Carboxylesterase 1 (also known as hCE-1)
CES-2	Carboxylesterase 2 (also known as hCE-2)
CHAPS	3-[(3-Cholamidopropyl)dimethylammonio]-1-propanesulfonate
CHI	Chromatographic hydrophobicity index
CHIlogD	Chromatographic hydrophobicity index distribution coefficient
ChromlogD	Chromatographic distribution coefficient

ChromlogP	Chromatographic partition coefficient
Cl _b	Blood clearance
CLND	Chemiluminescent nitrogen detection
clogP	Calculated partition coefficient
C _{max}	Maximum concentration
CMR	Calculated molar refractivity
c-Myc	v-Myc myelocytomatosis viral oncogene homologue
cPent	Cyclopentyl
CpG	Cytosine-phosphate-guanine
CTCL	Cutaneous T-cell lymphoma
CYP450	Cytochrome P450
dba	Dibenzylideneacetone
DCM	Dichloromethane
DEL	Deoxyribonucleic acid encoded library
ΔG	Change in Gibbs free energy
DIPEA	<i>N,N</i> -diisopropylethylamine
DMEM	Dulbecco's modified Eagle's medium
DMF	<i>N,N</i> -dimethylformamide
DMPK	Drug metabolism and pharmacokinetics
DMSO	Dimethylsulfoxide
DNA	Deoxyribonucleic acid
DPU	Discovery Performance Unit
DTT	Dithiothreitol
EBV	Epstein–Barr virus
EC ₅₀	Half maximal effective concentration
EC ₁₇₀	170% of maximal effective concentration
EDC	<i>N</i> -(3-Dimethylaminopropyl)- <i>N</i> -ethylcarbodiimide
ee	Enantiomeric excess
ELT	Encoded library technology
ESM	Esterase sensitive motif
Et	Ethyl
EtOAc	Ethyl acetate
EtOH	Ethanol
F	Oral bioavailability
FAC	1-(2'-deoxy-2'-fluoro-β- <i>D</i> -arabinofuranosyl)cytosine

FaSSIF	Fasted state simulated intestinal fluid
FCS	Foetal calf serum
FDA	Food and Drug Administration
FLINT	Fluorescence intensity
FP	Fluorescence polarisation
FRET	Forster resonance energy transfer
GI	Gastrointestinal
Gly	Glycine
GM-CSF	Granulocyte-macrophage colony stimulating factor
GPCR	G-protein coupled receptor
GSK	GlaxoSmithKline
HAC	Heavy atom count
HATU	<i>O</i> -(7-Azabenzotriazol-1-yl)- <i>N,N,N,N</i> -tetramethyluronium hexafluorophosphate
hCE-1	Human carboxylesterase 1
hCE-2	Human carboxylesterase 2
HDAC	Histone deacetylase
HEPES	4-(2-Hydroxyethyl)-1-piperazineethanesulfonic acid
hERG	Human ether-à-go-go-related gene
His	Histidine
HIV	Human immunodeficiency virus
HPLC	High-performance liquid chromatography
HPV	Human papilloma virus
HSA	Human serum albumin
HSV	Herpes simplex virus
HTRF	Homogeneous time resolved fluorescence
HTS	High throughput screening
HWB	Human whole blood
IC ₅₀	Half maximal inhibitory concentration
IL-10	Interleukin 10
IL-6	Interleukin 6
IND	Investigational new drug
IPA	Isopropyl alcohol
IR	Infra red
iv	Intravenous
JMJD3	Jumonji domain-containing protein 3

LBF	Liver blood flow
LC	Liquid chromatography
LCMS	Liquid chromatography–mass spectrometry
LCMS/MS	Liquid chromatography–tandem mass spectrometry
LE	Ligand efficiency
LHMDS	Lithium bis(trimethylsilyl)amide
LLE	Lipophilic ligand efficiency
logD	Distribution coefficient
logP	Partition coefficient
LPS	Lipopolysaccharide
MAP	Mitogen-activated protein
mChromlogD	Measured chromatographic distribution coefficient
MCP-1	Monocyte chemotactic protein 1
MDAP	Mass-directed auto-preparative HPLC
MDCK2	Madin–Darby canine kidney 2
Me	Methyl
MLA	Mouse lymphoma assay
MLL	Multiple mixed lineage
MNT	Micronucleus test
MPER	Mammalian protein extraction reagent
MS	Mass spectrometry
MSD	Meso Scale Discovery
mwt	Molecular weight
N/A	Not available
nBuLi	<i>n</i> -Butyllithium
NCC	No cell control
NMC	NUT midline carcinoma
NMP	<i>N</i> -Methyl-2-pyrrolidone
NMR	Nuclear magnetic resonance
NOE	Nuclear Overhauser effect
NUT	Nuclear protein in testes
PBMC	Peripheral blood mononuclear cell
PCA	Principal component analysis
PCAF	P300/cAMP-response element-binding protein-associated factor
PCR	Polymerase chain reaction

Pd/C	Palladium on carbon
Pd(PPh ₃) ₄	Tetrakis(triphenylphosphine)palladium(0)
PEPPSI-SIPr	Pyridine-enhanced precatalyst preparation stabilisation and initiation catalyst [1,3-bis(2,6-diisopropylphenyl)imidazolidene) (3-chloropyridyl) palladium(II) dichloride]
PFI	Property forecast index
Ph	Phenyl
PK	Pharmacokinetics
pK _a	Acid dissociation constant
po	<i>per os</i> (Latin; by mouth)
ppm	Parts per million
PSA	Polar surface area
pTSA	<i>para</i> -Toluene sulfonic acid
R&D	Research and development
RA	Rheumatoid arthritis
rt	Retention time
SAR	Structure-activity relationship
SCX	Sulfonic acid, strong cation exchange
SDM	Site-directed mutant
Ser	Serine
SFI	Solubility forecast index
siRNA	Small interfering ribonucleic acid
S _N Ar	Nucleophilic aromatic substitution
SPE	Solid phase extraction
ssDNA	Single-stranded deoxyribonucleic acid
t _{1/2}	Half-life
<i>t</i> Bu	Tertiary butyl
TFA	Trifluoroacetic acid
THF	Tetrahydrofuran
THP	Tetrahydropyran
THQ	Tetrahydroquinoline
TI	Therapeutic index
TLC	Thin layer chromatography
TLR4	Toll-like receptor 4
TMS	Tetramethylsilane

TNF _α	Tumour necrosis factor alpha
TR-FRET	Time-resolved Forster resonance energy transfer
Trp	Tryptophan
UPLC	Ultra-performance liquid chromatography
UV	Ultraviolet
VG	Vivid green
VR	Vivid red
V _{ss}	Volume of distribution
WPF	Tryptophan proline phenylalanine

References

“The more that you read, the more things you will know.”

I Can Read With My Eyes Shut! Dr Seuss

- 1.01. S.M. Paul, D.S. Mytelka, C.T. Dunwiddle, C.C. Persinger, B.H. Munos, S.R. Lindborg, A.L. Schacht; *Nat. Rev. Drug Discovery* **2010**, *9*, 203-214.
- 1.02. M.P. Gleeson, A. Hersey, D. Montanari, J. Overington; *Nat. Rev. Drug Discovery* **2011**, *10*, 197-208.
- 1.03. P.D. Leeson, B. Springthorpe; *Nat. Rev. Drug Discovery* **2007**, *6*, 881-890.
- 1.04. P.D. Leeson; J.R. Empfield; *Annu. Rep. Med. Chem.* **2010**, *45*, 393-407.
- 1.05. C.A. Lipinski, F. Lombardo, B.W. Dominy, P.J. Feeney; *Adv. Drug Delivery Rev.* **1997**, *23*, 3-25.
- 1.06. J.A. DiMasi, L. Feldman, A. Seckler, A. Wilson; *Clin. Pharmacol. Ther.* **2010**, *87*, 272-277.
- 1.07. Editorial; *Nat. Biotechnol.* **2010**, *28*, 1031-1032.
- 1.08. M.F. Fraga, E. Ballestar, M.F. Paz, S. Ropero, F. Setien, D. Heine-Suñer, J.C. Cigudosa, M. Urioste, J. Benitez, M. Boix-Chornet, A. Sanchez-Aguilera, C. Ling, E. Carlsson; P. Poulsen, A. Vaag, Z. Stephan, T.D. Spector, Y.-Z. Wu, C. Plass, M. Esteller; *Proc. Natl. Acad. Sci. U. S. A.* **2005**, *102*, 10604-10609.
- 1.09. J. Qui; *Nature*, **2006**, *441*, 143-145.
- 1.10. A. Portela; M. Esteller; *Nat. Biotechnol.* **2010**, 1057-1068.
- 1.11. L. Kruidenier; *Presentation: Epinova Seminar Series, GlaxoSmithKline* **2010**, 4th March.
- 1.12. T.D. Heightman; *Expert Opin. Ther. Targets* **2011**, *15*, 729-740.
- 1.13. U.S. Food and Drug Administration; FDA Approves New Drug for Skin Cancer, Zolanza. *Press release* 2006, P06-162.
- 1.14. P.A. Marks, R. Breslow; *Nat. Biotechnol.* **2007**, *25*, 84-90.
- 1.15. C. Monneret; *Anti-Cancer Drugs* **2007**, *18*, 363-370.
- 1.16. M. Paris, M. Porcelloni, M. Binaschi, D. Fattori; *J. Med. Chem.* **2008**, *51*, 1505-1529.
- 1.17. S.V. Frye, T. Heightman, J. Jin; *Annu. Rep. Med. Chem.* **2010**, *45*, 329-343.
- 1.18. P. Filippakopoulos, J. Qi, S. Picaud, Y. Shen, W.B. Smith, O. Fedorov, E.M. Morse, T. Keates, T.T. Hickman, I. Felletar, M. Philpott, S. Munro, M.R. McKeown, Y. Wang, A.L. Christie, N. West, M.J. Cameron, B. Schwartz, T.D. Heightman, N. La Thangue, C.A. French, O. Wiest, A.L. Kung, S. Knapp, J.E. Bradner; *Nature* **2010**, *468*, 1067-1073.
- 1.19. E. Nicodeme, K.L. Jeffrey, U. Schaefer, S. Beinke, S. Dewell, C. Chung, R. Chandwani, I. Marazzi, P. Wilson, H. Coste, J. White, J. Kirilovsky, C.M. Rice, J.M. Lora, R.K. Prinjha, K. Lee, A. Tarakhovsky; *Nature* **2010**, *468*, 1119-1123.

- 1.20. A. Villagra, F. Cheng, H.-W. Wang, I. Suarez, M. Glozak, M. Maurin, D. Nguyen, K.L. Wright, P.W. Atadja, K. Bhalla, J. Pinilla-Ibarz, E. Seto, E.M. Sotomayor; *Nat. Immunol.* **2009**, *10*, 92-100.
- 1.21. F. De Santa, V. Narang, Z.H. Yap, B.K. Tusi, T. Burgold, L. Austenaa, G. Bucci, M. Caganova, S. Notarbartolo, S. Casola, G. Testa, W.-K. Sung, C.-L. Wei, G. Natoli; *EMBO J.* **2009**, *28*, 3341-3352.
- 1.22. J.W. Tamkun, R. Deuring, M.P. Scott, M. Kissinger, A.M. Pattatucci, T.C. Kaufman, J.A. Kennison; *Cell* **1992**, *68*, 561-572.
- 1.23. S.R. Haynes, C. Dollard, F. Winston, S. Beck, J. Trowsdale, I.B. Dawid; *Nucleic Acids Res.* **1992**, *20*, 2603.
- 1.24. J.E. Brownell, C.D. Allis; *Curr. Opin. Genet. Dev.* **1996**, *6*, 176-184.
- 1.25. B.M. Turner; *BioEssays*, **2000**, *22*, 836-845.
- 1.26. C. Chung; *Prog. Med. Chem.*, **2012**, *51*, 1-55.
- 1.27. B. Florence, D.V. Faller; *Front. Biosci.* **2001**, *6*, d1008-1018.
- 1.28. S.-Y. Wu, C.-M. Chiang; *J. Biol. Chem.* **2007**, *282*, 13141-13145.
- 1.29. Y. Nakamura, T. Umehara, K. Nakano, M.K. Jang, M. Shirouzu, S. Morita, H. Uda-Tochio, H. Hamana, T. Terada, N. Adachi, T. Matsumoto, A. Tanaka, M. Horikoshi, K. Ozato, B. Padmanabhan, S. Yokoyama; *J. Biol. Chem.* **2007**, *282*, 4193-4201.
- 1.30. P. Filippakopoulos, J. Qi, S. Picaud, Y. Shen, W.B. Smith, O. Fedorov, E.M. Morse, T. Keates, T.T. Hickman, I. Felletar, M. Philpott, S. Munro, M.R. McKeown, Y. Wang, A.L. Christie, N. West, M.J. Cameron, B. Schwartz, T.D. Heightman, N. La Thangue, C.A. French, O. Wiest, A.L. Kung, S. Knapp, J.E. Bradner; *Nature* **2010**, *468*, 1067-1073.
- 1.31. M.Y. Teo, P. Crotty, M. O'Sullivan, C.A. French, J.M. Walshe; *J. Clin. Oncol.* **2011**, *29*, e336-e339.
- 1.32. D.E. Bauer, C.M. Mitchell, K.M. Strait, C.S. Lathan, E.B. Stelow, S.C. Luer, S. Muhammed, A.G. Evans, L.M. Sholl, J. Rosai, E. Giraldi, R.P. Oakley, C. Rodriguez-Galindo, W.B. London, S.E. Sallan, J.E. Bradner, C.A. French; *Clin. Cancer Res.* **2012**, *15*, 5773-5779.
- 1.33. E. Nicodeme, K.L. Jeffrey, U. Schaefer, S. Beinke, S. Dewell, C. Chung, R. Chandwani, I. Marazzi, P. Wilson, H. Coste, J. White, J. Kirilovsky, C.M. Rice, J.M. Lora, R.K. Prinjha, K. Lee, A. Tarakhovskiy; *Nature* **2010**, *468*, 1119-1123.
- 1.34. J.E. Delmore, G.C. Issa, M.E. Lemieux, P.B. Rahl, J. Shi, H.M. Jacobs, E. Kastiris, T. Gilpatrick, R.M. Paranal, J. Qi, M. Chesi, A.C. Schinzel, M.R. McKeown, T.P. Heffernan, C.R. Vakoc, P. Leif Bergsagel, I.M. Ghobrial, P.G. Richardson, R.A. Young, W.C. Hahn, K.C. Anderson, A.L. Kung, J.E. Bradner, C.S. Mitsiades; *Cell*, **2011**, *146*, 904-917.

- 1.35. M.A. Dawson, R.K. Prinjha, A. Dittmann, G. Giotopoulos, M. Bantscheff, W.-I. Chan, S.C. Robson, C. Chung, C. Hopf, M.M. Savitski, C. Huthmacher, E. Gudgin, D. Lugo, S. Beinke, T.D. Chapman, E.J. Roberts, P.E. Soden, K.R. Auger, O. Mirguet, K. Doehner, R. Delwel, A.K. Burnett, P. Jeffrey, G. Drewes, K. Lee, B.J.P. Huntly, T. Kouzarides; *Nature*, **2011**, *478*, 529-533.
- 1.36. H. Mahdi, B.A. Fisher, H. Källberg, D. Plant, V. Malmström, J. Rönnelid, P. Charles, B. Ding, L. Alfredsson, L. Padyukov, D.P.M. Symmons, P.J. Venables, L. Klareskog, K. Lundberg; *Nat. Genet.*, **2009**, *41*, 1319-1324.
- 1.37. B. Huang, X.-D. Yang, M.-M. Zhou, K. Ozato, L.-F. Chen; *Mol. Cell. Biol.* **2009**, *29*, 1375-1387.
- 1.38. S.-Y. Wu, A.-Y. Lee, S.Y. Hou, J. K. Kemper, H. Erdjument-Bromage, P. Tempst, C.-M. Chiang; *Genes Dev.* **2006**, *20*, 2383-2396.
- 1.39. F. Wang, H. Liu, W.P. Blanton, A. Belkina, N.K. Lebrasseur, G.V. Denis; *Biochem. J.*, **2010**, *425*, 71-83.
- 1.40. A study to investigate the safety, pharmacokinetics, pharmacodynamics, and clinical activity of GSK525762 in subjects with NUT Midline Carcinoma (NMC) and other cancers: <http://clinicaltrials.gov/show/NCT01587703> Retrieved 5th February 2014.
- 1.41. A Phase I, dose-finding study of the bromodomain (Brd) inhibitor OTX015 in haematological malignancies: <http://clinicaltrials.gov/ct2/show/NCT01713582> Retrieved 5th February 2014.
- 1.42. A Phase 1 study evaluating CPI-0610 in patients with progressive lymphoma: <http://clinicaltrials.gov/ct2/show/NCT01949883> Retrieved 5th February 2014.
- 1.43. D. Bailey, R. Jahagirdar, A. Gordon, A. Hafiane, S. Campbell, S. Chatur, G.S. Wagner, H.C. Hansen, F.S. Chiacchia, J. Johansson, L. Krimbou, N.C.W. Wong, J. Genest; *J. Am. Coll. Cardiol.* **2010**, *55*, 2580-2589.
- 1.44. S. Picaud, C. Wells, I. Felletar, D. Brotherton, S. Martin, P. Savitsky, B. Diez-Dacal, M. Philpott, C. Bountra, H. Lingard, O. Fedorov, S. Müller, P.E. Brennan, S. Knapp, P. Filippakopoulos; *Proc. Natl. Acad. Sci. U. S. A.* **2013**, *110*, 19754-19759.
- 1.45. Clinical Trial for Dose Finding and Safety of RVX000222 in Subjects With Stable Coronary Artery Disease (ASSERT): <http://clinicaltrials.gov/ct2/show/NCT01058018> Retrieved 5th February 2014.
- 1.46. S. Picaud, D. Da Costa, A. Thanasopoulou, P. Filippakopoulos, P.V. Fish, M. Philpott, O. Fedorov, P. Brennan, M.E. Bunnage, D.R. Owen, J.E. Bradner, P. Taniere, B. O'Sullivan, S. Müller, J. Schwaller, T. Stankovic, and S. Knapp; *Cancer Res.* **2013**, *73*, 3336-3346.

- 1.47. O. Mirguet, Y. Lamotte, F. Donche, J. Toum, F. Gellibert, A. Bouillot, R. Gosmini, V.-L. Nguyen, D. Delannée, J. Seal, F. Blandel, A.-B. Boullay, E. Boursier, S. Martin, J.-M. Brusq, G. Krysa, A. Riou, R. Tellier, A. Costaz, P. Huet, Y. Dudit, L. Trottet, J. Kirilovsky, E. Nicodeme; *Bioorg. Med. Chem. Lett.* **2012**, *22*, 2963-2967.
- 1.48. P. Bamborough, H. Diallo, J.D. Goodacre, L. Gordon, A. Lewis, J.T. Seal, D.M. Wilson, M.D. Woodrow, C. Chung; *J. Med. Chem.*, **2012**, *55*, 587-596.
- 1.49. D.S. Hewings, M. Wang, M. Philpott, O. Fedorov, S. Uttarkar, P. Filippakopoulos, S. Picaud, C. Vuppusetty, B. Marsden, S. Knapp, S.J. Conway, T.D. Heightman; *J. Med. Chem.*, **2011**, *54*, 6761-6770.
- 1.50. C. Chung, E. Nicodeme; *International Patent Application* **2011**, WO2011054843.
- 1.51. R. Macarron; *Drug Discovery Today* **2006**, *11*, 277-279.
- 1.52. S. Brenner, R.A. Lerner; *Proc. Natl. Acad. Sci. USA* **1992**, *89*, 5381-5383.
- 1.53. M.A. Clark; *Curr. Opin. Chem. Biol.* **2010**, *14*, 396-403.
- 1.54. Z.J. Gartner, M.W. Kanan, D.R. Liu; *J. Am. Chem. Soc.* **2002**, *124*, 10304-10306.
- 1.55. Z.J. Gartner, M.W. Kanan, D.R. Liu; *Angew. Chem., Int. Ed.* **2002**, *41*, 1796-1800.
- 1.56. B.N. Tse, T.M. Snyder, Y. Shen, D.R. Liu; *J. Am. Chem. Soc.* **2008**, *130*, 15611-15627.
- 1.57. D.R. Halpin, J.A. Lee, S.J. Wrenn, P.B. Harbury; *PLoS Biol.* **2004**, *2*, e175.
- 1.58. A. Furka, F. Sebestyén, M. Asgedom, G. Dibó; *Int. J. Pept. Protein Res.* **1991**, *37*, 487-493.
- 1.59. S.J. Wrenn, R.M. Weisinger, D.R. Halpin, P.B. Harbury; *J. Am. Chem. Soc.* **2007**, *129*, 13137-13143.
- 1.60. B. Morgan, S. Hale, C.C. Arico-Muendel, M. Clark, R. Wagner, D.I. Israel, M.L. Gefter, M.J. Kavarana, S.P. Creaser, G.J. Franklin, P.A. Centrella, R.A. Acharya, D. Benjamin, N.J.V. Hansen; *International Patent Application* **2007**, WO2007053358.
- 1.61. M.A. Clark, R.A. Acharya, C.C. Arico-Muendel, S.L. Belyanskaya, D.R. Benjamin, N.R. Carlson, P.A. Centrella, C.H. Chiu, S.P. Creaser, J.W. Cuzzo, C.P. Davie, Y. Ding, G.J. Franklin, K.D. Franzen, M.L. Gefter, S.P. Hale, N.J.V. Hansen, D.I. Israel, J. Jiang, M.J. Kavarana, M.S. Kelley, C.S. Kollmann, F. Li, K. Lind, S. Mataruse, P.F. Medeiros, J.A. Messer, P. Myers, H. O'Keefe, M.C. Oliff, C.E. Rise, A.L. Satz, S.R. Skinner, J.L. Svendsen, L. Tang, K. van Vloten, R.W. Wagner, G. Yao, B. Zhao, B.A. Morgan; *Nat. Chem. Biol.* **2009**, *5*, 647-654.
- 1.62. M. Margulies, M. Egholm, W.E. Altman, S. Attiya, J.S. Bader, L.A. Bemben, J. Berka, M.S. Braverman, Y.-J. Chen, Z. Chen, S.B. Dewell, L. Du, J.M. Fierro, X.V. Gomes, B.C. Godwin, W. He, S. Helgesen, C.H. Ho, G.P. Irzyk, S.C. Jando, M.L.I. Alenquer, T.P. Jarvie, K.B. Jirage, J.-B. Kim, J.R. Knight, J.R. Lanza, J.H. Leamon, S.M. Lefkowitz, M. Lei, J. Li,

- K.L. Lohman, H. Lu, V.B. Makhijani, K.E. McDade, M.P. McKenna, E.W. Myers, E. Nickerson, J.R. Nobile, R. Plant, B.P. Puc, M.T. Ronan, G.T. Roth, G.J. Sarkis, J.F. Simons, J.W. Simpson, M. Srinivasan, K.R. Tartaro, A. Tomasz, K.A. Vogt, G.A. Volkmer, S.H. Wang, Y. Wang, M.P. Weiner, P. Yu, R.F. Begley, J.M. Rothberg; *Nature* **2005**, *437*, 376-380.
- 1.63. I. Kola, J. Landis; *Nat. Rev. Drug Discovery* **2004**, *3*, 711-715.
- 1.64. D.F. Veber, S.R. Johnson, H.-Y. Cheng, B.R. Smith, K.W. Ward, K.D. Kopple; *J. Med. Chem.* **2002**, *45*, 2615-2623.
- 1.65. A.K. Ghose, V.N. Viswanadhan, J.J. Wendoloski; *J. Comb. Chem.*, **1999**, *1*, 55-68.
- 1.66. M.P. Gleeson; *J. Med. Chem.*, **2008**, *51*, 817-834.
- 1.67. T.W. Johnson, K.R. Dress, M. Edwards; *Bioorg. Med. Chem. Lett.*, **2009**, *19*, 5560-5564.
- 1.68. J.D. Hughes, J. Blagg, D.A. Price, S. Bailey, G.A. DeCrescenzo, R.V. Devraj, E. Ellsworth, Y.M. Fobian, M.E. Gibbs, R.W. Gilles, N. Greene, E. Huang, T. Krieger-Burke, J. Loesel, T. Wager, L. Whiteley, Y. Zhang; *Bioorg. Med. Chem. Lett.* **2008**, *18*, 4872-4875.
- 1.69. D.A. Price, J. Blagg, L. Jones, N. Greene, T. Wager; *Expert Opin. Drug Metab. Toxicol.* **2009**, *5*, 921-931.
- 1.70. D. Muthas, S. Boyer, C. Hasselgren; *MedChemComm* **2013**, *4*, 1058-1065.
- 1.71. P. Kirkpatrick; *Nat. Rev. Drug Discovery* **2012**, *11*, 900-901.
- 1.72. M.V.S. Varma, R.S. Obach, C. Rotter, H.R. Miller, G. Chang, S.J. Steyn, A. El-Kattan, M.D. Troutman; *J. Med. Chem.* **2010**, *53*, 1098-1108.
- 1.73. K. Sugano, M. Kansy, P. Artursson, A. Avdeef, S. Bendels, L. Di, G.F. Ecker, B. Faller, H. Fischer, G. Gerebtzoff, H. Lennernaes, F. Senner; *Nat. Rev. Drug Discovery* **2010**, *9*, 597-614.
- 1.74. A.L. Hopkins; C.R. Groom; A. Alex; *Drug Discovery Today* **2004**, *9*, 430-431.
- 1.75. R.J. Young, D.V. Green, C.N. Luscombe, A.P. Hill; *Drug Discovery Today* **2011**, *16*, 822-830.
- 1.76. T.J. Ritchie, S.J.F. Macdonald; *Drug Discovery Today*, **2009**, *14*, 1011-1020.
- 1.77. J.H. Lin, A.Y.H. Lu; *Pharmacol. Rev.* **1997**, *49*, 403-449.
- 1.78. G. Valsami, P. Macheras; *Mol. Inf.* **2011**, *30*, 112-121.
- 1.79. M. Vertzoni, J. Dressman, J. Butler, J. Hempenstall, C. Reppas; *Eur. J. Pharm. Biopharm.* **2005**, *60*, 413-417.
- 1.80. P.V. Balimane, Y.-H. Han, S. Chong; *AAPS J.* **2006**, *8*, E1-E13.
- 1.81. R.S. Obach; *Drug Metab. Dispos.* **1999**, *27*, 1350-1359.

- 1.82. M. Chiba, Y. Ishii, Y. Sugiyama; *AAPS J.* **2009**, *11*, 262-276.
- 1.83. J.H. Duffus, M. Nordberg, D.M. Templeton; *Pure Appl. Chem.*, **2007**, *79*, 1153-1344.
- 1.84. R. Urso, P. Blardi, G. Giorgi; *Riv. Eur. Sci. Med. Farmacol.* **2002**, *6*, 33-44.
- 1.85. V.J. Stella, W.N.A. Charman, V.H. Naringrekar; *Drugs*, **1985**, *29*, 455-473.
- 1.86. S.C. Alley, N.M. Okeley, P.D. Senter; *Curr. Opin. Chem. Biol.* **2010**, *14*, 529-537.
- 1.87. L.A. Needham, A.H. Davidson, L.J. Bawden, A. Belfield, E.A. Bone, D.H. Brotherton, S. Bryant, M.H. Charlton, V.L. Clark, S.J. Davies, A. Donald, F.A. Day, D. Krige, V. Legris, J. McDermott, Y. McGovern, J. Owen, S.R. Patel, S. Pintat, R.J. Testar, G.M.A. Wells, D. Moffat, A.H. Drummond; *J. Pharmacol. Exp. Ther.* **2011**, *339*, 132-142.
- 2.01. M.Y. Teo, P. Crotty, M. O'Sullivan, C.A. French, J.M. Walshe; *J. Clin. Oncol.* **2011**, *29*, e336-e339.
- 2.02. Helium: An Excel based user tool for SAR analysis:
<http://www.chemaxon.com/library/helium-an-excel-based-user-tool-for-sar-analysis/>
Retrieved 19th March 2012.
- 2.03. TIBCO Spotfire® professional: <http://spotfire.tibco.com/products/spotfire-professional/exploratory-data-analysis.aspx> Retrieved 19th March 2012.
- 2.04. T.J. Ritchie, S.J.F. Macdonald; *Drug Discovery Today*, **2009**, *14*, 1011-1020.
- 2.05. C.A. Lipinski, F. Lombardo, B.W. Dominy, P.J. Feeney; *Adv. Drug Delivery Rev.* **1997**, *23*, 3-25.
- 2.06. E.J. Ariëns; *Eur. J. Clin. Pharmacol.* **1984**, *26*, 663-668.
- 2.07. R.S. Brown, T.G. Traylor; *J. Am. Chem. Soc.*, **1973**, 8025-8032.
- 2.08. Synthesised by Robert Watson, *Epinova DPU*, GSK Stevenage.
- 2.09. S. Chen, R. Chen, M. He, R. Pang, Z. Tan, M. Yang; *Bioorg. Med. Chem.* **2009**, *17*, 1948-1956.
- 2.10. H. Suzuki, N.S.M. Aly, Y. Wataya, H.-S. Kim, I. Tamai, M. Kita, D. Uemura; *Chem. Pharm. Bull.*, **2007**, *55*, 821-824.
- 2.11. J.F. Gerster, K.J. Lindstrom, R.L. Miller, M.A. Tomai, W. Birmachu, S.N. Bomersine, S.J. Gibson, L.M. Imbertson, J.R. Jacobson, R.T. Knafla, P.V. Maye, N. Nikolaidis, F.Y. Oneyemi, G.J. Parkhurst, S.E. Pecore, M.J. Reiter, L.S. Scribner, T.L. Testerman, N.J. Thompson, T.L. Wagner, C.E. Weeks, J.-D. Andre, D. Lagain, Y. Bastard, M. Lupu; *J. Med. Chem.* **2005**, *48*, 3481-3491.
- 2.12. O. Prakash, H. Batra, H. Kaur, P.K. Sharma, V. Sharma, S.P. Singh, R.M. Moriarty; *Synthesis* **2001**, 541-543.
- 2.13. R.M. Moriarty, C.J. Chany II, R.K. Vaid, O. Prakash, S.M. Tuladhar; *J. Org. Chem.* **1993**, *58*, 2478-2482.

- 2.14. D. Yang, D. Fokas, J. Li, L. Yu, C.M. Baldino; *Synthesis* **2005**, 47-56.
- 2.15. P.A. Barsanti, C. Hu, K.B. Pfister, M. Sendzik, J. Sutton; *International Patent Application* **2011**, WO2011026904.
- 2.16. C. Bissantz, C. GrundSchober, H. Ratni, M. Rogers-Evans, P. Schnider; *International Patent Application* **2007**, WO2007009906.
- 2.17. Y. Ogino, N. Ohtake, Y. Nagae, K. Matsuda, M. Moriya, T. Suga, M. Ishikawa, M. Kanesaka, Y. Mitobe, J. Ito, T. Kanno, A. Ishihara, H. Iwaasa, T. Ohe, A. Kanatani, T. Fukami; *Bioorg. Med. Chem. Lett.* **2008**, *18*, 5010-5014.
- 2.18. T.T. Wager, S.R. Mente, T.W. Butler, G.F. Fuller Jr.; *International Patent Application* **2007**, WO2007069053.
- 2.19. A.J. Carpenter, K.A. Al-Barazanji, K.K. Barvian, M.J. Bishop, C.S. Britt, J.P. Cooper, A.S. Goetz, M.K. Grizzle, D.L. Hertzog, D.M. Ignar, R.O. Morgan, G.E. Peckham, J.D. Speake, W.R. Swain; *Bioorg. Med. Chem. Lett.* **2006**, *16*, 4994-5000.
- 2.20. A. El-Faham, R. Subirós-Funosas, F. Albericio; *Eur. J. Org. Chem.* **2010**, *19*, 3641-3649.
- 2.21. K. Mortelmans, E. Zeiger; *Mutat. Res., Fundam. Mol. Mech. Mutagen.* **2000**, *455*, 29-60.
- 2.22. J. Clements; *Mutat. Res., Fundam. Mol. Mech. Mutagen.* **2000**, *455*, 97-110.
- 2.23. Performed by Matthew Walker, *Exploratory Development Sciences*, GSK Stevenage.
- 2.24. H.K. Lee, Y.S. Lee, E.J. Roh, H. Rhim, J.Y. Lee, K.J. Shin; *Bioorg. Med. Chem. Lett.* **2008**, *18*, 4424-4427.
- 2.25. G. Basarab, B. Dangel, P.R. Fleming, M.B. Gravestock, O. Green, S.I. Hauck, P. Hill, K.G. Hull, G. Mullen, B. Sherer, F. Zhou; *International Patent Application* **2006**, WO2006087543.
- 2.26. S.R. Chemburkar, J. Bauer, K. Deming, H. Spiwek, K. Patel, J. Morris, R. Henry, S. Spanton, W. Dziki, W. Porter, J. Quick, P. Bauer, J. Donaubaue, B.A. Narayanan, M. Soldani, D. Riley, K. McFarland; *Org. Process Res. Dev.* **2000**, *4*, 413-417.
- 2.27. M. Vertzoni, J. Dressman, J. Butler, J. Hempenstall, C. Reppas; *Eur. J. Pharm. Biopharm.* **2005**, *60*, 413-417.
- 2.28. Experiments designed and performed by Tom Hayhow, *Epinova DPU*, GSK Stevenage.
- 2.29. P.L. Gould; *Int. J. Pharm. (Amsterdam, Neth.)* **1986**, *33*, 201-217.
- 2.30. H.J. Droogendijk, H.J.C. Kluin-Nelemans, J.J. van Doormaal, A.P. Oranje, A.A. van de Loosdrecht, P.L.A. van Daele; *Cancer* **2006**, *107*, 345-351.
- 2.31. J.P. Guthrie; *Can. J. Chem.* **1978**, *56*, 2342-2354.
- 2.32. D.P. Tashkin; *Expert Opin. Pharmacother.* **2010**, *11*, 2077-2085.

- 2.33. O.A. el Seoud, A.M. Chinelatto, M.R. Shimizu; *J. Colloid Interface Sci.* **1982**, *88*, 420-427.
- 2.34. H.A. Friedel, D.M. Campoli-Richards, K.L. Goa; Sultamicillin. *Drugs* **1989**, *37*, 491-522.
- 2.35. M. Boolell, M.J. Allen, S.A. Ballard, S. Gepi-Attee, G.J. Muirhead, A.M. Naylor, I.H. Osterloh, C. Gingell; *Int. J. Impotence Res.* **1996**, *8*, 47-52.
- 2.36. R.A. Evangelista, F.-T.A. Chen, A. Guttman; *J. Chromatogr., A* **1996**, *745*, 273-280.
- 2.37. J. Bryan; *Pharm. J.* **2007**, *279*, 404-405.
- 2.38. A.T.M Serajuddin; *Adv. Drug Delivery Rev.* **2007**, *59*, 603-616.
- 2.39. Data not shown. Experiments performed under the supervision of Dominic Beaumont, *Platform Technology and Science*, GSK Harlow.
- 2.40. X. Chen, J.S. Cordes, J.A. Bradley, Z. Sun, J. Zhou; *J. Pharmacol. Toxicol. Methods* **2006**, *54*, 261-272.
- 2.41. E.H. Demont, K.L. Jones, R.J. Watson; *International Patent Application* **2013**, WO2013024104A1.
- 2.42. K.L. Jones *et al.*; *Manuscript and author list in preparation.*
- 2.43. K.L. Jones; *Presentation: Drug Design and Medicinal Chemistry Conference, Berlin* **2014**, 8th May.
- 3.01. G. Gregoriadis; *Trends Biotechnol.* **1995**, *13*, 527-537.
- 3.02. K. Kataoka, A. Harada, Y. Nagasaki; *Adv. Drug Delivery Rev.*, **2001** *47*, 113-131.
- 3.03. L. Zhang, F.X. Gu, J.M. Chan, A.Z. Wang, R.S. Langer, O.C. Farokhzad; *Clin. Pharmacol. Ther.* **2008**, *83*, 761-769.
- 3.04. S.C. Alley, N.M. Okeley, P.D. Senter; *Curr. Opin. Chem. Biol.* **2010**, *14*, 529-537.
- 3.05. L.A. Needham, A.H. Davidson, L.J. Bawden, A. Belfield, E.A. Bone, D.H. Brotherton, S. Bryant, M.H. Charlton, V.L. Clark, S.J. Davies, A. Donald, F.A. Day, D. Krige, V. Legris, J. McDermott, Y. McGovern, J. Owen, S.R. Patel, S. Pintat, R.J. Testar, G.M.A. Wells, D. Moffat, A.H. Drummond; *J. Pharmacol. Exp. Ther.* **2011**, *339*, 132-142.
- 3.06. U.S. Food and Drug Administration; FDA Approves New Drug for Skin Cancer, Zolanza. *Press release* 2006, P06-162.
- 3.07. Y. Ma, R.M. Pope; *Curr. Pharm. Des.*, **2005**, *11*, 569-580.
- 3.08. C. Uphoff, H.G. Drexler; *Leuk. Lymphoma*, **2000**, *39*, 257-270.
- 3.09. T. Satoh, M. Hosokawa; *Annu. Rev. Pharmacol. Toxicol.*, **1998**, *38*, 257-288.
- 3.10. G.J. Ossenkoppele, B. Lowenberg, P. Zachee, N. Vey, D. Breems, A.A. Van de Loosdrecht, A.H. Davidson, G. Wells, L. Needham, L. Bawden, M. Toal, L. Hooftman, P.M. Debnam; *Br. J. Haematol.*, **2013**, *162*, 191-201.

- 3.11. Chroma Therapeutics Press Release: <http://www.chromatherapeutics.com/press-releases/Press-Release-23.pdf> Retrieved 26th November 2013.
- 3.12. E. Nicodeme, K.L. Jeffrey, U. Schaefer, S. Beinke, S. Dewell, C. Chung, R. Chandwani, I. Marazzi, P. Wilson, H. Coste, J. White, J. Kirilovsky, C.M. Rice, J.M. Lora, R.K. Prinjha, K. Lee, A. Tarakhovsky; *Nature* **2010**, *468*, 1119-1123.
- 3.13. Work carried out within Encoded Library Technology (ELT) group, *Platform Technology and Science*, GSK Boston.
- 3.14. Compounds designed and synthesised by Mythily Vimal, *Computational and Structural Chemistry*, GSK Stevenage.
- 3.15. B. Davies, T. Morris; *Pharm. Res.*, **1993**, *10*, 1093-1095.
- 3.16. R.J. Young, D.V.S. Green, C.N. Luscombe, A.P. Hill; *Drug Discovery Today* **2011**, *16*, 822-830.
- 3.17. D. Yang, D. Fokas, J. Li, L. Yu, C.M. Baldino; *Synthesis* **2005**, 47-56.
- 3.18. Synthesised at BioDuro: <http://www.bioduro.com/> (Retrieved 25th April 2013).
- 3.19. J.W. Williams, J.F. Morrison; *Methods Enzymol.* **1979**, *63*, 437-467.
- 3.20. J. Hambleton, S.L. Weinstein, L. Lem, A.L. DeFranco; *Proc. Natl. Acad. Sci. U. S. A.* **1996**, *93*, 2774-2778.
- 3.21. H.T. Aung, K. Schroder, S.R. Himes, K. Brion, W. van Zuylen, A. Trieu, H. Suzuki, Y. Hayashizaki, D.A. Hume, M.J. Sweet, T. Ravasi; *FASEB J.*, **2006**, *20*, 1315-1327.
- 3.22. T. Imai; *Drug Metab. Pharmacokinet.*, **2006**, *21*, 173-185.
- 3.23. Assays performed at Cyprotex: <http://www.cyprotex.com/> (Retrieved 19th May 2013).
- 4.01. T.J. Ritchie, S.J.F. Macdonald; *Drug Discovery Today*, **2009**, *14*, 1011-1020.
- 4.02. N.M. Aston, P. Bamborough, J.B. Buckton, C.D. Edwards, D.S. Holmes, K.L. Jones, V.K. Patel, P.A. Smee, D.O. Somers, G. Vitulli, A.L. Walker; *J. Med. Chem.* **2009**, *52*, 6257-6269.
- 4.03. K. Babaoglu, K. Bjornson, H. Guo, R.L. Halcomb, J.O. Link, H. Liu, M.L. Mitchell, J. Sun, R.W. Vivian, L. Xu; *International Patent Application* **2001**, WO2012003498A1.
- 4.04. V. Farina, S. Kapadia, B. Krishnan, C. Wang, L.S. Liebeskind; *J. Org. Chem.* **1994**, *59*, 5905-5911.
- 4.05. S. Saaby, K.R. Knudsen, M. Ladlow, S.V. Ley; *Chem. Commun.* **2005**, *23*, 2909-2911.
- 4.06. R.K. Reddy, M.D. Erion, Q. Dang; *International Patent Application* **2008**, WO2008019309.
- 4.07. Synthesised by Jack Brown, *Epinova DPU*, GSK Stevenage.
- 4.08. Work underway by Craig Robertson, Industrial PhD student, *University of Strathclyde and GSK*.

- 4.09. D. Yang, D. Fokas, J. Li, L. Yu, C.M. Baldino; *Synthesis* **2005**, 47-56.
- 4.10. Compounds and intermediates synthesised by Jack Brown, Robin Carton, Anet Varghese and Katherine Jones, *Epinova DPU*, GSK Stevenage.
- 5.01. R.J. Young, D.V.S. Green, C.N. Luscombe, A.P. Hill; *Drug Discovery Today*, **2011**, *16*, 822-830.
- 5.02. M. Vertzoni, J. Dressman, J. Butler, J. Hempenstall, C. Reppas; *Eur. J. Pharm. Biopharm.* **2005**, *60*, 413-417.
- 5.03. M. Hosokawa, T. Satoh; In *Toxicology of organophosphate and carbamate compounds*, R.C. Gupta, Ed; Elsevier Academic Press: California, **2006**, 219-232.
- 5.04. GSK public policy issues – Use of non-human primates (NHPs) in the discovery and development of medicines and vaccines.
<http://www.gsk.com/content/dam/gsk/globals/documents/pdf/use%20of%20non%20human.pdf>
 Retrieved: 28th October 2013.
- 5.05. J.H. Duffus, M. Nordberg, D.M. Templeton; *Pure Appl. Chem.*, **2007**, *79*, 1153-1344.
- 5.06. Work underway by Craig Robertson, Industrial PhD student, *University of Strathclyde and GSK*.
- 5.07. Accelrys available chemicals directory (ACD):
<http://accelrys.com/products/databases/sourcing/available-chemicals-directory.html> Retrieved 28th October 2013.
- 5.08. D. Weininger; *J. Chem. Inf. Model.*, **1988**, *28*, 31-36.
- 5.09. Helium: an excel based user tool for SAR analysis, ChemAxon:
<https://www.chemaxon.com/library/helium-an-excel-based-user-tool-for-sar-analysis/>
 Retrieved 28th October 2013.
- 5.10. J.H. Ward Jr.; *J. Am. Stat. Assoc.*, **1963**, *58*, 236-244.
- 5.11. F.A. Day, D.F. Launay, M.H. Charlton, D.F.C. Moffat; *International Patent Application* **2010**, WO2010043865.
- 5.12. A.H. Davidson, D.F.C. Moffat, F.A. Day, A.D.G. Donald; *International Patent Application* **2008**, WO2008040934.
- 5.13. D.F.C. Moffat, S. Pintat, S. Davies; *International Patent Application* **2009**, WO2009060160.
- 5.14. A.D.G. Donald, D.F.C. Moffat, A.J. Belfield, C.L. North, S.A.W. Jones; *International Patent Application* **2010**, WO2010097586.
- 5.15. L.A. Needham, A.H. Davidson, L.J. Bawden, A. Belfield, E.A. Bone, D.H. Brotherton, S. Bryant, M.H. Charlton, V.L. Clark, S.J. Davies, A. Donald, F.A. Day, D. Krige, V. Legris,

- J. McDermott, Y. McGovern, J. Owen, S.R. Patel, S. Pintat, R.J. Testar, G.M.A. Wells, D. Moffat, A.H. Drummond; *J. Pharmacol. Exp. Ther.* **2011**, 339, 132-142.
- 5.16. A. Varghese; *Industrial Placement Report* **2013**, University of Leeds.
- 5.17. D. Yang, D. Fokas, J. Li, L. Yu, C.M. Baldino; *Synthesis* **2005**, 47-56.
- 5.18. K.C. Nicolaou, P.S. Baran, Y.-L. Zhong; *J. Am. Chem. Soc.*, **2001**, 123, 3183-3185.
- 5.19. A.H. Drummond, R.J. Testar; *International Patent Application* **2010**, WO2010122294.
- 5.20. R. Fischer, S. Lehr, D. Feucht, O. Malsam, M.J. Hills, H. Kehne, C.H. Rosinger; *German Patent Application* **2006**, DE102006018828.
- 5.21. T.W. Johnson, K.R. Dress, M. Edwards; *Bioorg. Med. Chem. Lett.*, **2009**, 19, 5560-5564.
- 5.22. A. Hill, R. Young; *Drug Discovery Today*, **2010**, 15, 648-655.
- 5.23. D.A. Smith, B.C. Jones, D.K. Walker; *Med. Res. Rev.*, **1996**, 16, 243-266.
- 5.24. J.T. Goodwin, R.A. Conradi, N.F.H. Ho, P.S. Burton; *J. Med. Chem.*, **2001**, 44, 3721-3729.